Subfertility in grazing dairy cows: insights from a multi-omic exploration of the uterine microenvironment

---

A thesis

submitted in partial fulfilment

of the requirements for the Degree of

Doctor of Philosophy

at

Lincoln University

by

Nicolas Aranciaga

Lincoln University

2021

Abstract of a thesis submitted in partial fulfilment of the

requirements for the Degree of Doctor of Philosophy.

Subfertility in grazing dairy cows: insights from a multi-omic exploration of the uterine microenvironment

by

Nicolas Aranciaga

Dairy cow subfertility is a worldwide issue arising from multiple factors. One of its main manifestations is around 30% early pregnancy loss by day 7 of gestation in seasonal, pasture-grazed dairy herds. Pregnancy loss has a substantial impact on the seasonal grazing dairy cow as the mating period is short (six to nine weeks in length), and cows need to conceive while under strong metabolic stress to support their peak milk production. Factors in the uterine luminal fluid (ULF), on which the early embryo depends for sustenance and growth, appear to determine a portion of early pregnancy losses, and it is hypothesised that those factors improve with increasing days postpartum.

The present study examined the molecular composition of uterine luminal fluid (ULF) in day-7 pregnant dairy cows. Eighty cows were inseminated, and their uteri flushed 7 days later at two different oestrus cycles within three months of calving. Embryos recovered in those flushing samples were graded to estimate their potential viability and relate it to uterine suitability for pregnancy. The molecular milieu of ULF was investigated using three techniques: label-free quantitative proteomic analysis by LC-MS/MS, targeted metabolomic analysis by GC-MS/MS, and metabolic fingerprinting by REIMS (direct infusion mass spectrometry). For a more comprehensive perspective of the animals' conditions, potentially relevant variables at the cow-level were also measured and analysed. Moreover, links between embryo quality and differentially abundant molecules were investigated at the biochemical pathway level and by uni- and multivariate analyses, to screen for potential biomarkers of uterine suitability and to develop a predictive modelling pipeline.

Clear indications of differences across time postpartum were observed in the cow-level variables, signifying contrasting metabolic conditions between early- and mid-postpartum, with interaction between the actual time (days postpartum) and the number of oestrus events (oestrus after calving). Concomitantly, 33% more good- and excellent-quality embryos were found with increased days and oestrus cycles postpartum, reflecting a general positive effect of postpartum recovery on reproductive function.

A total of 1504 proteins were detected and measured in ULF, of which 472 had not been previously reported in this fluid. The abundance of 20 proteins varied relating to embryo quality, with various suggested roles in uterine function and embryogenesis-related pathways. Some of those proteins were macrophage migration inhibitory factor, phospholipase A2, myostatin, alpha-1-antiproteinase and prostaglandin reductase 1, involved in immune and development processes. Two proteins, cystatin C and pyruvate kinase M2, were more abundant in ULF with degenerate embryos (4-16 cells) and thus were considered promising protein biomarker candidates.

For biological validation, the effect of those proteins was tested on *in vitro* embryo culture system, together with cathepsin B, a protease potentially relevant to embryo quality. Different concentrations of each test protein were added to culture media; their effect was assessed based on development to tight morula and blastocyst stages, as well as embryo grade. Some evidence of a positive (of cystatin C) or negative (of pyruvate kinase M) effect on embryo development was observed.

Targeted metabolomic analysis of ULF showed 31 compounds' abundance varying along days and/or oestrus cycles after calving, with most (n = 25) decreasing with increasing days postpartum. These were chiefly carbohydrates (e.g. xylulose, ribose, fructose), and organic acids (e.g. malic, ethylmalonic and glyceric acids). Based on metabolomics data, pathways dysregulated at early postpartum included glycine, serine, and threonine metabolism, glycerolipid metabolism, beta alanine metabolism, pentose and glucuronate interconversions, cysteine, and methionine metabolism. Joint pathway analysis of proteomics and metabolomics data uncovered differentially regulated metabolic, signalling, and immune processes across oestrus cycles. Furthermore, dysregulation of protein metabolism and EGFR1 signalling in ULF appear to influence embryo development past the 16-cell stage.

A method for rapid metabolic fingerprinting based on a novel mass spectrometry technology (rapid evaporative ionisation mass spectrometry, REIMS) was tested for potential diagnostic applications. The method was successful at obtaining a distinct spectral profile of ULF, however its implementation for assessing uterine receptivity necessitates further instrumental optimisation.

Multivariate analyses (PCA and PLS-DA) of proteomic and metabolomic data suggested that the molecular microenvironment of the uterus is determined by the interaction of multiple factors at the animal level, and modelling of these intricate mechanisms is more challenging than previously thought.

In conclusion, this project's results advanced the characterisation of the molecular environment of bovine ULF. This study also provided evidence of links between molecular abundance of proteins and metabolites in the uterine environment to cow postpartum recovery and putatively to embryo quality, pinpointing metabolic and signalling pathways as potential mechanisms of action. The relevance of these molecular changes for diagnosing pregnancy suitability requires further research, of which concurrent analysis of follicular and uterine fluids at early postpartum is particularly promising.

Keywords: embryo, proteomics, metabolomics, modelling, pastoral farm system, agriculture, systems biology, uterine fluid, dairy cows, pregnancy

Publications

Papers

A modified version of Chapter 1, written by this thesis's author and supervisory team, has been published as follows: Aranciaga, N., Morton, J.D., Berg, D.K. and Gathercole, J.L., 2020. **Proteomics and metabolomics in cow fertility: a systematic review.** *Reproduction*, *160*(5), pp.639-658. 10.1530/REP-20-0047

Conference proceedings

Aranciaga, N., Morton, J.D., Hefer, C.A., Berg, D.K., and Gathercole, J.L. **Multi-omics approach to understanding dairy cow subfertility**. Multi-omics to mechanisms conference, European Molecular Biology Laboratory, Heidelberg, Germany. Poster presentation and lightning talk. September 2019.

Aranciaga, N., Morton, J.D., Berg, D.K., Gathercole, J.L. and Ross, A.B. **Optimising sample preparation for bovine uterine fluid metabolomics**. Australia and New Zealand Metabolomics Conference, Auckland, New Zealand. Poster presentation and lightning talk. September 2018.

Aranciaga, N., Gathercole, J.L., Berg, D.K., and Morton, J.D. **Biomarkers for contrasting early embryo development in cow uterus**. Australasian Proteomics Society Symposium, Lorne, Australia. Poster presentation. February 2018.

N.B. *appendices can be found in the last part of this thesis. Figures and tables in the appendices are noted e.g. "Fig. A1", "Supplementary Table S1.1", etc.*

Acknowledgements

During my PhD journey I have had the privilege to spend time and work with many of the best people I have ever met.

Firstly, I want to express my gratitude to my supervisors in equal manner; they have all been crucial for the success of this lengthy endeavour. To my main supervisor Jim Morton, for helping me connect my findings back to the bigger picture. He also provided fundamental comments to help me create order out of the massive amount of data that I got to play with. Jim, I am fortunate to have someone that is so good at their job. After every meeting with you I felt energised and a lot more motivated to do research. You rock!

To my associate supervisor Jess Gathercole, for spending many hours teaching me the magical world of molecular biology, for encouraging me and shaping me into something resembling a budding scientist. Jess, you have probably the best social skills of anyone I've ever encountered and I'm very happy to see you getting more students and continuing your path to scientific excellence. Thanks for becoming my friend along the way.

To my associate supervisor Deb Berg, for her limitless patience when answering my questions on animal physiology and embryo development. Deb, you are an incredibly driven scientist; your passion for your work is rarely seen in this environment in which admin eats out at the actual science. You are a role model.

Thanks to Deb, Robin MacDonald, Marty Berg, Natalie Lansdaal and Steph Delaney for treating the cows well, carrying out the animal-side work (sampling and inseminating), and performing the embryo culture experiments (Deb and Robin). Robin was also incredibly patient, organised, and helpful at sorting out technical stuff and teaching me embryo culture, together with Deb.

A heartfelt thank you also goes to the funders of this project: dairy farmers through DairyNZ Inc.'s programme DRCX1302, co-funded by Ministry of Business, Innovation and Employment (MBIE) and AgResearch. Without your generous support none of this would have happened. I also appreciate the multiple chances I was given to present this work at national and international forums. This was important to raise the profile of this field and showcase the hard work that the NZ dairy industry is doing to make farming more humane and sustainable.

I would also like to thank the many scientists and science-minded people from Agresearch that provided crucial assistance for the completion of this project, especially all the members of the

Proteins and Metabolites team at Agresearch. Stephen Haines, Ancy Thomas, Jeff Plowman, Erin Lee, and Ines Weissenbacher for assistance with instrument operation. Santanu Deb Choudhury, Arvind Subbaraj and Jennie Juengel, for revising my manuscripts. Duane Harland and Anita Grosvenor, for useful feedback on my presentations and advice on how science works. Alasdair Noble, Charles Hefer, Chikako van Hoten and Aurélie Laugraud for providing critical comments on bioinformatics and statistics over numerous meetings. Alastair Ross and Evelyne Maes became (unofficial) advisors in this project, with fundamental input into experimental planning and analysis strategies. My fellow PhD students and other office neighbours (Noémie, Catherine, Fionnuala, Sarah, Marina, Jennifer, Kim, and other short-time residents of the shared office) for putting up with some of my eccentricities and generally being awesome at creating a great environment to work in.

The Toastmasters bunch (especially Sonya Scott, Paul Middlewood and Chris Gregg) contributed hugely to my personal and professional development during my time in NZ. It was a pleasure and an honour to be member and president of the club, it has certainly made me a better human being.

As strange as it sounds, I did have a life before enrolling as a postgraduate student. I feel blessed that my parents Cristina and Gustavo put their best effort into raising me and my siblings. My siblings Joaquín and Ailén have also been immensely supportive, especially in recent years, and I really appreciate it. My partner Kee has also supported me at the distance and showed a great deal of patience waiting for me to finish my doctorate in a faraway land.

My many other friends that had a nice word for me when I needed it and made my life easier and more plentiful: Alex, Amy, Azusa, Eleana and Linh, Erica, Estelle, Jennel, Jorie, Nacho, Qianqian, Virginia, Zhen, and many others. I would not have been made it without you!

Abbreviations

AA: amino acid

ANOVA: analysis of variance

AU: arbitrary units

BCS: body condition score

BHB: beta hydroxybutyrate

CatB: cathepsin B

CysC: cystatin C

CL: corpus luteum

CV: coefficient of variation

Dpp: days postpartum

DTT: dithiothreitol

E2: oestradiol

EGFR1: epithelial growth factor receptor 1

ESPL: exclusion scheduled precursor list

ET: embryo transfer

EV: extracellular vesicle

FDR: false discovery rate, as defined by Benjamini and Hochberg (1995)

FF: follicular fluid

GC-MS/MS: gas chromatography coupled with tandem mass-spectrometry

GO: gene ontology

IVF/C/M: *in vitro* culture/fertilisation/maturation (of embryos or oocytes)

IAM: iodo-acetamide

IFNT: interferon tau

IMPaLA: integrated molecular pathway level analysis online tool

KEGG: Kyoto Encyclopaedia of Genes and Genomes

LC-MS/MS: liquid chromatography coupled with tandem mass-spectrometry

LFQ: label-free quantitation

LC-MS: liquid chromatography coupled with (single) mass-spectrometry

LOESS: locally weighted scatter-plot smoother

miRNA: micro ribonucleic acid

m/z: mass over charge

NCBI: National Centre for Biotechnology Information

NEFA: non-esterified fatty acids

OC: oestrus after calving (1 or 3)

OLF: oviduct luminal fluid

O-PLSDA: orthogonal partial least squares discriminant analysis

P4: progesterone

PCA: principal component analysis

PKM(2): pyruvate kinase subtype M(2)

PTM: posttranslational modifications

Q^2: goodness of prediction (predicted variation)

QC: quality control

QC-RFSC: quality control random forests signal correction

R^2: goodness of fit (explained variation)

REIMS: rapid evaporative ionisation mass spectrometry

Rt: retention time

SDC: sodium deoxycholate

sPLSDA: sparse partial least squares discriminant analysis

SPS: (uterine) size and position score

TCEP: Tris (2-carboxyethyl) phosphine

TIC: total ion chromatogram

ULF: uterine luminal fluid

Trials, experiments, and other work-specific terms

I: grade 1 embryos (tight morulae and blastocysts)

II: grade 2 embryos (tight morulae and blastocysts)

III: grade 3 embryos (tight morulae and blastocysts)

IV: 4- to 16-cell embryos (no 2-cell embryo was found in the present study)

V: 1- cell embryos or oocytes

VI: equivalent to NR, a class in the EQ1b system

Exp M1: Metabolomics experiment 1, protocol optimisation

Exp M2: Metabolomics experiment 2, testing heavy proline as a dilution tracer

Exp M3: Metabolomics experiment 3, preliminary REIMS metabolomic fingerprinting

Exp M4: Metabolomics experiment 4, main GC-MS/MS metabolomics experiment

Exp M5: Metabolomics experiment 5, main REIMS metabolomic fingerprinting experiment

Exp P1: Proteomics experiment 1, protocol optimisation

Exp P2: Proteomics experiment 2, variation sources preliminary trial

Exp P3: Proteomics experiment 3, main proteomics trial

Exp E1: Embryo *in vitro* culture experiment 1, supplementing cystatin C (CysC)

Exp E2: Embryo *in vitro* culture experiment 2, supplementing cathepsin B (CatB)

Exp E3: Embryo *in vitro* culture experiment 3, supplementing pyruvate kinase M (PKM)

EQ1: embryo quality classification 1 (five groups, I-V)

EQ1b: embryo quality classification 1 (like EQ1, plus including ULF with no embryo recovered as "VI")

EQ2: embryo quality classification 2, with two groups, I (optimal) vs III-V (suboptimal)

EQ3 embryo quality classification 3, with two groups, I-III (pregnant) vs IV-V (non-pregnant)

Farm Trial 1: small preliminary trial to test the use of tracer.

Farm Trial 2: main trial (2017)

Farm Trial 3: main trial (2018)

NR: non-recovery, e.g. ULF samples where no embryo was found (equivalent to EQ1b class "VI")

Table of Contents

Abstract ..... **ii**

Keywords: embryo, proteomics, metabolomics, modelling, pastoral farm system, agriculture, systems biology, uterine fluid, dairy cows, pregnancy ..... **iv**

Publications ..... **v**

Acknowledgements ..... **vi**

Abbreviations ..... **viii**

Table of Contents ..... **xii**

List of Tables ..... **xvii**

List of Figures ..... **xxi**

1 Introduction **1**

1.1 Background – dairy cow subfertility 1

1.1.1 Key events of early pregnancy in cow 2

1.1.2 Determinants of reproductive success 3

1.1.3 Challenges for the postpartum dairy cow 3

1.1.4 Omics technologies and biomarker discovery 10

1.1.5 Secretomics of bovine ULF 16

1.2 Rationale and aims of this work 17

2 Animal and sample collection **19**

2.1 Introduction 19

2.2 Materials and methods 19

2.2.1 Reagents and consumables 19

2.2.2 Farm and animal management 20

2.2.3 Phenotypical parameters 20

2.2.4 Experimental design 21

2.2.5 Statistical analysis 29

2.3 Results and discussion 30

2.3.1 Overall descriptive statistics and year effect 30

2.3.2 Effect of oestrus after calving (OC) and days post-partum (dpp) on animal phenotype 32

2.3.3 Embryo phenotype 35

2.4 Conclusions 43

3 Proteomics method development 44

3.1 Introduction 44

3.2 Materials 44

3.2.1 Reagents 44

3.2.2 Samples 45

3.3 Methods: sample preparation 45

3.3.1 ULF sample pre-processing 45

3.3.2 Extraction and processing 46

3.3.3 Protein reduction, alkylation, and digestion 47

3.3.4 Chromatography and mass spectrometry 49

3.3.5 Software analysis 51

3.3.6 Variation sources – pilot trial 52

3.4 Results and discussion 53

3.4.1 Sample pre-processing 53

3.4.2 Sample processing, extraction, albumin removal 54

3.4.3 Digestion 55

3.4.4 LC and MS parameters, use of Exclusion Lists 56

3.4.5 Software analysis 59

3.4.6 Optimal protocol summary 62

3.4.7 Proteomic analysis 63

3.4.8 Variation sources 64

4 Metabolomics method development 67

4.1 Introduction 67

4.1.1 Variability of sample volume 67

4.1.2 Aims....67
4.2 Materials and methods.... 68
4.2.1 Reagents and samples....68
4.2.2 Experimental design....68
4.3 Results and discussion 74
4.3.1 Experiment M1: development of optimal GC-MS/MS protocol....74
4.3.2 Experiment M2: Tracer 76
4.3.3 Targeted metabolomics: optimal protocol 80
4.3.4 Experiment M3: Optimisation of direct infusion mass spectrometry for metabolomic fingerprinting 81
4.4 Conclusions 83
5 Proteomic analysis....85
5.1 Introduction 85
5.2 Materials and methods.... 85
5.2.1 Assessment of blood contamination 85
5.2.2 Protocol for ULF sample analysis 86
5.2.3 Experimental design....86
5.2.4 Informatic and statistical analysis....87
5.3 Results and discussion 89
5.3.1 Blood contamination....89
5.3.2 Quality control assessment....89
5.3.3 Protein identification and ULF proteome meta-analysis 91
5.3.4 Protein functional analysis of ULF....93
5.3.5 Molecular factors determining embryo quality....97
5.4 Conclusions 111
6 Metabolomics....112
6.1 Introduction 112
6.2 Methods.... 112

6.2.1 Experimental design....112
6.3 Results and discussion....115
6.3.1 Experiment M4: targeted metabolomics....115
6.3.2 Integrated analysis: embryo quality and molecular changes postpartum....120
6.3.3 Experiment M5: metabolic fingerprinting....133
6.4 Summary, further remarks and conclusions....136

7 *In vitro* embryo culture....138
7.1 Introduction....138
7.1.1 Background....138
7.1.2 Aims....140
7.2 Materials and methods....140
7.2.1 Reagents and consumables....140
7.2.2 Experimental procedures....142
7.3 Results and discussion....147
7.3.1 Descriptive parameters across experiments....147
7.3.2 Effect of the test proteins on *in vitro* embryo development....149
7.3.3 Conclusions and recommendations....156

8 Discussion, conclusions, and further research....157
8.1 Recap – biological model and approach....157
8.2 Molecular and systemic determinants of subfertility....157
8.3 Technical aspects....159
8.4 Perspectives....160
8.5 Conclusion....160

References....162

A ppendices....193
A.1 Chapter 2....193
A.2 Chapter 4....194
A.3 Chapter 5....198

A.4 Chapter 6..... 205

List of Tables

Table 2-1 Different approaches to *in vivo* theriogenology experiments. 22

Table 2-2 Embryo classification schemes used, based on size and grade. 28

Table 2-3 Descriptive statistics in variables measured across all animals used in Farm Trials 2 and 3 together, by year, and statistical differences by t-test.....30

Table 2-4 Descriptive statistics of animals used and effect of the number of oestrus cycles after calving (OC) or days post-partum (dpp) on phenotypic variables, tested by paired t-test (OC) or linear regression (dpp). 34

Table 2-5 Proportions of embryo phenotypes found in ULF according to number of observed oestrus events postpartum.. 37

Table 2-6 Phenotype descriptive statistics according to embryo class (EQ1b). P- and q-values correspond to regression of EQ1 and EQ1b to the cow level variables.. 39

Table 2-7 Post-flushing embryo culture outcomes per grade.. 42

Table 3-1 Liquid Chromatography programme settings for long and short runs. 49

Table 3-2 Comparison of number of proteins identified between processing methods. 54

Table 3-3 Number of proteins identified with each combination of liquid chromatography and mass spectrometry settings trialled.. 58

Table 3-4 Most frequent post-translational modifications and putative mutations as identified by PEAKS Studio's Spider search tool. 61

Table 4-1 Latin square - methodological combinations for GC-MS/MS metabolomics optimisation experiments. 69

Table 5-1 Run order in a batch (example).. 87

Table 5-2 Number of proteins reported in studies surveying the bovine ULF proteome.....93

Table 5-3 Proteins classified as secreted by different bioinformatic tools.. 96

Table 5-4 Proteins in significantly higher abundance in third vs first oestrus postpartum.. 98

Table 5-5 Proteins in different abundance in ULF containing embryos of different quality (EQ1) at flushing on day 7. 105

Table 5-6 Differentially abundant proteins in ULF grouped according to EQ2 (III to V, i.e. 1-16 cell and grade 3 embryos, vs I -grade 1-) EQ3 (V and IV vs III-I) classification systems....107

Table 5-7 Functional categories and pathways impacted in ULF containing contrasting embryo quality, by Metascape overrepresentation analysis of proteomics data. 110

Table 6-1 Metabolites identified in ULF by untargeted or broadly targeted experiments.....117

Table 6-2 KEGG pathways significantly overrepresented in the full list of metabolites identified with respect to the whole bovine metabolome (~2100 compounds) using the MetaboAnalyst Pathway Overrepresentation tool.. 118

Table 6-3 Summary of results of statistical tests and modelling.. 122

Table 6-4 Differentially abundant metabolites across dpp and OC, at a q-value <0.05 123

Table 6-5 Enriched pathways in ULF according to metabolite abundance changes by OC and dpp, with q<0.05 and impact>0.3.. 125

Table 6-6 Significantly impacted pathways and functions across oestrus cycles postpartum by joint Wilcoxon enrichment analysis of proteins and metabolites using ImPALA web tool v12. 128

Table 6-7 Significantly dysregulated pathways and functions in non-pregnant uterine luminal fluid (ULF), i.e. EQ3 embryo quality IV and V (arrested at 1-16 cell state) by joint pathway enrichment analysis of proteins and metabolites. 131

Table 6-8 Features detected in REIMS (negative ionisation mode) at a significantly different abundance between ULF harbouring embryos of different grade (EQ1) by Kruskal-Wallis test.....135

Table 7-1 Overall combined embryo development parameters at day 7 of *in vitro* culture throughout the experiments described in this chapter. 148

Table 7-2 Effect on embryo development parameters of different concentrations of CysC and ammonium bicarbonate in culture medium by generalised linear models. 149

Table 7-3 Effect of the addition of CatB at different concentrations to culture medium on embryo development parameters by generalised linear models.....150

Table 7-4 Effect of the addition of pyruvate kinase M (PKM) at different concentrations to culture medium on embryo development parameters by generalised linear models. a. 150

Table A-1 Isotope-labelled proline (tracer) peak areas per sample.....194

Supplementary tables

Table S1-1 Studies investigating proteomics and metabolomics of bovine ULF.....217

Table S2-1 Details of the daily feed regime for cows either pregnant and non-lactating (dry), or milking, for the years 2017 and 2018. 219

Table S2-2 Instrument quality assurance values for oestradiol, progesterone NEFA and BHB concentration tests. 220

Table S2-3 Viability estimates according to embryo quality, from similar studies in literature…….221

Table S3-1a,b Top 5 proteins used to generate an Exclusion Scheduled Precursor List (ESPL) and MS/MS peptide list. ……222

Table S5-1 proteins detected most consistently across untargeted proteomic studies of bovine uterine luminal fluid (ULF). ……223

Table S5-2 curated entries of proteins previously unreported in bovine ULF. ……227

Table S5-3 full list of proteins identified in the present study and similar studies surveyed……229

Table S5-4 proteins identified as containing *Sec* signal peptides and thus putatively secreted through the classical secretion path as determined by SignalP analysis. ……365

Table S5-5 general linear model analysis of protein abundance (Exp. P3) across dpp and OC……373

Table S6-1 compounds detected in this study using broadly targeted or untargeted approaches, or both. ……395

Table S6-2 pathways to which metabolites detected in this study were mapped, as per Metaboanalyst overrepresentation analysis against the bovine metabolome……401

Table S6-3 univariate analysis of ULF metabolomics data, according to EQ1 (a), EQ2 (b) and EQ3 (c) embryo classification systems. ……404

Table S6-4 differentially regulated pathways across oestrus after calving (OC) by Metaboanalyst metabolites only……416

Table S6-5 enrichment results IMPaLA OC joint analysis……418

Table S6-6 enrichment results IMPaLA EQ2 joint analysis……489

Table S6-7 enrichment results IMPaLA EQ3 joint analysis……561

Table S6-8a differential abundance in OC of proteins in impacted pathways (joint analysis)……564

Table S6-8b differential abundance in OC of metabolites in impacted pathways (joint analysis)……568

Table S6-8c proteins in the epithelial growth factor receptor (EGFR1) pathway……575

Table S6-9 univariate analysis of ULF according to EQ1 embryo classification of REIMS features in negative ionisation mode. ……577

Table S7-1a,b Earle's salts and TCM 199 medium composition. ……581

Table S7-2 Exp. E1, E2, E3: raw data - number of embryos classified by stage and grade in each run (replicate). ……584

Table S7-3 embryo development parameters reported in experiments conducting in vitro embryo culture. ……587

Table S7-4a, b, c general linear models analysis: Exp. E1 (CysC, a), Exp. E2 (CatB, b) and Exp. E3 (PKM, c) ……588

List of Figures

Figure 1-1 Stages of development of pre-fertilisation and early pregnancy. 2

Figure 1-2 Schematic relationship between dairy cow feed requirements and herbal production, assuming a stocking rate of 3.3 cows/ha.....4

Figure 2-1 Synchronisation method for Farm Trial 1, testing the effect of isotope-labelled proline as tracer for dilution estimation. 21

Figure 2-2 Experimental design of Farm Trials 2 and 3.. 22

Figure 2-3 Photographs of day 7 embryos taken at 50x in a Nikon SMZ1500 stereo microscope.. .27

Figure 2-4 Schematic summary of the embryo quality classification systems employed. 29

Figure 3-1 Method combinations tested for sample preparation in this project's proteomics workflow. 47

Figure 3-2 Experimental design of a preliminary experiment (Exp. P2) to assess the degree of technical variation to total variation. 53

Figure 3-3 Processing protocol parameters trialled.....55

Figure 3-4 Protocol parameters trialled (digestion preparation).....56

Figure 3-5 Liquid chromatography and mass spectrometry parameters trialled.. 57

Figure 3-6 Software tools and parameters trialled.. 62

Figure 3-7 Principal component analysis (PCA) plot using the peptide features detected by LC-MS/MS analysis of uterine luminal fluid in the preliminary proteomics experiment to assess the degree of technical to total variation.....65

Figure 3-8 Pareto plot showing number of proteins in each range of percentage of coefficient of variation (CV) due to technical aspects vs total CV, which includes technical and biological variation (bars).. 66

Figure 4-1 Experimental workflows trialled for GC-MS/MS protocol optimisation to analyse ULF.. 69

Figure 4-2 Number of metabolites detected per replicate following each workflow combining either filtrate or whole uterine fluid with mono- or biphasic extraction. 74

Figure 4-3 Principal Component Analysis (first two components) showing the degree of similarity between technical replicates.....75

Figure 4-4 GC-MS/MS analysis (Exp. M2 - tracer): representative chromatograms for each type of sample.....78

Figure 4-5 Tracer peak areas of the different types of samples.. 79

Figure 4-6 REIMS (rapid evaporative ionisation mass spectrometry) reproducibility assessed by PCA. 83

Figure 5-1 Total ion chromatograms corresponding to QC pooled samples diluted 1:10 in Experiment P3. 90

Figure 5-2 Peptide sequence coverage of bovine serum albumin (BSA) standard, as obtained from a Mascot peptide web search, throughout the experiment. 91

Figure 5-3 Venn diagram showing proteins reported in the four studies with the highest number of proteins reported. 94

Figure 5-4 Venn diagram showing number of proteins classified as secreted by different informatic tools. 97

Figure 6-1 Venn diagram showing metabolites identified by targeted analysis, untargeted analysis, or both. 116

Figure 7-1 Experimental workflow of this embryo culture experiment. 143

Figure 7-2 Formulae for adjusting sperm preparation for *in vitro* fertilisation experiments. 145

Figure 7-3 Overview of Embryo experiments 1-3 (Exp. E1-3): composition of the controls and treatments in each experiment. 146

Figure A-8-1 PCA plot (PC1 and PC2) using normalised protein abundance as features. 193

Figure A-8-2 GC-MS/MS chromatogram example. A, qualifier ion chromatogram; B, quantifier ion chromatogram.. 195

Figure A-8-3 Example chromatograms obtained by REIMS metabolic fingerprinting, showing distinct degrees of signal-to-noise ratio according to ionisation mode. 196

Figure A-8-4 PCA of ULF sample replicates analysed in REIMS, after removal of features present in blanks, in negative or positive ionisation mode.. 197

Figure A-8-5 Graphic representation of batch correction done on sample intensity, LC-MS/MS Exp. P3. 198

Figure A-8-6 Peptide sequences of cystatin C and cystatin B 199

Figure A-8-7 PCA of proteomic features in ULF bearing embryos of different quality, according to the EQ3 classification system.. 200

Figure A-8-8 Treemap displaying enriched GO terms using all proteins identified in Exp. P3. 204

Figure A-8-9 Graphic representation of batch correction done on sample intensity, GC-MS/MS Exp. M4.. 206

Figure A-8-10 KEGG pathways overrepresented in the metabolite sets identified by targeted analysis or untargeted analysis vs the background of all compounds identified in this study. 207

Figure A-8-11 Relevant pathways differentially regulated across days postpartum (dpp) or oestrus after calving (OC).. 208

Figure A-8-12 PCA using auto-scaled metabolite abundance, coloured by embryo grade (EQ1). .209

Figure A-8-13 OPLS-DA showing predictive component 1 (x-axis) and orthogonal component 1 (variation unrelated to embryo grade) (y-axis), using embryo classification system EQ2 or EQ3.....210

Figure A-8-14 Graphic representation of batch correction done on sample intensity, REIMS Exp. M5.....212

Figure A-8-15 PCA of all samples; variables are peak area values from REIMS analysis in positive ionisation mode. 214

Figure A-8-16 PCA of all samples; variables are peak area values from REIMS analysis in negative ionisation mode. 216

1

Introduction

1.1 Background – dairy cow subfertility

Dairy cows' reproductive performance has been on the decline in the last decades in New Zealand and all over the world, and the causes are still being debated (Lucy 2001, Thatcher et al. 2011). This generalised impaired fertility is related to changes in cow physiology and management associated with increased milk production (LeBlanc 2010). More specifically, there seems to be a combination of various physiological and management factors at play, including: 1) genetic (breed, strain within breed), 2) diet and management, 3) endocrine and 4) reproductive tract factors (Evans and Walsh 2011). The latter are the focus of the present investigation, specifically the uterine luminal fluid (ULF).

The dairy industry is one of the leading economic sectors in New Zealand, accounting for a contribution of 8.2 billion dollars to the country's total GDP (Anonymous 2018). It is subject to political and commercial pressure to improve environmental performance, while required to stay competitive in the international market (von Keyserlingk et al. 2013). Therefore, efforts into optimising all aspects of the industry need to be addressed, including management and genetic factors (Jay and Morad 2007).

There has been a worldwide increase of milk production starting in the early 20th century (Royal et al. 2000). This increase is reflected in some of the most common parameters to measure milk production, namely total milk volume and milk solids (protein and fat) weight. These parameters differ in their significance: New Zealand's pricing system is based upon milk solids weight, with a deduction made for volume produced (Harris and Kolver 2001). In New Zealand, milk solids weight per cow per lactation increased 43% (259 kg/y to 372 kg/y) from 1992/1993 to 2008 (NZ Dairy Report Anonymous 2018). Concomitant to this, the rate of cows in-calf within six weeks of the seasonal planned start of mating decreased by about 20% (Burke et al. 2008).

Substantial economic losses, management difficulties and animal welfare concerns (Lucy 2001) have motivated a great deal of research to unravel the mechanisms of reduced fertility. Considerable progress to halt the decline in dairy cow fertility has been made in recent years using genetic approaches (Berglund 2008, García-Ruiz et al. 2016), but genetic variation in female fertility has a multifactorial basis that slows down genetic selection (Dennis et al. 2018).

1.1.1 Key events of early pregnancy in cow

Lonergan and Forde (2014) provide a succinct description of the main events taking place before embryo implantation in cattle (Figure 1-1). In brief, embryonic development starts after ovulation and fertilisation of the oocyte, which takes place in the oviduct. The resulting embryo migrates towards the uterus while increasing in cell number without increasing in volume through a series of cleavage stages. The bovine embryo enters the uterus 4 to 5 days after fertilisation at approximately the 16-cell to morula stage. The morula stage embryo undergoes compaction before completing its first lineage decision at the blastocyst stage. At this stage, approximately 7 days after fertilization, it consists of a trophectoderm which develops further to form the placenta, and an inner cell mass that eventually becomes the foetus. Around day 9, the spherical blastocyst hatches from the zona pellucida and commences to grow and change its shape from spherical to ovoid with the inner cell mass changing to a flattened embryonic disc. From day 12 to 14, the elongating embryo starts a transition period preceding a rapid increase in length: the 2 mm ovoid conceptus at day 13 reaches a length of around 60 mm by day 16, although considerable variation is observed between individuals (Berg et al. 2010, Ribeiro et al. 2016b). It is at this stage that the embryo begins gastrulation and the third cell lineage (the mesoderm) appears. Up to day 19, conceptuses (which comprise the embryo and extra-embryonic membranes) can be recovered by simple uterine flushing, but after that point the elongated conceptus starts to implant, its trophectoderm attaching to the luminal epithelium of the endometrium (Lonergan and Forde 2014). Throughout this period, the endometrial tissue also goes through increasingly conspicuous changes that allow for embryonic development and posterior implantation (Forde et al. 2011, Forde et al. 2012a), and constitutes an interdependent system with the endometrium and the extracellular fluid (uterine luminal fluid, ULF) that permeates them, reviewed in the next section. These changes of endometrial tissue modify the ULF biomolecular background (Rodriguez-Alonso, 2020a) and are important for the context of this research.

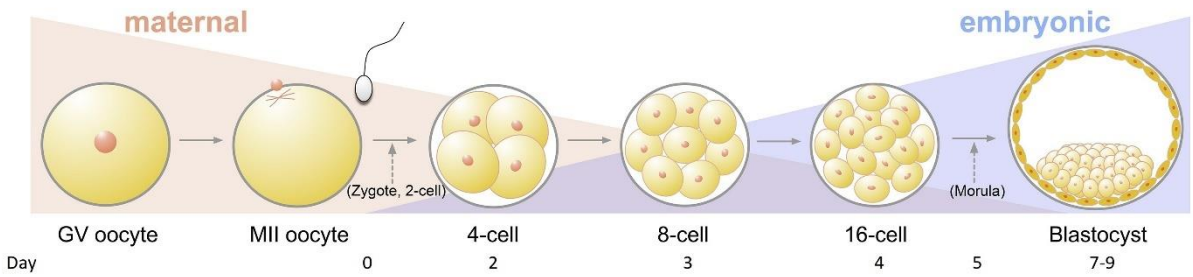

Figure 1-1 Stages of development of pre-fertilisation and early pregnancy. Adapted from Graf *et al.* (2014). Abbreviations: GV: germinal vesicle; MII: meiosis II.

1.1.2 Determinants of reproductive success

The development and birth of a healthy calf is a long process that depends on three main elements. These are paternal (comprehensively reviewed by Ceciliani et al. 2017), maternal, and the embryo itself (Artus et al. 2020). The relevance of this distinction between maternal and embryo factors is illustrated by studies assessing their relative effects: a previous meta-analysis of 46 sets of data comprising 4560 recipient cows using either embryo transfer or animals inseminated and concurrently receiving embryo transfer, demonstrated clear independent effects of embryos and recipient cows on embryo survival to parturition (McMillan 1998). More recently, Maillo et al. (2012) and Rizos et al. (2010) transferred good quality embryos synchronised with the recipient's day of oestrus -at either day 2 or day 7-; five or seven days after, they found embryos of markedly better quality in heifers and dry cows than in lactating cows, demonstrating the strong effect of the oviductal and uterine environments on embryo growth. Complementary molecular evidence of the same phenomenon was supplied by Moraes et al. (2018a), who transferred *in vivo* produced day-7 high-quality embryos to high and lower fertility beef heifers, describing substantial differences in the uterine transcriptomics of these animal groups at day 17 (ten days after embryo transfer, i.e. ET). These studies provide decisive evidence of the role of the uterine environment in pregnancy success, to a large extent independent of embryo quality (Lonergan et al. 2016).

1.1.3 Challenges for the postpartum dairy cow

Fertility problems can and should be considered from long before mating and conception. Coming into oestrus is arguably the first stage on the way to delivering a healthy calf; indeed, a prolonged post-partum anovulatory interval is considered a major form of infertility in New Zealand dairy cattle (McNaughton et al. 2003). This is especially critical in New Zealand and other countries with seasonal grazing dairying systems in which a circannual cycle needs to be maintained in order to synchronise feed requirements with pasture availability over the course of the year (Figure 1-2) (Roche et al. 2011). The peripartum and early postpartum period (one month before to two-three months after calving) are indeed the most critical period for the cows' health, in which their immune response needs to be strong enough to clear uterine pathogens while avoiding a hyperinflammatory state that is detrimental for physiological recovery and subsequent pregnancy (LeBlanc 2014). Along with the immune challenges, cows undergo high levels of metabolic stress due to much of their energy being diverted from physiological sustenance and recovery postpartum to milk production (Chagas et al. 2007). This substantial metabolic challenge results in a negative energy balance, whereby more energy is required than the cow can obtain by feed intake (Butler 2000).

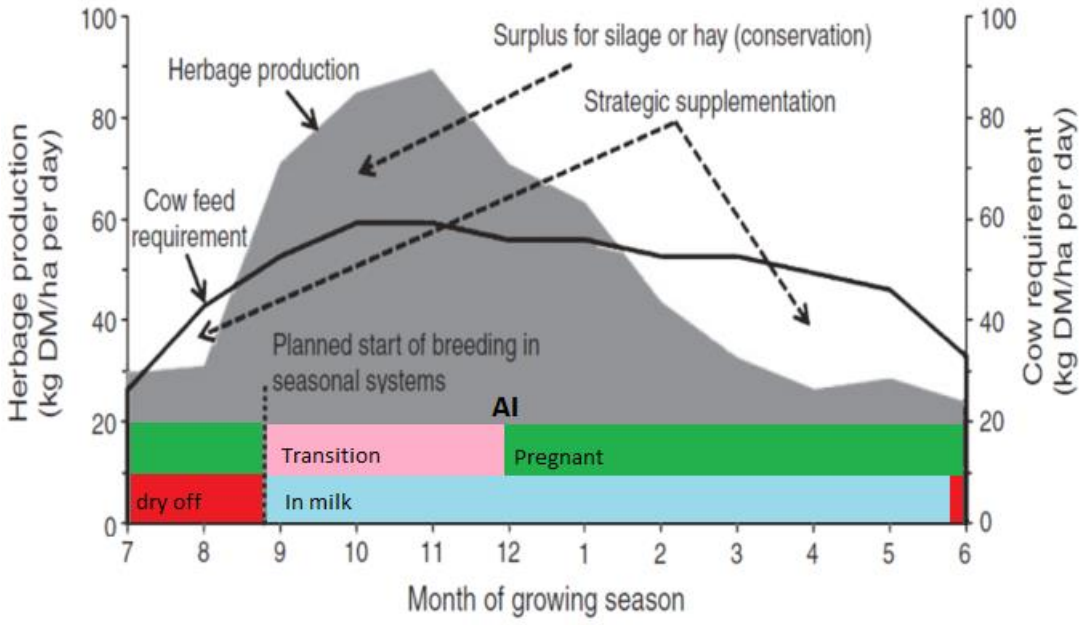

Figure 1-2 Schematic relationship between dairy cow feed requirements and herbal production, assuming a stocking rate of 3.3 cows/ha. To maintain a circannual (yearly) cycle to synchronise peaks in feed requirement and grass availability, cows need to get pregnant as soon as possible after calving. AI: artificial insemination. Modified from Roche et al. (2011).

The consequences of negative energy balance often include mobilisation of fat reserves and ketosis, indicated by loss of body condition score (BCS; Roche et al. 2009) and by higher blood concentrations of non-esterified fatty acids and beta-hydroxybutyrate, respectively (LeBlanc et al. 2011). Another aspect related to energetic disequilibrium is realised by lower concentrations of circulating glucose, diverted to milk production (Lucy et al. 2014), in what is called “uncoupling of the somatotropic axis” (Lucy et al. 2001). This entails ensuing low concentrations of insulin and high concentrations of growth hormone (“GH”, also called somatotropin), while decreasing expression of GH receptors (Lucy et al. 2001). A reduced number of GH receptors results in diminished secretion of insulin-like growth factor 1 (IGF1) (Lucy et al. 2014), a key hormonal link between metabolism and reproductive function (Kim 2014). IGF1 is instrumental in growth regulation in most mammal tissues (Jones and Clemmons 1995) and fundamental in postpartum recovery of reproductive functions (Garcia-Garcia 2012), hence the magnitude of this somatotropic axis destabilisation on resumption of ovulation (Chagas et al. 2007).

In addition to physiologically recovering from the adverse metabolic situation detailed, cows need to undergo uterine involution before their reproductive tract can successfully support embryo development (Breuel et al. 1993). This process is delayed by the metabolic and endocrine issues just examined (Scully et al. 2013) and is a sizable cause of subfertility in its own, considering that in

seasonal grazing systems like New Zealand cows must get pregnant by 85-90 days postpartum (dpp) to keep the annual calving-to-calving interval (Scully et al. 2013, Roche et al. 2017). While these morphological aspects have been well characterised, molecular changes in the reproductive tract along early postpartum and their relationship with resumption of cyclicity are still poorly understood (Wathes et al. 2009, Ribeiro et al. 2016a, Bauersachs et al. 2017, Forde et al. 2017, Edelhoff et al. 2020).

Suitability for pregnancy across the postpartum period

Due to the strong and often long-lasting effect of peripartum stress on the cow's health discussed, a trend for reproductive performance to improve later in the postpartum period is generally seen (Roche et al. 2009, Ferraz et al. 2016).

A classic study examining the effect of BCS on high producing dairy cows was conducted by Carvalho et al. (2014). In their first experiment, higher (≥2.75) versus lower (≤2.50) body condition score (BCS) at time of artificial insemination (AI) resulted in higher pregnancy rates (Carvalho et al. 2014). In their second experiment, 70-day pregnancy rates of cows that lost, maintained, or gained BCS from calving to 21 dpp were 23%, 36%, and 78%, respectively, but no effect of BCS changes was observed in one of the farms (Carvalho et al. 2014). In their third experiment, super-ovulated cows that lost the most weight from calving to 63 dpp had a significantly lower proportion of transferable embryos and higher proportion of degenerate embryos, all at day 7. This implies that in their animal model, body weight loss (as a result of negative energy balance) had a more pivotal effect on pregnancy than absolute body weight or BCS when these are within the intermediate range (2.25-3:25 in a 5-point scale). Santos et al. (2009) found a significant effect of BCS change between calving and AI (at around 65 dpp), but also of absolute values at each timepoint. Finally, Vasconcelos et al. (2006) compared pregnancy rates of lactating high producing dairy cows that underwent AI or ET (from non-lactating Holstein donors) from 50 to >500 dpp. They found 40% higher rates of pregnancy at day 25 in the ET vs AI group (59% vs 36%) in what may indicate lactation effects on oocytes; however, higher milk production was also associated to higher embryo death after ET (Vasconcelos et al. 2006) and thus presumably on uterine effects. Leroy et al. (2005a) described reduced pregnancy rates following ET of high producing lactating cows around a year after calving, showing that milk production can affect fertility independently from postpartum stress. In some cases, no effect of dpp on embryo survival was observed, though only after an average of 65 (Ferraz et al. 2016), 80 (Chebel et al. 2008) and 165 (Demetrio et al. 2007) dpp. Importantly, ET is normally conducted with day-7 embryos to synchronised recipients (Chebel et al. 2008) and for research purposes (Demetrio et al. 2007, Block et al. 2010, Ferraz et al. 2016, Gómez et al. 2020, Hansen 2020); this system implies that oocyte

growth, oviductal and early uterine phases are all bypassed, and determining the crucial steps is not possible (Vasconcelos et al. 2006, Demetrio et al. 2007).

Bates and Saldias (2019) showed a positive effect of higher dpp on pregnancy rates independent of BCS. This may be related to presence of clinical or subclinical conditions as suggested by (Ribeiro et al. 2016a). Finally, it may be that either undergoing pregnancy, lactation, or both, has long-lasting detrimental effects on fertility compared to nulliparous heifers, regardless of lack of metabolic stress at the time of AI (Berg et al. 2010).

Hormonal interventions

As a way of simplifying reproductive management and often remediating subfertility and infertility in cows, hormonal treatments are commonly implemented (Santos et al. 2004, Lima et al. 2010). Macmillan (2010) provides an excellent description of the characteristics and evolution of reproductive synchronisation technologies. Briefly, treatments mimic the natural patterns of hormonal fluctuations across oestrus and typically consist of luteolytic compounds (prostaglandin F_2-alpha or its synthetic analogues, cloprostenol) i.e. to induce luteolysis, sometimes combined with gonadotropin-releasing hormone (GnRH) analogues before and after to synchronise oestrus (Macmillan 2010). In the case of anoestrus lactating cows (i.e. that do not resume cycling), an additional therapeutic intervention is implemented by intravaginally placing a controlled internal drug release (CIDR) device four to nine days after insemination, for six to 12 days; the mechanisms by which this locally-supplied progesterone increases pregnancy rates are unclear (Macmillan and Peterson 1993). Evidence for effects of progesterone supplementation ranging from positive to null (Van Cleeff et al. 1992, Van Cleeff et al. 1996, Larson et al. 2007, Lamb et al. 2010, Herlihy et al. 2012) and negative (Santos et al. 2004, Saint-Dizier et al. 2019) has emerged. In normal physiological conditions, numerous molecular processes appear to be regulated by progesterone that are likely to determine fertility (Forde et al. 2010, Forde et al. 2012b, França et al. 2017, Simintiras et al. 2019a, b, Simintiras et al. 2019c). One important process dependent on progesterone is ULF secretion, which in turns influences embryo growth and its production of interferon tau (Lucy et al. 2014), examined later.

Periods of reproductive wastage

Wiltbank et al. (2016) describes five pivotal stages of pregnancy loss. Firstly, fertilisation failure often occurs because of heat stress or high progesterone concentrations near the time of insemination due to incomplete lysis of the corpus luteum (CL) (Pugliesi et al. 2014) and can represent up to 20% of the losses (Ryan et al. 1993). In the next pivotal stage (day 0-7 after insemination), which accounts for 30 to 40% of all the losses (Berg et al. 2017), the most common causes include oocyte quality problems

(Sartori et al. 2002) and postpartum metabolic issues (McDougall et al. 2011). During the following stages the embryo failures tend to be lower, and are associated with ill-timed elongation and imbalances in ULF (Stage 3, day 8-day 28 after AI, 20-30% losses), inadequate placentome formation and vascular development problems (Stage 4, second month, 5-20% losses) and unilateral twins (Stage 5, third month, 2% losses), as reviewed by Wiltbank et al. (2016).

Uterine, oviductal and follicular fluids

Uterine and oviductal luminal fluids

Systemic determinants of bovine fertility have been extensively discussed by Garnsworthy et al. (2008) with a focus on the interaction between feeding, lactation status, metabolic balance and hormones. Those aspects certainly influence fertility, but an understanding of the local conditions of the reproductive tract is crucial. A review by Evans and Walsh (2011) highlighted the importance of the uterine microenvironment, emphasising the role of factors such as presence of pathogenic bacteria and concentration of hormones and other important molecules.

There is vast evidence that the local conditions in the oviduct and uterus, including chemical composition and viscosity of fluids, temperature gradients and ciliary motility (Hunter 2012) affect reproductive outcomes in several ways (Rodríguez-Alonso et al. 2020a). For instance, reproductive biofluids exert a considerable effect on sperm transport and thus can substantially influence fertilisation (reviewed by Salilew-Wondim et al. 2012). The oviductal isthmus cells also capacitate spermatozoa, thus augmenting the efficiency of the fertilisation process and reducing the likelihood of polyspermy (Wiltbank et al. 2016). Recent studies continue to reveal other important roles of the oviduct on early pregnancy, showing physiologically relevant changes in its molecular composition across the oestrus cycle (Lamy et al. 2016a, Lamy et al. 2016b, Banliat et al. 2019b), a positive effect of oviductal hormone supplementation on embryos cultured *in vitro* (Banliat et al. 2019a), and interactions between OLF proteins and the early bovine embryo (Banliat et al. 2020). However, sampling the bovine oviduct *in vivo* is notoriously more challenging than sampling ULF, with only one technique reported recently by Papp et al. (2019). Another important consideration is that the oviductal environment has been replicated much more successfully than that of the uterus: transfer of embryos cultured *in vitro* up to day 7 (i.e. during the period when embryos develop in the oviduct and early uterine phase) generally results in successful pregnancies (Lonergan and Forde 2014), whereas no *in vitro* culture system has been able to physiologically emulate the elongation phase that can only occur in a later uterine phase (Ramos-Ibeas et al. 2020b, Isaac and Pfeffer 2021). These were determinants for the present research to be aimed at exploring uterine luminal fluid (ULF).

Reproductive biofluids such as OLF and especially ULF surround and provide nourishment to the early conceptus (embryo and accompanying placental structures) up to implantation around day 19 (Spencer et al. 2016). Both biofluids contain many kinds of molecules, such as proteins (including enzymes, growth factors and cytokines), amino acids, sugars, lipids and inorganic ions (reviewed by Roberts and Bazer 1988). The precise origin of molecules found in these fluids is often uncertain, but is likely a result of several processes: active secretion from endometrial tissues (Roberts and Bazer 1988) and the conceptus (Forde and Lonergan 2017), as well as molecules derived from epithelial cell renewal and apoptosis (Mondéjar et al. 2012) and maternal blood (Faulkner et al. 2012). When considering that experimental procedures are required to characterise these fluids, another component is added to the mixture: molecules released into the ULF because of damage due to sampling (Papp et al. 2019). These processes are further described next.

Concerning molecules actively released to ULF by endometrium cells, two processes intervene: one regulated by both endocrine mechanisms independent of the presence of an embryo, i.e. hormonal fluctuations that are determined by the oestrus cycle (Forde et al. 2014a, Tribulo et al. 2019) and by metabolic status (Harlow et al. 2018), and the paracrine influence of an embryo (Sponchiado et al. 2017). In that regard, a first stage of embryo-maternal communication in uterus has been shown to commence at least at day 7 after conception (Sponchiado et al. 2017), with limited evidence of oviductal transcriptome differences induced by embryo presence in bovine at day 3 (Maillo et al. 2015, Rodríguez-Alonso et al. 2020a) and by porcine sperm at insemination (Almiñana et al. 2014). A second stage of embryo-maternal communication is the period classically known as “maternal recognition of pregnancy” (Spencer et al. 2016), when significant molecular and physiological changes start to occur in the uterus as a consequence of the presence of an embryo (Mamo et al. 2012). This stage is triggered by interferon tau (IFNT) -the most widely known pregnancy recognition molecule in cows and sheep- signalling at around day 14 of pregnancy (Robinson et al. 2006). Blood components are known to be exuded to ULF through the uterine epithelium (Hunter 2012), but secretions from the endometrial tissues are still indispensable for pregnancy success, as evidenced by the fact that uterine gland *knock-out* ewes failed to sustain pregnancies after day 5 (Gray et al. 2002). A remarkable contribution to elucidating this was the work of Faulkner et al. (2012), which showed that many proteins are differentially abundant in bovine ULF compared to plasma. Hugentobler et al. (2007a,b; 2008) also found different concentrations of amino acids, energy substrates and ions respectively, providing evidence that ULF is not simply a by-product of blood, but that active regulation is involved to regulate its composition.

The uterine environment also differs between nulliparous (heifers) and multiparous (second or third lactation) cows: in a study by Rizos et al. (2010), good quality embryos (2-4 cell) were transferred to

nulliparous (i.e. virgin heifers) and lactating moderately productive dairy cows at day 2 after ovulation. Upon flushing at day 7, they found that more embryos were recovered from nulliparous than lactating cows and those tended to be of better quality, showing that a percentage of the losses depends on oviductal and uterine environment and that the uterus of a lactating dairy cow may be less capable of supporting early embryo development (Rizos et al. 2010).

Follicular fluid and oocyte quality

Another crucial determinant of reproductive success is oocyte quality (Camargo et al. 2006). Oocyte growth inside the follicle is a slow process that lasts about six months in cattle (Lussier et al. 1987). During this period, the oocyte acquires the competence to undergo meiotic maturation by an interaction between the oocyte and the theca and granulosa cells (Senbon et al. 2003) and accumulates transcripts and proteins that will guide the maturation, fertilisation, and initiate embryo development (Kruip et al. 2000). Oocyte quality is related to its follicular environment and reflects events and conditions occurring presently as well as months earlier, and this is particularly relevant considering the impact of diseases: both those systemic and local can affect reproduction well after disease resolution (Gilbert 2019). This influence does not only occur in the uterine environment, but also at the level of ovary and oocyte production (Gilbert 2019). In fact, bacterial lipopolysaccharide or endotoxin (a harmful compound produced by many microorganisms) due to infection can be found in follicular fluid in higher concentrations than in systemic circulation or even in the infected uterus (Groebner et al. 2011b, Gilbert 2019).

Due to the abovementioned relevance of the local conditions of the ovaries and uterus, different experimental approaches can be taken. For instance, some studies have studied endometrial tissue samples *in vivo* (Katagiri and Moriyoshi 2013) or post-mortem (Berendt et al. 2005, Belaz et al. 2016), or in a simpler and less invasive strategy, through analysis of uterine flushings (ULF) (Muñoz et al. 2012, Forde et al. 2014a). Additionally, analysing ULF is a convenient approach because it lacks high abundance cellular proteins and has a much less complex proteome, compared to endometrial tissue (Spencer et al. 2008).

Interplay of fluids within the reproductive tract

To date, little research has been reported on the specific molecular interdependence of oviduct and uterine fluids. The exchange of fluids within the reproductive tract is complex; fluid transfer has been shown between OLF and ULF at the utero-tubal junction (Hunter et al. 2011), by a counter-current mechanism between ovary, oviduct, uterus and blood (Einer-Jensen and Hunter 2005) and likely also through peritoneal fluid (Hunter et al. 2007). Research by Hugentobler et al. (2007a,b; 2008; 2010) has shown a similar composition of the metabolome of OLF and ULF, but with distinct differences

across animals, time of oestrus, and with progesterone concentration in blood. Therefore, although changes at the animal level are likely to affect sections of the reproductive tract following similar trends (Leroy et al. 2018, Jordaens et al. 2020), inferences between phenomena occurring in OLF and ULF must be done with caution.

1.1.4 Omics technologies and biomarker discovery

To understand the factors underlying this and other physiological conundrums, the trend in clinical and veterinary biochemistry has shifted in the last 30 years from investigating a few molecules in classical studies towards high-throughput methods (commonly referred to as 'omics') analysing hundreds or thousands of compounds.

Genomics and transcriptomics are the earliest examples of omics technologies and have been instrumental in determining processes underlying the physiology of reproduction. Genomics has been used to refine selection for fertility traits in addition to the standard production traits (Ortega et al. 2017). Transcriptomic data, on the other hand, furthered our knowledge of changes in gene expression, as well as how genes function as part of networks and pathways (Borrageiro et al. 2018). Improvements in both equipment and data processing have increased the popularity and volume of the more recently developed proteomic and metabolomic fields. Proteins and metabolites are closer to phenotype than genomic traits and tend to be highly informative of the organism's functional state, while also reflecting genetic factors (Nagana Gowda and Raftery 2016). Moreover, post-translational regulation processes hinder quantitative predictions of protein levels based on transcript abundance, and therefore proteomics offers unique advantages over transcriptomics (Arnold and Frohlich 2011). Insight from transcriptomics studies in this area has been reviewed by Forde and Lonergan (2012) and Ulbrich et al. (2013). Metabolomic analysis, in turn, has proven useful for exploratory experiments and biomarker discovery and validation (Nagana Gowda and Raftery 2016).

Proteomics

Proteomics is the large-scale investigation of the total protein complement of a given biological system (Aebersold and Mann 2003). For its study, two main experimental platforms exist, one consisting of gel separation of proteins dependent on their size (and often also isoelectric point), and "gel-free" whereby proteins are dissolved in liquid and undergo separations through chromatography and are detected and measured by mass spectrometry. Gel-free approaches are the most widely used nowadays due to its higher coverage in number of protein species detected (Baggerman et al. 2005). More specifically, most proteomic research in recent years has employed

liquid chromatography – tandem mass spectrometry (LC-MS/MS) because of its robustness, speed, sensitivity and throughput (Rappsilber et al. 2003). The analysis's output consists of a list of masses corresponding to precursor and product ions (chiefly peptide sequence resulting from peptide precursor ion fragmentation) together with their retention time. Informatic tools are used to determine the peptide sequence of the ions detected using information from databases, and quantify them (Aebersold and Mann 2003).

Metabolomics

Metabolites are a heterogeneous group of molecules sharing the common trait of a low molecular weight (i.e. under 1500 Da). Because metabolites are closest to an individual's phenotype, they are especially relevant when looking for biomarkers for the biological conditions studied (Smolinska et al. 2012).

Different techniques are currently in use for metabolomic analysis. Some of the most widely used include the abovementioned LC-MS/MS, gas chromatography-tandem mass spectrometry (GC-MS/MS) and nuclear-magnetic resonance (NMR). The latest is the least labour-demanding, but at the expense of reduced sensitivity (More et al. 2015). Gas chromatography coupled to tandem mass spectrometry (GC-MS/MS) was chosen as the main platform for metabolomic analysis in this project due to suitability for analysis of low molecular weight compounds related to known biochemical pathways, as well as its high resolution, separation efficiency and reproducibility compared to liquid chromatography or NMR (Bedair and Sumner 2008). The existence of proven systems for broad targeted methods can improve the number of compounds identified compared to untargeted analysis (Rochat 2016).

Metabolic fingerprinting using direct infusion mass spectrometry

Another type of metabolomic analysis is characterised by direct mass spectrometry techniques, based on ambient ionisation (Cooks et al. 2006). The main advantage of this type of technology is its ease of implementation and speed, often requiring minimal or no sample preparation (Black et al. 2016). A new technique in this realm is rapid evaporative ionisation mass spectrometry (REIMS), originally developed for real-time recognition of tumorous tissue in cancer surgery (Balog et al. 2010). Mass spectra patterns obtained produce a "fingerprint" (a distinctive pattern) of the sample analysed, but are generally unable to reliably identify specific molecular species in the samples (van Ruth et al. 2003). In recent years this technique has been applied to study many types of sample aiming for high-throughput or industrial applications, particularly in meat (reviewed by Ross et al. 2020), but also in fruit (Arena et al. 2020) and bacterial cultures (Bodai et al. 2018). However, to the

knowledge of the author, no reports of this technique being used on liquid samples have been published.

Application of direct MS analysis can help bridge the gap between laboratory and on-site applications (Ren et al. 2014). However, it is unlikely to substitute MS platforms with a chromatographic separation step such (e.g. LC- or GC-MS/MS) for scientific research purposes, due to its generally lower resolutive power and reproducibility, as well as its limited ability for compound identification (van Ruth et al. 2003, Ross et al. 2020).

Data analysis approaches

The instrumental analysis stage examined is fundamental in an omics workflow. However, further data handling, processing and integration are equally important. A brief description of the procedures employed in this project are presented next, while details of their application are presented in the respective methodology section of each chapter.

Multivariate analysis and modelling

It is common practice in an omics experiment to obtain a visual overview of the data generated as a first assessment of the results. Typically, this is done by principal component analysis (PCA), a multivariate method that - among other applications - can provide a readily interpretable means of identifying trends in the data, especially clustering and outliers (Jolliffe 1986). Indeed, PCA can extract a small number of feature patterns that represent most of the variation present in the original data, as well as the general relationships between measurements (Worley and Powers 2013). PCA is an unsupervised method, that is, no information regarding the factor(s) of interest is used in identifying trends in the data; colour- or shape-coding are usually implemented after the analysis for visualisation purposes only (Worley and Powers 2013). Conversely, partial least squares discriminant analysis (PLS-DA) is a supervised method: it aims to appraise how useful are the omics measurements at predicting one or more response variables, e.g. a disease or an altered physiological condition compared to healthy or normal individuals (Worley and Powers 2016). Two variants of PLS-DA were chosen for this analysis: orthogonal (OPLS-DA) and sparse (sPLS-DA). Compared to standard PLS-DA, its orthogonal variety provides a more analyst-friendly output: the variation that is predictive of group/condition from the condition-unrelated variation is segregated in different axes of a two-dimensional plot (Bylesjö et al. 2006). One caveat is that only binary classification is possible with OPLS-DA (Bylesjö et al. 2006). Conversely, sPLS-DA performs feature selection and parameter tuning with the aim of generating models with better predicting ability than standard PLS-DA at reduced computational power requirements (Lê Cao et al. 2011).

Two parameters are useful when evaluating a model's performance, R^2 and Q^2. R^2 represents the goodness of fit, i.e. how well is the data in the training set reproduced mathematically by the model; Q^2 quantifies the predictive performance of the model (how well it predicts data in a new/test set) (Eriksson et al. 1994). There is a compromise between goodness of fit (to the training data) and predictive ability (to new, test data) and applying cross-validation procedures can be useful for estimating these parameters and tuning the model consequently according to the goals of the analysis (Eriksson et al. 1994). Furthermore, PLS-DA approaches have measures to prevent overfitting, i.e. the production of models that adjust to and accurately explain a relationship between factors and dependent variables in the training set, but perform poorly when predicting new data (Hawkins 2004).

Univariate analysis

Statistical analysis of individual variables is highly relevant in omics research, particularly for biomarker discovery (discussed later). To test for differences in a variable across groups, Student's t-test is usually employed when there are two groups, and ANOVA when there are three groups or more. Those tests are known as parametric, i.e. they require that certain conditions be met (normal distribution of residues, independent sampling, and uniform variance across all the range of values). When one or more of those assumptions is not met, two options are possible: transforming the data (applying a function such as logarithm, power, etc.) to meet the assumptions for parametric tests, or using a non-parametric alternative, i.e. Mann Whitney U test instead of Student's T test, or Kruskal-Wallis instead of ANOVA (Thompson 1986).

From a theoretical point of view, ANOVA is a special case of regression analysis in which the predictor variables are strictly categorical (Thompson 1986). Binomial regression analysis was performed in Chapter 7 to estimate the quantitative relationship between a factor (the supplementation of a test protein) and the response variable (embryo development).

An important concept when conducting univariate analysis on omics experiments is false discovery rate (FDR). Because many features (hundreds or thousands) are analysed in each experiment, the likelihood of false positives increases substantially; for example, testing differences in 1000 variables at a 5% significance will result in an average of 50 variables found different when they are not. Multiple testing correction is therefore necessary to control the number of false positives. False discovery rate (Benjamini and Hochberg 1995) is one of the most widely used methods to this effect,

$$\mathrm{FDR} = E\left[\frac{\mathrm{FP}}{\mathrm{FP}+\mathrm{TP}}\right] = E\left[\frac{\mathrm{FP}}{\mathrm{R}}\right] \text{ if } R > 0; 0 \text{ otherwise.}$$

whose formula is (Benjamini and Hochberg 1995), where E=chosen threshold, FP= false positives, TP= true positives, and R is the number of H0 (null hypotheses) rejected. FDR is then the proportion of the rejected null hypotheses which are erroneously rejected (Benjamini and Hochberg 1995).

Multiomics and pathway analyses

In addition to the approaches presented above, to make sense of the substantial amount of information generated by omics analyses and identify trends within, multi-omics integrated investigation is highly beneficial. Integrated approaches can serve to uncover new biological phenomena, which would not be readily apparent from any single analysis (Weston and Hood 2004, Li et al. 2013). One of the most widely used integrated analysis methods is pathway analysis, whereby pathways are defined as "models describing the interactions of genes, proteins, or metabolites within cells, tissues or organisms, not simple lists of genes" (Mitrea et al. 2013). Related methodologies that are sometimes erroneously referred to as pathway analysis include functional classification based on specific aspects of the molecules studied. A typical approach for gene and protein data is Gene Ontology (GO) term enrichment analysis, which delivers insight on important molecular functions, cellular components and biological processes most closely linked to the phenomenon of interest (Ashburner et al. 2000). It is necessary to examine the purpose of this classification system to avoid misguided conclusions. According to Schulz et al. (2009), ontologies in the biomedical realm aim to offer "a system of domain-independent distinctions to structure domain-specific theories with the goal of integrating and retrieving data and fostering interoperability". The authors also emphasise that simplifications necessary to encode biological facts to ontology terms inevitably result in some errors and underrepresentation (Schulz et al. 2009). As new information is added to the knowledgebase, it becomes more reliable, however it is a broad exploratory tool that can provide leads but hardly strong empirical results. In the present work, two types of pathway analysis approaches are used. Pathway overrepresentation analysis tests the biological interrelationships of features with significance values under a defined threshold are analysed (Mitrea et al. 2013). In the other type, pathway enrichment analysis, all features are considered regardless of their statistical significance, to discover subtle yet consistent changes in biological processes (Mitrea et al. 2013); many enrichment analysis methods also consider the relative position of the molecules within the pathway (Bayerlová et al. 2015). Lastly, when referring to pathway analyses results, the terms "impact", "enrichment" and "overrepresentation" refer to

equivalent phenomena, merely pointing at an atypical behaviour of a certain biological process. Since mechanistic knowledge of reaction dynamics is usually not available in these tools, the specific changes within the pathway still require manual curation and analysis (Nguyen et al. 2019).

The ultimate goal of omics studies and their integration is embodied in the concept of "systems biology", that is, the fine-grained understanding of interactions and functional relationships between physical entities in the cell and at higher levels of organisation (Kitano 2002). Systems-level understanding of biology requires substantial amount of ''omics'' data, requiring improved throughput, agility, comprehensiveness, and precision (Feng et al. 2008, Zhang et al. 2010). One key goal of systems biology is to allow for reliable predictions of the system-wide effect of a given perturbation at the molecular level, but this has not been realised yet.

Biomarker discovery

A biomarker is defined as ''a characteristic that is objectively measured and evaluated as an indicator of normal biologic or pathogenic processes or pharmacological responses to a therapeutic intervention'' (Chakravarty 2003). An ideal biomarker is easy to measure with minimally invasive procedures and therefore it is natural that urine and blood have been investigated extensively for biomarker discovery (Nagana Gowda and Raftery 2016). Results for fertility traits, however, have been mixed. Molecular analyses of bovine plasma (Hailemariam et al. 2014) and urine (Dervishi et al. 2018) have shown potential for diagnosing metritis (inflammation of the uterus caused by bacterial infection) but to the author's knowledge measurement of canonical biochemical biomarkers, i.e. progesterone (P4), non-esterified fatty acids (NEFA), and beta hydroxybutyrate (BHB), in blood, milk or urine has consistently failed to reliably predict or diagnose fertility parameters without additional information (Pieterse et al. 1990, Breukelman et al. 2012).

In contrast, omics studies of local conditions within the maternal reproductive tract might shed light onto this, as exemplified by the work of (Mikolajczyk et al. 2006): the authors assessed the potential of leukaemia inhibitory factor (LIF) as an indicator of fertility in both blood and uterine fluid in humans. The concentration of LIF in blood did not correlate with fertility, but its concentration in uterine fluid did, highlighting the importance of obtaining samples in the affected organ (in this case, the reproductive tract) to aid in the identification of molecules or pathways relevant to the condition of interest.

Taken together, proteomics and metabolomics of extracellular fluids can be referred to as "secretomics", which in its most common usage is defined as "the global identification of factors

secreted by cells or tissues at any given time under particular physiologic, pathologic or experimental conditions" (Dominguez et al. 2010). This topic is presented next.

1.1.5 Secretomics of bovine ULF

A systematic review was published as part of the present work that compiles and discusses proteomic and metabolomic research of the cow reproductive biofluids (OLF, ULF and follicular fluid) with a focus on the interaction between inflammation, disease and fertility (Aranciaga et al. 2020). Surveyed studies that conducted proteomic and metabolomic investigations of ULF are presented in Table S1-1. Some important points discussed in the review are technical (reproducibility across studies and effect of breed, management, sampling and reporting), key molecules underlying reproductive issues, biomarker candidates of endometritis and fertility, as well as differences in reproductive biofluid molecular composition due to hormones and pregnancy status. Three main conclusions ensued from the systematic review. Firstly, that higher technical standards are required to establish a "healthy cow" benchmark to compare to. Secondly, that supplementation of specific compounds to improve fertility is promising but more research is needed to elucidate its effect on the molecular milieu of the reproductive tract. Thirdly, that further development of *in vivo* and highly localised sampling procedures of reproductive organs is paramount.

Immediate antecedents of the present work

In previous work by this group a similar trial was conducted on commercial farms in 2014-2015 (Berg et al. 2017). Seasonal pasture-grazed New Zealand crossbred dairy cows were artificially inseminated (AI) and their uteri were either flushed on day 7 or day 15 or scanned for conception at day 28/35 or day 70, including examination and grading of embryos when present. In accordance with the results of Butler (2000), and Diskin and Morris (2008), most embryo loss (30%) occurred within the first 7 days following fertilisation (Berg et al. 2017). In this biological model (representative of the average NZ herd), parameters such as cow age, milk production, calving body condition score (BCS), or change in BCS from calving to insemination were not found to significantly affect embryo survival. On the other hand, cow and sire used for insemination, progesterone concentration at day 7, dpp and the number of oestrous cycles after calving (OC) were all associated with increased conception rates (Berg et al. 2017). In the same study, cows inseminated on their first OC carried a viable embryo at day 7 only in 30% of the cases, whereas 60% of cows inseminated in their third OC had a viable embryo by day 7. This is likely related to the intense metabolic stress that dairy cows suffer in the early postpartum period, in which physiological recovery and uterine involution compete for energy supply with the udders in their peak milk production. Berg et al. (2017) also assessed causes of fertilisation failure by parentage testing, to differentiate between oocytes not penetrated by sperm

and those penetrated by sperm (eggs) that failed to progress further; results showed that 85% of the oocytes and embryos recovered at day 7 had been penetrated by sperm (Berg et al. 2017). This indicates that failure of sperm to reach the site of fertilisation or to penetrate the oocyte were not major factors in conception loss.

The importance of uterine conditions for the preimplantation period accounting for most pregnancy failures in New Zealand dairy cows motivated the present research, examining the uterine environment at seven days after insemination. Importantly, research using different breeds and production systems, such as highly producing US Holstein cows and beef heifers, has been markedly different, and this is discussed in Chapter 8.

1.2 Rationale and aims of this work

The starting hypothesis of this work was that there are differences in one or more biochemical pathways regarding two factors: between cows that get pregnant versus those that do not; and between those pregnant on their first oestrus cycle after calving (OC1) from those that only get pregnant on their third oestrus after calving (OC3), and that these differences can be determined by proteomic and metabolomic analysis of their uterine fluid. Thus, the aim of this study was to investigate molecular differences in the ULF microenvironment between different physiological states (OC1 and OC3) through proteomic and metabolomic analysis of uterine flushings at day 7 after insemination. More specifically, the analysis involved extracting both proteins and metabolites present in ULF, processing the samples and analysing them by liquid chromatography-tandem mass spectrometry (LC-MS/MS) for proteomics and gas chromatography-tandem mass spectrometry (GC-MS/MS) and REIMS (rapid evaporative ionisation-mass spectrometry) for metabolomics.
Blood samples were also analysed for concentration of progesterone and metabolites indicative of energy balance: circulating concentrations of NEFA and BHB are useful to assess the relative adaptation to negative energy balance conditions (Herdt 2000). The concentration of serum NEFA indicates the degree of depletion of fat reserves, whereas BHB concentration manifests fat oxidation in liver (LeBlanc 2010). Progesterone concentration was determined both to confirm oestrous status and to determine potential correlations with molecular changes in ULF (Costello et al. 2010).

The same pattern of insemination followed by collection of uterine flushes and blood samples was repeated in two consecutive breeding seasons and is presented in detail in Chapter 2. Data from omics experiments were analysed separately as well as integrated under a multi-omics holistic approach, and biological validation of the effect of potential biomarker candidates was tested by *in vitro* embryo culture experiments.

Main aim

To gain insight in biochemical processes underlying uncharacterised pregnancy losses and to obtain proteomic and metabolomic markers from the ULF of New Zealand dairy cows correlated to already determined differences in pregnancy rate that can be used to estimate the probability of a successful pregnancy.

Perspectives

Results from metabolomics and proteomics analyses may be instrumental to selecting individuals with a desirable genotype, devising a supplementation treatment to improve embryo development in uterus and during in vitro culture of embryos. Bovine in vitro embryo production is used worldwide and in 2018 over one million *in vitro* bovine embryos were produced, accounting for 69% of bovine embryos (Viana 2019).

2

Animal and sample collection

2.1 Introduction

As stated in Chapter 1, the aim of this work was to unravel the proximal factors (i.e. in the uterus) causing differential embryo development, as well as their interplay with distal factors (at the animal level). For this, a suitable animal model was devised taking into account the characteristics of the seasonal pasture grazed dairy cow (with a focus on the New Zealand herd) and minimising the number of covariates, particularly bull effect (Berg et al. 2010) by using semen from a single sire with high breeding value for conception rate, and uniform management conditions. The methodology of choice was inseminating early post-partum cows at two timepoints and flushing their uterine luminal fluid (ULF) seven days post-insemination with saline solution. This allowed sampling the molecules in the ULF as well as recovering an embryo when present, to assess its reproductive outcome.

This chapter describes the animals used in different trials in the present work, the trial design and outcomes regarding both cows' and embryos' phenotypes. Farm Trial 1 was a preliminary trial to test the application of an internal standard of sample concentration, whereas Farm Trials 2 and 3 used cows from the main herd located at the research dairy farm and followed the same protocols in consecutive years, using different animals each year (i.e. subgroups within the main herd). In each of Farm Trials 2 and 3, the same cows were sampled in both their first and third spontaneous OC (oestrus after calving), to determine the effect of increased recovery time (both in number of oestrus cycles and days postpartum) after calving on reproductive performance.

2.2 Materials and methods

2.2.1 Reagents and consumables

Cloprostenol 250 ug/ml (estroPlan, synthetic analogue to prostaglandin F2a) was purchased from Parnell Laboratories (Auckland, New Zealand). Eazi-breed CIDR (controlled internal drug release inserts containing 1.38 g progesterone) were sourced from Zoetis Ltd. (Auckland, New Zealand). Isotonic sterile saline (0.9% sodium chloride intravenous infusion) and Hartmans solution (Ringer's lactate solution) containing 3.17 g/l sodium lactate, 6 g/l sodium chloride, 400 mg/l potassium chloride, and 270 mg/l calcium chloride dihydrate were bought from Baxter (Toongabbie, NSW, Australia). Bomacaine (Lignocaine hydrochloride monohydrate 20 mg/ml) used as an epidural analgesia was acquired from Bomac Laboratories (Auckland, New Zealand). Bovine serum albumin (BSA) (20% w/v)

was purchased from ICP Bio Ltd. (Auckland, New Zealand) and leupeptin from Sigma-Aldrich (St. Louis, MO, USA). Synthetic releasing analogue of GnRH (Gonadotrophin Releasing Hormone, Receptal, 4 µg/ml buserelin) was supplied by (MSD animal health, Wellington, NZ).

Metricheck devices were bought from Simcro (Hamilton, New Zealand). E-Z Way filters with pore size of 64 microns were bought from SPI-MFG (Canton, TX, USA). "Red-top" plastic tubes (regular tubes without any anticoagulant or preservative added) for blood sample collection were purchased from Vacutainer (Becton Dickinson, Auckland, New Zealand). Fifteen-ml plastic tubes were acquired from Eppendorf (Hamburg, Germany), and Foley three-way embryo collection catheters (size 20) from Minitube (Tiefenbach, Germany).

2.2.2 Farm and animal management

All animal handling was done in accordance with the 1999 Animal Protection Regulations of New Zealand and with prior approval of the Ruakura Animal Ethics Committee (register number: AE Applications 14255 and 14432).

Cows were maintained at the AgResearch's Tokanui Farm (38°03'51.4"S 175°19'50.8"E). The farm operates under a seasonal pastoral system, predominately grazed on annual and perennial ryegrass and white clover, supplemented with silage and minerals (Table S2-1). The research farm's yearly average production was 1.33 kg milk solids/day/cow in 2017 and 1.59 in 2018 with peak occurring on the 29th and 25th October, respectively. Calving occurred during July through to September in 2017 and 2018 and breeding (artificial insemination) commenced the first week in October in both years.

2.2.3 Phenotypical parameters

Production and physiological parameters of each individual cow were collected daily through a cow monitoring and milking management digital system, DataFlow^{TM} (SCR Ltd., Netanya, Israel). Additional information was gathered by MINDA (LIC, Hamilton, New Zealand), a tool for herd management and visual assessment on-farm. Information from these resources was made available for this project.

The information extracted from the sources cited above included breed composition, age, calving date, average daily milk production, live weight, and semen batch.

The herd was predominately Friesian (F) and crossbred animals, crossbred defined as less than 12/16 Friesian. These included Jersey and Ayrshire. One variable tested was the proportion of Friesian genetics. For this, the proportion values were logit-transformed; to avoid infinite values, 0.01 was added or subtracted when the proportions were 0 or 1, respectively.

2.2.4 Experimental design

Farm Trial 1: use of tracer

Farm Trial 1 determined the feasibility of adding an internal standard to the flushing media, with the purpose of accounting for dilution and recovery efficiency of the flushing procedure (analysed in Experiment M2, section 4.3). Non-lactating Friesian cows (n=12) were synchronised using a fixed-time AI programme employing a CIDR as per Macmillan and Peterson (1993) to ensure all animals were at day 7 at the time of flushing. The animal synchronisation method and experimental design is presented in Figure 2-1.

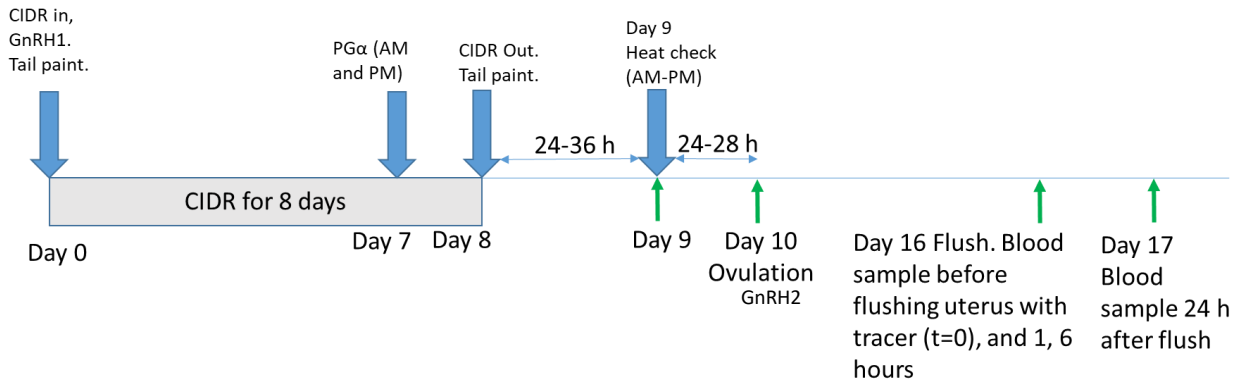

Figure 2-1 Synchronisation method for Farm Trial 1, testing the effect of isotope-labelled proline as tracer for dilution estimation. Doses: Day 0, Receptal 2.5 ml (10 µg buserelin, i.e. "GnRH1") + Progesterone 1.38 g. Day 7, estroPLAN (500 mg cloprostenol, i.e. "$PGF_2\alpha$"), 2 ml each AM and PM. Day 10, Receptal 2.5 ml (10 µg buserelin)

Details of the processing and analysis of these samples are described in section 4.3.

Farm Trials 2 and 3: uterine fluid collection with embryo recovery

Cows for Farm Trials 2 and 3 were selected using the same enrolment scheme in both years (Figure 2-2):

1 Daily monitoring of oestrous behaviour during morning milking.

2 Cows were enrolled and inseminated on their first spontaneous oestrus after calving (OC1), followed by uterine flushing at day 7.

3 A second dose of 500 mg cloprostenol (a progesterone analogue) on day 15 of first oestrus was administered to cows that failed to exhibit a return to oestrus (i.e. day 15 after AI and day 8 after flushing) to cause luteolysis, ensuring a return to heat, especially important in the cases where an embryo was not recovered.

4 Track and report OC2 and OC3, without experimental interventions.

5 During OC3, the AI and flushing procedure was repeated as per 1).

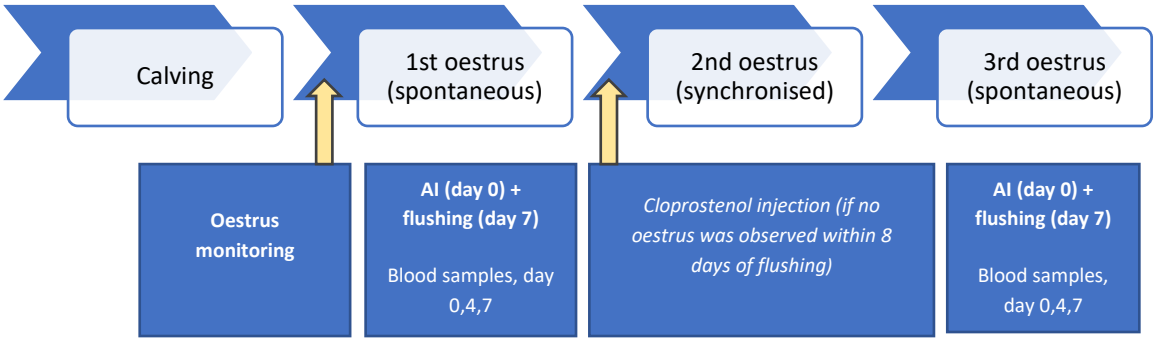

Figure 2-2 Experimental design of Farm Trials 2 and 3. The flushing process includes embryo recovery and ULF sample collection.

In Farm Trials 2 and 3, the approach taken was to minimise hormonal interventions as this is known to affect fertility parameters (Van Cleeff et al. 1996), so cows were inseminated when they came to oestrus naturally. This had the purpose of reflecting the natural postpartum evolution of the cow: in ewes, distinct dissimilarities were found in the OLF proteome of animals experiencing synchronised vs spontaneous oestrus (Soleilhavoup et al. 2016). Practical and ethical implications (Chenault et al. 2003) were also taken into consideration.

Other studies have chosen a different strategy: by exerting a higher degree of manipulation (synchronising and transferring embryos from the same donor or donors) it is easier to distinguish the effects of the uterine environment from the oocyte quality. Key elements of the two approaches are summarised in Table 2-1. The implications of this trade-off are further discussed in Chapter 8.

Table 2-1 Different approaches to *in vivo* theriogenology experiments.

Present work	**Gegenfurtner et al. (2020), Shorten et al. (2018), and others**
Naturally cycling	Synchronised
No CIDR	CIDR (progesterone supplementation) represents an extra disturbance
Long sampling period that does not overlook differences in recovery and resuming oestrus in cows	Easier to sample and account for season effect, and to distinguish embryonic from maternal factors
Artificial insemination	Embryo transfer

Enrolment

All cows in the milking herd were monitored daily for oestrous behaviour during the morning milking. Tail paint was used as the oestrus detection aid. In this method, a strip of enamel paint is applied on the animals' first coccygeal vertebra (i.e. the area near the base of the tail). When an animal comes into heat, her rubbing behaviour increases substantially and is highly prone to being mounted by other cows, causing the paint on her back to wear off. A day after the paint is applied, an operator assesses the amount of paint left in a scale from 5 (intact) to 0 (completely rubbed off; Macmillan and Curnow 1977). Cows were tail painted when they joined the milking herd four days after calving and reapplied as required. Only animals with tail paint scores 0 or 1 (bare or rubbed, indicative of being receptive to mounting by other cows) were selected for enrolment. Tail paint colour was changed after enrolment on first oestrus (insemination) and subsequent second and third oestrus.

Cows exhibiting their first oestrus after calving were drafted from the herd and further assessed before enrolment (i.e. inseminated) only if fulfilling the following criteria:

1. No history of calving difficulties; no mastitis, metritis, and metabolic disease within the first 21 days.
2. At least ≥24 days post-partum (i.e. a commonly accepted regular period of post-partum uterine recovery; Roberts 1986, Humblot 2001). Furthermore, no embryos are recovered from NZ dairy cows less than 24 days post-partum (Deb Berg, personal communication). Enrolment preference was given to cows 2 to 7 years of age, but cows greater than 7 years of age (n=6) were enrolled to achieve the minimum number of 80 cows to achieve statistical power at the 10% level.
3. Body Condition Score (BCS) greater than 3.0 (in a 5 point scale where 1=emaciated and 5=obese; Roche et al. 2004).
4. OC1 observed before the 15th of September. This ensured OC3 would occur during the six weeks of the routine artificial insemination on the farm.

Animal Evaluation and Insemination

Cows drafted from the main herd were inseminated after the morning milking. Verification of oestrus was determined by good uterine tone and the presence of a large follicle at insemination. The same inseminators (n=2) were used for both years. Cows enrolled were inseminated using frozen-thawed semen from a high-conception Friesian bull (Greenwell TF Blitz, Bull Code 108237; Berg et al. 2017).

Before insemination, uterine involution was assessed by rectal palpation of uterine horns for uterine tone and the uterine position in the pelvic cavity. The cow was assigned a uterine size and position score (SPS) based on the criteria of Young et al. (2017). An SPS1 score indicated that the uterus was positioned entirely within the pelvic cavity; SPS2 score indicated the cervix is within the pelvic cavity and the uterine horns were outside the pelvic cavity and a SPS3 was the cervix and uterine horns lie outside of the pelvic cavity. Uterine horns were examined by sonography using a SonoSite M-Turbo Ultrasound system. The presence of fluid in the uterine lumen was recorded and both uterine horn diameters were measured at the greater curvature of the horns and recorded. Uterine health was determined by the presence of purulent vaginal discharge score using the Metricheck device consisting of a 50-cm-long stainless-steel rod with a 4-cm hemisphere of silicon used to retrieve vaginal contents. Using this method, vaginal secretion scores $\geq$ 2 indicate purulent vaginal discharge endometritis (McDougall et al. 2007). Thus, only cows with scores <2 were enrolled.

Blood sampling

Blood serum samples were taken at AI (day 0) of all enrolled cows via coccygeal venepuncture into a 10 ml red top (i.e. regular plastic) tube. Subsequent blood samples were taken at the same time in the morning at day 4 and day 7. Blood samples were incubated upright at room temperature for no longer than 60 minutes to allow clotting, then centrifuged at 3,000 *g* for 10 min. Resulting serum was sub-aliquoted and stored at -20^{o}C for analysis of oestradiol, progesterone, non-esterified fatty acids (NEFA) and beta-hydroxybutyrate (BHB) at day 0, and the latter three at days 4 and 7 of both first and third oestrus cycles.

Progesterone and oestradiol concentrations analysis in blood serum were performed by Liggins Institute, University of Auckland, using an electrochemiluminescence immunoassay kit through an Elecsys e41 (2018) or COBAS e601 (2019) analyser. Two quality controls were performed, at the middle and top of the range of detection. The average CV (coefficient of variation) for the controls were 6.14% and 4.31% (mid concentration range) and 2.8% and 3.57% (high concentration range) for oestradiol and progesterone respectively (Table S2-2). NEFA & BHB analysis were performed by New Zealand Veterinary Pathology (NZVP); the CV of the controls were 5.87% (BHB) and 1.47% (NEFA) (Table S2-2).

Sonography

Sonography was performed as described by Jaureguiberry et al. (2017). A portable ultrasound machine, SonoSite M-Turbo Ultrasound system (Fujifilm, Bothell WA, USA) fitted with a 5-8 MHz sector array transducer was used to scan both ovaries. All images were saved after measurements with the in-built callipers. Before insemination, the side of the preovulatory was verified, and the uterine horn

diameters were measured. The uterine diameters were defined as the distance between the inner echogenic boundaries of the uterine lining in each of the dimensions of the image. On day 2 ultrasonography was used to verify ovulation and to measure and record the dimensions (length and width) of the developing CL (corpus luteum).

On embryo recovery day (day 7) the ovary was scanned after flushing. The image of the CL was captured on the screen at its maximum area. The horizontal and vertical diameters were measured using the electronic callipers to determine the mean maximum cross-sectional diameter of the CL and its inner vacuole (if present). The luteal area (mm^2) was calculated as $A= \pi \times r^2$. The radius (r) was calculated as 0.5 x mean maximum cross-sectional area.

Uterine flushing and embryo grading

Seven days after insemination (i.e. day 7) non-surgical uterine flushing was performed in the uterine horn ipsilateral to the CL (corpus luteum). Prior to flushing, 5 ml epidural analgesic (Bomacaine) was administered. A silicon ET Foley three-way embryo collection catheter was placed into the ipsilateral uterine horn, to ensure approximately one third of the anterior uterine horn was flushed with isotonic sterile saline solution (ISS- Ledgard et al. (2012). The uterine horn was massaged gently to ensure the ISS solution reached the anterior tip of the horn and to recover the majority of ISS solution. The ISS containing the uterine contents was passed through an E-Z Way Filter (stainless steel pore size of 64 microns) chosen to prevent protein binding, to capture both flushing debris and the embryo while the fluid passed through the filter and was collected in a 50 ml polypropylene collection tube (Eppendorf AG, Hamburg, Germany). To prevent proteolytic degradation by endogenous and exogenous proteases, leupeptin (a protease inhibitor) to a final concentration of 10 µM was added immediately after collection and ULF samples were placed on ice. Next, samples were centrifuged at 2,500 *g* for 10 mins at 4°C to remove cellular debris. The supernatant was aliquoted into 15 ml plastic tubes and snap-frozen on dry ice. Samples were held at -80°C until analysis.

The filter was immediately searched for an embryo using a Nikon SMZ1500 stereo microscope. When no embryo was found upon inspection of the filter, a second flush (methodologically identical to the first) was performed using embryo-flushing medium (300 to 500 ml per horn) and an embryo was searched in this second flush. Flushing medium consisted of Hartmann solution, containing potassium chloride (0. 04%), sodium chloride (0.6%), sodium lactate (0.322%) and calcium chloride (0.027%) supplemented with 1 ml of M-3-morpholinopropane-1-sulfonic acid (MOPS), pH 7.4, and 1 ml of BSA (20% w/v). The final concentration of the flushing medium was 1mM MOPS and 0.02% w/v BSA, pH 7.4.

Embryo grading and classification

The fluid recovered from the flush using embryo-flushing medium was searched using a stereomicroscope as detailed above and repeated up to three times. In all cases an embryo was found, it was evaluated for stage and grade according to the International Embryo Transfer Society (IETS) scoring system (Bo and Mapletoft 2018).

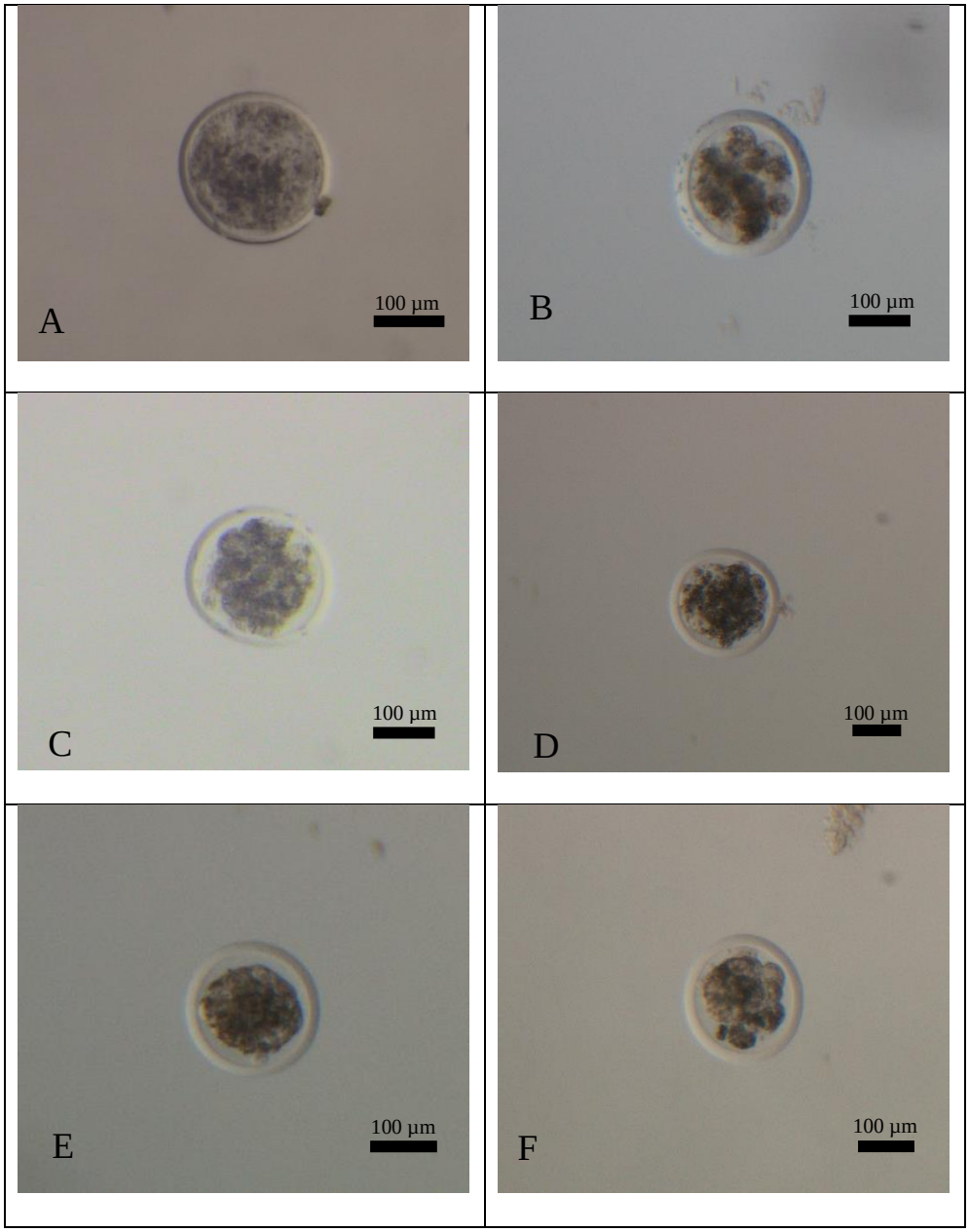

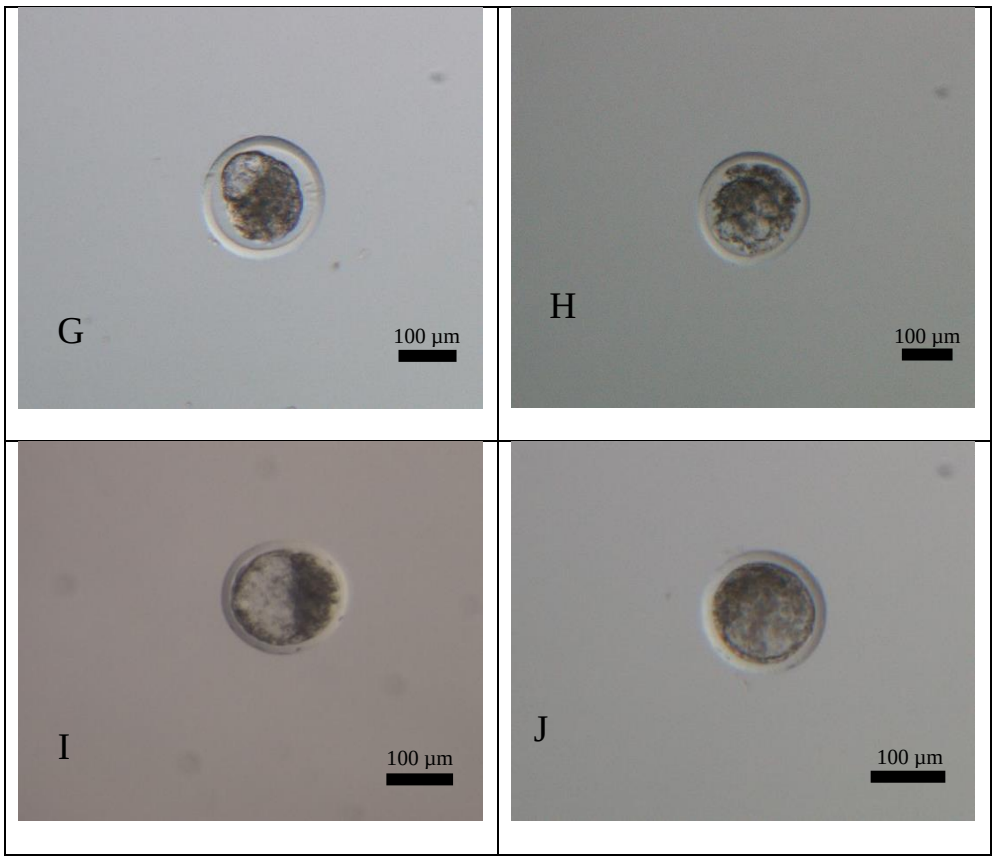

Figure 2-3 Photographs of day 7 embryos taken at 50x in a Nikon SMZ1500 stereo microscope. A) One cell zygote (class V), B) Degenerate 8-cell (class IV), C) Grade 2 morula (class II), D) Grade 3 morula (class III), E) Grade 1 tight morula (class I), F) Grade 3 tight morula (class III), G) Grade 1 early blastocyst (class I), H) Grade 3 early blastocyst (class III), I) Grade 1 blastocyst (class I), J) Grade 3 blastocyst (class III).

Briefly, two embryo phenotypical factors were considered. Firstly, embryo size (i.e. developmental stage) was measured by counting the number of cells in the embryo up to the 16-cell stage using microscopy (60x). Embryos at higher developmental stages were named according to standard convention (morula, compact morula, early blastocysts, and blastocysts).

Embryo grade was defined following the four-values scale developed by (Bo and Mapletoft 2018), one of the most widely used measures of bovine embryo quality. Based on the morphological integrity of the embryos (symmetry, size, colour, density), they are graded from grade 1 (best) to grade 4 (dead or degenerate). For reference, Figure 2-3 shows pictures of embryos of different developmental stages and grades at day 7.

Three different embryo classification systems were devised. The first system, EQ1, used all classifiable embryos, excluding ULF discarded due to the animal being diagnosed as sick. It was devised *a priori* on the basis of being the most biologically accurate, having five classes corresponding to distinct embryo phenotypes and designated with roman numerals throughout this

work: 1 cell oocytes/embryos (i.e. potentially due to fertilisation failure, “V”), 4- to 16-cell (development potentially blocked; in this study, no 2-cell embryos were recovered, “IV”), grade 3 (low quality embryo at the right development stage, i.e. tight morula or blastocyst, “III”), grade 2 (good quality at an adequate development stage, “II”), and grade 1 (excellent quality, “I”). A variant of this system (“EQ1b”) was also used in this chapter, in which ULF flushings where no embryo was recovered were encoded as class “VI”.

Two simpler, binary classification systems (EQ2 and EQ3) were also established. Under EQ2, I embryos were classed as “optimal” and V, IV and III as “suboptimal” (Table 2-2 and Figure 2-4), responding to both biological and technical issues. Class II embryos were excluded from this binary classification because of the likely overlap with classes I and III embryos. Indeed, reducing the overlap between juxtaposed classes is important for modelling purposes: predictive models tend to be significantly more accurate when the number of groups or classes is smallest and most divergent (Smith et al. 2000). System EQ3 was devised to test the hypothesis that two broad embryo stage groups (16 cells or under -i.e. classes V and IV- vs tight morula stage or more advanced development -i.e. classes III, II and I) were determined by a general physiological conditions of the cow, affecting all stages of embryo development, and termed “pregnant” and “non-pregnant”, respectively.

Table 2-2 Embryo classification schemes used, based on size and grade.

Phenotype	**EQ1**	***EQ1b***	**EQ2**	**EQ3**
Grade 1	I	*I*	Optimal	Pregnant
Grade 2	II	*II*		
Grade 3	III	*III*	Suboptimal	
4 to 16 cells	IV	*IV*		Non-pregnant
1 cell	V	*V*		
Infected	~~N/A~~	~~*N/A*~~	~~N/A~~	~~N/A~~
Non-recovery (NR)	~~N/A~~	*VI*	~~N/A~~	~~N/A~~

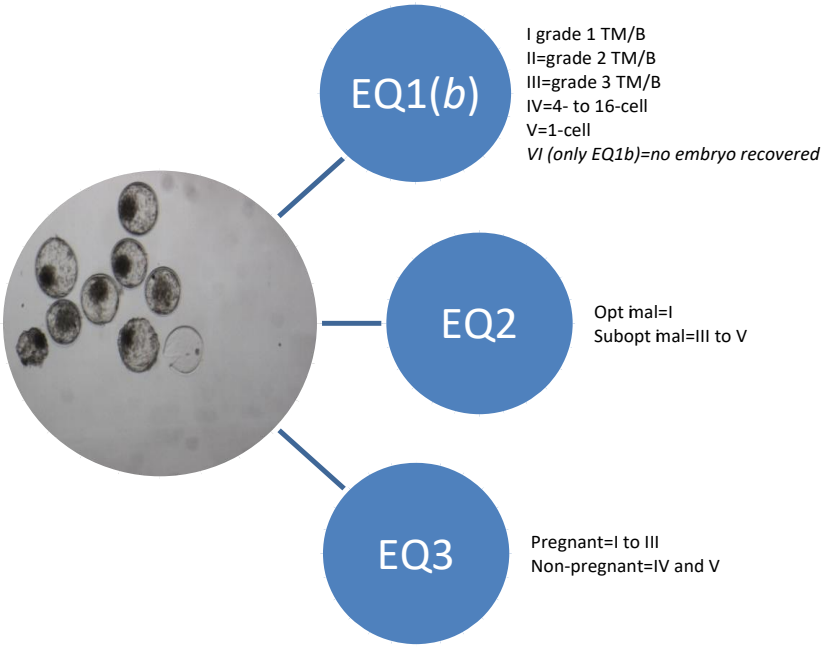

Figure 2-4 Schematic summary of the embryo quality classification systems employed.

In vitro culture after flushing

To gain additional understanding of the phenomena driving the observed embryo phenotypes, a subset (50%) of tight morulae and early blastocysts retrieved from ULF flushings were cultured for an additional 24 h. A detailed description of these techniques and tools is presented in Chapter 7. In brief, recovered tight morulae and early blastocysts were immediately placed in EMCARE Holding solution (ICP bio, Auckland, New Zealand), washed twice, placed in 0.25 ml embryo transfer straws, transported to laboratory within 3 h, washed twice in LSOF medium, and individually placed in a 10 µl drop of LSOF overlaid with mineral oil (Sigma). Embryos were cultured overnight at 7% O_2, 5% CO_2 and 88% N_2 in a modular incubator at 38.5°C. The following morning, embryos were evaluated for stage and grade as described above (Bo and Mapletoft 2018).

2.2.5 Statistical analysis

R statistical software v4.0.2 (R Core Team 2019) was used for all statistical analysis. Effect of oestrus number after calving (OC) and year on the phenotypic parameters were analysed by t-test (paired for OC and unpaired for year). Missing values were imputed using the predictive mean matching method of the *mice* ("Multivariate Imputation by Chained Equations") package v3.11.0 (Buuren and Groothuis-Oudshoorn 2010). Effect of days post-partum (dpp) at insemination on the phenotypic parameters was tested by a general linear model (regression). In all cases, non-normally distributed variables were log-transformed to satisfy the conditions for t-test. Statistical analysis of embryo proportions was carried out by Fisher's Exact test using R's *fisher.test* base function.

Embryo phenotype analyses

A research question posed was whether the ULF samples where no embryo was recovered were reflecting a biological phenomenon or a result of technical issues. This was evaluated in two ways: by observing the results of a PCA procedure using proteomics data as variables (following the methods described in Chapter 5) to check for clustering or outliers, and secondly by determining differences between embryo phenotypes by univariate analysis.

2.3 Results and discussion

In this section, an overview of the animals' data is presented first, along with differences in phenotypical parameters at the cow level (BCS, hormonal concentrations in blood, etc.) by calving year (i.e. Farm Trials 2 vs 3). Then, the effects of OC and dpp in both years were tested on the same parameters at the individual and group (trial) level respectively. Lastly, the effect of calving season, dpp and OC, along with cow phenotypical parameters on embryo recovery and quality were tested. Additionally, when many univariate tests are conducted simultaneously, it is likely that some of those are false positives (i.e. p-values<0.05 by chance). Therefore, besides p-value, a q-value (the proportion of tests showing significant differences that are expected to be false, also known as False Discovery Rate) is reported, for multiple test correction (Benjamini and Hochberg 1995). The same FDR criterion (0.05, i.e. 5%) was used throughout this project.

2.3.1 Overall descriptive statistics and year effect

Descriptive statistics for cows used in Farm Trials 2 and 3 are displayed in Table 2-3, in total and by year. Differences between years were assessed by t-test. Significant differences in five parameters were found between cows in the two milking seasons (i.e. years): average daily milk production in the week of calving and the weeks before and after (all q<0.001), serum progesterone (P4) at day 7 (q<0.027), and SPS score (q<0.028). Animals from the 2018 milking season showed higher milk production and serum concentration of P4, and lower SPS score. Importantly, as a commercial decision by the farm managers, a decrease in dry matter intake in 2017 of 3 kg (19%), may have also contributed to some of the differences observed.

Table 2-3 Descriptive statistics in variables measured across all animals used in Farm Trials 2 and 3 together, by year, and statistical differences by t-test. Values are expressed as means ± standard deviation. Abbreviations: Avg, average; BHB, beta-hydroxybutyrate; CL, corpus luteum; dpp, days postpartum; E2, oestradiol; NEFA, non-esterified fatty acids; O, oestrus; P4, progesterone; EQ1, embryo classification system 1 (see text).

Variable	Overall	Farm Trial 2 (2017)	Farm Trial 3 (2018)	p-value	q-value
% Friesian ancestry	70±28	74±26	67±30	0.156	0.305
Age (y)	5.19±1.89	5.36 ± 2.51	5.1 ± 1.21	0.36	0.532
Avg. BHB (mM)	0.55±0.12	0.58 ± 0.12	0.55 ± 0.09	0.152	0.305
Avg. daily milk yield (L). O+ 1 week	18.42±3.31	16.71 ± 3.2	19.69 ± 2.88	<0.001	<0.001
Avg. daily milk yield (L). O week	18.55±3.58	16.92 ± 3.77	19.69 ± 2.95	<0.001	<0.001
Avg. daily milk yield (L). O-1 week	18.56±3.42	17.12 ± 3.77	19.57 ± 2.82	<0.001	<0.001
Avg. horn section area (cm^2)	6.91 ± 2.31	Not measured	6.91 ± 2.31	NA	NA
Avg. NEFA (mM)	0.45±0.34	0.44 ± 0.22	0.42 ± 0.27	0.577	0.701
Avg. P4 (ng/ml)	2.18±0.87	2.11 ± 0.87	2.41 ± 0.85	0.002	0.061
Body condition score (BCS)	3.95±0.44	3.91 ± 0.3	3.97 ± 0.49	0.511	0.643
BHB day 0 (mM)	0.53±0.18	0.54 ± 0.18	0.55 ± 0.16	0.676	0.766
BHB day 4 (mM)	0.54±0.18	0.56 ± 0.18	0.55 ± 0.14	0.605	0.709
BHB day 7 (mM)	0.59±0.18	0.63 ± 0.21	0.56 ± 0.13	0.04	0.167
CL area day 2 (cm^2)	1.36±0.99	1.17 ± 0.58	1.46 ± 1.16	0.084	0.19
CL area day 7 (cm^2)	5.06±2.09	4.84 ± 2.15	5.24 ± 1.63	0.174	0.305
CL area of luteal tissue day 7 (-vac)[1]	1.09±0.62	0.9±0.52	1.4±0.65	0.021	0.059
Dpp	58±6.84	56.15 ± 21.29	61.16 ± 22.63	0.977	1
E2 day 0 (ng/ml)	20.04±11.5	21.35 ± 11.78	19.02 ± 11.29	0.179	0.305
Flush vol. recovered (ml)	17.21±4.51	17.04 ± 3.45	17.53 ± 4.94	0.46	0.619
Metriscore	1.08±0.35	1.1 ± 0.36	1.05 ± 0.33	0.474	0.619
NEFA day 0 (mM)	0.6±0.46	0.54 ± 0.29	0.63 ± 0.49	0.191	0.31
NEFA day 4 (mM)	0.42±0.57	0.4 ± 0.28	0.35 ± 0.29	0.251	0.388
NEFA day 7 (mM)	0.34±0.29	0.37 ± 0.31	0.28 ± 0.23	0.08	0.055
P4 day 0 (ng/ml)	0.34±0.64	0.29 ± 0.49	0.38 ± 0.75	0.377	0.534

P4 day 4 (ng/ml)	1.62±0.82	1.62 ± 0.96	1.62 ± 0.7	1	1
P4 day 7 (ng/ml)	4.73±1.98	4.45 ± 1.72	5.19 ± 1.91	0.007	0.028
EQ1	3.48±2.05	3.82 ± 2.05	3.22 ± 2.04	0.051	0.123
Size and position score (SPS)	1.55±0.57	1.81 ± 0.57	1.47 ± 0.55	0.006	0.027
Tail paint score	0.35±0.56	0.45 ± 0.59	0.28 ± 0.52	0.048	0.123

1 CL area of the luteal tissue Is the CL area minus the area of the vacuole.

Metabolic clearance rate was not measured in this study, but a 20% increase in dry matter intake for moderate milk yield cattle would be expected to increase liver blood flow and thus metabolic clearance rate for progesterone (Sangsritavong et al. 2002). A lower SPS score, indicating reproductive tracts better suited for pregnancy, was possibly related to differences in dry matter intake, although uterine location and size result from the interaction of many different factors (de Rezende et al. 2020). Furthermore, no significant differences were found in most of the physiological and biochemical parameters analysed, suggesting a high degree of inter-year consistency. In further analyses, groups were balanced regarding the proportion of individuals per year so that these differences would not affect embryo development analyses.

2.3.2 Effect of oestrus after calving (OC) and days post-partum (dpp) on animal phenotype

The effect of OC on the animal level parameters was examined by paired t-test, and effect of dpp at insemination by general linear models (regression). There was a general agreement between variables significantly different between OC and according to dpp (Table 2-4); two points of discrepancy between OC and dpp were blood beta hydroxybutyrate (BHB) concentrations and effect on embryo phenotype, discussed below.

Milk yield in the week of oestrus, and the weeks before and after, all decreased with both OC and dpp, signifying the cows' transitioning out of their peak milk production. Because of lower milk yield, along with more time for recovery from the previous pregnancy, body condition score (BCS) was higher at third OC ($p<0.001$), implying a positive energy balance. This is reflected by the metabolic indicators measured: blood concentrations of non-esterified fatty acids (NEFA) and BHB decreased with dpp at day 0 ($p<0.001$) or tended to decrease at days 4 and 7 ($p=0.056$ and $p=0.087$ respectively) of oestrus, indicative of the improvement in metabolic status over time (Bernabucci et al. 2005). Similarly, average uterine horn size decreased with dpp ($p=0.017$) and OC ($p=0.03$). An interesting finding was that tail paint score was significantly lower at OC3 ($p<0.001$), suggesting that with increased time after calving, animals display clearer oestrus behaviour when in heat and this

contributes to their overall reproductive performance. The increased concentration of oestradiol in cows on OC3 and along dpp is likely an important determinant of this heightened in-heat behaviour (Lyimo et al. 2000).

Perhaps related to the overall metabolic conditions of the animals, oestradiol, and progesterone concentrations in blood at insemination (day 0) were higher at OC3 (all at $q<0.001$). One contributing factor of this difference is that the lower milk production by OC3 is accompanied by a decrease in feed intake, and consequently, lower metabolic clearance (Sangsritavong et al. 2002).
In more detail, the process linking feed intake and hormonal concentration is as follows. Higher feed consumption causes increased liver function, to convert blood glucose into glycogen. This increase in liver function brings about a rise in blood flow through liver, and hormones present in blood (e.g. progesterone and oestradiol) are metabolised at a higher speed because of this augmented blood flow rate (Parr et al. 1993).
In this case, it is possible that reduced dry matter intake later postpartum caused the amount of blood filtered by the liver to decrease, hence the amount of sexual hormones metabolised and excreted was also reduced. So, even though the secretion rate might remain stable, it stays in the circulation for longer and exerts a stronger effect (Diskin et al. 2006). These are hypothetical considerations, as feed intake was not measured in this study.

No differences in area were found for CL at day 2 but CL tissue area (CL total area minus vacuole area) at day 7 increased with OC and dpp. Progesterone concentrations at the three timepoints measured however, were not different by OC ($p>0.4$) or dpp ($p>0.31$). This suggests that in this study, although progesterone is produced by the CL, CL size is not correlated to the amount of progesterone found in systemic circulation, being affected by the interaction of the processes discussed. This is in line with the results of Scully et al. (2015), who examined CL tissue area, CL blood flow, uterine homogeneity and progesterone concentrations. They found differences between pregnant and non-pregnant beef heifers at day 16, but not at days 7 and 14 of pregnancy: specifically, non-pregnant cows showed a clear reduction of CL size from day 16 after insemination, whereas the CL of pregnant cows maintained its size (Scully et al. 2015).

Effect of days postpartum on embryo quality

An effect on embryo quality according to EQ1b (embryos classed from I to V in decreasing order of quality, plus non-recovery encoded as VI; $q<0.001$) and trend on EQ1 (embryos classed I to V; $q=0.073$) was observed for dpp but not OC. Specifically, embryos of higher quality were recovered as time postpartum increased. This agrees with the results of Berg et al. (2017), who showed that both dpp and OC affect conception outcome, dpp more strongly than OC.

Trends along OC and dpp in the variables examined tend to agree, though some discrepancies were also observed. These small discrepancies are unsurprising when observing a typical occurrence in breeding patterns in cattle herds: there is an overlap in OC across the season, i.e. at a given timepoint some cows will be expressing their OC1 while others are experiencing OC2 or even OC3. For example, in the present study, early cycling cows in this herd resumed ovulation (OC) at 11 dpp, while the last OC1 registered was at 70 dpp, by which point 20% of the herd had experienced their OC3. Based on the factors examined above, the physiological state of a cow can be distinctly different between early and late cyclers. This finding is important to establish the relevance of this study with similar studies from the literature. Furthermore, the effect of those parameters on embryo quality phenotype was examined next. A final consideration is that early pregnancies of day-7 transferred embryos occurring in winter were associated with smaller embryo size at day 14 of pregnancy compared to those in spring or autumn, though it is unclear whether seasonal effects were acting at the recipient level, on the oocytes, or both (Berg et al. 2010).

Table 2-4 Descriptive statistics of animals used and effect of the number of oestrus cycles after calving (OC) or days post-partum (dpp) on phenotypic variables, tested by paired t-test (OC) or linear regression (dpp). Values are mean±standard deviation. q-values: corrected for false discovery rate (FDR). Bold: significantly different variables by OC. Underlined: significantly different variables by dpp. Abbreviations: Avg, average; BHB, beta hydroxybutyrate; CL, corpus luteum; dpp, days postpartum; E2, oestradiol; NEFA, non-esterified fatty acids; O, oestrus; P4, progesterone; EQ1(b), embryo classification system 1 (see text).

	Oestrus after calving (OC)				days postpartum (dpp)		
Variables	**OC1**	**OC3**	**p-value**	**q-value**	**p-value**	**q-value**	**adj. R^2**
Avg. BHB (mM)	**0.59 ± 0.11**	**0.54 ± 0.09**	**0.002**	**0.002**	**0.072**	**0.119**	**0.013**
Avg. daily milk yield (l). O+ 1 week	**19.22 ± 3.35**	**17.63 ± 3.18**	**0.002**	**0.003**	**0.001**	**0.003**	**0.054**
Avg. daily milk yield (l). O week	**19.5 ± 3.55**	**17.51 ± 3.35**	**>0.001**	**>0.001**	**>0.001**	**0.001**	**0.07**
Avg. daily milk yield (l). O-1 week	**19.28 ± 3.4**	**17.78 ± 3.38**	**0.003**	**0.008**	**>0.001**	**0.001**	**0.063**
Avg. horn section area (cm^2)	**7.44 ± 2.01**	**6.38 ± 2.47**	**0.003**	**0.037**	**0.017**	**0.032**	**0.046**
Avg. NEFA (mM)	**0.59 ± 0.23**	**0.27 ± 0.13**	**>0.001**	**>0.001**	**>0.001**	**>0.001**	**0.376**
Body condition score (BCS)	**3.83 ± 0.31**	**4.09 ± 0.53**	**0.001**	**0.001**	**0.007**	**0.014**	**0.046**

BHB day 0 (mM)	**0.61 ± 0.18**	**0.48 ± 0.12**	**>0.001**	**>0.001**	**>0.001**	**>0.001**	**0.078**
BHB day 4 (mM)	**0.59 ± 0.16**	**0.51 ± 0.15**	**0.001**	**0.001**	**0.05**	**0.087**	**0.016**
BHB day 7 (mM)	**0.56 ± 0.18**	**0.62 ± 0.16**	**0.004**	**0.041**	**0.031**	**0.056**	**0.02**
CL area day 2 (cm^2)	1.28 ± 1.03	1.43 ± 0.97	0.344	0.523	0.367	0.465	-0.001
CL area luteal tissue day 7 (-vac; cm^2)	3.94 ± 1.92	4.38 ± 1.65	0.355	0.169	>0.001	0.001	0.063
Days postpartum (dpp)	**38.89 ± 11.27**	**70.31 ± 18.62**	**>0.001**	**>0.001**	**NA**	**NA**	**NA**
E2 day 0 (ng/ml)	**14.39 ± 9.19**	**25.62 ± 10.9**	**>0.001**	**>0.001**	**>0.001**	**>0.001**	**0.137**
Metriscore	1.07 ± 0.3	1.06 ± 0.39	0.8	0.981	0.885	0.909	-0.006
NEFA day 0 (mM)	**0.78 ± 0.47**	**0.4 ± 0.23**	**>0.001**	**>0.001**	**>0.001**	**>0.001**	**0.171**
NEFA day 4 (mM)	**0.53 ± 0.28**	**0.21 ± 0.18**	**>0.001**	**>0.001**	**>0.001**	**>0.001**	**0.259**
NEFA day 7 (mM)	**0.46 ± 0.29**	**0.18 ± 0.14**	**>0.001**	**>0.001**	**>0.001**	**>0.001**	**0.262**
P4 day 0 (ng/ml)	0.29 ± 0.8	0.39 ± 0.47	0.306	0.485	0.71	0.771	-0.005
P4 day 4 (ng/ml)	1.62 ± 0.84	1.62 ± 0.8	0.969	1	0.483	0.553	-0.003
P4 day 7 (ng/ml)	4.95 ± 2.03	4.79 ± 1.68	0.564	0.798	0.207	0.303	0.003
EQ1	2.46±1.41	2.17±1.33	0.249	0.426	0.056	0.073	0.021
EQ1b	3.68 ± 2.04	3.28 ± 2.07	0.193	0.319	>0.001	>0.001	0.126
Size and position score (SPS)	1.55 ± 0.54	1.53 ± 0.6	0.839	0.997	0.922	0.922	-0.008
Tail paint score	**0.49 ± 0.61**	**0.15 ± 0.4**	**>0.001**	**>0.001**	**>0.001**	**0.001**	**0.07**

2.3.3 Embryo phenotype

The question of what is considered a viable embryo is not trivial. Studies in this area report viability estimates based on embryo grades that span a large range and with limited agreement (Table S2-3), though morphological grade is generally a better indicator of viability than developmental stage (tight morula, early blastocyst, etc.) at the time of transfer (Chebel et al. 2008). Other parameters have been associated with viability, including amino acid turnover (Sturmey et al. 2010, Hemmings et al. 2012) and release of other metabolites into the culture medium (Muñoz et al. 2014, Gomez et al. 2018), though these are only useful when *in vitro* culture is performed.

Incorporating differences in viability according to embryo stage in addition to embryo grade was intended in the present study but was not feasible due to a particularity of the experimental design chosen. Enrolled cows in Farm trials 2 and 3 cycled naturally at the oestrus events used in the experiments, without the use of synchronising protocols. Because heat detection was carried out by a technician observing the cows twice a day, the exact time of heat and insemination were within a 12 h range. In this timeframe an embryo can develop from a tight morula to an early blastocyst, or from early blastocyst to hatched blastocyst (Alvarez et al. 2008); this implies that differences in embryo size observed at flushing could be related to ULF factors just as they could simply be a consequence of a few hours' difference in ovulation time. Conversely, embryo grade is a time-agnostic parameter (Hasler 2001), and thus was chosen as the main embryo classification phenotypic factor. One working hypothesis of this work is that there is a trend of increased viability with development from class V to class I. An exception/addition to this system were embryos of 16 cells or under (before compaction), including one cell embryos/oocytes, that were considered non-viable based on their delayed or arrested development. Finally, in 33% of ULF flushing samples no embryo was recovered ("NR", non-recovery, discussed in a subsequent section).

Trends by year and oestrus number

Similar proportions of embryo phenotypes were observed in Farm Trials 2 and 3 (conducted in 2017 and 2018 respectively) and between OC1 and OC3 in both years (Table 2-5). Recovery rates (i.e. proportion of ULF flushing samples where an embryo was found) was consistent across cycles (65% in OC1 and 67% in OC3). One important difference was a much higher proportion of excellent and good embryos (I and II) relative to total embryos recovered in OC3 compared to OC1 (78.9% vs 55.9%), and lower number of III embryos (7% vs 22%) (Fisher's chi-square p=0.0151). Similar proportions were found in the experiment of Berg et al. (2017) in NZ dairy cows conducted in several farms which reported that an increasing number of OC improved conception outcome to day 70. This is intimately related to the time after calving needed for uterine involution and to restore general metabolic function, as discussed in Chapter 1 and above. Of note, in two cases, ULF flushings recovered were turbid and not clear; ULF samples were examined under 200x phase contrast microscope (Nikon), finding that the turbidity of the fluid was due to eukaryotic cells, i.e. not caused by bacterial infection. Those samples were excluded from the data set.

Potential determinants of embryo development

No significant difference was found in the proportion of embryos under the 16-cell stage (i.e. classes IV and V) in both oestrus cycles (chi square p=0.2). A possibility is that those were predominantly caused by ULF-unrelated factors, not measured in the present work. Thus, OLF or FF factors

(affecting oocyte quality) may constitute primary determinants of embryo development. The 8- to 16-cell stage is a critical development milestone as activation of the embryonic genome must occur for further embryo development, and this milestone occurs while the embryo resides in the oviduct (Moussa et al. 2015). The ULF molecular milieu thus may affect embryo quality and determine embryo fate only beyond the 16-cell developmental threshold (Zhang and Smith 2015), i.e. after it started increasing its signal transduction apparatus (Misirlioglu et al. 2006). A higher proportion of embryo failure during OC1 may be related to cows having higher serum NEFA concentrations during the week of insemination. This hypothesis is supported by plentiful evidence (Van Hoeck et al. 2014, Leroy et al. 2018, Jordaens et al. 2020) that oocytes and early developmental embryos are more susceptible to high NEFA concentrations than later stage embryos. Alternatively, it is possible that oocyte quality was similar for both cycles or better at OC1, having started developing before the animal experience the peripartum metabolic shock (Britt 1991, Galvão et al. 2010), but that the oviduct was under severe metabolic compromise. Conflicting evidence exists, however: Matoba et al. (2012) observed no detrimental effect of metabolic stress -and associated higher concentrations of NEFA in blood- in postpartum (7-85 dpp) dairy cows on oocyte ability to develop to blastocyst stage. The implications of NEFA-induced embryo loss are further discussed in Chapter 8.

Significance of time-dependent embryo losses

The concurrent decrease of single cell embryos and increase in 4-16 cells from OC1 to OC3 might be evidencing the interaction of oocyte and uterine factors affecting embryo development in different ways at several timepoints (McMillan 1998). That is, oocyte quality is possibly the main determinant of embryo development, but that OLF and ULF also affect embryo viability substantially (Lonergan et al. 2016), as shown *in vitro* (Lopera-Vasquez et al. 2017, Hamdi et al. 2018) and *in vivo* (Katagiri and Moriyoshi 2013, Tríbulo et al. 2018). From this standpoint, good quality oocytes may develop to grade 3, 2 or 1 depending on ULF factors. Bad quality oocytes, conversely, may either not be fertilised and remain at the 1-cell stage in suboptimal OLF, or progress up to the 16-cell stage in optimal OLF environments; both cases constitute early embryonic death (Ahmad et al. 1997). This and other scenarios are explored in subsequent chapters, including comparisons of molecular composition of ULF harbouring embryos of different grades and sizes, except for those where no embryo was recovered. Non-recovery is discussed next.

Table 2-5 Proportions of embryo phenotypes found in ULF according to number of observed oestrus events postpartum. *significantly different ($p<0.05$) by Fisher's chi square test.

	Oestrus 1 (OC1)	Oestrus 3 (OC3)	Total (OC 1 and 3)

Embryo stage and grade	Number and % of embryos recovered	Number and % of embryos recovered	Number and % of embryos recovered
Compact morula and blastocysts -Total (I-III)	46 (78.0%)	49 (86.0%)	95 (81.9%)
Excellent and good (Grades 1-2, I-II)	*33 (55.9%)*	*45 (78.9%)**	*78 (67.2%)*
Poor (Grade 3, III)	*13 (22.0%)*	*4 (7.0%)**	*17 (14.7%)*
Morula (IV)	1 (1.7%)	0	1 (0.9%)
2-16 cell (IV)	3 (5.1%)	6 (10.5%)	9 (7.8%)
Single cell (V)	9 (15.3%)	2 (3.5%)	11 (9.5%)
Total embryos	59	57	116

Cow phenotype effect on embryo quality

The effect of the parameters measured on the enrolled animals on the embryos found upon flushing their uteri was determined by regression analysis, using the systems designed as EQ1 and EQ1b as explained above (Table 2-6). Metriscore (p=0.03), tail paint score (p=0.04, q=0.17) and NEFA blood concentration at day 4 (p-0.07, q=0.28) were found to differ (or tend to differ) between classes according to EQ1 (embryo quality system excluding NR, Figure 2-4). The first two parameters are intrinsically subjective, i.e. highly dependent on the personnel in charge of the measurements and thus affected by a higher degree of variability. It is however interesting that a relationship was observed between these parameters and embryo quality. These results may be interpreted as follows: cows with low tail paint score (tail paint rubbed off), displaying stronger heat behaviour at oestrus tend to be in a better hormonal and metabolic condition and better prepared for pregnancy (Cummins et al. 2012, Diskin et al. 2015). Additionally, cows with low metriscore have lower intrauterine bacterial load, resulting in less inflammatory perturbations to the embryo environment (Jaureguiberry et al. 2017).

This supports the theory behind the EQ3 system presented above, where distinct effects of oocyte quality (long and short term) and uterine milieu (chiefly short term) determine embryo quality sequentially. The trend of a significant effect of NEFA at day 4 is noteworthy, though unlikely to become a useful factor for prediction of uterine suitability because of two reasons: high variability within groups, and absence of effect at other timepoints, coinciding with the analysis of Santos and Ribeiro (2018). Finally, the absence of effect of progesterone blood concentrations on embryo quality

observed could be related to factors not tested here and that have been shown essential for pregnancy, such as the number of hormonal receptors in endometrium (Diedrich et al. 2007).

Table 2-6 Phenotype descriptive statistics according to embryo class (EQ1b). P- and q-values correspond to regression of EQ1 and EQ1b to the cow level variables. Underlined are variables with a significant effect on embryo quality or tending to significance. Abbreviations: Avg, average; BHB, beta-hydroxybutyrate; CL, corpus luteum; dpp, days postpartum; E2, oestradiol; NEFA, non-esterified fatty acids; O, oestrus; P4, progesterone; Q1(b), embryo classification system 1 (see text).

							EQ1		EQ1b	
Variable	**I**	**II**	**III**	**IV**	**V**	**VI**	**p-val.**	**q-val.**	**p-val.**	**q-val.**
Age (y)	5.21±1	5.43±2	4.8±2	5.67±1	6.47±3	4.84±2	0.17	0.53	0.72	0.89
Avg. daily milk yield (l) O week	18±4	18±4	20±4	18±3	18±3	18±3	0.44	0.79	0.69	0.89
Avg. daily milk yield (l) O+1 week	19±3	18±4	19±4	19±3	17±2	18±3	0.83	0.93	0.48	0.89
Avg. daily milk yield (l) O-1 week	18±3	18±4	20±3	18±3	18±3	18±3	0.31	0.71	0.76	0.89
Body condition score (BCS)	3.86±0	3.91±0	4±1	4.19±0	3.78±0	4.03±0	0.73	0.92	0.28	0.89
BHB average (mM)	0.39±0.3	0.43±0.3	0.5±0.3	0.31±0.2	0.51±0.2	0.43±0.2	0.4	0.79	0.39	0.89
BHB day 0 (mM)	0.55±0.2	0.51±0.2	0.6±0.2	0.53±0.2	0.56±0.2	0.54±0.2	0.56	0.79	0.28	0.89
BHB day 4 (mM)	0.58±0.2	0.5±0.2	0.6±0.2	0.53±0.1	0.57±0.2	0.55±0.1	0.79	0.93	0.65	0.89
BHB day 7 (mM)	0.59±0.2	0.57±0.2	0.5±0.2	0.66±0.1	0.57±0.2	0.62±0.2	0.96	0.97	0.39	0.89

CL area day 7 (- vac; cm^2)	4.65±1.8	4.38±1.4	4.7±1.5	4.87±1.5	4.25±1.3	3.3±2	0.52	0.79	0.04	0.89
CL area day 2 (cm^2)	1.17±0.6	1.6±1.3	1.1±0.6	1.7±1.9	1.31±0.8	1.41±1.1	0.88	0.94	0.48	0.89
Days postpartum (dpp)	66±21	57±20	48±19	74±24	53±21	44±19	0.08	0.29	0.94	0.94
E2 day 0 (ng/ml)	21±13	20±11	17±9	20±10	19±9	20±12	0.71	0.92	0.63	0.89
Flush recovered (ml)	17±4	18±5	18±5.2	16±4.2	18±4	17±4.1	0.26	0.71	0.67	0.89
Friesian ancestry (%)	76±7	74±11	95±12	66±8	83±9	89±9	0.67	0.91	0.07	0.36
Uterine horn avg. area (cm^2)	6.68±2.8	7.09±2.5	5.98±2.2	6.75±2	6.33±1.6	7.53±1.7	0.29	0.71	0.79	0.89
Metriscore	1±0.01	1±0.03	1.03±0.1	1.13±0.4	1.55±1	1.06±0.2	0.03	0.01	0.71	0.89
NEFA average (mM)	0.57±0.1	0.53±0.1	0.56±0.1	0.57±0.1	0.56±0.1	0.57±0.1	0.82	0.93	0.78	0.89
NEFA day 0 (mM)	0.59±0.5	0.62±0.4	0.6±0.5	0.48±0.4	0.61±0.4	0.59±0.4	0.47	0.79	0.83	0.89
NEFA day 4 (mM)	0.32±0.3	0.32±0.3	0.5±0.4	0.24±0.2	0.51±0.3	0.37±0.3	0.07	0.28	0.36	0.89
NEFA day 7 (mM)	0.25±0.2	0.33±0.3	0.4±0.3	0.22±0.2	0.41±0.3	0.34±0.3	0.13	0.45	0.58	0.89
P4 average (ng/ml)	2.34±0.6	2.28±0.6	2.2±0.8	2.21±0.8	2.22±0.9	2.28±1.1	0.33	0.71	0.62	0.89
P4 day 0 (ng/ml)	0.26±0.2	0.24±0.2	0.3±0.6	0.24±0.1	0.3±0.4	0.52±1.1	0.54	0.79	0.41	0.89
P4 day 4 (ng/ml)	1.75±0.7	1.49±0.6	1.7±0.9	1.82±0.7	1.45±0.8	1.56±1	0.43	0.79	0.74	0.89
P4 day 7 (ng/ml)	5.01±1.6	5.09±1.7	4.8±1.4	4.56±1.9	4.92±2.3	4.71±2.2	0.33	0.71	0.84	0.89

SPS	1.53±0.6	1.46±0.5	1.6±0.5	1.29±0.5	2±1.3	1.54±0.5	0.97	0.97	0.49	0.89
Tail paint score	0.18±0.4	0.28±0.5	0.6±0.8	0.11±0.3	0.5±0.5	0.44±0.6	0.04	0.17	0.09	0.89

Non-recovery (NR) of embryos

Due to the considerable proportion of ULF without embryos recovered (NR, "non-recovery") and some differences observed between statistical analyses of EQ1 and EQ1b -different only by inclusion or not of NR ULF flushings as "class VI"-, this was examined further. Cow phenotype parameters measured were not different from animals for which an embryo was found in ULF flushing samples (Table 2-6). This agreed with PCA and univariate methods using proteomic features of ULF samples, in which no clustering of NR samples and no significantly different protein abundance (of NR compared to other groups) were observed (described in Chapter 5).

In other studies, pregnancy determination was conducted by measuring interferon-tau (IFNT). This protein, secreted exclusively by the early embryo (Robinson et al. 2006) is responsible for the maternal recognition of pregnancy in ruminants (Ealy and Yang 2009). Detection of IFNT in ULF during embryo elongation (day 12 to 16) has been used to diagnose pregnancy status in ULF samples in which no embryo was recovered (Ribeiro et al. 2016b, Shorten et al. 2018). Research employing untargeted proteomics has reported detection of interferon tau at days 16 (Forde et al. 2014a), 17 (Moraes et al. 2020a) and 19 (Gegenfurtner et al. 2019a). Conversely, IFNT was not detected in this study or other experiments examining ULF containing a single day-7 (Muñoz et al. 2012, Beltman et al. 2014) or day-10 (Forde et al. 2014a) embryo. However, evidence of IFNT secretion of day-7 embryos from *in vitro* research is abundant (reviewed by Forde and Lonergan 2017). Taken together, these results suggest that embryos likely produce IFNT from at least day 7 of pregnancy, and that its concentration could not be used here to ascertain embryo presence because IFNT would be present in concentrations below the sensitivity limit of detection of most untargeted proteomic techniques. Lastly, cows with NR at OC1 had, in OC3, the highest proportion of good embryos (60%) and the lowest of NR (17%).

The lack of correlation between the parameters measured and the non-recovery of an embryo in ULF flushing samples suggest that no negative phenotypical trait in certain animals caused the absence of a recovered embryo. Instead, non-recovery of an embryo is likely the product of technical difficulties (i.e. embryo not captured by the flushing medium or not found during screening of the flushing sample) as opposed to being caused by an abnormal, detrimental physiological process. A compilation of studies which recovered day-6 to day-8 embryos from single ovulating lactating cows

had an overall embryo recovery rate of 64.9% (648/998) (Wiebold 1988, Ryan et al. 1993, Sartori et al. 2002, Cerri et al. 2009a, Cerri et al. 2009b), with conditions nearly identical to this work. Roche et al. (1981) reported embryo recovery rates of 84% and 75% at days 8 and 14 respectively, higher than the average likely due to two reasons: flushing heifers, known for better fertility performance (Sartori et al. 2002) and post-mortem, reducing the odds of missing the embryo (Velazquez et al. 2010).

In vitro culture post-flushing

Table 2-7 shows the proportion of embryos of each grade with an outcome reflecting improvement, no change, or worsened after 24 h cultured *in vitro*. A chi-square test of independence was carried out to ascertain the relationship between embryo culture outcome and grade of embryo at flushing. No significant differences were found (chi-square p=0.28), indicating that *in vitro* culture of day-7 embryos for 24 h did not produce different outcomes depending on the original grade of the embryo.

These results may be interpreted as indicating that the culture medium is neutral, slightly better than a detrimental ULF but worse than a healthy (beneficial) ULF. More than half of the embryos (56%) did not change quality, suggesting that the embryo fate is determined by day 7 in most cases. It is also possible that the stress from flushing and changing environment brought about most of the decrease in grade observed (Maillo et al. 2016, Ramos-Ibeas et al. 2020a). The small number of embryos (n=5) that improved after 24 h of *in vitro* culture was insufficient to constitute a group for statistical analysis. However, future studies are likely to benefit from following this relatively simple yet insightful experimental procedure, with potential prognostic value for pregnancy success (Alvarez et al. 2008).

Table 2-7 Post-flushing embryo culture outcomes per grade. An increase or decrease in embryo grade was interpreted as per standard ETS classification system.

Both oestrus	Total n	Improved	Same	Worsened
Grade 1	14	N/A	8	6

Grade 2	17	2	11	4
Grade 3	12	3	7	2

2.4 Conclusions

In the experiments described in this chapter, distinct phenotypical changes were determined related to the time between calving and first expressed oestrus, both in number of oestrus events after calving (OC) and days post-partum (dpp). Longer post-partum interval measured by dpp significantly improved reproductive outcome because of generally ameliorated metabolic (energy) and morpho-physiologic (uterine involution) status. Many phenotypical variables were tested at cow level, including blood concentration of progesterone and metabolites, CL dimensions and BCS, and others. Of those, three (metriscore, tail paint score, and NEFA at day 4) were found to have (or tend to have) an effect on embryo quality phenotype. However, none of those was deemed a significant contributing factor, i.e. with a high potential of application in predicting pregnancy suitability of a cow, in agreement with the findings of a recent multi-herd study in New Zealand (Bates and Saldias 2019).

As mentioned earlier, a key feature of this investigation is the use of the same animal at two distinctly different physiological stages from the early postpartum period through to the planned start of mating, the first of its kind to the knowledge of the author. This was deemed important to reduce sources of variability (particularly genetic) and to increase statistical power by performing paired analyses. The phenotypical variability observed is within normal parameters in a typical herd and thus reflects real conditions.

To better understand the relationship between embryo phenotype, number of OC and dpp, and uterine environment, Chapters 5 and 6 examine the molecular composition of ULF in relation to those factors.

3

Proteomics method development

3.1 Introduction

In omics, a methodological approach that is sound, reliable, and efficient is key to maximise the quantity and quality of information extracted from samples. Prior to analysis of the experimental sample set, there were two fundamental premises directing method optimisation. One was to separate the metabolite-rich from the protein-rich fractions (reducing the total volume of sample needed, important in case samples had to be reanalysed). Another reason was to remove both the protease inhibitor and salts from the samples before proteomic analysis as those can be detrimental by affecting protein folding, which can effect trypsin's ability to digest the protein and thus result in a decreased proteome coverage (Ananthi et al. 2011).

Both the proteomics and metabolomics workflows include multiple customisable steps. Indeed, adjusting parts of the protocols is important for analysis of samples of different characteristics (Álvarez-Sánchez et al. 2010). This chapter describes the process of optimising several points in the workflow to maximise coverage and reproducibility.

For proteomics method development, the process was divided into four parts: 1) extraction, 2) digestion (including reduction and alkylation), 3) instrument analysis, and 4) informatic analysis. Combinations were tested in triplicate unless otherwise stated.

Optimised methods were selected according to the number of proteins identified. After protocol optimisation, to assess whether the setup was effective, Proteomics Experiment 2 (Exp. P2) describes a pilot trial carried out to estimate the magnitude of technical variation compared to biological variation in proteomics and determine the feasibility of this approach.

3.2 Materials

3.2.1 Reagents

Water, acetonitrile, formic acid and methanol, all LC-MS grade, were sourced from Thermo fisher (Waltham, MA, USA). SDC (sodium deoxycholate) was bought from Acros Organics (Geel, Belgium); acrylamide, from BioRad (Hercules, CA, USA), and sodium bicarbonate from Fluka (Munich, Germany). DTT (dithiothreitol), SDS (sodium dodecyl sulphate), TCEP (tris(2-carboxyethyl)

phosphine), IAM (iodoacetamide), urea and thiourea were purchased from Sigma-Aldrich (St. Louis, MO, USA). Chloroform was bought from Mallinckrodt (St. Louis, MO, USA).

Five-ml spin filter columns with 10 kDa molecular weight cut-off (Microsep® advance) were bought from Pall (Hamilton, New Zealand), and Slide-a-lyzer 3.5 kDa (12 ml) dialysis casettes from Thermo Fisher (Waltham, MA, USA).

3.2.2 Samples

ULF (uterine flushing) samples were obtained from a similar trial conducted by this research group in 2015 and were used here for the specific purpose of protocol optimisation. Both the animals and the sampling method used in that trial were identical to those in trials carried out in this project (Farm Trials 2 and 3, described in Chapter 2). In detail, 20 cycling cows from several farms in central Waikato (New Zealand) were inseminated and flushed as described in section 2.1. A 5 ml aliquot of each uterine flushing was pooled for 100 ml final volume. All further method development was conducted using this pool as the sample except where otherwise noted.

3.3 Methods: sample preparation

3.3.1 ULF sample pre-processing

Two protocols to isolate the protein fraction from the ULF were trialled, in both cases employing 5 ml of uterine flushing.

a Dialysis using Slide-a-lyzer (Thermo Fisher) dialysis cassettes (3.5 kDa molecular cut-off weight).

b Filtering using a 5 ml Microsep® advance spin filter device (Pall, Hamilton, New Zealand) with a 10 kDa molecular weight cut-off.

Protein concentration of the retentates (high molecular weight fraction) resulting from the spin-filtering (P_0) and the dialysis (P_D) were determined using DirectDetect® (Merck Millipore, Mairangi Bay, New Zealand) as described by Strug et al. (2014). Next, a volume containing 250 µg of protein from each sample was dried by a Centrivap benchtop vacuum concentrator (Labconco, Kansas City, KA, USA) at 45 °C for 3 h, and resuspended in 60 µl of 0.1 M ammonium bicarbonate (P_0). Likewise, the filtrate resulting from the centrifugation was dried down by Centrivap (M_0). Both fractions were kept at -80 °C until analysis via either proteomic (section 3.3.2) or metabolomic (section 5.2) workflows.

3.3.2 Extraction and processing

A common approach in proteomics experiments is to process sample material, with the aim of reducing the amount of potential contamination.

In this work, five sample processing methods were trialled, using sample P_0 (Fig. 3-1) as a starting point: a) none, b) protein denaturation with urea solution, c) chloroform-methanol extraction, d) addition of sodium deoxycholate before digestion and e) use of an albumin depletion kit.

Protein denaturation with urea solution

As described by Deb-Choudhury et al. (2014), 400 µl of denaturing solution (7 M urea, 2 M thiourea, 50 mM DTT and SDS 1%) were added to P_0 and centrifuged at 14,000 *g* for 30 min at 4°C resulting in sample P_U.

The denaturing solution used is incompatible with LC-MS analysis. Therefore, this protocol (P_U) was followed by chloroform-methanol extraction as detailed next.

Chloroform-methanol extraction

A standard chloroform-methanol protein precipitation (Wessel and Flügge 1984) was tried, both preceded by extraction in urea buffer (P_U to produce P_{UCM} - Figure 3-) and as a first step (P_0 to produce P_{CM}). In brief, 400 µl of methanol were added to 100 µl protein solution (250 µg total protein resuspended in 100 µl of sample). After vortexing for 20 s, 100 µl chloroform were added and vortexed again. Subsequently 300 µl water were added, vortexed and then spun 1 min at 14,000 *g* (Eppendorf benchtop centrifuge 5424, Eppendorf AG, Hamburg, Germany). Next, after the removal of the top aqueous layer, 400 µl methanol were added, vortexed and spun again 2 min at 14,000 *g*. Upon methanol removal, samples were dried by Centrivap (P_{UCM}, P_{CM}) or resuspended in 50 µl of 0.1 M ammonium bicarbonate before addition of sodium deoxycholate (P_{CMS}).

Addition of sodium deoxycholate

Sodium deoxycholate is a detergent shown to improve protein solubility and digestion (Koehn et al. 2011). The effect of using this reagent on protein identification was tested as follows: addition of sodium deoxycholate (final concentration 1% v/v) to the 0.1 M ammonium bicarbonate solution prior to the first step in the digestion protocol (i.e. reduction) using filtered samples (P_0 to produce P_S) or extracted by methanol-chloroform (P_{CM} to produce P_{CMS}, Figure 3-1). Sodium deoxycholate was precipitated after digestion by the addition of 10% formic acid, upon which the mixture was centrifuged 5 min at 10,000 *g* and the clear tryptic digest transferred into a fresh 1.5 ml tube.

Albumin depletion

A small number of proteins (chiefly albumin) make up a disproportionally high percentage of the total protein complement in uterine fluid (Beltman et al. 2014), and this may obscure detection of less abundant proteins (Faulkner et al. 2011). To address this, a kit for physical removal of albumin (AlbuminOUT™ Spin Columns, G-Biosciences, St. Louis, MO, USA) was trialled according to the manufacturer's instructions. In short, 50 µl of albumin-binding buffer and 100 µl of resuspended uterine flushing were transferred into a 1.5 ml Eppendorf tube. After mixing by pipette, it was centrifuged at 10,000 *g* for 5 min at 4 °C. The supernatant was added to a previously conditioned AlbuminOUT™ Spin Column and incubated 2 min at room temperature. The flow-through was collected and re-applied to the column. It was spun at 1,000 *g* for 5 s, whereupon the albumin-free flow-through fraction (P_{AO}) was dried by Centrivap and stored at -80 °C for digestion.

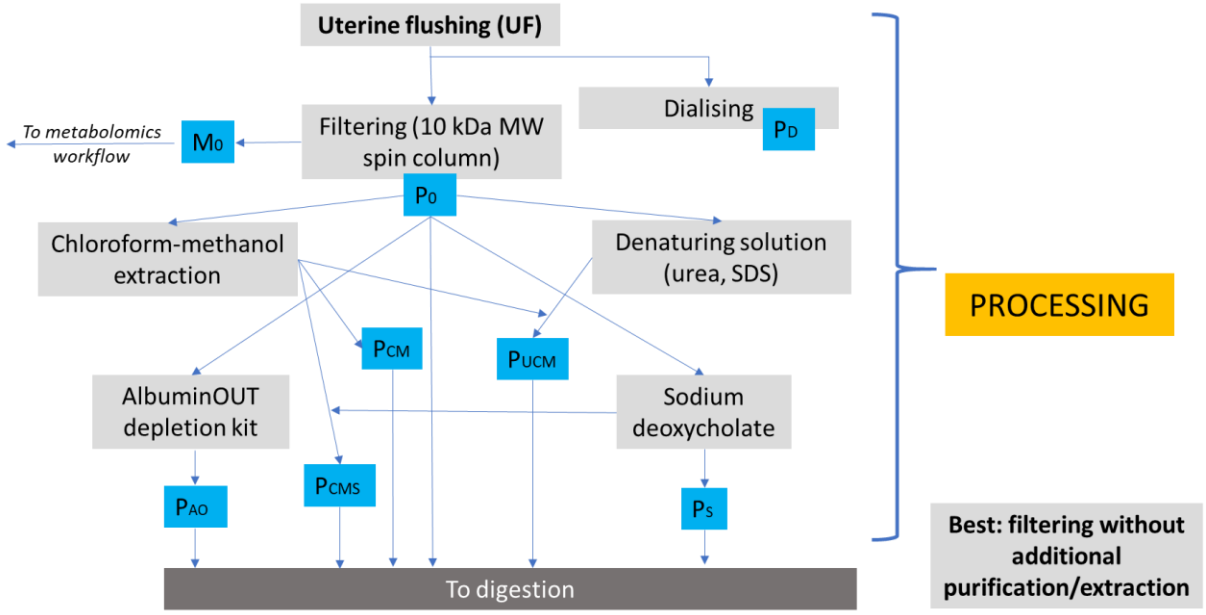

Figure 3-1 Method combinations tested for sample preparation in this project's proteomics workflow.

3.3.3 Protein reduction, alkylation, and digestion

Reduction and alkylation

Digestion of proteins was performed following the standard protocol by Shevchenko et al. (1996) for bottom-up proteomics with modifications in the reagents used for the reduction and alkylation steps. Through those processes, disulphide bonds are first reduced and then alkylated. This process allows tryptic cleavage of proteins into medium-sized peptides that can be analysed by standard mass spectrometry methods (Bantscheff et al. 2007).

Firstly, samples P_D, P_0, P_{UCM}, P_{CM}, P_{CMS}, P_S, P_{A0}, resulting from all combinations trialled in section 3.3.2 were re-suspended in 50 µL of 0.1 M ammonium bicarbonate. For protein reduction, two reagents were tested. Twenty µL of either 100 mM TCEP or DTT were added to the samples and incubated 45 min at 56 °C on a thermomixer (Eppendorf Thermomixer R Mixer 5355, Eppendorf AG, Hamburg, Germany) at 600 rpm.

For alkylation two reagents were also tested, iodoacetamide (IAM) and acrylamide. Either 20 µL 150 mM IAM (0.028g of IAM in 1000 µL of 50 mM NH_4HCO_3, prepared fresh) or acrylamide (1.5 g/ml acrylamide in 50 mM NH_4HCO_3, prepared fresh) (Mineki et al. 2002) were added after reduction and incubated in the dark at room temperature for 30 min on a thermomixer at 600 rpm.

The addition of acetonitrile as an adjuvant to digestion was also tried out as follows: after alkylation, tryptic digestion was performed by addition of 5 µg of sequencing grade porcine trypsin (Promega, Madison, WI, USA) overnight (16 h) at 37°C on a thermomixer (1:50 w/w trypsin to protein) with or without adding acetonitrile to a final concentration of 10% v/v.

The digests were dried and re-suspended in 50 µL of 0.1% formic acid and were either used for mass spectrometry analysis or extracted as detailed next.

Solid phase extraction

Extraction matrices are commonly used for cleaning up and fractionating samples before proteomic analysis (Żwir-Ferenc and Biziuk 2006). For this, after digestion, tryptic peptides resulting from the previous step were extracted using Empore® disks (Meng et al. 2008) in either a three-step or four-step fashion.

In brief, Empore® (C18 47-mm) solid extraction disks (Supelco, Bellefonte, PA, USA) were cut in squares of 4 mm^2 of area and conditioned by sequential 1-min incubations in acetonitrile, methanol, and water. Two 4 mm^2 squares conditioned Empore® were immersed directly into the peptide extract and centrifuged briefly. Peptide extraction was carried out for 2.5 h at room temperature (21 °C) on a thermomixer at 600 rpm. Subsequently, Empore disks from each sample were then placed in separate vials containing 100 µL of 0.1% (m/w) formic acid. Samples were washed by pipetting up and down 5 times and then formic acid was discarded.

Further to this step, two different peptide elution methods were tested, a three-step and a four-step elution. For the three-step elution, the Empore disks were placed in 100 µL of 10 mM ammonium formate: acetonitrile 10:90 v/v and vortexed for 60 min. Next, the Empore disks were transferred to

a tube containing 100 µl of 10 mM ammonium formate: acetonitrile 40:60 v/v and vortexed for 60 min. Lastly, the procedure was repeated by transferring the disks to ammonium formate: acetonitrile 75:25 and vortexed for 60 min.

The four-step elution was performed in a similar fashion, with elution mixtures of ammonium formate: acetonitrile 90:10, 75:25, 50:50, and 25:75.

In both cases, all fractions were spun in Centrivap to dryness and stored at -20 °C until analysis.

3.3.4 Chromatography and mass spectrometry

Liquid chromatography programme

Two liquid chromatography methods were tested (Table 3-1). In both cases, the mobile phase consisted in mixtures of solvent A (0.1% formic acid in MS-grade water), and B (98% acetonitrile, 0.1% formic acid). The long gradient involved increasing from 2% to 20% B in 45 min, and 20% to 45% B in 15 min, and up to 95% B, for a total run time of 85 min at a flow rate of 1 µl/min. The short gradient run was 2 to 10% B in 2 min, then 10 to 25% B in 8 min, 25 to 95% in 4 min and maintained for a further 5 min, for 28 min total running time. After the run, in both programmes a re-equilibration of 2% B was programmed before the following run.All samples were diluted 10x using 0.1% v/v formic acid (FA).

Table 3-1 Liquid Chromatography programme settings for long and short runs.

Long programme		**Short programme**	
Duration (min)	% B	Duration (min)	% B
0	2	0	2
0	2	0	2
2	2	1	2
47	20	3	10
62	45	11	25
66	95	15	95
71	95	20	95

73	2	22	2
85	2	28	2

Mass spectrometry instrumental setup

MS/MS analysis was carried out on a nanoAdvance UPLC, coupled to a maXis impact HD (Qq-TOF) mass spectrometer equipped with a CaptiveSpray source operated at 1500 V (Bruker). Two µl of sample was loaded on a C18AQ Nanotrap column (Bruker, C18AQ, 75 µm × 2 cm, 3 µm, 200 Å). The trap column was then switched in line with the analytical column (ProntoSil C18AQ, 100 µm × 15 cm, 3 µm particles, 200 Å pore size, NanoLCMS Solutions Oroville, CA, USA). The column oven temperature was 50 °C. A mix of air and gas-phase acetonitrile was injected around the emitter spray tip through a nanoBooster™ (Bruker, Bremen, Germany) to support liquid desolvation and increase ionisation efficiency; settings were 3 l/min, dry temperature 150 °C. Samples were measured in auto MS/MS mode, in the mass range of m/z 350-1200.

Mass spectrometry acquisition settings

Mass spectrometry setups allow adjusting several settings. Trying all possible combinations was deemed impractical, therefore 25 runs with different parameters were performed using the same pooled sample. Some of them were trialled in short gradient LC runs for time-saving purposes, and if presenting an improvement over the by-default conditions, tried again using the long gradient LC run. Combinations of the following were tested (default values in **bold**, settings that are enabled only upon activation of a previous parameter in *italics*).

<u>Scan and fragmentation</u>

1 a) Number of precursors (**10** or 5) OR
b) Cycle time (3 or 5 seconds)

2 a) Acquire MS/MS spectra for empty intervals (tick/**not**)
b) *[Empty interval] Time slice (1 seconds)*

3 Absolute threshold (**1000** counts)

4 a) Active exclusion (tick/**<u>not</u>**)
b) *(Active exclusion) Exclude after **1** spectrum*
c) *(Active exclusion) Release after 0.2, 1, **1.5** minutes*

5 a) Smart exclusion (tick/**not**)
b) *[Smart exclusion) 5x or 10x*

<u>Precursor acquisition control</u>

6 MS/MS low threshold (**1000** cts)
7 Low - frequency (**1**, 5, 10 Hz)
8 MS/MS high threshold (**100,000** cts)
9 High - frequency (10, 15, **20** Hz)

Exclusion Scheduled Precursors List (ESPL)

A technical limitation of data dependent acquisition methods for tandem MS is that only a limited number of molecules detected in the first MS scan are fragmented and scanned on the second step. This biases the detection towards peptides derived from the most abundant proteins in the sample (Aebersold and Mann, 2003). One workaround is to exclude those abundant, likely unimportant (for the biological question at hand) peptides from being fragmented and analysed. Aside from physical removal methods as AlbuminOUT™ Spin Columns described earlier, it is possible to create a list of peptides from those most abundant proteins along with their m/z and retention time and set the MS programme to not select them for fragmentation. This feature is known as Exclusion Scheduled Precursors List (ESPL) (Zerck et al. 2013).

The same pooled sample was injected three times and the list of all peptide species identified was surveyed. From this list, m/z and retention time of the peptides corresponding to one of the five most abundant proteins by sum of peak areas of the top-3 peptides (Table S3.1a) were used to create a list of peptides to exclude; a fragment example is in Table S3.1b.

3.3.5 Software analysis

Two proteomics packages were trialled: ProteinScape Version: 4.0.3 315, Build id: 20161220-0956 (Bruker Daltonics Inc) and PEAKS Studio v.10.0, build 20190129 (BSI, Waterloo, Canada). Proteinscape searching against Swissprot was used during the method optimisation stages of sample processing and digestion, while PEAKS studio was used after. Peptide-spectrum match searches against three databases were performed, namely Swissprot, Uniprot (which includes Swissprot and TrEMBL) and NCBI.

Different search engines were used for protein identification. Proteinscape employs Mascot v. 2.5.1 (Matrix Science, UK). PEAKS Studio has its proprietary search engine (PEAKS DB) with variants (PTM for extra post-translational modifications and Spider for amino acid substitutions); it also allows searches using Mascot v 2.5.1 (Matrix Science, UK) and Xtandem! v. Alanine (2017.02.01). Searches using external search engines need to be combined with a tool called “InChorus search” with a search result from a PEAKS proprietary search algorithm.

A further step was setting parameters at different levels of stringency. These included choice of post-translational modifications (both fixed and variable), mutations, peptide and protein score thresholds, and minimum unique peptides per protein identified.

Parameters kept stable were enzyme trypsin semi-specific, de novo score (ALC%) threshold 50%, peptide-spectrum match (PSM) false discovery rate of 1%, maximum 3 missed cleavages per peptide.

3.3.6 Variation sources – pilot trial

A pilot trial (Exp. P2) was set up according to Maes et al. (2015). Briefly, 5 ml ULF samples from 5 cows enrolled in a previous similar trial were used. Twenty ml were processed from samples of an additional cow in that trial, and from it resulted 6 technical (preparation) replicates (4A-F) (Figure 3-2). One of the biological replicates was injected 4 times to appraise the extent of variation due to analysis in the instrument. Samples were run both in single MS (for quantification) and tandem MS/MS, to identify the proteins detected.

Two different approaches were employed to evaluate relative contributions to variation: an analytical method dependent on identifications; as well as a multivariate, unsupervised method independent of identifications, and therefore able to capture a higher proportion of variation.

The multivariate, unsupervised method was conducted by importing raw MS data to ProfileAnalysis, v2.1.265 (Bruker, Bremen, Germany). Signals for each compound (including adducts with other ions, as well as charge states +2 to +5) were combined. Peak areas for each feature were log-transformed to reduce heteroscedasticity. Next, Principal Component Analysis (PCA) was performed to examine similarity between samples and replicates of different types.

The analytical method was based on identified proteins. Specifically, it consisted on tabulating the areas obtained by label free quantitation (LFQ) using PEAKS following the optimised method detailed in section 3.4.6. The MS/MS runs provided identifications, whereas peak areas were calculated from (single) MS runs.

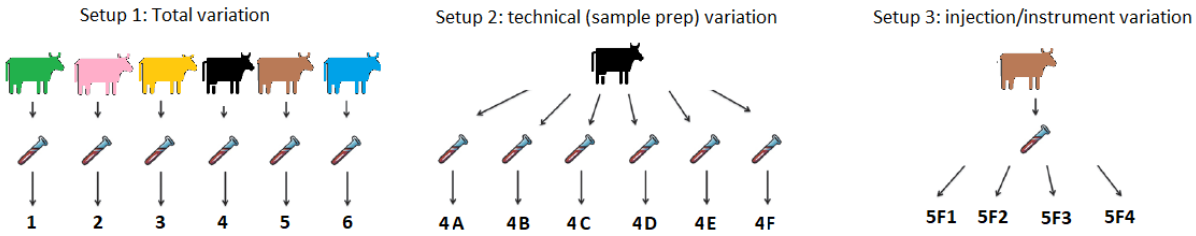

Figure 3-2 Experimental design of a preliminary experiment (Exp. P2) to assess the degree of technical variation to total variation. Uterine flushing (ULF) samples of 6 cows were processed as per protocol 4.1 (1-6). Six technical replicates from one ULF were prepared and run as independent samples (4A-4F). Another ULF sample was run four times by LC-MS/MS (5F1-5F4).

Label free quantitation (LFQ)

As established earlier, differences in amounts of proteins identified were assessed by LFQ, by MS (single MS) signal intensity; this is explained in detail in section 5.2.3. Briefly, mass error tolerance was 20 ppm, whereas Rt (retention time) shift tolerance was 2 min. Most parameters were left as default, including auto-detection of reference sample (taken as the centre for retention time alignment) and training samples (used to calculate the feature vector quality). Significance method was PEAKSQ, and data was normalised by total ion current.

To link identifications to quantification data, all six biological replicates were run in MS/MS mode and incorporated as a separate group in the LFQ analysis. Both the sum of peak areas from all peptides as well as the top-3 peptides of each protein were exported.

3.4 Results and discussion

The objective of these experiments was to define the most efficient workflow. This included optimising the number of experimental steps to the minimum without sacrificing effectiveness, as technical variation is introduced in each stage. Thus, when the addition of a reagent resulted in only marginal improvements it was discarded, to reduce time and cost of processes or assays.

3.4.1 Sample pre-processing

Number of proteins identified are displayed in Table 3-2. The dialysis method resulted in 55±6 proteins identified compared to 160±5 identified in the retentate product of the filtering method. Considering the additional disadvantage of losing the low MW fraction by dialysing, all further sample preparation was conducted using the retentate product of the spin filter process. Further method optimisation was attempted to maximise the number of proteins identified.

Table 3-2 Comparison of number of proteins identified between processing methods. Values presented as means ± standard error of the mean.

Method (fraction)	Proteins
P_D (dialysis)	*55*±6
P_0 (retentate after filtering)	160±5
P_{CM} (chloroform-methanol extraction)	110±3
P_{UCM} (urea, chloroform-methanol)	70±2
P_S (addition of sodium deoxycholate (SDC))	161±4
P_{CMS} (chloroform-methanol, SDC)	133±3
P_{AO} (retentate after Albumin depletion)	68±5

3.4.2 Sample processing, extraction, albumin removal

Both urea extraction and addition of sodium deoxycholate (SDC) have been reported to enhance detection by MS and reduce the amount of non-proteinaceous contaminants (Masuda et al. 2008). Regarding ULF samples, urea extraction resulted in 70±2 proteins identified (P_{UCM}) compared to 160±5 using the retentate (P_0). Chloroform-methanol extraction also reduced the number of proteins identified (110±3 vs 160±5 proteins). As of the effect of SDC, it brought about an improvement over the use of chloroform-methanol extraction alone, but an average of only one extra protein was identified when this was used compared to without addition of SDC (133±3 for P_{CMS}, 161±5 P_S, 160±5 P_0). This minimal gain did not justify including this step.

Albumin removal using resin columns (P_{AO}) also resulted in a lower number of proteins identified, compared to the unprocessed retentate (P_0) (68±5 vs 160±5). In summary, no denaturation or extraction step improved protein identification over the use of unprocessed retentate of spin-column filtering (P_0). Therefore, unprocessed retentate of ULF was used thereafter. Steps are depicted in Figure 3-3.

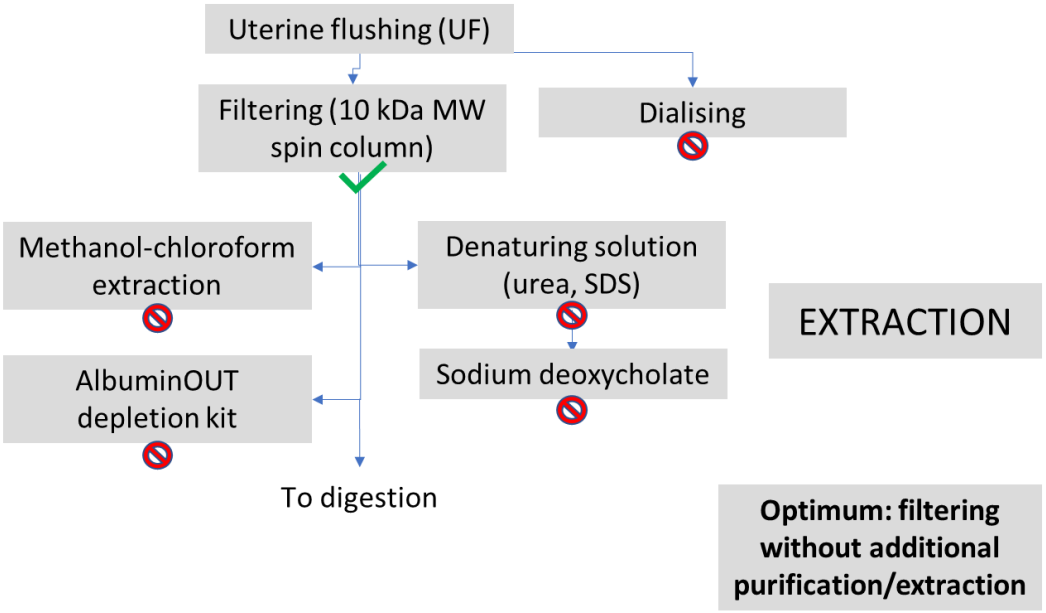

Figure 3-3 Processing protocol parameters trialled. Filtering without additional processing was chosen as the preferred method.

3.4.3 Digestion

Iodised alkylation reagents such as IAM may generate artefacts, specifically non-biological post-translational modifications (Nielsen et al. 2008). Thus, acrylamide, an alternative alkylation reagent, was also trialled. In order of decreased performance, the combinations trialled produced the following number of proteins identified: DTT + IAM = 160 proteins; DTT + acrylamide, 133 proteins; TCEP + IAM, 129 proteins; TCEP + acrylamide, 118 proteins). DTT was clearly the optimal reduction reagent in this setup, whereas for alkylation, the higher number of protein identifications motivated in the selection of IAM as the preferred option, also considering the extremely toxic nature of acrylamide. As mentioned earlier, the use of IAM results in well-characterised modifications of proteins, especially carbamidomethylation of cysteine (Nielsen et al. 2008). Thus, this was included in subsequent protein searches as a variable post-translational modification (PTM).

Incorporation of a digestion adjuvant -acetonitrile (ACN)- to a final concentration of 10% v/v resulted in decreased number of identified proteins in this setup (120±11 vs 160±5 under the same parameters without addition of acetonitrile) and was therefore not further performed.

Solid phase extraction

Neither 3- and 4-step solid phase extraction protocols, used for clean-up prior to LC-MS, increased the number of proteins identified, while substantially increasing sample preparation (by 1 h per

fraction) and running time (extra 85 minutes per fraction). Specifically, 141±10 (4 fractions) and 153±8 (3 fractions) proteins were identified, as opposed to 160±5 proteins without any solid phase extraction.

Summarising, the optimal digestion protocol included reduction of ULF proteins with DTT, alkylation with IAM, and no solid phase extraction or addition of acetonitrile as a digestion adjuvant (Figure 3-4).

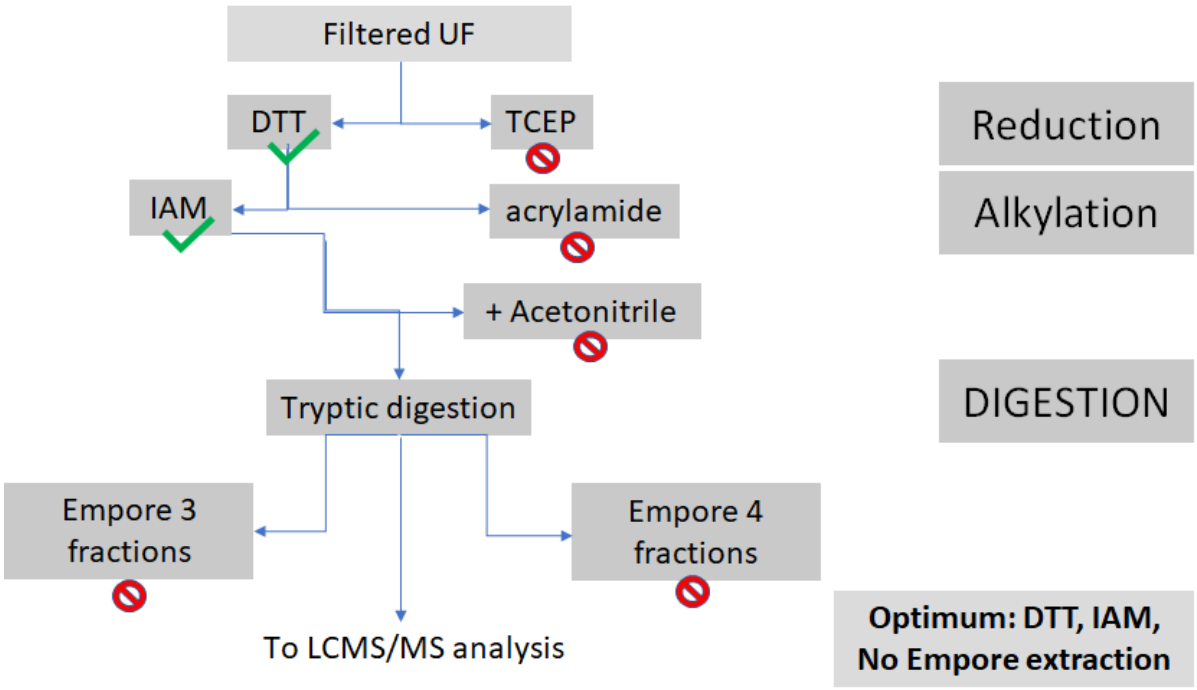

Figure 3-4 Protocol parameters trialled (digestion preparation). Chosen protocol was reduction with DTT, alkylation with IAM, no acetonitrile added as an adjuvant, no solid phase extraction with Empore disks.

3.4.4 LC and MS parameters, use of Exclusion Lists

Liquid chromatography

The average number of proteins in the short gradient programme was 84±13, whereas the long programme resulted in 160±5 identified proteins. Because there were no substantial differences in reproducibility, the long gradient programme was used hereafter. Table 3-3 shows the effect of selected permutations on number of proteins identified, using Proteinscape. Alternative settings provided substantially less protein identifications than the standard method (160±5), therefore the standard setting was chosen (Figure 3-5).

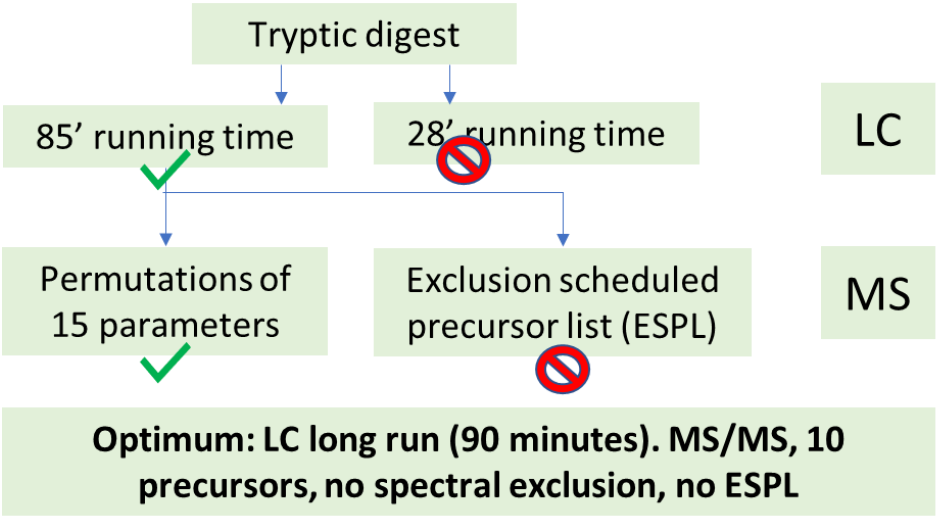

Figure 3-5 Liquid chromatography and mass spectrometry parameters trialled. Optimal settings were 85 minutes LC programme, and default MS fragmentation settings.

Table 3-3 Number of proteins identified with each combination of liquid chromatography and mass spectrometry settings trialled. First row for each LC method (in dark gray) are runs analysed with default parameters.

LC Programme	1.a) Precursors	1.b) Cycle time (s)	2.a) Acquire spectra for empty intervals	2.b) Time slice	3) Absolute threshold	4.a) Active exclusion	4.b) Exclude after *n* spectra	4.c) Release after *n* min	5.a) Smart exclusion	6. MS/MS low-counts	7. MS/MS low - freq	8. MS/MS high-counts	9.MS/MS high - freq	Proteins
Long	10	NA	No	No	1000	No	NA	NA	No	1000	1	100000	20	160
Long	10	NA	Yes	2	1000	No	NA	NA	5	1000	1	100000	20	134
Long	10	3	No	No	1000	No	NA	NA	No	1000	1	100000	10	99
Long	10	NA	No	No	1000	No	NA	NA	No	1000	1	100000	15	99
Long	10	NA	No	No	1000	No	NA	NA	No	1000	5	100000	20	95
Long	10	NA	No	No	1000	No	NA	NA	No	1000	10	100000	20	101
Long	10	NA	No	No	1000	Yes	NA	0.2	5	1000	1	100000	20	100
Long	10	NA	No	No	1000	Yes	NA	0.2	5	1000	1	100000	20	83
Long	10	NA	No	No	10000	Yes	NA	0.2	5	1000	1	100000	20	77
Long	10	NA	No	No	10000	No	NA	NA	No	1500	0.1	100000	20	97
Long	2	NA	No	No	1000	No	NA	NA	5	1500	0.1	10000	0.5	28
Long	10	NA	No	No	5000	Yes	NA	NA	5	1000	1	100000	20	86
Long	10	3	No	No	1000	No	NA	NA	No	1500	0.1	100000	20	91
Long	10	NA	No	No	1000	No	NA	NA	No	1500	0.1	10000	0.5	62
short	10	NA	No	No	1000	No	NA	NA	No	1000	1	100000	20	84
Short	10	NA	No	No	1000	No	NA	NA	No	1000	1	100000	15	38
Short	2	NA	No	No	1000	No	NA	NA	No	1500	0.1	10000	0.5	9
Short	10	NA	No	No	1000	Yes	NA	0.2	No	1500	0.1	10000	0.5	34
Short	10	NA	No	No	1000	No	NA	NA	No	1500	0.1	10000	0.5	23
Short	10	NA	No	No	5000	No	NA	NA	No	1000	1	100000	20	28
Short	5	NA	No	No	1000	No	2	NA	5	1000	1	100000	20	32
Short	10	NA	Yes	2	1000	No	NA	NA	5	1000	1	100000	20	49
Short	20	NA	Yes	1	1000	No	NA	NA	No	1000	1	100000	20	50
Short	10	NA	No	No	1000	No	NA	NA	No	1000	1	100000	10	67
Short	5	NA	No	No	1000	No	NA	NA	No	1000	1	100000	15	70
Short	10	NA	No	No	1000	No	2	1	No	1000	10	100000	20	77
Short	10	NA	No	No	1000	No	1	NA	No	1000	5	100000	20	53

Exclusion Scheduled Precursors List (ESPL)

The creation, importing and application of the exclusion list in the MS control software, otofControl v. 4.4.4.4 (Bruker, Bremen, Germany) required strict parameters. These included file format, specific rules for naming files and entering data, step order to import into the software, etc. Moreover, anecdotal evidence from colleagues using the same instrument suggested that this software was optimised for inclusion scheduled precursor lists and that exclusion lists might not work simply because of software limitations (Evelyne Maes, personal communication).

A peptide list corresponding to albumin (most abundant protein in ULF samples) or the top-5 proteins was generated from the results of the optimised run (top row, Table 3-). Different ESPL were added to the MS method used in 14 separate runs. Although some peptide fragments in the list were effectively excluded, this did not result in greater number of identifications. In fact, some fragments outside of the set m/z and Rt ranges were also excluded by the instrument during analysis. The application of ESPL thus resulted in 75±17 proteins identified, compared to the original 160 of the run from which the exclusion list was derived. Therefore, this approach was discarded.

To sum up, the settings chosen were a long programme for LC runs, default settings in MS/MS analysis, and no application of ESPL (Figure 3-6).

3.4.5 Software analysis

Software package and databases

Instrumental steps described so far were assessed by number of proteins identified as well as inter-replicate consistency using Proteinscape. Subsequently, to select the best protein identification software, the performance of Proteinscape and PEAKS studio (specifically, using PEAKS DB as the search tool) were compared using Uniprot. Protein identifications were higher using PEAKS studio compared to Proteinscape (235±14 vs 160±5), likely due to its improved algorithm that uses both database searches as well as *de novo* peptide identification, thus augmenting the number of peptides identified (Zhang et al. 2012). From this point on, all further optimisation was performed using PEAKS studio.

Next, the implementation of different protein databases (NCBI, Uniprot and Swissprot) using PEAKS DB as the search tool was trialled. Number of proteins identified were 321±7 for NCBI, 235±11 for Uniprot and 208±14 for Swissprot. The non-curated nature of the NCBI database resulted in the highest number of proteins but also in a high degree of redundancy, that is, many of the proteins

identified were in fact the same protein under different accession numbers. With regards to the other two databases, Uniprot -which comprises the curated database of Swissprot and its automatically annotated supplement TrEMBL (O'Donovan et al. 2002)- was chosen due to its balance between number of proteins identified and the reliability of the matches.

Search engine

InChorus search is a functionality of PEAKS studio that incorporates results from up to four search engines, increasing number of hits and confidence, as positive identifications resulting from different algorithms are more reliable (Shteynberg et al. 2013). Quantification using PEAKS studio requires both simple (MS) and tandem (MS/MS) data; the method optimisation for identification belong in the second category.

MS/MS chromatography data from a run using the optimised parameters as per above were analysed using the four main search tools in PEAKS studio: PEAKS DB, PEAKS PTM, Spider and InChorus. In that order, the number of proteins identified using the standard run and searching against Uniprot was 235, 276, 279 and 327. An important caveat is that quantification using InChorus identification is not supported in PEAKS studio. Therefore, the other three search tools were considered further for use in label-free quantification experiments.

Protein search parameters

PEAKS Studio includes an algorithm that detects the most common post-translational modifications (PTM) and incorporates them into the following steps of the search (PEAKS PTM search). Based on the number of PTM across all proteins identified, carbamylation (M) was set as fixed modification, whereas carbamidomethylation (C) ubiquitin (CKST), deamidation (NQ) and methylation (KR) were set as variable modifications.

Mass error tolerance parameters were examined using Spider, a search tool in PEAKS Studio that repeats the peptide search of unassigned spectra against proteins already identified in a PEAKS DB search, potentially increasing coverage and identifying new mutations. Combinations tested were precursor mass error (5 or 10 ppm), and fragment ion tolerance (0.05 or 0.02 Da). The combination that resulted in the highest number of identifications was 10 ppm and 0.02 Da (279 proteins), whereas 5 ppm and 0.05 Da was the least effective (198 proteins), in both cases at 1% false discovery rate (Benjamini and Hochberg 1995).

A key distinction between Spider and PEAKS PTM is that the first search tool considers the existence of amino acids (AA) mutations in its search. A lengthy list of mutations was suggested by results from Spider. A tBLASTn search (https://blast.ncbi.nlm.nih.gov/) showed that at least twenty of them had

not been reported in the NCBI library. The substantial number of suggested mutations that are unreported in the NCBI library points at an overconfident algorithm (Table 3-4). PEAKS PTM results were deemed more reliable and constituted the preferred search tool to use in LFQ experiments.

To summarise, the optimal software setup was PEAKS Studio, using Uniprot as the database. The most suitable search engine was PEAKS PTM for quantification and InChorus for identification purposes only, with one unique peptide required to accept an identified protein (Figure 3-7).

Table 3-4 Most frequent post-translational modifications and putative mutations as identified by PEAKS Studio's Spider search tool. Position indicates what amino acids this modification is searched on; "#PSM" is the number of peptide-spectrum match instances this modification was found.

Name	Position (AA)	#PSM
Carbamidomethyl	C	1828
Ubiquitin	CKST	1743
Deamidation	NQ	496
Ala -> Gln	Q	346
Gly -> Asn	NQ	184
Methylation	KR	84
Val -> Arg	R	79
Phosphorylation	STY	40

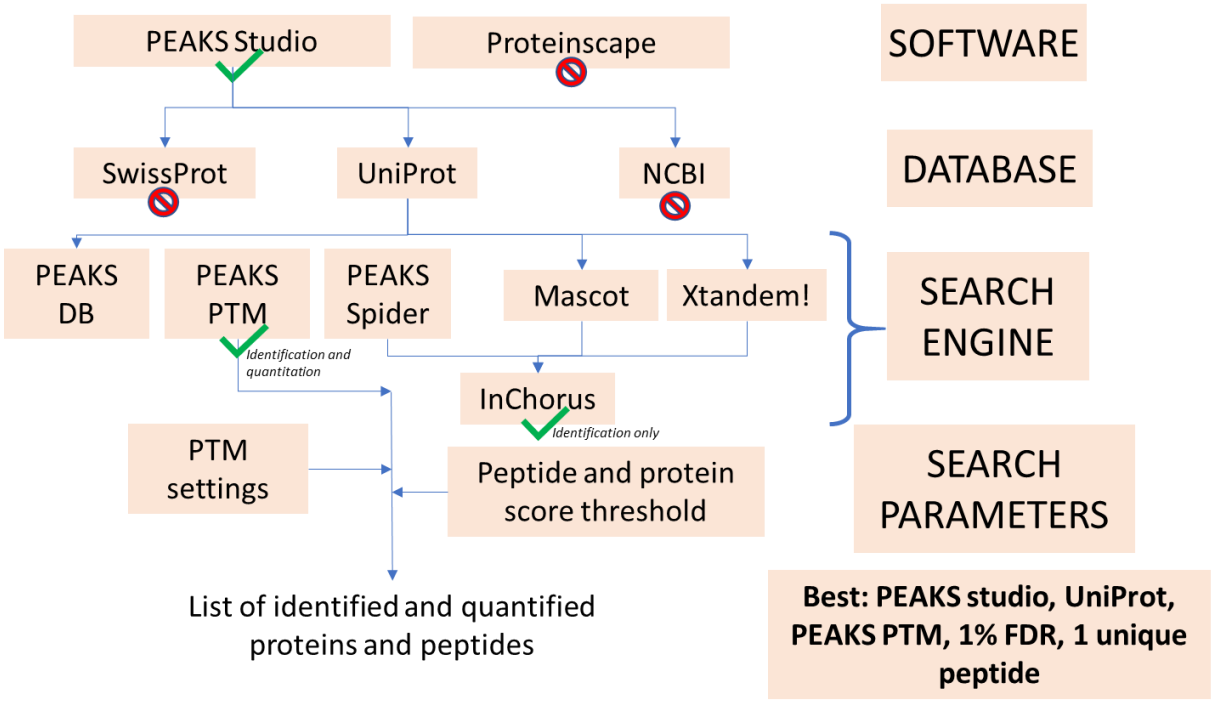

Figure 3-7 Software tools and parameters trialled. Optimal options were PEAKS Studio, using Uniprot as protein database, with PEAKS PTM for quantitation, and InChorus for identification purposes only. Other settings are detailed in text, section 3.4.3.

3.4.6 Optimal protocol summary

Sample preparation

Firstly, 5 ml spin filter columns 10 kDa molecular weight cut-off Microsep® advance (Pall, Hamilton, New Zealand) were rinsed with saline solution (Baxter, Toongabbie, Australia) twice to remove glycerol (which interfered with metabolomics analysis) and left to dry under a fume hood. Then, 5 ml aliquots were taken from each ULF sample and centrifuged in said spin filter columns to fractionate them.

The protein content of the retentates was measured using DirectDetect® (Merck Millipore, Mairangi Bay, New Zealand) plates. A volume containing 250 µg was taken and dried using a Centrivap benchtop vacuum concentrator (Labconco, Kansas City, KA, USA) at 45 °C for 3 h, following which were resuspended in 60 µl of 0.1 M ammonium bicarbonate (Fluka Munich, Germany). Then, samples were reduced with 20 µl of 100 mM DTT (Sigma-Aldrich, St. Louis, MO, USA). for 45 min at 56 °C on a thermomixer (Eppendorf Thermomixer R Mixer 5355, Eppendorf AG, Hamburg, Germany) at 600 rpm, followed by alkylation with 20 µL 150mM IAM (Sigma-Aldrich, St. Louis, MO, USA) (solution in ammonium bicarbonate) in the dark at room temperature for 30 min on a thermomixer at 600 rpm.

Tryptic digestion was performed by addition of 5 µg of sequencing grade porcine trypsin (Promega, Madison, WI, USA) overnight (16 h) at 37 °C on a thermomixer (1:50 w/w trypsin to protein). Finally,

the digests were dried and re-suspended in 50 µl of 0.1% formic acid (Thermo-fisher, Waltham, MA, USA) in LC-grade water (Thermo-fisher, Waltham, MA, USA) and used for LC-MS/MS analysis.

LC-MS/MS analysis

Five µl of the peptide digest were added to 45 µl 0.1% FA and this 1:10 dilution was used for LC analysis. The mobile phase consisted in mixtures of solvent A (0.1% formic acid in MS-grade water, v/v), and B (98% acetonitrile, 0.1% formic acid, v/v). Elution was with a gradient from 2% to 20% B in 45 min, and 20% to 45% B in 15 min, and up to 95% B, for a total run time of 85 min at a flow rate of 1 µl/min. LC-MS and LC-MS/MS analysis was carried out on an UltiMate 3000 RSLC nano UHPLC (Thermo Fisher), coupled to an Impact HD (Q-TOF) mass spectrometer equipped with a CaptiveSpray source (Bruker, Bremen, Germany). Two µl of sample were loaded on a Dionex Nanotrap column (5 mm × 300µm inner diameter, with 5 µm C18 beads, Thermo Fisher). The trap column was then switched in line with the analytical column (ProntoSil C18AQ, 100 µm × 15 cm, 3 µm particles, 200 Å pore size, NanoLCMS Solutions Oroville, CA, USA). The column oven temperature was 50 °C. A mix of air and gas-phase acetonitrile was injected around the emitter spray tip through a nanoBooster™ (Bruker, Bremen, Germany) to support liquid desolvation and increase ionisation efficiency; settings were 3 l/min, dry temperature 150 °C.

Samples were measured in auto MS/MS mode, in the mass range of m/z 350-1200. One MS scan from m/z 350-1200 at 1 Hz was followed by tandem MS scans of the top 10 precursor ions at 1-20 Hz by CID (collisional induced dissociation), and with dynamic exclusion of 90 s, with ions reconsidered if intensity increased more than 4-fold within the exclusion period). Up to 10 precursors were selected for fragmentation. The LFQ (Label-Free Quantitation) method employed was based on two types of information: protein identification (obtained through tandem MS, i.e. MS/MS runs) and protein quantification (single MS runs). For identification-purposed (MS/MS) analysis, 64 ULF samples (picked at random and run throughout) were run undiluted to maximise the number of peptide ions detected. Thus, when analysed with single MS (i.e. without fragmentation) samples were diluted 1:10 to prevent signal saturation. PEAKS Studio's functionality was used to link precursor ions of these runs to those identified in MS/MS runs.

3.4.7 Proteomic analysis

PEAKS Studio v.10.0, build 20190129 (BSI Inc., Waterloo, Canada) was used for proteomic analysis, specifically by PEAKS PTM, with protein identification augmented by InChorus search, a multi-engine search tool that incorporates results from Mascot, X!Tandem, and the PEAKS de novo search engine. Protein identification was performed searching against an in-house database comprising all bovine Uniprot sequences (40690 sequences), downloaded from Uniprot on 14/02/2020 (Uniprot

Consortium 2018), with the following parameters: semi-specific trypsin as enzyme, maximum 3 missed cleavages per peptide, precursor mass error 10 ppm, and fragment ion tolerance 0.02 Da. Carbamylation (M) was set as fixed modification, whereas ubiquitin (CKST), carbamidomethylation (C), deamidation (NQ) and methylation (KR) were set as variable modifications. Protein quantification by PEAKSQ significance method followed a label-free approach, with mass error tolerance of 20 ppm and retention shift tolerance of 2 min. Settings for export were: minimum one unique peptide per protein group, de novo score (ALC%) threshold 50% and peptide-spectrum match (PSM) false discovery rate 1%. For quantification, the top hit of each protein group was used, and protein abundance was calculated as the peak area sum of the top-3 unique peptides, normalised by total ion current (TIC) of each sample divided by the reference sample chosen automatically by PEAKS studio.

Informatic analysis

PEAKS Studio v.10.0, build 20190129 (BSI, Waterloo, Canada) was used for software analysis.

Protein identification was performed searching against Uniprot (Uniprot Consortium 2018) with the following parameters: semi-specific trypsin as enzyme, de novo score (ALC%) threshold 50%, peptide-spectrum match (PSM) false discovery rate 1%, maximum 3 missed cleavages per peptide, precursor mass error 10 ppm, and fragment ion tolerance 0.02 Da. Carbamylation (M) was set as fixed modification, whereas ubiquitin (CKST), carbamidomethylation (C), deamidation (NQ) and methylation (KR) were set as variable modifications.

Protein quantification followed a label-free approach, with mass error tolerance of 0.01 Da, and Rt shift tolerance of 2 min. Most parameters were left as default, including auto-detection of reference sample (taken as the centre for retention time alignment) and training samples (used to calculate the feature vector quality). Significance method was PEAKSQ, and data normalised by total ion chromatogram (TIC).

3.4.8 Variation sources

The aim of this trial was to assess the proportion of variation corresponding to true biological differences as opposed to error stemming from technical factors. This was necessary to confirm whether this setup would be suitable for the large-scale analysis to be carried out as the main proteomics experiment.

Multivariate analysis

One approach employed to assess relative importance of variation sources was a PCA using features directly, bypassing the identification step so that all features could be included in the analysis. In the main trials presented in further chapters, identifying the proteins detected was important and thus a different method was employed.

The clustering of samples according to the first two principal components confirmed that injection replicates are the most reproducible, followed by technical (e.g. sample preparation) replicates, whereas those two groups and the other four biological replicates did not cluster (Figure 3-8). Note one slight outlier among the technical replicates (pointed by a green arrow).

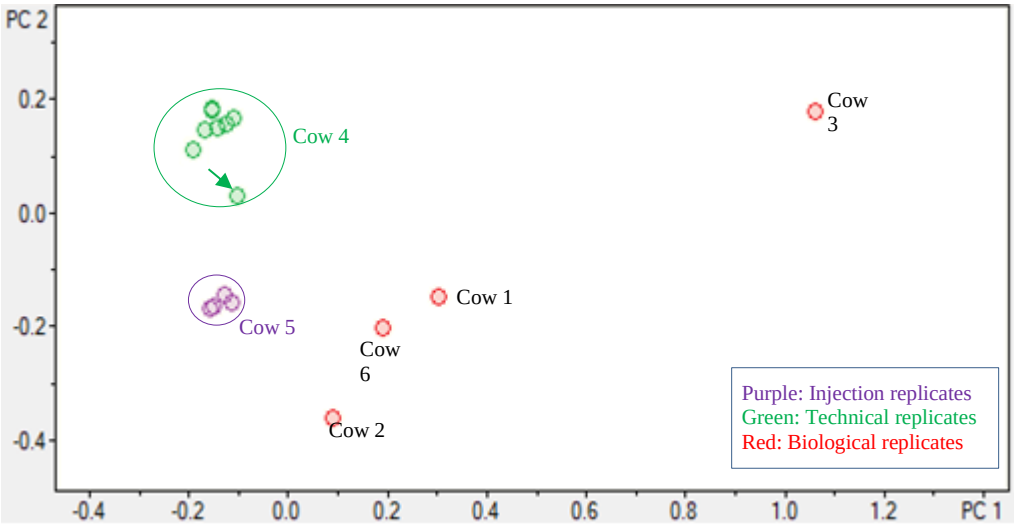

Figure 3-8 Principal component analysis (PCA) plot using the peptide features detected by LC-MS/MS analysis of uterine luminal fluid in the preliminary proteomics experiment to assess the degree of technical to total variation.

Univariate analysis

To obtain a numeric estimate of the differences observed in the principal component analysis, protein abundance (sum of top-3 peptide peak areas) identified by PEAKS as detailed in section 3.4.6 were tabulated and grouped to estimate the proportion of variation of three origins: LC injection, technical (i.e. sample preparation, which also includes LC injection), and total (biological, technical and injection). The coefficient of variation (CV) for each type of replicate was calculated to obtain the proportion of technical variation to total variation.

A total of 332 proteins were identified, out of which 300 were consistently detected, i.e. in at least 70% of the samples in each group. Injection CV was under 20% for more than 200 proteins. Total technical variation was less than 30% of the total variation for 108 proteins (40% of the protein set)

i.e. 70% of the variation detected was biological. A similar number of proteins presented technical variation between 30 and 60% of the total, while a further 44 proteins evidenced between 60 to 90%. Some 20% of the proteins had technical variations in the range of the total, which indicates that potentially the biological differences between samples could be obscured by variability in the setup (Figure 3-9).

Taking the results of both assessment methods together the conclusion was that the biological component in the variation of most of the proteins was likely to be detectable and quantifiable.

In conclusion, the procedures presented in this chapter resulted in a satisfactory level of performance to carry out the main proteomics experiment using this instrumental setup (Exp. P3, Chapter 5).

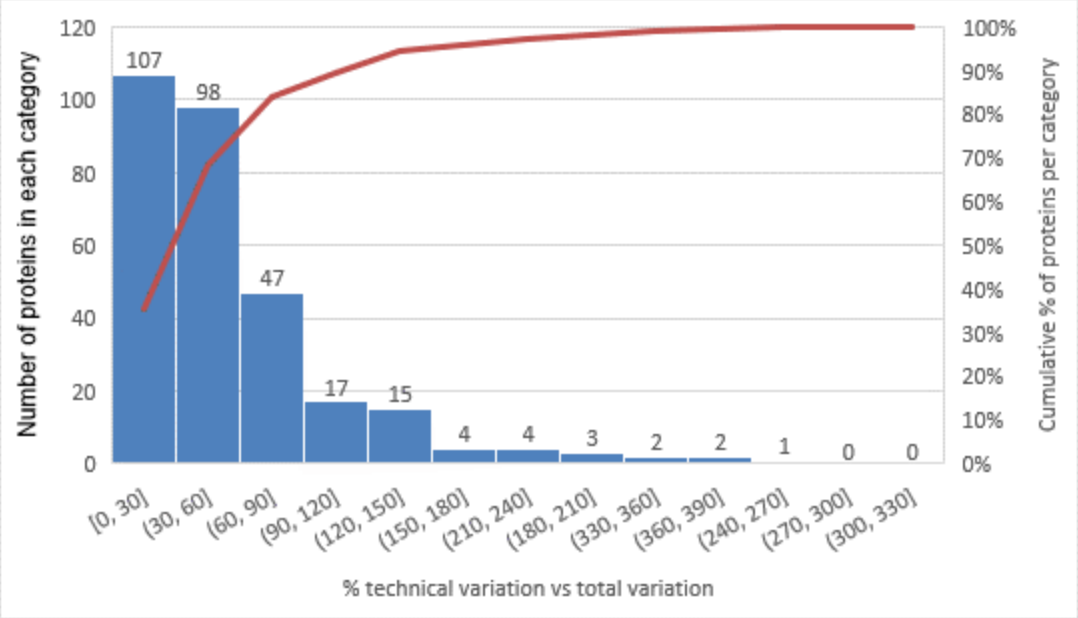

Figure 3-9 Pareto plot showing number of proteins in each range of percentage of coefficient of variation (CV) due to technical aspects vs total CV, which includes technical and biological variation (bars). Red line represents the cumulative proportion of proteins in each range.

4

Metabolomics method development

4.1 Introduction

As described in Chapter 1, metabolites are the endpoint of many endogenous processes and highly informative about their functional state, while also reflecting genetic factors. Because metabolites are closest to an individual's phenotype, they are especially relevant when looking for biomarkers for the biological conditions being studied (Smolinska et al. 2012). In addition to individual biomarker discovery, a deeper understanding of metabolic pathways evolving throughout the postpartum period relevant to embryo development may result in improved herd fertility parameters.

In addition to characterising changes in the ULF molecular landscape that putatively influence early embryo development, a potential application of a metabolomic fingerprinting method was tested using rapid evaporative ionisation mass spectrometry (REIMS), an instrumental platform based on direct infusion mass spectrometry. One of the goals of this project was to test if a molecular fingerprint of ULF is feasible, with the aim of assessing its potential to identify a receptive uterus before embryo transfer.

4.1.1 Variability of sample volume

Uterine flushing *in vivo* presents a key challenge: the volume of ULF originally sampled is unknown and complete recovery of the liquid is never obtained, complicating comparisons of abundance of molecules across samples (Velazquez et al. 2010). Thus, to account for differences in recovery efficiency of the flushing process, and potentially of the fluid dilution, a small trial was designed to test the use of an isotopic tracer.

The molecule tested in this work as a tracer was stable-isotope-labelled proline. It is not present naturally in the animal yet mimics a biological compound (native proline). This was added to the flushing medium as an internal standard to account for dilution and recovery efficiency of the flushing procedure. Stable isotopes have been successfully employed to study nitrogen flux and energy expenditure (Klein and Klein 1987) as well as other nutritional parameters (Iyengar 2002), and proven to be safe for human application, including in infants (Klein and Klein 1987).

4.1.2 Aims

The main aim was to develop an experimental method to characterise the ULF metabolome effectively and reliably (Metabolomics Experiment 1, "Exp. M1"). A secondary aim was to test the

application of a tracer molecule as an internal standard to account for variation caused by dilution of ULF during flushing, as well as testing the safety of its application (Exp. M2). Finally, Exp. M3 evaluated the use of a direct infusion mass spectrometry technique (REIMS) to generate a metabolomic fingerprint of ULF, in a first step to appraise the potential of this approach as a diagnostic tool for uterine receptivity in a further experiment.

ULF flushing samples have not been extensively measured using metabolomics, so it was important to ensure that protocols developed for blood plasma were appropriate. Therefore, different approaches were trialled in two steps of the GC-MS/MS workflow, and their suitability determined by coverage (number of metabolites detected) as well as technical reproducibility.

4.2 Materials and methods

4.2.1 Reagents and samples

Chloroform was bought from Mallinckrodt (St. Louis, MO, USA). LC-quality water and methanol were sourced from Thermo fisher (Waltham, MA, USA); trimethylsilyltrifluoroacetamide (MSTFA) with 1% trimethylchlorosilane (TMCS) and methoxamine-hydrochloride solution in pyridine (30 mg/ml) were obtained from Sigma-Aldrich (St. Louis, MO, USA). Medical-grade saline solution 0.9% NaCl was acquired from Baxter (Toongabbie, NSW, Australia).

Alkane retention index standards (C7-C33) were bought from Restek Corporation (Bellefonte, PA, USA). Internal standard mix (Alanine d4, Benzoic acid d5, Leucine d10, Citric acid d4, Glucose 1,2 13C2, Tyrosine d2, Stearic acid d35 and Tryptophan d5, Methyl nonadecanoate, all 4 µg/ml) was prepared in-house from chemicals sourced from Cambridge Isotope Laboratories (Tewksbury, MA, US). Isotope-labelled L-Proline ($^{13}C_5$, 99%; ^{15}N, 99%) was also sourced from Cambridge Isotope Laboratories.

4.2.2 Experimental design

Experiment M1: pre-fractionation and extraction for GC-MS/MS

The method was optimised for uterine fluid by testing two pre-fractionation alternatives and two extraction methods in a 2x2 design (Table 4-8) using 5 ULF pooled technical replicates per treatment. The effect of pre-fractionation was assessed by comparing ULF samples as described in section 3.3.1, specifically a) unprocessed ULF flushing fluid, or b) filtrate from ULF spin column filtration (fraction of low molecular weight, < 10 kDa).

Table 4-8 Latin square - methodological combinations for GC-MS/MS metabolomics optimisation experiments.

	Monophasic extraction (M)	**Biphasic extraction (B)**
Whole ULF (W)	5 technical replicates (**WM**)	5 technical replicates (**WB**)
ULF Filtrate (F)	5 technical replicates (**FM**)	5 technical replicates (**FB**)

A second aspect was the extraction protocol, either monophasic (Jiye et al. 2005) or biphasic (Armirotti et al. 2014). Two outcome variables were examined to decide the most suitable approach for Experiment M4 (main GC-MS/MS metabolomics experiment, Chapter 6): number of transitions or features (metabolites) identified for each combination of methods and reproducibility. This was assessed by two independent methods. Analytically, the number of features detected whose peak areas presented a coefficient of variation equal to or lower than 10% was determined, across technical replicates. A second parameter considered was the degree of clustering in non-supervised statistical analysis (PCA). This parameter indicates similarity between replicates, both qualitatively and quantitatively, and thus it is a useful tool to compare treatments (Lenz et al. 2016).

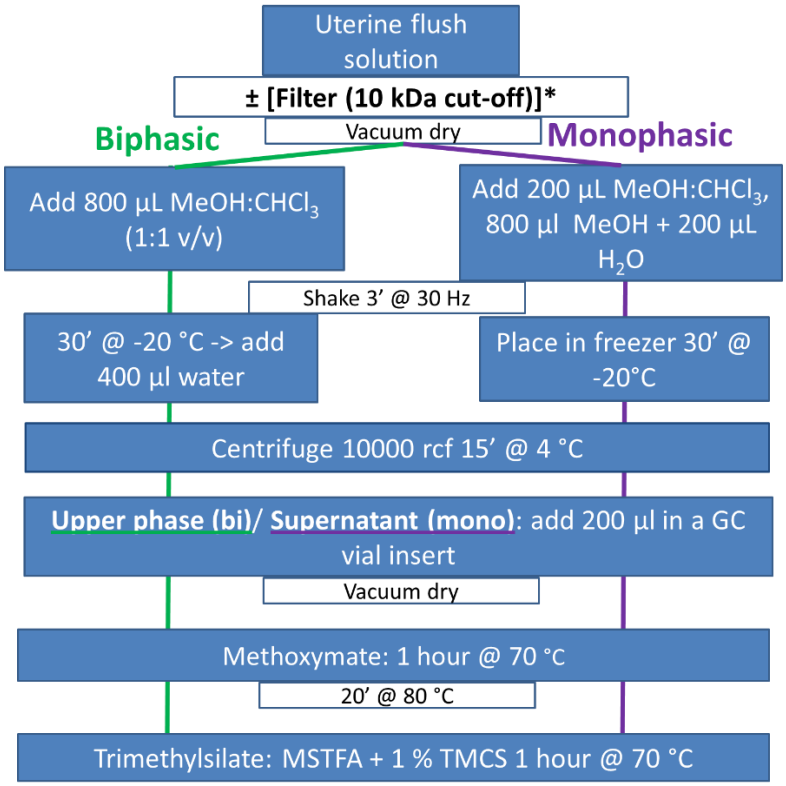

Figure 4-3 Experimental workflows trialled for GC-MS/MS protocol optimisation to analyse ULF. *Filtered with centrifugal spin columns as detailed in Chapter 3. Abbreviations: $CHCl_3$, chloroform; GC, gas chromatography; MeOH, methanol; MSTFA, methyl-silyl trifluoroacetamide; Rcf, relative centrifugal force; TMCS: trimethyl-silyl chloride.

In all cases, targeted analysis was used for optimisation, with centring and auto-scaling as the default data pre-treatment. This process results in each variable (i.e. metabolite peak area) having a mean of zero and variance equal to one (Jackson 2005). Its main feature is that all variables are given equal weight, reflecting the premise that in living beings, relative abundance cannot be taken as a proxy of biological importance (van den Berg et al. 2006). An alternative analysis strategy investigated was full-scan (untargeted) GC-MS/MS analysis, using the parameters presented in the following section.

Sample processing methods

Samples used were described in 2.2.4 (Farm Trials 2 and 3). Workflows are depicted in Figure 4-3, The first step tested in this experiment was pre-processing, as described in 3.3.1. In brief, 5 ml aliquots from a pool of ULF from 20 different cows were filtered using Microsep® spin filter columns with 10 kDa molecular weight cut-off (Pall, Hamilton, New Zealand), which resulted in a retentate and a filtrate fraction ("F"). Both the filtrate fraction and whole ("W") ULF 5 ml aliquots were dried down by vacuum centrifuge concentrator (Labconco, Kansas City, KA, USA) and kept at -80 °C until analysis.

The two extraction methods were similar except for the initial steps. Briefly, the dried fraction was re-suspended in 50 µl LC-grade water, and 10 µl of internal standard (IS) mix was subsequently added. Then, 450 µl of a mixture of chloroform: methanol (1:1 v/v) (biphasic) or 450 µl of methanol: water (4:1 v/v) (monophasic) was added and shaken for 3 min at 30 Hz in a bead shaker (Qiagen, Stockach, Germany). For the biphasic extraction, tubes were placed at -20 °C for 30 min and then 200 µl of water were added.

From this point on, the workflows were the same. The samples were shaken for a further 3 min at 30 Hz and centrifuged at 10,000 rcf for 15 min at 4 °C. A 200 µl aliquot of the upper phase (biphasic) or supernatant (monophasic) were transferred to a GC glass vial insert and dried completely in vacuum centrifuge concentrator at 35 °C for 2 h. Samples were then derivatised using a two-step procedure. Methoxymation was accomplished by addition of 30 µl of methoxamine-hydrochloride solution in pyridine (30 mg/ml) and incubating for 1 h at 40 °C. Sylilation was conducted by adding 30 µL of N-Methyl-N-trimethylsilyltrifluoroacetamide (MSTFA) with 1% (w/v) trimethylchlorosilane (TMCS) and incubating for 1 h at 40 °C.

Targeted analysis

Samples were analysed using a broad-based targeted GC-MS/MS metabolomics method. For this, GC was performed on a BPX5 capillary column with 0.25 mm internal diameter, 0.25 µm film thickness, and 30 m length (SGE Ltd, Australia). One µL of derivatised sample was injected at a starting

temperature of 60 °C for 2 min then ramped to 320 °C at 15 °C/min and held for 3 min, using He as the carrier gas at a constant linear velocity of 39 cm/s.

A Shimadzu 8040 GC-MS/MS instrument (Shimadzu, Kyoto, Japan) was employed for mass spectrometry analysis, with the following settings: interface temperature 280 °C, the ion source 200 °C, ionisation voltage 70 eV. Mass measured range was 45 to 600 m/z, at a 0.2 s interval.

Mass spectrometry parameters were predetermined and optimised for the same system and column based on injection of standards as part of the Smart Metabolites Database package (Shimadzu, Kyoto, Japan). This commercially developed method package for targeted metabolomics contains 452 multiple reaction monitoring (MRM) transitions, totalling 311 unique metabolites. These metabolites cover a broad range of compound classes including organic acids, energy metabolism intermediates, amino acids, some fatty acids, and mono- and di-saccharides.

In this technical approach, metabolite identification is based on two factors. One is retention index (Gonzalez and Nardillo 1999), that is, retention time relative to a series of alkane standards (C7–C33) injected during the same batch. This allows reliable comparisons independent of actual retention time between batches and even across different GC-MS platforms. The second is MRM transition, where a compound must have not only the right initial fragment from the initial electron impact ionisation fragmentation (precursor ion), but also the correct fragment after further fragmentation (product ion), and a roughly similar intensity (peak area) ratio between precursor and product ion (Hansen et al. 2011). Peaks were automatically integrated and each of the 452 transitions further checked manually for correct qualifier/quantifier ion ratio and retention time.

All peak areas were normalised using internal standards (Jonsson et al. 2005). This approach aims to standardise samples' peak areas by adding the same amount of internal standard (IS) mix to all samples; differences in the peak areas of these compounds are a measure of the magnitude of technical error. Specifically, values of peak areas of IS for all samples were tabulated, centred, and autoscaled (transformed so that each variable had a mean of 0 and a standard deviation of 1, to correct for magnitude differences across variables). Next, principal component analysis (PCA) was performed using R statistical software v4.0.2 (R Team 2019). The first component of the PCA represents the dimension with the highest amount of variability across samples due to all IS peak areas; the (loading) value of each sample in this component is considered to summarise variation arising from differences in peak areas of all IS. Lastly, all metabolite peak areas in the samples were divided by the loading value of the first component of the PCA in that sample, and the resulting values were used thereafter for all further analyses.

Afterwards, two parameters were evaluated. Firstly, the number of features detected in each group (coverage) and the number of those with coefficients of variation (CV) lower than 10% within each group were assessed. Secondly, sample clustering in non-supervised statistical analysis (PCA) was examined. The tightness of clustering indicates both qualitative and quantitative similarity between replicates (Worley and Powers 2013). Plots were produced using the R package *ggplot2* (Wickham 2016).

Untargeted analysis

Settings were identical to those for targeted analysis except that instead of measuring set transitions, a full scan of ions in the region of 30 to 650 m/z was performed.

Experiment M2: heavy proline as tracer to estimate sample dilution

The animals used in this experiment were sampled in Farm Trial 1 and were similar in breed to those in the main herd. Differences were that the animals were synchronised to be at the same cycling stage (oestrus), were not lactating, and that due to the novel use of a xenobiotic they were kept separated in a containment unit. Further details of the animals and the schedule of synchronisation and sampling have been presented in section 2.2.4.

The molecule chosen as tracer was isotope-labelled L-Proline ($^{13}C_5$, 99%; ^{15}N, 99%), a compound commonly used as an internal standard for technical variation introduced during sample preparation in metabolomics experiments (Koek et al. 2006). This proline is identical to the naturally most abundant proline isotopical form except for its molecular weight (6 Da heavier). This property enables its detection as a separate peak in mass spectrometry analysis even though its chromatographic retention time is the same as native proline.

Procedure

Firstly, three tracer concentrations (0.1, 1 or 10 µg/ml) in a range based on the report of Koek et al. (2006) were tested to determine the optimal concentration for detection; this was 1 µg/ml. Flushing medium was prepared by adding 1 ml of tracer stock solution (500 µg/ml) to 500 ml of saline solution for a final volume of 1 µg/ml. Uterine flushing was performed as detailed in 2.2.4, using 30 ml of flushing medium. The flushed liquid was collected, snap-frozen and kept at -80 °C. ULF samples of six animals were further analysed, following filtration and extraction as per 4.2.2.

A 5 ml blood sample was taken from all animals at four times: t0 (immediately before flushing), and at 1, 6 and 24 h (t1, t6, t24) post-flushing, and stored as plasma according to the protocol in section 2.2.4. Plasma samples from two animals at all timepoints were further analysed by GC-MS/MS.

Along with ULF and plasma samples, the following were analysed: a saline blank, three aliquots of tracer-spiked flushing medium, standards of heavy proline dissolved in LC-MS grade water (i.e. stock solution of 4.2 mg/ml and a dilution at 1 µg/ml, both as positive controls), and a QC pool made of aliquots of all other sample types to assess instrument performance. Except for the standards of heavy proline, all other sample types were filtered and extracted as per 4.2.2. Gas chromatography and tandem mass spectrometry equipment and settings used were described in section 4.2.2.

Chromatogram peaks for tracer were manually checked, tracer peak areas quantified and tabulated. Transfer to bloodstream was assessed based on the abundance differences between tracer peak areas of ULF and blood samples.

Experiment M3: Metabolomic fingerprinting by direct infusion mass spectrometry

Fourteen ULF samples as described in 3.2.2 from a previous similar trial were used to refine the direct infusion mass spectrometry technique (REIMS). In brief, 2 ml of ULF sample were pipetted into a foil cup (Wilton Inc., Wellington, New Zealand) and vaporised using a handheld monopolar device ("iKnife") fitted with a diathermy electrosurgical generator (Erbe VIO 50C, Erbe Medical UK Ltd, UK) at 50 V cutting mode in triplicate measurement, with cone voltage set to 100 V and heater bias to 20 V. The MS data was acquired in both positive and negative ionisation mode using a Waters Xevo® G2 qToF mass spectrometer with REIMS interface (Waters Corp. Wilmslow, UK), run in resolution mode at 100 µl/min isopropanol flow rate, with a scan time of 0.5 s and a mass range of m/z 50-1500. The instrument was calibrated using 5 mM sodium formate in isopropanol (infused via REIMS's matrix inlet) prior to analysis. Sample measurement consisted in sliding the tip of the knife along the surface of the ULF sample for 2 s (positive ionisation mode) or 4 s (negative ionisation mode), three to four times per sample, with a 15 s window between burns to allow time for clearing the signal. Data processing was conducted as described by Ross et al. (2020). In brief, the sample files were split into separate files for each replicate using ProGenesis Bridge (Waters). Mass alignment and baseline subtraction were carried out with the same software, with 0.1 Da mass tolerance for feature selection. ProGenesis QI (Waters) was employed for noise correction. Mass adjustment for all features were adjusted to an internal lock-mass peak area of ion 121.25 m/z (an adduct of protonated isopropanol) in positive mode, and peak area of ion 325.3 m/z (consistently the largest peak, putatively identified as arginylasparagine) in negative mode. In both ionisation modes, peak intensity was normalised to total ion current.

4.3 Results and discussion

4.3.1 Experiment M1: development of optimal GC-MS/MS protocol

Coverage and univariate analysis of reproducibility

All method combinations were equally effective in terms of coverage, i.e. 209-211 features identified, out of a total 452 features scanned for in the mass spectrometry package used (Figure 4-2). This was considered satisfactory, especially in light of other studies using the same method reporting 159 compounds detected in human plasma (Uji et al. 2017) and 91 detected in soybean (Makino et al. 2020). When examining the number of reproducible features (i.e. with CV <10%), the most robust combination was filtering and biphasic extraction (96 highly reproducible features), followed by non-filtered and monophasic extraction (81), filtered and monophasic (70) and lastly, non-filtered and biphasic (20). On closer inspection, compounds higher in filtrate fractions compared to whole samples were mostly amino acids and other organic acids, whereas the main differences between monophasic and biphasic extractions were in monosaccharide concentrations.

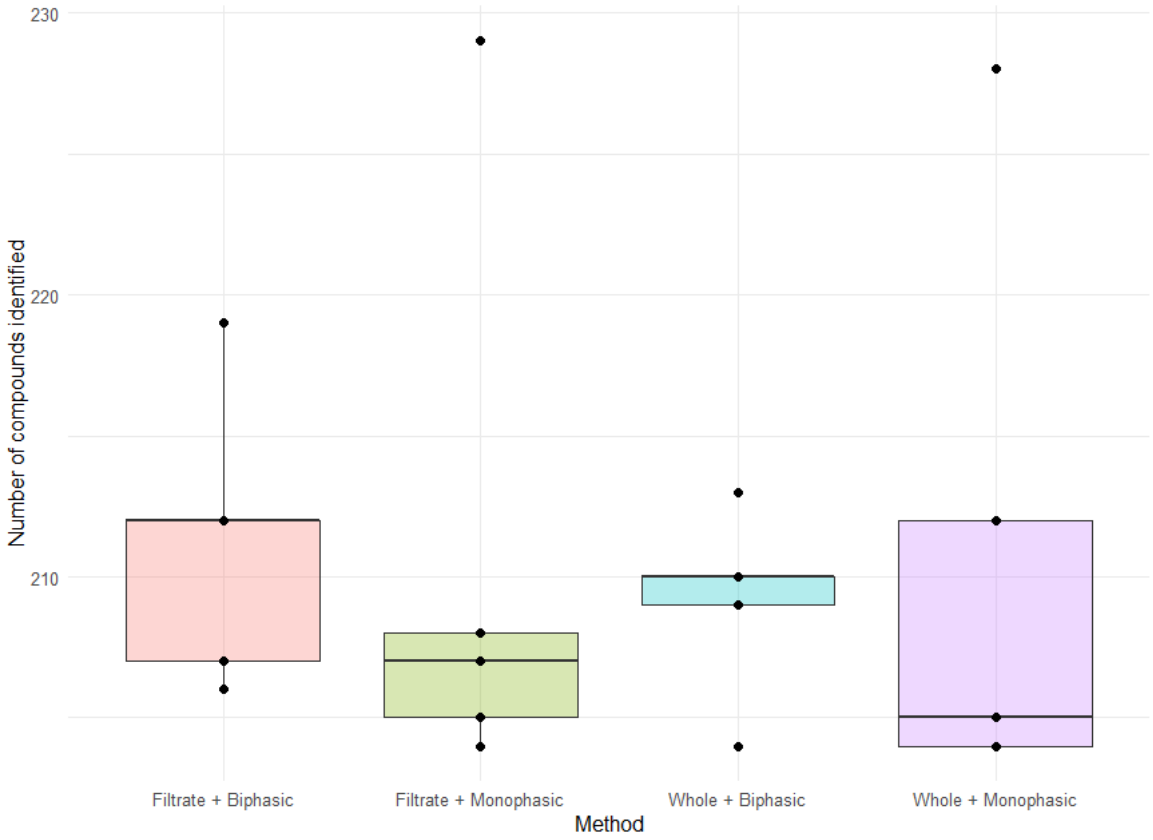

Figure 4-2 Number of metabolites detected per replicate following each workflow combining either filtrate or whole uterine fluid with mono- or biphasic extraction. N=5 technical replicates.

There are some reports of trends for sample processing methods to favour extraction of specific metabolite classes, such as lipids by monophasic extraction (Calderón et al. 2019), and sugar phosphates by biphasic extraction (Prasannan et al. 2018). However, this last study also suggested that despite differences in specific metabolites, both types of extraction can be used to adequately extract all the predominant metabolite classes (Prasannan et al. 2018), which was also evident in this study. Differences in the metabolites detected according to the platform employed are further examined in Chapter 6.

Multivariate analysis of reproducibility

Reproducibility was further assessed by visual inspection of a PCA plot displaying the first two principal components. Samples in the FB group (filtrate fraction, processed by biphasic method) presented by far the tightest clustering in the two dimensions encompassing the most variance in a PCA (Figure 4-3).

Considering results from both univariate and multivariate analyses, FB (filtrate and biphasic extraction) was the methodology of choice for the main experiment (Exp. M4).

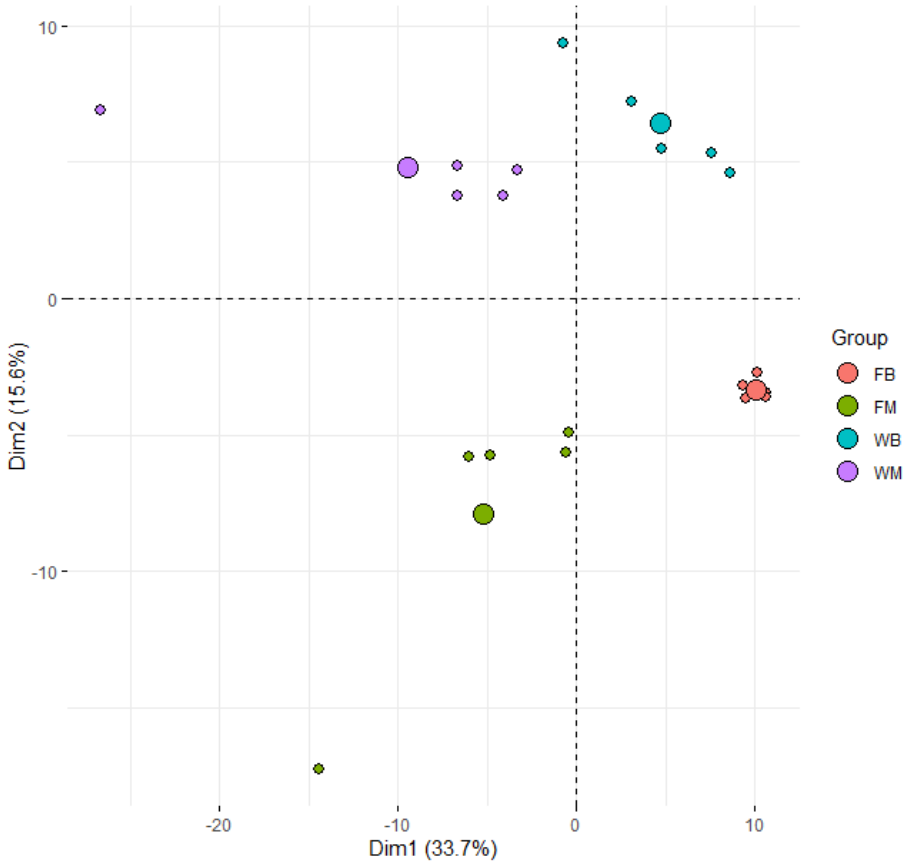

Figure 4-3 Principal Component Analysis (first two components) showing the degree of similarity between technical replicates. Abbreviations: FB, filtrate biphasic; FM, filtrate monophasic; WB, whole ULF biphasic; WM, whole ULF monophasic.

Untargeted analysis

Samples were analysed by an alternative approach. Instead of pre-selecting specific ions for fragmentation, all ions in the 30-650 m/z window were analysed and fragmented. This resulted in a high number of features detected (532). However, only 86 were identified by the m/z of the precursor and product ions in mass spectrometry analysis, due to not all metabolites being well characterised and included in metabolite libraries. The overlaps and differences between the metabolites identified by each approach are examined in Chapter 6. For the present work, compound identification was crucial and therefore the targeted method was selected.

Glycerol contamination

Following preliminary runs, an unexpectedly high glycerol peak was detected in the spectra of filtered samples which saturated the detector and interfered with closely eluting compounds. By comparing spectra with those obtained from non-filtered samples, the source of the glycerol contamination was found to be the plastic filters in the spin columns. A simple washing with saline solution followed by centrifuging 10 min at 10,000 *g* was able to remove most of the glycerol from the columns and improved accurate detection of three compounds that were otherwise saturated by the glycerol signal (data not shown).

4.3.2 Experiment M2: Tracer

Tracer peak annotation and identification

The goals of this experiment were to determine the validity of quantifying tracer peak area as a proxy of dilution during sampling, and to confirm no transfer occurred from uterine lumen to bloodstream.

The first step was sample preparation and measurement by GC-MS/MS. ULF samples from 6 cows (both whole and their filtered fraction <10 kDa, Table 4.1) and plasma samples from two cows at four timepoints (before flushing, and 1, 6 and 24 h after) were processed and analysed, along with QC pooled samples, saline solution blanks (negative control), aliquots of tracer-spiked flushing medium, and standards of tracer dissolved in MS grade water, i.e. stock solution of 4.2 mg/ml and a dilution at 5 µg/ml (both as positive controls).

Next, manual inspection of peaks was carried out to verify that the area values reported by the automatic software analysis corresponded to the tracer. Representative chromatograms of tracer transitions in the six types of samples (ULF, QC pools, saline blanks, saline spiked with tracer, tracer stock solution, and plasma) are displayed in Figure 4-4. For identification of the tracer peak, the Rt and qualifier to quantifier ion ratios were taken as standard to which the other runs were compared. The most prevalent peak in ULF, QC and plasma samples was classed as an unidentified compound. This was a transition ion of the same weight (147>73.1 m/z) eluting 2 s after the tracer peak. Closer

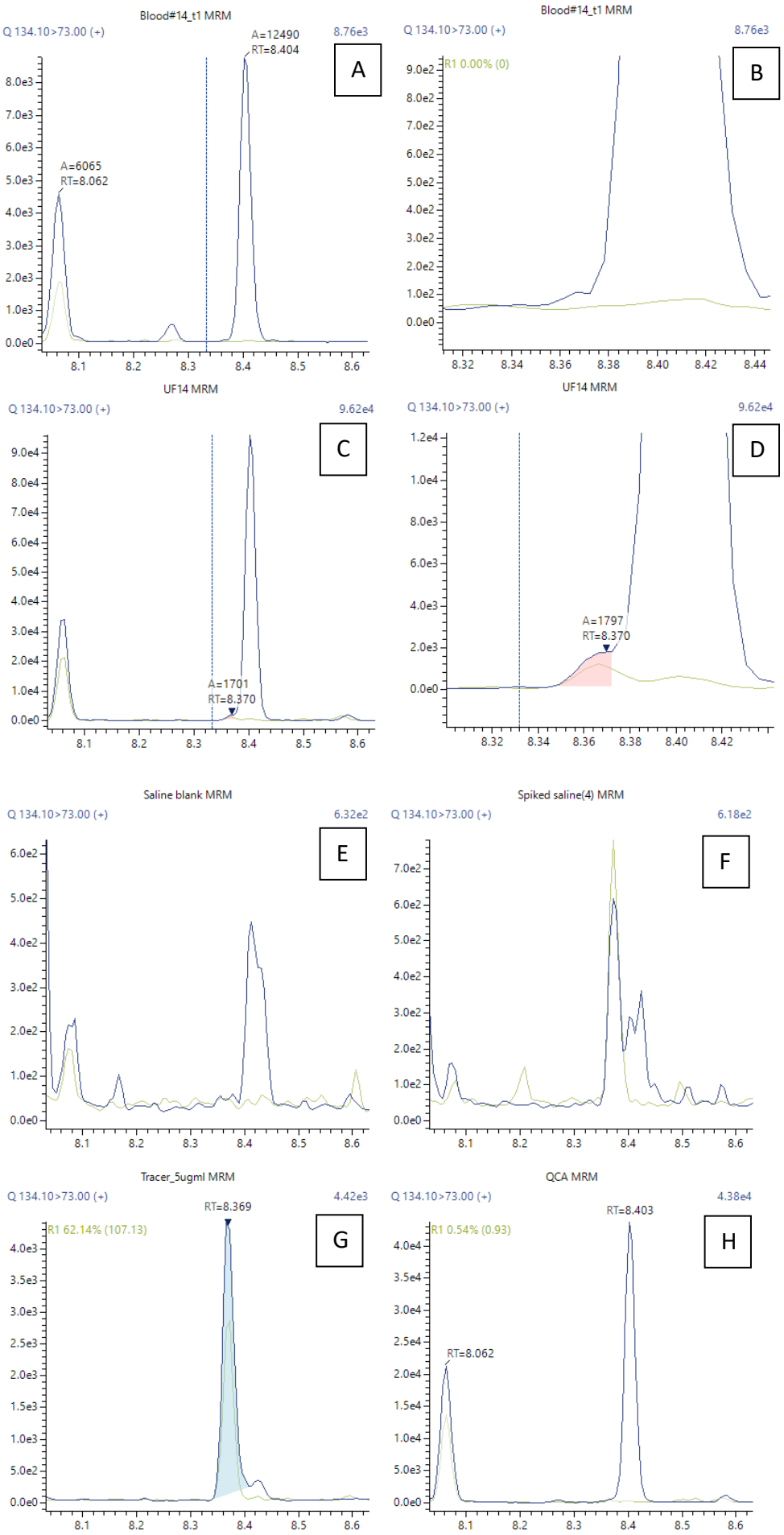
Blood#14_t1 MRM
Q 134.10>73.00 (+)
8.76e3
A=12490
RT=8.404
A=6065
RT=8.062
A
Blood#14_t1 MRM
Q 134.10>73.00 (+)
8.76e3
R1 0.00% (0)
B
UF14 MRM
Q 134.10>73.00 (+)
9.62e4
A=1701
RT=8.370
C
UF14 MRM
Q 134.10>73.00 (+)
9.62e4
A=1797
RT=8.370
D
Saline blank MRM
Q 134.10>73.00 (+)
6.32e2
E
Spiked saline(4) MRM
Q 134.10>73.00 (+)
6.18e2
F
Tracer_5ugml MRM
Q 134.10>73.00 (+)
4.42e3
R1 62.14% (107.13)
RT=8.369
G
QCA MRM
Q 134.10>73.00 (+)
4.38e4
R1 0.54% (0.93)
RT=8.403
RT=8.062
H

Figure 4-4 GC-MS/MS analysis (Exp. M2 - tracer): representative chromatograms for each type of sample. A: plasma sample from cow #14 at t1, i.e. taken 1 h after flushing B: detail from A. C: ULF flushing sample. D: detail of C (8x zoom). E: saline blank. F: spiked saline (flushing medium), batch 7. G: Tracer standard. H: Quality control pool A (QCA).

examination evidenced a small peak of tracer in ULF and QC samples, preceding and partially co-eluting with the dominant peak (Figure A-8-2). Even though both the automatic and manual peak annotation were performed as consistently as possible, some error is unavoidable as the overlap between peaks hinders unequivocal delimitation.

After peak verification, quantification was carried out using the quantifier ion peak areas (transition 189>73.1) as per the software developer's specifications. Worthy of note, the qualifier transition was a suitable candidate for quantification as none appeared in plasma samples or blank. In fact, similar trends were observed as when using quantifier transition; however, because of its lower intensity, this resulted in an increased error. In consequence, quantifier ion peak area was used hereafter.

Tracer peak quantification

The stock solution presented a peak of considerable intensity (over 400,000 arbitrary units). An aliquot of the stock solution was diluted to the same concentration as the samples (1 µg/ml); its peak area of 6457 units was taken as a reference of this concentration. In the case of spiked flushing medium, the three aliquots taken from different batches were technical replicates and expected to present peaks at least at the same level of the ULF samples, if not more, as no dilution would have occurred by the volume of fluid originally present in the uterine lumen. The discrepancies observed between what could be considered technical replicates, might be related to the high amount of salt that did not dissolve fully in the small volumes of solvents added during the extraction and derivatisation stages. The replicate with the biggest peak area (3560 units) is likely representative of the spiked flushing medium. This indicates a potential decrease of 45% of tracer amount during the filtering and chemical extraction steps.

QC runs represent injection replicates, whose purpose was to determine differences in the instrument performance across this experiment; their areas varied up to 30%, which is not surprising at low intensities (i.e. under 10,000, and especially under 1,000; Table A-1). However, the peak areas of other compounds with higher intensities were similar and therefore the reproducibility of this experiment was considered satisfactory.

Regarding ULF samples, the volume recovered in each case was within an 8 ml range (19 to 27 ml), and the peak areas of tracer ranged from 461 to 4487 arbitrary units. The implications of this are discussed next.

Transfer to blood

As mentioned, no tracer peak was observed for plasma samples (Figure 4-5, Table A-11). Inspection of the tracer peak area values in blood samples at different timepoints showed that the biggest areas corresponded to T0 samples, i.e. before flushing and therefore before any tracer could have entered the bloodstream. The absence of a detectable amount of tracer in blood samples in this experiment was potentially caused by the substantial dilution that would have occurred if any amount of tracer had indeed entered the bloodstream. The concentration of tracer added to the flushing medium was optimal to measure it in uterine fluid -of an estimated volume of under 10 ml (Schultz et al. 1971)-. On the other hand, the total amount of blood in a cow is usually in the range of 20 to 25 l (Reynolds 1953). Had any material transfer occurred, it would have resulted in a change below the limit of detection sensitivity of the instrument.

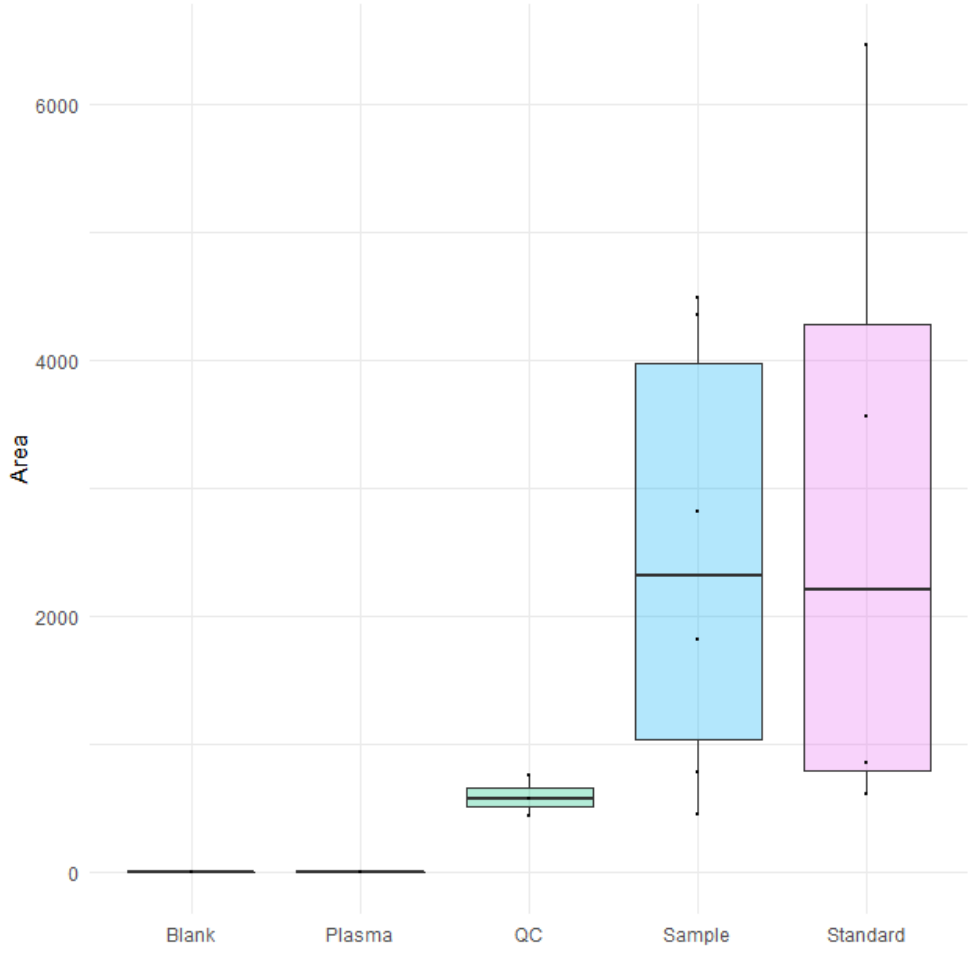

Figure 4-5 Tracer peak areas of the different types of samples. QC, quality control (pooled ULF) samples. Area is expressed in arbitrary units (AU).

Applicability of the tracer approach for dilution estimates

Aside from the use of heavy proline as a tracer, other strategies to calculate dilution and volume were considered. One is the use of a readily diffusible molecule that can spread freely between blood

and ULF. In a successful example of a similar technique, urea has been effective for dilution calculations when performing lung epithelial fluid flushing in humans (Rennard et al. 1986), based on the assumption that urea can diffuse almost unrestrained throughout body fluids and compartments (Taylor et al. 1965). However, the application of this strategy for ULF requires extensive method development and validation, and this was deemed outside the scope of the present work.

The biological rationale motivating this experiment was that differences in the degree of uterine involution might be an important factor in the differences in reproductive performance observed in this animal model (Berg et al. 2017). Uterine involution has been highly relevant and indicative of recovery post-partum and readiness for a pregnancy (Kiracofe 1980), directly as well as indirectly by determining post-partum disease (Sheldon et al. 2006). While this preliminary data showed consistency in the recovered volumes, these cows were synchronised to day 7 of oestrus and the uterus was well involved as these cows were not lactating. Greater variation in the recovered flushing medium volume was likely to occur in dairy cows 23 to 80 days postpartum in Farm Trials 2 and 3. This is because when the uterine horns are not contained within the pelvis, some fluid can be trapped in the uterine horns as these cannot be lifted sufficiently to allow all flushing liquid to flow down. Thus, along with implementing the tracer approach described, SPS score (indicative of the position of the reproductive tract in the pelvic cavity as explained in Chapter 2) was included as a variable in the analysis. Moreover, another factor that can affect fluid recovery are technical issues, especially the catheter balloon not making a tight seal of the uterine walls; this results in some fluid escaping the catheter and not being recovered.

In summary, the results of this preliminary trial pointed at the uterine flushing method producing a measurable degree of mixing and dilution between the ULF and the flushing medium. The differences observed justified its use in the main trials (Farm Trials 2 and 3, analysed in chapters 5 and 6), considering that the safety of tracer application to lactating animals was confirmed due to negligible or undetectable transfer from uterus to general circulation. SPS score was also considered important as a covariate to account for recovery differences.

4.3.3 Targeted metabolomics: optimal protocol

Based on the methods trialled in Exp. M1, the protocol to be used for sample analysis in the main experiment was decided. It was decided that the tracer (i.e. isotope-labelled proline) be added to the saline solution to make up the flushing medium, at the tested concentration of 1 µg/ml. Following is the detailed method.

Protocol

Firstly, 5 ml spin filter columns 10 kDa molecular weight cut-off Microsep® advance (Pall, Hamilton, New Zealand) were rinsed with saline solution twice to remove glycerol and left to dry under a fume hood. Then, 5 ml aliquots were taken from each (tracer-spiked) ULF sample and centrifuged in said spin filter columns to fractionate them. The filtrate (4.8 ± 0.2ml) was collected and dried down in a Centrivap benchtop vacuum concentrator (Labconco, Kansas City, KA, USA) at 45 °C for 3 h and kept at -80 °C until analysis.

Next, the dried fraction was resuspended in 50 µl water, and 10 µl of internal standard mix (Alanine d4, Benzoic acid d5, Leucine d10, Citric acid d4, Glucose 1,2 13C2, Tyrosine d2, Stearic acid d35 and Tryptophan d5, Methyl nonadecanoate, all 4 µg/ml, prepared in-house from chemicals sourced from Cambridge Isotope Laboratories, Tewksbury, MA, US) was added. Biphasic extraction was carried out by adding 450 µl of a mixture of chloroform (Mallinckrodt, St. Louis, MO, USA): methanol (Thermo-fisher, Waltham, MA, USA) (1:1 v/v) and shaken for 3 min at 30 Hz in a bead shaker (Qiagen, Stockach, Germany). Tubes were placed at -20 °C for 30 min and then 200 µl of MS-grade water (Thermo-fisher, Waltham, MA, USA) were added. The samples were shaken for a further 3 min at 30 Hz and centrifuged at 10,000 *g* for 15 min at 4 °C. Two hundred µl of the upper phase (biphasic) were transferred to a GC glass vial insert and dried completely in vacuum centrifuge concentrator (Labconco, Kansas City, KA, USA) at 35 °C for 2 h. Samples were then derivatised using a two-step derivatisation procedure. Methoxymation was accomplished by addition of 30 µl of methoxamine-hydrochloride solution in pyridine (30 mg/ml) (Sigma-Aldrich, St. Louis, MO, USA) and incubating for 1 h at 40 °C. Sylilation was conducted by adding 30 µL of N-Methyl-N-trimethylsilyltrifluoroacetamide (MSTFA) with 1% trimethylchlorosilane (TMCS) (Sigma-Aldrich, St. Louis, MO, USA). and incubating for 1 h at 40 °C.

4.3.4 Experiment M3: Optimisation of direct infusion mass spectrometry for metabolomic fingerprinting

Direct infusion mass spectrometry analysis with REIMS was carried out as per usual practice in this laboratory (Ross et al. 2020), which typically employs solid sample matrices like meat or, occasionally, vegetables. Despite REIMS being a technology optimised for analysis of solid samples, it was possible to analyse (i.e. obtain spectra) ULF samples. However, this was not the case with plain water. It is likely that the presence of sodium chloride in the flushing solution (main constituent of ULF samples) was the cause of this difference, by making ULF conductive enough for application of this technique.

Reproducibility

In negative mode, a total of 4933 features (ions) were detected, of which 2862 were kept after removing those in blanks, for a final number of 2294 after removing features not quantified (i.e. zeroes). Similar values were observed for analysis in positive mode (4971 features detected; 2238 only in ULF samples, of which 1533 were quantified). Sampling in positive mode produced cleaner burns (i.e. more clearly defined peaks in total ion chromatogram) and therefore sample reproducibility based on features obtained in this ionisation mode was expected to be higher (Figure A-8-). However, this did not result in visible improvements in technical reproducibility, i.e. outlier burns (technical replicates) were observed by multivariate analysis (PCA) in both modes (Figure A-8-4).

In this regard, a matrix effect has been reported, whereby certain materials produce cleaner spectra in either positive (fruit; Arena et al. 2020) or negative (bacterial cultures; Bodai et al. 2018) polarity, however this phenomenon has not been studied in depth.

Averaging technical replicates considered reliable for each cow, PCA plotting showed a trend towards clustering based on embryo quality, though the low number of samples precluded conclusive interpretations (Figure 4-6).

In summary, a measurable metabolomic fingerprint was achieved by REIMS in both positive and negative ionisation mode; thus, this approach was suitable for the main metabolomic fingerprinting experiment (Exp. M5).

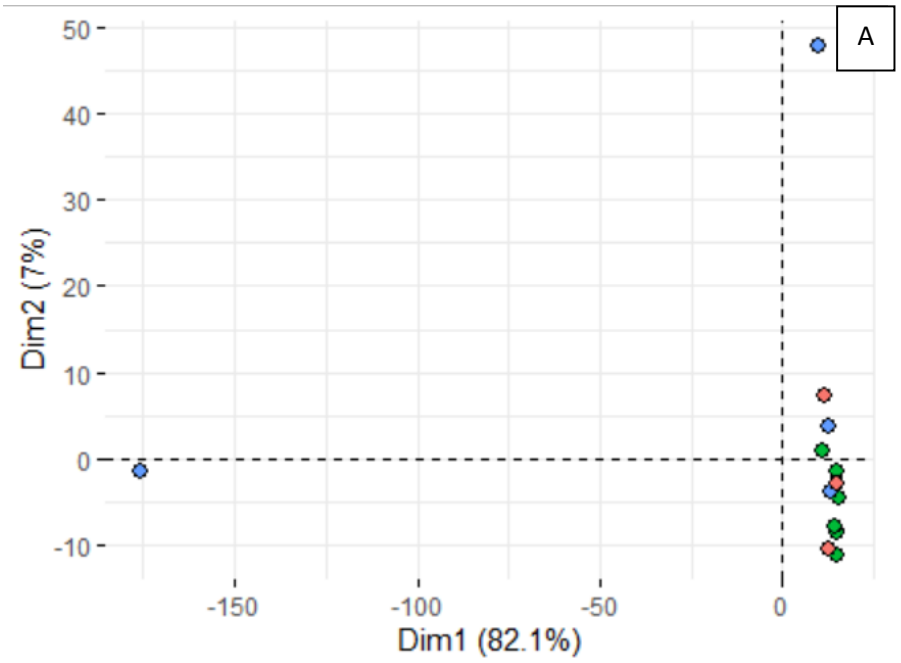

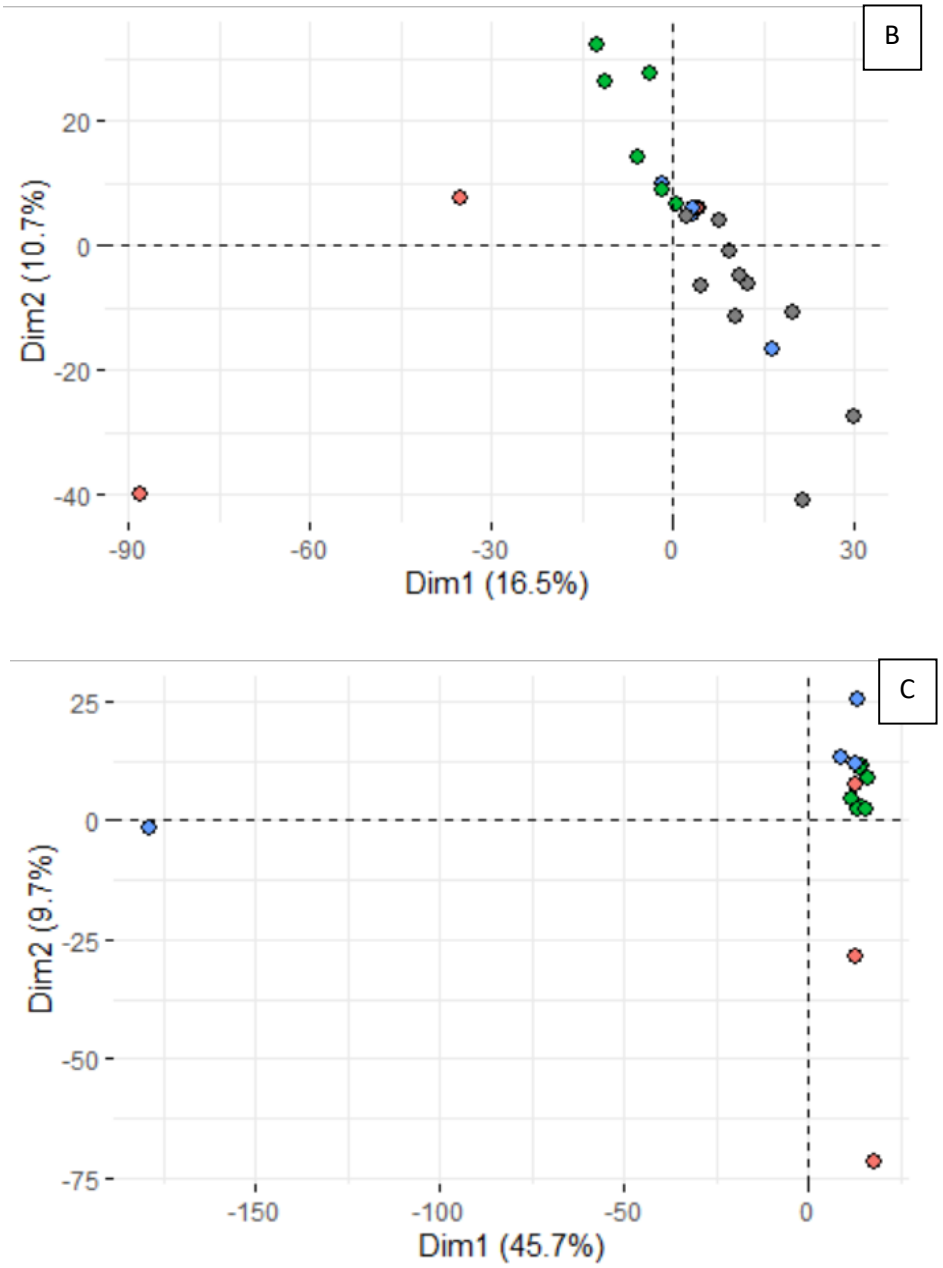

Figure 4-6 REIMS (rapid evaporative ionisation mass spectrometry) reproducibility assessed by PCA. A, positive ionisation mode; B, negative ionisation mode; C: combined. Colours indicate embryo quality: Red, non-viable (1-16 cells); blue, potentially viable (Grade3); green, viable (Grade 1-2).

4.4 Conclusions

Several alternatives were trialled at different steps of the method for broad targeted metabolomic analysis. This process concluded with the choice of filtrate ULF extracted by a biphasic method as the optimal protocol to use in the main experiment in this project. Moreover, the targeted approach assayed was deemed more suitable for this experiment than the untargeted due to the difference in number of compounds identified (Exp. M1). In addition, application of isotope-labelled proline as a

tracer, assayed in Exp. M2, enabled measuring the degree of flushing-induced dilution of ULF across samples. This, as well as the confirmation of the safety of its use, motivated the decision of adding tracer to flushing medium in the main metabolomics experiment (Chapter 6).

Lastly, the untargeted, ambient mass spectrometry approach tested in Exp. M3 was effective at obtaining a metabolic fingerprint of ULF and therefore suitable for measuring the main experimental cohorts in this project (Farm Trials 2 and 3, analysed in Chapter 6).

5

Proteomic analysis

5.1 Introduction

This part of the project aimed to explore relationships between abundance of protein species in bovine uterine luminal fluid (ULF) with embryo phenotypes sampled and with days post-partum or number of oestrus after calving (OC). This investigation was accomplished by liquid chromatography – tandem mass spectrometry (LC-MS/MS)-based molecular analysis of ULF samples collected in Farm Trials 2 and 3 over two years at OC1 and OC3, as explained in Chapter 2.

This chapter is organised as follows. Firstly, presence and degree of blood contamination and technical reproducibility throughout the experiment were assessed. Afterwards, the ULF proteome - as detected in this experiment- was analysed qualitatively by itself and compared with previous studies. This comprised number of proteins identified, functional analysis (Gene Ontology terms and pathways represented), and proteins predicted to be secreted. Next, univariate analysis was carried out to determine differences in the molecular composition of ULF containing embryos of dissimilar quality. Lastly, the dataset was explored by multivariate analyses, firstly unsupervised (PCA) followed by supervised (sPLS-DA and OPLS-DA). The predictive potential of the models created was evaluated by cross-validation.

5.2 Materials and methods

All ULF samples corresponding to the main experiment were prepared according to the optimised protocol as described in section 3.4.6, with the following modifications.

5.2.1 Assessment of blood contamination

A low to moderate degree of tissue damage is a regular occurrence during uterine flushing (Velazquez et al. 2010). This can constitute an issue because, as described in Chapter 1, ULF and blood share a sizable portion of their proteome (Faulkner et al. 2012). Differentiating which biofluid those common proteins originated from is not feasible, and this can severely affect quantitative protein abundance determinations (Helfrich et al. 2020). Blood contamination creates a red tinge caused by the high concentration of haemoglobin and this can be indicative of the degree of blood present in the sample (Guise and Gwazdauskas 1987). In this study, sample colour was assessed visually before spin column filtration according to Martins et al. (2018), a step not undertaken in the preliminary trial as pooled samples were used. Colour was recorded on a scale from 0 (completely

transparent) to 4 (deeply red tinted samples). This classification had the primary purpose of estimating the degree of blood contamination; a second purpose was to appraise the protein concentration of the samples to ensure they were within the detection range of the method, as explained below.

Protein concentration of the retentate (high molecular weight fraction) was determined using DirectDetect® (Merck Millipore, Mairangi Bay, New Zealand) as described by Strug et al. (2014). Samples with a colour score ≥ 2 were diluted 1:10 with distilled water before the measurement to keep readings within the concentration range 0.5-5 mg/ml protein. In this range, there is a linear relationship between infrared absorbance and protein concentration and therefore allows for the most accurate estimates.

5.2.2 Protocol for ULF sample analysis

The full protocol is detailed in section 3.4.6. In short, sample preparation consisted of filtering ULF using 10 kDa cut-off spin-columns, without any denaturing or extraction steps, noting their colour in a scale from 0 to 4. Next, protein concentration was measured using DirectDetect; and then a volume of retentate containing 250 µg of protein was reduced with DTT, alkylated with IAM, and digested with trypsin. The LC programme involved a gradient separation (described fully in chapter 3) between 2% B to 95 % B with a total length of 85 minutes followed by re-equilibration at 2% B.

5.2.3 Experimental design

All samples were prepared and run in a randomised order using the "random" function in MS Excel v.2002 (Microsoft Inc., Build 12527.21330). The LFQ (Label-Free Quantitation) method employed to quantify proteins in the samples followed the specifications of Dong et al. (2020). Briefly, this approach requires two types of information: protein identification (obtained through tandem MS, i.e. MS/MS runs) and protein quantification (single MS runs). Both types of runs were included in each batch. For identification-purposed (MS/MS) analysis, ULF samples were run undiluted to maximise the number of peptide ions detected. This resulted in many peaks reaching the detector's maximum intensity threshold, detrimental for reliable quantification. Thus, when analysed with single MS (i.e. without fragmentation) samples were diluted 1:10 to enable quantification, using PEAKS Studio's functionality to link precursor ions of these runs to those identified in MS/MS runs. The sum of the top-3 peptides for each protein was used to calculate abundance.

Quality control system

Based on the system proposed by Bittremieux et al. (2018), two types of quality control (QC) were carried out as one of the methods to assess the system's performance throughout the experiment.

First, a bovine serum albumin (BSA) standard at a concentration of 5 µM was run twice in each batch as routine so comparisons to historical QC runs in our lab could be made. It was run in a shorter LC programme (28 minutes total time, as described in 3.3.4) to save instrument time. The peak areas of six of the most consistent ions were plotted across time to evaluate the performance of the mass spectrometry system. Table 5-9 shows an example of the sample run list of a batch. Additionally, a pooled QC sample was run in a standard 85 min LC programme (the same as the ULF samples). For this, 20 ULF samples were pooled for a QC pool to be injected in every batch. These pool QC samples were also used for batch correction, as explained later.

Table 5-9 Run order in a batch (example). Green: ULF test samples - quantitation. Pink: ULF samples – protein identification. Purple: ULF pooled sample (control). Blue: BSA standard (control). Grey: blank.

Sample	Type
1160 1.18	ULF sample (MS)
1026 3.17	ULF sample (MS)
1118 3.18	ULF sample (MS)
1118 3.18	ULF sample (MS)
1167 3.18	ULF sample (MS)
BSA	QC_A (MS/MS)
2020 3.18	ULF sample (MS)
1105 3.18	ULF sample (MS)
1114 3.18	ULF sample (MS)
1165 1.18	ULF sample (MS)
Pool	QC_B (MS/MS)
1116 1.18	ULF sample (MS/MS)
BSA	QC_A (MS/MS)
Column clean	Blank (MS/MS)

5.2.4 Informatic and statistical analysis

PEAKS studio using Uniprot was used for protein identification and LFQ, specifically by using the PEAKS PTM algorithm. Batch correction was applied using the QC-RFSC (Quality Control Random

Forests Signal Correction) algorithm choosing the LOESS (Locally Estimated Scatterplot Smoothing) method in the W4M Galaxy web-based tool (Dunn et al. 2011).

Univariate analysis

Embryo classification was performed as detailed in Chapter 2. Then, to determine differentially abundant proteins between groups, protein abundance measured in arbitrary units was firstly square-root transformed, to correct for pronounced right-skewness, i.e. distributions where the mean is to the right of the median, with many zero values.

Then, differences in molecules' abundance in ULF between embryo classes (EQ1-3) or oestrus after calving (OC) were assessed either by ANOVA or Kruskal-Wallis non-parametric test (for variables that did not satisfy the criteria of distribution normality and/or homogeneity of variance), and linear regression to test for the effect of dpp. All statistical tests were performed using the R base package v4.0.2 (R Team 2019), using a 5% false discovery rate (FDR) to correct for multiple testing (Benjamini and Hochberg 1995), and this was expressed as "q-value". To determine which groups were different, Tukey test (parametric) was performed using R *base* package, or Dunn test (non-parametric) was done using the package *pgirmess* 1.6.9 (Giraudoux et al. 2018).

Proteins detected - comparisons with other studies

Results from ten articles on untargeted proteomic investigation were collected. As different protein nomenclature systems were used across the relevant studies, the identifiers were converted to Uniprot accession numbers using DAVID v. 6.8, updated May 2016 (Huang et al. 2009). Uniprot identifiers were considered unique proteins for the purpose of this comparison. Protein name conversion resulted in 2.3% of the proteins not being mapped (165/7168).

Secreted protein analysis

This analysis was performed according to Pillai et al. (2017). Firstly, SignalP v5.0 (http://www.cbs.dtu.dk/services/SignalP) (Almagro Armenteros et al. 2019b) was used to predict which proteins identified were potentially secreted via the classical secretory pathway, by identifying N-terminal motifs that direct proteins for secretion. In parallel, Outcyte v1.0 (Zhao et al. 2019) was employed to predict proteins secreted by non-classical pathways. Next, TargetP v2.0 (www.cbs.dtu.dk/services/TargetP) was used to exclude mitochondria-bound proteins (Almagro Armenteros et al. 2019a), with further refinement through Phobius (http://phobius.sbc.su.se/) (Käll et al. 2004, 2007) to remove membrane proteins (i.e. those with transmembrane regions) and potentially expand the list of secreted proteins.

Functional and pathway analysis

Functional and gene ontology (GO) analyses were performed using GO::TermFinder (Boyle et al. 2004) concomitantly with the REVIGO visualisation tool (Supek et al. 2011). Metascape (updated 16/09/2020; Zhou et al. 2019) was used for overrepresentation analysis. These tools are diverse in their scope, update frequency, and algorithm used.

Multivariate analysis

Multivariate analyses and modelling (PCA, sPLS-DA, and OPLS-DA) were conducted using MetaboAnalyst v4.0 and R, packages *mixOmics* v4.0 (Rohart et al. 2017) and *ropls* v3.8 (Thévenot et al. 2015). Predictive performance was assessed by 10-fold cross-validation. In this process the original dataset is divided in 10 subsets at random and models are subsequently fit to 9 of those and tested on the subset left out, in turn. The performances of all the models thus produced are averaged and indicated by a EQ2 value that goes from 1 (perfect predictive performance) to 0 and negative, i.e. no predictive use or overfit (Worley and Powers 2013).

5.3 Results and discussion

5.3.1 Blood contamination

There was a statistically significant positive relationship between colour and protein concentration (R^2 = 0.28, $p<0.001$). Additionally, after visual assessment, 11 samples (out of 189) were considered contaminated with blood (colour code ≥2.5). These samples, on average, were of a slightly smaller volume compared to clear ULF samples at 14.56 ml, whereas the average of transparent samples was 17.69 ml. However, no statistically significant relationship was observed between ULF volume of samples and colour by linear regression analysis ($p>0.3$). In this regard, it was hypothesised that rough flushing might have both hindered sampling medium recovery and caused haemorrhages. However, only five samples had especially low volumes recovered (under 8 ml); all other red samples were recovered at volumes near average. This complicates appraising the degree to which an abnormally shaped uterus hampers flushing and causes injuries and haemorrhages. Nonetheless, since it is not possible to determine whether the proteins and metabolites detected in these samples originated in ULF or blood, those 11 samples were removed from further analysis.

5.3.2 Quality control assessment

The batch correction method employed considers intensity differences in each of the peptides to adjust for systematic error. For this, a LOESS (Locally Estimated Scatterplot Smoothing) regression model was fitted to the intensity values of the peptides in the pool QC samples. This method fits simple models to segments of the data, building a function that describes trends in the variation

across samples and generates a smooth curve through the sample set (Cleveland and Devlin 1988). In this case, the median intensity of peptides in the pool samples was taken as the scaling factor.

Pooled QC samples – chromatography and MS quality control

Figure 5-4 shows an example of the QC chromatograms overlaid. Most of the relevant features stayed within the set 2 min Rt tolerance set. No clear trend in overall intensity changes was observed (Figure 5-4). Overall, good reproducibility was observed throughout the instrumental analysis, that lasted for 25 days of continuous LC-MS/MS runs.

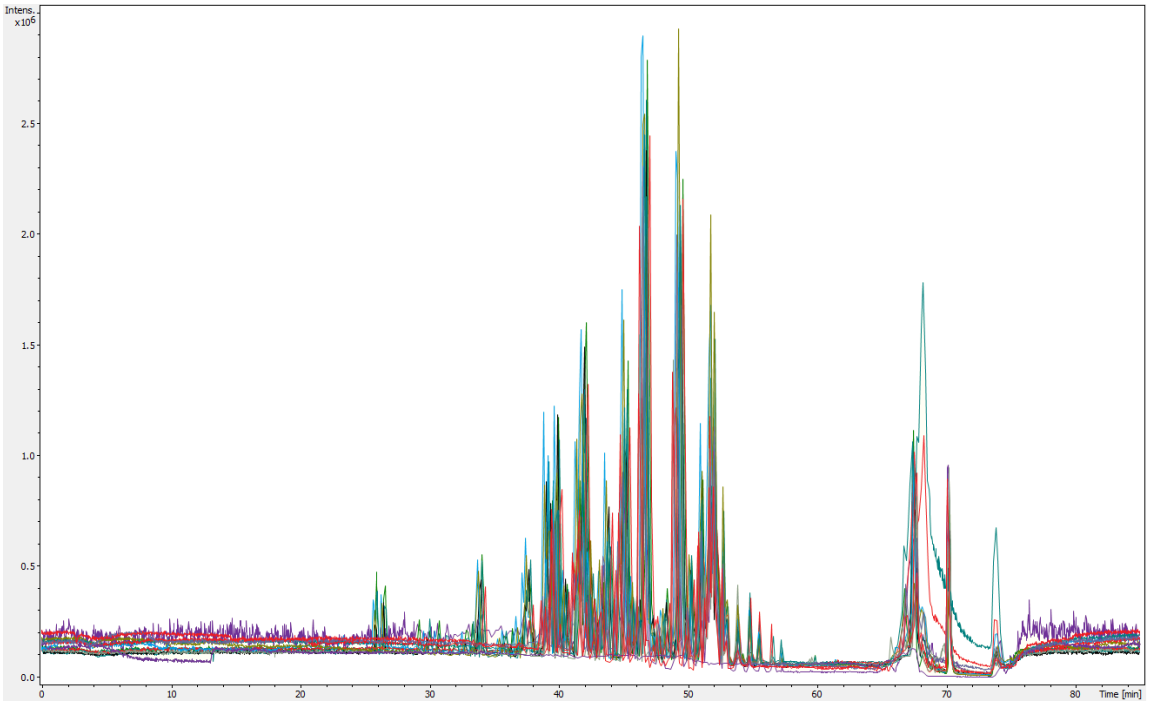

Figure 5-4 Total ion chromatograms corresponding to QC pooled samples diluted 1:10 in Experiment P3. N=20 runs.

Bovine serum albumin (BSA): MS quality control

As an additional method of quality control, BSA standards were run using a short LC programme (28 min, details in 3.4.4) at the end of every batch. The shape of the chromatogram and the sequence coverage of the peptides detected were evaluated on the spot to determine whether the instrument was performing adequately or whether it required tuning.

Sequence coverage average were similar throughout the experiment, with an even spread on either side of the mean (Figure 5-5). This was one indication that instrument performance remained within acceptable boundaries throughout the experiment. There was a slight tendency to decrease, likely indicative of the normal wearing of the pre-column. According to standard practice in this research group, coverage values under 70%, or two under 75% in succession, indicate that a long step of column clean (i.e. running a blank to remove peptides and residues from the column) or tuning is necessary.

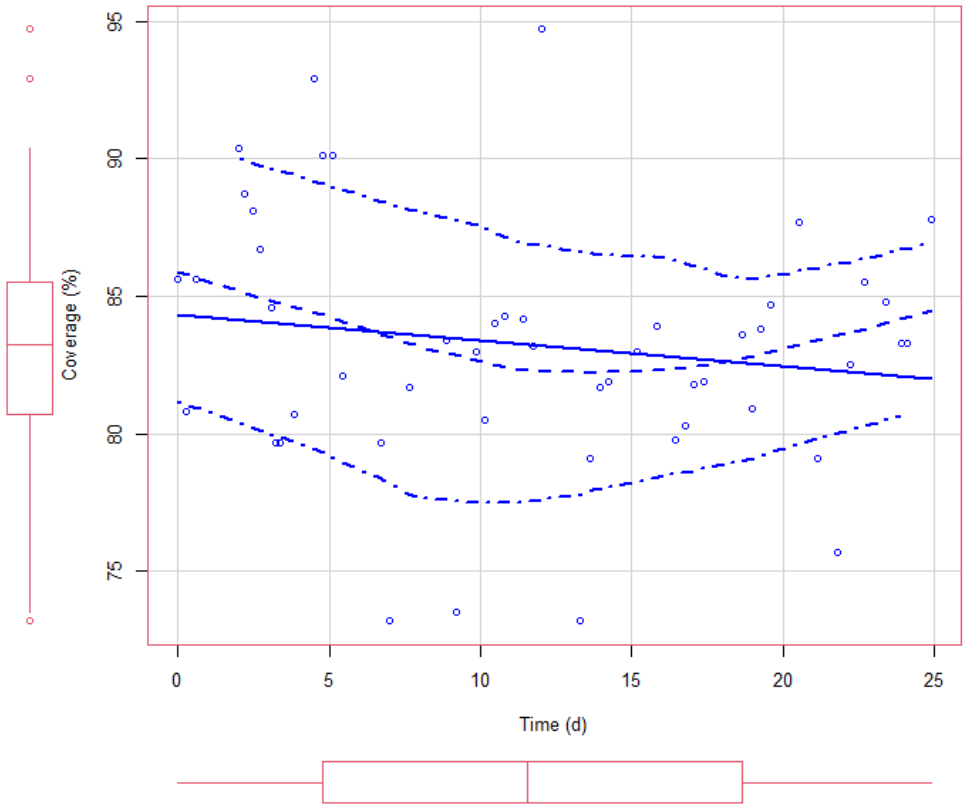

Figure 5-5 Peptide sequence coverage of bovine serum albumin (BSA) standard, as obtained from a Mascot peptide web search, throughout the experiment. Time in days. Solid line: linear regression; dashed line: LOESS (locally estimated scatterplot smoothing) non-linear polynomic regression; dash-dotted line: smoothed conditional spread (LOESS line fitted to values below and above the mean regression line).

5.3.3 Protein identification and ULF proteome meta-analysis

Informatic analysis of all samples resulted in a total of 1504 proteins detected in this experiment, of which 1173 could be quantified. To put these findings in context, a list was compiled of proteins reported in studies surveyed characterising the bovine ULF proteome as described in the Introduction (Table 5-). This list comprised eleven articles in addition to the present study. The number of proteins reported per study ranged from 37 to over 3300; this was related to differences in confidence parameters employed as well as technical capabilities. For example, while most studies provided the total list of proteins identified, some reported only proteins statistically different between groups (Muñoz et al. 2012, Beltman et al. 2014). Moreover, in addition to the significance score assigned by the proteomics software, Beltman et al. (2014) further filtered peptides manually, considering only those containing ion series of at least 4 amino acid residues. Regarding technical capabilities, the performance of tools used in virtually all stages of proteomic analysis is in constant improvement, and this is a notable determinant of the amount and quality of the information collected, including reported protein quantity and reliability (Lössl et al. 2016).

This study included a larger number of animals than previous studies of a similar type. The number of animals and total samples analysed per study in the literature averaged 18, ranging from 6 (Beltman et al. 2014) to 25 (Moraes et al. 2020a, Moraes et al. 2020b), compared to 92 in the present study. The median number of samples analysed -i.e. because animals were analysed at more than one time point in some studies, e.g. (Mullen et al. 2012, Muñoz et al. 2012, Forde et al. 2014a)- was 33, ranging from n=6 for Muñoz et al. (2012), Beltman et al. (2014), to n=64 in the previous studies, whereas n=184 was used in the present study. Notably, some studies sampling a reduced number of animals used longer LC separation programmes (Helfrich et al. 2020, Moraes et al. 2020a), and this is conducive to a higher number of distinct peptides being detected (Moraes et al. 2020a). The large number of samples analysed in this research implied finding a compromise between peptide detection (depth) and number of samples run (width). However, the analysis resulted in a considerable number of proteins reported at 1504 even with shorter run times because of the higher number of samples.

Next, shared and unique proteins were assessed. A total of 6914 proteins (Uniprot knowledgebase entries) were surveyed. Only 66 proteins were present in more than 50% of the studies, i.e. at least in six out of the 11 studies (Table S5-1). In addition, 4426 entries were detected in only one study, and no protein was identified in more than eight studies out of the eleven surveyed. For illustrative purposes, Figure 5-6 shows the overlap in identified proteins across the four studies that reported the highest number of proteins identified, including the current work. In this case it is perhaps clearer that these recent studies have all identified a similar number of unique proteins, and that the proteins detected in more than one study are evenly spread throughout, i.e. there are no outlier studies. Proteins reported by the four most comprehensive represent a “core” proteomic signature of bovine ULF, constituted by the most consistently abundant proteins (Table S5-1).

As discussed in Chapter 1, several factors likely underlie these findings. Some are differences in animals sampled (including breed), sampling method (and associated contamination with cellular debris and/or blood), and sample processing. It is appropriate to compare these 11 studies as in all studies, mass spectrometry was performed in DDA (data-dependent acquisition) mode. The stochastic nature of the precursor selection favours fragmentation and analysis of the most abundant peptides and entails under-sampling of peptides with low and medium abundance (Liu et al. 2004). Wider application of the most advanced DIA (data-independent acquisition) setups will most certainly contribute to increasing inter-experimental reproducibility (Doerr 2015). The author is not aware of any reported experiments employing DIA to investigate the ULF proteome, and such a platform was not available for this project.

From the 1504 proteins (Uniprot entries) identified in this study, 472 had not been reported in bovine ULF by the surveyed articles; moreover, 43 were Swissprot manually curated entries (Table S5-2). The full list of proteins detected in this and other studies can be found in Table S5.3. This contributes to advancing the characterisation of the total protein complement of the bovine ULF. Next, a qualitative exploration of the ULF proteome was undertaken.

5.3.4 Protein functional analysis of ULF

The full set of proteins detected in the present study were analysed using Go::TermFinder, assessing their relative representation across ontology categories. As expected from any given tissue or biofluid, a wide variety of molecular functions and biological processes was observed (Figure A-8-898a,b,c).

Table 5-2 Number of proteins reported in studies surveying the bovine ULF proteome. Number of Animals (samples): number between brackets indicates the number of samples analysed when animals were sampled more than once.

Study	Proteins reported	Unique to the study	Animals N (samples)
Munoz et al. 2012	39	5	8 (16)
Beltman et al. 2014	40	4	6
Faulkner et al. 2013	89	-	20
Faulkner et al. 2012	197	16	6
Forde et al. 2015	242	26	8
Mullen et al. 2012	702	492	18 (36)
Moraes et al. 2020	776	73	25
Forde et al. 2014	887	414	16 (64)
Gegenfurtner et al. 2020	1737	391	12
Helfrich et al. 2020	2648	916	5
Harlow et al. 2018	3316	1690	16
Present study	1504	472	92 (184)
Total	7003	4499	-

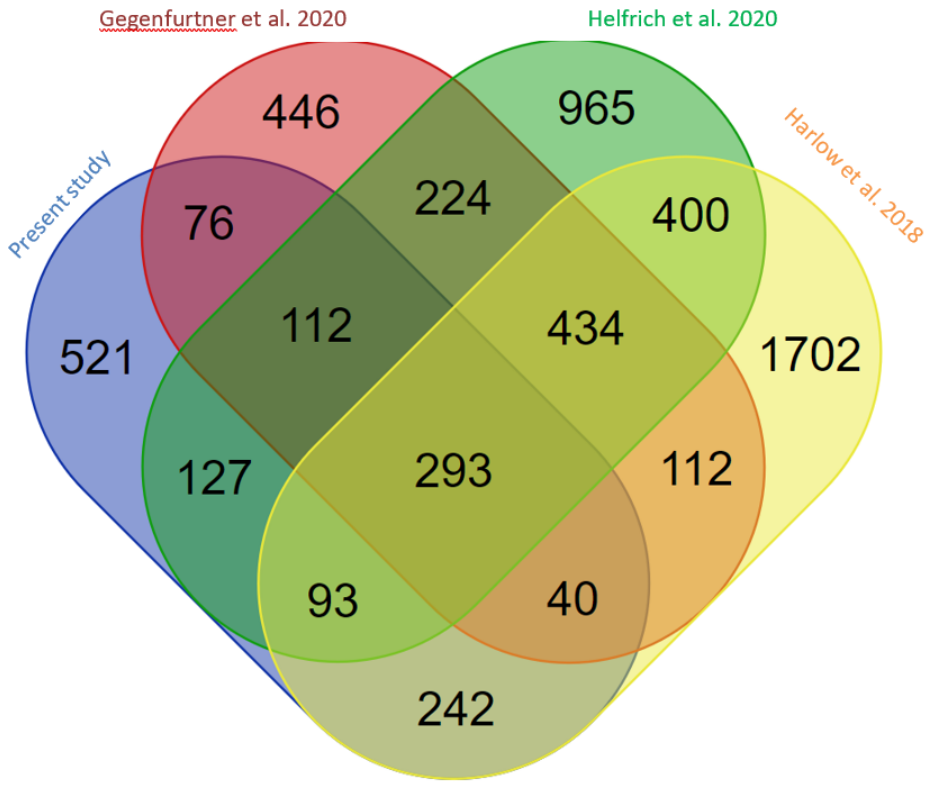

Figure 5-6 Venn diagram showing proteins reported in the four studies with the highest number of proteins reported. A protein was considered a unique Uniprot accession identifier.

GO molecular function showed that 41% of the proteins are classified as "binding proteins" and 35% as having "catalytic activity"; less represented functions included "molecular function regulator" (6%), "structural molecule molecular transducer activity" (4%), "transcription regulator activity" (2%), "transporter activity" (1.5%) and "molecular transducer activity" (0.5%). By the very nature of this type of analysis, these terms are very general; for instance, "binding proteins" are defined as "proteins that interact selectively with any protein or protein complex", whereas "catalytic activity" refers to all enzymes. These will be discussed considering the specific classes and pathways defined next. Regarding GO cellular processes, no dominant class was found. The most prevalent classes were metabolic proteins (21%) and regulators (18%). "Response to stress" and "immune system processes" accounted for 7% and 1% of the proteins, respectively. Based on the findings of the review article conducted as part of this project (Aranciaga et al. 2020) a larger proportion of proteins involved in these processes was expected, due to their fundamental roles in the physiology of the reproductive tract. However, it is important to bear in mind that the number of proteins of a given class does not correlate to its class's biological importance (Pascovici et al. 2012). This classification provides an overview of two aspects of the molecular activity within ULF. To examine the roles of these processes in the physiology of postpartum recovery and embryo development, the specific functions of relevant molecules and classes are discussed later.

Finally, GO cellular component classification showed that 62% of the proteins are annotated as "cytosolic", whereas 9% were classed as "membrane proteins" and 14% as "extracellular proteins". The implications of a high proportion of proteins in an extracellular fluid being classified as (intra)cellular are examined next.

Protein origin and cellular location

Proteins detected in a biofluid would typically be expected to be secreted; the results of the gene ontology classification however do not support this. Nonetheless, this is not at odds with similar studies that identified a similarly low proportion of typically extracellular proteins, in ULF (Forde et al. 2014a; 20%, Gegenfurtner et al. 2019a; 14%) and oviduct fluid (Lamy et al. 2016a; 28%). Some important considerations are examined next.

The question of the origin of a protein is intimately related to its function. Distinguishing physiologically relevant compounds from those that are present as a by-product of an unrelated process is key for this research. As reviewed in Chapter 1, the contents of fluids in the reproductive tract (including proteins) originate from several sources. These consist of cellular debris due to physiological processes (Mondéjar et al. 2012), sampling-introduced artefacts (Papp et al. 2019), as well as molecules secreted by uterine cells, both expressed by those cells (Roberts and Bazer 1988) or originating from blood transfer (McRae 1988). Many of those proteins considered secreted go through the classical secretory pathway, i.e. containing a signal peptide to the endoplasmic reticulum for further processing and extracellular secretion, known as the *Sec* signal peptide (von Heijne 1990). Others are believed to be transported by alternative and potentially undescribed mechanisms (Gegenfurtner et al. 2019a). One such alternative mechanism might be exosomes (small membrane-bound vesicles of endocytic origin): Almiñana et al. (2017) posit that exosomes play a key role in oviduct-embryo communication. Supporting this are the reports of Passaro et al. (2016) and Harlow et al. (2018) that over half of the proteins detected in ULF were categorised as exosomal according to Gene Ontology. Analysis of secreted proteins by a set of specialised informatic tools was carried out to formulate hypotheses regarding their relative importance and function.

Secreted protein analysis

A total of 1115 proteins were used in four informatic tools, namely SignalP, TargetP, Phobius, and Outcyte. The algorithms they use are optimised for different uses, however they all have a function to predict secretion via the classical secretion pathway, via Golgi apparatus and granular endoplasmic reticule; these contain signal peptides known as *Sec*, typically characterised by a 5-16 sequence of hydrophobic amino acids (von Heijne 1990). Altogether, 408 proteins were predicted to be secreted by at least one of the tools, out of which 224 contained a *Sec* signal peptide (SP) and 184 were identified by other, alternative means ("Outcyte unconventional secretion"). There was a significant

overlap between proteins classified as secreted with *Sec* signal peptide by the different tools (Table 5-310 and Figure 5-7). SignalP is considered the most reliable tool for this determination because it is optimised for identification of signal peptide and its location within the protein sequence (list in Table S5-4); therefore, those identified by SignalP plus those identified by at least two other tools were considered secreted for functional analyses next.

Proteins predicted to belong in other cellular locations (transmembrane, translocating to mitochondria, intracellular) were all considered equal for the purpose of the present work; i.e., they were not expected in the extracellular space but were detected in ULF. Additionally, tools whose main purpose is not related to identifying putatively secreted proteins (particularly Phobius) indeed identified the least putatively secreted proteins (but none was unique to it).

The results of this analysis are useful in themselves for their contribution to a deeper characterisation of the ULF proteome, and were also considered to select molecules to test on *in vitro* embryo culture as examined after.

Table 5-310 Proteins classified as secreted by different bioinformatic tools. Secreted-SP: secreted by the classical secretion pathway, i.e. containing a *Sec* signalling peptide.

List names	number of distinct elements	Unique to one tool
OutCyte (unconventional)	223	184
Outcyte (secreted-SP)	56	8
Phobius (secreted-SP)	179	0
SignalP (secreted-SP)	209	26
TargetP (secreted-SP)	184	2
Overall number of unique elements	**408**	**220**

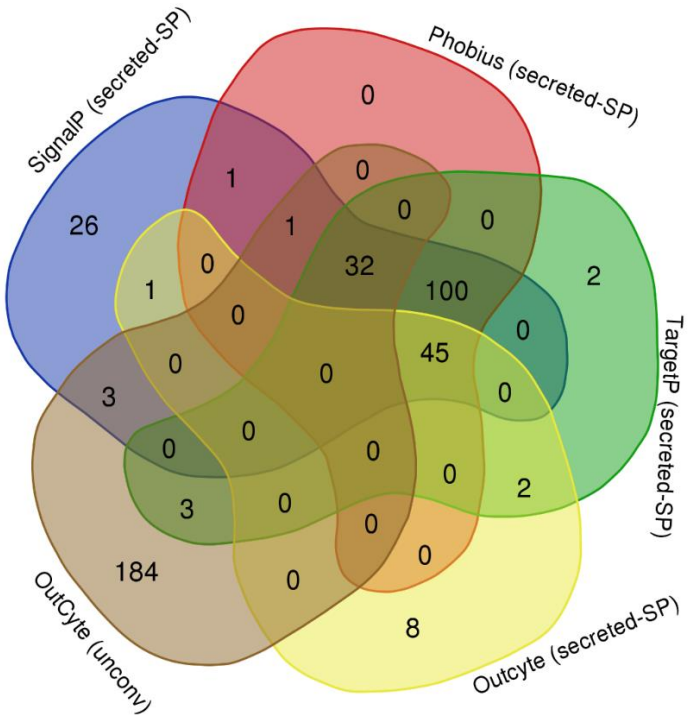

Figure 5-7 Venn diagram showing number of proteins classified as secreted by different informatic tools.

5.3.5 Molecular factors determining embryo quality

Further to assessing molecular differences in ULF related to embryo quality, differences between oestrus cycles were considered. As seen in Chapter 2, the proportion of cows with embryos of excellent and good quality was higher for pregnancies in the third oestrus event after calving, in agreement with (Berg et al. 2017) who showed improved fertility outcome with more oestrus cycles after calving. It is therefore relevant to factor in oestrus number when examining the relationship between embryo quality and molecule abundance, and as an independent metric of animal health.

Embryo quality, dpp and OAC - Univariate analysis

Protein abundance (measured as the sum of the areas of the top-3 peptides of each protein, batch-corrected and square-root transformed) of proteins detected in more than 50% of the samples was evaluated by either ANOVA and Tukey tests, or Kruskal-Wallis and Dunn test for proteins that did not satisfy the assumptions for parametric tests. Applying a data transformation to the molecule abundance data improves the likelihood of it fitting the assumptions for parametric tests (Osborne 2010). Even in the case of some of the transformed features which do not conform to the normality of residues and homoscedasticity assumptions for parametric tests, this type of data transformation tends to increase the statistical power of non-parametric tests (Osborne 2010). In this case, the skewness of the raw data (median 1.29, mean 1.64) was reduced substantially after square-root transformation (median 0.098, mean 0.22, where 0 represents no skewness or a Gaussian

distribution). In addition, even after data transformation, the standard deviations were relatively large (relative standard deviation of 35%, on average), illustrating the high amount of within-class variation.

From the quantifiable proteins, a total of 388 proteins were protein group replicates, i.e. in which the peptides quantified to estimate the protein's abundance were the same as in one or more other proteins. Protein replicates included both strictly replicate entries, considered essentially the same protein but found as additional entries in the Trembl database, as well as homologues sharing most of their primary sequence (>50%; Pearson 2013). For the purpose of statistical analysis, these are replicates and testing those individually has no practical advantage and results in decreased statistical power. Therefore, only the top hit in each protein group was analysed by ANOVA; this resulted in a dataset of 653 proteins.

Number of oestrus cycles after calving (OAC) and days postpartum (dpp)

Firstly, the effect of dpp on protein abundance was examined by linear regression, using OC as a covariate. No protein was found to be significantly affected by dpp (Table S5-5). A trend for interaction effects of dpp and OC (q=0.065) was found for one uncharacterised protein, however upon examination of the scatterplot this was caused by an outlier. Thus, it did not present high potential for practical applications and was not pursued further.

Table 5-411 Proteins in significantly higher abundance in third vs first oestrus postpartum. Abbreviations: FC, fold change; OAC, oestrus after calving; q-value, false discovery rate according to Benjamini and Hochberg (1995).

Protein	Gene	p-value	q-value	Trend	FC
Peroxyredoxyn 5	PRDX5	0.011	0.035	OAC3>OAC1	1.56
Haemopexin	HPX	0.007	0.048	OAC3>OAC1	1.38

Two proteins were found to be in significantly higher abundance in ULF at OC3 compared to OC1: peroxiredoxin 5 and haemopexin (Table 5-411). Peroxiredoxins are proteins typically found in mitochondria and peroxisomes, and fulfil signalling and protective functions related to reactive oxygen species, particularly hydrogen peroxide (Chae et al. 1994). They are proposed to play important roles in embryo development by regulating the redox balance of the embryo cells, together with other enzymes such as dehydrogenases, catalases (Guerin et al. 2001). Peroxiredoxin 5 expression has been reported from the immature bovine oocyte to after the 16 cell stage embryo (Leyens et al. 2004). Here it was found in higher abundance in OC3 (p=0.011). Despite being classified as intracellular, this protein

was also found in ULF of both cycling (Harlow et al. 2018, Helfrich et al. 2020) and pregnant (Forde et al. 2015) cows.

Haemopexin is a protein known for binding haem molecules and transporting them to the liver for its clearance (Tolosano and Altruda 2002). It is also known as an acute-response protein, i.e. whose synthesis is induced following an inflammatory event (Baumann and Gauldie 1994). This protein was found in ULF of cycling animals of Holstein and Montebeliarde breeds (Gegenfurtner et al. 2019b) and was reported to be downregulated from day 0 to day 35 of pregnancy (Rawat et al. 2016). Faulkner et al. (2012) found haemopexin to be in half the abundance in ULF compared to blood plasma. It is not clear however why this protein was higher at OC3 in this experiment, when postpartum inflammation is assumed to have diminished. The putative role of these proteins is further discussed later in the context of molecular changes relative to embryo quality.

To expand on the molecular changes in the postpartum ULF, a comprehensive analysis of differences across oestrus cycles after calving is presented in Chapter 6 using joint pathway analysis.

Protein abundance effect on embryo quality phenotype

The proteins found differentially expressed by ANOVA (parametric) or Kruskal-Wallis (non-parametric) were classified in positive or negative according to which groups were different as determined by Tukey (parametric) or Dunn (non-parametric) tests. Results of univariate statistical analyses, along with what differences between groups are displayed in Table 5-5 (EQ1 system) and Table 5- (EQ2, EQ3). The groups were detailed earlier (Figure 2-4). Briefly, the EQ1 system considered 5 embryo classes (Roman numerals I to V) in decreasing order of quality: I-III correspond to grade 1-3 tight morulae and blastocysts, respectively. IV and V designate embryos in arrested development (4-16 cell), and one-cell (possible fertilisation failure), respectively. The EQ2 system contrasts “Optimal” (class I) with “Suboptimal” (grouping classes III-V), whereas the EQ3 classification contrasts “Pregnant” (grouping classes I-III) with “Non-pregnant” (grouping classes IV and V). A total of 18 proteins were found in differential abundance between ULF holding embryos of contrasting quality, as discussed next.

Proteins negatively associated with embryo quality

This section discusses the 11 proteins found to be upregulated in ULF with poorer quality embryos (chiefly class IV) according to the EQ1 classification system explained earlier, and how these proteins relate to fertility in the context of literature.

Dihydropteridine reductase (DHPR) was found in the highest abundance in class IV embryos of 4-16 cells. This is an enzyme that produces tetrahydrobiopterin (BH-4), an essential cofactor for phenylalanine, tyrosine, and tryptophan hydroxylases; it is also involved in folate biosynthesis

(Varughese et al. 1992). In human, deficiency of DHPR due to recessive mutations manifests in many diseases, the most conspicuous of which is phenylketonuria (Blau 2016). Pregnancies of human mothers with phenylketonuria present several problems including spontaneous abortion and intrauterine growth retardation (Rouse et al. 1997). In a human kidney cell line, wild-type DHPR played an important role in protecting the cells against oxidative stress, but mutant DHPR failed to have these beneficial effects (Gu et al. 2017). Rodríguez-Alonso et al. (2020a) found DHPR to be more abundant in oviduct fluid of pregnant vs cycling cows, i.e. opposite to what was found here, though the spatial (oviduct vs uterus) and temporal (day 3 vs day 7) conditions tested were different.

Two proteins from one protein family, cystatin B and C, were found in highest abundance in class IV (4-16 cell) embryos. Upon examination of the peptide sequences identified, all of them were common to both proteins, i.e. no peptide fragment unique to either was detected (Figure A-8-6). This is a common occurrence in the proteomics field, in which a protein family is reported instead of a protein, due to the lack of means to establish which variant or variants were detected (Miller et al. 2019). Cystatins are a family of cysteine protease inhibitors found in most eukaryotes and many prokaryotes (Kordiš and Turk 2009). Both cystatins B and C are involved in multiple processes through interaction with and regulation of cathepsins (Kos et al. 2014), some of the most prominent being bone remodelling, inflammation, and cancer aetiology (Abrahamson et al. 2003). It is precisely the cathepsin-cystatin interplay that is often investigated. Cystatin B mRNA was found downregulated in oestrogen-receptor-knockout mice (Winuthayanon et al. 2015), showing a positive association with a healthy reproductive function. It was also found in day 16 and 19 of pregnant bovine ULF and in the secretome of day 16 embryos *in vitro*, but not found at days 10 or 13 of pregnancy, or in cyclic animals (Forde et al. 2015). The different timepoints analysed preclude a direct comparison to the results in this study, but further research into the role of cystatin B is promising.

Cystatin C is produced by nearly all organs and is found in biological fluids, including blood; it is also the most abundant and potent endogenous inhibitor of cathepsins (Lafarge et al. 2010). Cystatin C is the main cathepsin inhibitor regulated in tissue remodelling events (Lerner and Grubb 1992) and chronic inflammatory diseases (Henskens et al. 1994). The interplay between cathepsin B and cystatin C, its main inhibitor *in vivo*, determines several processes related to pregnancy (Afonso et al. 1997). One of those processes is immune status regulation (Høglund et al. 2019), a major factor in pregnancy establishment that can result in maternal rejection of the partially allogenic embryo (Ott 2019). Another important process governed by the interaction of cathepsin B and cystatin C is tissue remodelling (Kos et al. 2014). This is relevant in this context due to the significant and rapid morphological changes within the reproductive tract in the female to allow for pregnancy. Indeed, anomalous patterns of cathepsin B and cystatin C abundance were responsible for failed

implantation in mice (Afonso et al. 1997). Another study in murine (Baston-Buest et al. 2010) showed that the embryonic expression of cystatin C is involved in apoptotic protection against cathepsins released during implantation, and that higher expression of cystatin C during metestrus might also indicate a signal from the cow that its proliferative endometrium is not ready to bear an embryo.

Whether the difference in abundance observed was for cystatin B, cystatin C, or both is up for discussion. Gegenfurtner et al. (2019b) found cystatin B in all OLF samples but cystatin C only in some of them. Moraes et al. (2020a) found cystatin B but not C-); Malo Estepa (2020) found both B and C in culture medium of day-16 embryos (i.e. secreted by embryo). Helfrich 2020 found both cystatins in at least 5 out of 6 animals. An important source of insight was the secreted protein analysis described earlier in this chapter: cystatin C but no other proteins in the cystatin group were classified as putatively secreted -through non-conventional mechanisms- by OutCyte, concurring with the report of Huh et al. (1995) in mice.

Acyl-CoA-binding protein (ACBP or DBI) was found in higher abundance in class IV embryos (4-16 cells) vs class II and III embryos and has been reported as a crucial factor in early pregnancy in mice, as DBI-knockout embryos do not develop past the 32-cell stage (Landrock et al. 2010). It was also reported by Berendt et al. (2005) to be 7.3-fold more abundant in pregnant uterine tissue compared to cyclic, at day 18 of pregnancy or oestrus. No evidence of a negative effect of this protein was found, but its potential role in energy supply to the embryo is examined in its pathway context later.

S100A2 functions as a calcium sensor and modulator, contributing to cellular calcium signalling and interacting with other proteins, thus indirectly play a role in many physiological processes (Rust et al. 2000). S100 proteins tend to be overexpressed in disease, mediating inflammation and with antimicrobial activity (Lukanidin and Sleeman 2012) and are known to be induced by progesterone(Moraes et al. 2018b). S100A8 and S100A9 were found to be higher in cyclic day 7 UF compared to day 13 and may modulate maternal immune function. S100A4 exhibited the opposite trend (Mullen et al. 2012) and was suggested to be detrimental to embryo development at day 7 of pregnancy by an altered balance between pro-and anti-inflammatory processes (Beltman et al. 2014). S100A2 transcription was upregulated in pregnant animals, deemed to be important in inflammatory regulation (Moraes et al. 2018a). Again, the reason for this protein to be higher abundance in ULF holding embryos of suboptimal quality is likely to be the result of a compensation mechanism against an undetermined detrimental factor.

Unc-80-homolog, NALCN channel complex subunit (UNC80) is a membrane protein found in higher abundance in class IV embryos compared to all the rest. No reports of this protein were found in studies examining the proteome of ULF in any mammal. Its transcript RNA, however, has been reported in 9 different tissues in cows according to the Bgee database of mammal transcriptomics

(Bastian et al. 2020), including sperm, nervous system and muscle. Mutations in its human homolog cause infantile hypotonia, a condition characterised by intrauterine growth retardation and frequently foetal death (Perez et al. 2016). Being a membrane protein, it is unlikely to be present in ULF due to active secretion. Nonetheless, whether UNC80 was detected in ULF in this study due to biological phenomena (i.e. apoptosis) or because of disturbances during sampling necessitates targeted research.

ATP synthase subunit beta is part of a mitochondrial enzymatic complex that produces ATP (adenosine triphosphate, the main energy token in cells across all domains of life) by leveraging potential energy from a transmembrane gradient (Mulkidjanian et al. 2009). It was found in higher abundance in retained placenta compared to normal placenta in cows (Ner-Kluza et al. 2019), but its function in this context is largely unknown except for its involvement in anabolism, as detailed in the pathway analysis section later.

Macrophage migration inhibitory factor (MIF) is a well-characterised protein with regulatory capacity in immune response and inflammation (Baugh and Bucala 2002), and regulated by interferons in sheep (Satterfield et al. 2009). It was reported to be upregulated in bovine pregnancy with a suggested regulatory role in vascular development of extraembryonic tissues from at least day 18 of pregnancy (Paulesu et al. 2012). Forde et al. (2015) found MIF in similar abundance in ULF of cyclic and pregnant cows at days 10-19 of the cycle or pregnancy, whereas Gegenfurtner et al. (2019b) found it in higher abundance in OLF of dairy cows with low breeding value for fertility, i.e. of low genetic potential for reproductive performance (Pryce et al. 2004); further studies are needed to verify the potential of MIF as a genetic fertility biomarker. This is a central molecule in the myeloid activation pathway, as explained in the next section.

Pyruvate kinase M2 (PKM2) was first characterised with regards to its function in glycolysis, i.e. as a rate-limiting enzyme synthesising pyruvate from G3P (Tanaka et al. 1967). There are four pyruvate kinase isoenzymes in mammals, which are L, R, M1 and M2. The L and R isozymes are generated from the PKLR by differential splicing of RNA; the M1 and M2 forms are produced from the PKM gene by differential splicing (Takenaka et al. 1996). L isoenzyme (PKL) is mainly found in the liver, R isoenzyme (PKR) is mainly found in red blood cells, M1 isoenzyme (PKM1) is mainly found in heart, muscle and brain. The M2 isoenzyme (PKM2) is present in most adult human tissues, but is detectable only in early foetal tissues as well as in most cancer cells, upregulated as part of a mechanism of protection against cancer proliferation (Steták et al. 2007). Originally believed to be nuclear, it has also been annotated as cytosolic, secreted and exosomal (Luo and Semenza 2012), rendering it an interesting candidate for biomarker discovery. It is also possible that its higher abundance in ULF, as found in this study, might indicate an abnormally increased metabolism and that this is detrimental at the

pathway level. Most importantly, PKM2 is suggested to be a gatekeeper of cellular growth, apoptosis and survival (Harris et al. 2012) and might be an important modulator of uterine remodelling.

Alpha-1-antiproteinase (SERPINA1) is an extracellular inhibitor of serine proteases whose primary target is elastase, but it also has a moderate affinity for plasmin, thrombin and other proteases (Silverman et al. 2001). In ULF, SERPINA1 along with SERPINF2 and SERPIND1 were more abundant on day 17 of pregnancy in sub-fertile compared to highly fertile beef heifers, all associated to haemostasis (blood coagulation) pathways, but no differences were found between cyclic and pregnant animals (Moraes et al. 2020a). Conversely, it was reported in higher abundance in pregnant vs cycling oviduct fluid in cows (Rodríguez-Alonso et al. 2020a). Many SERPINs (A3-1, A3-7, A3-8, D1 and H1) were detected in oviduct fluid (Pillai et al. 2017, Gegenfurtner et al. 2019b), potentially involved in zona pellucida-sperm interactions (Cesari et al. 2010). SERPINA1 mRNA was found downregulated in oestrogen-receptor-knockout mice (Winuthayanon et al. 2015). The apparent discrepancies between studies suggest that SERPINA1 plays an important role in pregnancy, but whose spatiotemporal pattern is more complex than can be assessed by untargeted studies. An interpretation of this protein being more abundant in class IV embryos is that it may indicate an underlying detrimental process, instead of directly hindering normal embryo development.

Prostaglandin reductase 1 (PTGR-1) is an enzyme involved in the degradation of prostaglandins, i.e. to halt the pro-inflammatory effects of prostaglandin signalling (Mesa et al. 2015). It was detected in bovine ULF in several studies (Mullen et al. 2012, Harlow et al. 2018, Helfrich et al. 2020), but not found to be differentially abundant in response to the factors studied (pregnancy status or feeding regime). In equine ULF it was significantly upregulated by pregnancy at day 13 (Smits et al. 2017) and has been reported to be present in cytoplasm (Mesa et al. 2015) and exosomes (Gonzales et al. 2009) in humans. Its higher abundance in poor quality embryos, together with some of the aforementioned proteins (S100A2, SERPINA1) suggests that an abnormal regulation of inflammation is hindering embryo development in those animals. Additionally, a similar enzyme, prostaglandin reductase 2, was found to physically interact with bovine embryos at 4-16 cells and morulae *in vitro* and suggests signalling or regulatory roles of classical metabolic enzymes (Banliat et al. 2020).

Proteins positively related to embryo quality phenotype

This section discusses the seven proteins found to be upregulated in ULF with good quality embryos according to the EQ1, EQ2 and EQ3 classification systems explained above, and how these proteins relate to fertility in the context of the literature.

Eukaryotic translation initiation factor 5A-1 is a nuclear protein known as a marker for cellular proliferation (Nilsson et al. 2004), and has been associated with vulvar cancer in humans (Cracchiolo et al. 2004). It is also significantly more abundant in the blastocyst stage compared to previous stages

of development in bovine embryos (Demant et al. 2015). In this study, its lower abundance in in grade III embryos is suggestive of a poorer development of these. However, no clear tendency was apparent across classes.

Plasminogen is a secreted protease that participates in thrombolysis and extracellular proteolysis (Ponting et al. 1992). Its gene expression was significantly upregulated in endometrium of cows with severe negative energy balance at two weeks postpartum potentially indicating abnormal tissue remodelling (Wathes et al. 2009). In ULF, it was also found to fluctuate throughout the bovine oestrus cycle, increasing ten-fold from day 7 to day 13 (Mullen et al. 2012). It was higher in oviduct fluid of cyclic vs pregnant cows in the isthmus but not the ampulla region at day 3.5 after oestrus (Rodríguez-Alonso et al. 2020a). Both reports showcase the precise regulation of proteomic changes in relation to embryo development. In this experiment it was lower in ULF containing class IV embryos, but no differences were observed among the other classes.

Membrane-associated guanylate kinase inverted 3 is a protein known to be downregulated in gliomas (a type of brain cancer) and that functions as a tumour suppressor (Ma et al. 2015). In this study, it was in lower abundance in ULF containing class V and III embryos, with no other reports of its being detected in ULF. Being a membrane protein its involvement in embryo development needs further research.

Phospholipase A2 activating protein (PLAA), as its name indicates, regulates PLA2 and thus the production of lyso-phospholipids and prostaglandin precursors from arachidonic acid (Murakami and Kudo 2002). Its induction by tumour necrosis factor (TNF)-alpha has been shown to perpetuate an inflammatory status in HeLa tumoral cells (Zhang et al. 2008). In this study, PLAA exhibited a linear trend from worse to best quality embryos (class V to class I), which may be related to the increased amounts of prostaglandin precursors induced by pregnancy (Sponchiado et al. 2017). PLAA was however detected at very low intensity and therefore its quantitation is not as reliable as most other proteins analysed here. The role of PLA2 is discussed later.

Triosephosphate isomerase (TIM) is a metabolic enzyme that converts dihydroxyacetone phosphate to D-glyceraldehyde-3-phosphate in both gluconeogenesis and glycolysis (Rodríguez-Almazán et al. 2008) and it is found in cytosol, extracellular space and exosomes (Gonzales et al. 2009). It was found in higher abundance in ULF of pregnant vs cyclic ULF at day 8 (Muñoz et al. 2012) and in day 16 of pregnancy compared to day 10 (Forde et al. 2014a). In another study also conducted in beef heifers, no significant differences were found in the abundance of TIM in ULF holding viable or nonviable embryos at day 7 of pregnancy (Beltman et al. 2014). Joint pathway analysis results presented in Chapter 6 suggest that this enzyme -linking the galactose metabolism to the pentose phosphate pathways- might be increasing the interconversion of monosaccharides (galactose to fructose and

ribose). Fructose, but not galactose, was reported to be an energy substrate of cultured sheep granulosa cells (Campbell et al. 2010). In this case, higher abundance of TIM might improve embryo quality by increasing fructose concentration for use as an energy source. This is further discussed in Chapter 6.

Delta-aminolevulinic acid dehydratase -ALAD(H)-, also known as porphobilinogen synthase, was lowest in ULF containing class III embryos. It catalyses the conversion of aminolevulinic acid to porphobilinogen and is thus involved in production of heme chemical group and other pyrrolic compounds (Tanaka et al. 2011). Polymorphisms in this gene in human mothers are associated with differential levels of heavy metals in placenta (Kayaaltı et al. 2016). In cows, transcription of this gene was downregulated in endometrium at day 16 after oestrus in pregnant vs cyclic cows (Forde et al. 2012a). This protein was also found in 4 fold higher abundance at the preovulatory vs postovulatory bovine oviduct fluid, and this could indicate a role of ALAD in sperm capacitation (Lamy et al. 2016a).

Costars family protein (ABRACL) was also found in lower abundance in ULF with class III embryos. It intervenes in the regulation of actin filament-based processes (Gaudet et al. 2011) and is thus an important modulator of cell motility (Pang et al. 2010). It is also upregulated in human oesophageal carcinoma cells (Fan et al. 2020). Little information on any potential role on reproduction is available on this protein, but the results obtained herein warrant further investigation.

Phospholipase A2 (PLA2) was highest in ULF with class I embryos compared to classes III-V, i.e. “optimal” vs “suboptimal” embryos, under the EQ2 system (Table 5-6). This secreted protein is considered pro-inflammatory; it hydrolyses phospholipids and releases arachidonic acid, a key precursor of eicosanoids, i.e. prostaglandins and leukotrienes (Dennis 1994). It is activated by PLAA, as explained earlier. In rats, PLA2 is under regulation of oestrogen, indirectly modulated by progesterone (Dey et al. 1982). Knock-out mice lacking PLA2 present defective metabolism of eicosanoids, and this manifests in impaired reproduction in two ways: parturition complications in the maternal side, and non-functional macrophages and ultimately in major neurological and cardiac disfunctions in embryos (Bonventre et al. 1997). In cows, uterine infection often causes a switch in production of prostaglandins from F-type to E-type by inhibiting phospholipase A2. This prevents luteolysis and results in abnormal extension of luteal phases, greatly hindering reproductive performance (Sheldon et al. 2009).

Table 5-5 Proteins in different abundance in ULF containing embryos of different quality (EQ1) at flushing on day 7. Values are relative to protein amount in ULF containing class I (grade 1) embryos. Highlighted in red/green: potential biomarkers of suboptimal/optimal ULF. V: one-cell embryos; IV: 4-16 cell embryos; III, II, I: embryos of grade 1,2,3. Letter superscripts indicate statistical differences.

Protein name	p-value	q-value	V	IV	III	II	I
Dihydropteridine reductase	<0.001	0.001	0.79^{ab}	**1.34^{a}**	**0.71^{b}**	**0.84^{b}**	**1^{b}**
Cystatin-B/C	<0.001	0.001	**0.78^{b}**	**1.49^{a}**	**0.83^{b}**	**0.77^{b}**	**1^{b}**
Eukaryotic translation initiation factor 5A-1	<0.001	0.002	0.84^{ab}	**1.2^{a}**	**0.65^{b}**	0.89^{ab}	**1^{a}**
Acyl-CoA-binding protein (ACBP)	0.001	0.006	0.99^{ab}	**1.26^{a}**	**0.76^{b}**	0.79^{ab}	**1^{a}**
Protein S100-A2 (Protein S-100L)	0.001	0.007	**0.77^{a}**	**2.73^{b}**	**0.86^{b}**	**0.95^{b}**	**1^{b}**
Glutamic acid-rich-like protein (obsolete)	0.001	0.008	**0.75^{b}**	**1.44^{a}**	**0.75^{b}**	**0.9^{b}**	1^{ab}
Unc-80 homolog, NALCN channel complex subunit	0.001	0.011	0.97^{ab}	**1.72^{a}**	**0.72^{b}**	**0.88^{b}**	**1^{b}**
ATP synthase subunit beta	0.001	0.012	1^{abc}	**1.13^{a}**	**0.82^{b}**	0.82^{abc}	1^{bc}
Plasminogen	0.009	0.012	0.96^{ab}	**0.55^{a}**	**1^{b}**	**1.15^{b}**	**1^{b}**
Membrane-associated guanylate kinase inverted 3	0.009	0.013	**0.71^{b}**	0.91^{a} ^{b}	**0.81^{b}**	**1.14^{a}**	1^{ab}
Macrophage migration inhibitory factor (MIF)	0.002	0.021	0.85^{ab}	**1.17^{a}**	**0.82^{b}**	**0.86^{b}**	1^{ab}
Pyruvate kinase (Fragment) (PKM2)	0.002	0.023	0.94^{ab}	**1.34^{a}**	**0.78^{b}**	**0.92^{b}**	1^{ab}
Phospholipase A2 activating protein (PLAA)	0.003	0.026	**0.3^{b}**	**0.3^{b}**	0.5^{ab}	0.7^{ab}	**1^{a}**
Triosephosphate isomerase (TIM)	0.004	0.032	0.84^{ab}	**1.08^{a}**	**0.78^{b}**	0.9^{ab}	**1^{a}**
Alpha-1-antiproteinase (Serpin A1)	0.004	0.038	0.97^{ab}	**1.4^{a}**	**0.95^{b}**	**0.97^{b}**	**1^{b}**
Delta-aminolevulinic acid dehydratase (ALADH)	0.004	0.038	0.73^{ab}	**1.1^{a}**	**0.63^{b}**	0.8^{ab}	**1^{a}**
Costars family protein ABRACL	0.006	0.048	1.02^{ab}	1.05^{a} ^{b}	**0.63^{b}**	0.79^{ab}	**1^{a}**
Prostaglandin reductase 1 (PTGR-1)	0.006	0.049	0.56^{ab}	**1.61^{a}**	**0.56^{b}**	**0.67^{b}**	**1^{ab}**

MSTN (myostatin, or growth/differentiation factor 8) is a secreted negative regulator of skeletal muscle growth (Carnac et al. 2006), found in lower abundance in class I embryos in this work. Defects in MSTN are the cause of the double-muscle phenotype or muscular hypertrophy, a recessive disease frequently found in the Asturiana de los Valles and Belgian blue cattle breeds, but not in other breeds such as Holstein (Bellinge et al. 2005). This disease is characterized by an increased number of muscle fibres, with an increase in muscle mass of 20-25% (Kambadur et al. 1997). Low levels of MSTN are found up to day-29 bovine embryos and increase from day 31 up until late gestation (Cassar-Malek et al. 2007). Furthermore, MSTN-knock-out bovine foetuses showed downregulated genes in essential

developmental processes -ribosomal and extracellular matrix proteins like collagens-, and upregulation of others -translation, cell cycle and apoptosis- (Cassar-Malek et al. 2007). Animals in this work were not found to present this mutation according to the SPIDER tool of PEAKS Studio, though full genotyping would be required to confirm these preliminary findings. Although high variability in the abundance of this protein was found in ULF in this work, the evidence presented justifies further research.

Nicotinate phosphoribosyltransferase (NAPRTase) is a cytosolic enzyme that catalyses anabolism of NAD^+ (nicotinamide adenine dinucleotide), an important redox cofactor in all living cells (Schomburg and Stephan 1996). In this work, it was found in higher abundance in ULF containing class I and IV embryos vs classes III and V, a classification based on the theory presented earlier (EQ3). Allelic variants in genes in the "nicotinate and nicotinamide metabolism" pathway were significantly associated with the likelihood of suffering cystic ovary syndrome in Canadian Holstein cows (Guarini et al. 2019), indicating its potential importance in reproductive performance. Moreover, decrease of this enzyme in human oocytes is posited as one of the main factors linking age with reduced fertility (Massudi et al. 2012, Bertoldo et al. 2020). In this latter work, supplementation of a NAD agonist restored fertility to aged reproductively impaired mice, underlining the potential of this enzyme and the processes it regulates for non-invasive fertility treatment (Bertoldo et al. 2020).

Table 5-6 Differentially abundant proteins in ULF grouped according to EQ2 (III to V, i.e. 1-16 cell and grade 3 embryos, vs I -grade 1-) EQ3 (V and IV vs III-I) classification systems. q-value: false discovery rate (see text for details). FC: fold change.

Protein	Gene	p-value	q-value	Trend	FC
Phospholipase A2	PLA2	0.0037	0.052	Optimal>Suboptimal (EQ2)	2.27
Myostatin	GF8	0.01	0.087	Optimal<Suboptimal (EQ2)	0.52
NAPRTase	NAPRT	0.0053	0.0538	Pregnant>Non-pregnant (EQ3)	1.59

Biomarker candidates' potential for validation

The proteins presented were assessed for their potential to be assayed on *in vitro* embryo culture. Aspects considered were putative effect on embryo development, cellular location, magnitude of difference between good and poor-quality embryos, antecedents in literature, and availability.

Upon extensive consideration, proteins found to be positively related to embryo quality were excluded because it is more technically challenging to test a positive effect compared to a negative effect on *in vitro* embryo culture (Zullo et al. 2016a). Then, out of the negative proteins, some had

contradictory evidence in literature to what was observed here: dihydropteridine reductase, Acyl-CoA-binding protein, S100A2, SERPINA1, prostaglandin reductase. Membrane proteins (both cell and mitochondria) were also excluded, i.e. UNC80, ATP synthase subunit beta.

Cystatin C was the only cystatin determined to be secreted and thus chosen as a potential biomarker to try through *in vitro* embryo culture. Pyruvate kinase M2, in turn, was classified as intracellular by Outcyte, Phobius and SignalP. However, there is evidence of its extracellular location by several studies (reviewed by Hsu and Hung 2018). Its multiplicity of functions rendered it of special interest.

The effect of some of those proteins was tested in *in vitro* embryo culture experiment (Chapter 7).

Pathway and functional analysis

As previously mentioned, one way to gain understanding of complex biological data is by ontology and pathway investigation. Overrepresentation analysis and enrichment analyses are two of the most widely used approaches; here these were carried out using Metascape.

Overrepresentation assesses the proportion of proteins of a certain class (being cellular component, molecular function, biological process, or pathway) over a user-decided threshold (usually statistical significance and/or fold change) to the whole set of proteins detected in the study, i.e. background. In this type of analysis, all proteins are considered equally important and depends heavily on the user's choice. Pathway enrichment analysis, on the other hand, takes an input of all proteins identified together with a measure reflecting its difference between two or more conditions tested (usually fold change). Unlike overrepresentation, it tests for coordinate trends in the proteins within each pathway, assessing the likelihood of a pathway being up- or down-regulated.

Table 5 shows the functional categories impacted according to genes in differential abundance between favourable and unfavourable conditions, i.e. inputting fold change values of all proteins in differential abundance between EQ1-3.

According to overrepresentation analysis, differentially regulated GO biological processes in ULF containing embryos of different classes, in order of increasing FDR (q-value), were "myeloid leukocyte activation", "cofactor metabolic process", "generation of precursor metabolites and energy", "response to wounding", "proteolysis in cellular catabolic processes" and "monocarboxylic acid metabolic process". The definitions provided below were obtained from the GO website (Ashburner et al. 2000, Gaudet et al. 2011).

At first sight, these processes are not particularly relevant to the extracellular liquid matrix that constitutes ULF. The q-value assigned to each is useful to assess how reliable each term is but is not a

rigid parameter meant to preclude consideration and discussion. Therefore, terms above the specified significance threshold of 0.05 will still be examined, albeit more briefly.

Firstly, “cofactor metabolic process” has been rendered obsolete because “it is not meaningful to group metabolic processes that are not all chemically related by the fact that they may be used as a cofactor” (https://www.ebi.ac.uk/QuickGO, 02/12/2020).

“Myeloid leukocyte activation” is defined as “a change in the morphology or behaviour of a myeloid leukocyte resulting from exposure to an activating factor such as a cellular or soluble ligand” and is part of the bigger class of “immune system processes”. Most of the proteins in this pathway were negatively associated with embryo quality phenotype (CST3, MIF, SERPINA1, PKM, NAPRT, PLG), whereas ALAD was the only positively associated with embryo quality ($p<0.001$, $q=0.003$). An activation of this pathway is typical at the onset of pregnancy in cows (Ott 2019), but the result obtained here strongly suggests an abnormal hyperactivation of myeloid leukocytes -macrophages and dendritic cells- (Kamat et al. 2016). This disruption of the delicate balance required for allowing the semi-allogenic embryo to develop while fending off detrimental bacteria often results in pregnancy loss (Ott 2019).

Generation of precursor metabolites and energy, i.e. “the chemical reactions and pathways resulting in the formation of precursor metabolites, substances from which energy is derived, and any process involved in the liberation of energy from these substances”. The weak tendency for dysregulation of this pathway ($p<0.001$, $q=0.151$) was associated with poorer embryo quality in this work, signified by higher levels of ATP5F1B, PKM, QDPR, SH3BGRL3, CST3 and MSTN. The discussion presented earlier around each of these proteins showcases their diversity and complicates simple interpretations of this category’s dysregulation. However, Simintiras et al. (2019a) have shown that progesterone reduced total metabolite abundance at day 12 of oestrus, exemplifying the “goldilocks principle of embryo development” coined by Leese et al. (2016): although satisfying the metabolic requirements of the embryo is crucial, when an upper threshold is crossed the results are as negative as insufficiency. It is possible thus that in the present work an increased metabolic status at the cow level brought about negative effects on embryo quality; this is examined in the next chapter.

Table 5-7 Functional categories and pathways impacted in ULF containing contrasting embryo quality, by Metascape overrepresentation analysis of proteomics data.

Impact	GO	Description	Proteins	p-value	q-value
Detrimental	GO:0002274	myeloid leukocyte activation	ALAD, CST3, MIF, SERPINA1, PKM, NAPRT, PLG	<0.001	0.003
Detrimental	GO:0051186	cofactor metabolic process (obsolete)	ALAD, DBI, PKM, QDPR, NAPRT, ATP5F1B, MAGI3	<0.001	0.085
Detrimental	GO:0006091	generation of precursor metabolites	ATP5F1B, PKM, QDPR, SH3BGRL3, CST3, MSTN	<0.001	0.151
Detrimental	GO:0009611	response to wounding	CST3, MSTN, SERPINA1, PKM, PLG, S100A2	<0.001	0.166
Beneficial	GO:0051603	proteolysis in cellular catabolic process	ALAD, PLG, PLAA	0.001	0.933
Detrimental	GO:0032787	monocarboxylic acid metabolic process	MIF, PKM, PLAA, PTGR1	0.001	0.933

Proteins in the “response to wounding”, i.e. “any process that results in a change in state or activity of a cell or an organism (in terms of movement, secretion, enzyme production, gene expression, etc.) as a result of a stimulus indicating damage to the organism”, and a subgroup of the “response to stress” mechanisms showed a weak tendency to enrichment in this work ($p<0.001$, $q=0.166$). This is seemingly at odds with the report of Gegenfurtner et al. (2019b) in oviduct fluid of Montebeliarde (of high genetic potential for fertility traits) vs Holstein (of low genetic potential for fertility traits) cattle. There, they reported that response to wounding was higher in Montebeliarde compared to Holstein, however the location (oviduct) and timeframe (day 3 after oestrus) were dissimilar and thus may not be directly comparable. They also showed that metabolic stress due to calving and milking increased proteins involved in defence response (Gegenfurtner et al. 2019b), pointing at an increase in “response to wounding” proteins being responsible for at least part of the well-characterised differences in fertility between breeds.

"Proteolysis in cellular catabolic processes" and "monocarboxylic acid metabolic process" had q-values of 0.93, indicating a high likelihood of their significance being spurious.

Multivariate analysis and modelling

Unsupervised multivariate analysis determined trends in the proteomics composition of ULF samples. Protein abundance values were auto-scaled, as referred to in Chapters 3 and 4. No trends or clustering was observed related to embryo quality (by either of the classification systems employed, EQ1-3); Figure A-8- shows principal components 1 and 2 of an example PCA plot according to protein abundance features.

Supervised analysis (OPLS-DA) was also performed to ascertain whether a model was both able to fit (explain) data and to predict the response variable (embryo viability or oestrus number) based on tendencies in explanatory variables (protein abundances). In all cases, the parameter representing degree of fit (R^2) was relatively high (consistently over 0.5) but lacked predictive power ($Q^2<0$ for OPLS-DA); these results are discussed in Chapter 6 where they are integrated with the analysis of metabolomics data.

5.4 Conclusions

The present chapter investigated the proteomic composition of ULF and its relationship with embryo quality under different frameworks. Many proteins were identified in this work for the first time in ULF proteome. Moreover, comparisons between studies showed moderate overlap in the protein complement identified in each. Further research is needed to identify the most consistent components of ULF and other biofluids, particularly using newer technological approaches.

Univariate analysis showed differences in ULF protein abundance related to embryo phenotype. Some potential biomarker candidates were identified, of which SERPINA1, PKM2 and Cystatin C showed high potential for application and were considered for experimental validation purposes. Results from metabolomic and joint analyses (presented in the next chapter) were also considered to expand the list of potential biomarker candidates for validation assays.

6

Metabolomics

6.1 Introduction

As detailed in Chapter 1, the metabolome is an important component of the uterine environment of the dairy cow and highly influential on embryo development. Following the method optimisation process described in chapter 4, two metabolomics experiments were carried out to analyse the molecular composition of ULF samples collected from Farm trials 2 and 3. These trials encompassed the spring reproductive seasons of two years (2017 and 2018) in a herd at Tokanui farm in the Waikato area of New Zealand, as specified in Chapter 2.

The two main metabolomic experiments of this project are described herein. Experiment M4 was based on GC-MS/MS targeted metabolomics and was performed to identify metabolites and biological processes underlying uterine physiology differences related to the contrasting embryo development observed. Integration at functional and pathway levels with proteomics data (Chapter 5) was also performed. Experiment M5 used REIMS direct infusion mass spectrometry analysis as a proof of concept to establish whether the metabolic fingerprint obtained could model or predict embryo fate or, alternatively, other relevant physiological parameters. In this case, relevant spectral features were putatively identified.

This chapter had two main goals. Firstly, to characterise the ULF metabolome qualitatively (including comparisons with previous related studies) and quantitatively, including integrating these data with proteomics data for a systems-level analysis. Secondly, to determine molecules relevant to embryo development directly or through the influence of other factors, especially oestrus after calving (OC).

6.2 Methods

6.2.1 Experimental design

Reagents along with their origin are specified in 4.2.1. Samples used were obtained in Farm Trials 2 and 3, section 2.2.3. In both experiments, all steps of sample preparation and analysis in instrument were randomised using the random function in MS Excel, blocking by year and OC. Further specifications were followed to ensure inter-sample and inter-batch consistency in these lengthier experiments, and these are detailed next.

Targeted metabolomic analysis of ULF flushings: Experiment M4

Experiment M4 (targeted metabolomics) followed the protocol detailed in 4.4.7 with the following differences: tracer (heavy proline) peak areas were calculated as detailed in 4.3.2. Quality control (QC) procedures were like those detailed for proteomics in Chapter 5. Specifically, in both Exp. M4 and M5, a pool of at least 20 samples was produced, and aliquots of this pool were run at regular intervals (every 10 ULF samples). Batches consisted of ten ULF samples preceded and followed by a QC injection. At the end of the batch, a hexane blank and a water blank were also run to confirm the absence of carryover.

Metabolites detected - comparisons with other studies

Results from five previous studies on untargeted or broadly targeted metabolomic analysis of ULF were collected. As different metabolite nomenclature systems were used across the relevant studies, the identifiers were batch-converted to HMDB, KEGG and/or PubChem ID using MetaboAnalyst web tool v4.0.

Metabolomic fingerprinting of ULF using direct infusion-MS: Experiment M5

Experiment M5 was carried out in a similar manner as described for Exp. M3 (Chapter 4). In brief, each batch was made up of 10 samples, which were analysed in positive and negative modes, with a QC sample analysed at the beginning and end of each batch. The iKnife handheld device was slid on the surface of each ULF sample placed in a foil cup to vaporise it and this was siphoned into the REIMS machine to generate a mass spectrum. The iKnife was wiped clean in between samples with a paper towel and ethanol. At the end of each batch, a saline blank was analysed, and the handheld device was thoroughly scrubbed. The instrument was also cleaned by isopropanol infusion for 15 minutes before proceeding to the next batch.

Informatic and statistical analysis

Informatic analysis was performed in a similar manner as detailed in Chapter 5 for Exp. P3. Specifically, a spreadsheet containing peak areas for each identified metabolite (Exp. M4) or feature (Exp. M5) in each sample (ULF, QC, blanks) was produced and analysed using the statistic and bioinformatic approaches explained in Chapter 5. Batch correction was applied using the QC-RFSC (Quality Control Random Forests Signal Correction) algorithm choosing the LOESS (Locally Estimated Scatterplot Smoothing) method in the W4M Galaxy web-based tool (Dunn et al. 2011). This method was chosen over those presented in Chapter 4 -i.e. normalisation by internal standards (Jonsson et al. 2005) in Exp. M4 and by total ion chromatogram area for Exp. M5 (Ross et al. 2020)- due to its improved consistency when conducting a large experiment with several batches.

Univariate analysis

Generalised linear model analysis (multiparametric regression) was performed to determine changes in the molecular composition of ULF through time (in dpp and OC). Then, the potential effect of metabolites and dpp or OC on embryo quality (according to the systems developed, i.e. EQ1, EQ2 and EQ3 as described in Chapter 2) was assessed in a similar manner using the *GLM* function of the base package in R 4.0.2 - R Team (2019).

Multivariate analysis and modelling

In brief, PCA, sPLS-DA and OPLS-DA were performed using the R packages mixOmics v4.0 (Rohart et al. 2017) and ropls v3.8 (Thévenot et al. 2015).

Functional and pathway analysis

Enrichment (using KEGG, the Kyoto Encyclopaedia of Genes and Genomes) and overrepresentation pathway analyses were performed using IMPaLA version 12 (build January 2019) (http://impala.molgen.mpg.de/) (Kamburov et al. 2011) and metaboAnalystR v5.0 (https://www.metaboanalyst.ca/) (Pang et al. 2020), on all KEGG pathways (metabolic and gene-only, regulatory pathways). Impact score, i.e. "the sum of the importance measures of the matched metabolites normalised by the sum of the importance measures of all metabolites in each pathway" (Xia and Wishart 2010) higher than 0.3 was also used as a threshold of relevance.

For over-representation analysis the formula Impala uses is:

$$\forall_{i \in pathways}, p_i = \sum_{j=k_i}^{\min(K, N_i)} \frac{\binom{N_i}{j}\binom{M - N_i}{K - j}}{\binom{M}{K}}$$

pathways p where N_i is the effective size of pathway i, M is the overall number of genes or metabolites available to be picked, K is the number of genes or metabolites picked and k_i is the number of genes or metabolites picked from the pathway.

6.3 Results and discussion

6.3.1 Experiment M4: targeted metabolomics

Quality control assessment

Acceptable reproducibility was achieved in experiments, with intra- and inter-batch effects relatively small; these were adjusted by the LOESS method as described (Figure A-8-910). However, the replacement of a component (the detector) in the GC instrument resulted in noticeably lower sharpness and intensity of peaks in Exp. M4 compared to those from preliminary experiments (Exp. M1 and M2). This was not apparent in the periodic checks during the running of the samples. It however resulted in a lower number of metabolite transitions detected (122 in this experiment compared to the >200 detected in Exp. M2 and M3, Chapter 4). Nonetheless, this number is within the range of many recent articles in this area, most of which identified less than 200 compounds, with the exception of (Moraes et al. 2020a, Moraes et al. 2020b) who reported over 600 compounds, most of which were lipids with multiple isomer variants; this is examined next.

On a different note, the use of heavy proline as a tracer to estimate uterine volume and degree of ULF dilution by sampling medium was not employed in Exp. M4 due to inconsistent patterns observed in the peak areas for these transitions. The tracer approach was considered a useful strategy that did not fulfil its purpose as intended, potentially due to instrument issues.

The data obtained was further analysed in perspective to previous work, and in terms of individual molecules, classes, and pathways.

Metabolite identification and comparisons to previous studies

The bovine metabolome is estimated to be constituted by about 50,000 by genomic-scale inference, although only around 2,100 have been experimentally detected (Foroutan et al. 2020). Their research group created a database – the "Bovine Metabolome Database" (https://bovinedb.ca)- including both detected and predicted metabolites in 10 biofluids and tissues, though coverage in the reproductive tract is limited (Foroutan et al. 2020).

To characterise the ULF metabolome in this study, results from a combination of broad targeted and untargeted GC-MS/MS analysis were examined. To examine metabolome coverage, all compounds identified in Exp. M1 were considered: 278 transitions totalling 209 compounds after removing duplicates and internal standards. In addition, compounds identified by full scan, untargeted GC-MS/MS analysis were included: the 94 features matches were mapped to PubChem id's resulting in 81 unique compounds (i.e. some features were fragments of the same compound). This resulted in a combined total of 242 unique metabolites mapped to metabolic networks. A Venn diagram shows

the overlap between the two approaches (Figure 6-181); the full compound list is displayed in Table S6-1.

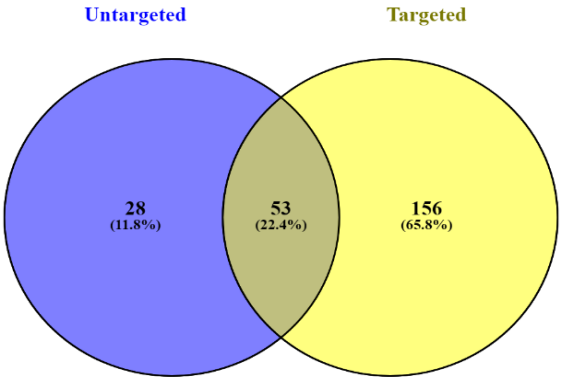

Figure 6-18 Venn diagram showing metabolites identified by targeted analysis, untargeted analysis, or both.

Comparisons to other studies: meta-analysis

A list of metabolites detected in the studies analysed from the literature was assembled to contextualise the findings of this study in a manner analogue as that described in the previous chapter for proteomics data. For this, metabolite identifiers reported in studies conducting untargeted or broadly targeted metabolomic analysis of bovine ULF were converted to standard names using the batch conversion tool in Metaboanalyst 5.0 (Pang et al. 2020). Compounds successfully identified were pooled to create a "background dataset" to be used for pathway overrepresentation analysis (described next). Results obtained in one experiment and published in more than one article were grouped (Moraes et al. 2020a, Moraes et al. 2020b) and (Simintiras et al. 2019a, b, Simintiras et al. 2019c).

Next, overlap between the compounds reported across studies was analysed, along with other relevant parameters (total number of compounds and number of animals sampled; Table 6-1). It's important to consider here that comparisons suffer of a certain degree of inexactness because of missing data (i.e. incomplete lists available), as well as nomenclature issues. These include notation discrepancies (i.e. "2-3-Bisphosphoglyceric acid" vs "2,3-Diphosphoglyceric acid" or "Prolyl hydroxyproline" vs "Prolyl-Hydroxyproline"), mismatches, and ambiguous entries (particularly

isomers that cannot be resolved by traditional mass spectrometry, such as fatty acids and enantiomers of AA); consequently, lists were manually checked and corrected.

A total of 1382 unique compounds were surveyed from the studies; the present study reports 242, above the mean of 219 compounds reported per study. Of those compounds, 1194 (86%) were reported in one study only; the average number of unique compounds was 125 (132 in the present study). As was the case with the proteomics meta-analysis, the number of animals sampled in this study (92) and samples analysed (184) were substantially higher than the average (18 and 23, respectively), and more than twice as high as the second largest study (35 animals; Simintiras et al. 2019a).

The studies surveyed were less diverse in the instrumental platforms employed and scope than was observed with the meta-analysis of proteomics in the previous chapter. This seems sensible, considering that metabolomics (i.e. the large-scale analysis of small molecules) is a newer field and in fact almost all studies surveyed were performed in the period 2016-2020 using a small number of instruments and informatic analysis tools. While most studies detected metabolites classified as lipids, these were mainly polar (phospholipids, eicosanoids, carnitines). Only two studies (Simintiras et al. 2019b, Moraes et al. 2020b) analysed specifically the hydrophobic fraction of ULF by lipid-centred methods ("lipidomics"), both reaching the conclusion that pregnancy induces an increase in phospholipid content in ULF with the likely purpose of conceptus membrane biogenesis.

Table 6-112 Metabolites identified in ULF by untargeted or broadly targeted experiments. Animals(samples): number between brackets indicates the number of samples analysed when animals were sampled more than once.

Study	Metabolites reported	Unique to the study	Animals (samples) N
Tribulo et al. 2018	95	35	4 (16)
Simintiras et al. 2019	141	49	35
Sponchiado et al. 2019	201	137	18
Ribeiro et al. 2016	301	217	30
Moraes et al. 2020	627	613	25
Present study	**242**	**132**	**92 (184)**
Total	1382	1194	-

No compound was detected in all studies; the most reported (in five studies out of six) were taurine, succinic acid, L-malic acid, L-threonine, L-glutamine and L-tyrosine. One hundred and seventy compounds were detected in more than one study, predominantly amino acids and derivatives, organic acids and carbohydrates, similarly to the compounds detected in experiments in the present study.

Two points summarise the results of this meta-analysis. Firstly, there was limited overlap in the metabolite sets reported between studies, underlining the importance of more descriptive analysis of this biofluid; this will be greatly aided by newly developed tools for identification in untargeted studies and by multi-tissue analyses (Foroutan et al. 2020). Secondly, the present study contributed to expand the known universe of metabolites present in ULF by an additional

Functional analysis of compounds detected in this study

Next, to assess pathway coverage of the approaches trialled, all compounds detected in the present study by both targeted and untargeted analysis were entered in Metaboanalyst's Pathway enrichment tool. Out of the 242 compounds, 231 were mapped to 33 pathways (Table S6-2). Pathways enriched (i.e. with more components in the list than expected by taking a sample at random from the total metabolome) with false discovery rate (FDR) under 5% (q< 0.05) are shown in Table 6-13. Most of those pathways were related to amino acid metabolism or central carbon metabolism, which partly reflects the fact that most compounds included in the targeted method package were indeed amino acids and organic acids. This is further discussed next.

Table 6-13 KEGG pathways significantly overrepresented in the full list of metabolites identified with respect to the whole bovine metabolome (~2100 compounds) using the MetaboAnalyst Pathway Overrepresentation tool. Hits: number of compounds detected vs total n of compounds in pathway. q-value= false discovery rate-adjusted significance value.

Metabolite set	Hits	P-value	q-value
Aminoacyl-tRNA biosynthesis	20/48	<0.001	2.29E-04
Arginine biosynthesis	9/14	<0.001	0.00103
Valine, leucine and isoleucine biosynthesis	6/8	<0.001	0.00391
Citrate cycle (TCA cycle)	8/20	<0.001	0.0412
Fructose and mannose metabolism	8/20	<0.001	0.0412

As mentioned before, the choice of analysing the hydrophilic fraction is a determining factor of the type of metabolites detected in the present study; a choice certainly influenced by the fact that ULF is water-based (Roberts and Bazer 1988). Similar results were obtained when classifying all compounds in this study by chemical class: the most relevant metabolite class were “organic acids and derivatives” (45%), followed by “organic oxygen compounds” (15%), “lipids and lipid-like molecules” (11%), and “organo-heterocyclic compounds” and “benzenoids” (7% each).

The same analysis was repeated including all compounds surveyed from previous studies in the meta-analysis, provided they could be mapped to HMDB identifiers (i.e. excluding most lipids), a total of 823 metabolites. No pathway was significantly enriched, suggesting that the proportions of metabolite classes detected across studies match the class proportions in the KEGG database. Integration between general metabolomic tools (e.g. MetaboAnalyst) and specialised lipidomics informatic tools such as Lipid Ontology (Molenaar et al. 2019) will greatly aid to attain a more comprehensive and objective view of the metabolome of this and other biofluids and tissues.

In conclusion, the metabolites within significantly enriched pathways detected in the present study are likely relevant to biological functions in ULF, but not necessarily in the manner described by the canonical pathways listed above. All those processes are in fact known to occur in the cytoplasm and/or the mitochondria (TCA cycle), though abundance differences in ULF could be related to endometrial cell metabolism (Belaz et al. 2016). To gain an accurate picture of the functionally important molecules in ULF in relation to embryo quality, uni- and multivariate analyses were conducted, discussed next.

Comparisons between targeted and untargeted approaches in this study

The metabolites detected by either GC-MS/MS approach in the present study were contrasted to define their scope and usefulness.

Untargeted analysis GC-MS/MS analysis

Enrichment analysis showed that the aminoacyl-tRNA biosynthesis pathway was significantly enriched ($q<0.001$) in compounds identified only by untargeted analysis when compared to the total set of metabolites detected in this study, consistently identifying 15 amino acids. When adding the 28 compounds identified by both methods, other pathways enriched at the $q<0.05$ level were “galactose metabolism and starch and sucrose metabolism” (both constituted by carbohydrates and other molecules like myo-inositol), “valine, leucine and isoleucine biosynthesis” and “alanine, aspartate and glutamate metabolism” (including amino acids and organic acids), and “glyoxylate and dicarboxylate metabolism” (AA, glyceric and glycolic acids - Figure A-8-10a).

Targeted analysis GC-MS/MS analysis

The metabolite set detected by the targeted method tended to be enriched (i.e. identified more compounds in these than expected if all compounds were equally likely to be detected) in the following KEGG pathways ($p < 0.005$; $q < 0.1$): "Glycine, serine and threonine metabolism" (3-phosphoglyceric acid, glycine, sarcosine, glyceric acid, 2-phosphoglyceric acid and L-cysteine), "taurine and hypotaurine metabolism" (L-cysteine, 3-sulfinoalanine and hypotaurine), "glycerolipid metabolism" (glycerol, glyceric acid, dihydroxyacetone phosphate and 2-phosphoglyceric acid) and "glutathione metabolism" (glycine, L-cysteine, pyroglutamic acid, ornithine, putrescine - Figure A-8-10B). An important consideration is that pathway analysis is biased against methods with reduced identification potential -i.e. the untargeted approach- (Karnovsky and Li 2020). Furthermore, in all the above analyses, the overlap between pathways exemplifies their interconnectedness and is a timely reminder that this powerful analysis tool still requires human curation for interpretation and to avoid false inferences, as demonstrated by Nguyen et al. (2019). In their work they tested the performance of several pathway analysis tools on well-characterised datasets as well as on fabricated data; their conclusions show that methods that consider pathway structure are better at finding biologically meaningful differences but that all methods are biased (Nguyen et al. 2019). The authors also warned about pathways related to amino acid metabolism appearing to be overrepresented; these pathways are very well characterised, and this often results in a pronounced bias that requires careful manual checking (Nguyen et al. 2019). In the present work, pathway analyses were conducted on three of the most widely used platforms, all of which consider pathway internal structure: Metaboanalyst for metabolomics data only, Metascape for proteomics data only, and ImPALA for joint omics analyses.

Summarising, the pathway enrichment results of targeted vs untargeted metabolomics indicate that specific molecule classes (amino acids, organic acids, and carbohydrates) are preferentially detected and measured using GC-MS/MS under both approaches. In this analysis, a key difference between targeted and untargeted approaches was the number of identified compounds. Based on these observations, further work in this area may be carried out using targeted analysis when the identity of the metabolites is crucial for the research question, and untargeted when maximising the number of features is more important regardless of the identity of the individual features, such as for predictive modelling purposes.

6.3.2 Integrated analysis: embryo quality and molecular changes postpartum

Data from both omics' workflows (Exp. P3 and M4) was also explored by multivariate approaches to assess the potential of models to predict embryo quality and OC. In all cases, individual and interactive effects of embryo quality, OC and dpp on molecule abundance in ULF were also explored. Then, metabolomic data were analysed in a univariate approach to determine differences in the

abundance of individual chemical species in ULF. Lastly, metabolite abundance both by itself and conjunctly with proteomics data (presented in Chapter 5) was analysed to identify biochemical pathways impacted by time postpartum (OC and dpp) and related to embryo quality (EQ1-EQ3).

Multivariate analysis

In the case of targeted analysis, from the total 451 metabolites within the Smart Metabolites database, 122 were present in at least 70% of the sample runs and QC (107 unique compounds) and these were used for statistical and biomarker analysis.

PCA was carried out using both metabolomic data only, as well as together with the abovementioned protein dataset to conform a joint dataset. In turn, PCA were plotted and coloured based on the following parameters: the three embryo quality systems (EQ1-3), OC (1 or 3), and year (2017 or 2018). No clear clustering by any of those variables was observed, or clear outliers (example plot in Figure A-8-). This points at the absence of a single dominant physiological parameter determining the molecular composition of bovine ULF. Instead, the interplay between post-partum recovery, ULF molecular composition and embryo quality requires different analytical approaches, some of which are presented next.

Binary classification using orthogonal partial least-squares discriminant analysis (OPLSDA)

Modelling and classification using the metabolomic and joint data through sPLSDA (sparse Partial Least Square-Discriminant Analysis) was attempted for systems EQ1-3 and OC. In addition, OPLSDA was performed for systems EQ2, EQ3 and OC, as it only allows binary classification. EQ2 compared ULF containing III, IV and V embryos ("undesirable" group) vs I embryos ("desirable"), while EQ3 contrasted ULF containing embryos hypothesised to have originated from bad quality oocytes (IV and V) vs good quality oocytes (I to III). All models created were tested by 10-fold cross-validation to estimate their fit and predictive power. Negative Q^2 were obtained in all cases (Table 6-3), i.e. the models generated had no predictive power or were overfitted (Lê Cao et al. 2011). In summary, predictive models based on multivariate analysis (sPLSDA) of joint omics data were not able to predict number of oestrus cycles postpartum (OC) (Q^2 = -0.12) or embryo quality, in the EQ1 (Q^2=-0.032), EQ2 (Q^2=-0.33) or EQ3 (Q^2=-0.14) classification systems. Figure A-8-1313a,b shows representative plots of OPLS-DA (EQ2 and EQ3).

Univariate analysis – days postpartum and oestrus after calving

Metabolomics data was analysed to determine effects of dpp, OC and their interaction by general linear models (Table 6-4144). Nine metabolites were significantly affected by both dpp and OC (phosphoric acid, ethylmalonic acid, malic acid, ribulose, 2-aminoethanol, glycerol, D-xylulose, glyceric acid and arabinose; $q<0.05$), in all cases decreasing with time postpartum. Other metabolites

that decreased with dpp were cysteine, uridine, inositol, N-acetylmannosamine, 3-hydroxypropionic acid, ribonolactone, threonic acid, rhamnose, xylitol, succinic acid, inosine, ribose and lyxose. Metabolites with an upward trend in concentration along dpp were 3-aminopropanoic acid, putrescine, beta alanine, 2-hydroxyisovaleric acid, and lactic acid. Two metabolites were significantly different (both at q=0.047) between OC but not by dpp, ribose 5-phosphate (2.2-fold higher in OC3) and fructose (1.95-fold higher in OC1). Additionally, metoprolol (an antihypertensive drug) was detected here, though it is likely a misidentification as these animals were not exposed to this substance. Finally, no interactive effect of OC and dpp was found for any metabolite, that is, no joint effect significantly different than their sum was found. It also signifies that in all cases the trends were in the same direction (either decreasing or increasing with dpp and OC).

Table 6-3 Summary of results of statistical tests and modelling. sPLS-DA/OPLS-DA: sparse/orthogonal Partial Least Squares Discriminant Analysis.

		Univariate analysis		sPLSDA		OPLSDA	
Experiment	**Variable**	**n features q<0.05**	**n features 0.05<q<0.1**	**R^2**	**Q^2**	**R^2**	**Q^2**
M4	EQ1	0	0	0.1	-0.15	N/A (>2 classes)	
M4	EQ2	0	0	0.11	-0.46	0.309	-0.625
M4	EQ3	0	0	0.005	-0.17	0.267	-0.426
M4	OC	11	8	0.049	0.047	0.28	0.1
M4	dpp	28	2	N/A (regression)			
P3	EQ1	18	0	0.029	-0.25	N/A (>2 classes)	
P3	EQ2	0	2	0.0007	-0.208	0.138	-0.011
P3	EQ3	0	1	0.174	-0.079	0.219	-0.124
P3	OC	2	0	0.05	0.037	0.257	-0.073
P3	dpp	0	0	N/A (regression)			
Joint	EQ1	N/A	N/A	0.58	-0.032	N/A (>2 classes)	
Joint	EQ2	N/A	N/A	0.035	-0.33	0.1	-0.13
Joint	EQ3	N/A	N/A	0.11	-0.14	0.194	-0.167
Joint	OC	N/A	N/A	0.054	-0.12	0.215	-0.151

An interesting difference in metabolite abundance that was not accounted for in pathway analysis was a higher abundance of lactic acid (lactate) at OC3. The early embryo (up to the morula state) has been shown to depend chiefly on pyruvate for growth (Khurana and Niemann 2000), with lactate showing similar energetic support for embryo development *in vitro* (Takahashi and First 1992) and *in vivo* (reviewed by Li and Winuthayanon 2017). Lactate is also one of the most abundant metabolites in oviduct fluid exosomes (Gatien et al. 2019). Its concentration in oviduct fluid across oestrus has been reported to be up to eightfold higher than in plasma and ULF (Hugentobler et al. 2007b), though appears not to be determined by sexual hormones (progesterone or oestradiol) in blood, ULF or oviduct fluid (Hugentobler et al. 2010). Additionally, higher lactate concentrations in uterine and oviduct fluids can support higher amounts of lactic acid bacteria, of known positive effect on postpartum recovery (faster uterine involution, higher prostaglandin-F_2alpha in blood - Deng et al. (2015)) and uterine health, regulating E. coli-produced-inflammation (Genís et al. 2017) and decreasing incidence of metritis (Genís et al. 2018). The increased lactate abundance in ULF at OC3 could also be partly responsible of increased fertilisation rate by a higher energy supply for sperm (Sengupta et al. 2020), In the conditions of the present work, it is not possible to determine whether contrasting abundance of lactate or other molecules respond to differential secretion, consumption or interconversion, but considering the work cited, lactate warrants further research.

Table 6-414 Differentially abundant metabolites across dpp and OC, at a q-value <0.05. *not naturally occurring. #metabolites higher in OC3 and increasing with dpp. Bold: significant effect of both dpp and OC.

	Days postpartum			Oestrus after calving			Interaction	
Name	p-value	q-value	R^2	p-value	q-value	Fold change	p-value	q-value
Phosphoric acid	<0.001	<0.001	0.149	0.002	0.016	1.77	0.72	1
Ethylmalonic acid	<0.001	<0.001	0.067	0.001	0.011	1.6	0.44	0.7
Cysteine	<0.001	<0.001	0.101	*0.017*	*0.078*	*1.68*	0.17	0.27
Uridine	<0.001	0.0014	0.09	*0.047*	*0.174*	*1.6*	0.38	0.61
Malic acid	<0.001	0.002	0.078	0.001	0.008	2.45	0.21	0.34
Ribulose	<0.001	0.002	0.093	0.001	0.009	2.18	0.55	0.88
2-Aminoethanol	<0.001	0.002	0.101	0.001	0.014	1.5	0.79	1

	Days postpartum			Oestrus after calving			Interaction	
Name	p-value	q-value	R^2	p-value	q-value	Fold change	p-value	q-value
Glycerol	<0.001	0.003	0.077	0.003	0.027	1.39	0.64	1
Inositol	<0.001	0.004	0.057	*0.173*	*0.341*	*1.27*	0.57	0.91
N-Acetylmannosamine	<0.001	0.004	0.055	*0.19*	*0.357*	*1.26*	0.62	0.99
Metoprolol*	<0.001	0.004	0.044	*0.232*	*0.389*	*1.32*	0.39	0.62
3-Hydroxypropionic acid	<0.001	0.005	0.098	*0.013*	*0.066*	*1.82*	0.31	0.5
D-Xylulose	<0.001	0.005	0.072	0.008	0.047	1.82	0.31	0.5
Ribonolactone	0.001	0.007	0.069	*0.013*	*0.066*	*1.47*	0.21	0.34
Glyceric acid	0.003	0.016	0.068	0.002	0.016	1.64	1	1
Threonic acid	0.003	0.017	0.088	*0.037*	*0.142*	*1.58*	0.14	0.22
3-Aminopropanoic acid[#]	0.004	0019	0.034	*0.066*	*0.222*	*0.74*	0.14	0.22
Putrescine[#]	0.004	0.019	0.031	*0.079*	*0.25*	*0.65*	0.21	0.34
Arabinose	0.005	0.021	0.049	0.008	0.047	1.7	0.57	0.91
Rhamnose	0.006	0.024	0.016	*0.132*	*0.329*	*1.86*	0.15	0.24
Beta alanine[#]	0.007	0.027	0.026	*0.12*	*0.319*	*0.78*	0.9	1
Xylitol	0.008	0.032	0.046	*0.018*	*0.081*	*1.56*	0.14	0.22
Succinic acid	0.009	0.033	0.074	*0.284*	*0.431*	*1.22*	0.89	1
2-Hydroxyisovaleric acid[#]	0.011	0.039	0.037	*0.804*	*0.89*	*0.5*	0.14	0.22
Inosine	0.013	0.045	0.027	*0.561*	*0.695*	*1.24*	0.09	0.19
Lactic acid[#]	0.014	0.045	0.038	*0.428*	*0.608*	*0.73*	0.95	1
Ribose	0.014	0.045	0.04	*0.013*	*0.066*	*1.6*	0.83	1

	Days postpartum			Oestrus after calving			Interaction	
Name	p-value	q-value	R^2	p-value	q-value	Fold change	p-value	q-value
Lyxose	0.015	0.047	0.04	*0.011*	*0.061*	*1.62*	0.87	1
Ribose 5-phosphate[#]	*0.061*	*0.161*	*0.007*	**0.008**	**0.047**	0.45	0.34	0.54
Fructose	*0.117*	*0.256*	*0.008*	**0.007**	**0.047**	1.95	0.12	0.23

Univariate analysis – embryo quality

No significant difference was observed in metabolite abundance between embryo quality classes under the systems examined (EQ1, EQ2, EQ3: Tables S6-3a, b and c, respectively). This suggested that embryo quality differences respond to distinct (though likely interrelated) factors, but this was further tested by joint pathway analysis.

Pathway analysis

For pathway enrichment analysis, metabolite abundance values were entered in the MetaboAnalyst web tool and analysed for differential regulation across dpp and OC. /Forty-five pathways represented by more than 2 related compounds were found (Table S6-4). Pathways within the criteria established for further analysis (q<0.05 and impact>0.3) are displayed in **Table** 6-5 and Figure A-8-11.

Table 6-**5 Enriched pathways in ULF according to metabolite abundance changes by OC and dpp, with q<0.05 and impact>0.3.** Matches: differentially abundant metabolites vs metabolites in pathway detected in the experiment. Abbreviations: dpp, days postpartum; OC, oestrus after calving.

KEGG Pathway name	Matches	p (dpp)	q (dpp)	Impact (OC)	p (dpp)	q (dpp)	Impact (dpp)
Pentose and glucuronate interconversions	3/5	0.009	0.033	0.42	0.004	0.018	0.42
beta-Alanine metabolism	4/8	<0.001	0.007	0.4	0.004	0.017	0.4
Cysteine and methionine metabolism	5/10	0.023	0.073	0.34	0.004	0.024	0.34
Glycerolipid metabolism	2/4	<0.001	<0.001	0.34	0.007	0.003	0.34
Glycine, serine, and threonine metabolism	7/11	0.23	0.49	0.59	0.019	0.038	0.59

In a study of plasma metabolomics at three timepoints of pregnancy some of the same pathways were found altered; from day 0 (artificial insemination) to both days 17 and 45 of pregnancy these were glycerophospholipid metabolism, pentose and glucuronate interconversions and glycerolipid metabolism (Guo and Tao 2018). On day 45, pathways differentially regulated vs day 0 were thiamine metabolism, pantothenate and CoA biosynthesis, inositol phosphate metabolism and pentose phosphate (Guo and Tao 2018).

Here, pathways with an impact factor higher than 0.3 were selected for discussion. A superscript was added to each differentially abundant molecule in each pathway to indicate the trend across time (higher in OC1 or OC3) and their significance (plain: $p<0.05$ and $q<0.1$; underlined: $q<0.05$).

Glycerolipid metabolism (glycerol$^{\underline{OC1}}$, D-glycerate$^{\underline{OC1}}$) was posited by Sun et al. (2015) to be one of the most ubiquitous and impactful pathways across rumen, milk, serum and urine. Moreover, higher abundance of glycerol and D-glycerate in ULF at OC1 could be related to higher triacyl glyceride lipids, rendering glycerol and NEFA as products (Nayeri and Stothard 2016). In support of this, substantially higher concentrations of NEFA in serum were found at OC1 vs OC3 (Chapter 2). Higher concentrations of saturated fatty acids (particularly palmitic and stearic acids) in blood are known to be also mirrored by their abundance in follicular fluid (Leroy et al. 2004) and to markedly reduce oocyte quality (Leroy et al. 2005b). Also, as detailed in Chapter 1, oocyte development occurs in a period of up to six months before ovulating (Lussier et al. 1987). Upregulation of this pathway, therefore, suggests low quality oocytes developing during early postpartum as an (or potentially the most) important cause of poorer quality embryos on OC3.

Another factor that could be involved in this pathway being upregulated at OC1 is that this occurs at the beginning of spring (end of August and beginning of September), with temperatures typically in the range of 5-15°C, whereas OC3 occurred on average 42 days later (Chapter 2, Table 2 -4) , on early-mid October with temperatures 3 to 4 degrees warmer on average (www.weather-atlas.com). Glycerolipid metabolism, and particularly extracellular lipolysis, is known to increase with lower temperatures for thermogenesis, i.e. to maintain an adequately warm body temperature (Prentki and Madiraju 2008). It is suggested that farm management decisions on provision of shelter and/or housing consider this factor in their reproductive remediation strategies.

Beta alanine metabolism (3-hydroxypropanoate$^{\underline{OC1}}$, beta alanine$^{\underline{OC3}}$, L-aspartate^{OC1}, uracil^{OC3}): higher concentrations of beta alanine at OC3 might indicate increased catabolism of carnosine, a known antioxidant molecule (Boldyrev et al. 2013), which is less required in an improved redox environment compared to earlier postpartum (Ledgard et al. 2009). Carnosine was not detected in this study; the only reference of its detection in bovine ULF was by Groebner et al. (2011c), who found it in fourfold higher abundance in ULF containing *in vitro* produced vs cloned (somatic cell nuclear transfer)

embryos. However, a similar study by the same research group failed to detect both carnosine and beta alanine in bovine ULF (Groebner et al. 2011a). Beta alanine in cyclic cow ULF was found to increase from day 3 to reach a maximum at day 5 and then decrease at day 7 (Tribulo et al. 2019). It is also possible that increased abundance of L-aspartate in ULF at OC3 results in an increased abundance of beta alanine without a relevant physiological purpose related to fertility. The implications of this pathway being impacted at OC1 require further investigation.

Pentose and glucuronate interconversions (D-xylulose**OC1**, xylitol**OC1**, L-arabinose**OC1**, ribulose**OC1**, D-glucuronate**OC1**): this pathway was downregulated by OC3 in this study. Guo and Tao (2018) reported decrease of metabolites in this pathway at day 17 and 45 of pregnancy in cows' serum. In the present study, the relatively high abundance of ribulose, xylulose and xylitol feed D-ribulose 5-phosphate into the pentose phosphate pathway, with the potential aim of producing NADPH to regulate the redox balance of the endometrial cells (Agarwal et al. 2012). Endometrial cells can be exposed to high oxidising activity product of the antibacterial defensive action of eosinophils and their secreted enzymes (Klebanoff and Smith 1970). Additionally, a metabolite matching xylulose and ribulose was found in 6-fold higher abundance in day 12 of oestrus in cow ULF vs cows at 14 and 16 days, and at the three timepoints in cows receiving progesterone supplementation (Simintiras et al. 2019c). D-glucuronate, also in this pathway, was also suggested to be regulated by both timepoint within the oestrus cycle and blood progesterone concentration, in the same study (Simintiras et al. 2019c).

Cysteine and methionine metabolism (L-cystathionine**OC1**, L-serine**OC3**, L-cysteine**OC3**, (S)-2-aminobutanoate^{OC1}, pyruvate^{OC1}) in the present work was activated at OC3, with both L-cysteine and L-serine in higher abundance, and L-cystathionine (their precursor) in lower abundance. In apparent contraposition, cows under a hormonal manipulation to have reduced corpus luteum (CL) and smaller dominant follicle had lower concentration of cystathionine at day 7 of oestrus (França et al. 2017). Although L-methionine was not detected in the present work, it is conceivable that this amino acid would also be produced in higher amounts at OC3, but its temporal regulation is unclear (Tribulo et al. 2019). Methionine metabolism modulation was suggested to considerably affect bovine embryo growth *in vitro*, where concentrations of methionine under or over 5 mM decreased embryo development (Ikeda et al. 2011). Rumen-protected methionine supplementation has shown improvement in certain parameters positively correlated to fertility (Stella 2017) but its effectiveness to improve reproductive function per se has not been proven (reviewed by Aranciaga et al. 2020).

Glycine, serine and threonine metabolism (glycine**OC1**, L-threonine**OC3**, L-cystathionine**OC1**, sarcosine **OC3**, D-glycerate**OC1**, L-cysteine**OC3**, pyruvate^{OC1}) was reported by Sun et al. (2015) as one of the most impacted in cows fed alfalfa (high protein diet) vs corn stove (low protein diet), with alfalfa-fed cows having higher concentration of D-glycerate in urine and creatine in milk. Glycine and serine are non-

essential amino acids and can be interconverted or converted to other amino acids (L-serine, L-threonine, L-aspartate) through several different biochemical reactions. This pathway was activated at OC3: glycine, L-cystathionine and D-glycerate (precursors) were in higher abundance in ULF at OC1 and at OC3 it shifted towards the products (particularly L-threonine and L-cysteine). Cysteine supplementation was reported to have a positive effect on embryo development *in vitro* (Caamano et al. 1998), whereas threonine was less abundant in ULF of pregnant compared to cyclic heifers at day 7 and 10 of pregnancy (Forde et al. 2014b), suggesting sizable consumption by the early embryo.

Other pathways approaching the threshold were "Inositol phosphate metabolism" (myo-inositol$^{\underline{\mathbf{OC1}}}$, D-glucuronate$^{\underline{\mathbf{OC1}}}$, activated in heifers with successful vs unsuccessful pregnancies (Salilew-Wondim et al. 2010), "Pyrimidine metabolism" (uridine$^{\underline{\mathbf{OC1}}}$, uracil$^{\underline{\mathbf{OC3}}}$, beta alanine$^{\underline{\mathbf{OC3}}}$) and "Galactose metabolism" (sucrose$^{\underline{\mathbf{OC3}}}$, lactose$^{\underline{\mathbf{OC1}}}$, alpha-D-galactose^{OC1}, D-glucose same^{OC1}, glycerol$^{\underline{\mathbf{OC1}}}$, D-mannose^{OC3}, myo-inositol$^{\underline{\mathbf{OC1}}}$).

Joint pathway analysis

One of the standard tools for multiomic functional and pathway analyses (IMPaLA) was used for joint pathway enrichment analysis of protein and metabolite abundances. This tool searches against 12 databases and employs an algorithm that requires more extensive manual curation than the other tools used in the present work. This is an important consideration when examining this kind of biological probing: pathway and functional analysis is meant to be the starting point for generating hypotheses and should not be taken as a definite explanation of the phenomena of interest but instead should form the basis of future experimental planning.

Because this method of analysis requires inputting a fold-change value for each compound, this tool was not suitable for pathway analysis of the EQ1 system for embryo classification or changes along days postpartum. Thus, differentially regulated pathways according to binary factors were used, i.e. oestrus cycle after calving and embryo systems EQ2 and EQ3.

The analysis of differentially regulated pathways between OC1 and OC3 resulted in 18 pathways or processes significantly impacted (Table 6-6 and Table S6-5), whereas no differential pathway was observed according to EQ2 (q=1, Table S6-6) and three pathways or functions were or tended to be differentially regulated according to EQ3 (q<0.1, Table S6-7). Potential implications are described next.

Table 6-6 Significantly impacted pathways and functions across oestrus cycles postpartum by joint Wilcoxon enrichment analysis of proteins and metabolites using ImPALA web tool v12.

	Proteins	Metabolites			Joint			
Pathway	**detected vs total (n)**	**p-value**	**q-value**	**detected vs total (n)**	**p-value**	**q-value**	**p-value**	**q-value**
Metabolism	126/1972	<0.001	<0.001	43/1384	0.004	1	<0.001	<0.001
Metabolism of lipids	19/664	<0.001	0.003	12/620	0.012	1	<0.001	<0.001
TCR (T cell antigen receptor)	24/245	<0.001	0.001	0/0	1	1	<0.001	<0.001
Immune System	113/1840	<0.001	<0.001	1/136	1	1	<0.001	<0.001
Neutrophil degranulation	68/490	<0.001	0.001	0/4	1	1	<0.001	0.001
Biological oxidations	16/231	<0.001	0.028	8/321	0.016	1	<0.001	0.003
Innate Immune System	98/1077	<0.001	0.001	1/99	1	1	<0.001	0.003
Metabolism of amino acids and derivatives	26/342	<0.001	0.006	22/285	0.406	1	<0.001	0.008
Gene expression (Transcription)	26/1373	<0.001	0.019	4/66	0.25	1	<0.001	0.017
JAK-STAT signalling after Interleukin-12 stimulation	16/36	<0.001	0.017	0/0	1	1	<0.001	0.018
Signal Transduction	67/2647	<0.001	0.204	16/271	0.025	1	<0.001	0.033
Glycolysis / Gluconeogenesis	17/68	<0.001	0.037	3/31	0.25	1	<0.001	0.034
Phase II - Conjugation	12/115	<0.001	0.204	7/148	0.031	1	<0.001	0.035
EGFR1	44/457	<0.001	0.035	0/4	1	1	<0.001	0.035
RNA Polymerase II Transcription	25/1236	<0.001	0.031	2/52	0.5	1	<0.001	0.038

Metabolic reprogramming in colon cancer	17/42	<0.001	0.237	8/35	0.039	1	<0.001	0.046
Metabolism of proteins	114/2008	<0.001	0.047	12/269	0.38	1	<0.001	0.046
Metabolism of carbohydrates	22/264	<0.001	0.237	16/137	0.051	1	<0.001	0.049
Generic Transcription Pathway	*23/1107*	<0.001	*0.065*	*2/49*	*0.5*	*1*	*0.001*	*0.073*
Cellular responses to stress	*29/345*	<0.001	*0.069*	*3/48*	*0.5*	*1*	*0.001*	*0.076*

Differentially regulated pathways between OC1 vs OC3

An unexpected finding was that, in the pathways and functions significantly impacted between OC1 and OC3, proteins within each pathway were consistently more abundant and metabolites less abundant at OC3. In pathway analysis, contrasting changes within a pathway are ubiquitous and reflect the static nature of these experiments, as we are still unable to model elusive dynamic changes in cells and biofluids (Kitano 2002). Metabolite abundance is also known to vary faster and to a higher degree than other biomolecules in response to system perturbations (Woelders et al. 2011). In addition, metabolites tend to participate in more different pathways and processes than proteins (Altmae et al. 2014), and thus protein trends might be more dependable in this case.

Most pathways identified as impacted were not biochemical routes but, rather, tissue- or organ-level processes and general GO functions (Gene Ontology Consortium 2019). Some terms were exceedingly general and may thus offer limited insight beyond what was described for the pathway analysis with metabolites alone (Table S6-4), particularly in metabolism (general metabolism, metabolism of lipids, of carbohydrates, and proteins, metabolic reprogramming in colon cancer). Metabolism of amino acids and derivatives as well as glycolysis/gluconeogenesis appear to be more active in the ULF environment earlier postpartum in relationship with an increased energetic need for tissue remodelling and fighting off pathogens (Esposito et al. 2014). The opposite trends between protein and metabolite abundances may signify a time-dependent process whereby higher amounts of metabolites upregulate protein expression, and this increase is only detected days or weeks after (Breier 1999). Some of these functions are examined next in the context of their potential influence on the embryo. Other general terms were RNA polymerase II transcription, gene expression

(transcription), and signal transduction. In line with the pathway analyses presented in Chapter 5, some interesting similarities point at differential regulation of immune signalling factors, with terms including “T-cell antigen receptor”, “innate immune system”, ”Jak-STAT signalling after IL-12 stimulation”, “EGFR1 (epithelial growth factor receptor 1)”. Other impacted processes include “phase-II conjugation” involved in detoxifying xenobiotics, “cellular responses to stress” and “biological oxidations”; the significance of most proteins in these processes to be more abundant in OC3 may reflect a physiological status better able to cope with oxidative stress (De Maio 1999), compared to earlier at OC1. For each of the impacted pathways, Tables S6-8a,b display the relative abundance between proteins and metabolites, respectively.

Differentially regulated pathways between pregnant and non-pregnant ULF (EQ3)

Results presented in Table 6-7 are somewhat less conclusive than previous pathway analysis findings due to their significance values ($0.05<q<0.1$) being above the previously established threshold ($q<0.05$). However, the exploratory nature of the present study justifies a short discussion. Three functions were found (“general metabolism”, $q<0.001$) or tended to be (“metabolism of proteins” and “EGFR1”, $q<0.1$) generally upregulated in ULF containing class IV-V embryos, i.e. non-pregnant according to the EQ3 classification system.

Table 6-7 Significantly dysregulated pathways and functions in non-pregnant uterine luminal fluid (ULF), i.e. EQ3 embryo quality IV and V (arrested at 1-16 cell state) by joint pathway enrichment analysis of proteins and metabolites.

	Proteins			Metabolites			Joint	
Pathway	**detected vs total (n)**	**p-value**	**q-value**	**detected vs total (n)**	**p-value**	**q-value**	**p-value**	**q-value**
Metabolism	125/1972	1.20E-05	0.0549	45/1384	0.00309	1	6.68E-07	0.000667
Metabolism of proteins	113/2008	0.000137	0.185	13/269	0.127	1	0.000209	0.069
EGFR1	44/457	8.66E-05	0.185	0/4	1	1	8.66E-05	0.078

Upregulation of “metabolism” and “metabolism of proteins” points to a heightened molecular activity in ULF, potentially caused by systemic metabolic stress and/or inflammation, of autoimmune or infectious origin (Gilbert 2019). This molecular hyperactivity results in excessive production of reactive oxygen species as a by-product of many chemical reactions and is generally associated with decreased viability in both somatic cells and embryos (Leese et al. 2007).

The trend for a general dysregulation of the EGFR1 pathway is particularly interesting as EGF regulates several processes essential for embryo development (cell cycle, transcription and apoptosis) and substantially increases bovine embryo blastocyst rate *in vitro* (Lonergan et al. 1996). This pathway consists of 322 compounds and 219 reactions, originating in the extracellular space and with signalling routes in cytoplasm, mitochondria and nucleus (Oda et al. 2005). Importantly, Katagiri and Takahashi (2004) reported dysregulation in this pathway (by marked differences in EGF concentrations in endometrial tissue) as a potential mechanism of subfertility in repeat breeder cows. Furthermore, Katagiri and Moriyoshi (2013) found evidence for progesterone and oestradiol regulation of EGF, signifying the importance of this signalling pathway for reproductive function.

Whereas the specific mechanisms affecting fertility within this pathway are not identifiable in a multiomics exploratory analysis like this, six proteins with the most contrasting patterns in the OC vs EQ3 pathway analyses were chosen for deeper scrutiny. That is, proteins higher in non-pregnant ULF and at OC1, or higher in pregnant ULF and at OC3, representing most likely indicators of poor and good uterine suitability, respectively. These were keratin 18, albumin, plectin, KIAA1217, E3 ubiquitin-protein ligase CBL, and actin-related protein 2 (Table S6-8c).

Keratin 18 (KRT18) is a cytoskeleton protein expressed in bovine embryos from the morula stage and considered a marker of trophectoderm specification (Madeja et al. 2013). Its expression was associated with improved quality and higher cell number of cloned bovine embryos (Bang et al. 2015). In addition, KRT18 gene knockdown reduced blastocyst formation but its function appears to overlap with other factors (Goossens et al. 2010). In the present work, the higher abundance of KRT18 protein in non-pregnant ULF (containing IV and V embryos) appears to be opposite to previous findings. Here, KRT18 might be fulfilling a different function in ULF, such as endometrial epithelium growth (Brewer et al. 2020), as suggested by its higher abundance at OC1, when uterine remodelling is more active (Scully et al. 2013).

Albumin is one of the most abundant proteins in both blood and ULF (Guise and Gwazdauskas 1987, Alavi-Shoushtari et al. 2006) and has well-known beneficial effects on embryo development, including as a carrier of embryokines, an amino acid source, and a regulator of pH, redox state and osmotic pressure (Otsuki et al. 2013). The involvement of albumin in the EGFR1 may be by eliciting pro-inflammatory responses, though this was reported in human kidney (Reich et al. 2005) and may not be relevant in this context.

Plectin is a cytoskeleton protein whose distribution in the rat uterine epithelium is regulated during the embryo implantation period and appears to modulate it (Png and Murphy 2002). In human, it appears to be important in endometrial epithelial integrity (Singh and Aplin 2015) and its expression is downregulated in women with endometriosis (Kao et al. 2003). Its function in bovine has not been

tested, though Papp et al. (2019) reported plectin to be the tenth most abundant protein in bovine OLF. Its higher abundance at OC3 and in good embryos suggests its potential as a biomarker for a receptive reproductive tract.

KIAA1217 is related to spinal embryonic development in mice (Kandasamy et al. 2010) and a mutation in its gene has been reported to be correlated to lower fertility in cow (Mesbah-Uddin et al. 2018). KIAA1217 expression was upregulated by ethanol exposure of porcine blastocysts *in vitro* (Pagé-Larivière et al. 2017). In their study, ethanol-induced oxidative damage resulted in lower proportions of blastocysts due to developmental arrest and activated oxidative stress control pathways (Pagé-Larivière et al. 2017). In the present work, the trend for a higher abundance of KIAA1217 in ULF of non-pregnant and OC1 indicates that a similar oxidative effect may have been present, due to other oxidisers.

E3 ubiquitin-protein ligase CBL is a regulator of numerous signalling pathways within immune and growth processes, and particularly relevant in apoptosis (Smirnova et al. 2009). A mutation in its gene causes development impairment in Ayrshire cattle (Venhoranta 2015). Here, the higher abundance of this protein in pregnant and OC3 ULF could be related to endometrial function.

Actin-related protein 2 abundance fulfils roles as transcription factor and DNA repair in addition to its function in the cytoskeleton (Nolen and Pollard 2007). Its inhibition by miRNA in bovine ovarian granulosa cells appeared to induce apoptosis necessary for normal follicular development (Ahmad 2014). The reasons for its higher abundance in non-pregnant and OC1 ULF remain unclear.

All in all, several processes were found that may underlie the distinct molecular environments of ULF at OC1 vs OC3, at the general metabolism, immune, and signalling-endocrine levels. Some of those processes appear to affect embryo fate, namely dysregulation of EGFR1.

Furthermore, differences observed when contrasting pathway analysis results from the different approaches (proteomics and metabolomics data alone, or jointly) may arise from the diverse types of data input, algorithms and the databases supported. Conducting pathway analysis by these tools resulted in a more comprehensive perspective of the range of processes potentially involved in uterine physiology and embryo development, though at the expense of low agreement between the results from each approach.

6.3.3 Experiment M5: metabolic fingerprinting

Quality control

In Exp. M5 using REIMS, both intra- and inter-batch variation was substantially higher than in experiments with GC-MS/MS (Exp. M4), likely caused by subtle differences in pressure applied when

operating the iKnife handheld device; these were adjusted by the LOESS method as described (Figure A-8-). Next, features present in blanks or with highest abundance in saline spiked with tracer were subtracted from all samples as a first processing step. A total of 3429 (2501) features were detected originally in positive (negative) ionisation mode, of which 1153 (550) features remained after excluding features in blanks (i.e. non-biologically relevant features) as explained above.

As previously observed in the preliminary test (Exp. M3), analysis in positive ionisation mode performed better than in negative mode, with cleaner burns and consistently high peak intensities. This is exemplified by peak areas per feature: average raw abundances and standard deviation were 62.1±28.2 arbitrary units for positive and 44.7±26.9 for negative ionisation mode.

Univariate analysis

Univariate analysis was performed as explained above for features acquired in both positive and negative ionisation modes and using the three embryo classification systems detailed above (Table S6-9). Feature abundance was only different between groups for seven features in negative ionisation mode (Table 6-8158). Potential identifications were assigned to three of those. It is important to bear in mind that the reliability of these putative identifications is lower compared to those obtained by tandem mass spectrometry instruments; for definite identification, a targeted (multiple reaction monitoring) method should be used (Ross et al. 2020). No statistically significant difference in abundance of features was detected in either positive or negative mode between OC1 and 3, EQ2 or EQ3 (data not shown).

Putatively identified compounds

Based on m/z of the ion features significantly different between class III embryos vs other embryo classes (under the EQ1 classification system), three compounds were tentatively identified. As explained earlier, definite identification requires either a tandem mass spectrometry method (i.e. with a fragmentation) or implementing some method of orthogonal separation (e.g. ion mobility chromatography (Kyle et al. 2016), therefore caution needs to be exercised when extracting conclusions from these putative identifications.

Arachidyl-behenate is a wax monoester found in higher abundance in ULF harbouring class III embryos compared to classes IV or V. There is evidence of this metabolite class to be important in defence (Rawlings 1995) and they make up a substantial proportion of the *vernix caseosa*, the waxy, white substance covering new-born human babies, and also cows, though in smaller amounts (Parrish and Fountaine 1952).

Another compound, putatively identified as 2-methyl-1,3-thiazolidine-2-carboxamide, was significantly lower in ULF containing grade 3 embryos compared to 1-16 cell embryos. This

metabolite has been putatively identified in human samples but not empirically confirmed. Its biological function has not been defined; however, a close structural analogue, AS604872 ((2S)-3-([1,1'-biphenyl]-4-ylsulfonyl)-N-[(R)-phenyl(2-pyridinyl)methyl]-1,3-thiazolidine-2-carboxamide) is a drug used as an PGF_2-alpha (prostaglandin) antagonist and has been shown to inhibit uterine contractions (Chollet et al. 2007). Whether 2-methyl-1,3-thiazolidine-2-carboxamide is acting as a prostaglandin antagonist in the ULF in the present study demands further investigation.
Finally, a compound putatively identified as a prostaglandin or phospholipid was found in higher abundance in ULF harbouring class III embryos. As discussed in the attached review paper (Aranciaga et al. 2020), these lipids fulfil crucial functions relevant to fertility and many have been found specifically associated to uterine suitability, including 1-stearoyl-GPC (18:0) and 1-palmitoyl-GPC (16:0), both increased by exogenous progesterone supplementation at days 12-13 post ovulation (Simintiras et al. 2019b).

Table 6-815 Features detected in REIMS (negative ionisation mode) at a significantly different abundance between ULF harbouring embryos of different grade (EQ1) by Kruskal-Wallis test. Abbreviations: MW, molecular weight; III, grade 3 embryos; IV, 4- to 16-cell embryos; V, 1 cell embryos

p-value	q-value	m/z	Trend	Potential id	HMDB
>0.001	0.001	539.6951	III>rest	None	N/A
0.005	0.001	626.6677	III>rest	None	N/A
0.001	0.003	533.7749	III>rest	None	N/A
0.003	0.016	655.6149	III> (IV, V)	Many; arachidyl behenate (fatty acid ester)	LMFA07010061
0.007	0.043	825.5636	III>rest	Many (phospholipids/prostaglandins)	HMDB0010611
0.01	0.049	181.0208	III< (IV, V)	2-methyl-1,3-thiazolidine-2-carboxamide	HMDB0062599

Fingerprinting related to embryo quality – multivariate analysis and modelling

PCA was performed to gain an overview of the samples. No clustering was observed when colouring the samples by oestrus cycle or embryo quality by any of the described classification systems (EQ1, EQ2, EQ3) in positive (Figure A-8-) or negative (Figure A-8-) ionisation mode.

Models based on OPLS-DA did not present potential to predict embryo quality (i.e. negative values for the Q^2 parameter) using features from either ionisation mode or both together (Table 6-).

To sum up, Exp. M5 was conducted analysing ULF samples of all cows in Farm Trials 2 and 3 with the goal of obtaining a rapid metabolic fingerprint that could help assess parameters of interest. While good quality molecular spectra were generated, very limited correlations were observed between spectral features and the variables analysed. This suggests that the technical variation and low sensitivity associated with this instrumental setup may not be optimal for metabolomic measurements of ULF. In a study investigating meat metabolite fingerprinting using the REIMS detector, replacing the standard handheld sampling device (as was used here) for a robot-operated laser system improved the signal-to-noise ratios 17-fold and the model classification accuracy two-fold (Genangeli et al. 2019), offering an appealing possibility for further studies like the present. Other slightly more laborious but comparably versatile tools, such as direct analysis in real time-mass spectrometry (DART-MS), can achieve excellent detection sensitivity at the expense of minimum sample preparation required (Gross 2014) and may be more suitable for ULF metabolic fingerprinting.

6.4 Summary, further remarks and conclusions

Two experiments were carried out to survey the ULF metabolome from different angles: Experiment M4 based on GC-MS/MS to quantify known metabolites, and Experiment M5 to obtain a rapid metabolic fingerprint. One of the goals of these experiments was to obtain insight on important metabolic processes affecting embryo quality (with further integration with proteomics data in the targeted analysis), and to shortlist potential biomarkers of uterine suitability for pregnancy, encompassing embryo phenotype observed and number of oestrus events after calving (OC). Whereas no direct significant association was observed between metabolite abundance and embryo quality, the abundance of several metabolites was found to differ across time postpartum and this may be useful for assessing the metabolic status of the animals and, by extension, allowing estimating their readiness for pregnancy. Further studies are needed for empirical validation of these findings. Alternatively, it is possible that the metabolic mechanisms most directly regulating embryo development implied chemical classes with relatively low coverage in the metabolite package used. Two of those groups evidenced to play important endocrine and metabolic roles in the oviductal and uterine environments are fatty acids (Ribeiro et al. 2016c) and phospholipids (Belaz et al. 2016, Banliat et al. 2019a, Simintiras et al. 2019b). Improving coverage by the use of two or more orthogonal (complementary) technologies is generally recommended (Goldansaz et al. 2017). This could be attained by concomitant analysis using instrumental techniques such as LC-MS/MS (both the typical reverse-phase setup and the rapidly rising hydrophilic interaction liquid chromatography ;

Tang et al. 2016). As mentioned in Chapter 1, a key aspect of metabolomics is that no single technique can detect more than a few classes in this heterogenic realm, compared to other omics (Bedair and Sumner 2008, Álvarez-Sánchez et al. 2010, Beale et al. 2018).

Analyses from Chapters 5 and 6 showed some indications of the ULF molecular influences on embryo viability, and an indirect influence of time postpartum. Yet, the limited agreement in impacted pathways and processes between proteins and metabolites suggest that embryo quality is at least partly determined through processes not measured herein. Based on the copious literature on early pregnancy loss (Artus et al. 2020, Rodríguez-Alonso et al. 2020b), it is hypothesised that the interaction of oocyte, oviductal and uterine factors at different degrees determine embryo quality phenotype at day 7.

Another goal was to examine the feasibility of using analysis by one or both instrumental platforms for predictive modelling of embryo quality based on metabolite features in ULF. PCA and OPLS-DA of the metabolomic, proteomic or joint data delivered models with good fit but limited prognostic potential. The implications of these results and suggested avenues for improvement are presented in Chapter 8.

7

In vitro embryo culture

7.1 Introduction

For empirical validation of the two proteins (cystatin C and pyruvate kinase M) shortlisted as most relevant to embryo development in Chapter 5, a set of *in vitro* embryo culture experiments was conducted to directly test the protein effect on the embryo. Additionally, to test the potentially embryo-protective effect of cystatin C (CysC), one of its most typical antagonists *in vivo* (cathepsin B, CatB) was also assayed.

7.1.1 Background

Embryo culture *in vitro* is a widely used biotechnology for applications such as increased genetic gain and improvement in cattle and other livestock, as well as for fertilisation and developmental research (Camargo et al. 2006). Extensive research on *in vitro* reproductive technologies has resulted in significant progress in the efficacy of their application; standard procedures for *in vitro* maturation (IVM), *in vitro* fertilisation (IVF) and *in vitro* culture (IVC) have become less complex and result in high proportions of transferable quality embryos (Block et al. 2009).

An *in vitro* model was deemed suitable for testing the effect of those proteins. Although there are clear discrepancies in embryonic outcome between *in vivo* and *in vitro* grown embryos (Rizos et al. 2002), embryo culture is an extensively validated process that allows a high degree of control over the conditions in which an oocyte progresses to become a blastocyst around day 7 after fertilisation (Tríbulo et al. 2019), matching the time course for this *in vivo* trial.

As stated in Chapter 5, two potential biomarkers were selected for biological validation *in vitro*: pyruvate kinase M2 (PKM2) and cystatin C (CysC). As explained earlier, PKM2 is a protein involved in regulatory processes aside from its classical role in the glycolysis pathway (Mazurek et al. 2005), including immunity regulation and tumour differentiation (Luo and Semenza 2012). CysC is a protease inhibitor, prominently expressed in mammal reproductive tissues and with sperm-capacitation function in humans (Lee et al. 2018), and regulated by interferon tau (IFNT) in cows, thus likely important in embryo development (Spencer et al. 2007). Importantly, it is widely reported to protect the embryo from damage by proteases, one of which is cathepsin B (CatB; Baston-Buest et al. 2010). CatB was included as a test protein in the present set of experiments to help determine a protective function of CysC that would otherwise not be apparent in the absence of the detrimental effect of a peptidase.

Cathepsin B

CatB is a cystatin-peptidase involved in numerous physiological processes, including apoptosis, inflammation, protein metabolism, hormone processing and immunity (Turk et al. 2012). As discussed in Chapter 5, alterations in the balance between cathepsins (peptidases/proteases) and cystatins (protease inhibitors) result in a variety of disorders (reviewed by Kos et al. 2014) including disruption of embryo implantation in mice (Afonso et al. 1997).
In cows, increased CatB concentration is associated with autophagy in *in vitro* matured oocytes (Li et al. 2019). High expression and activity of CatB were found in poor quality bovine embryos growing *in vivo*, and this effect was reversed *in vitro* by supplementing E-64, a synthetic inhibitor of multiple proteases, among which is CatB (Balboula et al. 2010). Similar observations were reported by Yamanaka et al. (2018) examining developmental competence of bovine embryos affected by heat shock.

CatB was not detected by untargeted proteomic analysis in the present study, possibly because of a combination of low relative amount and co-elution with more abundant proteins. This is a feature of data-dependent acquisition mass-spectrometry discussed earlier when examining the relatively meagre overlap between proteins identified in different studies (Section 5.3.3). However, CatB is a well characterised component of uterine secretions, having been reported in several studies of bovine reproductive tract (Mullen et al. 2012, Harlow et al. 2018, Helfrich et al. 2020) and in other mammals such as rat (Balan et al. 2001), pig (Song et al. 2010) and human (Dasari et al. 2007).

Technical considerations

The concentration ranges of the proteins to be tested were estimated from literature. For CatB this was 15-90 ng/ml based on the results of Tsai et al. (2009) whereas for PKM and CysC the concentrations chosen span the typical range tested in similar experiments (Saugandhika et al. 2015, Gomez et al. 2017, Algarra et al. 2018), i.e. 0.1-10 μg/ml. Regarding the time of application, no protein was added before day 2, i.e. in which the first embryo cleavages are expected. This was decided so that fertilisation failure, chiefly dependent on oocyte quality (Rizos et al. 2002) would not obscure effects of the proteins added in the culture medium. CysC and CatB were added at both day 2 and day 5 (at early and late embryo culture, i.e. the oviductal and uterine phases), whereas PKM was added at day 4 to coincide with the time when embryos enter the uterus *in vivo* (Hackett et al. 1993).

Another important consideration was the source of the proteins tested. Proteins expressed in mammalian cell lines or of mammalian origin to *in vitro* embryo culture are more biologically relevant compared to more economical alternatives (e.g. *Escherichia coli* and *Saccharomyces cerevisiae*), primarily due to abnormal patterns of folding and post-translational modifications in

unicellular organisms (Berlec and Štrukelj 2013). Thus, proteins that were expressed from mammalian cell lines were chosen. Due to the lack of suitable bovine alternatives, human CatB (homology to bovine 83.6%), human CysC (66.4% overall homology to bovine, >90% homology in N-terminal and C-terminal active sites), and mouse PKM (96.4% homology to bovine) were used.

This set of experiments was designed in two stages, the first experiment added each of the test proteins individually to IVC medium (three replicates). Depending on the outcomes of those experiments, a second stage would be conducted using an appropriate concentration of the test proteins.

7.1.2 Aims

The experiments in this part of the project were conducted to test the effect of selected proteins at several concentrations on key parameters of embryo development *in vitro*, early embryo development, kinetics of development to day 5, and embryo development to day 7, and to create an activity curve based on the concentration of any protein(s) shown to affect embryo development.

7.2 Materials and methods

Briefly, three experiments, each testing the effect of one of the selected proteins, were carried out in triplicate. Embryo experiment 1 ("Exp. E1") tested the effect of CysC on proportion of a) cleaved embryos , b) degenerate embryos less than eight cells, c) degenerate embryos greater than eight cells , d) tight morulae and blastocysts (TM-B), e) total blastocysts (B), and f) blastocysts of grade 1 or 2 (B1-2). Proportions of B and B1-2 were evaluated at day 7. Embryo experiments 2 and 3 (Exp. E2 and E3) evaluated the same criteria to assess the effect of CatB and PKM, respectively.

7.2.1 Reagents and consumables

In this section, consumables and media used are listed. Then, subsections for each experimental stage present the equipment, consumables, and media reagents employed.

Costar® plastic Stripettes were acquired from Sigma (St. Louis, MO, USA). Pasteur (glass) pipettes were acquired from Interlab (Wellington, NZ); Falcon® polystyrene petri dishes 30 and 60 mm were acquired from Corning Inc. (Corning, NY, USA) and 90 mm-sized petri dishes from Citotest (Haimen, China). Mineral oil used was Light oil (Sigma, St. Louis, MO, USA). Base culture medium: TCM-199 with Earl's salts and L-glutamine, without sodium bicarbonate, was bought from Gibco 31100035, Life Technologies, Auckland. This is a standard base medium containing a mixture of vital nutrients, including energy substrates, amino acids, vitamins, and minerals (details in Table S7-1). *In vitro*

fertilisation and embryo culture media was prepared in house and based on Synthetic Oviduct Fluid ("SOF"; Tervit et al. 1972) modified by Thompson et al. (2000).

Oocyte recovery (aspiration medium):

Sterile 15 ml Falcon® polypropylene conical centrifuge tubes were bought from Corning Inc. (Corning, NY, USA). Oocytes were recovered under vacuum using a sterile bung and blunt needle (18" gauge) developed and crafted in-house. Aspiration pump was a Cook Veterinary Products model VMAR 5100 (Cook, SA, Australia) and active vacuum was 40 to 45 mm Hg of negative pressure. Sterile 0.9% saline solution was bought from Baxter (Toongabbie, NSW, Australia). Aspiration medium H199: HEPES-buffered version of TCM 199 comprising 20 mM HEPES, 5 mM $NaHCO_3$, 50 µg/ml kanamycin sulphate (Sigma K1377) supplemented with 2% fetal calf serum (v/v; Moregate, Australia NZ Batch 48827103) and 1.85 µl/ml of liquid heparin (Multiparin, 5000 international units/ml).

Oocyte maturation (IVM medium):

Stock solutions: TCM 199 + 10% Foetal calf serum supplemented with 10 µg/ml porcine follicle stimulating hormone (Folltrophin V; Bioniche), 1 mg/ml oestradiol (Sigma) and 10 mM/ml cysteamine (Sigma). Final concentrations were 10 µg/ml follicle stimulating hormone, 1 µg/mL oestradiol and 10 µM of cysteamine. H-199: see above under oocyte recovery. B-199: TCM-199 medium supplemented with 25 mM sodium bicarbonate, 0.33 mM sodium pyruvate, 10 % (v/v) foetal calf serum (FCS).

Fertilisation (IVF-SOF medium):

IVF-PPHH: IVFSOF supplemented with 1 µl/ml heparin, 1 µl/ml pyruvate and 10 µl/ml 1-penicillamine-hypotaurine. Final concentrations were 10 µg/mL of heparin (Sigma H3149 100KU), 1 mM of pyruvate (Sigma P4562), 10 µM hypotaurine (Sigma H1384) and 20 µM penicillamine (Sigma P4875). HSOF: HEPES buffered (20 mM Hepes, 5 mM $NaHCO_3$) synthetic oviduct fluid (SOF) medium supplemented with 8 mg/ml bovine serum albumin (IVP grade, gamma irradiated, MP Biomedicals NZ, Auckland). Nidacon Bovipure™ and Bovidilute™ were purchased from Tek-Event, Sydney, NSW, Australia.

In vitro culture

Modular incubator chamber MIC-101 (Lab supply, NZ) for culture in low O_2 environment was placed in Contherm Biocell (Model 1200, Thermofisher, NZ) for *in vitro* culture. ESOF/LSOF (early/late synthetic oviduct fluid) is a biphasic media (Thompson 2000) supplemented with 8 mg/ml BSA: LSOF contains 10 µM of 2,4-dinitrophenol (DNP; Aldrich D198501). Modified ESOF and LSOF (mESOF and mLSOF) were ESOF/LSOF without BSA, supplemented with 1 mg/ml polyvinyl alcohol (PVA; Sigma

P8136) with the addition of CatB or CysC. Modified LOSF for PKM was LSOF without 2,4-dinitrophenol added.

Proteins

Recombinant human CatB (CTSB) protein was acquired from Creative Biomart (Shirley, NY, US). Segment: Arg18-Ile339, fused to His tag at C-terminus, was expressed in a human 293 cell line (HEK293). Human CysC (CSTX) purified from human urine was bought from Byorbyt (Cambridge, UK), kept in ammonium bicarbonate (NH_4HCO_3) buffer. Recombinant mouse pyruvate kinase (PKM) protein was acquired from Cusabio Technology (Houston, TX, US) at a purity of at least 90% and treated for endotoxin removal; no specific isoform was available (i.e. isoform M2), however homology of the protein purchased to bovine PKM2 was 96%. It was N-t 10xHis-tagged and C-t Myc-tagged was expressed in a mammalian cell line and kept in Tri-based buffer with 6% trehalose.

7.2.2 Experimental procedures

Ovaries were sourced from local abattoirs predominantly from Friesian, Jersey, or Friesian–Jersey cross dairy cows. Oocytes were aspirated, matured, and fertilised using standard *in vitro* embryo production (IVP) techniques (Thompson et al. 2000). Furthermore, presumptive zygotes were cultured *in vitro* for 24 h in ESOF to ensure a homogenous population of embryos were selected ($\geq$4-cells). These embryos were transferred into mESOF which included one of the potential biomarker proteins (as determined in chapter 6) to test their effect on embryo development. Embryos were transferred to mLSOF on day 5 of *in vitro* culture (fertilisation = day 1) and graded on day 7.

All media and culture plates were prepared in a laminar flow hood using a pipettor and sterile pipette tips. Ovaries were collected and maintained in saline solution at 30 °C. Oocyte/embryo manipulations were performed on a warm stage of the stereomicroscope set at 37.5±1°C.

For reference, day of IVF is considered day 1, whereas the day into culture is day 2. Figure 7-1 provides a schematic representation of the experimental steps undertaken.

Oocyte recovery

Bovine ovaries collected at the abattoir in thermos flasks filled with pre-warmed (30 °C) 0.9% saline solution were transported back to the aspiration lab within 1 h. The ovaries were rinsed with warm (30 °C) saline solution twice to remove blood and miscellanea tissue and fluid. Follicles between 3 and 10 mm in diameter were punctured with an 18” blunt needle and the follicular fluid plus the cumulus cell oocyte complex (COC) were collected in 15 ml conical tubes containing 1.5 ml of pre-warmed aspiration medium under vacuum.

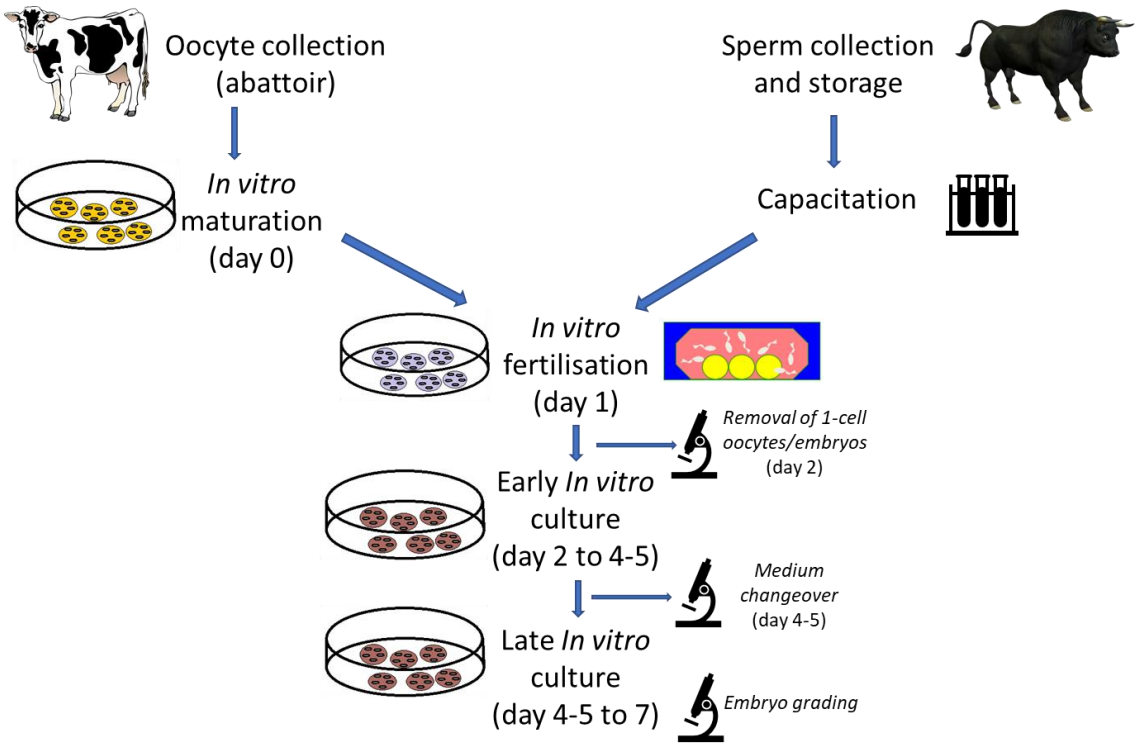

Figure 7-1 Experimental workflow of this embryo culture experiment.

Maturation (IVM) day 0

A 60 mm sterile plastic petri dish containing 12 x 40 µl drops of IVM medium were overlaid with 8 ml pre-gassed mineral oil and pre-equilibrated for 2 h at 38.5 °C and 5% CO_2 prior to aspiration.

The pellet resulting from aspiration, containing the COCs, was transferred to a 90 mm petri dish containing fresh aspiration medium. The contents of the dishes were searched for COCs, and these were transferred into a 35 mm petri dish containing 3 ml H199 + 10% FCS. High quality COCs were selected based upon morphological characteristics previously described by Thompson et. al. (2000). The selected COCs were washed once in 3 ml H199 + 10% FCS, followed by a final wash in 3 ml of B199 + 10% FCS. Groups of 10 COCs in a 10 µl total volume were placed into a 40 µl IVM medium drops (total drop volume 50 µl) and incubated for 20-22 h at 38.5 °C under 5% CO_2 in air.

Fertilisation (IVF, day 1)

Oocyte and plate preparation for IVF

A 60 mm sterile plastic petri dish containing 12 x 30 µl drops of IVFSOF medium was overlaid with 8 ml pre-gassed mineral oil and pre-equilibrated for 2 h at 38.5 °C and 5% CO_2 prior to gamete addition. To prepare oocytes for IVF, they were removed from the IVM drops using a 200 µl pipettor and transferred to a wash 35 mm petri dish containing warm HSOF. The oocytes were transferred to a second wash dish of HSOF and then to a third 35 mm petri dish of equilibrated IVFSOF. Five oocytes

in 10 µl of IVFSOF medium were transferred into each IVF drop awaiting sperm addition. The IVF plate was placed in an incubator (38.5 °C and 5% CO_2 in air) awaiting sperm addition.

Semen preparation

Frozen– thawed spermatozoa from the same Friesian bull as in Farm Trials A, B and C (Blitz GL295 @ 1.5 million sperm/ml) was used throughout the entire data set.

To obtain healthy, motile sperm and exclude immotile or abnormal sperm, white blood cells and miscellanea components of semen a two-layer gradient for density gradient centrifugation was performed. Frozen-thawed sperm was placed on a Nidacon Bovipure™ gradient of colloidal silica particles and then centrifuged, causing spermatozoa to precipitate to the bottom of the tube. In this system, the sperm with the best motility and intact morphology tend to accumulate towards the bottom (Moohan and Lindsay 1995). Briefly, a 1 ml, two-layer gradient of 40% and 80% Bovipure™ gradient was prepared according to manufactures protocol. To make the gradient, 0.5 ml of 80% solution was pipetted into a 15 ml conical centrifuge tube and carefully overlaid with 0.5ml of 40% solution. This Bovipure™ gradient was used for sperm selection as explained next.

Sperm straws (stored in liquid nitrogen at -80 °C) were thawed in a water bath 30-35 °C for 30 s, dried with a tissue and wiped with ethanol (70% v/v). Next, the contents of the straw were emptied into a sterile 5 ml Falcon tube. Using a sterile glass Pasteur pipette, the thawed semen was aspirated and gently laid on top of the Bovipure™ gradient. The gradient was centrifuged at 300 *g* for 15 min. During centrifugation oocytes were prepared for IVF as described in the previous section. Immediately after centrifugation, the gradient supernatant was aspirated with a sterile Pasteur pipette and discarded. A clean Pasteur pipette was used to carefully remove the sperm pellet at the bottom of the centrifuge tube and transfer the sperm to an empty tube. One ml of HSOF was carefully added, mixed gently, and centrifuged at 300 *g* for a further 5 min. Immediately after centrifugation, the supernatant was removed, and the sperm pellet was resuspended in 200 µl of equilibrated IVFSOF medium. A 10 µl aliquot of this was diluted 1:20 with water for sperm count; the remaining volume of the sperm preparation was measured for subsequent calculations.

The sperm concentration of the diluted aliquot was estimated using a haemocytometer. This consists of a counting chamber and a cover glass and is commonly used to determine the concentration of cells in any fluid medium. To fill the counting grids, 10 µl out of the diluted sperm solution were introduced into each side. The haemocytometer was then placed under the microscope and the spermatozoa heads in 25 large squares (i.e. 400 small squares) were counted at 400x. The counts in both sides were averaged, and the sperm concentration calculated using the following formula:

$$\frac{Vol.measured\ of\ undiluted\ sperm(A) \times Average\ number\ of\ sperm\ counted(B) = Total\ volume(C)}{37.5\left(dilution\ factor\ for\ 1.5million\frac{sperm}{ml}\right)}$$

$$Total\ Vol.(C) - Vol.undiluted\ sperm\ prep. = Vol.of\ IVF\ media\ add(D)$$

$$Number\ of\ fertilised\ group\ IVF\ drops\ (E) \times insemination\ Vol.(F) = Total\ Vol.of\ sperm\ prep.for\ group\ IVF(G)$$

Figure 7-2 Formulae for adjusting sperm preparation for *in vitro* fertilisation experiments.

Sperm, 10 µl (i.e. 15,000 spermatozoa), was added to each 40 µl drop containing five oocytes for a final drop volume of 50 µl. The final sperm concentration was 3,000 spermatozoa per oocyte. The plates were placed in an incubator for 24 h at 38.5 °C and 5% CO_2 in air.

In vitro embryo culture (IVC, day 2)

The following day, embryos (25-55 per treatment, balanced per treatment in each run) were placed in culture for six days in a gassed modular incubator chamber. A modular incubator chamber was set up by placing a small amount of sterile water at the bottom (to humidify), sealed, and kept at 38.5 °C in a hot air incubator. An indicator plate of B199 + FCS was placed in modular incubator chamber to monitor the chamber's pH environment. In detail, IVC plates were prepared by making 20 µl drops of ESOF x 5 with a central wash drop of 40 µl in a 35 mm petri dish. The drops of medium were overlaid with 3 ml of gassed mineral oil and placed in the modular incubator chamber, gassed for 5 min (5% CO_2, 7% O_2, 88% N_2) to purge atmospheric air and returned to incubator running at 38.5 °C.

On day 2 (24 h post-fertilisation), the cumulus cells were removed from the presumptive zygotes. This was accomplished by transferring the embryos to an Eppendorf tube containing HSOF, vortex-shaking for 2 min and centrifuging briefly. The bottom half of the medium which contained the zygotes, was transferred to 35 mm petri dish containing HSOF. The Eppendorf tube was rinsed once with HSOF, quickly centrifuged and the entire tube contents was placed into the 35 mm petri dish containing the cumulus free zygotes. Zygotes were washed twice by placing into 35 mm dishes containing 2.5 ml HSOF. After the final wash, zygotes were transferred into a central wash drop of an IVC plate. Embryos in groups of 10 were moved to drops and plates were placed in the modular incubator chamber and re-gassed for 5 min (in an atmosphere of 5% CO_2, 7% O_2, 88% N_2) and returned to an incubator. On day 2, only embryos ≥ 4 cells were transferred into fresh mESOF drops with the addition of the test proteins where applicable (for Exp. E1 and E2). The number of unfertilised oocytes and 1 – 3 cell embryos was recorded and not cultured further. On day 5 (CysC and CatB, i.e. Exp. E1 and E2), embryos were changed to fresh drops containing mLSOF medium supplemented with a test protein when applicable. For this, mLSOF plates were equilibrated in the

gassed modular incubator chamber overnight, embryos were transferred from IVC plates to the central wash drops of new plates and then into culture drops. Cleavage and tight morula rates were recorded, plates were returned to the modular incubator chamber, re-gassed, and cultured for a further two days. In Exp. E3 (testing PKM), on day 4 only embryos at ≥ 8-cell stage were taken through to mLSOF, in controls and treatments, to test the effect of this protein after the oviduct phase. This was decided to prevent potential differences in bioavailability of pyruvate in the medium that could affect embryo metabolism, which was not the focus of this study.

On day, 7 plates were removed from the modular incubator chamber for embryo development scoring. In a similar fashion as detailed in Chapter 2, the number (proportion) and quality of the following phenotypes were recorded: oocytes, cleaved embryos, tight morulae, blastocysts, hatched blastocysts. Tight morulae and early blastocysts were cultured for a further 24 h (i.e. day 8) to determine if they develop to the blastocyst stage and were re-graded.

The experimental design was as follows (Figure 7-3). In Exp. E1, controls adding BSA (as per typical protocol in the laboratory) were included, but similar results with the controls without BSA were observed (Table S7-2) therefore these were not included in subsequent runs.

A dilution control (i.e. adding to each IVC drop 15 µl of distilled, sterile water) was included in Exp. E2 to test for a potential effect of the addition of the small volume of liquid containing a protein. No effect of dilution was found (i.e. similar proportions of embryo development were observed between standard controls and dilution controls). Therefore, these were further treated as replicates of the standard controls.

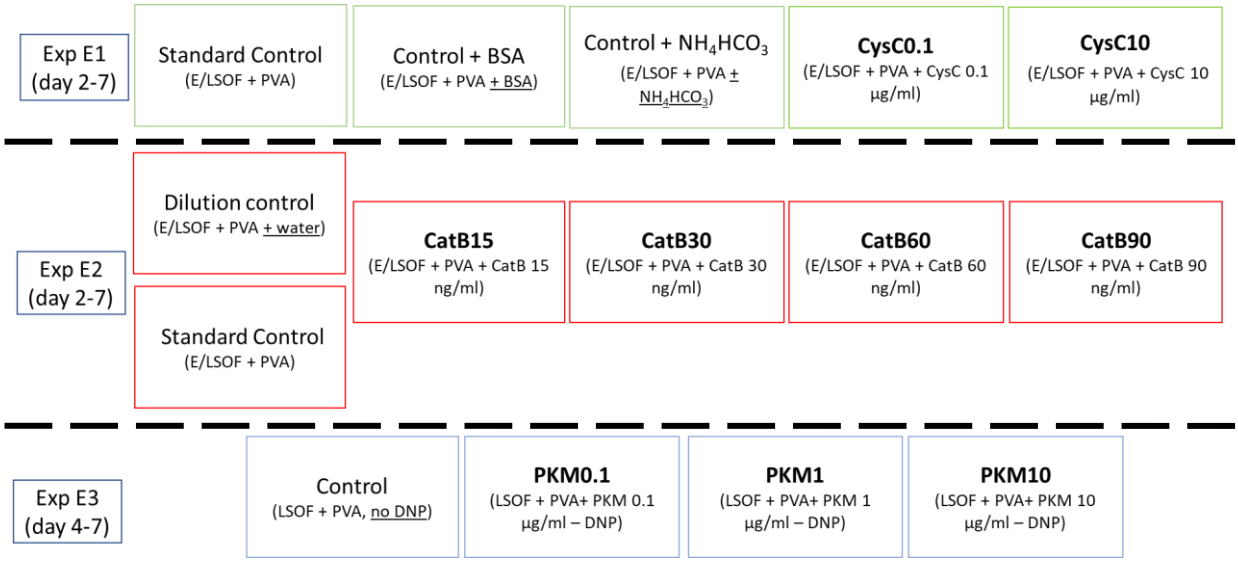

Figure 7-3 Overview of Embryo experiments 1-3 (Exp. E1-3): composition of the controls and treatments in each experiment. Treatments (addition of the test proteins) occurred from day 2 to 7 (Exp. E1 and E2) or day 4 to 7 (Exp. E3). Abbreviations: BSA, bovine

serum albumin; CatB, cathepsin B; CysC, cystatin C; DNP, 2,4-dinitrophenol; E/LSOF, Early/late synthetic oviduct fluid; PKM, pyruvate kinase M; PVA, polyvinyl alcohol.

In embryo experiment 1 ("Exp. E1"), CysC was dissolved in a buffer containing ammonium bicarbonate, with known detrimental effects on embryo quality (Gardner and Lane 1993) because of recommendations form the protein supplier. Therefore, a control containing the maximum concentration of NH_4HCO_3 used (1mM) was added.

Statistical analysis

Outcome variables (i.e. proportions) were logit-transformed, i.e. to the natural logarithm of the odds ratio, logit(p) = ln(p/(1-p)). They were then checked for normality of distribution. Experiments E1, E2 and E3 (testing the effect of each of the proteins, CatB, CysC, and PKM) were analysed separately. Generalised linear regression models and ANOVA were performed using R 4.0.2 (R Team 2019) as follows:

For experiment E1 (CysC): **Var ~ CysC concentration + Run + NH_4HCO_3 concentration**

For experiment E2 (CatB): **Var ~ CatB concentration + Run**

For experiment E3 (PKM): **Var ~ PKM concentration + Run**

In each case, the test protein concentration was included as the main explanatory variable and run was added as a random effect, whereas "Var" is the (logit-transformed) variable, i.e. % of one cell oocytes/embryos at day 2, % developed to TM on day 5, % total development to TM-B on day 7, % B at day 7, % B1-2 at day 7, % of embryos less than 8 cells at day 7, and % of embryos greater than 8 cells (degenerate or morulae stage) at day 7.

7.3 Results and discussion

7.3.1 Descriptive parameters across experiments

Three experiments were conducted in triplicate, each testing the effect of one target protein. The first steps of the experiments were identical; treatments were conducted differently from the timepoint of medium changeover at day 4 (Exp. E3) or day 5 (Exp. E1 and E2).

A total of 1802 oocytes were cultured in the three experiments; the raw data is displayed in Table S7-2. Out of those, at day 2, 79 oocytes or 1-cell zygotes were removed to eliminate the confounding effect of oocyte quality on embryo development (Table 7-1). Thus, the overall cleavage rate, i.e. in which embryonic cell division was observed, was 94.1% (1690 embryos out of 1802 oocytes placed into culture). A midway determination of development kinetics showed that 21.6% of the embryos

had reached the tight morula stage by day 5. Replicates from Exp. E3 were not included in this calculation as they were transferred to fresh mLSOF at day 4.

The overall rates of development at day 7 of culture were as follows: 20.4% (257/1259) embryos of had arrested ≤ 8 cell stage, 22.8% (287/1259) embryos > 8-cell (including degenerate and morulae), and 56.9% (716/1259) transferable embryos (i.e. tight morulae and blastocysts, TM-B). The proportion of blastocysts (B) out of all or viable embryos was 44.2% (557/1259) and 77.78% (557/716) respectively. Blastocysts of grades 1 and 2 (i.e. of transferable quality, B1-2) were 26.4% (332/1259) and 46.41% (332/716) of all or viable embryos, respectively. Most development parameters observed were better than those reported in similar recent studies (Table S7-3): cleavage was 94.1% (vs 73%), 56.9% (vs 44%) TM-B/cleaved embryos, B/cleaved embryos (44.2% vs 31%), while the proportion of B1-2/cleaved embryos (26.4% vs 39%) was worse than the two studies that reported it (Zullo et al. 2016a, Zullo et al. 2016b). However, the media used in the latter studies (Zullo et al. 2016a, Zullo et al. 2016b) were supplemented with bovine serum, BSA and hormones, all of which is known to improve embryo development (Thompson et al. 2000, Gilardi et al. 2004, Camargo et al. 2006) and thus are not directly comparable to the present study. To sum up, the experimental setup of these embryo culture experiments was of comparable quality to those reported in similar studies.

Table 7-1 Overall combined embryo development parameters at day 7 of *in vitro* culture throughout the experiments described in this chapter.

Day	Variable	Proportion		Percentage		Average from literature	
2	Cleavage rate (>1 cell)	1259/1338		94.1		73	
5	*Tight morulae (kinetics)*	*365/563**		*64.8*		*N/A*	
7	≤8-cell	257/1259		20.4		N/A	
7	> 8-cell degenerate and morulae	287/1259		22.8		N/A	
7	Tight morulae and blastocysts (TM-B)	716/1259		56.9		44	
		of TM-B	**of cleaved embryos**	**of TM-B**	**of cleaved embryos**	**of TM-B**	**of cleaved embryos**
7	Blastocysts	557/716	557/1259	77.8	44.2	N/A	31

7	Blastocysts grades 1 and 2	332/716	332/1259	46.4	26.4	N/A	39

*in experiment E3, medium changeover occurred at day 4 and thus is not included in this calculation.

7.3.2 Effect of the test proteins on *in vitro* embryo development

The three proteins tested were not found to exert a clear, concentration-dependent effect on the embryo development parameters measured (Table 7-2, Table 7-3 and Table 7-44). Generalised linear model analysis showed similar figures, with the following differences. Higher %TM-B (p=0.04) and %B (p=0.07) at day 7 in CysC0.1 (Table S7-4a), of a complex interpretation because of the interaction effect of ammonium bicarbonate, as examined later. Lower development to TM at day 5 was observed in CatB15 (Table S7-4b), which however did not result in any difference at day 7. Lastly, a tendency (p<0.1) for lower proportion of TM-B at day 7 was found in PKM1 (Table S7-4c), though a difference was only observed in replicate 3 (Table S7-2), precluding confident conclusions.

Table 7-2 Effect on embryo development parameters of different concentrations of CysC and ammonium bicarbonate in culture medium by generalised linear models. Results expressed as mean percentage (to total embryos cleaved) ± standard deviation. Green (red) font: positive (negative) parameters. Abbreviations: B, blastocyst; B1-2, blastocyst grade 1 or 2., CysC, cystatin C; deg, degenerate; dev., development; TM, tight morula.

CysC (µg/ml)	**0**		**0.1**	**10**	**p-value (CysC)**		**p-value (interaction)**
NH_4HCO_3 (mM)	**0 (standard control)**	**1 (NH_4HCO_3 control)**	**0.01**	**1**		**p-value (NH_4HCO_3)**	
% Dev. to TM on Day 5 (kinetics)	43±12.3	28±11.5	34.1±7.4	36.9±4.9	0.42	0.23	0.8
% Total Dev. (TM and B) on Day 7	73±13.2^{a}	50.3±6.3^{b}	53.9±5.1^{b}	52.6±8.5^{b}	0.28	0.048	0.71
% B Day 7	63.7±12.9^{a}	20.7±12.7^{c}	44.9±12.2^{ab}	31±5.2^{bc}	0.42	0.005	0.14
% B1-2 Day 7	33.8±11.3^{a}	9.1±1^{b}	31.5±5^{a}	18.8±9^{ab}	0.41	0.008	0.17
% < 8-cells	9.1±5^{b}	27±3^{a}	30±8^{a}	16±13^{ab}	0.55	0.02	0.38
% total deg > 8-cells	20.6±13^{a}	8.3±5^{b}	20.1±5.3^{a}	16±9.6^{ab}	0.63	0.03	0.29

The absence of clear, significant effects of supplementing the chosen proteins on embryo development parameters measured is likely underpinned by several distinct factors. Two of the most determining aspects were a detrimental effect of ammonium bicarbonate -a solubilising aid of CysC in the formulation used- on several parameters of embryo development, and significant inter-run variations (Table S7-2). These factors are discussed next. Additionally, because no clear effect of the proteins tested was found, coupled with the strong confounding effect of ammonium bicarbonate, experiments of co-supplementation of those proteins were not carried out, though the possibility of an interaction effect cannot be discarded.

Table 7-3 Effect of the addition of CatB at different concentrations to culture medium on embryo development parameters by generalised linear models. Results expressed as mean percentage (to cleaved) ± standard deviation. Green (red) font: positive (negative) parameters. Abbreviations: B, blastocyst; B1-2, blastocyst grade 1 or 2., CatB, cathepsin B; deg, degenerate; dev., development; std, standard; TM, tight morula.

CatB (ng/ml)	0 (std or dilution controls)	*15*	*30*	*60*	*90*	p-value
% Dev. to TM on Day 5 (kinetics)	30.7±11.8	21.2±7.7	24.5±7	30±8.6	29±8.7	0.69
% Total Dev. (TM and B) on Day 7	52.5±14.8	48.8±4.7	56.6±4.8	50.5±11.5	53.4±1.8	0.94
% B Day 7	40.7±12.4	34.1±9.7	51.2±6.3	40.3±10.2	36.7±7.1	0.5
% B1-2 Day 7	28.1±5.6	19.9±6.6	34±2.9	22.4±7.8	25±8.8	0.27
% <8 cells	24±10.8	32.8±1.7	27.4±8	20.7±7.8	24.6±6.7	0.61
% total deg + >8cells	24±5.2	18.4±3.1	18.3±6.2	27.6±2.4	21.1±8.5	0.33

Table 7-4 Effect of the addition of pyruvate kinase M (PKM) at different concentrations to culture medium on embryo development parameters by generalised linear models. Results expressed as mean percentage (to total embryos cleaved) ± standard deviation. Green (red) font: positive (negative) parameters. Abbreviations: B, blastocyst; B1-2, blastocyst grade 1 or 2., deg, degenerate; dev., development; PKM, pyruvate kinase M; TM, tight morula.

PKM (µg/ml)	0 (control - DNP)	0.1	1	10	p-value
% Total Dev. (TM - B) Day 7	60±4.3	63.9±6.9	48.7±9.2	59.3±10	0.32
% B Day 7	46.9±7.2	42.9±5.1	41.3±8.6	43.3±7.3	0.87

% B1-2 Day 7	24.2±6.9	24.8±2.6	23.2±3.6	26.3±14.3	0.99
% <8 cells	12.1±10.2	16.5±1.2	23.2±12.2	6.2±8.7	0.32
% total deg + >8cells	27.9±10.3	19.6±5.7	17.3±7	33±15.3	0.47

Effect of ammonium bicarbonate on embryo development

Ammonium bicarbonate showed a strong detrimental effect on most embryo development parameters measured for CysC. This can be observed from contrasting outcomes from standard controls and controls with the addition of 1 mM ammonium bicarbonate (Table S7-2). All parameters measured at day 7 were worse in ammonium bicarbonate controls ($p<0.05$): % TM-B (50.3±6.3 vs 73±13.2), % B (20.7±12.7 vs 63.7±12.9), % B1-2 (9.1±1 vs 33.8±11.3), % ≤ 8-cell (27±3 vs 9.1±5) and % > 8-cell degenerate and morulae (8.3±+5 vs 20.6±13).

Interestingly, a non-statistically significant interaction effect of ammonium bicarbonate and CysC was suggested in some of those parameters (% B and % B1-2; $p<0.15$). In those, the CysC10 treatment might have compensated for some of the negative effect of ammonium bicarbonate seen in the ammonium bicarbonate controls, both with 1 mM NH_4HCO_3. Thirty one percent of cleaved embryos in CysC10 treatment became blastocysts at day 7, significantly lower than 73±13.2 % in standard controls but tending to be higher than in ammonium bicarbonate controls (20.7±12.7 %). A similar trend was seen for % B1-2 at day 7: 18.8±9, 9.1±1 and 33.8±11.3 in Cys10, ammonium bicarbonate control and standard control, respectively. Trends were inconclusive for the treatment CysC0.1, generally showing better embryo development than CysC at 10 µg/ml and ammonium bicarbonate control but lower than standard controls. Whether the intermediate values observed for CysC0.1 are caused by CysC, ammonium bicarbonate or their interaction cannot be determined in this experimental design. Overall, these results point at a strong negative influence of ammonium bicarbonate at these relatively high concentrations and suggest that CysC supplementation may partially offset the impact of ammonium toxicity, though it is unclear through what mechanism, this is worth further consideration in future work.

Ammonium toxicity is a well-known issue in embryo IVP. Ammonia (Gardner and Lane 1993) and ammonium bicarbonate (Ménézo et al. 1993) exert a considerable negative effect on mammal embryo growth and quality at concentrations as low as 75 µM, particularly from cleavage to hatching -i.e. morula and blastocyst stages- (Gardner and Lane 1993). In the same work, one mechanism proposed to underlie this negative effect is excessive conversion of alpha-ketoglutarate to glutamate by glutamate dehydrogenase (alpha-ketoglutarate + NADH + $NH4^+$ ---> glutamate + NAD^+ + H_20), reducing alpha-ketoglutarate abundance and thus disrupting the TCA cycle (Gardner and Lane 1993). Other possible mechanisms mediating the negative effect of ammonium bicarbonate are an increase

of pH (Gardner and Lane 1993) or a disruption of calcium transport by competitively using membrane cation transporters (Hammon et al. 2000, Lin et al. 2020). This detrimental effect is usually a side effect of amino acid supplementation to *in vitro* culture medium, a practice that substantially stimulates embryo development (Gardner and Lane 1993). This is a noteworthy difference between *in vivo* and *in vitro* growth: ammonium concentration is kept within physiologically-compatible parameters *in vivo* by endogenous mechanisms (Guerin et al. 2001). However, when culturing embryos *in vitro* there is typically a build-up resulting from two main processes: as a result of spontaneous breakdown of amino acids at temperatures over 35 °C, and as a by-product of embryo metabolism (Wale and Gardner 2015). Medium changeover -as performed in this work- prevents the accumulation of toxic by-products (Gardner and Lane 1993) but also of potentially beneficial paracrine factors that underlie the better developmental performance of embryos cultured in groups compared to individually (Fujita et al. 2005).

More replicates would be required to formulate hypotheses about an embryo-protective effect of CysC that is only apparent in the presence of intense stress, as caused by ammonium bicarbonate in this experiment. For future similar experiments, removal of ammonium bicarbonate by dialysis and replacement with another protein-solubilisation adjuvant would be an important step to appropriately test the effect of a target protein without interference. If this were not possible, adding ammonium bicarbonate to the same final concentration in all treatments is another option, though less preferable because its effect could mask the effect of the test protein. Finally, considering that ammonium toxicity is widespread in embryo IVP, research on molecules to reduce this toxicity would be an important endeavour.

Run effects

Random (run) effects were found significant for one or more measures of embryo development in most experiments (Tables S7-2, S7-4a,b,c). These effects can result from several components. Regarding the biological origin of the embryos, all semen used was taken from the same high conception outcome bull, and were furthermore from the same batch, minimising variations in this respect (Ponsart et al. 2001). Supporting this, the proportion of one-cell embryos per replicate run was constantly <3% and not significantly different between runs (data not shown). To the same effect, all chemicals and consumables used in all experiments belonged to the same batch.

Another crucial factor is the source of ovaries for oocyte collection. There are reports of sizeable differences in oocyte quality (determined by *in vitro* culture performance in a similar manner as in the present work) at the breed (Fischer et al. 2000), herd (Lopes et al. 2006), cow (Domínguez 1995), follicle (Lonergan et al. 1994) and individual oocyte (Humblot et al. 2005) levels. In this project, all ovaries came from the same abattoir, and the utmost care was taken to harvest oocytes from

healthy ovaries and follicles of normal appearance. However, it was not possible to choose the cows from which the ovaries were taken, and little information was available as to whether they were predominantly dairy or beef cattle on a given day. To interpret the inter-experimental differences observed, two aspects deserve consideration in this context. One is that many cows whose ovaries were sourced might have been culled due to reproductive issues, many of which would not affect ovarian morphology and could therefore go unnoticed (Dubuc and Denis-Robichaud 2017). Another one is differences in the oestrus cycle stage at which the animals were when slaughtered, a crucial determinant of oocyte capability and embryo development (Hagemann et al. 1999). In addition, although technical variation was kept to the minimum as stated above, a small effect of inter-experimental differences in other aspects (pipetting, manipulation time, etc.) cannot be ruled out.

An important consideration when relating these results to those of other studies is the way experimental outcomes are presented. Most papers on both molecular biology and embryo culture report mean values ± SEM (standard error of the mean). This parameter expresses the confidence in the mean value considering the (square root of the) number of observations but not the spread or variability across replicates. This effectively precludes the reader from assessing consistency and repeatability across replicates and experiments. In fact, it was not possible to determine whether the inter-run differences observed here were excessive, normal, or even lower than those reported in other articles. In this work, standard deviation of the mean (square root of the variance) was chosen to reflect experimental outcomes more accurately and transparently. Similar considerations apply to the use of bar plots compared to the clearer and more apparent use of strip charts and/or boxplots as used here.

Finally, it is conceivable that a greater number of replicates would have reduced the effects of random variation across runs that potentially obscured any effect caused by the addition of the proteins tested. The number of replicates in similar studies went from two (Leroy et al. 2005b) to seven (Hill and Gilbert 2008) with a median of four.

Biochemical considerations

Other considerations about testing the effect of the supplementation of a molecule to embryo IVC are the concentration range, timing of supplementation, and the use of complementary technologies to assess embryo quality and development.

The protein concentrations used were decided based on an extensive literature search. Concentrations of CatB used here were chosen based on the work of Tsai et al. (2009) in human blood, who used ELISA for measurements. For the other two proteins, no reports of absolute concentration in biological fluids was found. Thus, the range found in several similar studies was

adopted, as explained in the introduction of this chapter. This leads to a logical means of optimising this experiment: by using targeted proteomics, e.g. by multiple reaction monitoring using spiked peptides as described by Deutsch et al. (2019) and discussed in the review performed as part of this doctoral project (Aranciaga et al. 2020). Knowledge of the actual concentrations of these proteins *in vivo* is likely to result in an experiment that better mimics the conditions in which embryo development and fate are decided. Importantly, an in-depth embryological investigation was beyond the scope of this thesis.

The timing of supplementation could also be adjusted: supplementing selected proteins/metabolites only at specific stages can significantly alter experimental outcome, as examined in the introduction of this chapter. The equivalences between *in vivo* and *in vitro* developmental stages are as follows: IVM (day 0 to 1) mimics the final step of oocyte maturation in the follicle; IVF (day 1 to 2) represents the early oviduct phase -including the fertilisation process and the initial hours of development (Miller 2018)-, early IVC (day 2 to 4-5) the late oviduct phase and the late IVC (day 4-5 to 7) the early uterine phase.

The parameters analysed here are typical indicators of an effect on embryo development but are not the only ones. Some were not analysed here due to practical limitations and the fact that embryo culture was not the focus of this thesis; they may have shown an effect of the tested proteins. Common response variables analysed in similar embryology studies are cell numbers of the whole blastocyst and of its main parts -the inner cell mass and the outer trophectoderm-, apoptotic cells (with differential staining immunohistochemistry), interaction or absorption of supplemented molecules, and lipid micro-drop accumulation. The distinction between apoptosis, necrosis and embryonic senescence is only starting to be investigated but is extremely promising (Ramos-Ibeas et al. 2020a).

The outcomes from a study comparable to the present, published recently (Sang et al. 2020), provide valuable insight into the results presented here. In their study, Sang et al. (2020) tested the effect of several putative embryokines discovered *in vivo,* i.e. embryotrophic factors -CLP, IL-8, LIF, BMP-4, IL-6; Tríbulo et al. (2018)- on IVC from day 5 to day 7. They found no differences in development rates (cleavage, development to blastocyst, etc.) though some subtler changes were observed in other parameters: in the number of total cells or cells in the inner cell mass, in transcript abundance of important genes, or in growth rate in male vs female embryos, dependent on the specific molecule added (Sang et al. 2020). The authors' interpretation on the relatively minor effect of these molecules is related to oocyte effects. They posit that most embryos are likely derived from suboptimal oocytes not capable of becoming blastocysts, regardless of the molecular milieu, and that only a small number of the embryos placed in culture are intrinsically viable and may manifest

differential development related to specific embryokines after fertilisation (Sang et al. 2020). Their conclusion is that regulatory molecules (embryokines) are more likely to affect the physiology of the blastocyst that is formed rather than determine whether the early embryo becomes a blastocyst (Sang et al. 2020). This suggests that *in vitro* culture should include more that the median of four replicates in future studies to reduce the confounding effect of the variability between ova, sperm and embryos.

Regarding the outcome variables tested, it is noteworthy that visual grading of embryos is one out of many ways of estimating potential reproductive success. In a study by Tao et al. (2013), embryo groups graded as of good or bad quality at day 3 of IVC showed no differences in implantation and pregnancy rates. Similarly, Alvarez et al. (2008) showed that when poor quality (grade 3) embryos -derived from live donor cows- developed to blastocysts, pregnancy rates were equal to good quality blastocysts. This indicates that visual assessment of embryo quality is not always a good predictor of pregnancy success. It is also possible that the proteins tested in this study exert an effect on embryo morphology at day 7 after insemination but whose main effect would only become apparent later in pregnancy, as reported by Kruip et al. (2000). Lastly, recent evidence links transcriptional profiles of genes in stress response with embryo survival after transfer of both *in vitro* (Zolini et al. 2020b) and *in vivo* (Zolini et al. 2020a) produced embryos, opening a new realm for improved selection of transferrable embryos.

If the effect of the selected test proteins is mediated by an interaction with maternal structures or secreted molecules, it follows that no differences were observed on embryo development when those were absent. Co-culture with oviduct cells *in vitro* has been suggested to better mimic the environment of the reproductive tract by adding embryotrophic factors or removing toxic products (Bavister 1992). Indeed, embryos co-cultured with oviduct cells showed substantially improved blastocyst rate at day 7.5 in a recent study by Sponchiado et al. (2020) and could be a key missing element in the experiments described in this chapter. However, co-culture technologies still face important challenges: despite improvements on *in vitro* development rates, co-culture has been linked to detrimental effects later in pregnancy (Camous et al. 1984), during the neonatal period (Young et al. 1998), and in adult life (Siqueira et al. 2017).

Lastly, the molecular factors in the reproductive tract that are crucial for embryo development is largely unknown. A recent study (Banliat et al. 2020) shed light on this, reporting that only 0.03% (56/1707) proteins in oviduct fluid (OLF) interacted physically with embryos *in vitro* (i.e. were detected in OLF-treated embryos but not in controls). This suggests that a vast majority of proteins in the reproductive tract fulfil physiological functions in the cow and are not strong determinants of pregnancy by themselves.

7.3.3 Conclusions and recommendations

Based on these experiments, it is strongly suggested that, when using products containing ammonium bicarbonate, this should be removed prior to adding it to oocytes or embryos in culture. Regarding the protein concentration ranges tested, they were within physiological typical boundaries. It is possible that higher concentrations produce an effect on embryo development, but its biological meaning would be limited.

To sum up, the present experiment showed the negative impact of ammonium bicarbonate on IVP embryos. No significant effect of the supplementation of CysC, CatB and PKM was observed in embryo development. However, some tendencies for differences were apparent for some of the treatments -protein concentrations-, namely for improved development to TM-B stages with 0.1 or 10 µg/ml CysC (in the presence of ammonium bicarbonate), and less TM-B when adding 1 µg/ml PKM to embryo culture. These could not be confirmed in this experiment due to having three replicates -with sizable inter-replicate variation- but deserve further consideration. While the experimental design is likely adequate, future similar experiments will benefit from increasing the number of replicates (runs), ensuring the absence of detrimental molecules such as ammonium bicarbonate, and measuring other parameters such as cell numbers, expression of key developmental genes, and uptake by the embryo of the test molecule(s).

In conclusion, the experiments presented in this chapter provide important insight on factors relevant to embryo culture *in vitro* and to testing the effect of supplementing specific molecules on embryo development.

8

Discussion, conclusions, and further research

8.1 Recap – biological model and approach

This project aimed to provide insight into direct determinants of dairy cow subfertility, a pressing multifactorial issue in New Zealand and across the world. This was attempted through ascertaining the influence on early embryo development of biologically relevant molecules -metabolites and proteins- present in bovine uterine luminal fluid (ULF). This effect and overall molecular changes were studied at two timepoints in the early and mid-postpartum period, i.e. at first and third oestrus after calving (OC1 and OC3). These goals were fulfilled in this work, advancing the characterisation of the molecular environment of bovine ULF and determining that multiple interacting factors at the animal and organ levels intervene in ULF composition and likely affect embryo fate.

Here a unique animal model was employed, determining changes in the uterine tract of a large group of cows at contrasting physiological situations across the postpartum period, and investigating implications of those changes on embryo early development *in vivo*. The day-7 timepoint was chosen in the present work because the first week of pregnancy was associated with the highest embryo losses in this animal model (moderately producing grazing dairy cows), of around 30% of inseminations (Diskin and Morris 2008, Berg et al. 2017). As previously discussed, sampling ULF *in vivo* from animals pregnant by a single embryo as in the present work may not detect subtle molecular differences caused by the embryo itself in its surrounding fluid/endometrial microenvironment. Rather, in the present study, the embryo functioned as a sensor to appraise the ULF molecular milieu due to maternal factors.

8.2 Molecular and systemic determinants of subfertility

Untargeted LC-MS/MS proteomic experiments allowed the comprehensive characterisation of the ULF proteome in relation to embryo quality and time postpartum. Of the 1504 proteins detected, 472 are reported here for the first time in bovine ULF, to the knowledge of the author. This is an important contribution towards characterising this relatively unexplored biofluid. Only two proteins showed a statistically significant trend over time, whereas 20 proteins were significantly related to embryo quality.

The proteins found to be correlated with embryo quality in the present work might exert disparate effects at different points in the postpartum period. However, no statistically significant interaction effects of these proteins' abundances with dpp or OC were found on embryo quality (Chapter 5). A

possibility is that the lower reproductive performance observed at OC1 might be caused indirectly by a strong metabolic imbalance (Moyes et al. 2013). As presented in Chapter 1, one of the manifestations of this metabolic imbalance is an increase in NEFA in blood in the early postpartum period, which is accompanied by a heightened systemic oxidative status until around day 30 postpartum (Bernabucci et al. 2005). This mechanism may have impacted the reproductive tract at several levels, i.e. at the ovary (follicular fluid) oviduct (oviduct luminal fluid) and/or uterus (ULF) (Jordaens et al. 2020).

GC-MS/MS metabolomic experiments (Exp. M1, M2 and M4) resulted in 132 compounds not previously reported in bovine ULF. Change patterns in metabolites' abundances were dissimilar to those observed in proteins: while no significant associations were found between metabolite abundance and embryo quality, 31 compounds fluctuated along dpp and/or OC. An interpretation of the seemingly divergent trends in proteins and metabolites in ULF (metabolite abundance changes in time, protein changes correlated to embryo quality) can be extrapolated from the review of Roche et al. (2009). They discuss how some processes (e.g. body fat mobilisation) are predominantly regulated by genetic factors, while others (e.g. lipogenesis) are modulated mostly by the metabolic conditions (Roche et al. 2009).

Interaction between the proteins and metabolites studied at the biological function level in ULF was determined by joint pathway analysis, with several processes fluctuating between the two timepoints examined. These processes encompassed metabolism, regulation of transcription, signalling and defence. This points at the ULF environment at OC1 being generally more metabolically active, in part likely due to incomplete postpartum recovery. The ULF at OC3 contained a higher abundance of enzymes in the pathways impacted, which may account for its improved ability to cope with stress and better host an embryo. The EGFR1 signalling pathway also appeared to be differentially regulated between ULF containing >16-cells vs <16-cells embryos. This central pathway to development may be affecting embryo development in a myriad of ways and is a promising target for future studies.

Cow-level (Chapter 2) and uterine molecular (Chapters 5-6) variables were associated with differential embryo quality, but in the present work links between those systemic and local factors were not apparent by multivariate analysis. Furthermore, PCA and PLS-DA analyses of molecular data evidenced a high degree of variation within groups in all the variables scrutinised, i.e. no variable showed definite clusters or clear separation between classes, with two implications.

Firstly, that the molecular composition of ULF is a result of complex interactions between the cow-level phenotypical variables measured, and likely others. Thus, no variable, or small subset of variables, appears to be a key determining factor of the ULF molecular milieu. Secondly, that

potentially subtle molecular signatures of uterine suitability may be manifested predominantly at levels of regulation other than those measured herein. Important regulatory processes of uterine function and early embryo have been described for mRNA transcription (Bauersachs et al. 2017), DNA methylation (O'Doherty et al. 2017), protein post-translational modifications (Bhojwani et al. 2006), and protein stability and degradation (Deutsch et al. 2014). In addition, the extracellular vesicle fraction of ULF was not isolated in the present work and thus some potentially relevant signal molecules within (Almiñana et al. 2018, Koh et al. 2020) could provide valuable additional insight.

The proteins selected for biological validation by *in vitro* embryo culture (cystatin C, cathepsin B and pyruvate kinase M) were not found to consistently affect the embryonic development parameters measured. In these experiments a detrimental effect of ammonium bicarbonate on embryo development to the blastocyst stage was observed, and the data suggests potential detrimental effects of PKM on blastocyst rate and a protective effect of CysC against ammonium bicarbonate-induced damage. More *in vitro* studies are needed to better understand the molecular dynamics of early embryo development. State-of-the-art oviduct and endometrial cell culture systems have been shown to closely mimic the endocrine and morphological properties of the organs *in vivo* (Jordaens et al. 2020) and constitute an excellent strategy for future work due to practical, logistic and ethical purposes (Rodríguez-Alonso et al. 2020b).

Integrative studies conjunctly assessing the molecular milieu of follicular, oviductal and uterine fluids will greatly help clarify the spatiotemporal nature of the pregnancy losses observed here, and better understand the interaction between these microenvironments. Furthermore, there is an increasing amount of evidence on carry-over effects of metabolic and disease conditions on reproductive performance (Britt 1991, Gilbert 2019). This implies that measurements across time (ideally starting weeks before calving) may provide essential insight to ascertain the direct mechanisms determining readiness for pregnancy.

8.3 Technical aspects

The proof-of-concept test of a rapid metabolic fingerprinting platform (REIMS) on ULF samples (Exp. M3 and M5) succeeded at obtaining good quality spectra and determine a small subset of metabolic features potentially associated to embryo quality differences. However, its sensitivity appeared to be insufficient for determinations of subtle changes associated with the phenomena of interest in this work. Replacing the sampling setup for an automated system (as opposed to the standard handheld device employed in this work) or trialling similar techniques originally developed for liquid samples (e.g. DART-MS) may form the basis of a diagnostic application for health and pregnancy parameters.

Some suggestions to improve the scope, precision, and consistency of the proteomic and metabolomic data generated include the use of data-independent acquisition methods (Doerr 2015) for improved coverage in LC-MS/MS proteomic analyses and the incorporation of orthogonal technologies to GC-MS/MS (e.g. hydrophilic interaction chromatography, "HILIC"; Tang et al. 2016) for detection of additional metabolite classes.

8.4 Perspectives

A multifactorial approach will likely be necessary for understanding molecular pathways underlying dairy cows' reproductive function. Ameliorating it will also require a similarly multifaceted strategy, with each factor representing a small percentage of improvement that can however compound for greater total gains (Diskin et al. 2015). This is especially true in countries with predominantly grazing dairy systems that have a higher dependence on timely and compact calving seasons (Brownlie et al. 2014). These factors include genetic improvements (Crowe et al. 2018), management -i.e. housing and quality of feed adjustments peripartum (Sawa and Bogucki 2011)-, potentially reducing milking frequency in the first one or two weeks postpartum (Stelwagen et al. 2013), and setting the voluntary waiting time to about day 24 (Humblot 2001), as longer waiting times imply risking impregnating oocytes produced peripartum, of lower quality (Britt 1991); after 3 months postpartum, longer waits do not improve reproductive outcome in moderate producing dairy cows (Stadnik 2017).

In addition, further studies may test differences in development of dairy and beef embryos transferred to early postpartum dairy cows. This could help determine whether production of a beef calf represents a viable alternative to culling, for dairy cows not pregnant on time to keep up with the annual calving pattern.

8.5 Conclusion

The present work provided evidence for links between proteins and metabolites associated with (and potentially determinant of) postpartum recovery and embryo quality. Worthy of note, proteins related to immune processes such as myeloid leukocyte activation and response to wounding tended to be in higher abundance in ULF holding poorer quality embryos. The abundance of many metabolites changed with time postpartum; at OC1 the "pentose and glucuronate conversion" pathway was upregulated, whereas "cysteine and methionine metabolism" and "glycine, serine and threonine metabolism" were downregulated, accounting for time-specific molecular signatures of the uterine environment. Additionally, dysregulation of protein metabolism and EGFR1 signalling is putatively associated with embryo development beyond the 16-cell stage. Targeted studies are needed for empirical validation of these findings.

Important future avenues of related research include integration with other omics (genomics, epigenomics, lipidomics, etc.), tissues (endometrium) and fluids (follicular fluid) for systems biology modelling, as well as more comprehensive and large-scale *in vitro* assays for validation of potential biomarkers.

References

Abrahamson, M., et al. (2003). "Cystatins." Biochemical Society Symposium **70**: 179-199.

Aebersold, R. and M. Mann (2003). "Mass spectrometry-based proteomics." Nature **422**(6928): 198-207.

Afonso, S., et al. (1997). "The expression and function of cystatin C and cathepsin B and cathepsin L during mouse embryo implantation and placentation." Development **124**(17): 3415-3425.

Agarwal, A., et al. (2012). "The effects of oxidative stress on female reproduction: a review." Reproductive Biology and Endocrinology **10**(1): 49-59.

Ahmad, I. (2014). "Investigation of miRNAs enrichment and degradation in bovine granulosa cells during follicular development." Published doctoral dissertation, University of Bohn.

Ahmad, N., et al. (1997). "Relationships of hormonal patterns and fertility to occurrence of two or three waves of ovarian follicles, before and after breeding, in beef cows and heifers." Animal Reproduction Science **49**(1): 13-28.

Alavi-Shoushtari, S. M., et al. (2006). "A study of the uterine protein variations during the estrus cycle in the cow: a comparison with the serum proteins." Animal Reproduction Science **96**(1-2): 10-20.

Algarra, B., et al. (2018). "Effects of recombinant OVGP1 protein on in vitro bovine embryo development." Journal of Reproduction and Development **64**(5): 433-443.

Almagro Armenteros, J. J., et al. (2019a). "Detecting sequence signals in targeting peptides using deep learning." Life Science Alliance **2**(5): e201900429.

Almagro Armenteros, J. J., et al. (2019b). "SignalP 5.0 improves signal peptide predictions using deep neural networks." Nature Biotechnology **37**(4): 420-423.

Almiñana, C., et al. (2014). "The battle of the sexes starts in the oviduct: modulation of oviductal transcriptome by X and Y-bearing spermatozoa." BMC Genomics **15**(1): 293.

Almiñana, C., et al. (2017). "Oviduct extracellular vesicles protein content and their role during oviduct–embryo cross-talk." Reproduction **154**(3): 253-268.

Almiñana, C., et al. (2018). "Deciphering the oviductal extracellular vesicles content across the estrous cycle: implications for the gametes-oviduct interactions and the environment of the potential embryo." BMC Genomics **19**(1): 1-27.

Altmae, S., et al. (2014). "Guidelines for the design, analysis and interpretation of 'omics' data: focus on human endometrium." Human Reproduction Update **20**(1): 12-28.

Álvarez-Sánchez, B., et al. (2010). "Metabolomics analysis I. Selection of biological samples and practical aspects preceding sample preparation." Trends in Analytical Chemistry **29**(2): 111-119.

Alvarez, R., et al. (2008). "Transfer of Bovine Blastocysts Derived from Short-term In Vitro Culture of Low Quality Morulae Produced In Vivo." Reproduction in Domestic Animals **43**(3): 257-260.

Ananthi, S., et al. (2011). "Comparative proteomics of human male and female tears by two-dimensional electrophoresis." Experimental eye research **92**(6): 454-463.

Anonymous (2018). "New Zealand Dairy Statistics 2017-18." from www.dairynz.co.nz/dairystats, accessed 04/07/2018.

Aranciaga, N., et al. (2020). "Proteomics and metabolomics in cow fertility: a systematic review." Reproduction **160**(5): 639.

Arena, K., et al. (2020). "Exploration of Rapid Evaporative-Ionization Mass Spectrometry as a shotgun approach for the comprehensive characterization of Kigelia africana (Lam) Benth. Fruit." Molecules **25**(4): 962.

Armirotti, A., et al. (2014). "Sample preparation and orthogonal chromatography for broad polarity range plasma metabolomics: application to human subjects with neurodegenerative dementia." Analytical Biochemistry **455**: 48-54.

Arnold, G. J. and T. Frohlich (2011). "Dynamic proteome signatures in gametes, embryos and their maternal environment." Reproduction, Fertility and Development **23**(1): 81-93.

Artus, J., et al. (2020). "Preimplantation development in ungulates: A 'ménage à quatre'scenario." Reproduction **159**(3): R151-R172.

Ashburner, M., et al. (2000). "Gene ontology: tool for the unification of biology. The Gene Ontology Consortium." Nature Genetics **25**(1): 25-29.

Baggerman, G., et al. (2005). "Gel-based versus gel-free proteomics: a review." Combinatorial Chemistry & High-throughput Screening **8**(8): 669-677.

Balan, K., et al. (2001). "Cathepsin B and complement C3 are major comigrants in the estrogen-induced peroxidase fraction of rat uterine fluid." Journal of Submicroscopic Cytology and Pathology **33**(3): 221-230.

Balboula, A., et al. (2010). "Intracellular cathepsin B activity is inversely correlated with the quality and developmental competence of bovine preimplantation embryos." Molecular Reproduction and Development **77**(12): 1031-1039.

Balog, J., et al. (2010). "Identification of Biological Tissues by Rapid Evaporative Ionization Mass Spectrometry." Analytical Chemistry **82**(17): 7343-7350.

Bang, J. I., et al. (2015). "Quality improvement of transgenic cloned bovine embryos using an aggregation method: Effects on cell number, cell ratio, embryo perimeter, mitochondrial distribution, and gene expression profile." Theriogenology **84**(4): 509-523.

Banliat, C., et al. (2019a). "Intraoviductal concentrations of steroid hormones during in vitro culture changed phospholipid profiles and cryotolerance of bovine embryos." Molecular Reproduction and Development **86**(6): 661-672.

Banliat, C., et al. (2019b). "Stage-dependent changes in oviductal phospholipid profiles throughout the estrous cycle in cattle." Theriogenology **135**: 65-72.

Banliat, C., et al. (2020). "Identification of 56 Proteins Involved in Embryo-Maternal Interactions in the Bovine Oviduct." International Journal of Molecular Sciences **21**(2): 17.

Bantscheff, M., et al. (2007). "Quantitative mass spectrometry in proteomics: a critical review." Analytical and Bioanalytical Chemistry **389**(4): 1017-1031.

Bastian, F. B., et al. (2021). "The Bgee suite: integrated curated expression atlas and comparative transcriptomics in animals." Nucleic Acids Research **49**(1): 831-847.

Baston-Buest, D. M., et al. (2010). "The embryo's cystatin C and F expression functions as a protective mechanism against the maternal proteinase cathepsin S in mice." Reproduction **139**(4): 741.

Bates, A. J. and B. Saldias (2019). "A comparison of machine learning and logistic regression in modelling the association of body condition score and submission rate." Preventive Veterinary Medicine **171**: 104765.

Bauersachs, S., et al. (2017). "Effect of metabolic status on conceptus-maternal interactions on day 19 in dairy cattle: II. Effects on the endometrial transcriptome." Biology of Reproduction **97**(3): 413-425.

Baugh, J. A. and R. Bucala (2002). "Macrophage migration inhibitory factor." Critical Care Medicine **30**(1): S27-S35.

Baumann, H. and J. Gauldie (1994). "The acute phase response." Immunology Today **15**(2): 74-80.

Bavister, B. D. (1992). "Co-culture for embryo development: is it really necessary?" Human Reproduction **7**(10): 1339-1341.

Bayerlová, M., et al. (2015). "Comparative study on gene set and pathway topology-based enrichment methods." BMC Bioinformatics **16**(1): 334.

Beale, D. J., et al. (2018). "Review of recent developments in GC-MS approaches to metabolomics-based research." Metabolomics **14**(11): 152.

Bedair, M. and L. W. Sumner (2008). "Current and emerging mass-spectrometry technologies for metabolomics." Trends in Analytical Chemistry **27**(3): 238-250.

Belaz, K. R., et al. (2016). "Phospholipid Profile and Distribution in the Receptive Oviduct and Uterus During Early Diestrus in Cattle." Biology of Reproduction **95**(6): 127.

Bellinge, R. H., et al. (2005). "Myostatin and its implications on animal breeding: a review." Animal Genetics **36**(1): 1-6.

Beltman, M. E., et al. (2014). "Global proteomic characterization of uterine histotroph recovered from beef heifers yielding good quality and degenerate day 7 embryos." Domestic Animal Endocrinology **46**: 49-57.

Benjamini, Y. and Y. Hochberg (1995). "Controlling the false discovery rate: a practical and powerful approach to multiple testing." Journal of the Royal Statistical Society: series B (Methodological) **57**(1): 289-300.

Berendt, F. J., et al. (2005). "Holistic differential analysis of embryo-induced alterations in the proteome of bovine endometrium in the preattachment period." Proteomics **5**(10): 2551-2560.

Berg, D., et al. (2017). Conception and embryo losses in New Zealand seasonal pasture-grazed dairy cattle. InCalf Symposium 2017.

Berg, D., et al. (2010). "Embryo loss in cattle between Days 7 and 16 of pregnancy." Theriogenology **73**(2): 250-260.

Berglund, B. (2008). "Genetic improvement of dairy cow reproductive performance." Reproduction in Domestic Animals **43**(s2): 89-95.

Berlec, A. and B. Štrukelj (2013). "Current state and recent advances in biopharmaceutical production in Escherichia coli, yeasts and mammalian cells." Journal of Industrial Microbiology & Biotechnology **40**(3): 257-274.

Bernabucci, U., et al. (2005). "Influence of body condition score on relationships between metabolic status and oxidative stress in periparturient dairy cows." Journal of Dairy Science **88**(6): 2017-2026.

Bertoldo, M. J., et al. (2020). "NAD+ repletion rescues female fertility during reproductive aging." Cell Reports **30**(6): 1670-1681.e1677.

Bhojwani, M., et al. (2006). "Molecular analysis of maturation processes by protein and phosphoprotein profiling during in vitro maturation of bovine oocytes: a proteomic approach." Cloning Stem Cells **8**(4): 259-274.

Bittremieux, W., et al. (2018). "Quality control in mass spectrometry-based proteomics." Mass Spectrometry Reviews **37**(5): 697-711.

Black, C., et al. (2016). "The current and potential applications of Ambient Mass Spectrometry in detecting food fraud." Trends in Analytical Chemistry **82**: 268-278.

Blau, N. (2016). "Genetics of phenylketonuria: Then and now." Human Mutation **37**(6): 508-515.

Block, J., et al. (2009). "Effect of addition of hyaluronan to embryo culture medium on survival of bovine embryos in vitro following vitrification and establishment of pregnancy after transfer to recipients." Theriogenology **71**(7): 1063-1071.

Block, J., et al. (2010). "Efficacy of in vitro embryo transfer in lactating dairy cows using fresh or vitrified embryos produced in a novel embryo culture medium." Journal of Dairy Science **93**(11): 5234-5242.

Bo, G. and R. Mapletoft (2018). "Evaluation and classification of bovine embryos." Animal Reproduction **10**(3): 344-348.

Bodai, Z., et al. (2018). "Effect of Electrode Geometry on the Classification Performance of Rapid Evaporative Ionization Mass Spectrometric (REIMS) Bacterial Identification." Journal of the American Society for Mass Spectrometry **29**(1): 26-33.

Boldyrev, A. A., et al. (2013). "Physiology and pathophysiology of carnosine." Physiological Reviews **93**(4): 1803-1845.

Bonventre, J. V., et al. (1997). "Reduced fertility and postischaemic brain injury in mice deficient in cytosolic phospholipase A2." Nature **390**(6660): 622-625.

Borrageiro, G., et al. (2018). "A review of genome-wide transcriptomics studies in Parkinson's disease." European Journal of Neuroscience **47**(1): 1-16.

Boyle, E. I., et al. (2004). "GO::TermFinder--open source software for accessing Gene Ontology information and finding significantly enriched Gene Ontology terms associated with a list of genes." Bioinformatics **20**(18): 3710-3715.

Breier, B. H. (1999). "Regulation of protein and energy metabolism by the somatotropic axis." Domestic Animal Endocrinology **17**(2): 209-218.

Breuel, K. F., et al. (1993). "Factors affecting fertility in the postpartum cow: role of the oocyte and follicle in conception rate." Biology of Reproduction **48**(3): 655-661.

Breukelman, S. P., et al. (2012). "Characterisation of pregnancy losses after embryo transfer by measuring plasma progesterone and bovine pregnancy-associated glycoprotein-1 concentrations." The Veterinary Journal **194**(1): 71-76.

Brewer, A., et al. (2020). "Qualitative and quantitative differences in endometrial inflammatory gene expression precede the development of bovine uterine disease." Scientific Reports **10**(1): 18275.

Britt, J. H. (1991). Impacts of early postpartum metabolism on follicular development and fertility. American Association of Bovine Practitioners: Proceedings of the Annual Conference, 39-43.

Brownlie, T. S., et al. (2014). "Reproductive performance of seasonal-calving, pasture-based dairy herds in four regions of New Zealand." New Zealand Veterinary Journal **62**(2): 77-86.

Burke, C., et al. (2008). Building towards the InCalf programme for New Zealand. Proceedings of Dairy Cattle Veterinarians Conference:18-22.

Butler, W. (2000). "Nutritional interactions with reproductive performance in dairy cattle." Animal Reproduction Science **60**: 449-457.

Buuren, S. v. and K. Groothuis-Oudshoorn (2010). "mice: Multivariate imputation by chained equations in R." Journal of Statistical Software **45**: 1-68.

Bylesjö, M., et al. (2006). "OPLS discriminant analysis: combining the strengths of PLS-DA and SIMCA classification." Journal of Chemometrics: A Journal of the Chemometrics Society **20**(8-10): 341-351.

Caamano, J., et al. (1998). "Promotion of development of bovine embryos produced in vitro by addition of cysteine and β-mercaptoethanol to a chemically defined culture system." Journal of Dairy Science **81**(2): 369-374.

Calderón, C., et al. (2019). "Comparison of simple monophasic versus classical biphasic extraction protocols for comprehensive UHPLC-MS/MS lipidomic analysis of Hela cells." Analytica Chimica Acta **1048**: 66-74.

Camargo, L. S. d. A., et al. (2006). "Factors influencing in vitro embryo production." Animal Reproduction **3**(1): 19-28.

Camous, S., et al. (1984). "Cleavage beyond the block stage and survival after transfer of early bovine embryos cultured with trophoblastic vesicles." Reproduction **72**(2): 479-485.

Campbell, B. K., et al. (2010). "The effect of monosaccharide sugars and pyruvate on the differentiation and metabolism of sheep granulosa cells in vitro." Reproduction **140**(4): 541.

Carnac, G., et al. (2006). "Myostatin: biology and clinical relevance." Mini Reviews in Medicinal Chemistry **6**(7): 765-770.

Carvalho, P. D., et al. (2014). "Relationships between fertility and postpartum changes in body condition and body weight in lactating dairy cows." Journal of Dairy Science **97**(6): 3666-3683.

Cassar-Malek, I., et al. (2007). "Target genes of myostatin loss-of-function in muscles of late bovine fetuses." BMC Genomics **8**: 63.

Ceciliani, F., et al. (2017). A Systems Biology Approach to Dairy Cattle Subfertility and Infertility. In: Periparturient Diseases of Dairy Cows. B. N. Ametaj. Cham, Springer International Publishing**:** 93-119.

Cerri, R. L. A., et al. (2009a). "Effect of fat source differing in fatty acid profile on metabolic parameters, fertilization, and embryo quality in high-producing dairy cows." Journal of Dairy Science **92**(4): 1520-1531.

Cerri, R. L. A., et al. (2009b). "Effect of source of supplemental selenium on uterine health and embryo quality in high-producing dairy cows." Theriogenology **71**(7): 1127-1137.

Cesari, A., et al. (2010). "Regulated serine proteinase lytic system on mammalian sperm surface: there must be a role." Theriogenology **74**(5): 699-711 e691-695.

Chae, H. Z., et al. (1994). "Thioredoxin-dependent peroxide reductase from yeast." Journal of Biological Chemistry **269**(44): 27670-27678.

Chagas, L. M., et al. (2007). "Invited review: New perspectives on the roles of nutrition and metabolic priorities in the subfertility of high-producing dairy cows." Journal of Dairy Science **90**(9): 4022-4032.

Chakravarty, A. (2003). "Surrogate markers: their role in regulatory decision process." Food and Drug Administration, http://www.fda.gov/cder/Offices/Biostatistics/Chakravarty_376/sld016.htm.

Chebel, R., et al. (2008). "Factors affecting success of embryo collection and transfer in large dairy herds." Theriogenology **69**(1): 98-106.

Chenault, J., et al. (2003). "Intravaginal progesterone insert to synchronize return to estrus of previously inseminated dairy cows." Journal of Dairy Science **86**(6): 2039-2049.

Chollet, A., et al. (2007). "Tocolytic effect of a selective FP receptor antagonist in rodent models reveals an innovative approach to the treatment of preterm labor." BMC Pregnancy and Childbirth **7**(1): S16.

Cleveland, W. S. and S. J. Devlin (1988). "Locally weighted regression: an approach to regression analysis by local fitting." Journal of the American statistical association **83**(403): 596-610.

Consortium, G. (2019). "The Gene Ontology resource: 20 years and still GOing strong." Nucleic Acids Research **47**(D1): D330-D338.

Consortium, U. (2018). "UniProt: a worldwide hub of protein knowledge." Nucleic Acids Research **47**(D1): D506-D515.

Cooks, R. G., et al. (2006). "Ambient mass spectrometry." Science **311**(5767): 1566-1570.

Costello, L. M., et al. (2010). "Retinol-binding protein (RBP), retinol and -carotene in the bovine uterus and plasma during the oestrous cycle and the relationship between systemic progesterone and RBP on Day 7." Reproduction, Fertility and Development **22**(8): 1198-1205.

Cracchiolo, B. M., et al. (2004). "Eukaryotic initiation factor 5A-1 (eIF5A-1) as a diagnostic marker for aberrant proliferation in intraepithelial neoplasia of the vulva." Gynecologic Oncology **94**(1): 217-222.

Crowe, M. A., et al. (2018). "Reproductive management in dairy cows - the future." Irish Veterinary Journal **71**(1): 1-13.

Cummins, S. B., et al. (2012). "Genetic merit for fertility traits in Holstein cows: II. Ovarian follicular and corpus luteum dynamics, reproductive hormones, and estrus behavior." Journal of Dairy Science **95**(7): 3698-3710.

Dasari, S., et al. (2007). "Comprehensive Proteomic Analysis of Human Cervical−Vaginal Fluid." Journal of Proteome Research **6**(4): 1258-1268.

De Maio, A. (1999). "Heat shock proteins: facts, thoughts, and dreams." Shock **11**(1): 1-12.

de Rezende, E. V., et al. (2020). "Factors related to uterine score and its influence on pregnancy per artificial insemination in crossbred dairy cows." Livestock Science **241**: 104231.

Deb-Choudhury, S., et al. (2014). "Effect of cooking on meat proteins: mapping hydrothermal protein modification as a potential indicator of bioavailability." Journal of Agricultural and Food Chemistry **62**(32): 8187-8196.

Demant, M., et al. (2015). "Proteome analysis of early lineage specification in bovine embryos." Proteomics **15**(4): 688-701.

Demetrio, D., et al. (2007). "Factors affecting conception rates following artificial insemination or embryo transfer in lactating Holstein cows." Journal of Dairy Science **90**(11): 5073-5082.

Deng, Q., et al. (2015). "Intravaginally administered lactic acid bacteria expedited uterine involution and modulated hormonal profiles of transition dairy cows." Journal of Dairy Science **98**(9): 6018-6028.

Dennis, E. A. (1994). "Diversity of group types, regulation, and function of phospholipase A2." Journal of Biological Chemistry **269**(18): 13057-13060.

Dennis, N., et al. (2018). "Combining genetic and physiological data to identify predictors of lifetime reproductive success and the effect of selection on these predictors on underlying fertility traits." Journal of Dairy Science **101**(4): 3176-3192.

Dervishi, E., et al. (2018). "Urine metabolic fingerprinting can be used to predict the risk of metritis and highlight the pathobiology of the disease in dairy cows." Metabolomics **14**(6): 83.

Deutsch, D. R., et al. (2019). Proteomics of bovine endometrium, oocytes and early embryos. Reproduction in Domestic Ruminants VIII, Bioscientifica. **8**.

Deutsch, D. R., et al. (2014). "Stage-specific proteome signatures in early bovine embryo development." Journal of Proteome Research **13**(10): 4363-4376.

Dey, S. K., et al. (1982). "Phospholipase A2 activity in the rat uterus: Modulation by steroid hormones." Prostaglandins **23**(5): 619-630.

Diedrich, K., et al. (2007). "The role of the endometrium and embryo in human implantation." Human Reproduction Update **13**(4): 365-377.

Diskin, M. G. and D. G. Morris (2008). "Embryonic and early foetal losses in cattle and other ruminants." Reproduction in Domestic Animals **43 Suppl 2**: 260-267.

Diskin, M. G., et al. (2006). "Embryo survival in dairy cows managed under pastoral conditions." Animal Reproduction Science **96**(3-4): 297-311.

Diskin, M. G., et al. (2015). "Pregnancy losses in cattle: potential for improvement." Reproduction, Fertility and Development **28**(2): 83-93.

Doerr, A. (2015). "DIA mass spectrometry." Nature Methods **12**(1): 35-35.

Dominguez, F., et al. (2010). "Embryologic outcome and secretome profile of implanted blastocysts obtained after coculture in human endometrial epithelial cells versus the sequential system." Fertility and sterility **93**(3): 774-782, e771.

Domínguez, M. M. (1995). "Effects of body condition, reproductive status and breed on follicular population and oocyte quality in cows." Theriogenology **43**(8): 1405-1418.

Dong, Z., et al. (2020). "Proteomic Profiling of Stem Cell Tissues during Regeneration of Deer Antler: A Model of Mammalian Organ Regeneration." Journal of Proteome Research **19**(4): 1760-1775.

Dubuc, J. and J. Denis-Robichaud (2017). "A dairy herd-level study of postpartum diseases and their association with reproductive performance and culling." Journal of Dairy Science **100**(4): 3068-3078.

Dunn, W. B., et al. (2011). "Procedures for large-scale metabolic profiling of serum and plasma using gas chromatography and liquid chromatography coupled to mass spectrometry." Nature Protocols **6**(7): 1060-1083.

Ealy, A. D. and Q. E. Yang (2009). "Control of interferon-tau expression during early pregnancy in ruminants." American Journal of Reproductive Immunology **61**(2): 95-106.

Edelhoff, I. N. F., et al. (2020). "Inflammatory diseases in dairy cows: Risk factors and associations with pregnancy after embryo transfer." Journal of Dairy Science **103**(12): 11970-11987.

Einer-Jensen, N. and R. Hunter (2005). "Counter-current transfer in reproductive biology." Reproduction **129**(1): 9.

Eriksson, L., et al. (1994). "Multi and Megavariate Data Analysis, Principles and Applications; Umetrics AB: Umea, Sweden, 2001." 43-111.

Esposito, G., et al. (2014). "Interactions between negative energy balance, metabolic diseases, uterine health and immune response in transition dairy cows." Animal Reproduction Science **144**(3): 60-71.

Evans, A. C. and S. W. Walsh (2011). "The physiology of multifactorial problems limiting the establishment of pregnancy in dairy cattle." Reproduction, Fertility and Development **24**(1): 233-237.

Fan, S., et al. (2020). "miR-145-5p overexpression inhibits the proliferation, migration and invasion of esophageal carcinoma cells by targeting ABRACL." BioMed Research International 2021: 1-10.

Faulkner, S., et al. (2011). "Immunodepletion of albumin and immunoglobulin G from bovine plasma." Proteomics **11**(11): 2329-2335.

Faulkner, S., et al. (2012). "A comparison of the bovine uterine and plasma proteome using iTRAQ proteomics." Proteomics **12**(12): 2014-2023.

Feng, X., et al. (2008). "Mass spectrometry in systems biology: An overview." Mass Spectrometry Reviews **27**(6): 635-660.

Ferraz, P. A., et al. (2016). "Factors affecting the success of a large embryo transfer program in Holstein cattle in a commercial herd in the southeast region of the United States." Theriogenology **86**(7): 1834-1841.

Fischer, A., et al. (2000). "Estimates of heterosis for in vitro embryo production using reciprocal crosses in cattle." Theriogenology **54**(9): 1433-1442.

Forde, N., et al. (2015). "'Conceptualizing' the endometrium: identification of conceptus-derived proteins during early pregnancy in cattle." Biology of Reproduction **92**(6): 156.

Forde, N., et al. (2011). "Conceptus-induced changes in the endometrial transcriptome: how soon does the cow know she is pregnant?" Biology of Reproduction **85**(1): 144-156.

Forde, N., et al. (2012a). "Evidence for an early endometrial response to pregnancy in cattle: both dependent upon and independent of interferon tau." Physiological Genomics **44**(16): 799-810.

Forde, N. and P. Lonergan (2012). "Transcriptomic analysis of the bovine endometrium: What is required to establish uterine receptivity to implantation in cattle?" The Journal of Reproduction and Development **58**(2): 189-195.

Forde, N. and P. Lonergan (2017). "Interferon-tau and fertility in ruminants." Reproduction **154**(5): F33-F43.

Forde, N., et al. (2014a). "Proteomic analysis of uterine fluid during the pre-implantation period of pregnancy in cattle." Reproduction **147**(5): 575-587.

Forde, N., et al. (2012b). "Effects of low progesterone on the endometrial transcriptome in cattle." Biology of Reproduction **87**(5): 124.

Forde, N., et al. (2014b). "Amino acids in the uterine luminal fluid reflects the temporal changes in transporter expression in the endometrium and conceptus during early pregnancy in cattle." PLoS One **9**(6): e100010.

Forde, N., et al. (2017). "Effect of lactation on conceptus-maternal interactions at the initiation of implantation in cattle: I. Effects on the conceptus transcriptome and amino acid composition of the uterine luminal fluid." Biology of Reproduction **97**(6): 798-809.

Forde, N., et al. (2010). "Effect of pregnancy and progesterone concentration on expression of genes encoding for transporters or secreted proteins in the bovine endometrium." Physiological Genomics **41**(1): 53-62.

Foroutan, A., et al. (2020). "The bovine metabolome." Metabolites **10**(6): 233-249.

França, M. R., et al. (2017). "Evidence of endometrial amino acid metabolism and transport modulation by peri-ovulatory endocrine profiles driving uterine receptivity." Journal of Animal Science and Biotechnology **8**(1): 54-63.

Fujita, T., et al. (2005). "Effect of group culture and embryo-culture conditioned medium on development of bovine embryos." Journal of Reproduction and Development **52**(1): 137-142.

Galvão, K., et al. (2010). "Effect of early postpartum ovulation on fertility in dairy cows." Reproduction in Domestic Animals **45**(5): e207-e211.

Garcia-Garcia, R. M. (2012). "Integrative control of energy balance and reproduction in females." ISRN Veterinary Science **2012**: 121389.

García-Ruiz, A., et al. (2016). "Changes in genetic selection differentials and generation intervals in US Holstein dairy cattle as a result of genomic selection." Proceedings of the National Academy of Sciences **113**(28): E3995-E4004.

Gardner, D. K. and M. Lane (1993). "Amino acids and ammonium regulate mouse embryo development in culture." Biology of Reproduction **48**(2): 377-385.

Garnsworthy, P. C., et al. (2008). "Integration of physiological mechanisms that influence fertility in dairy cows." Animal **2**(8): 1144-1152.

Gatien, J., et al. (2019). "Metabolomic profile of oviductal extracellular vesicles across the estrous cycle in cattle." International Journal of Molecular Sciences **20**(24): 6339.

Gaudet, P., et al. (2011). "Phylogenetic-based propagation of functional annotations within the Gene Ontology consortium." Briefings in Bioinformatics **12**(5): 449-462.

Gegenfurtner, K., et al. (2019a). "Genetic merit for fertility alters the bovine uterine luminal fluid proteome." Biology of Reproduction **102**(3): 730-739.

Gegenfurtner, K., et al. (2019b). "Influence of metabolic status and genetic merit for fertility on proteomic composition of bovine oviduct fluid." Biology of Reproduction **101**(5): 893-905.

Genangeli, M., et al. (2019). "Tissue classification by rapid evaporative ionization mass spectrometry (REIMS): comparison between a diathermic knife and CO 2 laser sampling on classification performance." Analytical and Bioanalytical Chemistry **411**(30): 7943-7955.

Genís, S., et al. (2018). "Pre-calving intravaginal administration of lactic acid bacteria reduces metritis prevalence and regulates blood neutrophil gene expression after calving in dairy cattle." Frontiers in Veterinary Science **5**(135): 1-10.

Genís, S., et al. (2017). "A combination of lactic acid bacteria regulates Escherichia coli infection and inflammation of the bovine endometrium." Journal of Dairy Science **100**(1): 479-492.

Gilardi, S., et al. (2004). "Efeito de diferentes meios de cultivo no desenvolvimento e proporção do sexo de embriões bovinos produzidos in vitro." Arquivo Brasileiro de Medicina Veterinária e Zootecnia **56**(5): 623-627.

Gilbert, R. O. (2019). "Symposium review: Mechanisms of disruption of fertility by infectious diseases of the reproductive tract." Journal of Dairy Science **102**(4): 3754-3765.

Giraudoux, P., et al. (2018). "pgirmess: Spatial analysis and data mining for field ecologists." R package version **1**(9).

Goldansaz, S. A., et al. (2017). "Livestock metabolomics and the livestock metabolome: A systematic review." PLoS One **12**(5): e0177675.

Gomez, E., et al. (2018). "Differential release of cell-signaling metabolites by male and female bovine embryos cultured in vitro." Theriogenology **114**: 180-184.

Gomez, E., et al. (2017). "Hepatoma-derived growth factor: Protein quantification in uterine fluid, gene expression in endometrial-cell culture and effects on in vitro embryo development, pregnancy and birth." Theriogenology **96**: 118-125.

Gómez, E., et al. (2020). "Metabolomic Profiling of Bos taurus Beef, Dairy, and Crossbred Cattle: A Between-Breeds Meta-Analysis." Journal of Agricultural and Food Chemistry **68**(32): 8732-8743.

Gonzales, P. A., et al. (2009). "Large-scale proteomics and phosphoproteomics of urinary exosomes." Journal of the American Society of Nephrology **20**(2): 363-379.

Gonzalez, F. and A. Nardillo (1999). "Retention index in temperature-programmed gas chromatography." Journal of Chromatography A **842**(1-2): 29-49.

Goossens, K., et al. (2010). "Suppression of keratin 18 gene expression in bovine blastocysts by RNA interference." Reproduction, Fertility and Development **22**(2): 395-404.

Graf, A., et al. (2014). "Genome activation in bovine embryos: review of the literature and new insights from RNA sequencing experiments." Animal Reproduction Science **149**(1-2): 46-58.

Gray, C. A., et al. (2002). "Evidence that absence of endometrial gland secretions in uterine gland knockout ewes compromises conceptus survival and elongation." Reproduction **124**(2): 289-300.

Groebner, A. E., et al. (2011a). "Increase of essential amino acids in the bovine uterine lumen during preimplantation development." Reproduction **141**(5): 685.

Groebner, A. E., et al. (2011b). "Immunological mechanisms to establish embryo tolerance in early bovine pregnancy." Reproduction, Fertility and Development **23**(5): 619-632.

Groebner, A. E., et al. (2011c). "Reduced amino acids in the bovine uterine lumen of cloned versus in vitro fertilized pregnancies prior to implantation." Cellular Reprogramming **13**(5): 403-410.

Gross, J. H. (2014). "Direct analysis in real time—a critical review on DART-MS." Analytical and Bioanalytical Chemistry **406**(1): 63-80.

Gu, Y.-t., et al. (2017). "Protective effect of dihydropteridine reductase against oxidative stress is abolished with A278C mutation." Journal of Zhejiang University-Science B **18**(9): 770-777.

Guarini, A. R., et al. (2019). "Genetics and genomics of reproductive disorders in Canadian Holstein cattle." Journal of Dairy Science **102**(2): 1341-1353.

Guerin, P., et al. (2001). "Oxidative stress and protection against reactive oxygen species in the pre-implantation embryo and its surroundings." Human Reproduction Update **7**(2): 175-189.

Guise, M. B. and F. C. Gwazdauskas (1987). "Profiles of Uterine Protein in Flushings and Progesterone in Plasma of Normal and Repeat-Breeding Dairy Cattle." Journal of Dairy Science **70**(12): 2635-2641.

Guo, Y. S. and J. Z. Tao (2018). "Metabolomics and pathway analyses to characterize metabolic alterations in pregnant dairy cows on D 17 and D 45 after AI." Scientific Reports **8**(1): 5973.

Hackett, A. J., et al. (1993). "Location and status of embryos in the genital tract of superovulated cows 4 to 6 days after insemination." Theriogenology **40**(6): 1147-1153.

Hagemann, L. J., et al. (1999). "Development during single IVP of bovine oocytes from dissected follicles: interactive effects of estrous cycle stage, follicle size and atresia." Molecular Reproduction and Development: Incorporating Gamete Research **53**(4): 451-458.

Hailemariam, D., et al. (2014). "Identification of predictive biomarkers of disease state in transition dairy cows." Journal of Dairy Science **97**(5): 2680-2693.

Hamdi, M., et al. (2018). "Bovine oviductal and uterine fluid support in vitro embryo development." Reproduction, Fertility and Development **30**(7): 935-945.

Hammon, D. S., et al. (2000). "Effects of ammonia during different stages of culture on development of in vitro produced bovine embryos." Animal Reproduction Science **59**(1): 23-30.

Hansen, M., et al. (2011). "Determination of steroid hormones in blood by GC–MS/MS." Analytical and Bioanalytical Chemistry **400**(10): 3409-3417.

Hansen, P. J. (2020). "The incompletely fulfilled promise of embryo transfer in cattle—why aren't pregnancy rates greater and what can we do about it?" Journal of Animal Science **98**(11) 1-20.

Harlow, K., et al. (2018). "Diet impacts pre-implantation histotroph proteomes in beef cattle." Journal of Proteome Research **17**(6): 2144-2155.

Harris, B. and E. Kolver (2001). "Review of Holsteinization on intensive pastoral dairy farming in New Zealand." Journal of Dairy Science **84**: E56-E61.

Harris, I., et al. (2012). "PKM2: A gatekeeper between growth and survival." Cell Research **22**(3): 447-449.

Hasler, J. F. (2001). "Factors affecting frozen and fresh embryo transfer pregnancy rates in cattle." Theriogenology **56**(9): 1401-1415.

Hawkins, D. M. (2004). "The Problem of Overfitting." Journal of Chemical Information and Computer Sciences **44**(1): 1-12.

Helfrich, A. L., et al. (2020). "Novel sampling procedure to characterize bovine subclinical endometritis by uterine secretions and tissue." Theriogenology **141**: 186-196.

Hemmings, K. E., et al. (2012). "Amino acid turnover by bovine oocytes provides an index of oocyte developmental competence in vitro." Biology of Reproduction **86**(5): 165, 161-112.

Henskens, Y., et al. (1994). "Cystatins S and C in human whole saliva and in glandular salivas in periodontal health and disease." Journal of Dental Research **73**(10): 1606-1614.

Herdt, T. H. (2000). "Ruminant adaptation to negative energy balance: Influences on the etiology of ketosis and fatty liver." Veterinary Clinics: Food Animal Practice **16**(2): 215-230.

Herlihy, M. M., et al. (2012). "Presynchronization with Double-Ovsynch improves fertility at first postpartum artificial insemination in lactating dairy cows." Journal of Dairy Science **95**(12): 7003-7014.

Hill, J. and R. Gilbert (2008). "Reduced quality of bovine embryos cultured in media conditioned by exposure to an inflamed endometrium." Australian veterinary journal **86**(8): 312-316.

Høglund, R. A., et al. (2019). "Human cysteine cathepsins degrade immunoglobulin G in vitro in a predictable manner." International Journal of Molecular Sciences **20**(19): 4843.

Hsu, M.-C. and W.-C. Hung (2018). "Pyruvate kinase M2 fuels multiple aspects of cancer cells: from cellular metabolism, transcriptional regulation to extracellular signaling." Molecular Cancer **17**(1): 35.

Huang, D. W., et al. (2009). "Bioinformatics enrichment tools: paths toward the comprehensive functional analysis of large gene lists." Nucleic Acids Research **37**(1): 1-13.

Hugentobler, S., et al. (2008). "Energy substrates in bovine oviduct and uterine fluid and blood plasma during the oestrous cycle." Molecular Reproduction and Development **75**(3): 496-503.

Hugentobler, S., et al. (2007a). "Ion concentrations in oviduct and uterine fluid and blood serum during the estrous cycle in the bovine." Theriogenology **68**(4): 538-548.

Hugentobler, S., et al. (2010). "Effects of changes in the concentration of systemic progesterone on ions, amino acids and energy substrates in cattle oviduct and uterine fluid and blood." Reproduction, Fertility and Development **22**(4): 684-694.

Hugentobler, S. A., et al. (2007b). "Amino acids in oviduct and uterine fluid and blood plasma during the estrous cycle in the bovine." Molecular Reproduction and Development **74**(4): 445-454.

Huh, C., et al. (1995). "Structural organization, expression and chromosomal mapping of the mouse cystatin-C-encoding gene (Cst3)." Gene **152**(2): 221-226.

Humblot, P. (2001). "Use of pregnancy specific proteins and progesterone assays to monitor pregnancy and determine the timing, frequencies and sources of embryonic mortality in ruminants." Theriogenology **56**(9): 1417-1433.

Humblot, P., et al. (2005). "Effect of stage of follicular growth during superovulation on developmental competence of bovine oocytes." Theriogenology **63**(4): 1149-1166.

Hunter, R. H. (2012). "Components of oviduct physiology in eutherian mammals." Biological Reviews **87**(1): 244-255.

Hunter, R. H., et al. (2007). "Peritoneal fluid as an unrecognised vector between female reproductive tissues." Acta Obstetricia et Gynecologica Scandinavica **86**(3): 260-265.

Hunter, R. H., et al. (2011). "Considerations of viscosity in the preliminaries to mammalian fertilisation." Journal of Assisted Reproduction and Genetics **28**(3): 191-197.

Ikeda, S., et al. (2011). "Importance of Methionine Metabolism in Morula-to-blastocyst Transition in Bovine Preimplantation Embryos." Journal of Reproduction and Development **58**(1)**: 91-99.**

Isaac, E. and P. L. Pfeffer (2021). "Growing cattle embryos beyond Day 8 – An investigation of media components." Theriogenology **161**: 273-284.

Iyengar, V. (2002). "Nuclear and isotopic techniques for addressing nutritional problems, with special reference to current applications in developing countries." Food and Nutrition Bulletin **23**(1): 3-10.

Jackson, J. E. (2005). A user's guide to principal components, John Wiley & Sons.

Jaureguiberry, M., et al. (2017). "Short communication: Repeat breeder cows with fluid in the uterine lumen had poorer fertility." Journal of Dairy Science **100**(4): 3083-3085.

Jay, M. and M. Morad (2007). "Crying over spilt milk: A critical assessment of the ecological modernization of New Zealand's dairy industry." Society and Natural Resources **20**(5): 469-478.

Jiye, A., et al. (2005). "Extraction and GC/MS analysis of the human blood plasma metabolome." Analytical Chemistry **77**(24): 8086-8094.

Jolliffe, I. T. (1986). Principal Components in Regression Analysis. Principal Component Analysis. I. T. Jolliffe. New York, NY, Springer New York**:** 129-155.

Jones, J. I. and D. R. Clemmons (1995). "Insulin-like growth factors and their binding proteins: biological actions." Endocrinology Reviews **16**(1): 3-34.

Jonsson, P., et al. (2005). "High-throughput data analysis for detecting and identifying differences between samples in GC/MS-based metabolomic analyses." Analytical Chemistry **77**(17): 5635-5642.

Jordaens, L., et al. (2020). "Altered embryotrophic capacities of the bovine oviduct under elevated free fatty acid conditions: an n vitro embryo–oviduct co-culture model." Reproduction, Fertility and Development **32**(6): 553-563.

Käll, L., et al. (2004). "A combined transmembrane topology and signal peptide prediction method." Journal of molecular biology **338**(5): 1027-1036.

Käll, L., et al. (2007). "Advantages of combined transmembrane topology and signal peptide prediction—the Phobius web server." Nucleic Acids Research **35**(suppl_2): W429-W432.

Kamat, M. M., et al. (2016). "Changes in Myeloid Lineage Cells in the Uterus and Peripheral Blood of Dairy Heifers During Early Pregnancy." Biology of Reproduction **95**(3).

Kambadur, R., et al. (1997). "Mutations in myostatin (GDF8) in double-muscled Belgian Blue and Piedmontese cattle." Genome Research **7**(9): 910-916.

Kamburov, A., et al. (2011). "Integrated pathway-level analysis of transcriptomics and metabolomics data with IMPaLA." Bioinformatics **27**(20): 2917-2918.

Kandasamy, K., et al. (2010). "NetPath: a public resource of curated signal transduction pathways." Genome biology **11**(1): 1-9.

Kao, L. C., et al. (2003). "Expression Profiling of Endometrium from Women with Endometriosis Reveals Candidate Genes for Disease-Based Implantation Failure and Infertility." Endocrinology **144**(7): 2870-2881.

Karnovsky, A. and S. Li (2020). Pathway Analysis for Targeted and Untargeted Metabolomics. Computational Methods and Data Analysis for Metabolomics. S. Li. New York, NY, Springer US**:** 387-400.

Katagiri, S. and M. Moriyoshi (2013). "Alteration of the endometrial EGF profile as a potential mechanism connecting the alterations in the ovarian steroid hormone profile to embryonic loss in repeat breeders and high-producing cows." Journal of Reproduction and Development **59**(5): 415-420.

Katagiri, S. and Y. Takahashi (2004). "Changes in EGF concentrations during estrous cycle in bovine endometrium and their alterations in repeat breeder cows." Theriogenology **62**(1): 103-112.

Kayaaltı, Z., et al. (2016). "Association between delta-aminolevulinic acid dehydratase polymorphism and placental lead levels." Environmental Toxicology and Pharmacology **41**: 147-151.

Khurana, N. K. and H. Niemann (2000). "Energy Metabolism in Preimplantation Bovine Embryos Derived In Vitro or In Vivo1." Biology of Reproduction **62**(4): 847-856.

Kim, J. W. (2014). "Modulation of the somatotropic axis in periparturient dairy cows." Asian-Australasian Journal of Animal Sciences **27**(1): 147-154.

Kiracofe, G. (1980). "Uterine involution: its role in regulating postpartum intervals." Journal of Animal Science **51**(suppl_II): 16-28.

Kitano, H. (2002). "Systems biology: a brief overview." Science **295**(5560): 1662-1664.

Klebanoff, S. and D. Smith (1970). "Peroxidase-mediated antimicrobial activity of rat uterine fluid." Gynecologic and Obstetric Investigation **1**(1): 21-30.

Klein, P. D. and E. R. Klein (1987). "Stable isotope usage in developing countries: Safe tracer tools to measure human nutritional status." IAEA Bulletin **29**(4): 41-44.

Koehn, H., et al. (2011). "Combination of acid labile detergent and C18 Empore™ disks for improved identification and sequence coverage of in-gel digested proteins." Analytical and Bioanalytical Chemistry **400**(2): 415-421.

Koek, M. M., et al. (2006). "Microbial Metabolomics with Gas Chromatography/Mass Spectrometry." Analytical Chemistry **78**(4): 1272-1281.

Koh, Y. Q., et al. (2020). "Exosomes from dairy cows of divergent fertility; Action on endometrial cells." Journal of Reproductive Immunology **137**: 102624.

Kordiš, D. and V. Turk (2009). "Phylogenomic analysis of the cystatin superfamily in eukaryotes and prokaryotes." BMC Evolutionary Biology **9**(1): 266.

Kos, J., et al. (2014). "The current stage of cathepsin B inhibitors as potential anticancer agents." Future Medicinal Chemistry **6**(11): 1355-1371.

Kruip, T. A., et al. (2000). "Environment of oocyte and embryo determines health of IVP offspring." Theriogenology **53**(2): 611-618.

Kyle, J. E., et al. (2016). "Uncovering biologically significant lipid isomers with liquid chromatography, ion mobility spectrometry and mass spectrometry." Analyst **141**(5): 1649-1659.

Lafarge, J.-C., et al. (2010). "Cathepsins and cystatin C in atherosclerosis and obesity." Biochimie **92**(11): 1580-1586.

Lamb, G. C., et al. (2010). "Control of the estrous cycle to improve fertility for fixed-time artificial insemination in beef cattle: A review1." Journal of Animal Science **88**(suppl_13): E181-E192.

Lamy, J., et al. (2016a). "Regulation of the bovine oviductal fluid proteome." Reproduction **152**(6): 629-644.

Lamy, J., et al. (2016b). "Steroid hormones in bovine oviductal fluid during the estrous cycle." Theriogenology **86**(6): 1409-1420.

Landrock, D., et al. (2010). "Acyl-CoA binding protein gene ablation induces pre-implantation embryonic lethality in mice." Lipids **45**(7): 567-580.

Larson, S. F., et al. (2007). "Pregnancy rates in lactating dairy cattle following supplementation of progesterone after artificial insemination." Animal Reproduction Science **102**(1): 172-179.

Lê Cao, K.-A., et al. (2011). "Sparse PLS discriminant analysis: biologically relevant feature selection and graphical displays for multiclass problems." BMC Bioinformatics **12**(1): 253.

LeBlanc, S. (2010). "Assessing the association of the level of milk production with reproductive performance in dairy cattle." Journal of Reproduciton and Development **56(S)**: S1-7.

LeBlanc, S. J. (2014). "Reproductive tract inflammatory disease in postpartum dairy cows." Animal **8**(S1): 54-63.

LeBlanc, S. J., et al. (2011). "Reproductive tract defense and disease in postpartum dairy cows." Theriogenology **76**(9): 1610-1618.

Ledgard, A. M., et al. (2012). "Effect of asynchronous transfer on bovine embryonic development and relationship with early cycle uterine proteome profiles." Reproduction, Fertility and Development **24**(7): 962-972.

Ledgard, A. M., et al. (2009). "Bovine endometrial legumain and TIMP-2 regulation in response to presence of a conceptus." Molecular Reproduction and Development **76**(1): 65-74.

Lee, R. K.-K., et al. (2018). "Expression of cystatin C in the female reproductive tract and its effect on human sperm capacitation." Reproductive Biology and Endocrinology **16**(1): 8.

Leese, H. J., et al. (2016). "Biological optimization, the Goldilocks principle, and how much is lagom in the preimplantation embryo." Molecular Reproduction and Development **83**(9): 748-754.

Leese, H. J., et al. (2007). "Embryo viability and metabolism: obeying the quiet rules." Human Reproduction **22**(12): 3047-3050.

Lenz, M., et al. (2016). "Principal components analysis and the reported low intrinsic dimensionality of gene expression microarray data." Scientific Reports **6**(1): 1-11.

Lerner, U. H. and A. Grubb (1992). "Human cystatin C, a cysteine proteinase inhibitor, inhibits bone resorption in vitro stimulated by parathyroid hormone and parathyroid hormone-related peptide of malignancy." Journal of Bone and Mineral Research **7**(4): 433-440.

Leroy, J., et al. (2005a). "Comparison of embryo quality in high-yielding dairy cows, in dairy heifers and in beef cows." Theriogenology **64**(9): 2022-2036.

Leroy, J. L., et al. (2018). "Negative energy balance and metabolic stress in relation to oocyte and embryo quality: an update on possible pathways reducing fertility in dairy cows." Animal Reproduction **14**(3): 497-506.

Leroy, J. L., et al. (2005b). "Non-esterified fatty acids in follicular fluid of dairy cows and their effect on developmental capacity of bovine oocytes in vitro." Reproduction **130**(4): 485-495.

Leroy, J. L. M. R., et al. (2004). "Metabolic changes in follicular fluid of the dominant follicle in high-yielding dairy cows early post partum." Theriogenology **62**(6): 1131-1143.

Leyens, G., et al. (2004). "Expression of peroxiredoxins in bovine oocytes and embryos produced in vitro." Molecular Reproduction and Development: Incorporating Gamete Research **69**(3): 243-251.

Li, C. Q., et al. (2013). "Subpathway-GM: identification of metabolic subpathways via joint power of interesting genes and metabolites and their topologies within pathways." Nucleic Acids Research **41**(9): e101-e101.

Li, J., et al. (2019). "Effect of autophagy induction and cathepsin B inhibition on developmental competence of poor quality bovine oocytes." Journal of Reproduction and Development **66**(1): 83-91.

Li, S. and W. Winuthayanon (2017). "Oviduct: roles in fertilization and early embryo development." Journal of Endocrinology **232**(1): R1-R26.

Lima, F. S., et al. (2010). "Economic comparison of natural service and timed artificial insemination breeding programs in dairy cattle." Journal of Dairy Science **93**(9): 4404-4413.

Lin, L.-Y., et al. (2020). "Ammonia exposure impairs lateral-line hair cells and mechanotransduction in zebrafish embryos." Chemosphere **257**: 127170.

Liu, H., et al. (2004). "A model for random sampling and estimation of relative protein abundance in shotgun proteomics." Analytical Chemistry **76**(14): 4193-4201.

Lonergan, P., et al. (1996). "Role of Epidermal Growth Factor in Bovine Oocyte Maturation and Preimplantation Embryo Development in Vitro1." Biology of Reproduction **54**(6): 1420-1429.

Lonergan, P., et al. (2016). "Embryo development in dairy cattle." Theriogenology **86**(1): 270-277.

Lonergan, P. and N. Forde (2014). "Maternal-embryo interaction leading up to the initiation of implantation of pregnancy in cattle." Animal **8**(S1): 64-69.

Lonergan, P., et al. (1994). "Effect of follicle size on bovine oocyte quality and developmental competence following maturation, fertilization, and culture in vitro." Molecular Reproduction and Development **37**(1): 48-53.

Lopera-Vasquez, R., et al. (2017). "Effect of bovine oviductal extracellular vesicles on embryo development and quality in vitro." Reproduction **153**(4): 461-470.

Lopes, A., et al. (2006). "Effect of days post-partum, breed and ovum pick-pp scheme on bovine oocyte recovery and embryo development." Reproduction in Domestic Animals **41**(3): 196-203.

Lössl, P., et al. (2016). "The diverse and expanding role of mass spectrometry in structural and molecular biology." EMBO Journal **35**(24): 2634-2657.

Lucy, M., et al. (2014). "Endocrine and metabolic mechanisms linking postpartum glucose with early embryonic and foetal development in dairy cows." Animal **8**(s1): 82-90.

Lucy, M., et al. (2001). "Changes in the somatotrophic axis associated with the initiation of lactation." Journal of Dairy Science **84**: E113-E119.

Lucy, M. C. (2001). "Reproductive loss in high-producing dairy cattle: where will it end?" Journal of Dairy Science **84**(6): 1277-1293.

Lukanidin, E. and J. P. Sleeman (2012). "Building the niche: the role of the S100 proteins in metastatic growth." Seminars in Cancer Biology **22**(3): 216-225.

Luo, W. and G. L. Semenza (2012). "Emerging roles of PKM2 in cell metabolism and cancer progression." Trends in Endocrinology and Metabolism **23**(11): 560-566.

Lussier, J., et al. (1987). "Growth rates of follicles in the ovary of the cow." Reproduction **81**(2): 301-307.

Lyimo, Z. C., et al. (2000). "Relationship among estradiol, cortisol and intensity of estrous behavior in dairy cattle." Theriogenology **53**(9): 1783-1795.

Ma, Q., et al. (2015). "MAGI3 negatively regulates Wnt/β-catenin signaling and suppresses malignant phenotypes of glioma cells." Oncotarget **6**(34): 35851-35865.

Macmillan, K. and R. Curnow (1977). "Tail painting—a simple form of oestrus detection in New Zealand dairy herds." New Zealand Journal of Experimental Agriculture **5**(4): 357-361.

Macmillan, K. and A. Peterson (1993). "A new intravaginal progesterone releasing device for cattle (CIDR-B) for oestrous synchronisation, increasing pregnancy rates and the treatment of post-partum anoestrus." Animal Reproduction Science **33**(1-4): 1-25.

Macmillan, K. L. (2010). "Recent Advances in the Synchronization of Estrus and Ovulation in Dairy Cows." Journal of Reproduction and Development **56**(S): S42-S47.

Madeja, Z. E., et al. (2013). "Changes in sub-cellular localisation of trophoblast and inner cell mass specific transcription factors during bovine preimplantation development." BMC Developmental Biology **13**(1): 1-17.

Maes, E., et al. (2015). "Determination of variation parameters as a crucial step in designing TMT-based clinical proteomics experiments." PLoS One **10**(3), article e0120115.

Maillo, V., et al. (2015). "Oviduct-Embryo Interactions in Cattle: Two-Way Traffic or a One-Way Street?" Biology of Reproduction **92**(6): 144.

Maillo, V., et al. (2016). "Maternal-embryo interaction in the bovine oviduct: Evidence from in vivo and in vitro studies." Theriogenology **86**(1): 443-450.

Maillo, V., et al. (2012). "Influence of lactation on metabolic characteristics and embryo development in postpartum Holstein dairy cows." Journal of Dairy Science **95**(7): 3865-3876.

Makino, Y., et al. (2020). "Influence of low O2 and high CO2 environment on changes in metabolite concentrations in harvested vegetable soybeans." Food Chemistry **317**: 126380.

Mamo, S., et al. (2012). "Conceptus-endometrium crosstalk during maternal recognition of pregnancy in cattle." Biology of Reproduction **87**(1): 6, 1-9.

Martins, T., et al. (2018). "Perturbations in the uterine luminal fluid composition are detrimental to pregnancy establishment in cattle." Journal of Animal Science and Biotechnology **9**: 70.

Massudi, H., et al. (2012). "Age-associated changes in oxidative stress and NAD+ metabolism in human tissue." PLoS One **7**(7): e42357.

Masuda, T., et al. (2008). "Phase Transfer Surfactant-Aided Trypsin Digestion for Membrane Proteome Analysis." Journal of Proteome Research **7**(2): 731-740.

Matoba, S., et al. (2012). "The association between metabolic parameters and oocyte quality early and late postpartum in Holstein dairy cows." Journal of Dairy Science **95**(3): 1257-1266.

Mazurek, S., et al. (2005). Pyruvate kinase type M2 and its role in tumor growth and spreading. Seminars in Cancer Biology, Elsevier.

McDougall, S., et al. (2011). "Relationships between cytology, bacteriology and vaginal discharge scores and reproductive performance in dairy cattle." Theriogenology **76**(2): 229-240.

McDougall, S., et al. (2007). "Association between endometritis diagnosis using a novel intravaginal device and reproductive performance in dairy cattle." Animal Reproduction Science **99**(1-2): 9-23.

McMillan, W. (1998). "Statistical models predicting embryo survival to term in cattle after embryo transfer." Theriogenology **50**(7): 1053-1070.

McNaughton, L., et al. (2003). Postpartum anoestrous intervals and reproductive performance in three genotypes of Holstein-Friesian dairy cattle managed in a seasonal pasture-based dairy system. Proceedings of the New Zealand Society of Animal Production, **63**:77-81.

McRae, A. C. (1988). "The blood–uterine lumen barrier and exchange between extracellular fluids." Reproduction **82**(2): 857-873.

Ménézo, Y., et al. (1993). Embryo quality and co-culture. Gamete and embryo quality, Proceedings of the Fourth Organon, Round Table Conference, Thessaloniki, Greece**:** 139-155.

Meng, W., et al. (2008). "One-Step Procedure for Peptide Extraction from In-Gel Digestion Sample for Mass Spectrometric Analysis." Analytical Chemistry **80**(24): 9797-9805.

Mesa, J., et al. (2015). "Human prostaglandin reductase 1 (PGR1): Substrate specificity, inhibitor analysis and site-directed mutagenesis." Chemico-Biological Interactions **234**: 105-113.

Mesbah-Uddin, M., et al. (2018). "Genome-wide mapping of large deletions and their population-genetic properties in dairy cattle." DNA Research **25**(1): 49-59.

Mikolajczyk, M., et al. (2006). "Leukaemia inhibitory factor and interleukin 11 levels in uterine flushings of infertile patients with endometriosis." Human Reproduction **21**(12): 3054-3058.

Miller, D. J. (2018). "Review: The epic journey of sperm through the female reproductive tract." Animal **12**(s1): s110-s120.

Miller, R. M., et al. (2019). "Improved Protein Inference from Multiple Protease Bottom-Up Mass Spectrometry Data." Journal of Proteome Research **18**(9): 3429-3438.

Mineki, R., et al. (2002). "In situ alkylation with acrylamide for identification of cysteinyl residues in proteins during one-and two-dimensional sodium dodecyl sulphate-polyacrylamide gel electrophoresis." Proteomics **2**(12): 1672-1681.

Misirlioglu, M., et al. (2006). "Dynamics of global transcriptome in bovine matured oocytes and preimplantation embryos." Proceedings of the National Academy of Sciences **103**(50): 18905-18910.

Mitrea, C., et al. (2013). "Methods and approaches in the topology-based analysis of biological pathways." Frontiers in Physiology **4**(278).

Molenaar, M. R., et al. (2019). "LION/web: a web-based ontology enrichment tool for lipidomic data analysis." GigaScience **8**(6): giz061.

Mondéjar, I., et al. (2012). "The Oviduct: Functional Genomic and Proteomic Approach." Reproduction in Domestic Animals **47**(s3): 22-29.

Moohan, J. M. and K. S. Lindsay (1995). "Spermatozoa selected by a discontinuous Percoll density gradient exhibit better motion characteristics, more hyperactivation, and longer survival than direct swim-upt." Fertility and sterility **64**(1): 160-165.

Moraes, J. G., et al. (2018a). "Uterine influences on conceptus development in fertility-classified animals." Proceedings of the National Academy of Sciences **115**(8): E1749-E1758.

Moraes, J. G. N., et al. (2020a). "Analysis of the uterine lumen in fertility-classified heifers: II. Proteins and metabolites." Biology of Reproduction **102**(3): 571-587.

Moraes, J. G. N., et al. (2018b). "Uterine influences on conceptus development in fertility-classified animals." Proceedings of the National Academy of Sciences **115**(8): E1749-E1758.

Moraes, J. G. N., et al. (2020b). "Analysis of the uterine lumen in fertility-classified heifers: I. Glucose, prostaglandins, and lipids." Biology of Reproduction **102**(2): 456-474.

More, T., et al. (2015). "Metabolomics and its integration with systems biology: PSI 2014 conference panel discussion report." Journal of Proteomics **127**(Part A): 73-79.

Moussa, M., et al. (2015). "Maternal control of oocyte quality in cattle “a review”." Animal Reproduction Science **155**: 11-27.

Moyes, K. M., et al. (2013). "Generation of an index for physiological imbalance and its use as a predictor of primary disease in dairy cows during early lactation." Journal of Dairy Science **96**(4): 2161-2170.

Mulkidjanian, A. Y., et al. (2009). "Co-evolution of primordial membranes and membrane proteins." Trends in Biochemical Sciences **34**(4): 206-215.

Mullen, M. P., et al. (2012). "Proteomic characterization of histotroph during the preimplantation phase of the estrous cycle in cattle." Journal of Proteome Research **11**(5): 3004-3018.

Muñoz, M., et al. (2012). "Proteome of the early embryo-maternal dialogue in the cattle uterus." Journal of Proteome Research **11**(2): 751-766.

Muñoz, M., et al. (2014). "Metabolomic prediction of pregnancy viability in superovulated cattle embryos and recipients with Fourier transform infrared spectroscopy." BioMed Research International **2014**: art. 608579.

Murakami, M. and I. Kudo (2002). "Phospholipase A2." The Journal of Biochemistry **131**(3): 285-292.

Nagana Gowda, G. and D. Raftery (2016). "Recent advances in NMR-based metabolomics." Analytical Chemistry **89**(1): 490-510.

Nayeri, S. and P. Stothard (2016). "Tissues, Metabolic Pathways and Genes of Key Importance in Lactating Dairy Cattle." Springer Science Reviews **4**(2): 49-77.

Ner-Kluza, J., et al. (2019). "Identification of protein patterns in bovine placenta at early-mid pregnancy - Pilot studies." Rapid Communications in Mass Spectrometry **33**(12): 1084-1090.

Nguyen, T.-M., et al. (2019). "Identifying significantly impacted pathways: a comprehensive review and assessment." Genome Biology **20**(1): 203.

Nielsen, M. L., et al. (2008). "Iodoacetamide-induced artifact mimics ubiquitination in mass spectrometry." Nature Methods **5**(6): 459.

Nilsson, J., et al. (2004). "Regulation of eukaryotic translation by the RACK1 protein: a platform for signalling molecules on the ribosome." EMBO reports **5**(12): 1137-1141.

Nolen, B. J. and T. D. Pollard (2007). "Insights into the influence of nucleotides on actin family proteins from seven structures of Arp2/3 complex." Molecular Cell **26**(3): 449-457.

O'Doherty, A. M., et al. (2017). "Imprinted and DNA methyltransferase gene expression in the endometrium during the pre- and peri-implantation period in cattle." Reproduction, Fertility and Development **29**(9): 1729-1738.

O'Donovan, C., et al. (2002). "High-quality protein knowledge resource: SWISS-PROT and TrEMBL." Briefings in Bioinformatics **3**(3): 275-284.

Oda, K., et al. (2005). "A comprehensive pathway map of epidermal growth factor receptor signaling." Molecular Systems Biology **1**: 2005.0010.

Ortega, M. S., et al. (2017). "Association of single nucleotide polymorphisms in candidate genes previously related to genetic variation in fertility with phenotypic measurements of reproductive function in Holstein cows." Journal of Dairy Science **100**(5): 3725-3734.

Osborne, J. (2010). "Improving your data transformations: Applying the Box-Cox transformation." Practical Assessment, Research, and Evaluation **15**(1): 12.

Otsuki, J., et al. (2013). "The redox state of recombinant human serum albumin and its optimal concentration for mouse embryo culture." Systems Biology in Reproductive Medicine **59**(1): 48-52.

Ott, T. L. (2019). "Symposium review: Immunological detection of the bovine conceptus during early pregnancy." Journal of Dairy Science **102**(4): 3766-3777.

Pagé-Larivière, F., et al. (2017). "Mechanisms Involved in Porcine Early Embryo Survival following Ethanol Exposure." Toxicological Sciences **156**(1): 289-299.

Pang, T.-L., et al. (2010). "Costars, a Dictyostelium protein similar to the C-terminal domain of STARS, regulates the actin cytoskeleton and motility." Journal of Cell Science **123**(21): 3745-3755.

Pang, Z., et al. (2020). "MetaboAnalystR 3.0: toward an optimized workflow for global metabolomics." Metabolites **10**(5): 186.

Papp, S. M., et al. (2019). "A novel approach to study the bovine oviductal fluid proteome using transvaginal endoscopy." Theriogenology **132**: 53-61.

Parr, R., et al. (1993). "Liver blood flow and metabolic clearance rate of progesterone in sheep." Research in Veterinary Science **55**(3): 311-316.

Parrish, D. and F. Fountaine (1952). "Contents of the alimentary tract of calves at birth." Journal of Dairy Science **35**(10): 839-845.

Pascovici, D., et al. (2012). "PloGO: Plotting gene ontology annotation and abundance in multi-condition proteomics experiments." Proteomics **12**(3): 406-410.

Passaro, C., et al. (2016). "73 Proteomic analysis of uterine luminal fluid on Day 7 of pregnancy in cattle." Reproduction, Fertility and Development **28**(2): 166.

Paulesu, L., et al. (2012). "Variation in macrophage migration inhibitory factor [MIF] immunoreactivity during bovine gestation." Placenta **33**(3): 157-163.

Pearson, W. R. (2013). "An introduction to sequence similarity ("homology") searching." Current Protocols in Bioinformatics **42**(1): 3.1.

Perez, Y., et al. (2016). "UNC80 mutation causes a syndrome of hypotonia, severe intellectual disability, dyskinesia and dysmorphism, similar to that caused by mutations in its interacting cation channel, NALCN." Journal of Medical Genetics **53**(6): 397.

Pieterse, M., et al. (1990). "Early pregnancy diagnosis in cattle by means of linear-array real-time ultrasound scanning of the uterus and a qualitative and quantitative milk progesterone test." Theriogenology **33**(3): 697-707.

Pillai, V. V., et al. (2017). "Profiling of proteins secreted in the bovine oviduct reveals diverse functions of this luminal microenvironment." PLoS One **12**(11): e0188105.

Png, F. Y. and C. R. Murphy (2002). "Cytoskeletal proteins in uterine epithelial cells only partially return to the pre-receptive state after the period of receptivity." Acta Histochemica **104**(3): 235-244.

Ponsart, C., et al. (2001). "Effects of the paternal origin of the donor cow on embryo production after superovulation in the Prim Holstein and Montbeliarde breeds." Theriogenology **55**(1): 369-380.

Ponting, C. P., et al. (1992). "Plasminogen: a structural review." Blood Coagulation & Fibrinolysis **3**(5): 605-614.

Prasannan, C. B., et al. (2018). "An improved method for extraction of polar and charged metabolites from cyanobacteria." PLoS One **13**(10): e0204273.

Prentki, M. and S. R. M. Madiraju (2008). "Glycerolipid metabolism and signaling in health and disease." Endocrinology Reviews **29**(6): 647-676.

Pryce, J., et al. (2004). "Fertility in the high-producing dairy cow." Livestock Production Science **86**(1-3): 125-135.

Pugliesi, G., et al. (2014). "Corpus luteum development and function after supplementation of long-acting progesterone during the early luteal phase in beef cattle." Reproduction in Domestic Animals **49**(1): 85-91.

Ramos-Ibeas, P., et al. (2020a). "Senescence and apoptosis during in vitro embryo development in a bovine model." Frontiers in Cell and Developmental Biology **8**(1646).

Ramos-Ibeas, P., et al. (2020b). "Embryonic disc formation following post-hatching bovine embryo development in vitro." Reproduction **160**(4): 579-589.

Rappsilber, J., et al. (2003). "Stop and go extraction tips for matrix-assisted laser desorption/ionization, nanoelectrospray, and LC/MS sample pretreatment in proteomics." Analytical Chemistry **75**(3): 663-670.

Rawat, P., et al. (2016). "Identification of potential protein biomarkers for early detection of pregnancy in cow urine using 2D DIGE and label free quantitation." Clinical Proteomics **13**(1): 15.

Rawlings, A. (1995). "Skin waxes: their composition, properties, structures and biological significance." Waxes The Oily Press, Dundee, UK: 223-258.

Reich, H., et al. (2005). "Albumin activates ERK via EGF receptor in human renal epithelial cells." Journal of the American Society of Nephrology **16**(5): 1266-1278.

Ren, Y., et al. (2014). "Direct mass spectrometry analysis of biofluid samples using slug-llow microextraction nano-electrospray ionization." Angewandte Chemie International Edition **53**(51): 14124-14127.

Rennard, S., et al. (1986). "Estimation of volume of epithelial lining fluid recovered by lavage using urea as marker of dilution." Journal of Applied Physiology **60**(2): 532-538.

Reynolds, M. (1953). "Plasma and blood volume in the cow using the T-1824 hematocrit method." American Journal of Physiology-Legacy Content **173**(3): 421-427.

Ribeiro, E. S., et al. (2016a). "Carryover effect of postpartum inflammatory diseases on developmental biology and fertility in lactating dairy cows." Journal of Dairy Science **99**(3): 2201-2220.

Ribeiro, E. S., et al. (2016b). "Biology of preimplantation conceptus at the onset of elongation in dairy cows." Biology of Reproduction **94**(4): 97, 91-18.

Ribeiro, E. S., et al. (2016c). "Role of lipids on elongation of the preimplantation conceptus in ruminants." Reproduction **152**(4): R115-126.

Rizos, D., et al. (2010). "Contribution of the female reproductive tract to low fertility in postpartum lactating dairy cows." Journal of Dairy Science **93**(3): 1022-1029.

Rizos, D., et al. (2002). "Consequences of bovine oocyte maturation, fertilization or early embryo development in vitro versus in vivo: Implications for blastocyst yield and blastocyst quality." Molecular Reproduction and Development **61**(2): 234-248.

Roberts, R. and F. Bazer (1988). "The functions of uterine secretions." Reproduction **82**(2): 875-892.

Roberts, S. J. (1986). "Veterinary obstetrics and genital diseases." Theriogenology, 3rd ed. , Woodstock, VT.

Robinson, R. S., et al. (2006). "In vivo expression of interferon tau mRNA by the embryonic trophoblast and uterine concentrations of interferon tau protein during early pregnancy in the cow." Molecular Reproduction and Development **73**(4): 470-474.

Rochat, B. (2016). "From targeted quantification to untargeted metabolomics: Why LC-high-resolution-MS will become a key instrument in clinical labs." Trends in Analytical Chemistry **84**: 151-164.

Roche, J., et al. (1981). "Reproductive wastage following artificial insemination of heifers." The Veterinary Record **109**(18): 401-404.

Roche, J., et al. (2004). "Relationships among international body condition scoring systems." Journal of Dairy Science **87**(9): 3076-3079.

Roche, J. R., et al. (2017). "Fertility and the transition dairy cow." Reproduction, Fertility and Development **30**(1): 85-100.

Roche, J. R., et al. (2011). "Nutrition × reproduction interaction in pasture-based systems: is nutrition a factor in reproductive failure?" Animal Production Science **51**(12): 1045-66.

Roche, J. R., et al. (2009). "Invited review: Body condition score and its association with dairy cow productivity, health, and welfare." Journal of Dairy Science **92**(12): 5769-5801.

Rodríguez-Almazán, C., et al. (2008). "Structural basis of human triosephosphate isomerase deficiency mutation e104d is related to alterations of a conserved water network at the dimer interface." Journal of Biological Chemistry **283**(34): 23254-23263.

Rodríguez-Alonso, B., et al. (2020a). "Spatial and pregnancy-related changes in the protein, amino acid, and carbohydrate composition of bovine oviduct fluid." International Journal of Molecular Sciences **21**(5): 1681.

Rodríguez-Alonso, B., et al. (2020b). "Challenges in studying preimplantation embryo-maternal interaction in cattle." Theriogenology **150**(2020): 139-149.

Rohart, F., et al. (2017). "mixOmics: An R package for 'omics feature selection and multiple data integration." PLoS Computational Biology **13**(11): e1005752.

Ross, A., et al. (2020). "Making complex measurements of meat composition fast: Application of rapid evaporative ionisation mass spectrometry to measuring meat quality and fraud." Meat Science: 108333 *(in press)*.

Rouse, B., et al. (1997). "Maternal phenylketonuria collaborative study (MPKUCS) offspring: facial anomalies, malformations, and early neurological sequelae." American Journal of Medical Genetics **69**(1): 89-95.

Royal, M., et al. (2000). "Declining fertility in dairy cattle: changes in traditional and endocrine parameters of fertility." Animal Science **70**(3): 487-501.

Rust, R. R., et al. (2000). "Structure of the negative regulatory domain of p53 bound to S100B (ββ)." Nature Structural Biology **7**(7): 570-574.

Ryan, D. P., et al. (1993). "Comparing early embryo mortality in dairy cows during hot and cool seasons of the year." Theriogenology **39**(3): 719-737.

Saint-Dizier, M., et al. (2019). "Composing the Early Embryonic Microenvironment: Physiology and Regulation of Oviductal Secretions." International Journal of Molecular Sciences **21**(1): 223.

Salilew-Wondim, D., et al. (2010). "Bovine pretransfer endometrium and embryo transcriptome fingerprints as predictors of pregnancy success after embryo transfer." Physiological Genomics **42**(2): 201-218.

Salilew-Wondim, D., et al. (2012). "Oviductal, endometrial and embryonic gene expression patterns as molecular clues for pregnancy establishment." Animal Reproduction Science **134**(1-2): 9-18.

Sang, L., et al. (2020). "Actions of putative embryokines on development of the preimplantation bovine embryo to the blastocyst stage." Journal of Dairy Science **103**(12): 11930-11944.

Sangsritavong, S., et al. (2002). "High feed intake increases liver blood flow and metabolism of progesterone and estradiol-17β in dairy cattle." Journal of Dairy Science **85**(11): 2831-2842.

Santos, J. and E. Ribeiro (2018). "Impact of animal health on reproduction of dairy cows." Animal Reproduction **11**(3): 254-269.

Santos, J., et al. (2009). "Risk factors for resumption of postpartum estrous cycles and embryonic survival in lactating dairy cows." Animal Reproduction Science **110**(3-4): 207-221.

Santos, J. E. P., et al. (2004). "The effect of embryonic death rates in cattle on the efficacy of estrus synchronization programs." Animal Reproduction Science **82-83**: 513-535.

Sartori, R., et al. (2002). "Fertilization and early embryonic development in heifers and lactating cows in summer and lactating and dry cows in winter." Journal of Dairy Science **85**(11): 2803-2812.

Satterfield, M. C., et al. (2009). "Discovery of candidate genes and pathways in the endometrium regulating ovine blastocyst growth and conceptus elongation." Physiological Genomics **39**(2): 85-99.

Saugandhika, S., et al. (2015). "Expression and purification of buffalo interferon-tau and efficacy of recombinant buffalo interferon-tau for in vitro embryo development." Cytokine **75**(1): 186-196.

Sawa, A. and M. Bogucki (2011). "Effect of housing system and milk yield on cow fertility." Archives of Animal Breeding **54**(3): 249-256.

Schomburg, D. and D. Stephan (1996). Nicotinate phosphoribosyltransferase. Enzyme Handbook 12: Class 2.3.2 — 2.4 Transferases. D. Schomburg and D. Stephan. Berlin, Heidelberg, Springer Berlin Heidelberg**:** 997-1001.

Schultz, R., et al. (1971). "A chemical study of uterine fluid and blood serum of normal cows during the oestrous cycle." Reproduction **27**(3): 355-367.

Schulz, S., et al. (2009). "Strengths and limitations of formal ontologies in the biomedical domain." Revista Electronica de Comunicacao, Informacao & Inovacao em Saude: RECIIS **3**(1): 31.

Scully, S., et al. (2015). "Ultrasound monitoring of blood flow and echotexture of the corpus luteum and uterus during early pregnancy of beef heifers." Theriogenology **83**(3): 449-458.

Scully, S., et al. (2013). "The Effect of Lactation on Post-Partum Uterine Involution in Holstein Dairy Cows." Reproduction in Domestic Animals **48**(6): 888-892.

Senbon, S., et al. (2003). "Interactions between the oocyte and surrounding somatic cells in follicular development: lessons from in vitro culture." Journal of Reproduction and Development **49**(4): 259-269.

Sengupta, P., et al. (2020). Fuel/Energy Sources of Spermatozoa. Male Infertility: Contemporary Clinical Approaches, Andrology, ART and Antioxidants. S. J. Parekattil, S. C. Esteves and A. Agarwal. Cham, Springer International Publishing**:** 323-335.

Sheldon, I. M., et al. (2009). "Defining postpartum uterine disease and the mechanisms of infection and immunity in the female reproductive tract in cattle." Biology of Reproduction **81**(6): 1025-1032.

Sheldon, I. M., et al. (2006). "Defining postpartum uterine disease in cattle." Theriogenology **65**(8): 1516-1530.

Shevchenko, A., et al. (1996). "Mass spectrometric sequencing of proteins from silver-stained polyacrylamide gels." Analytical Chemistry **68**: 850-858.

Shorten, P. R., et al. (2018). "A mathematical model of the interaction between bovine blastocyst developmental stage and progesterone-stimulated uterine factors on differential embryonic development observed on Day 15 of gestation." Journal of Dairy Science **101**(1): 736-751.

Shteynberg, D., et al. (2013). "Combining results of multiple search engines in proteomics." Molecular and Cellular Proteomics **12**(9): 2383-2393.

Silverman, G. A., et al. (2001). "The serpins are an expanding superfamily of structurally similar but functionally diverse proteins evolution, mechanism of inhibition, novel functions, and a revised nomenclature." Journal of Biological Chemistry **276**(36): 33293-33296.

Simintiras, C. A., et al. (2019a). "The influence of progesterone on bovine uterine fluid energy, nucleotide, vitamin, cofactor, peptide, and xenobiotic composition during the conceptus elongation-initiation window." Scientific Reports **9**(1): 7716.

Simintiras, C. A., et al. (2019b). "Progesterone alters the bovine uterine fluid lipidome during the period of elongation." Reproduction **157**(4): 399-411.

Simintiras, C. A., et al. (2019c). "Biochemical characterization of progesterone-induced alterations in bovine uterine fluid amino acid and carbohydrate composition during the conceptus elongation window." Biology of Reproduction **100**(3): 672-685.

Singh, H. and J. D. Aplin (2015). "Endometrial apical glycoproteomic analysis reveals roles for cadherin 6, desmoglein-2 and plexin b2 in epithelial integrity." Molecular Human Reproduction **21**(1): 81-94.

Siqueira, L. G., et al. (2017). "Postnatal phenotype of dairy cows is altered by in vitro embryo production using reverse X-sorted semen." Journal of Dairy Science **100**(7): 5899-5908.

Smirnova, N. P., et al. (2009). "Persistent fetal infection with bovine viral diarrhea virus differentially affects maternal blood cell signal transduction pathways." Physiological Genomics **36**(3): 129-139.

Smith, B. M., et al. (2000). Using auxiliary variables and implied constraints to model non-binary problems. In AAAI/IAAI: 182-187.

Smits, K., et al. (2017). "Proteome of equine oviducal fluid: effects of ovulation and pregnancy." Reproduction, Fertility and Development **29**(6): 1085-1095.

Smolinska, A., et al. (2012). "NMR and pattern recognition methods in metabolomics: From data acquisition to biomarker discovery: A review." Analytica Chimica Acta **750**(Supplement C): 82-97.

Soleilhavoup, C., et al. (2016). "Proteomes of the female genital tract during the oestrous cycle." Molecular and Cellular Proteomics **15**(1): 93-108.

Song, G., et al. (2010). "Cathepsin B, cathepsin L, and cystatin C in the porcine uterus and placenta: potential roles in endometrial/placental remodeling and in fluid-phase transport of proteins secreted by uterine epithelia across placental areolae." Biology of Reproduction **82**(5): 854-864.

Spencer, T., et al. (2007). "Fetal-maternal interactions during the establishment of pregnancy in ruminants." Society of Reproduction and Fertility Supplement **64**: 379-396.

Spencer, T. E., et al. (2016). "Insights into conceptus elongation and establishment of pregnancy in ruminants." Reproduction, Fertility and Development **29**(1): 84-100.

Spencer, T. E., et al. (2008). "Genes involved in conceptus-endometrial interactions in ruminants: insights from reductionism and thoughts on holistic approaches." Reproduction **135**(2): 165-179.

Sponchiado, M., et al. (2017). "Pre-hatching embryo-dependent and -independent programming of endometrial function in cattle." PLoS One **12**(4): e0175954.

Sponchiado, M., et al. (2020). "Molecular interactions at the bovine embryo–endometrial epithelium interface." Reproduction **160**(6): 887-903.

Stella, S. L. (2017). "Uterine immune mediators and lipid profiles of the preimplantation embryo and endometrial tissue in Holstein cows supplemented with rumen-protected methionine and observed neutrophil extracellular trap (NET) formation in the bovine endometrial tissue." Published doctoral dissertation, University of Illinois.

Stelwagen, K., et al. (2013). "Invited review: Reduced milking frequency: Milk production and management implications." Journal of Dairy Science **96**(6): 3401-3413.

Steták, A., et al. (2007). "Nuclear translocation of the tumor marker pyruvate kinase M2 induces programmed cell death." Cancer Research **67**(4): 1602-1608.

Strug, I., et al. (2014). "Development of a univariate membrane-based mid-infrared method for protein quantitation and total lipid content analysis of biological samples." Journal of Analytical Methods in Chemistry **2014**: 657079.

Sturmey, R. G., et al. (2010). "Amino acid metabolism of bovine blastocysts: a biomarker of sex and viability." Molecular Reproduction and Development **77**(3): 285-296.

Sun, H.-Z., et al. (2015). "Metabolomics of four biofluids from dairy cows: Potential Biomarkers for Milk Production and Quality." Journal of Proteome Research **14**(2): 1287-1298.

Supek, F., et al. (2011). "REVIGO summarizes and visualizes long lists of Gene Ontology terms." PLoS One **6**(7): e21800.

Takahashi, Y. and N. L. First (1992). "In vitro development of bovine one-cell embryos: Influence of glucose, lactate, pyruvate, amino acids and vitamins." Theriogenology **37**(5): 963-978.

Takenaka, M., et al. (1996). "Alternative splicing of the pyruvate kinase M gene in a minigene system." European Journal of Biochemistry **235**(1-2): 366-371.

Tanaka, R., et al. (2011). "Tetrapyrrole metabolism in Arabidopsis thaliana." The Arabidopsis book/American Society of Plant Biologists, **9**.

Tanaka, T., et al. (1967). "Crystallization, characterization and metabolic regulation of two types of pyruvate kinase isolated from rat tissues." The Journal of Biochemistry **62**(1): 71-91.

Tang, D.-Q., et al. (2016). "HILIC-MS for metabolomics: An attractive and complementary approach to RPLC-MS." Mass Spectrometry Reviews **35**(5): 574-600.

Tao, T., et al. (2013). "Influence of group embryo culture strategies on the blastocyst development and pregnancy outcome." Journal of Assisted Reproduction and Genetics **30**(1): 63-68.

Taylor, A. E., et al. (1965). "Permeability of the alveolar membrane to solutes." Circulation Research **16**(4): 353-362.

Team, R. C. (2019). "R version 3.6.2 A language and environment for statistical computing." R Foundation for Statistical Computing, Vienna, Austria.

Tervit, H., et al. (1972). "Successful culture in vitro of sheep and cattle ova." Reproduction **30**(3): 493-497.

Thatcher, W., et al. (2011). "Dietary manipulations to improve embryonic survival in cattle." Theriogenology **76**(9): 1619-1631.

Thévenot, E. A., et al. (2015). "Analysis of the human adult urinary metabolome variations with age, body mass index, and gender by implementing a comprehensive workflow for univariate and OPLS statistical analyses." Journal of Proteome Research **14**(8): 3322-3335.

Thompson, B. (1986). "ANOVA versus regression analysis of ATI designs: An empirical investigation." Educational and Psychological measurement **46**(4): 917-928.

Thompson, J., et al. (2000). "Effect of inhibitors and uncouplers of oxidative phosphorylation during compaction and blastulation of bovine embryos cultured in vitro." Journal of Reproduction and Fertility **118**(1): 47-56.

Tolosano, E. and F. Altruda (2002). "Hemopexin: Structure, function, and regulation." DNA and Cell Biology **21**(4): 297-306.

Tribulo, P., et al. (2019). "Changes in the uterine metabolome of the cow during the first 7 days after estrus." Molecular Reproduction and Development **86**(1): 75-87.

Tríbulo, P., et al. (2019). Production and culture of the bovine embryo. Comparative Embryo Culture, Springer**:** 115-129.

Tríbulo, P., et al. (2018). "Identification of potential embryokines in the bovine reproductive tract." Journal of Dairy Science **101**(1): 690-704.

Tsai, H.-T., et al. (2009). "Imbalanced serum concentration between cathepsin B and cystatin C in patients with pelvic inflammatory diesease." Fertility and Sterility **91**(2): 549-555.

Turk, B., et al. (2012). "Protease signalling: the cutting edge." EMBO Journal **31**(7): 1630-1643.

Uji, M., et al. (2017). "Exploration of serum biomarkers for predicting the response to Inchinkoto (ICKT), a Japanese traditional herbal medicine." Metabolomics **13**(12): 155.

Ulbrich, S. E., et al. (2013). "Transcriptional profiling to address molecular determinants of endometrial receptivity--lessons from studies in livestock species." Methods **59**(1): 108-115.

Van Cleeff, J., et al. (1992). "Plasma and milk progesterone and plasma LH in ovariectomized lactating cows treated with new or used controlled internal drug release devices." Animal Reproduction Science **27**(2-3): 91-106.

Van Cleeff, J., et al. (1996). "Effects of administering progesterone at selected intervals after insemination of synchronized heifers on pregnancy rates and resynchronization of returns to service." Theriogenology **46**(7): 1117-1130.

van den Berg, R. A., et al. (2006). "Centering, scaling, and transformations: improving the biological information content of metabolomics data." BMC Genomics **7**: 142.

Van Hoeck, V., et al. (2014). "Reduced oocyte and embryo quality in response to elevated non-esterified fatty acid concentrations: A possible pathway to subfertility?" Animal Reproduction Science **149**(1): 19-29.

van Ruth, S., et al. (2003). "Evaluation of three gas chromatography and two direct mass spectrometry techniques for aroma analysis of dried red bell peppers." International Journal of Mass Spectrometry **223-224**: 55-65.

Varughese, K. I., et al. (1992). "Crystal structure of rat liver dihydropteridine reductase." Proceedings of the National Academy of Sciences **89**(13): 6080.

Vasconcelos, J. L. M., et al. (2006). "Factors potentially affecting fertility of lactating dairy cow recipients." Theriogenology **65**(1): 192-200.

Velazquez, M. A., et al. (2010). "Sampling techniques for oviductal and uterine luminal fluid in cattle." Theriogenology **73**(6): 758-767.

Venhoranta, H. (2015). "Inherited developmental diseases related to reproductive failures in cattle." Dissertationes Scholae Doctoralis Ad Sanitatem Investigandam Universitatis Helsinkiensis.

Viana, J. (2019). Embryo industry on a new level: over one million embryos produced *in vitro*. Statistics of embryo production and transfer in domestic farm animals. P. J. Ross. Champaign, IL, USA, International Embryo Technology Society. **37**.

von Heijne, G. (1990). "The signal peptide." The Journal of Membrane Biology **115**(3): 195-201.

von Keyserlingk, M. A. G., et al. (2013). "Invited review: Sustainability of the US dairy industry." Journal of Dairy Science **96**(9): 5405-5425.

Wale, P. L. and D. K. Gardner (2015). "The effects of chemical and physical factors on mammalian embryo culture and their importance for the practice of assisted human reproduction." Human Reproduction Update **22**(1): 2-22.

Wathes, D. C., et al. (2009). "Negative energy balance alters global gene expression and immune responses in the uterus of postpartum dairy cows." Physiological Genomics **39**(1): 1-13.

Wessel, D. and U. Flügge (1984). "A method for the quantitative recovery of protein in dilute solution in the presence of detergents and lipids." Analytical Biochemistry **138**(1): 141-143.

Weston, A. D. and L. Hood (2004). "Systems biology, proteomics, and the future of health care: toward predictive, preventative, and personalized medicine." Journal of Proteome Research **3**(2): 179-196.

Wickham, H. (2016). ggplot2: elegant graphics for data analysis, Springer.

Wiebold, J. L. (1988). "Embryonic mortality and the uterine environment in first-service lactating dairy cows." Journal of Reproduction and Fertility **84**(2): 393-399.

Wiltbank, M. C., et al. (2016). "Pivotal periods for pregnancy loss during the first trimester of gestation in lactating dairy cows." Theriogenology **86**(1): 239-253.

Winuthayanon, W., et al. (2015). "Oviductal estrogen receptor alpha signaling prevents protease-mediated embryo death." Elife **4**: e10453.

Woelders, H., et al. (2011). "Systems biology in animal sciences." Animal **5**(7): 1036-1047.

Worley, B. and R. Powers (2013). "Multivariate analysis in metabolomics." Current Metabolomics **1**(1): 92-107.

Worley, B. and R. Powers (2016). "PCA as a practical indicator of OPLS-DA model reliability." Current Metabolomics **4**(2): 97-103.

Xia, J. and D. S. Wishart (2010). "MetPA: a web-based metabolomics tool for pathway analysis and visualization." Bioinformatics **26**(18): 2342-2344.

Yamanaka, K.-i., et al. (2018). "Heat-shock-induced cathepsin B activity during IVF and culture compromises the developmental competence of bovine embryos." Theriogenology **114**: 293-300.

Young, C., et al. (2017). "A reproductive tract scoring system to manage fertility in lactating dairy cows." Journal of Dairy Science **100**(7): 5922-5927.

Young, L. E., et al. (1998). "Large offspring syndrome in cattle and sheep." Reviews of Reproduction **3**(3): 155-163.

Zerck, A., et al. (2013). "Optimal precursor ion selection for LC-MALDI MS/MS." BMC Bioinformatics **14**(1): 56-64.

Zhang, F., et al. (2008). "Alteration in the activation state of new inflammation-associated targets by phospholipase A2-activating protein (PLAA)." Cellular Signalling **20**(5): 844-861.

Zhang, J., et al. (2012). "PEAKS DB: de novo sequencing assisted database search for sensitive and accurate peptide identification." Molecular and Cellular Proteomics **11**(4).

Zhang, K. and G. W. Smith (2015). "Maternal control of early embryogenesis in mammals." Reproduction, Fertility and Development **27**(6): 880-896.

Zhang, W., et al. (2010). "Integrating multiple 'omics' analysis for microbial biology: application and methodologies." Microbiology **156**(2): 287-301.

Zhao, L., et al. (2019). "OutCyte: a novel tool for predicting unconventional protein secretion." Scientific Reports **9**(1): 19448.

Zhou, Y., et al. (2019). "Metascape provides a biologist-oriented resource for the analysis of systems-level datasets." Nature Communications **10**(1): 1523.

Zolini, A. M., et al. (2020a). "Genes associated with survival of female bovine blastocysts produced in vivo." Cell and Tissue Research **382**(3): 665-678.

Zolini, A. M., et al. (2020b). "Molecular fingerprint of female bovine embryos produced in vitro with high competence to establish and maintain pregnancy†." Biology of Reproduction **102**(2): 292-305.

Zullo, G., et al. (2016a). "L-ergothioneine supplementation during culture improves quality of bovine in vitro–produced embryos." Theriogenology **85**(4): 688-697.

Zullo, G., et al. (2016b). "Crocetin improves the quality of in vitro–produced bovine embryos: Implications for blastocyst development, cryotolerance, and apoptosis." Theriogenology **86**(8): 1879-1885.

Żwir-Ferenc, A. and M. Biziuk (2006). "Solid phase extraction technique-trends, opportunities and applications." Polish Journal of Environmental Studies **15**(5): 677-690.

Appendices

A.1 Chapter 2

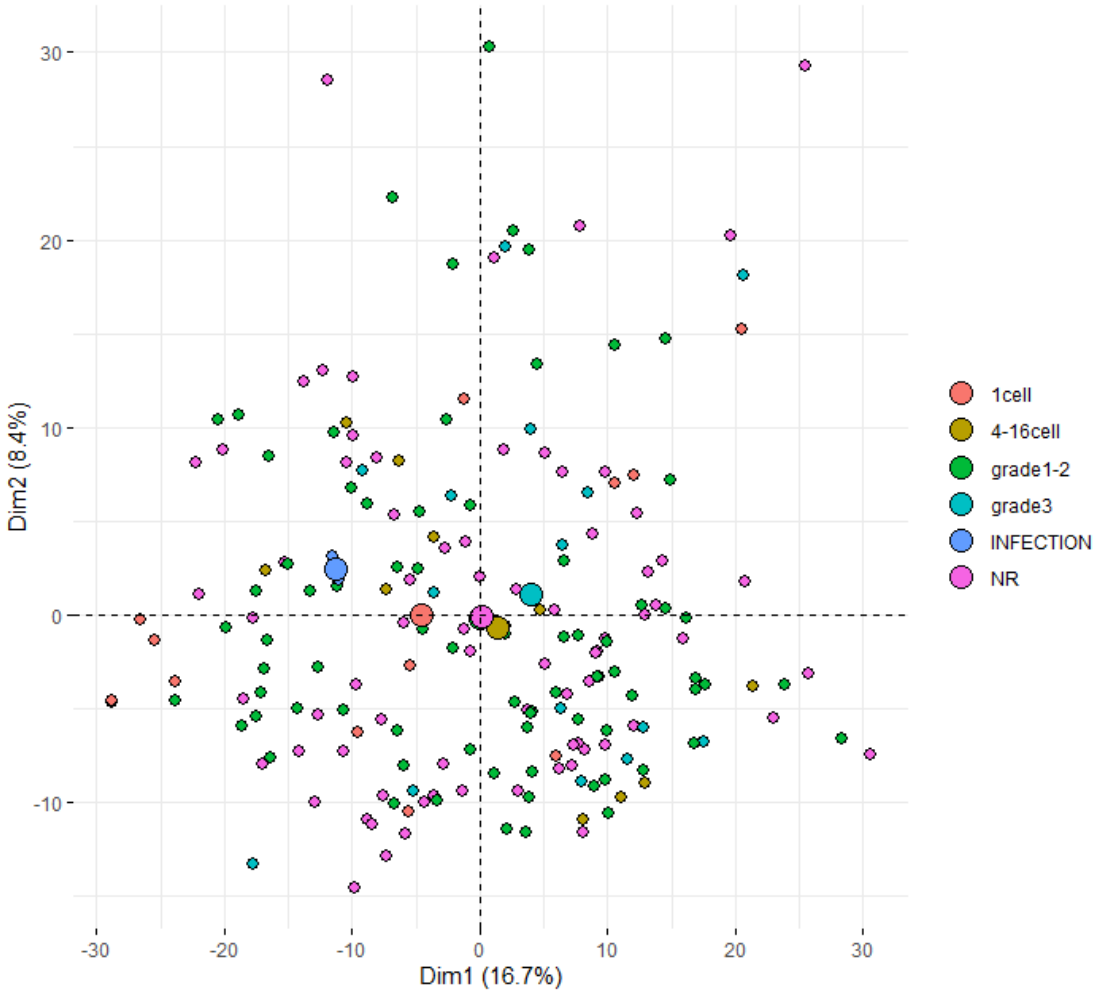

Figure A-8-1 PCA plot (PC1 and PC2) using normalised protein abundance as features. Abbreviations: NR, non-recovery (i.e. uterine flushing samples in which no embryo was found, EQ1b class VI)

A.2 Chapter 4

Table A-1 Isotope-labelled proline (tracer) peak areas per sample. Stock solution area in purple, positive controls in orange, blank in light green, plasma samples in light blue, ULF samples and QCs in yellow.

Sample	Type	Area
Tracer (stock)	Standard	450538
Tracer (5 µg/ml)	Standard	6457
Spiked saline(a)	Standard	3560
Spiked saline(b)	Standard	856
Spiked saline(c)	Standard	618
Blank	Blank	0
Plasma #1 T0	Plasma	0
Plasma #1 T1	Plasma	0
Plasma #1 T2	Plasma	0
Plasma #1 T6	Plasma	0
Plasma #1 T24	Plasma	0
Plasma #2 T0	Plasma	0
Plasma #2 T6	Plasma	0
Plasma #2 T24	Plasma	0
QCA	QC	760
QCB	QC	450
QCC	QC	577

ULF #1	Sample	**1824**
ULF #2	Sample	**4355**
ULF #3	Sample	**780**
ULF #4	Sample	**461**
ULF #5	Sample	**4487**
ULF #6	Sample	**2825**

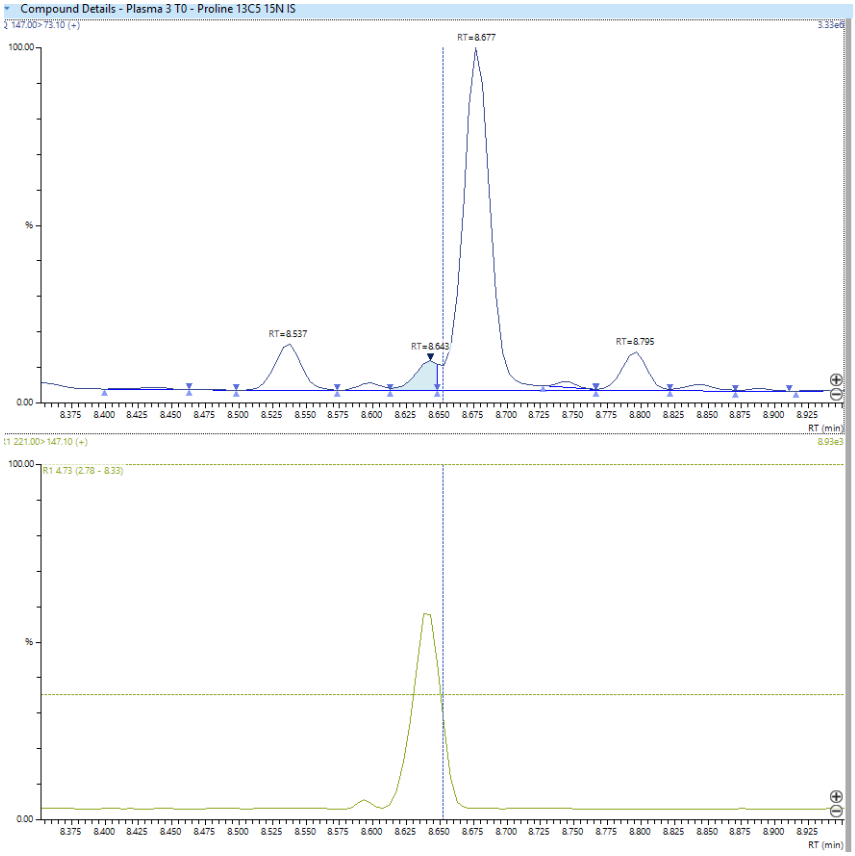

Figure A-8-2 GC-MS/MS chromatogram example. A, qualifier ion chromatogram; B, quantifier ion chromatogram. Coelution of both ions is required to validate feature identification.

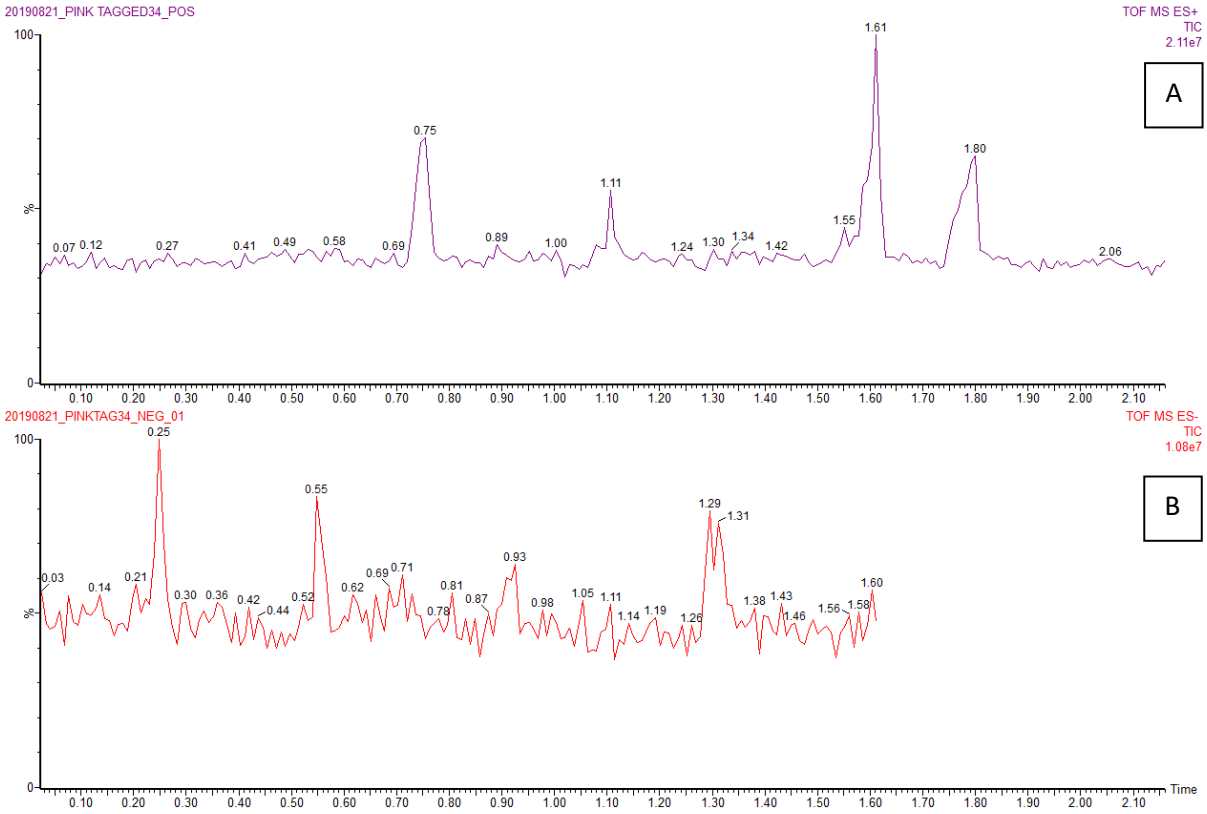

Figure A-8-3 Example chromatograms obtained by REIMS metabolic fingerprinting, showing distinct degrees of signal-to-noise ratio according to ionisation mode. A, positive ionisation mode; B, negative ionisation mode.

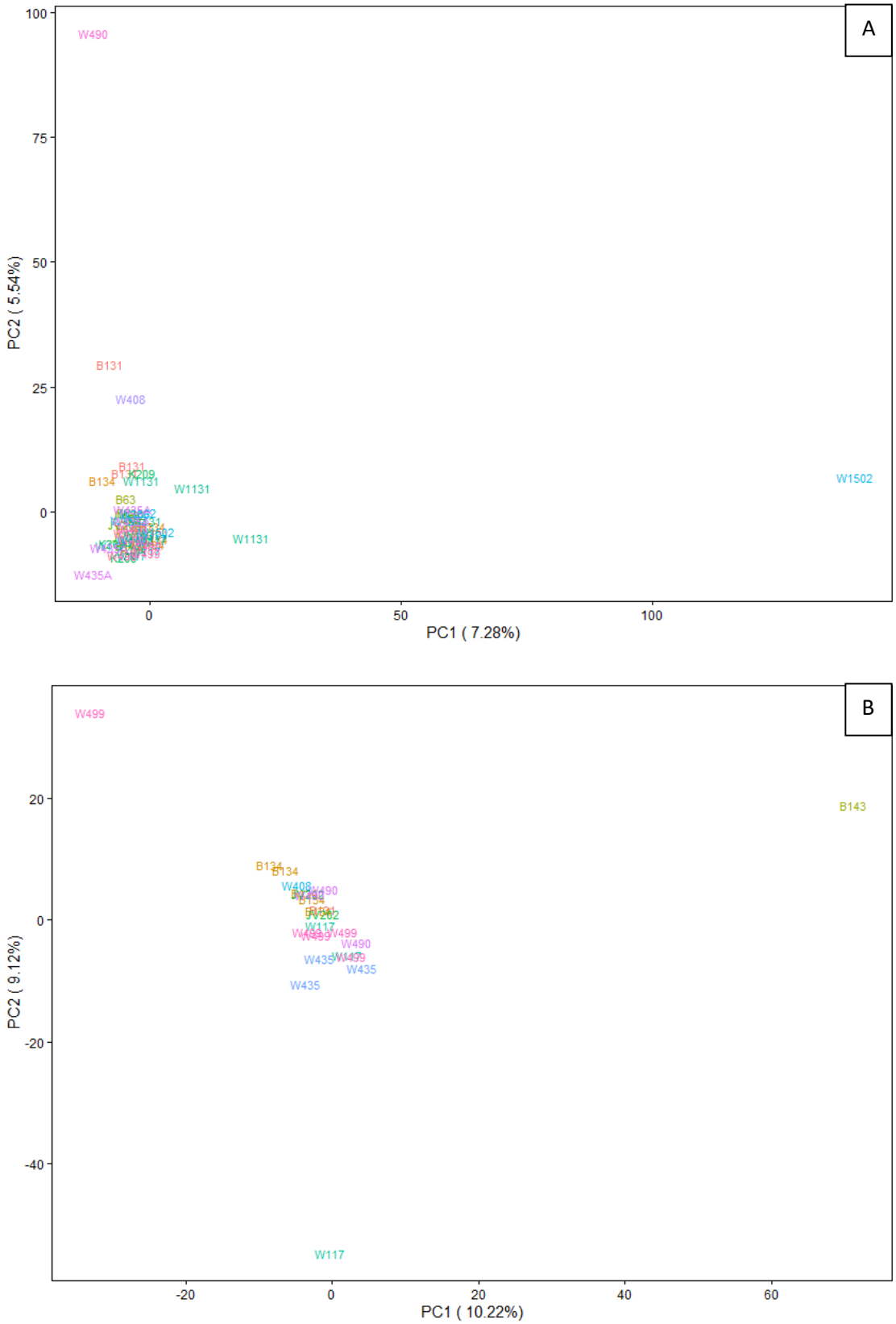

Figure A-8-4 PCA of ULF sample replicates analysed in REIMS, after removal of features present in blanks, in negative (A) or positive (B) ionisation mode. Colours indicate technical replicate samples of the same cows.

A.3 Chapter 5

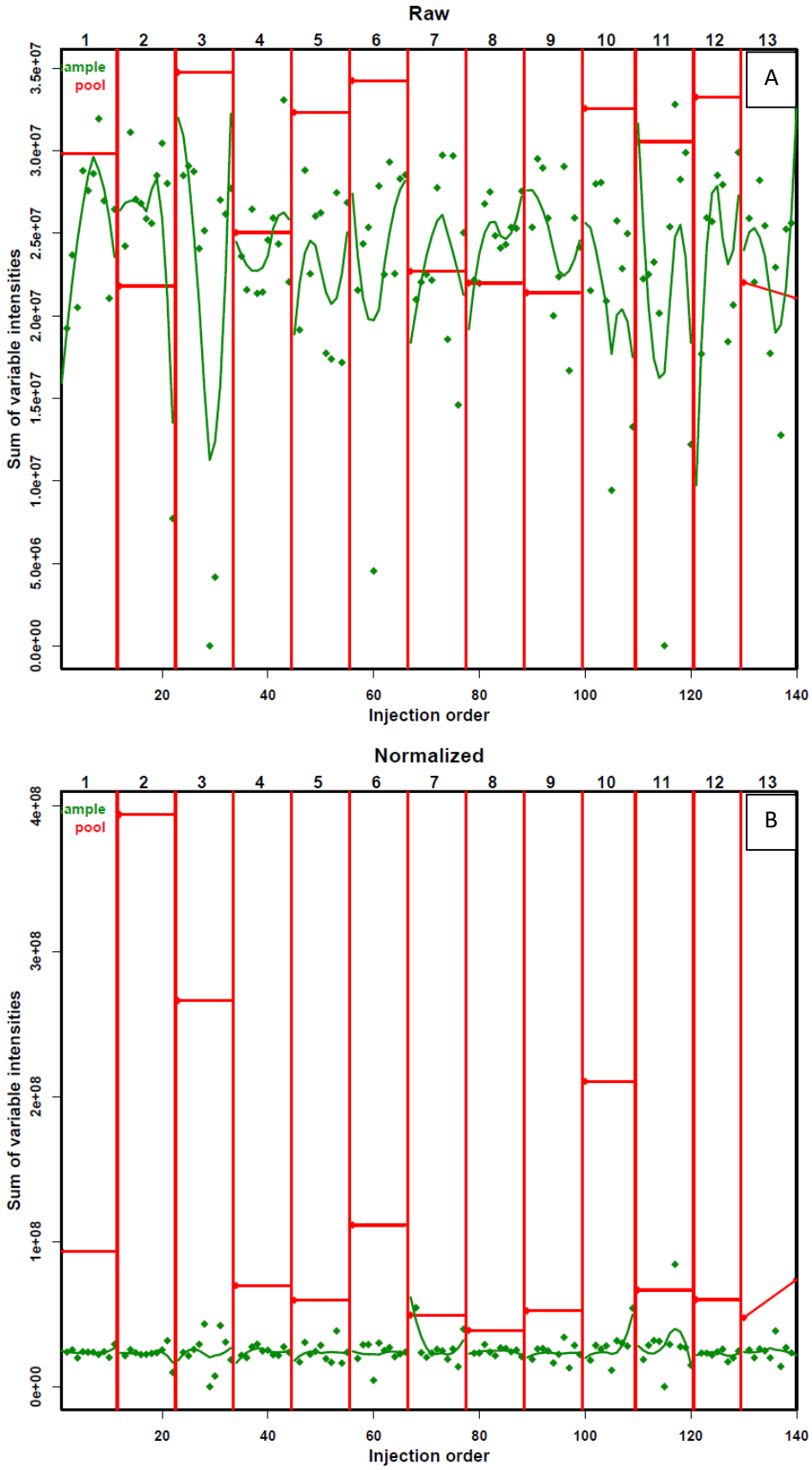

Figure A-8-5 Graphic representation of batch correction done on sample intensity, LC-MS/MS Exp. P3. A, raw values; B, batch-corrected values.

Figure A-8-6 Peptide sequences of cystatin C (A) and cystatin B (B).

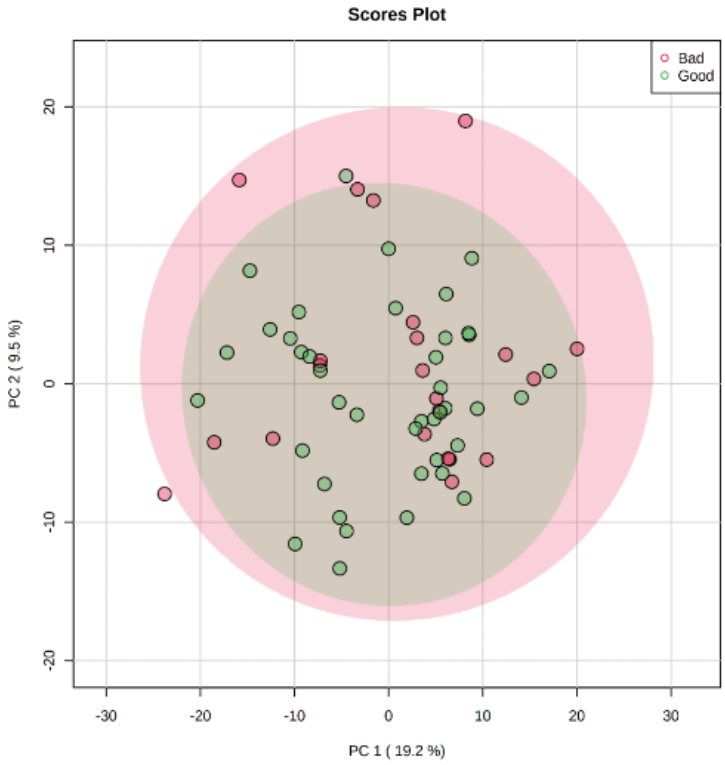

Figure A-8-7 PCA of proteomic features in ULF bearing embryos of different quality, according to the EQ3 classification system. "Bad", non-pregnant ULF (embryo classes IV and V); "good" pregnant ULF (embryo classes I, II and III). Coloured areas indicate Hotelling T2 confidence ellipses, i.e. the space of 95% confidence for each class.

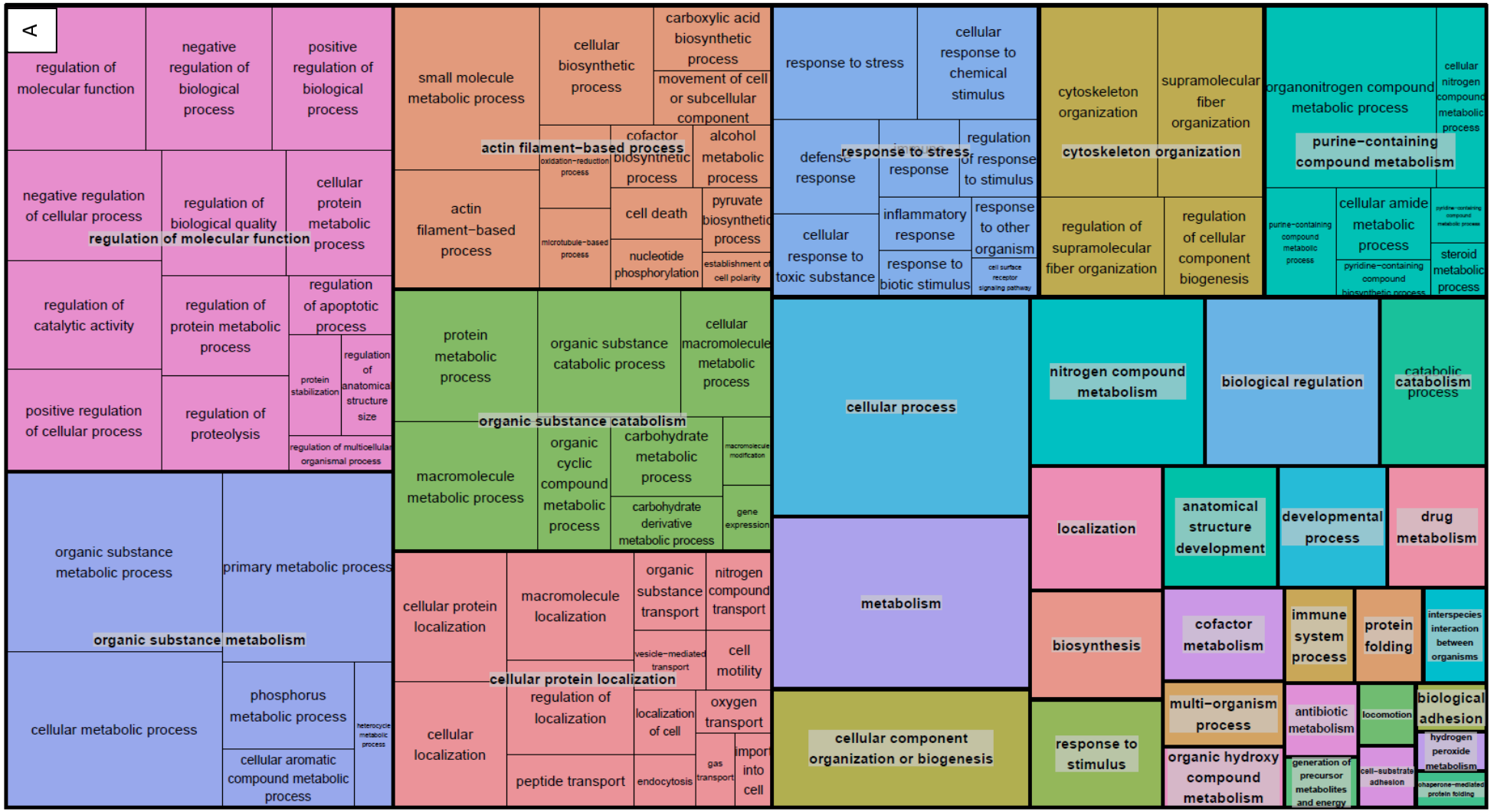
A
regulation of molecular function
negative regulation of biological process
positive regulation of biological process
negative regulation of cellular process
regulation of biological quality
cellular protein metabolic process
regulation of molecular function
regulation of catalytic activity
regulation of protein metabolic process
regulation of apoptotic process
positive regulation of cellular process
regulation of proteolysis
protein stabilization
regulation of anatomical structure size
regulation of multicellular organismal process
small molecule metabolic process
cellular biosynthetic process
carboxylic acid biosynthetic process
movement of cell or subcellular component
actin filament−based process
cofactor biosynthetic process
alcohol metabolic process
oxidation−reduction process
actin filament−based process
cell death
pyruvate biosynthetic process
microtubule−based process
nucleotide phosphorylation
establishment of cell polarity
protein metabolic process
organic substance catabolic process
cellular macromolecule metabolic process
organic substance catabolism
macromolecule metabolic process
organic cyclic compound metabolic process
carbohydrate metabolic process
macromolecule modification
carbohydrate derivative metabolic process
gene expression
response to stress
cellular response to chemical stimulus
response to stress
defense response
response to stress
regulation of response to stimulus
inflammatory response
response to other organism
cellular response to toxic substance
response to biotic stimulus
cell surface receptor signaling pathway
cytoskeleton organization
supramolecular fiber organization
cytoskeleton organization
regulation of supramolecular fiber organization
regulation of cellular component biogenesis
organonitrogen compound metabolic process
cellular nitrogen compound metabolic process
purine−containing compound metabolism
purine−containing compound metabolic process
cellular amide metabolic process
pyridine−containing compound metabolic process
pyridine−containing compound biosynthetic process
steroid metabolic process
cellular process
nitrogen compound metabolism
biological regulation
catabolic process
metabolism
localization
anatomical structure development
developmental process
drug metabolism
biosynthesis
cofactor metabolism
immune system process
protein folding
interspecies interaction between organisms
cellular component organization or biogenesis
response to stimulus
multi−organism process
antibiotic metabolism
locomotion
biological adhesion
organic hydroxy compound metabolism
generation of precursor metabolites and energy
cell−substrate adhesion
hydrogen peroxide metabolism
chaperone−mediated protein folding
organic substance metabolic process
primary metabolic process
organic substance metabolism
cellular metabolic process
phosphorus metabolic process
heterocycle metabolic process
cellular aromatic compound metabolic process
cellular protein localization
macromolecule localization
organic substance transport
nitrogen compound transport
vesicle−mediated transport
cell motility
cellular protein localization
cellular localization
regulation of localization
localization of cell
oxygen transport
peptide transport
endocytosis
gas transport
import into cell

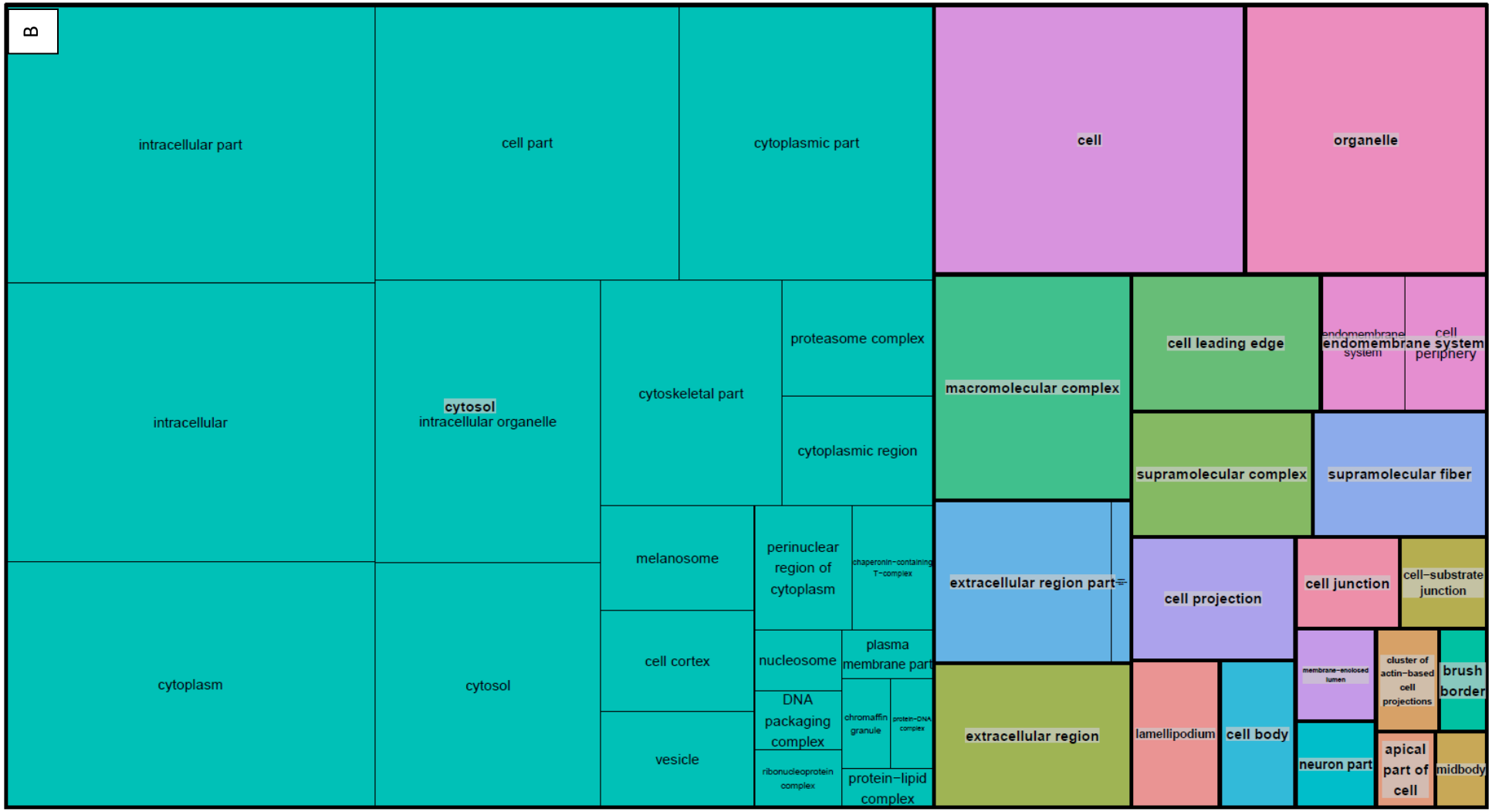
B
intracellular part
cell part
cytoplasmic part
intracellular
cytosol
intracellular organelle
cytoskeletal part
proteasome complex
cytoplasmic region
cytoplasm
cytosol
melanosome
perinuclear region of cytoplasm
chaperonin-containing T-complex
cell cortex
nucleosome
plasma membrane part
DNA packaging complex
chromaffin granule
protein-DNA complex
vesicle
ribonucleoprotein complex
protein-lipid complex
cell
organelle
macromolecular complex
cell leading edge
endomembrane system
cell periphery
supramolecular complex
supramolecular fiber
extracellular region part
cell projection
cell junction
cell-substrate junction
membrane-enclosed lumen
cluster of actin-based cell projections
brush border
extracellular region
lamellipodium
cell body
neuron part
apical part of cell
midbody

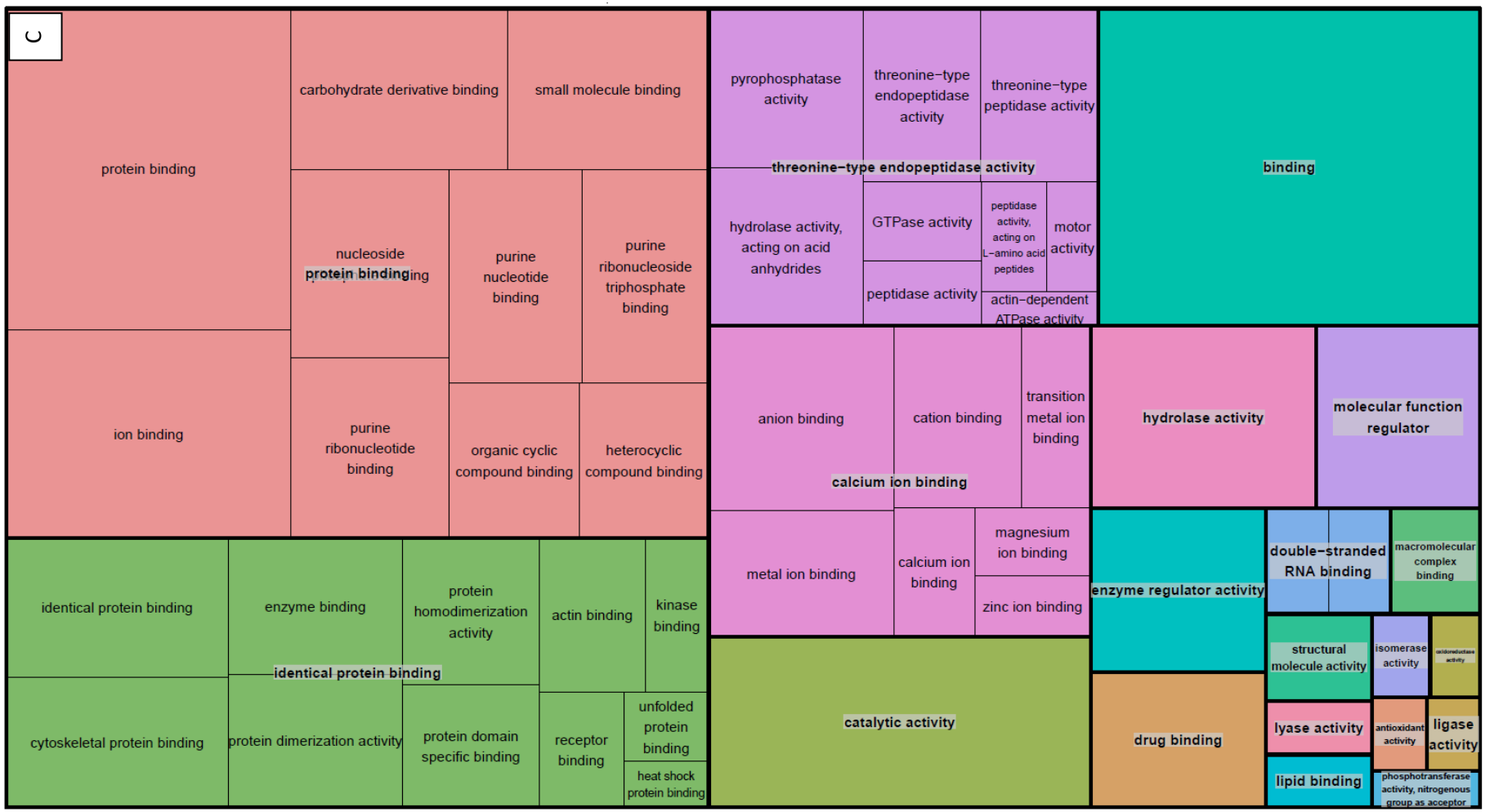
C
protein binding
carbohydrate derivative binding
small molecule binding
nucleoside protein binding
purine nucleotide binding
purine ribonucleoside triphosphate binding
ion binding
purine ribonucleotide binding
organic cyclic compound binding
heterocyclic compound binding
pyrophosphatase activity
threonine−type endopeptidase activity
threonine−type peptidase activity
threonine−type endopeptidase activity
hydrolase activity, acting on acid anhydrides
GTPase activity
peptidase activity, acting on L−amino acid peptides
motor activity
peptidase activity
actin−dependent ATPase activity
binding
anion binding
cation binding
transition metal ion binding
calcium ion binding
hydrolase activity
molecular function regulator
metal ion binding
calcium ion binding
magnesium ion binding
zinc ion binding
enzyme regulator activity
double−stranded RNA binding
macromolecular complex binding
structural molecule activity
isomerase activity
identical protein binding
enzyme binding
protein homodimerization activity
actin binding
kinase binding
identical protein binding
catalytic activity
drug binding
lyase activity
antioxidant activity
ligase activity
cytoskeletal protein binding
protein dimerization activity
protein domain specific binding
receptor binding
unfolded protein binding
heat shock protein binding
lipid binding
phosphotransferase activity, nitrogenous group as acceptor

Figure A-8-89 Treemap displaying enriched GO terms using all proteins identified in Exp. P3. A, biological process; B, cellular location; C, molecular function.

A.4 Chapter 6

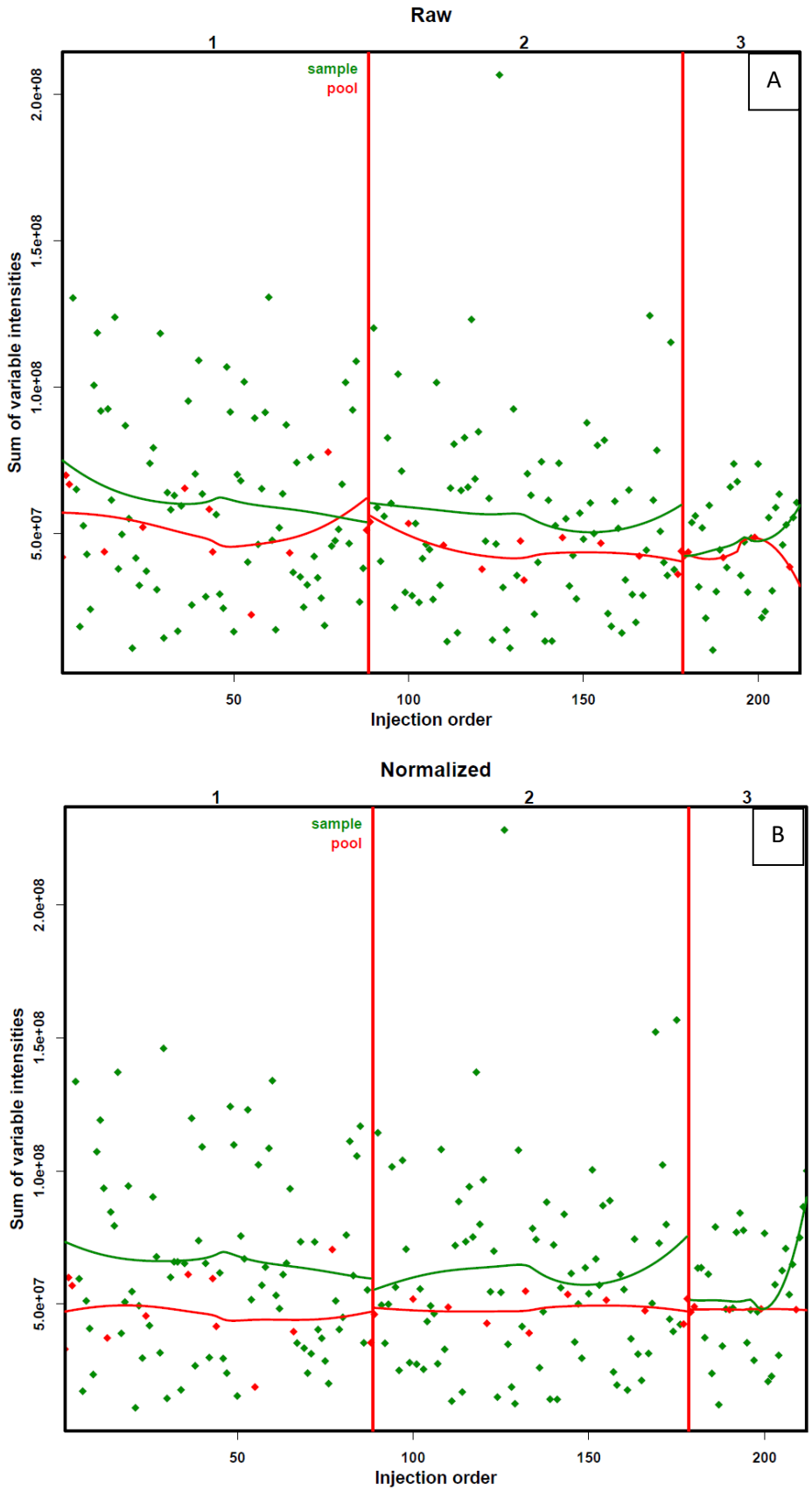
Raw
1
2
3
sample
pool
A
Sum of variable intensities
2.0e+08
1.5e+08
1.0e+08
5.0e+07
50
100
150
200
Injection order
Normalized
1
2
3
sample
pool
B
Sum of variable intensities
2.0e+08
1.5e+08
1.0e+08
5.0e+07
50
100
150
200
Injection order

Figure A-8-910 Graphic representation of batch correction done on sample intensity, GC-MS/MS Exp. M4. A, raw values. B, batch-corrected values.

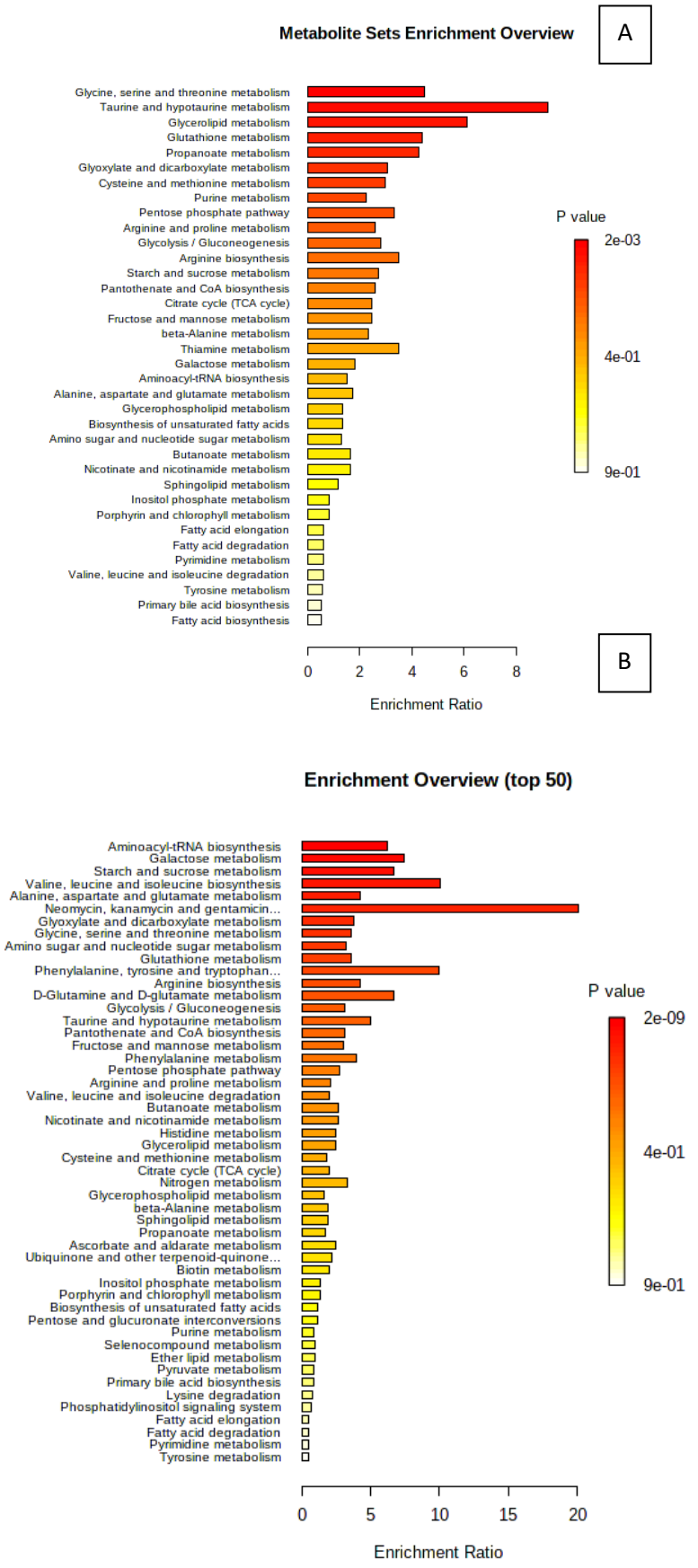

Figure A-8-10 KEGG pathways overrepresented in the metabolite sets identified by targeted analysis (A) or untargeted analysis (B) vs the background of all compounds identified in this study.

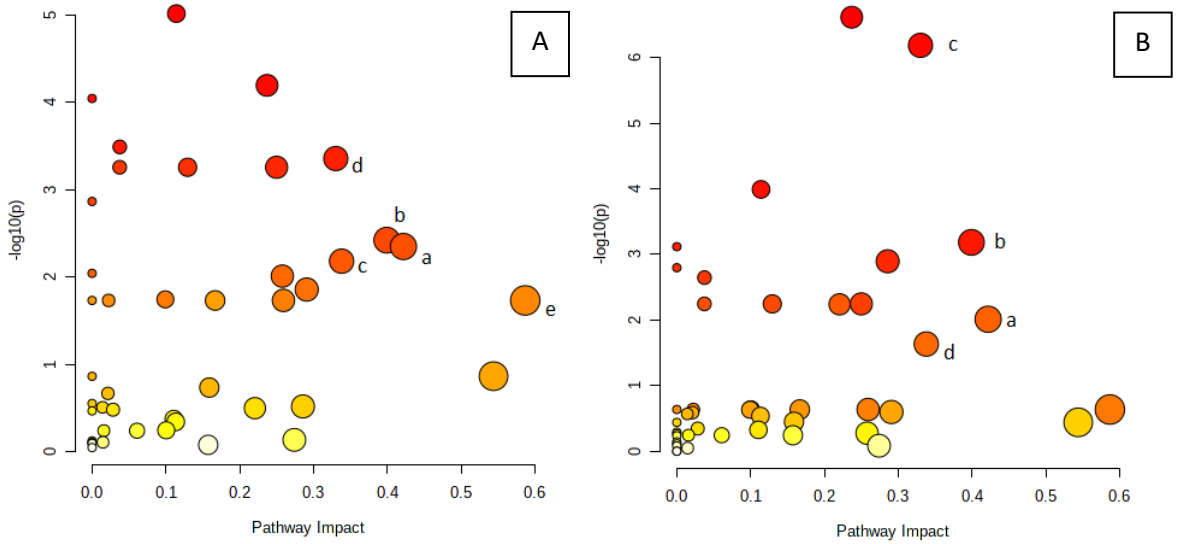

Figure A-8-11 Relevant pathways differentially regulated across days postpartum (dpp, subplot A) or oestrus after calving (OC, subplot B). a: Pentose and glucuronate interconversions, b: beta alanine metabolism, c: cysteine and methionine metabolism, d: glycerolipid metabolism, e: glycine, serine, and threonine metabolism.

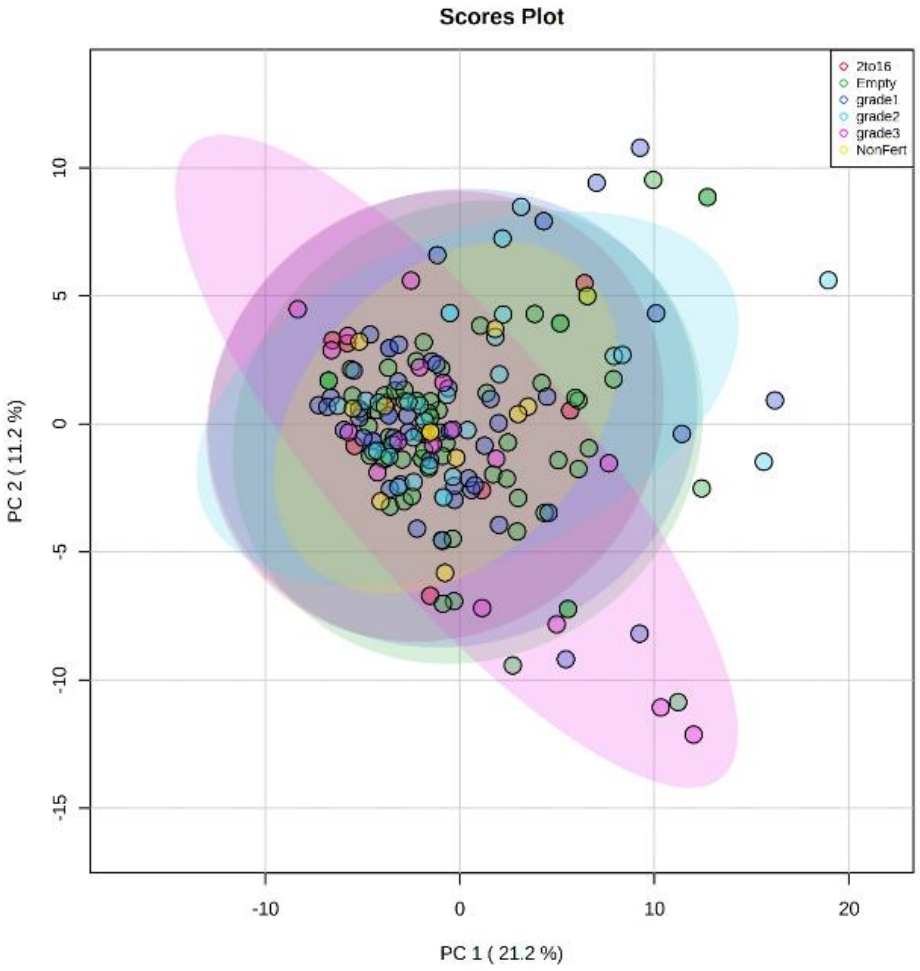

Figure A-8-12 PCA using auto-scaled metabolite abundance, coloured by embryo grade (EQ1). Coloured areas indicate Hotelling T2 confidence ellipses, i.e. the space of 95% confidence for each class.

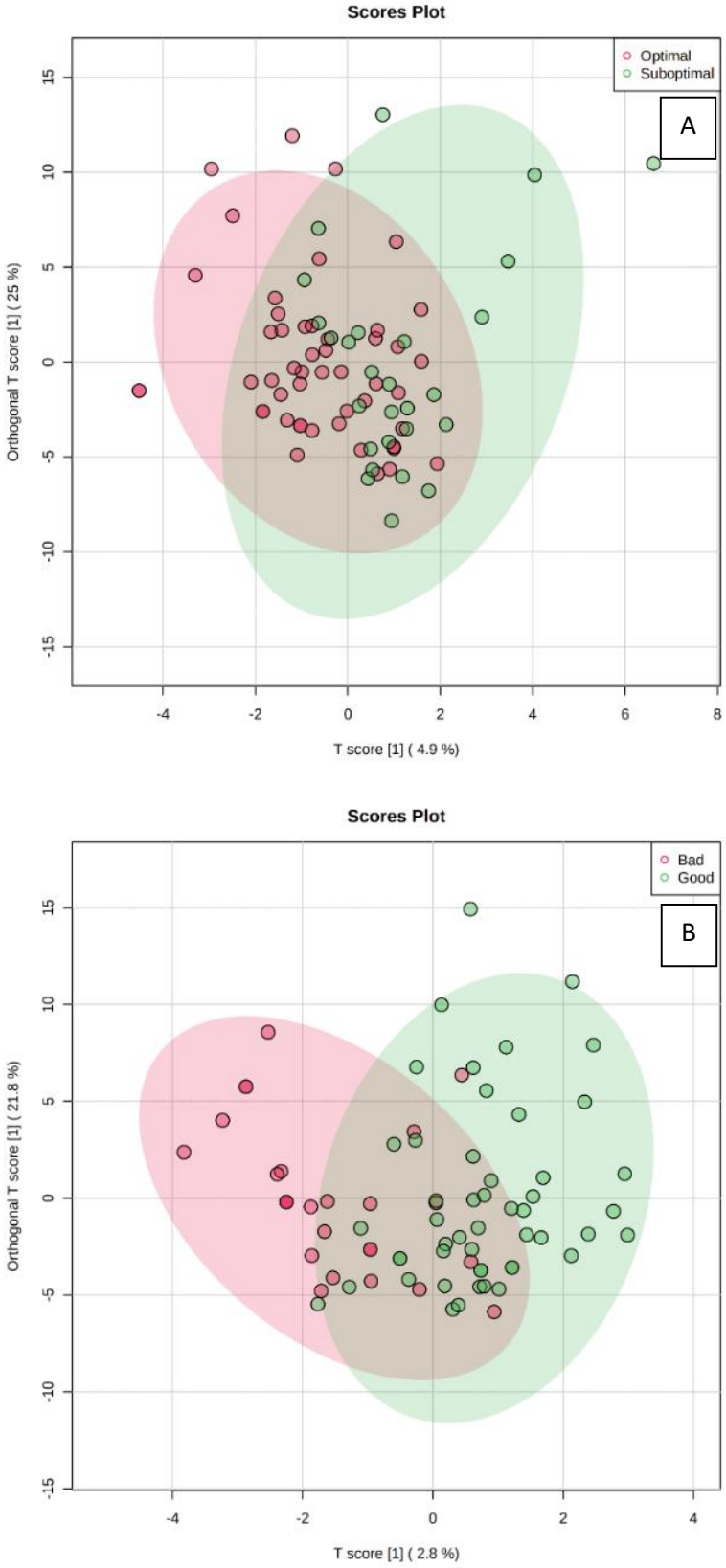

Figure A-8-13 OPLS-DA showing predictive component 1 (x-axis) and orthogonal component 1 (variation unrelated to embryo grade) (y-axis), using embryo classification system EQ2 (A) or EQ3 (B). "Optimal", embryo class I; "suboptimal", embryo classes III, IV, V; "bad" indicates non-pregnant ULF (embryo classes IV and V); "good", pregnant ULF (embryo

classes I, II and III). Coloured areas indicate Hotelling T2 confidence ellipses, i.e. the space of 95% confidence for each class.

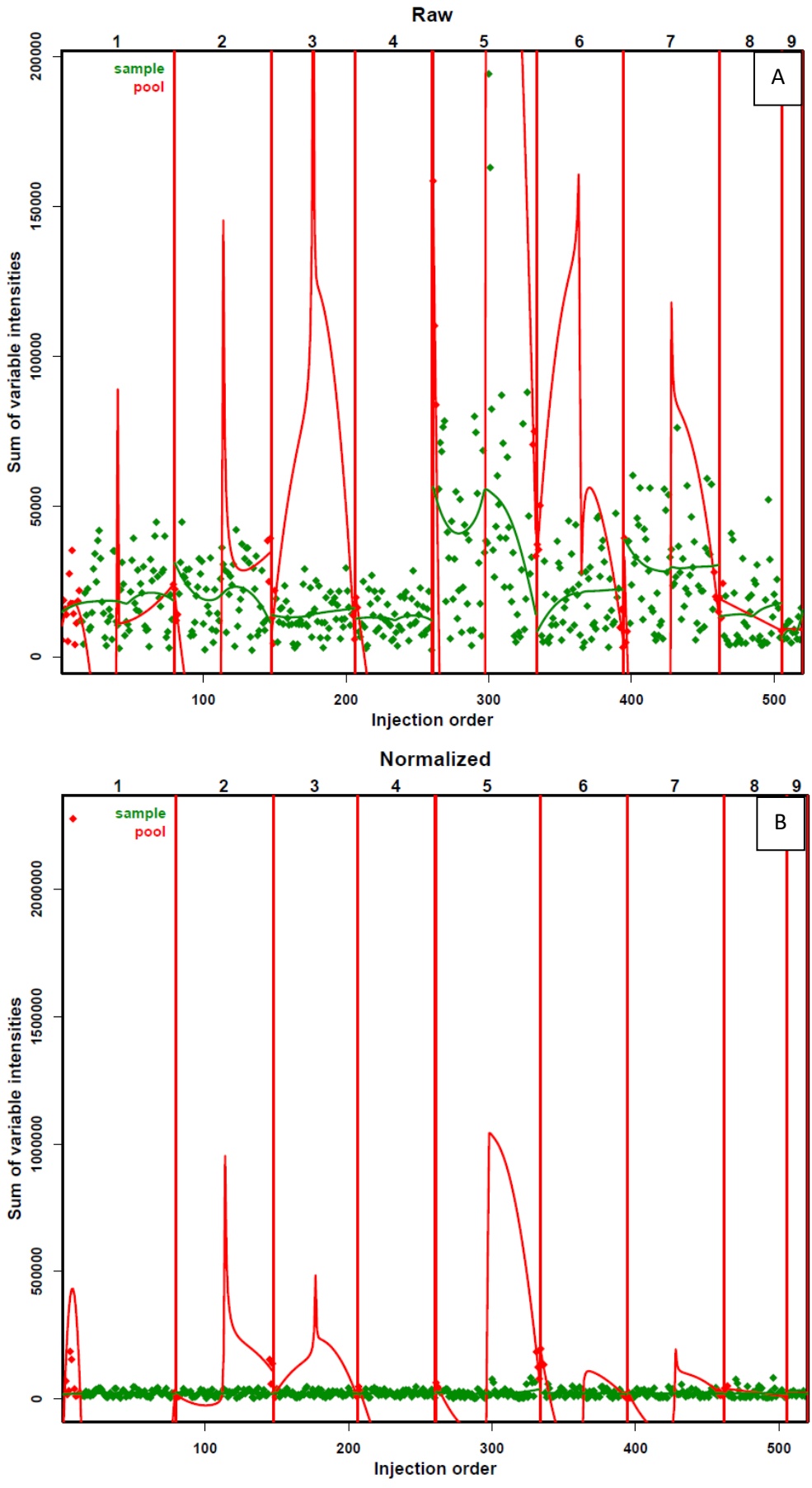

Figure A-8-14 Graphic representation of batch correction done on sample intensity, REIMS Exp. M5. A, raw values. B, batch-corrected values.

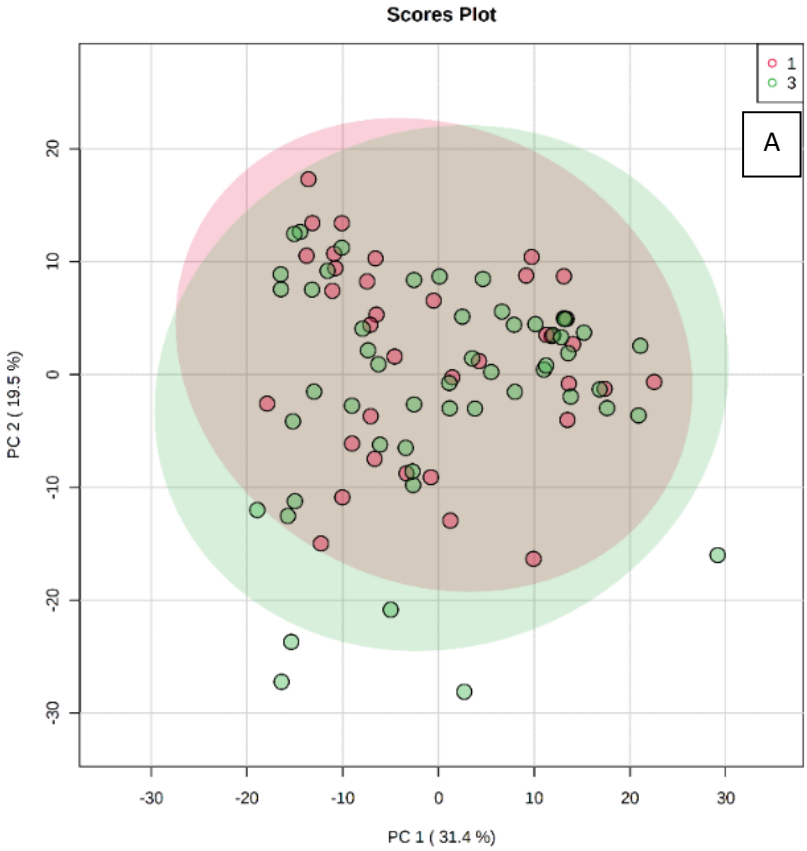
Scores Plot
1
3
A
PC 2 (19.5 %)
PC 1 (31.4 %)
-30
-20
-10
0
10
20
30

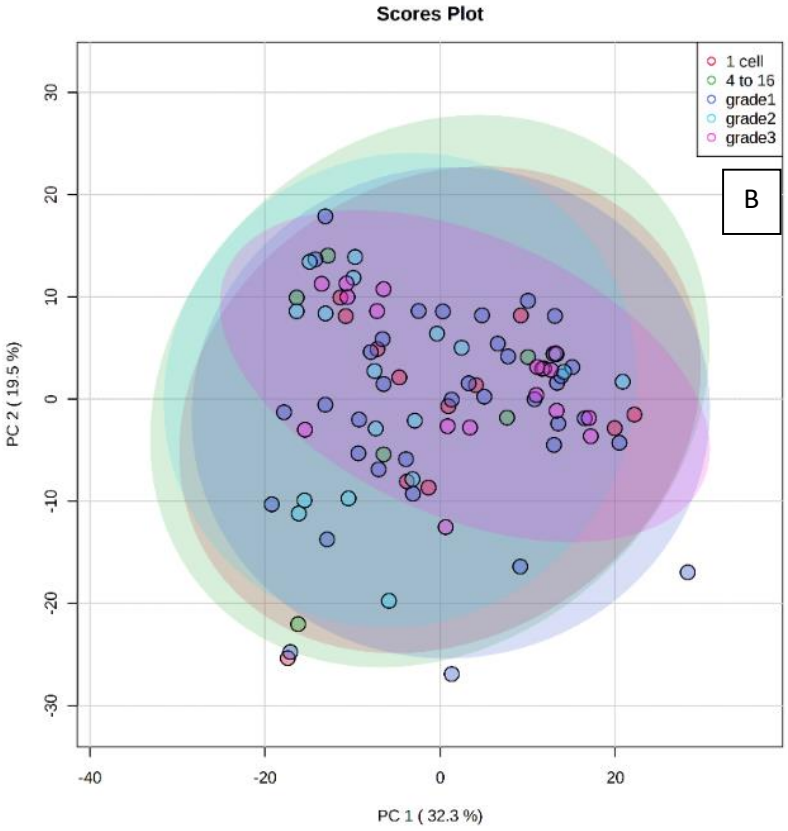
Scores Plot
1 cell
4 to 16
grade1
grade2
grade3
B
PC 2 (19.5 %)
PC 1 (32.3 %)
-40
-20
0
20
30
10
-10
-30

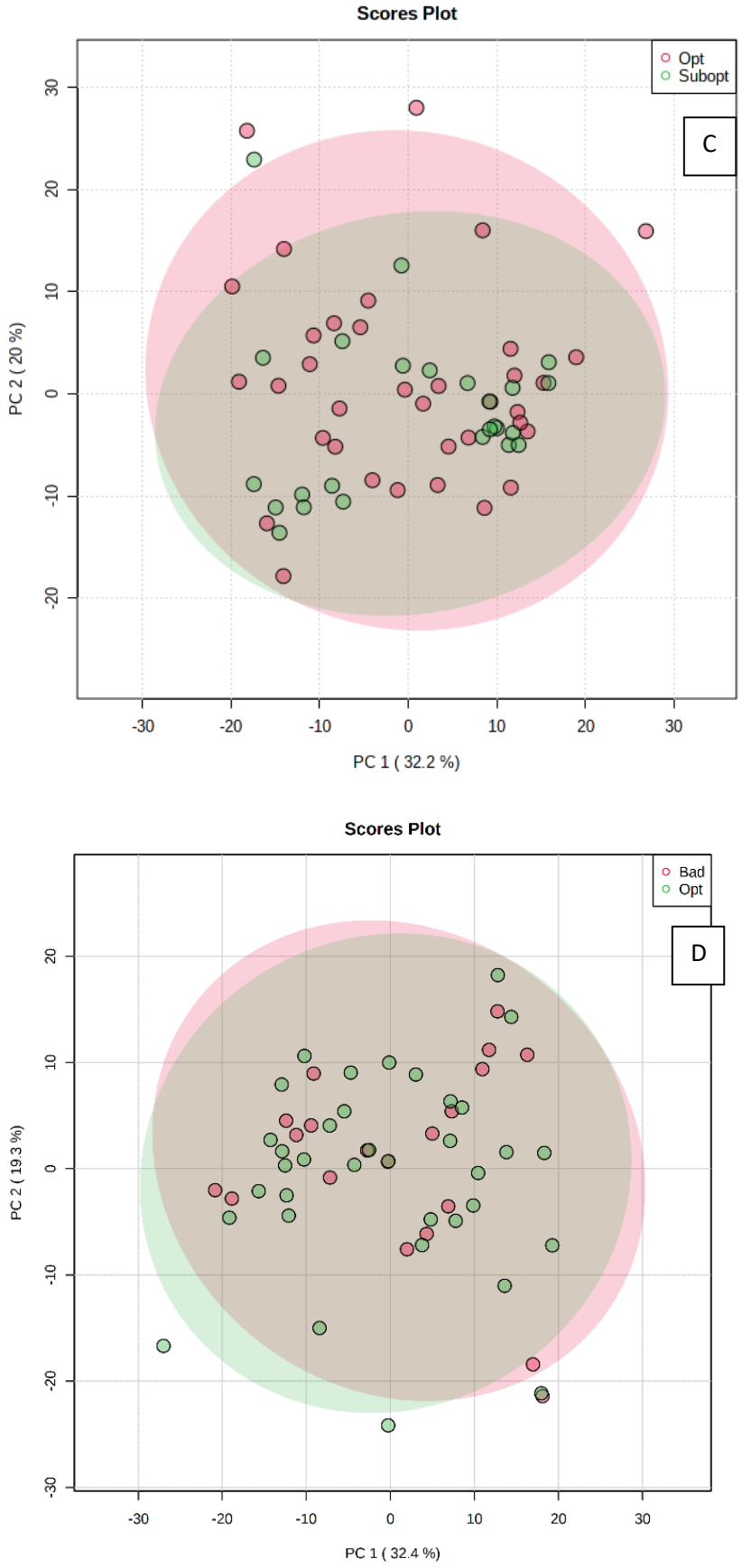

Figure A-8-15 PCA of all samples; variables are peak area values from REIMS analysis in positive ionisation mode. A, OC; B, EQ1; C, EQ2; D: EQ3. Coloured areas indicate Hotelling T2 confidence ellipses, i.e. the space of 95% confidence for each class.


Scores Plot
1
3
A
PC 2 (16.1 %)
PC 1 (33.3 %)
30
20
10
0
-10
-20
-40
-20
0
20
40
60

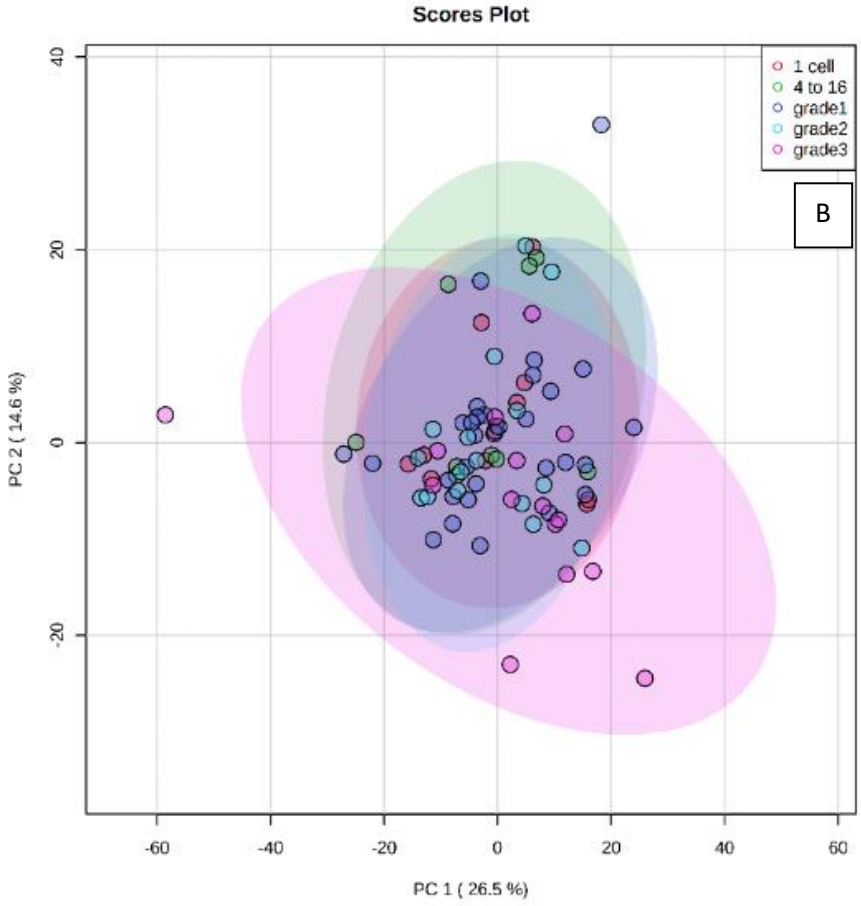
Scores Plot
1 cell
4 to 16
grade1
grade2
grade3
B
PC 2 (14.6 %)
PC 1 (26.5 %)
40
20
0
-20
-60
-40
-20
0
20
40
60

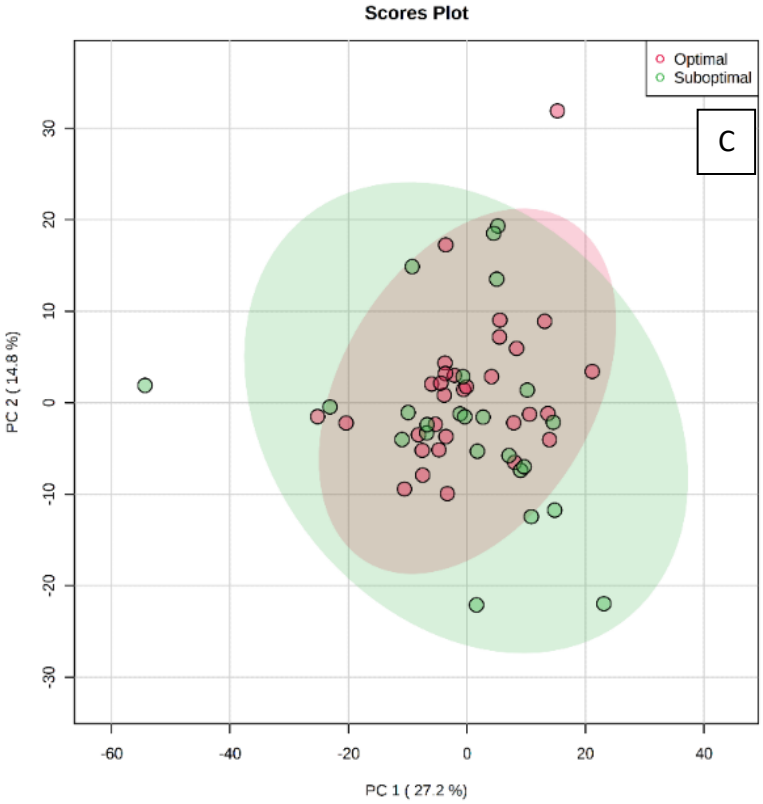

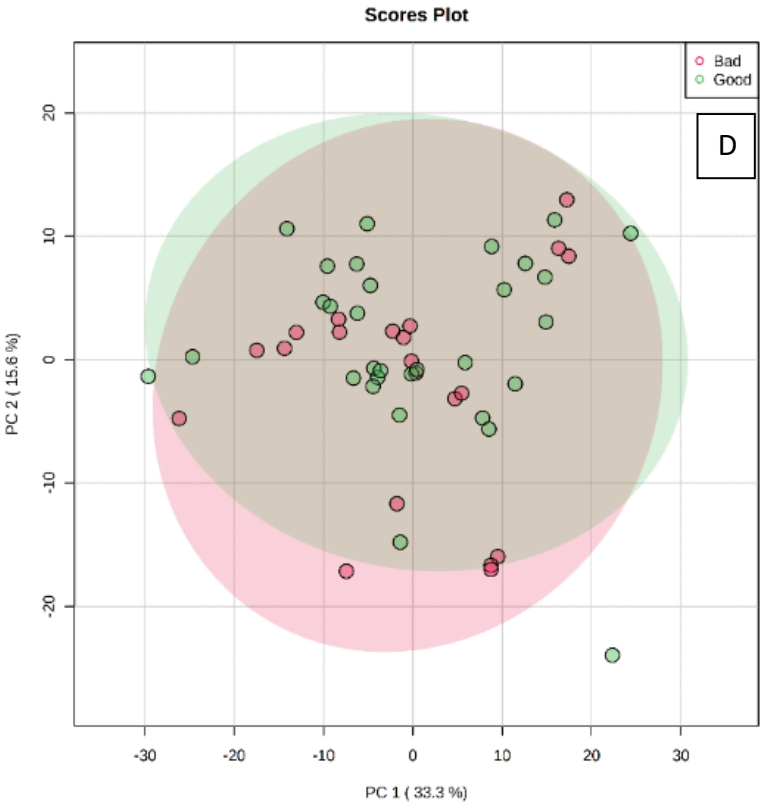

Figure A-8-16 PCA of all samples; variables are peak area values from REIMS analysis in negative ionisation mode. A, OC; B, EQ1; C, EQ2; D: EQ3. Coloured areas indicate Hotelling T2 confidence ellipses, i.e. the space of 95% confidence for each class.

Table S1-1 Studies investigating proteomics and metabolomics of bovine ULF. Abbreviations: AA, amino acids; AI, artificial insemination; ET, embryo transfer; M, metabolomics; P, proteomics; P4, progesterone; T, transcriptomics; ULF, uterine luminal fluid.

Reference	Collection day	Omics	Research subject
Beltman *et al.*, 2014	Preg: 7	P	Viable vs degenerate embryo
Faulkner *et al.*, 2012	Oestrus:7	P	ULF vs blood plasma proteomes
Faulkner *et al.*, 2013	Oestrus: 7,15	P	Low vs high P4 effect on ULF proteome
Forde *et al.*, 2013	Preg: 13-19	P, (T)	Effect of P4 on gene expression
Forde *et al.*, 2014a	Preg: 10-19	P, (T)	Protein changes in pregnancy
Forde *et al.*, 2014b	Preg+Oestrus: 10-19	M, (T)	Changes pregnant vs oestrus at different days
Forde *et al.*, 2015	Preg+Oestrus: 16	P, (T)	Effect of embryo on ULF composition
Forde *et al.*, 2016b	Preg: 19	M, (T)	AA consumption differences by embryo gender
Forde *et al.*, 2017	Preg: 19	M, (T)	Heifers, lactating and dry cows
Gegenfurtner *et al.*, 2019b	Pregnancy: 19	P	Effect of genetic merit on ULF proteome
Groebner *et al.*, 2011b	Oestrus: 12,15,18	M, (T)	Changes in 41 AA through oestrus
Harlow *et al.*, 2018	Oestrus: 9	P	Effect of diet on ULF composition
Helfrich *et al.*, 2020	*43-62 dpp*	P, (T)	Subclinical endometritis effect on ULF
Hugentobler *et al.*, 2007a	Oestrus: 0-14	M	Changes in [AA] through oestrus
Hugentobler *et al.*, 2010	Oestrus: 3,6	M	Effect of infused P4 on fluid composition
Ledgard *et al.*, 2012	Oestrus: 5,9,14	P	Asynchronic ET effect on proteome
Ledgard *et al.*, 2015	*15 and 42 dpp*	P	Subclinical endometritis vs healthy cows
Moraes *et al.*, 2020a	Preg+Oestrus: 17	M, (T)	Effect of preg. on ULF lipid composition
Moraes *et al.*, 2020b	Preg+Oestrus: 17	P, M, (T)	Effect of preg. on ULF proteome, metabolome
Mullen *et al.*, 2012	Oestrus: 7, 13	P	High fertility heifers' ULF proteome
Muñoz *et al.*, 2012	Preg+Oestrus: 8	P	Differences in ULF of i*n vivo* vs AI pregnancies

Passaro *et al.*, 2016	Preg+Oestrus: 7	P	Proteome changes induced by pregnancy
Ribeiro *et al.*, 2016	Preg+Oestrus: 15	M, (T)	Non-preg vs several embryo shapes
Simintiras *et al.*, 2019a	Oestrus: 12,13,14	M	Lipids (P4 suppl. effect)
Simintiras *et al.*, 2019b	Oestrus: 12,13,14	M	Nucleotides, vitamins, etc. (P4 suppl. effect)
Simintiras *et al.*, 2019c	Oestrus: 12,13,14	M	AA, carbohydrates (P4 suppl. effect)
Sponchiado *et al.*, 2019	Preg+Oestrus: 7	M, (T)	Embryo modulates ULF metabolome
Tribulo *et al.*, 2019	Oestrus: 0,3,5,7	M	Changes in ULF metabolome in early oestrus

Table S2-1 Details of the daily feed regime for cows either pregnant and non-lactating (dry), or milking, for the years 2017 and 2018.

	Farm Trial 1	Farm Trial 2 2017		Farm Trial 3 2018	
	Dry	Dry	Milking	Dry	Milking
Maize silage (kg)	3	2	2	3	2
Grass silage (kg)		3.5	3.5		
Mg oxide (g)	5	20	20	5	5
Sodium chloride (g)	10	10	10	10	10
Calimate (g)			75		50
Trace elements (g)		5	5		
Dicalcium phosphate (g)	10			10	
Zinc (g)	10			10	20
Total supplements (kg)	3.1	5.6	5.6	3.1	2.1
Pasture (Rye grass 70%, white clover 30%) (kg)	1.9	0.4	7.4	1.9	13.9
Total dry matter (kg)	**5**	**6**	**13**	**5**	**16**

Table S2-2 Instrument quality assurance values for oestradiol, progesterone NEFA and BOH concentration tests.

Quality Controls-mid range						
		date	Oestradiol	Progesterone	NEFA	BOH
		Expected	**87.8-107.3**	**7.54-8.68**	**1.48-1.72**	**0.65-0.95**
		mean	97.69	8.02	1.595	0.83
		std dev	6	0.35	0.024	0.049
		CV	6.14	4.31	1.47	5.87
Quality Control B-high range						
		date	Oestradiol	Progesterone	NEFA	BOH
		Expected	**471.6-576.4**	**16.46-18.94**	**2.3-2.66**	**1.41-1.71**
		mean	513.1	17.5	2.501	1.634
		std dev	14.38	0.62	0.019	0.117
		CV	2.8	3.57	0.73	7.11

Table S2-3 Viability estimates according to embryo quality, from similar studies in literature.

Article	Column1	Grade 1	Grade 2	Grade 3	Grade 4	TOTAL	G2/G1	G3/G1	Day	M	EB	MB	XB	HB
Farin (1999)		76	65	54		66	0.85	0.71	Day 43 rates					
Alkan (2019)		44.66	33.07			39	0.73		Day 30 rates					
Erdem (2019)		44.15	32.58			39	0.73		Day 30 rates					
Arreseigor 1998		57.1	52.9	31.2		46.5	0.92	0.55	Day 35					
Wright 1981		64	45	33		59	0.7	0.52	Day40-60	49	65	65	65	
Hasler 2001		73	68	56	47.5	68.2	0.93	0.77	Day50-60	66.9	70.3	70.9	71.4	56
AVERAGE							81	64						

Table S3-1 a. Top 5 proteins used to generate an Exclusion Scheduled Precursor List (ESPL). b. MS/MS peptide list. First 10 entries of ESPL made from albumin-only peptides; tolerance was 5 min (Rt), 0.05 Da (m/z).

A

Protein	Ranking
Serum albumin	1
Haemoglobin, subunit alpha	2
Serum transferrin	3
Haemoglobin, subunit beta	4
Lactotransferrin	5

B

Order	Sequence	m/z meas-ured	Rt (min)	m/z
1	R.RPCFSALTPDETYVPK.A	627.65	43.3	44.78
2	K.LGEYGFQNAL.I	556.27	48.46	48.49
3	R.MPCTED.Y	752.26	10.35	49.01
4	R.HPEYAVSVLLR.L	428.58	43.52	45.78
5	R.HPYFYAPELLYYANK.Y	630.31	53.42	53.45
6	R.PCFSALTPDETYVPK.A	862.91	47.7	47.74
7	F.YAPELLYYANK.Y	672.85	45.04	45.04
8	K.LFTFHAD.I	425.71	37.91	37.99
9	K.TVMENFVAFVDK.C	700.84	53.01	39.23
10	K.LGEYGFQN.A	464.21	30.58	31.17

Table S5-1 Proteins detected most consistently across untargeted proteomic studies of bovine uterine luminal fluid (ULF).

Protein names	Gene names	De-tected in stud-ies (N)
Carboxymethylenebutenolidase homolog	CMBL	8
Isocitrate dehydrogenase [NADP] (EC 1.1.1.42)	IDH1	8
Fructose-bisphosphate aldolase (EC 4.1.2.13)	ALDOA	7
Albumin	ALB	7
Branched-chain-amino-acid aminotransferase (EC 2.6.1.42)	BCAT1	7
GM2 ganglioside activator	GM2A	7
WAP four-disulfide core domain 2	WFDC2	7
DPP7 protein (Dipeptidyl peptidase 7)	DPP7	7
Acid sphingomyelinase-like phosphodiesterase	SMPDL3B	7
Phosphatidylethanolamine-binding protein 1 (PEBP-1) (Basic cytosolic 21 kDa protein) (HCNPpp) [Cleaved into: Hippocampal cholinergic neurostimulating peptide (HCNP)]	PEBP1 PBP PEBP	7
Ezrin (Cytovillin) (Villin-2) (p81)	EZR VIL2	7
Peroxiredoxin-2 (EC 1.11.1.24) (Thioredoxin-dependent peroxiredoxin 2)	PRDX2	7
Cytosolic non-specific dipeptidase (EC 3.4.13.18) (CNDP dipeptidase 2)	CNDP2	7
Keratin, type I cytoskeletal 19 (Cytokeratin-19) (CK-19) (Keratin-19) (K19)	KRT19	7
Phosphatidylethanolamine-binding protein 4	PEBP4	7
Inter-alpha (Globulin) inhibitor H4 (Plasma Kallikrein-sensitive glycoprotein)	ITIH4	6
FGG protein (Fibrinogen gamma-B chain)	FGG	6
Adenylyl cyclase-associated protein	CAP1	6
Cathepsin S (EC 3.4.22.27)	CTSS	6
Galectin-3-binding protein (Lectin galactoside-binding soluble 3-binding protein)	LGALS3BP	6
S-formylglutathione hydrolase (FGH) (EC 3.1.2.12) (Esterase D)	ESD	6
Coactosin-like protein	COTL1	6

Alkaline phosphatase, tissue-nonspecific isozyme (AP-TNAP) (TNSALP) (EC 3.1.3.1) (Alkaline phosphatase liver/bone/kidney isozyme)	ALPL	6
Arylsulfatase A (ASA) (EC 3.1.6.8) (Cerebroside-sulfatase)	ARSA	6
Leukocyte elastase inhibitor (LEI) (Serpin B1)	SERPINB1	6
Chloride intracellular channel protein 1	CLIC1	6
Enolase-phosphatase E1 (EC 3.1.3.77) (2,3-diketo-5-methylthio-1-phosphopentane phosphatase)	ENOPH1 MASA	6
Delta-aminolevulinic acid dehydratase (ALADH) (EC 4.2.1.24)	ALAD	6
Acyl-CoA-binding protein (ACBP) (Diazepam-binding inhibitor) (DBI)	DBI	6
Peroxiredoxin-6 (EC 1.11.1.27) (1-Cys peroxiredoxin) (1-Cys PRX) (Acidic calcium-independent phospholipase A2)	PRDX6 AOP2 GPX PHGPX	6
Phosphoglycerate kinase 1 (EC 2.7.2.3)	PGK1	6
Tubulin alpha-1D chain [Cleaved into: Detyrosinated tubulin alpha-1D chain]	TUBA1D	6
Phosphoglycerate mutase 1 (EC 5.4.2.11) (EC 5.4.2.4) (BPG-dependent PGAM 1) (Phosphoglycerate mutase isozyme B) (PGAM-B)	PGAM1	6
Heat shock 70kD protein binding protein (ST13 Hsp70 interacting protein) (ST13 protein)	ST13	6
Alpha-actinin-4 (Non-muscle alpha-actinin 4)	ACTN4	6
Isoaspartyl peptidase/L-asparaginase (EC 3.4.19.5) (EC 3.5.1.1) (Asparaginase-like protein 1)	ASRGL1	6
Clathrin heavy chain 1	CLTC	6
Annexin A2 (Annexin II) (Annexin-2) (Calpactin I heavy chain) (Calpactin-1 heavy chain)	ANXA2 ANX2	6
Gamma-ECS (EC 6.3.2.2) (Gamma-glutamylcysteine synthetase)	GCLC	6
Heat shock protein HSP 90-alpha	HSP90AA1 HSP90A HSPCA	6
Aspartate aminotransferase, cytoplasmic (cAspAT) (EC 2.6.1.1) (EC 2.6.1.3)	GOT1	6
L-lactate dehydrogenase A chain (LDH-A) (EC 1.1.1.27) (LDH muscle subunit) (LDH-M)	LDHA	6

Ubiquitin-like modifier-activating enzyme 1 (EC 6.2.1.45) (Ubiquitin-activating enzyme E1)	UBA1 UBE1	6
Plastin-1	PLS1	6
Malate dehydrogenase, cytoplasmic (EC 1.1.1.37) (Cytosolic malate dehydrogenase)	MDH1	6
Adenosylhomocysteinase (AdoHcyase) (EC 3.3.1.1) (S-adenosyl-L-homocysteine hydrolase)	AHCY	6
Parkinson disease protein 7 homolog (Maillard deglycase) (Parkinsonism-associated deglycase) (Protein DJ-1) (DJ-1) (Protein/nucleic acid deglycase DJ-1) (EC 3.1.2.-) (EC 3.5.1.-) (EC 3.5.1.124)	PARK7	6
Protein ABHD14B (EC 3.-.-.-) (Alpha/beta hydrolase domain-containing protein 14B) (Abhydrolase domain-containing protein 14B)	ABHD14B	6
Growth/differentiation factor 8 (GDF-8) (Myostatin)	MSTN GDF8 MH	6
Aldo-keto reductase family 1 member A1 (EC 1.1.1.2) (EC 1.1.1.33) (EC 1.1.1.372)	AKR1A1	6
N(G),N(G)-dimethylarginine dimethylaminohydrolase 2 (DDAH-2) (Dimethylarginine dimethylaminohydrolase 2) (EC 3.5.3.18) (DDAHII) (Dimethylargininase-2)	DDAH2	6
Phosphoserine aminotransferase (EC 2.6.1.52)	PSAT1	6
Ribonuclease inhibitor (Ribonuclease/angiogenin inhibitor 1)	RNH1	6
Cystatin E/M	CST6	6
Uncharacterized protein		
Triosephosphate isomerase (TIM) (EC 5.3.1.1) (Methylglyoxal synthase) (EC 4.2.3.3) (Triose-phosphate isomerase)	TPI1	6
Endoplasmic reticulum chaperone BiP (EC 3.6.4.10) (78 kDa glucose-regulated protein) (GRP-78)	HSPA5 GRP78	6
Rho GDP-dissociation inhibitor 1 (Rho GDI 1) (Rho-GDI alpha)	ARHGDIA	6
DPYSL3 protein (Dihydropyrimidinase like 3)	DPYSL3	6
Annexin A4 (35-beta calcimedin) (Annexin IV) (Annexin-4) (Carbohydrate-binding protein p33/p41)	ANXA4 ANX4	6
Glyceraldehyde-3-phosphate dehydrogenase (GAPDH) (EC 1.2.1.12) (Peptidyl-cysteine S-nitrosylase GAPDH) (EC 2.6.99.-)	GAPDH GAPD	6
Bifunctional purine biosynthesis protein ATIC (AICAR transformylase/inosine monophosphate cyclohydrolase) (ATIC)	ATIC PURH	6

3'(2'),5'-bisphosphate nucleotidase 1 (EC 3.1.3.7) (Bisphosphate 3'-nucleotidase 1)	BPNT1	6
EGF containing fibulin extracellular matrix protein 1 (EGF-containing fibulin-like extracellular matrix protein 1)	EFEMP1	6
Superoxide dismutase [Cu-Zn] (EC 1.15.1.1)	ECSOD	6
CD48 molecule	CD48	6

Table S5-2 Curated entries of proteins previously unreported in bovine ULF

Accession	*Protein names*	*Gene names*
E1BKK0	Transcription factor E2F8 (E2F-8)	E2F8
P0CG53	Polyubiquitin-B [Cleaved into: Ubiquitin]	UBB
P02672	Fibrinogen alpha chain [Cleaved into: Fibrinopeptide A; Fibrinogen alpha chain]	FGA
P33433	Histidine-rich glycoprotein (Histidine-proline-rich glycoprotein) (HPRG) (Fragments)	HRG
EQ3T056	L-lactate dehydrogenase A-like 6B (EC 1.1.1.27)	LDHAL6B
Q56K04	Cysteine-rich protein 1 (CRP-1)	CRIP1
P55206	C-type natriuretic peptide (SVSP15) [Cleaved into: CNP-22; CNP-29; CNP-53]	NPPC
P0C0S9	Histone H2A type 1 (H2A.1b)	
A4FV45	Transmembrane protein 214	TMEM214
EQ24K09	DNA (cytosine-5)-methyltransferase 1 (Dnmt1) (EC 2.1.1.37)	DNMT1
P38573	Uroplakin-1b (UP1b) (Uroplakin Ib) (UPIb)	UPK1B
EQ3SZZ0	Ribosome biogenesis protein BRX1 homolog (Brix domain-containing protein 2)	BRIX1
Q4U5R3	Proteasome activator complex subunit 1 (Proteasome activator 28 subunit alpha) (PA28a) (PA28alpha)	PSME1
Q9TTK4	Lysosomal-trafficking regulator	LYST
A5D989	Elongation factor 1-delta (EF-1-delta)	EEF1D
P31098	Osteopontin-K	
Q5E9T6	Leucine-rich glioma-inactivated protein 1	LGI1
P0CH28	Polyubiquitin-C [Cleaved into: Ubiquitin-related; Ubiquitin]	UBC
EQ3SZK4	FAST kinase domain-containing protein 4 (Protein TBRG4) (Transforming growth factor beta regulator 4)	TBRG4
Q6R8F2	Cadherin-1 (Epithelial cadherin) (E-cadherin) (CD antigen CD324) [Cleaved into: E-Cad/CTF1; E-Cad/CTF2; E-Cad/CTF3]	CDH1
P04973	Clathrin light chain A (Lca)	CLTA
EQ29RP1	Ubiquitin carboxyl-terminal hydrolase 1 (EC 3.4.19.12) (Deubiquitinating enzyme 1) (Ubiquitin thioesterase 1) (Ubiquitin-specific-processing protease 1)	USP1
EQ2TA29	Ras-related protein Rab-11A	RAB11A
EQ17QV3	Small ubiquitin-related modifier 3 (SUMO-3)	SUMO3

EQ3SZG8	Iron-sulfur cluster assembly 1 homolog, mitochondrial (HESB-like domain-containing protein 2) (Iron-sulfur assembly protein IscA)	ISCA1 HBLD2
EQ2KJC9	Alpha-aminoadipic semialdehyde dehydrogenase (Alpha-AASA dehydrogenase) (EC 1.2.1.31) (Aldehyde dehydrogenase family 7 member A1) (EC 1.2.1.3) (Antiquitin-1) (Betaine aldehyde dehydrogenase) (EC 1.2.1.8) (Delta1-piperideine-6-carboxylate dehydrogenase) (P6c dehydrogenase)	ALDH7A1
EQ32L81	Phosphatidate cytidylyltransferase, mitochondrial (EC 2.7.7.41) (CDP-diacylglycerol synthase) (CDP-DAG synthase) (Mitochondrial translocator assembly and maintenance protein 41 homolog) (TAM41)	TAMM41
EQ32LK1	Alanyl-tRNA editing protein Aarsd1 (Alanyl-tRNA synthetase domain-containing protein 1)	AARSD1
Q0P5D2	Cleavage and polyadenylation specificity factor subunit 6	CPSF6
P61285	Dynein light chain 1, cytoplasmic (Dynein light chain LC8-type 1)	DYNLL1 DNCL1
P20288	D(2) dopamine receptor (Dopamine D2 receptor)	DRD2
EQ1JP75	L-xylulose reductase (XR) (EC 1.1.1.10) (Dicarbonyl/L-xylulose reductase)	DCXR
EQ29RR5	Tuftelin-interacting protein 11 (Septin and tuftelin-interacting protein 1) (STIP-1)	TFIP11 STIP
EQ3T160	Nucleophosmin (NPM)	NPM1
EQ3T0S5	Fructose-bisphosphate aldolase B (EC 4.1.2.13) (Liver-type aldolase)	ALDOB
Q58DA7	Glutaredoxin-3 (PKC-interacting cousin of thioredoxin) (PICOT) (Thioredoxin-like protein 2)	GLRX3 TXNL2
A2VE01	Polyribonucleotide 5'-hydroxyl-kinase Clp1 (EC 2.7.1.78) (Polyadenylation factor Clp1) (Polynucleotide kinase Clp1) (Pre-mRNA cleavage complex II protein Clp1)	CLP1
P35478	Stefin-C	
A1A4R1	Histone H2A type 2-C (H2A-clustered histone 20)	H2AC20
O18738	Dystroglycan (Dystrophin-associated glycoprotein 1) [Cleaved into: Alpha-dystroglycan (Alpha-DG); Beta-dystroglycan (Beta-DG)]	DAG1
Q4ZHA6	Potassium voltage-gated channel subfamily B member 2	KCNB2
P31096	Osteopontin (Bone sialoprotein 1) (Secreted phosphoprotein 1) (SPP-1)	SPP1 OPN
EQ2HJB8	Tubulin alpha-8 chain (Alpha-tubulin 8)	TUBA8

Table S5-3 Full list of proteins identified in the present study and similar studies surveyed.

All	Article
A0A096LNF2	Aranciaga 2020
A0A0A0MP90	Aranciaga 2020
A0A0F7RPX0	Aranciaga 2020
A0A0F7RQ40	Aranciaga 2020
A0A0M4MD57	Aranciaga 2020
A0A0N4STN1	Aranciaga 2020
A0A140T831	Aranciaga 2020
A0A140T846	Aranciaga 2020
A0A140T887	Aranciaga 2020
A0A140T894	Aranciaga 2020
A0A140T8A5	Aranciaga 2020
A0A1K0FUD3	Aranciaga 2020
A0A3Q1LFG8	Aranciaga 2020
A0A3Q1LFQ2	Aranciaga 2020
A0A3Q1LGC4	Aranciaga 2020
A0A3Q1LGM4	Aranciaga 2020
A0A3Q1LHZ0	Aranciaga 2020
A0A3Q1LI44	Aranciaga 2020
A0A3Q1LI46	Aranciaga 2020
A0A3Q1LI93	Aranciaga 2020
A0A3Q1LJB2	Aranciaga 2020
A0A3Q1LJT1	Aranciaga 2020
A0A3Q1LK49	Aranciaga 2020
A0A3Q1LKJ1	Aranciaga 2020
A0A3Q1LKR8	Aranciaga 2020
A0A3Q1LKS8	Aranciaga 2020
A0A3Q1LKU1	Aranciaga 2020
A0A3Q1LL25	Aranciaga 2020
A0A3Q1LL35	Aranciaga 2020
A0A3Q1LL88	Aranciaga 2020
A0A3Q1LLB2	Aranciaga 2020
A0A3Q1LLT0	Aranciaga 2020
A0A3Q1LM10	Aranciaga 2020
A0A3Q1LM31	Aranciaga 2020
A0A3Q1LMA3	Aranciaga 2020
A0A3Q1LMV9	Aranciaga 2020
A0A3Q1LN27	Aranciaga 2020
A0A3Q1LN63	Aranciaga 2020
A0A3Q1LNX9	Aranciaga 2020
A0A3Q1LP76	Aranciaga 2020
A0A3Q1LP77	Aranciaga 2020
A0A3Q1LPA7	Aranciaga 2020
A0A3Q1LPD0	Aranciaga 2020
A0A3Q1LPD2	Aranciaga 2020
A0A3Q1LPF4	Aranciaga 2020
A0A3Q1LPG0	Aranciaga 2020
A0A3Q1LPL7	Aranciaga 2020
A0A3Q1LPY0	Aranciaga 2020
A0A3Q1LPY4	Aranciaga 2020
A0A3Q1LPZ4	Aranciaga 2020
A0A3Q1LQ12	Aranciaga 2020
A0A3Q1LQ34	Aranciaga 2020
A0A3Q1LQD7	Aranciaga 2020
A0A3Q1LQQ0	Aranciaga 2020
A0A3Q1LQQ5	Aranciaga 2020
A0A3Q1LQR2	Aranciaga 2020
A0A3Q1LQU4	Aranciaga 2020
A0A3Q1LR88	Aranciaga 2020
A0A3Q1LR94	Aranciaga 2020
A0A3Q1LRC3	Aranciaga 2020
A0A3Q1LRD8	Aranciaga 2020
A0A3Q1LRW4	Aranciaga 2020
A0A3Q1LRY6	Aranciaga 2020
A0A3Q1LSB6	Aranciaga 2020
A0A3Q1LSF0	Aranciaga 2020
A0A3Q1LSF9	Aranciaga 2020
A0A3Q1LSK2	Aranciaga 2020
A0A3Q1LSL4	Aranciaga 2020
A0A3Q1LSN0	Aranciaga 2020
A0A3Q1LSN6	Aranciaga 2020
A0A3Q1LSS0	Aranciaga 2020
A0A3Q1LT32	Aranciaga 2020
A0A3Q1LT59	Aranciaga 2020
A0A3Q1LTB0	Aranciaga 2020
A0A3Q1LTK7	Aranciaga 2020
A0A3Q1LTK9	Aranciaga 2020
A0A3Q1LTM0	Aranciaga 2020
A0A3Q1LTP0	Aranciaga 2020
A0A3Q1LTS9	Aranciaga 2020
A0A3Q1LTY4	Aranciaga 2020
A0A3Q1LU13	Aranciaga 2020
A0A3Q1LU27	Aranciaga 2020
A0A3Q1LU36	Aranciaga 2020
A0A3Q1LU85	Aranciaga 2020
A0A3Q1LUB2	Aranciaga 2020
A0A3Q1LUE9	Aranciaga 2020

A0A3Q1LUP1	Aranciaga 2020
A0A3Q1LUW6	Aranciaga 2020
A0A3Q1LV18	Aranciaga 2020
A0A3Q1LV21	Aranciaga 2020
A0A3Q1LV73	Aranciaga 2020
A0A3Q1LVA2	Aranciaga 2020
A0A3Q1LVA9	Aranciaga 2020
A0A3Q1LVC7	Aranciaga 2020
A0A3Q1LVC8	Aranciaga 2020
A0A3Q1LWH4	Aranciaga 2020
A0A3Q1LWK1	Aranciaga 2020
A0A3Q1LWV4	Aranciaga 2020
A0A3Q1LWV8	Aranciaga 2020
A0A3Q1LX34	Aranciaga 2020
A0A3Q1LX44	Aranciaga 2020
A0A3Q1LX69	Aranciaga 2020
A0A3Q1LX83	Aranciaga 2020
A0A3Q1LXG6	Aranciaga 2020
A0A3Q1LXM2	Aranciaga 2020
A0A3Q1LXR9	Aranciaga 2020
A0A3Q1LY19	Aranciaga 2020
A0A3Q1LY29	Aranciaga 2020
A0A3Q1LY31	Aranciaga 2020
A0A3Q1LY57	Aranciaga 2020
A0A3Q1LYE7	Aranciaga 2020
A0A3Q1LYV7	Aranciaga 2020
A0A3Q1LZ35	Aranciaga 2020
A0A3Q1LZ97	Aranciaga 2020
A0A3Q1LZK3	Aranciaga 2020
A0A3Q1LZN1	Aranciaga 2020

A0A3Q1LZU8	Aranciaga 2020
A0A3Q1M013	Aranciaga 2020
A0A3Q1M026	Aranciaga 2020
A0A3Q1M032	Aranciaga 2020
A0A3Q1M053	Aranciaga 2020
A0A3Q1M057	Aranciaga 2020
A0A3Q1M0D3	Aranciaga 2020
A0A3Q1M0K3	Aranciaga 2020
A0A3Q1M0M2	Aranciaga 2020
A0A3Q1M0T4	Aranciaga 2020
A0A3Q1M0U8	Aranciaga 2020
A0A3Q1M0V5	Aranciaga 2020
A0A3Q1M0Y7	Aranciaga 2020
A0A3Q1M103	Aranciaga 2020
A0A3Q1M104	Aranciaga 2020
A0A3Q1M124	Aranciaga 2020
A0A3Q1M193	Aranciaga 2020
A0A3Q1M1A9	Aranciaga 2020
A0A3Q1M1N7	Aranciaga 2020
A0A3Q1M1P3	Aranciaga 2020
A0A3Q1M1P4	Aranciaga 2020
A0A3Q1M1Z4	Aranciaga 2020
A0A3Q1M299	Aranciaga 2020
A0A3Q1M2A1	Aranciaga 2020
A0A3Q1M2A8	Aranciaga 2020
A0A3Q1M2E0	Aranciaga 2020
A0A3Q1M2E4	Aranciaga 2020
A0A3Q1M2H2	Aranciaga 2020
A0A3Q1M2Q2	Aranciaga 2020
A0A3Q1M2S8	Aranciaga 2020

A0A3Q1M352	Aranciaga 2020
A0A3Q1M3L6	Aranciaga 2020
A0A3Q1M3R8	Aranciaga 2020
A0A3Q1M3U5	Aranciaga 2020
A0A3Q1M3Z8	Aranciaga 2020
A0A3Q1M471	Aranciaga 2020
A0A3Q1M478	Aranciaga 2020
A0A3Q1M4K3	Aranciaga 2020
A0A3Q1M4L0	Aranciaga 2020
A0A3Q1M5R4	Aranciaga 2020
A0A3Q1M667	Aranciaga 2020
A0A3Q1M6A2	Aranciaga 2020
A0A3Q1M6C1	Aranciaga 2020
A0A3Q1M6C6	Aranciaga 2020
A0A3Q1M6K6	Aranciaga 2020
A0A3Q1M6S0	Aranciaga 2020
A0A3Q1M6S3	Aranciaga 2020
A0A3Q1M6W0	Aranciaga 2020
A0A3Q1M796	Aranciaga 2020
A0A3Q1M808	Aranciaga 2020
A0A3Q1M8A4	Aranciaga 2020
A0A3Q1M8H9	Aranciaga 2020
A0A3Q1M8I4	Aranciaga 2020
A0A3Q1M8I6	Aranciaga 2020
A0A3Q1M8I9	Aranciaga 2020
A0A3Q1M8L6	Aranciaga 2020
A0A3Q1M913	Aranciaga 2020
A0A3Q1M927	Aranciaga 2020
A0A3Q1M930	Aranciaga 2020
A0A3Q1M970	Aranciaga 2020

A0A3Q1M990	Aranciaga 2020
A0A3Q1M9I5	Aranciaga 2020
A0A3Q1M9P4	Aranciaga 2020
A0A3Q1M9W4	Aranciaga 2020
A0A3Q1MA07	Aranciaga 2020
A0A3Q1MA31	Aranciaga 2020
A0A3Q1MAJ0	Aranciaga 2020
A0A3Q1MAJ2	Aranciaga 2020
A0A3Q1MAM8	Aranciaga 2020
A0A3Q1MAU7	Aranciaga 2020
A0A3Q1MAV6	Aranciaga 2020
A0A3Q1MAZ2	Aranciaga 2020
A0A3Q1MB09	Aranciaga 2020
A0A3Q1MB39	Aranciaga 2020
A0A3Q1MB98	Aranciaga 2020
A0A3Q1MBL5	Aranciaga 2020
A0A3Q1MBP1	Aranciaga 2020
A0A3Q1MBP6	Aranciaga 2020
A0A3Q1MBQ7	Aranciaga 2020
A0A3Q1MBT3	Aranciaga 2020
A0A3Q1MBX2	Aranciaga 2020
A0A3Q1MC73	Aranciaga 2020
A0A3Q1MC82	Aranciaga 2020
A0A3Q1MCC9	Aranciaga 2020
A0A3Q1MCP9	Aranciaga 2020
A0A3Q1MCW7	Aranciaga 2020
A0A3Q1MCX8	Aranciaga 2020
A0A3Q1MD16	Aranciaga 2020
A0A3Q1MD56	Aranciaga 2020
A0A3Q1MDA4	Aranciaga 2020
A0A3Q1MDA5	Aranciaga 2020
A0A3Q1MDE6	Aranciaga 2020
A0A3Q1MDK7	Aranciaga 2020
A0A3Q1MDS1	Aranciaga 2020
A0A3Q1ME14	Aranciaga 2020
A0A3Q1MEU1	Aranciaga 2020
A0A3Q1MF14	Aranciaga 2020
A0A3Q1MF62	Aranciaga 2020
A0A3Q1MF86	Aranciaga 2020
A0A3Q1MFC3	Aranciaga 2020
A0A3Q1MFG3	Aranciaga 2020
A0A3Q1MFI5	Aranciaga 2020
A0A3Q1MFI7	Aranciaga 2020
A0A3Q1MFJ2	Aranciaga 2020
A0A3Q1MFK7	Aranciaga 2020
A0A3Q1MFL7	Aranciaga 2020
A0A3Q1MFR4	Aranciaga 2020
A0A3Q1MG04	Aranciaga 2020
A0A3Q1MG31	Aranciaga 2020
A0A3Q1MGK4	Aranciaga 2020
A0A3Q1MGT0	Aranciaga 2020
A0A3Q1MGU4	Aranciaga 2020
A0A3Q1MHC4	Aranciaga 2020
A0A3Q1MHG7	Aranciaga 2020
A0A3Q1MHJ3	Aranciaga 2020
A0A3Q1MHT0	Aranciaga 2020
A0A3Q1MI29	Aranciaga 2020
A0A3Q1MI98	Aranciaga 2020
A0A3Q1MIB0	Aranciaga 2020
A0A3Q1MIF4	Aranciaga 2020
A0A3Q1MIL5	Aranciaga 2020
A0A3Q1MIN7	Aranciaga 2020
A0A3Q1MJ46	Aranciaga 2020
A0A3Q1MJ74	Aranciaga 2020
A0A3Q1MJD9	Aranciaga 2020
A0A3Q1MJM1	Aranciaga 2020
A0A3Q1MJX6	Aranciaga 2020
A0A3Q1MK01	Aranciaga 2020
A0A3Q1MK05	Aranciaga 2020
A0A3Q1MK49	Aranciaga 2020
A0A3Q1MKI2	Aranciaga 2020
A0A3Q1MKQ7	Aranciaga 2020
A0A3Q1MKR2	Aranciaga 2020
A0A3Q1MKT5	Aranciaga 2020
A0A3Q1MKY2	Aranciaga 2020
A0A3Q1ML09	Aranciaga 2020
A0A3Q1ML26	Aranciaga 2020
A0A3Q1ML30	Aranciaga 2020
A0A3Q1ML78	Aranciaga 2020
A0A3Q1MLJ3	Aranciaga 2020
A0A3Q1MLP4	Aranciaga 2020
A0A3Q1MM55	Aranciaga 2020
A0A3Q1MM86	Aranciaga 2020
A0A3Q1MMY7	Aranciaga 2020
A0A3Q1MN08	Aranciaga 2020
A0A3Q1MN33	Aranciaga 2020
A0A3Q1MN44	Aranciaga 2020
A0A3Q1MN97	Aranciaga 2020
A0A3Q1MNN6	Aranciaga 2020
A0A3Q1MP70	Aranciaga 2020

A0A3Q1MPF1	Aranciaga 2020
A0A3Q1MQ34	Aranciaga 2020
A0A3Q1MQH2	Aranciaga 2020
A0A3Q1MQW8	Aranciaga 2020
A0A3Q1MQZ2	Aranciaga 2020
A0A3Q1MR74	Aranciaga 2020
A0A3Q1MR90	Aranciaga 2020
A0A3Q1MR92	Aranciaga 2020
A0A3Q1MRD9	Aranciaga 2020
A0A3Q1MRM3	Aranciaga 2020
A0A3Q1MRN4	Aranciaga 2020
A0A3Q1MS48	Aranciaga 2020
A0A3Q1MSF7	Aranciaga 2020
A0A3Q1MSP0	Aranciaga 2020
A0A3Q1MTF0	Aranciaga 2020
A0A3Q1MTI5	Aranciaga 2020
A0A3Q1MTT6	Aranciaga 2020
A0A3Q1MTU9	Aranciaga 2020
A0A3Q1MU19	Aranciaga 2020
A0A3Q1MU31	Aranciaga 2020
A0A3Q1MU51	Aranciaga 2020
A0A3Q1MUA3	Aranciaga 2020
A0A3Q1MUH1	Aranciaga 2020
A0A3Q1MUR2	Aranciaga 2020
A0A3Q1MUU1	Aranciaga 2020
A0A3Q1MV38	Aranciaga 2020
A0A3Q1MV83	Aranciaga 2020
A0A3Q1MVR5	Aranciaga 2020
A0A3Q1MWF7	Aranciaga 2020
A0A3Q1MWI6	Aranciaga 2020
A0A3Q1MXB7	Aranciaga 2020
A0A3Q1MY21	Aranciaga 2020
A0A3Q1MZC5	Aranciaga 2020
A0A3Q1MZI6	Aranciaga 2020
A0A3Q1MZY9	Aranciaga 2020
A0A3Q1N0C4	Aranciaga 2020
A0A3Q1N0Z7	Aranciaga 2020
A0A3Q1N147	Aranciaga 2020
A0A3Q1N1K0	Aranciaga 2020
A0A3Q1N1N6	Aranciaga 2020
A0A3Q1N1T6	Aranciaga 2020
A0A3Q1N2B9	Aranciaga 2020
A0A3Q1N2J5	Aranciaga 2020
A0A3Q1N3K8	Aranciaga 2020
A0A3Q1N3Q6	Aranciaga 2020
A0A3Q1N461	Aranciaga 2020
A0A3Q1N4K8	Aranciaga 2020
A0A3Q1N522	Aranciaga 2020
A0A3Q1N5F9	Aranciaga 2020
A0A3Q1N5G3	Aranciaga 2020
A0A3Q1N5N9	Aranciaga 2020
A0A3Q1N6D1	Aranciaga 2020
A0A3Q1N6F8	Aranciaga 2020
A0A3Q1N6L6	Aranciaga 2020
A0A3Q1N716	Aranciaga 2020
A0A3Q1N7K2	Aranciaga 2020
A0A3Q1N894	Aranciaga 2020
A0A3Q1N8B9	Aranciaga 2020
A0A3Q1N8C6	Aranciaga 2020
A0A3Q1N8Q5	Aranciaga 2020
A0A3Q1N9S5	Aranciaga 2020
A0A3Q1N9Y5	Aranciaga 2020
A0A3Q1NAY2	Aranciaga 2020
A0A3Q1NE05	Aranciaga 2020
A0A3Q1NE82	Aranciaga 2020
A0A3Q1NEW0	Aranciaga 2020
A0A3Q1NG86	Aranciaga 2020
A0A3Q1NGS3	Aranciaga 2020
A0A3Q1NH43	Aranciaga 2020
A0A3Q1NHQ0	Aranciaga 2020
A0A3Q1NHX9	Aranciaga 2020
A0A3Q1NJB1	Aranciaga 2020
A0A3Q1NJM8	Aranciaga 2020
A0A3Q1NKD1	Aranciaga 2020
A0A3Q1NKP5	Aranciaga 2020
A0A3Q1NLD8	Aranciaga 2020
A0A3Q1NLS8	Aranciaga 2020
A0A3Q1NM24	Aranciaga 2020
A0A3Q1NND6	Aranciaga 2020
A0A3Q1NNJ3	Aranciaga 2020
A0A3Q1NNJ8	Aranciaga 2020
A0A3Q1NNP6	Aranciaga 2020
A0A3S5ZP98	Aranciaga 2020
A0A3S5ZPB0	Aranciaga 2020
A0A3S5ZPB2	Aranciaga 2020
A0A3S5ZPK1	Aranciaga 2020
A0A3S5ZPM3	Aranciaga 2020
A0A452DHV9	Aranciaga 2020
A0A452DHX8	Aranciaga 2020
A0A452DHY4	Aranciaga 2020

A0A452DI24	Aranciaga 2020
A0A452DI25	Aranciaga 2020
A0A452DI45	Aranciaga 2020
A0A452DI66	Aranciaga 2020
A0A452DI72	Aranciaga 2020
A0A452DI85	Aranciaga 2020
A0A452DID1	Aranciaga 2020
A0A452DID9	Aranciaga 2020
A0A452DIE3	Aranciaga 2020
A0A452DIF5	Aranciaga 2020
A0A452DII8	Aranciaga 2020
A0A452DIL8	Aranciaga 2020
A0A452DIM3	Aranciaga 2020
A0A452DIS6	Aranciaga 2020
A0A452DIT4	Aranciaga 2020
A0A452DIW4	Aranciaga 2020
A0A452DIX3	Aranciaga 2020
A0A452DIY3	Aranciaga 2020
A0A452DJ01	Aranciaga 2020
A0A452DJ53	Aranciaga 2020
A0A452DJ82	Aranciaga 2020
A0A452DJE9	Aranciaga 2020
A0A452DJK6	Aranciaga 2020
A0A452DJS8	Aranciaga 2020
A0A452DK44	Aranciaga 2020
A0A452DKI9	Aranciaga 2020
A0A498UZ20	Aranciaga 2020
A0JN68	Aranciaga 2020
A0JNL5	Aranciaga 2020
A1A4N9	Aranciaga 2020
A1A4R1	Aranciaga 2020
A1L528	Aranciaga 2020
A1L548	Aranciaga 2020
A1L5B6	Aranciaga 2020
A2T1U6	Aranciaga 2020
A2VDX0	Aranciaga 2020
A2VE01	Aranciaga 2020
A2VE41	Aranciaga 2020
A3KMX4	Aranciaga 2020
A4FUA8	Aranciaga 2020
A4FUD0	Aranciaga 2020
A4FV12	Aranciaga 2020
A4FV45	Aranciaga 2020
A4FV56	Aranciaga 2020
A4IF97	Aranciaga 2020
A4IFI0	Aranciaga 2020
A4IFQ7	Aranciaga 2020
A4IFU5	Aranciaga 2020
A4IFV2	Aranciaga 2020
A4ZVC5	Aranciaga 2020
A5D785	Aranciaga 2020
A5D7A0	Aranciaga 2020
A5D7D1	Aranciaga 2020
A5D7E8	Aranciaga 2020
A5D7J6	Aranciaga 2020
A5D7Q2	Aranciaga 2020
A5D7R6	Aranciaga 2020
A5D7S8	Aranciaga 2020
A5D986	Aranciaga 2020
A5D9D1	Aranciaga 2020
A5D9D7	Aranciaga 2020
A5D9E1	Aranciaga 2020
A5D9H5	Aranciaga 2020
A5PJR3	Aranciaga 2020
A5PJV5	Aranciaga 2020
A5PJZ8	Aranciaga 2020
A5PK11	Aranciaga 2020
A5PK20	Aranciaga 2020
A5PK51	Aranciaga 2020
A5PK65	Aranciaga 2020
A5PK72	Aranciaga 2020
A5PK73	Aranciaga 2020
A6H6Y0	Aranciaga 2020
A6H714	Aranciaga 2020
A6H742	Aranciaga 2020
A6H768	Aranciaga 2020
A6H7A2	Aranciaga 2020
A6H7D3	Aranciaga 2020
A6H7E3	Aranciaga 2020
A6H7G2	Aranciaga 2020
A6H7H6	Aranciaga 2020
A6H7J7	Aranciaga 2020
A6QLL8	Aranciaga 2020
A6QLT9	Aranciaga 2020
A6QLU7	Aranciaga 2020
A6QLZ0	Aranciaga 2020
A6QM09	Aranciaga 2020
A6QNJ7	Aranciaga 2020
A6QNJ8	Aranciaga 2020
A6QNL5	Aranciaga 2020

A6QNM1	Aranciaga 2020
A6QNS1	Aranciaga 2020
A6QNX2	Aranciaga 2020
A6QP39	Aranciaga 2020
A6QPP2	Aranciaga 2020
A6QPZ0	Aranciaga 2020
A6QQ11	Aranciaga 2020
A6QQ85	Aranciaga 2020
A6QQA8	Aranciaga 2020
A6QQN6	Aranciaga 2020
A6QR56	Aranciaga 2020
A7E3D5	Aranciaga 2020
A7E3Q2	Aranciaga 2020
A7E3W2	Aranciaga 2020
A7E3W4	Aranciaga 2020
A7E3W7	Aranciaga 2020
A7MAZ5	Aranciaga 2020
A7MB40	Aranciaga 2020
A7MB62	Aranciaga 2020
A7MBA2	Aranciaga 2020
A7MBG0	Aranciaga 2020
A7MBI5	Aranciaga 2020
A7MBI7	Aranciaga 2020
A7YY28	Aranciaga 2020
A7YY37	Aranciaga 2020
A7Z014	Aranciaga 2020
A7Z055	Aranciaga 2020
A7Z057	Aranciaga 2020
A8E4L8	Aranciaga 2020
A8E646	Aranciaga 2020
A8YXX7	Aranciaga 2020
B0JYL8	Aranciaga 2020
B0JYM5	Aranciaga 2020
B0JYN6	Aranciaga 2020
B0JYP6	Aranciaga 2020
B0JYQ0	Aranciaga 2020
B3VTM3	Aranciaga 2020
B5B3R8	Aranciaga 2020
B6VAP7	Aranciaga 2020
B8Y9S9	Aranciaga 2020
B8Y9T0	Aranciaga 2020
C1K3N7	Aranciaga 2020
C6KEF7	Aranciaga 2020
D2U6Q4	Aranciaga 2020
D3U796	Aranciaga 2020
D4QBB3	Aranciaga 2020
D4QBB4	Aranciaga 2020
E1B726	Aranciaga 2020
E1B748	Aranciaga 2020
E1B864	Aranciaga 2020
E1B8H0	Aranciaga 2020
E1B8K6	Aranciaga 2020
E1B8Y9	Aranciaga 2020
E1B9E8	Aranciaga 2020
E1B9H0	Aranciaga 2020
E1B9K1	Aranciaga 2020
E1BAR2	Aranciaga 2020
E1BBY7	Aranciaga 2020
E1BCC9	Aranciaga 2020
E1BCL3	Aranciaga 2020
E1BDB0	Aranciaga 2020
E1BDF5	Aranciaga 2020
E1BE11	Aranciaga 2020
E1BE76	Aranciaga 2020
E1BEX4	Aranciaga 2020
E1BFV0	Aranciaga 2020
E1BG21	Aranciaga 2020
E1BG59	Aranciaga 2020
E1BGA6	Aranciaga 2020
E1BGV8	Aranciaga 2020
E1BH02	Aranciaga 2020
E1BH06	Aranciaga 2020
E1BH22	Aranciaga 2020
E1BH94	Aranciaga 2020
E1BI28	Aranciaga 2020
E1BI72	Aranciaga 2020
E1BJG5	Aranciaga 2020
E1BJP1	Aranciaga 2020
E1BKB7	Aranciaga 2020
E1BKQ7	Aranciaga 2020
E1BKU2	Aranciaga 2020
E1BKX7	Aranciaga 2020
E1BLV6	Aranciaga 2020
E1BLZ8	Aranciaga 2020
E1BM96	Aranciaga 2020
E1BMD1	Aranciaga 2020
E1BMG2	Aranciaga 2020
E1BNG8	Aranciaga 2020
E1BNR0	Aranciaga 2020
E1BP41	Aranciaga 2020

E1BP73	Aranciaga 2020
E1BPJ0	Aranciaga 2020
E1BPK6	Aranciaga 2020
E1BPP3	Aranciaga 2020
E2CT01	Aranciaga 2020
E3SAZ8	Aranciaga 2020
E3W9A0	Aranciaga 2020
E9QB09	Aranciaga 2020
E9RHW1	Aranciaga 2020
F1MAV0	Aranciaga 2020
F1MB19	Aranciaga 2020
F1MBV6	Aranciaga 2020
F1MC40	Aranciaga 2020
F1MC48	Aranciaga 2020
F1MCK2	Aranciaga 2020
F1MCY7	Aranciaga 2020
F1MD34	Aranciaga 2020
F1MD63	Aranciaga 2020
F1MD74	Aranciaga 2020
F1MDH3	Aranciaga 2020
F1MDS0	Aranciaga 2020
F1MET0	Aranciaga 2020
F1MG05	Aranciaga 2020
F1MGZ5	Aranciaga 2020
F1MHB8	Aranciaga 2020
F1MHL1	Aranciaga 2020
F1MIA9	Aranciaga 2020
F1MIJ5	Aranciaga 2020
F1MJ95	Aranciaga 2020
F1MJI7	Aranciaga 2020
F1MJI8	Aranciaga 2020
F1MJK3	Aranciaga 2020
F1MKS5	Aranciaga 2020
F1MKU4	Aranciaga 2020
F1ML12	Aranciaga 2020
F1MLH6	Aranciaga 2020
F1MLM2	Aranciaga 2020
F1MLS8	Aranciaga 2020
F1MLW7	Aranciaga 2020
F1MLW8	Aranciaga 2020
F1MLX9	Aranciaga 2020
F1MLZ4	Aranciaga 2020
F1MM32	Aranciaga 2020
F1MM57	Aranciaga 2020
F1MM83	Aranciaga 2020
F1MM86	Aranciaga 2020
F1MMK0	Aranciaga 2020
F1MMK2	Aranciaga 2020
F1MMK9	Aranciaga 2020
F1MMP5	Aranciaga 2020
F1MMR8	Aranciaga 2020
F1MNN6	Aranciaga 2020
F1MNV5	Aranciaga 2020
F1MNW5	Aranciaga 2020
F1MP31	Aranciaga 2020
F1MPE1	Aranciaga 2020
F1MPU0	Aranciaga 2020
F1MQ37	Aranciaga 2020
F1MQH8	Aranciaga 2020
F1MR60	Aranciaga 2020
F1MR96	Aranciaga 2020
F1MRD0	Aranciaga 2020
F1MRG7	Aranciaga 2020
F1MRN2	Aranciaga 2020
F1MRY9	Aranciaga 2020
F1MS05	Aranciaga 2020
F1MS40	Aranciaga 2020
F1MS53	Aranciaga 2020
F1MTC2	Aranciaga 2020
F1MTI7	Aranciaga 2020
F1MTP5	Aranciaga 2020
F1MTR1	Aranciaga 2020
F1MTV9	Aranciaga 2020
F1MU12	Aranciaga 2020
F1MU19	Aranciaga 2020
F1MU79	Aranciaga 2020
F1MUC5	Aranciaga 2020
F1MUP9	Aranciaga 2020
F1MUR6	Aranciaga 2020
F1MUZ9	Aranciaga 2020
F1MVK1	Aranciaga 2020
F1MW03	Aranciaga 2020
F1MWD3	Aranciaga 2020
F1MWI1	Aranciaga 2020
F1MWN1	Aranciaga 2020
F1MWQ2	Aranciaga 2020
F1MWR8	Aranciaga 2020
F1MWU9	Aranciaga 2020
F1MXF5	Aranciaga 2020
F1MY85	Aranciaga 2020

F1MYN5	Aranciaga 2020
F1MYQ7	Aranciaga 2020
F1MYS7	Aranciaga 2020
F1MYX5	Aranciaga 2020
F1MZ46	Aranciaga 2020
F1MZ92	Aranciaga 2020
F1MZ96	Aranciaga 2020
F1MZR1	Aranciaga 2020
F1N049	Aranciaga 2020
F1N076	Aranciaga 2020
F1N091	Aranciaga 2020
F1N093	Aranciaga 2020
F1N0E5	Aranciaga 2020
F1N0F2	Aranciaga 2020
F1N160	Aranciaga 2020
F1N161	Aranciaga 2020
F1N169	Aranciaga 2020
F1N1C9	Aranciaga 2020
F1N1I6	Aranciaga 2020
F1N2I5	Aranciaga 2020
F1N2L9	Aranciaga 2020
F1N2W0	Aranciaga 2020
F1N3J3	Aranciaga 2020
F1N3P2	Aranciaga 2020
F1N3Q7	Aranciaga 2020
F1N3U5	Aranciaga 2020
F1N3Y1	Aranciaga 2020
F1N458	Aranciaga 2020
F1N468	Aranciaga 2020
F1N469	Aranciaga 2020

F1N474	Aranciaga 2020
F1N4A6	Aranciaga 2020
F1N4K1	Aranciaga 2020
F1N4M7	Aranciaga 2020
F1N510	Aranciaga 2020
F1N5T0	Aranciaga 2020
F1N619	Aranciaga 2020
F1N647	Aranciaga 2020
F1N650	Aranciaga 2020
F1N694	Aranciaga 2020
F1N6C0	Aranciaga 2020
F1N6Y1	Aranciaga 2020
F1N712	Aranciaga 2020
F1N726	Aranciaga 2020
F1N789	Aranciaga 2020
F1N7D7	Aranciaga 2020
F1N7I3	Aranciaga 2020
F1N7X3	Aranciaga 2020
F2FB38	Aranciaga 2020
F2FB42	Aranciaga 2020
F2Z4C1	Aranciaga 2020
F2Z4D5	Aranciaga 2020
F2Z4F0	Aranciaga 2020
F2Z4F5	Aranciaga 2020
F2Z4G5	Aranciaga 2020
F2Z4I6	Aranciaga 2020
F2Z4J1	Aranciaga 2020
F6Q4T4	Aranciaga 2020
F6Q9Q9	Aranciaga 2020
F6QEU6	Aranciaga 2020

F6QH94	Aranciaga 2020
F6QND5	Aranciaga 2020
F6QQ60	Aranciaga 2020
F6QS88	Aranciaga 2020
F6R4P6	Aranciaga 2020
F6R9I4	Aranciaga 2020
F6RMV5	Aranciaga 2020
F8UZU9	Aranciaga 2020
G3MWT1	Aranciaga 2020
G3MWV5	Aranciaga 2020
G3MX65	Aranciaga 2020
G3MXG6	Aranciaga 2020
G3MXL6	Aranciaga 2020
G3MY44	Aranciaga 2020
G3MYC9	Aranciaga 2020
G3MYM8	Aranciaga 2020
G3MYZ3	Aranciaga 2020
G3MZE0	Aranciaga 2020
G3MZK6	Aranciaga 2020
G3MZU3	Aranciaga 2020
G3N022	Aranciaga 2020
G3N0D7	Aranciaga 2020
G3N0V0	Aranciaga 2020
G3N148	Aranciaga 2020
G3N1E4	Aranciaga 2020
G3N1F5	Aranciaga 2020
G3N1H5	Aranciaga 2020
G3N1U4	Aranciaga 2020
G3N1Y3	Aranciaga 2020
G3N2N7	Aranciaga 2020

G3N3Q3	Aranciaga 2020
G3X6I0	Aranciaga 2020
G3X6K8	Aranciaga 2020
G3X6L4	Aranciaga 2020
G3X6L9	Aranciaga 2020
G3X6N3	Aranciaga 2020
G3X6S5	Aranciaga 2020
G3X743	Aranciaga 2020
G3X757	Aranciaga 2020
G3X7I5	Aranciaga 2020
G3X7K5	Aranciaga 2020
G3X8A0	Aranciaga 2020
G5E531	Aranciaga 2020
G5E569	Aranciaga 2020
G5E580	Aranciaga 2020
G5E589	Aranciaga 2020
G5E5A8	Aranciaga 2020
G5E5A9	Aranciaga 2020
G5E5B0	Aranciaga 2020
G5E5C3	Aranciaga 2020
G5E5C8	Aranciaga 2020
G5E5H2	Aranciaga 2020
G5E5Q6	Aranciaga 2020
G5E5T5	Aranciaga 2020
G5E5V1	Aranciaga 2020
G5E5V6	Aranciaga 2020
G5E5Y5	Aranciaga 2020
G5E6J5	Aranciaga 2020
G5E6N4	Aranciaga 2020
G8JKV3	Aranciaga 2020
G8JKY5	Aranciaga 2020
H2CNR1	Aranciaga 2020
H9KUV2	Aranciaga 2020
K4JBR5	Aranciaga 2020
L7R4Y6	Aranciaga 2020
M5FJW2	Aranciaga 2020
M5FJZ9	Aranciaga 2020
M5FK91	Aranciaga 2020
M5FMU4	Aranciaga 2020
O02675	Aranciaga 2020
O02751	Aranciaga 2020
O18738	Aranciaga 2020
O18836	Aranciaga 2020
O46375	Aranciaga 2020
O46415	Aranciaga 2020
O62652	Aranciaga 2020
O77834	Aranciaga 2020
O97680	Aranciaga 2020
P00366	Aranciaga 2020
P00435	Aranciaga 2020
P00442	Aranciaga 2020
P00515	Aranciaga 2020
P00727	Aranciaga 2020
P00735	Aranciaga 2020
P00921	Aranciaga 2020
P00978	Aranciaga 2020
P01045	Aranciaga 2020
P01252	Aranciaga 2020
P01888	Aranciaga 2020
P01966	Aranciaga 2020
P02070	Aranciaga 2020
P02081	Aranciaga 2020
P02253	Aranciaga 2020
P02453	Aranciaga 2020
P02584	Aranciaga 2020
P02633	Aranciaga 2020
P02662	Aranciaga 2020
P02702	Aranciaga 2020
P04272	Aranciaga 2020
P05786	Aranciaga 2020
P07107	Aranciaga 2020
P07589	Aranciaga 2020
P08728	Aranciaga 2020
P09487	Aranciaga 2020
P0C0S9	Aranciaga 2020
P0CB32	Aranciaga 2020
P0CG53	Aranciaga 2020
P0CH28	Aranciaga 2020
P10096	Aranciaga 2020
P10103	Aranciaga 2020
P10462	Aranciaga 2020
P10575	Aranciaga 2020
P10790	Aranciaga 2020
P11019	Aranciaga 2020
P11116	Aranciaga 2020
P12763	Aranciaga 2020
P13214	Aranciaga 2020
P13696	Aranciaga 2020
P15497	Aranciaga 2020
P17248	Aranciaga 2020

P17697	Aranciaga 2020
P18203	Aranciaga 2020
P19035	Aranciaga 2020
P19120	Aranciaga 2020
P19660	Aranciaga 2020
P19803	Aranciaga 2020
P19858	Aranciaga 2020
P20000	Aranciaga 2020
P20004	Aranciaga 2020
P21752	Aranciaga 2020
P21856	Aranciaga 2020
P22226	Aranciaga 2020
P25417	Aranciaga 2020
P26285	Aranciaga 2020
P26452	Aranciaga 2020
P26882	Aranciaga 2020
P28800	Aranciaga 2020
P28801	Aranciaga 2020
P31408	Aranciaga 2020
P31754	Aranciaga 2020
P31976	Aranciaga 2020
P33046	Aranciaga 2020
P34955	Aranciaga 2020
P35466	Aranciaga 2020
P35478	Aranciaga 2020
P35604	Aranciaga 2020
P38657	Aranciaga 2020
P41541	Aranciaga 2020
P42899	Aranciaga 2020
P46193	Aranciaga 2020
P48034	Aranciaga 2020
P48427	Aranciaga 2020
P49951	Aranciaga 2020
P50227	Aranciaga 2020
P50397	Aranciaga 2020
P50448	Aranciaga 2020
P51122	Aranciaga 2020
P54149	Aranciaga 2020
P56701	Aranciaga 2020
P60661	Aranciaga 2020
P60902	Aranciaga 2020
P61157	Aranciaga 2020
P61603	Aranciaga 2020
P61955	Aranciaga 2020
P62157	Aranciaga 2020
P62261	Aranciaga 2020
P62326	Aranciaga 2020
P62935	Aranciaga 2020
P62992	Aranciaga 2020
P63048	Aranciaga 2020
P63103	Aranciaga 2020
P63258	Aranciaga 2020
P68103	Aranciaga 2020
P68138	Aranciaga 2020
P68250	Aranciaga 2020
P68252	Aranciaga 2020
P68401	Aranciaga 2020
P68509	Aranciaga 2020
P79098	Aranciaga 2020
P79126	Aranciaga 2020
P79136	Aranciaga 2020
P80177	Aranciaga 2020
P80311	Aranciaga 2020
P81187	Aranciaga 2020
P81265	Aranciaga 2020
P81287	Aranciaga 2020
P81644	Aranciaga 2020
P84080	Aranciaga 2020
Q08DB4	Aranciaga 2020
Q08DD1	Aranciaga 2020
Q08DD6	Aranciaga 2020
Q08DJ3	Aranciaga 2020
Q08DW2	Aranciaga 2020
Q08E18	Aranciaga 2020
Q08E20	Aranciaga 2020
Q0II59	Aranciaga 2020
Q0IIA4	Aranciaga 2020
Q0IIK5	Aranciaga 2020
Q0P570	Aranciaga 2020
Q0P5D6	Aranciaga 2020
Q0P5K3	Aranciaga 2020
Q0VCC0	Aranciaga 2020
Q0VCK0	Aranciaga 2020
Q0VCM5	Aranciaga 2020
Q0VCN1	Aranciaga 2020
Q0VCU1	Aranciaga 2020
Q0VCX2	Aranciaga 2020
Q0VCY8	Aranciaga 2020
Q0VD18	Aranciaga 2020
Q0VD27	Aranciaga 2020

Q0VD52	Aranciaga 2020
Q0VFX8	Aranciaga 2020
Q148C4	Aranciaga 2020
Q17QG8	Aranciaga 2020
Q17QK4	Aranciaga 2020
Q17QL7	Aranciaga 2020
Q17QQ2	Aranciaga 2020
Q17QV0	Aranciaga 2020
Q17QV3	Aranciaga 2020
Q17QX0	Aranciaga 2020
Q17R18	Aranciaga 2020
Q1JP75	Aranciaga 2020
Q1JPA2	Aranciaga 2020
Q1JPB0	Aranciaga 2020
Q1JPJ2	Aranciaga 2020
Q1LZA1	Aranciaga 2020
Q1P9Q3	Aranciaga 2020
Q1RMN8	Aranciaga 2020
Q1RMP3	Aranciaga 2020
Q27965	Aranciaga 2020
Q27970	Aranciaga 2020
Q27971	Aranciaga 2020
Q28908	Aranciaga 2020
Q29437	Aranciaga 2020
Q29443	Aranciaga 2020
Q29460	Aranciaga 2020
Q29RP1	Aranciaga 2020
Q29RR5	Aranciaga 2020
Q29RU4	Aranciaga 2020
Q2HJ49	Aranciaga 2020
Q2HJ81	Aranciaga 2020
Q2HJF0	Aranciaga 2020
Q2KHU0	Aranciaga 2020
Q2KI90	Aranciaga 2020
Q2KIC5	Aranciaga 2020
Q2KIF2	Aranciaga 2020
Q2KIL3	Aranciaga 2020
Q2KIT0	Aranciaga 2020
Q2KIU3	Aranciaga 2020
Q2KIV8	Aranciaga 2020
Q2KIX7	Aranciaga 2020
Q2KJ23	Aranciaga 2020
Q2KJ44	Aranciaga 2020
Q2KJ57	Aranciaga 2020
Q2KJ75	Aranciaga 2020
Q2KJ93	Aranciaga 2020
Q2KJC9	Aranciaga 2020
Q2KJD0	Aranciaga 2020
Q2KJE7	Aranciaga 2020
Q2KJF1	Aranciaga 2020
Q2KJG3	Aranciaga 2020
Q2KJH4	Aranciaga 2020
Q2KJH6	Aranciaga 2020
Q2KJH9	Aranciaga 2020
Q2NKY7	Aranciaga 2020
Q2T9X2	Aranciaga 2020
Q2TA29	Aranciaga 2020
Q2TA40	Aranciaga 2020
Q2TBI4	Aranciaga 2020
Q2TBR3	Aranciaga 2020
Q2TBU0	Aranciaga 2020
Q2TBX6	Aranciaga 2020
Q2YDE4	Aranciaga 2020
Q32L92	Aranciaga 2020
Q32LE5	Aranciaga 2020
Q32LG3	Aranciaga 2020
Q32LK1	Aranciaga 2020
Q32P66	Aranciaga 2020
Q32PB7	Aranciaga 2020
Q32PF2	Aranciaga 2020
Q32PI4	Aranciaga 2020
Q3B7M5	Aranciaga 2020
Q3MHF7	Aranciaga 2020
Q3MHG9	Aranciaga 2020
Q3MHH4	Aranciaga 2020
Q3MHL4	Aranciaga 2020
Q3MHL7	Aranciaga 2020
Q3MHM5	Aranciaga 2020
Q3MHN2	Aranciaga 2020
Q3MHN5	Aranciaga 2020
Q3MHP6	Aranciaga 2020
Q3MHY1	Aranciaga 2020
Q3MHY9	Aranciaga 2020
Q3SX44	Aranciaga 2020
Q3SYR8	Aranciaga 2020
Q3SYT9	Aranciaga 2020
Q3SYU2	Aranciaga 2020
Q3SYU9	Aranciaga 2020
Q3SYV4	Aranciaga 2020
Q3SZ54	Aranciaga 2020

Q3SZ62	Aranciaga 2020
Q3SZ65	Aranciaga 2020
Q3SZA5	Aranciaga 2020
Q3SZB6	Aranciaga 2020
Q3SZC4	Aranciaga 2020
Q3SZC6	Aranciaga 2020
Q3SZH7	Aranciaga 2020
Q3SZI4	Aranciaga 2020
Q3SZJ4	Aranciaga 2020
Q3SZN8	Aranciaga 2020
Q3SZR3	Aranciaga 2020
Q3SZV3	Aranciaga 2020
Q3SZZ0	Aranciaga 2020
Q3SZZ9	Aranciaga 2020
Q3T035	Aranciaga 2020
Q3T054	Aranciaga 2020
Q3T056	Aranciaga 2020
Q3T063	Aranciaga 2020
Q3T0B6	Aranciaga 2020
Q3T0C7	Aranciaga 2020
Q3T0D0	Aranciaga 2020
Q3T0E0	Aranciaga 2020
Q3T0K2	Aranciaga 2020
Q3T0M7	Aranciaga 2020
Q3T0P6	Aranciaga 2020
Q3T0Q4	Aranciaga 2020
Q3T0R1	Aranciaga 2020
Q3T0S5	Aranciaga 2020
Q3T0S6	Aranciaga 2020
Q3T0U1	Aranciaga 2020

Q3T0X5	Aranciaga 2020
Q3T0X8	Aranciaga 2020
Q3T0Y1	Aranciaga 2020
Q3T0Y5	Aranciaga 2020
Q3T0Z0	Aranciaga 2020
Q3T0Z7	Aranciaga 2020
Q3T101	Aranciaga 2020
Q3T145	Aranciaga 2020
Q3T147	Aranciaga 2020
Q3T149	Aranciaga 2020
Q3T160	Aranciaga 2020
Q3ZBD7	Aranciaga 2020
Q3ZBD9	Aranciaga 2020
Q3ZBG0	Aranciaga 2020
Q3ZBG1	Aranciaga 2020
Q3ZBH0	Aranciaga 2020
Q3ZBH5	Aranciaga 2020
Q3ZBN0	Aranciaga 2020
Q3ZBX9	Aranciaga 2020
Q3ZBY4	Aranciaga 2020
Q3ZBZ8	Aranciaga 2020
Q3ZC00	Aranciaga 2020
Q3ZC42	Aranciaga 2020
Q3ZC84	Aranciaga 2020
Q3ZC87	Aranciaga 2020
Q3ZCA8	Aranciaga 2020
Q3ZCC8	Aranciaga 2020
Q3ZCF3	Aranciaga 2020
Q3ZCG6	Aranciaga 2020
Q3ZCH0	Aranciaga 2020

Q3ZCH5	Aranciaga 2020
Q3ZCI4	Aranciaga 2020
Q3ZCI9	Aranciaga 2020
Q3ZCJ2	Aranciaga 2020
Q3ZCK3	Aranciaga 2020
Q3ZCK9	Aranciaga 2020
Q3ZCL8	Aranciaga 2020
Q4U5R3	Aranciaga 2020
Q4ZHA6	Aranciaga 2020
Q56JV4	Aranciaga 2020
Q56JW4	Aranciaga 2020
Q56JX6	Aranciaga 2020
Q56JY8	Aranciaga 2020
Q56K04	Aranciaga 2020
Q56K14	Aranciaga 2020
Q58CQ9	Aranciaga 2020
Q58CS3	Aranciaga 2020
Q58D57	Aranciaga 2020
Q58DA7	Aranciaga 2020
Q58DK5	Aranciaga 2020
Q58DU5	Aranciaga 2020
Q58DW0	Aranciaga 2020
Q59A32	Aranciaga 2020
Q5DPW9	Aranciaga 2020
Q5E946	Aranciaga 2020
Q5E947	Aranciaga 2020
Q5E956	Aranciaga 2020
Q5E983	Aranciaga 2020
Q5E984	Aranciaga 2020
Q5E987	Aranciaga 2020

Q5E995	Aranciaga 2020
Q5E9A1	Aranciaga 2020
Q5E9A3	Aranciaga 2020
Q5E9B1	Aranciaga 2020
Q5E9B7	Aranciaga 2020
Q5E9D5	Aranciaga 2020
Q5E9E2	Aranciaga 2020
Q5E9F5	Aranciaga 2020
Q5E9F7	Aranciaga 2020
Q5E9I6	Aranciaga 2020
Q5EA61	Aranciaga 2020
Q5EA67	Aranciaga 2020
Q5EAD2	Aranciaga 2020
Q5GN72	Aranciaga 2020
Q5H9M6	Aranciaga 2020
Q5KR47	Aranciaga 2020
Q687I9	Aranciaga 2020
Q6B855	Aranciaga 2020
Q6B856	Aranciaga 2020
Q6EWQ7	Aranciaga 2020
Q76LV1	Aranciaga 2020
Q7SIH1	Aranciaga 2020
Q861U5	Aranciaga 2020
Q862F3	Aranciaga 2020
Q862L1	Aranciaga 2020
Q862L2	Aranciaga 2020
Q862L8	Aranciaga 2020
Q862N7	Aranciaga 2020
Q862Q3	Aranciaga 2020
Q862S8	Aranciaga 2020

Q863C3	Aranciaga 2020
Q865V6	Aranciaga 2020
Q8MII0	Aranciaga 2020
Q8SPP7	Aranciaga 2020
Q95121	Aranciaga 2020
Q95140	Aranciaga 2020
Q95L54	Aranciaga 2020
Q95M18	Aranciaga 2020
Q95ND9	Aranciaga 2020
Q9BGI1	Aranciaga 2020
Q9BGI3	Aranciaga 2020
Q9BGU1	Aranciaga 2020
Q9TRY0	Aranciaga 2020
Q9TTK4	Aranciaga 2020
Q9TTK8	Aranciaga 2020
Q9TU03	Aranciaga 2020
Q9XSA7	Aranciaga 2020
Q9XSK7	Aranciaga 2020
Q9XSX1	Aranciaga 2020
U3Q4C5	Aranciaga 2020
V6F7P3	Aranciaga 2020
V6F7X3	Aranciaga 2020
V6F869	Aranciaga 2020
V6F9A2	Aranciaga 2020
V6F9A3	Aranciaga 2020
V6F9B4	Aranciaga 2020
A0A140T897	Aranciaga 2020
F1MB08	Aranciaga 2020
Q76LV2	Aranciaga 2020
A6QR28	Aranciaga 2020

P02672	Aranciaga 2020
A5PJE3	Aranciaga 2020
F1MD73	Aranciaga 2020
F1MJH1	Aranciaga 2020
A5PJ79	Aranciaga 2020
Q5E962	Aranciaga 2020
G5E513	Aranciaga 2020
A5D984	Aranciaga 2020
E1B9K8	Aranciaga 2020
A8QQK1	Aranciaga 2020
F1N7T6	Aranciaga 2020
Q2TBL6	Aranciaga 2020
G3N3L5	Aranciaga 2020
Q3SZV7	Aranciaga 2020
A3KMV5	Aranciaga 2020
A6H7J6	Aranciaga 2020
F1MN84	Aranciaga 2020
Q32S38	Aranciaga 2020
G3N0I4	Aranciaga 2020
A6QR15	Aranciaga 2020
F1MHF7	Aranciaga 2020
L7R5X3	Aranciaga 2020
A5D989	Aranciaga 2020
A0A0A0MP99	Aranciaga 2020
Q0VCM4	Aranciaga 2020
G5E619	Aranciaga 2020
B0JYN2	Aranciaga 2020
E1BCU6	Aranciaga 2020
Q5E9K0	Aranciaga 2020
A6QR19	Aranciaga 2020

A7E3S8	Aranciaga 2020
E1BH17	Aranciaga 2020
Q9N0V4	Aranciaga 2020
E1BEL8	Aranciaga 2020
F1MHV5	Aranciaga 2020
A6QPM9	Aranciaga 2020
Q95107	Aranciaga 2020
B0JYR3	Aranciaga 2020
F1N4E4	Aranciaga 2020
Q6R8F2	Aranciaga 2020
A6QLC4	Aranciaga 2020
P00829	Aranciaga 2020
G5E631	Aranciaga 2020
F1MCF1	Aranciaga 2020
Q28910	Aranciaga 2020
G3MZV0	Aranciaga 2020
Q3ZBV8	Aranciaga 2020
Q148F1	Aranciaga 2020
F1MX83	Aranciaga 2020
Q862H7	Aranciaga 2020
Q56J78	Aranciaga 2020
F1MMW8	Aranciaga 2020
F1N4R4	Aranciaga 2020
P04973	Aranciaga 2020
F1MV90	Aranciaga 2020
Q2HJ86	Aranciaga 2020
G5E604	Aranciaga 2020
Q5E9G3	Aranciaga 2020
F1MSZ6	Aranciaga 2020
P41361	Aranciaga 2020

E1BKM4	Aranciaga 2020
F1MGH3	Aranciaga 2020
Q29RK4	Aranciaga 2020
Q3SZK8	Aranciaga 2020
Q0VCX4	Aranciaga 2020
P52556	Aranciaga 2020
Q3T0W4	Aranciaga 2020
A7E350	Aranciaga 2020
Q0VC36	Aranciaga 2020
Q2T9S0	Aranciaga 2020
Q32PA4	Aranciaga 2020
Q2YDE9	Aranciaga 2020
G3N2F0	Aranciaga 2020
E1BLA8	Aranciaga 2020
O18879	Aranciaga 2020
F1MI18	Aranciaga 2020
F1MGU7	Aranciaga 2020
Q76I81	Aranciaga 2020
Q3T0Q6	Aranciaga 2020
Q2HJH2	Aranciaga 2020
A5D7A2	Aranciaga 2020
P63243	Aranciaga 2020
G3N3D0	Aranciaga 2020
E1BDE6	Aranciaga 2020
G3MX23	Aranciaga 2020
F1MGU5	Aranciaga 2020
F1MSB7	Aranciaga 2020
G1K1Z4	Aranciaga 2020
Q28034	Aranciaga 2020
Q2HJ57	Aranciaga 2020

Q3T169	Aranciaga 2020
P83939	Aranciaga 2020
Q2UVX4	Aranciaga 2020
P33097	Aranciaga 2020
E1B953	Aranciaga 2020
P48644	Aranciaga 2020
Q2KIT8	Aranciaga 2020
Q2HJH0	Aranciaga 2020
P48616	Aranciaga 2020
Q29S11	Aranciaga 2020
Q95M59	Aranciaga 2020
Q0VCS3	Aranciaga 2020
F1N1A3	Aranciaga 2020
F1N284	Aranciaga 2020
Q2KHW3	Aranciaga 2020
Q5E9T6	Aranciaga 2020
Q32PI5	Aranciaga 2020
A5D973	Aranciaga 2020
F1MX51	Aranciaga 2020
G3MZH0	Aranciaga 2020
G3MXD9	Aranciaga 2020
F1MMD7	Aranciaga 2020
Q3T052	Aranciaga 2020
A6QPH7	Aranciaga 2020
Q2KI84	Aranciaga 2020
A5PK49	Aranciaga 2020
O18789	Aranciaga 2020
F1MHP6	Aranciaga 2020
A3KN12	Aranciaga 2020
F1MHR6	Aranciaga 2020

P13135	Aranciaga 2020
G3MYJ0	Aranciaga 2020
G3X7M4	Aranciaga 2020
G3MXT4	Aranciaga 2020
Q28085	Aranciaga 2020
G3N2V5	Aranciaga 2020
B0JYN9	Aranciaga 2020
Q9TU25	Aranciaga 2020
A5PK69	Aranciaga 2020
P62998	Aranciaga 2020
A7MBG9	Aranciaga 2020
Q1JPH6	Aranciaga 2020
G3MXW7	Aranciaga 2020
Q32L81	Aranciaga 2020
F1MFT4	Aranciaga 2020
A2VDN7	Aranciaga 2020
F1MNG1	Aranciaga 2020
E1BEL7	Aranciaga 2020
P55206	Aranciaga 2020
Q3MHN0	Aranciaga 2020
F1MMI1	Aranciaga 2020
E1BAP8	Aranciaga 2020
Q9TS96	Aranciaga 2020
P61585	Aranciaga 2020
Q2NKU6	Aranciaga 2020
Q9N1C3	Aranciaga 2020
Q3SZ52	Aranciaga 2020
Q862Q9	Aranciaga 2020
Q3SZ43	Aranciaga 2020
K4JDS8	Aranciaga 2020

Q29RV1	Aranciaga 2020
F1MEN8	Aranciaga 2020
E1BNW1	Aranciaga 2020
A1L558	Aranciaga 2020
F1ME49	Aranciaga 2020
E1BN82	Aranciaga 2020
M5FMW2	Aranciaga 2020
E1BE15	Aranciaga 2020
G3MXR2	Aranciaga 2020
F1MQ84	Aranciaga 2020
A6QNS7	Aranciaga 2020
A0A140T861	Aranciaga 2020
Q28009	Aranciaga 2020
H7BWW2	Aranciaga 2020
E1BMS2	Aranciaga 2020
F1MQ57	Aranciaga 2020
F1MZ95	Aranciaga 2020
G3N1K4	Aranciaga 2020
G3N029	Aranciaga 2020
A5D987	Aranciaga 2020
Q8WMY2	Aranciaga 2020
Q0VCD7	Aranciaga 2020
Q2NL07	Aranciaga 2020
F1N431	Aranciaga 2020
F1MI46	Aranciaga 2020
P31098	Aranciaga 2020
P31096	Aranciaga 2020
A0A0M3T9B6	Aranciaga 2020
E1BP91	Aranciaga 2020
P38573	Aranciaga 2020

Q3SZC2	Aranciaga 2020
Q2NKZ1	Aranciaga 2020
F1MNQ4	Aranciaga 2020
Q6PVY3	Aranciaga 2020
Q0III3	Aranciaga 2020
E1BB08	Aranciaga 2020
Q45VK8	Aranciaga 2020
F1N5U0	Aranciaga 2020
F6RCB9	Aranciaga 2020
M1NM98	Aranciaga 2020
Q95M58	Aranciaga 2020
G3MXR5	Aranciaga 2020
E1BJL8	Aranciaga 2020
G3MWY4	Aranciaga 2020
F1N0N6	Aranciaga 2020
Q2TA22	Aranciaga 2020
Q07130	Aranciaga 2020
F1MJX4	Aranciaga 2020
G3N188	Aranciaga 2020
G3MY71	Aranciaga 2020
Q2KJ32	Aranciaga 2020
Q0VCP0	Aranciaga 2020
A4FUZ1	Aranciaga 2020
F1MW96	Aranciaga 2020
A7E322	Aranciaga 2020
F1N1A4	Aranciaga 2020
Q32LE4	Aranciaga 2020
G3N2Z0	Aranciaga 2020
G1K208	Aranciaga 2020
A4IFC3	Aranciaga 2020

Q29S21	Aranciaga 2020
E1B7J1	Aranciaga 2020
G3N309	Aranciaga 2020
E1B9R5	Aranciaga 2020
F1MQN0	Aranciaga 2020
K4JDR8	Aranciaga 2020
F1MFD0	Aranciaga 2020
Q2T9P4	Aranciaga 2020
A5D969	Aranciaga 2020
Q08E32	Aranciaga 2020
H9GW31	Aranciaga 2020
Q3SZ96	Aranciaga 2020
F1MG94	Aranciaga 2020
Q17QI3	Aranciaga 2020
Q1JPB6	Aranciaga 2020
Q3MHL8	Aranciaga 2020
E1BEE0	Aranciaga 2020
E1B8K5	Aranciaga 2020
A5PJ69	Aranciaga 2020
F1N4T4	Aranciaga 2020
A4ZZF8	Aranciaga 2020
Q3B7N2	Aranciaga 2020
F1MVW5	Aranciaga 2020
A2VDL8	Aranciaga 2020
G3N1R1	Aranciaga 2020
F1N679	Aranciaga 2020
Q0VC64	Aranciaga 2020
E1BP20	Aranciaga 2020
F1MIY8	Aranciaga 2020
E1B944	Aranciaga 2020

Q3ZCF0	Aranciaga 2020
F1MGY6	Aranciaga 2020
A6QLB7	Aranciaga 2020
E1BJZ1	Aranciaga 2020
Q0VCA5	Aranciaga 2020
F1N441	Aranciaga 2020
Q3ZC41	Aranciaga 2020
M5FMV8	Aranciaga 2020
F1MSP9	Aranciaga 2020
F1MG70	Aranciaga 2020
Q3T030	Aranciaga 2020
O46738	Aranciaga 2020
C7FE01	Aranciaga 2020
B9VPZ5	Aranciaga 2020
P24627	Aranciaga 2020
Q862H8	Aranciaga 2020
F1MZL6	Aranciaga 2020
F1MXJ5	Aranciaga 2020
Q3ZBV1	Aranciaga 2020
F1MNF8	Aranciaga 2020
Q3SZF2	Aranciaga 2020
B1P383	Aranciaga 2020
Q24K09	Aranciaga 2020
A0A0A0MP92	Aranciaga 2020
Q3SZQ8	Aranciaga 2020
Q3MHG3	Aranciaga 2020
F6S1Q0	Aranciaga 2020
P20288	Aranciaga 2020
Q58DM8	Aranciaga 2020
Q95KZ6	Aranciaga 2020

P67808	Aranciaga 2020
G3N2D7	Aranciaga 2020
F1N2D3	Aranciaga 2020
P33433	Aranciaga 2020
Q32PH8	Aranciaga 2020
E1BKW7	Aranciaga 2020
G3MXE8	Aranciaga 2020
A7YWR0	Aranciaga 2020
A5PKI0	Aranciaga 2020
E1BKK0	Aranciaga 2020
F1MKG1	Aranciaga 2020
F1MKA1	Aranciaga 2020
Q0IIF8	Aranciaga 2020
E1BP42	Aranciaga 2020
F2Z4E9	Aranciaga 2020
Q0P5D2	Aranciaga 2020
G3N2L2	Aranciaga 2020
A4IF88	Aranciaga 2020
G3X8B1	Aranciaga 2020
Q3SZG8	Aranciaga 2020
G5E648	Aranciaga 2020
Q5E951	Aranciaga 2020
F1MCF8	Aranciaga 2020
Q05FF2	Aranciaga 2020
B0JYL6	Aranciaga 2020
G3MZJ9	Aranciaga 2020
O46626	Aranciaga 2020
Q8SQ28	Aranciaga 2020
F1MHZ0	Aranciaga 2020
Q9MZT5	Aranciaga 2020

B8Y7I4	Aranciaga 2020
A7MBJ5	Aranciaga 2020
G3MXB5	Aranciaga 2020
P55859	Aranciaga 2020
F1MAZ3	Aranciaga 2020
F1N0J2	Aranciaga 2020
G3N2G7	Aranciaga 2020
F1MAZ1	Aranciaga 2020
P36225	Aranciaga 2020
G3N126	Aranciaga 2020
E1BFG0	Aranciaga 2020
A0A0A0MP89	Aranciaga 2020
A6QPQ2	Aranciaga 2020
H7BWW0	Aranciaga 2020
Q0IIM3	Aranciaga 2020
Q32LP2	Aranciaga 2020
F1MJJ8	Aranciaga 2020
Q9XSG3	Aranciaga 2020
Q3ZCJ7	Aranciaga 2020
F1MKZ5	Aranciaga 2020
Q2HJB8	Aranciaga 2020
Q5EAC6	Aranciaga 2020
G3MYE2	Aranciaga 2020
Q58DW5	Aranciaga 2020
Q08E58	Aranciaga 2020
P81282	Aranciaga 2020
F1MZ85	Aranciaga 2020
F1MZ83	Aranciaga 2020
F1MLV3	Aranciaga 2020
Q0II43	Aranciaga 2020

Q27991	Aranciaga 2020
Q3SZK4	Aranciaga 2020
E1BAI4	Aranciaga 2020
Q3T108	Aranciaga 2020
A0JN92	Aranciaga 2020
Q58DR7	Aranciaga 2020
Q2VYC3	Aranciaga 2020
F1MJV6	Aranciaga 2020
Q27984	Aranciaga 2020
E1BN16	Aranciaga 2020
Q3ZBU7	Aranciaga 2020
P25326	Aranciaga 2020
E1BBM1	Aranciaga 2020
A7MBI6	Aranciaga 2020
E1B8W0	Aranciaga 2020
F6QDN3	Aranciaga 2020
A6QP95	Aranciaga 2020
O02739	Aranciaga 2020
F1N2A2	Aranciaga 2020
Q862F5	Aranciaga 2020
Q862K7	Aranciaga 2020
P61285	Aranciaga 2020
F1ME41	Aranciaga 2020
F1MHG0	Aranciaga 2020
Q148J6	Aranciaga 2020
Q3MHR7	Aranciaga 2020
Q32PA1	Aranciaga 2020
P81948	Aranciaga 2020
F1MUX6	Aranciaga 2020
F1MR22	Aranciaga 2020

Q3MHP1	Aranciaga 2020
Q3ZBF7	Aranciaga 2020
A0A0A0MP93	Aranciaga 2020
A0A0A0MPA2	Aranciaga 2020
G8JL00	Aranciaga 2020
Q9XSC6	Aranciaga 2020
A1A4J1	Aranciaga 2020
F1MNW4	Aranciaga 2020
A1AG	Beltman 2014
ACBP	Beltman 2014
ALBU	Beltman 2014
ALDR	Beltman 2014
AMPN	Beltman 2014
APOA1	Beltman 2014
B2MG	Beltman 2014
CYC	Beltman 2014
DPYL2	Beltman 2014
ENOA	Beltman 2014
GDIR1	Beltman 2014
HBA	Beltman 2014
HBB	Beltman 2014
HS90A	Beltman 2014
HS90B	Beltman 2014
HSP7C	Beltman 2014
HSPB1	Beltman 2014
IDHC	Beltman 2014
KCRB	Beltman 2014
LDHB	Beltman 2014
NDKB	Beltman 2014
PA1B3	Beltman 2014

PNPH	Beltman 2014
PPIA	Beltman 2014
PRDX1	Beltman 2014
PRDX2	Beltman 2014
S10A4	Beltman 2014
SERA	Beltman 2014
TBA1B	Beltman 2014
TBA1C	Beltman 2014
TBA1D	Beltman 2014
TBB4A	Beltman 2014
TBB4B	Beltman 2014
TBB5	Beltman 2014
TERA	Beltman 2014
TKT	Beltman 2014
TPIS	Beltman 2014
TPM3	Beltman 2014
TRFE	Beltman 2014
ZA2G	Beltman 2014
1433E	Faulkner 2012
A0A0A0MP89	Faulkner 2012
A0A0A0MP92	Faulkner 2012
A0A0F6QNP7	Faulkner 2012
A0A0F7RPX0	Faulkner 2012
A0A140T843	Faulkner 2012
A0A140T879	Faulkner 2012
A0A140T897	Faulkner 2012
A0A140T8A5	Faulkner 2012
A0A140T8D4	Faulkner 2012
A1A4L7	Faulkner 2012
A1AG	Faulkner 2012

A1AT	Faulkner 2012
A1BG	Faulkner 2012
A1EA81	Faulkner 2012
A1L514	Faulkner 2012
A1L5B6	Faulkner 2012
A2MG	Faulkner 2012
A3KLR9	Faulkner 2012
A4IFI0	Faulkner 2012
A4IFQ7	Faulkner 2012
A4ZVC5	Faulkner 2012
A5PJE3	Faulkner 2012
A6H7J6	Faulkner 2012
A6QLB7	Faulkner 2012
A6QLL8	Faulkner 2012
A6QPX7	Faulkner 2012
A8KC76	Faulkner 2012
ACBP	Faulkner 2012
ACTB	Faulkner 2012
ACTC	Faulkner 2012
ALBU	Faulkner 2012
ALDR	Faulkner 2012
AMPN	Faulkner 2012
ANXA1	Faulkner 2012
ANXA2	Faulkner 2012
ANXA3	Faulkner 2012
ANXA4	Faulkner 2012
ANXA5	Faulkner 2012
AOCX	Faulkner 2012
APOA1	Faulkner 2012
APOA2	Faulkner 2012

APOH	Faulkner 2012
ARSA	Faulkner 2012
B0JYL8	Faulkner 2012
B0JYN6	Faulkner 2012
B0JYQ0	Faulkner 2012
B1B3F7	Faulkner 2012
B1B3F8	Faulkner 2012
B1B3F9	Faulkner 2012
B1B3G0	Faulkner 2012
B2MG	Faulkner 2012
B3RFM8	Faulkner 2012
B9VPZ5	Faulkner 2012
C6KEF7	Faulkner 2012
CAP1	Faulkner 2012
CATD	Faulkner 2012
CFAB	Faulkner 2012
CLUS	Faulkner 2012
CMGA	Faulkner 2012
CNDP2	Faulkner 2012
CO3	Faulkner 2012
CO4	Faulkner 2012
COF1	Faulkner 2012
D4QBB3	Faulkner 2012
D4QBB4	Faulkner 2012
E1BI28	Faulkner 2012
E1BJL8	Faulkner 2012
ENOA	Faulkner 2012
EZRI	Faulkner 2012
F16P1	Faulkner 2012
F1MAV0	Faulkner 2012

F1MB08	Faulkner 2012
F1MCF8	Faulkner 2012
F1MD73	Faulkner 2012
F1MGU7	Faulkner 2012
F1MIH9	Faulkner 2012
F1MLW7	Faulkner 2012
F1MMD7	Faulkner 2012
F1MMK2	Faulkner 2012
F1MMR6	Faulkner 2012
F1MN84	Faulkner 2012
F1MRD0	Faulkner 2012
F1MWQ2	Faulkner 2012
F1MX83	Faulkner 2012
F1MXZ0	Faulkner 2012
F1N076	Faulkner 2012
F1N2I5	Faulkner 2012
F1N3J3	Faulkner 2012
F1N430	Faulkner 2012
F1N4M7	Faulkner 2012
F1N5M2	Faulkner 2012
F1N650	Faulkner 2012
F6QVC9	Faulkner 2012
FETUA	Faulkner 2012
FIBA	Faulkner 2012
FIBB	Faulkner 2012
FIBG	Faulkner 2012
FUCO	Faulkner 2012
G1K122	Faulkner 2012
G3MX65	Faulkner 2012
G3N2D7	Faulkner 2012

G3N2H5	Faulkner 2012
G3X6N3	Faulkner 2012
G3X7A5	Faulkner 2012
G8JKZ8	Faulkner 2012
G9BHW9	Faulkner 2012
GDF8	Faulkner 2012
GDIB	Faulkner 2012
GNS	Faulkner 2012
GRP	Faulkner 2012
GSTM1	Faulkner 2012
GSTP1	Faulkner 2012
H6S1N4	Faulkner 2012
HBB	Faulkner 2012
HEMO	Faulkner 2012
HP20	Faulkner 2012
HP252	Faulkner 2012
HS90A	Faulkner 2012
HSP7C	Faulkner 2012
IDHC	Faulkner 2012
ITIH4	Faulkner 2012
K4JB97	Faulkner 2012
K4JBA2	Faulkner 2012
K4JBA5	Faulkner 2012
K4JBB0	Faulkner 2012
K4JBR5	Faulkner 2012
K4JBR9	Faulkner 2012
K4JBS4	Faulkner 2012
K4JBS8	Faulkner 2012
K4JBT0	Faulkner 2012
K4JDR8	Faulkner 2012

K4JDS3	Faulkner 2012
K4JDS8	Faulkner 2012
K4JDT2	Faulkner 2012
K4JF02	Faulkner 2012
K4JF05	Faulkner 2012
K4JF08	Faulkner 2012
K4JF13	Faulkner 2012
K4JF16	Faulkner 2012
K4JR71	Faulkner 2012
K4JR76	Faulkner 2012
K4JR81	Faulkner 2012
K4JR84	Faulkner 2012
K4JR88	Faulkner 2012
LGMN	Faulkner 2012
MDHC	Faulkner 2012
MIF	Faulkner 2012
NUCB1	Faulkner 2012
PARK7	Faulkner 2012
PDIA1	Faulkner 2012
PEBP1	Faulkner 2012
PEDF	Faulkner 2012
PGAM1	Faulkner 2012
PLBL2	Faulkner 2012
PPBT	Faulkner 2012
PPIA	Faulkner 2012
PPIB	Faulkner 2012
PRDX1	Faulkner 2012
PRDX2	Faulkner 2012
PRDX6	Faulkner 2012
PROF1	Faulkner 2012

Q0QEQ4	Faulkner 2012
Q0VBX6	Faulkner 2012
Q32L14	Faulkner 2012
Q32P72	Faulkner 2012
Q32PI4	Faulkner 2012
Q3SZQ8	Faulkner 2012
Q3SZZ9	Faulkner 2012
Q3T010	Faulkner 2012
Q3T0Z0	Faulkner 2012
Q3T141	Faulkner 2012
Q3ZBS7	Faulkner 2012
Q3ZC20	Faulkner 2012
Q5E962	Faulkner 2012
Q5EA67	Faulkner 2012
Q6VUQ8	Faulkner 2012
Q862H7	Faulkner 2012
Q864S5	Faulkner 2012
Q9BGI4	Faulkner 2012
R9QSM8	Faulkner 2012
RET4	Faulkner 2012
S100G	Faulkner 2012
S10AC	Faulkner 2012
SPA31	Faulkner 2012
SPA37	Faulkner 2012
SPA38	Faulkner 2012
THIO	Faulkner 2012
TIMP2	Faulkner 2012
TPIS	Faulkner 2012
TPM3	Faulkner 2012
TRFE	Faulkner 2012

TRFL	Faulkner 2012
UBA1	Faulkner 2012
V6F9A2	Faulkner 2012
VTDB	Faulkner 2012
ZA2G	Faulkner 2012
A0A0F6QNP7	Faulkner 2013
A0A140T897	Faulkner 2013
A0A140T8A5	Faulkner 2013
A1EA81	Faulkner 2013
A2MG	Faulkner 2013
A4IFI0	Faulkner 2013
A4ZVC5	Faulkner 2013
A5PJE3	Faulkner 2013
A6H7J6	Faulkner 2013
A6QPX7	Faulkner 2013
ACTB	Faulkner 2013
ALBU	Faulkner 2013
AMPN	Faulkner 2013
ANXA1	Faulkner 2013
ANXA4	Faulkner 2013
ANXA5	Faulkner 2013
APOH	Faulkner 2013
B0JYL8	Faulkner 2013
B1B3F8	Faulkner 2013
B1B3F9	Faulkner 2013
B1B3G0	Faulkner 2013
B2MG	Faulkner 2013
C6KEF7	Faulkner 2013
CAP1	Faulkner 2013
CATD	Faulkner 2013

CMGA	Faulkner 2013
CO3	Faulkner 2013
D4QBB4	Faulkner 2013
F16P1	Faulkner 2013
F1MAV0	Faulkner 2013
F1MB08	Faulkner 2013
F1MCF8	Faulkner 2013
F1MGU7	Faulkner 2013
F1MMD7	Faulkner 2013
F1MX83	Faulkner 2013
F1MXZ0	Faulkner 2013
F1N2I5	Faulkner 2013
F1N4M7	Faulkner 2013
F6QVC9	Faulkner 2013
FETUA	Faulkner 2013
FIBA	Faulkner 2013
G1K122	Faulkner 2013
G3MX65	Faulkner 2013
G3N2D7	Faulkner 2013
G8JKZ8	Faulkner 2013
H6S1N4	Faulkner 2013
HBB	Faulkner 2013
HSP7C	Faulkner 2013
IDHC	Faulkner 2013
K4JB97	Faulkner 2013
K4JBA2	Faulkner 2013
K4JBA5	Faulkner 2013
K4JBB0	Faulkner 2013
K4JBR5	Faulkner 2013
K4JBS4	Faulkner 2013

K4JBS8	Faulkner 2013
K4JBT0	Faulkner 2013
K4JDR8	Faulkner 2013
K4JDS3	Faulkner 2013
K4JDS8	Faulkner 2013
K4JDT2	Faulkner 2013
K4JF02	Faulkner 2013
K4JF05	Faulkner 2013
K4JF08	Faulkner 2013
K4JF13	Faulkner 2013
K4JF16	Faulkner 2013
K4JR71	Faulkner 2013
K4JR76	Faulkner 2013
K4JR81	Faulkner 2013
K4JR84	Faulkner 2013
K4JR88	Faulkner 2013
LGMN	Faulkner 2013
MIF	Faulkner 2013
PDIA1	Faulkner 2013
PLBL2	Faulkner 2013
PPIA	Faulkner 2013
Q0VBX6	Faulkner 2013
Q3SZZ9	Faulkner 2013
Q3ZC20	Faulkner 2013
Q5EA67	Faulkner 2013
Q9BGI4	Faulkner 2013
R9QSM8	Faulkner 2013
RET4	Faulkner 2013
S10AC	Faulkner 2013
TIMP2	Faulkner 2013

TRFE	Faulkner 2013
TRFL	Faulkner 2013
V6F9A2	Faulkner 2013
VTDB	Faulkner 2013
A0A0F7RQ40	Forde 2014
A0A0N4STN3	Forde 2014
A0A140T831	Forde 2014
A0A140T853	Forde 2014
A0A140T865	Forde 2014
A0A140T867	Forde 2014
A0A140T882	Forde 2014
A0A140T897	Forde 2014
A0A140T8A3	Forde 2014
A0A140T8A5	Forde 2014
A0JN36	Forde 2014
A0JN59	Forde 2014
A0JN92	Forde 2014
A0JND2	Forde 2014
A0JNJ0	Forde 2014
A0JNL5	Forde 2014
A1A4L7	Forde 2014
A1L502	Forde 2014
A1L555	Forde 2014
A1L568	Forde 2014
A1L595	Forde 2014
A1L5C0	Forde 2014
A2I7M9	Forde 2014
A2I7N1	Forde 2014
A2I7N2	Forde 2014
A2T1U6	Forde 2014

A2VDQ0	Forde 2014
A2VDW1	Forde 2014
A2VDX0	Forde 2014
A2VE52	Forde 2014
A2VE56	Forde 2014
A3KFF6	Forde 2014
A3KLR9	Forde 2014
A3KMV5	Forde 2014
A3KMV6	Forde 2014
A3KMX7	Forde 2014
A3KMY1	Forde 2014
A3KMY4	Forde 2014
A3KMY8	Forde 2014
A4D7S0	Forde 2014
A4D7S3	Forde 2014
A4FUA8	Forde 2014
A4FUD7	Forde 2014
A4FUG8	Forde 2014
A4FUW9	Forde 2014
A4FUY5	Forde 2014
A4FUZ0	Forde 2014
A4FV03	Forde 2014
A4FV18	Forde 2014
A4FV72	Forde 2014
A4FV94	Forde 2014
A4IF68	Forde 2014
A4IF70	Forde 2014
A4IF82	Forde 2014
A4IF91	Forde 2014
A4IFE0	Forde 2014

A4IFP2	Forde 2014
A4IFQ7	Forde 2014
A4IFV6	Forde 2014
A4ZZF8	Forde 2014
A5ACB9	Forde 2014
A5D7A5	Forde 2014
A5D7C6	Forde 2014
A5D7D1	Forde 2014
A5D7D5	Forde 2014
A5D7F2	Forde 2014
A5D7L9	Forde 2014
A5D7N5	Forde 2014
A5D7P0	Forde 2014
A5D7U3	Forde 2014
A5D9D1	Forde 2014
A5H027	Forde 2014
A5LIP3	Forde 2014
A5PJ79	Forde 2014
A5PJF6	Forde 2014
A5PJJ7	Forde 2014
A5PJU2	Forde 2014
A5PK21	Forde 2014
A5PK49	Forde 2014
A5PK65	Forde 2014
A5PK74	Forde 2014
A5PK77	Forde 2014
A5PK80	Forde 2014
A5PK87	Forde 2014
A5PKE1	Forde 2014
A5PKE3	Forde 2014

A5PKG8	Forde 2014
A5PKI3	Forde 2014
A5PKM0	Forde 2014
A6BMK7	Forde 2014
A6H701	Forde 2014
A6H742	Forde 2014
A6H754	Forde 2014
A6H7D3	Forde 2014
A6H7H0	Forde 2014
A6QL48	Forde 2014
A6QLA0	Forde 2014
A6QLB7	Forde 2014
A6QLC4	Forde 2014
A6QLF1	Forde 2014
A6QLJ7	Forde 2014
A6QLJ8	Forde 2014
A6QLL8	Forde 2014
A6QLN2	Forde 2014
A6QLP2	Forde 2014
A6QLS8	Forde 2014
A6QLV0	Forde 2014
A6QLY7	Forde 2014
A6QLZ0	Forde 2014
A6QLZ9	Forde 2014
A6QM00	Forde 2014
A6QM09	Forde 2014
A6QNP8	Forde 2014
A6QNU9	Forde 2014
A6QNX2	Forde 2014
A6QP06	Forde 2014

A6QP32	Forde 2014
A6QP58	Forde 2014
A6QP90	Forde 2014
A6QP92	Forde 2014
A6QP94	Forde 2014
A6QP98	Forde 2014
A6QPD1	Forde 2014
A6QPE1	Forde 2014
A6QPF3	Forde 2014
A6QPM3	Forde 2014
A6QPN6	Forde 2014
A6QPP2	Forde 2014
A6QPY4	Forde 2014
A6QPZ0	Forde 2014
A6QQ07	Forde 2014
A6QQ11	Forde 2014
A6QQ67	Forde 2014
A6QQI6	Forde 2014
A6QQN6	Forde 2014
A6QQP7	Forde 2014
A6QQS6	Forde 2014
A6QQS9	Forde 2014
A6QQU9	Forde 2014
A6QQX5	Forde 2014
A6QQZ4	Forde 2014
A6QR19	Forde 2014
A6QR20	Forde 2014
A6QR28	Forde 2014
A6QR64	Forde 2014
A7E2Y6	Forde 2014

A7E302	Forde 2014
A7E305	Forde 2014
A7E322	Forde 2014
A7E326	Forde 2014
A7E3S4	Forde 2014
A7E3S8	Forde 2014
A7E3W2	Forde 2014
A7E3W4	Forde 2014
A7LN90	Forde 2014
A7MB01	Forde 2014
A7MB14	Forde 2014
A7MB29	Forde 2014
A7MB31	Forde 2014
A7MB40	Forde 2014
A7MB59	Forde 2014
A7MBA2	Forde 2014
A7MBA6	Forde 2014
A7MBB6	Forde 2014
A7MBI5	Forde 2014
A7MBI6	Forde 2014
A7MBJ4	Forde 2014
A7MBK4	Forde 2014
A7YVI6	Forde 2014
A7YVI7	Forde 2014
A7YW33	Forde 2014
A7YWC9	Forde 2014
A7YWF3	Forde 2014
A7YWH4	Forde 2014
A7YWK3	Forde 2014
A7YY28	Forde 2014

A7YY55	Forde 2014
A7YY60	Forde 2014
A7Z028	Forde 2014
A7Z031	Forde 2014
A7Z042	Forde 2014
A7Z089	Forde 2014
A8E4L8	Forde 2014
A8KC67	Forde 2014
A8NGN2	Forde 2014
A8WFL7	Forde 2014
A8YXY5	Forde 2014
A8YXZ5	Forde 2014
A9CR99	Forde 2014
B0JYN6	Forde 2014
B0JYQ3	Forde 2014
B6DXC7	Forde 2014
C9EF40	Forde 2014
C9EF41	Forde 2014
D4QBB3	Forde 2014
D4QBB4	Forde 2014
D5HSX1	Forde 2014
D6C4G0	Forde 2014
D6C4G1	Forde 2014
D9ZDE4	Forde 2014
E1B709	Forde 2014
E1B757	Forde 2014
E1B778	Forde 2014
E1B7B4	Forde 2014
E1B7K5	Forde 2014
E1B7Q7	Forde 2014

E1B898	Forde 2014
E1B8J9	Forde 2014
E1B988	Forde 2014
E1B9Q4	Forde 2014
E1BAI4	Forde 2014
E1BAL6	Forde 2014
E1BAX4	Forde 2014
E1BB16	Forde 2014
E1BB27	Forde 2014
E1BB46	Forde 2014
E1BB52	Forde 2014
E1BBH1	Forde 2014
E1BBY7	Forde 2014
E1BCF2	Forde 2014
E1BCI2	Forde 2014
E1BCK4	Forde 2014
E1BDC9	Forde 2014
E1BDL3	Forde 2014
E1BEK2	Forde 2014
E1BFC2	Forde 2014
E1BFI7	Forde 2014
E1BFP1	Forde 2014
E1BFQ6	Forde 2014
E1BFU2	Forde 2014
E1BFU9	Forde 2014
E1BFX4	Forde 2014
E1BG25	Forde 2014
E1BGA4	Forde 2014
E1BGL2	Forde 2014
E1BGM1	Forde 2014

E1BH45	Forde 2014
E1BHH1	Forde 2014
E1BHL6	Forde 2014
E1BI28	Forde 2014
E1BI80	Forde 2014
E1BIU0	Forde 2014
E1BJ10	Forde 2014
E1BJI4	Forde 2014
E1BJT7	Forde 2014
E1BK18	Forde 2014
E1BKJ5	Forde 2014
E1BKK2	Forde 2014
E1BKT9	Forde 2014
E1BKX1	Forde 2014
E1BKX7	Forde 2014
E1BL45	Forde 2014
E1BLD1	Forde 2014
E1BLD2	Forde 2014
E1BLK3	Forde 2014
E1BM24	Forde 2014
E1BMI4	Forde 2014
E1BMJ6	Forde 2014
E1BMV7	Forde 2014
E1BMW6	Forde 2014
E1BN35	Forde 2014
E1BNH9	Forde 2014
E1BNJ2	Forde 2014
E1BNQ6	Forde 2014
E1BNY8	Forde 2014
E1BP65	Forde 2014

E1BP91	Forde 2014
E1BP98	Forde 2014
E1BPL6	Forde 2014
E9LZ03	Forde 2014
F1MAW5	Forde 2014
F1MB07	Forde 2014
F1MB09	Forde 2014
F1MBP8	Forde 2014
F1MCD1	Forde 2014
F1MCZ7	Forde 2014
F1MGY2	Forde 2014
F1MHR4	Forde 2014
F1MI83	Forde 2014
F1MI98	Forde 2014
F1MJQ2	Forde 2014
F1MKI1	Forde 2014
F1MKV7	Forde 2014
F1ML50	Forde 2014
F1MME2	Forde 2014
F1MME5	Forde 2014
F1MMU9	Forde 2014
F1MNS5	Forde 2014
F1MQ26	Forde 2014
F1MSS2	Forde 2014
F1MWK8	Forde 2014
F1MWU9	Forde 2014
F1MX49	Forde 2014
F1MXD4	Forde 2014
F1MYC9	Forde 2014
F1MYV7	Forde 2014

F1MYW2	Forde 2014
F1MZ01	Forde 2014
F1N0L3	Forde 2014
F1N0Q2	Forde 2014
F1N1U0	Forde 2014
F1N2I5	Forde 2014
F1N348	Forde 2014
F1N362	Forde 2014
F1N3H0	Forde 2014
F1N5R7	Forde 2014
F1N616	Forde 2014
F1N6E9	Forde 2014
F1N6X2	Forde 2014
F6Q234	Forde 2014
F8SUS8	Forde 2014
G3MYD7	Forde 2014
G3MYI7	Forde 2014
G3MYZ3	Forde 2014
G3N0S0	Forde 2014
G3N0V2	Forde 2014
G3X755	Forde 2014
G3X7D3	Forde 2014
G5E5C8	Forde 2014
G5E5J6	Forde 2014
G8CY11	Forde 2014
G8CY14	Forde 2014
G9HR25	Forde 2014
G9HR40	Forde 2014
H6V5E5	Forde 2014
H6V5F6	Forde 2014

H6V5G1	Forde 2014
H7BWW0	Forde 2014
H7BWW2	Forde 2014
J7ILV6	Forde 2014
K4JBR5	Forde 2014
K4JBS4	Forde 2014
K7QEC6	Forde 2014
K7QEP9	Forde 2014
K7QF92	Forde 2014
M5FJZ9	Forde 2014
M5FMU1	Forde 2014
O02674	Forde 2014
O02739	Forde 2014
O02741	Forde 2014
O18836	Forde 2014
O46375	Forde 2014
O46406	Forde 2014
O46414	Forde 2014
O46469	Forde 2014
O46728	Forde 2014
O46738	Forde 2014
O46739	Forde 2014
O46760	Forde 2014
O46773	Forde 2014
O46777	Forde 2014
O62644	Forde 2014
O62768	Forde 2014
O77578	Forde 2014
O77801	Forde 2014
O77834	Forde 2014

O77972	Forde 2014
O97680	Forde 2014
P00366	Forde 2014
P00442	Forde 2014
P00515	Forde 2014
P00516	Forde 2014
P00586	Forde 2014
P00727	Forde 2014
P00735	Forde 2014
P00921	Forde 2014
P00978	Forde 2014
P01030	Forde 2014
P01035	Forde 2014
P01044	Forde 2014
P01966	Forde 2014
P02070	Forde 2014
P02081	Forde 2014
P02584	Forde 2014
P02769	Forde 2014
P04261	Forde 2014
P04262	Forde 2014
P04272	Forde 2014
P05307	Forde 2014
P05689	Forde 2014
P05786	Forde 2014
P06394	Forde 2014
P06504	Forde 2014
P06868	Forde 2014
P07107	Forde 2014
P07688	Forde 2014

P08166	Forde 2014
P08168	Forde 2014
P08728	Forde 2014
P09487	Forde 2014
P0CB32	Forde 2014
P0DPE1	Forde 2014
P10096	Forde 2014
P10103	Forde 2014
P10462	Forde 2014
P10790	Forde 2014
P11023	Forde 2014
P12344	Forde 2014
P12763	Forde 2014
P13214	Forde 2014
P13621	Forde 2014
P13696	Forde 2014
P15103	Forde 2014
P15497	Forde 2014
P15696	Forde 2014
P16116	Forde 2014
P16368	Forde 2014
P17248	Forde 2014
P17697	Forde 2014
P17870	Forde 2014
P18203	Forde 2014
P18246	Forde 2014
P18902	Forde 2014
P19111	Forde 2014
P19120	Forde 2014
P19483	Forde 2014

P19803	Forde 2014
P19858	Forde 2014
P20000	Forde 2014
P20004	Forde 2014
P21856	Forde 2014
P24591	Forde 2014
P24627	Forde 2014
P25326	Forde 2014
P25417	Forde 2014
P25975	Forde 2014
P26779	Forde 2014
P26882	Forde 2014
P26892	Forde 2014
P27628	Forde 2014
P28053	Forde 2014
P28800	Forde 2014
P28801	Forde 2014
P30932	Forde 2014
P31081	Forde 2014
P31976	Forde 2014
P32120	Forde 2014
P32592	Forde 2014
P33097	Forde 2014
P33672	Forde 2014
P34955	Forde 2014
P35705	Forde 2014
P36225	Forde 2014
P38657	Forde 2014
P41361	Forde 2014
P45478	Forde 2014

P46193	Forde 2014
P48616	Forde 2014
P48644	Forde 2014
P48765	Forde 2014
P49951	Forde 2014
P50397	Forde 2014
P50448	Forde 2014
P52174	Forde 2014
P52175	Forde 2014
P52193	Forde 2014
P54228	Forde 2014
P55203	Forde 2014
P55859	Forde 2014
P56541	Forde 2014
P58351	Forde 2014
P60712	Forde 2014
P61286	Forde 2014
P62894	Forde 2014
P68250	Forde 2014
P69678	Forde 2014
P79098	Forde 2014
P79114	Forde 2014
P79136	Forde 2014
P79345	Forde 2014
P80109	Forde 2014
P80311	Forde 2014
P81187	Forde 2014
P81265	Forde 2014
P81425	Forde 2014
P82649	Forde 2014

P82928	Forde 2014
P83939	Forde 2014
Q01107	Forde 2014
Q03247	Forde 2014
Q04467	Forde 2014
Q05B55	Forde 2014
Q06807	Forde 2014
Q08D91	Forde 2014
Q08DC3	Forde 2014
Q08DD1	Forde 2014
Q08DD4	Forde 2014
Q08DE2	Forde 2014
Q08DI0	Forde 2014
Q08DK4	Forde 2014
Q08DN0	Forde 2014
Q08DP2	Forde 2014
Q08DU0	Forde 2014
Q08DU3	Forde 2014
Q08E20	Forde 2014
Q0IIE9	Forde 2014
Q0IIF8	Forde 2014
Q0IIH7	Forde 2014
Q0III5	Forde 2014
Q0III8	Forde 2014
Q0III9	Forde 2014
Q0IIM1	Forde 2014
Q0P569	Forde 2014
Q0P597	Forde 2014
Q0P5G1	Forde 2014
Q0P5H7	Forde 2014

Q0P5I2	Forde 2014
Q0P5I4	Forde 2014
Q0P5J6	Forde 2014
Q0PHW6	Forde 2014
Q0PNG1	Forde 2014
Q0QF29	Forde 2014
Q0V8B6	Forde 2014
Q0V8R6	Forde 2014
Q0VBY1	Forde 2014
Q0VC16	Forde 2014
Q0VCA3	Forde 2014
Q0VCA5	Forde 2014
Q0VCC0	Forde 2014
Q0VCE7	Forde 2014
Q0VCK0	Forde 2014
Q0VCK8	Forde 2014
Q0VCN9	Forde 2014
Q0VCS5	Forde 2014
Q0VCT3	Forde 2014
Q0VCW3	Forde 2014
Q0VCX2	Forde 2014
Q0VCX3	Forde 2014
Q0VD27	Forde 2014
Q0VD34	Forde 2014
Q148D3	Forde 2014
Q148E7	Forde 2014
Q148H5	Forde 2014
Q148H6	Forde 2014
Q148H7	Forde 2014
Q148I8	Forde 2014

Q148M5	Forde 2014
Q17QB3	Forde 2014
Q17QG8	Forde 2014
Q17QI7	Forde 2014
Q17QL2	Forde 2014
Q17QL3	Forde 2014
Q17QL7	Forde 2014
Q17QP7	Forde 2014
Q17QT0	Forde 2014
Q17QW4	Forde 2014
Q17QX0	Forde 2014
Q17R11	Forde 2014
Q17R18	Forde 2014
Q1ADE7	Forde 2014
Q1JP73	Forde 2014
Q1JPB0	Forde 2014
Q1JPG7	Forde 2014
Q1JPJ2	Forde 2014
Q1JPJ8	Forde 2014
Q1JQE5	Forde 2014
Q1JU88	Forde 2014
Q1LZ95	Forde 2014
Q1LZA1	Forde 2014
Q1LZB9	Forde 2014
Q1LZH9	Forde 2014
Q1MU36	Forde 2014
Q1P9Q3	Forde 2014
Q1RMI2	Forde 2014
Q1RMI8	Forde 2014
Q1RMM2	Forde 2014

Q1RMM7	Forde 2014
Q1RMM9	Forde 2014
Q1RMN0	Forde 2014
Q1RMP3	Forde 2014
Q1RMR4	Forde 2014
Q1RMV2	Forde 2014
Q1RMX4	Forde 2014
Q24JZ7	Forde 2014
Q24K02	Forde 2014
Q27965	Forde 2014
Q27970	Forde 2014
Q27975	Forde 2014
Q27984	Forde 2014
Q28017	Forde 2014
Q28035	Forde 2014
Q28046	Forde 2014
Q28115	Forde 2014
Q28193	Forde 2014
Q28205	Forde 2014
Q29437	Forde 2014
Q29443	Forde 2014
Q29451	Forde 2014
Q29465	Forde 2014
Q29RH8	Forde 2014
Q29RL9	Forde 2014
Q29RM3	Forde 2014
Q29RQ1	Forde 2014
Q29RR0	Forde 2014
Q29RR8	Forde 2014
Q29RS6	Forde 2014

Q29RT6	Forde 2014
Q29S21	Forde 2014
Q2HJ49	Forde 2014
Q2HJ57	Forde 2014
Q2HJ80	Forde 2014
Q2HJ86	Forde 2014
Q2HJE1	Forde 2014
Q2HJF0	Forde 2014
Q2HJH2	Forde 2014
Q2HJI8	Forde 2014
Q2KHT5	Forde 2014
Q2KHU0	Forde 2014
Q2KHW5	Forde 2014
Q2KHX8	Forde 2014
Q2KHZ6	Forde 2014
Q2KI13	Forde 2014
Q2KI38	Forde 2014
Q2KI62	Forde 2014
Q2KI65	Forde 2014
Q2KI90	Forde 2014
Q2KIB0	Forde 2014
Q2KIC1	Forde 2014
Q2KIF2	Forde 2014
Q2KII6	Forde 2014
Q2KIK1	Forde 2014
Q2KIK3	Forde 2014
Q2KIM0	Forde 2014
Q2KIS7	Forde 2014
Q2KIT0	Forde 2014
Q2KIU3	Forde 2014

Q2KIX7	Forde 2014
Q2KIY5	Forde 2014
Q2KIZ9	Forde 2014
Q2KJ26	Forde 2014
Q2KJ75	Forde 2014
Q2KJ97	Forde 2014
Q2KJB2	Forde 2014
Q2KJD7	Forde 2014
Q2KJF1	Forde 2014
Q2NL22	Forde 2014
Q2PS14	Forde 2014
Q2T9V3	Forde 2014
Q2T9W3	Forde 2014
Q2T9X5	Forde 2014
Q2TA06	Forde 2014
Q2TBI4	Forde 2014
Q2TBL4	Forde 2014
Q2TBL6	Forde 2014
Q2TBV0	Forde 2014
Q2TBV1	Forde 2014
Q2TBV3	Forde 2014
Q2TBX6	Forde 2014
Q2UVX4	Forde 2014
Q2YDI7	Forde 2014
Q2YDP6	Forde 2014
Q30287	Forde 2014
Q30289	Forde 2014
Q30291	Forde 2014
Q32KL2	Forde 2014
Q32KN6	Forde 2014

Q32KN8	Forde 2014
Q32KS2	Forde 2014
Q32KT7	Forde 2014
Q32KY6	Forde 2014
Q32L13	Forde 2014
Q32L96	Forde 2014
Q32L99	Forde 2014
Q32LE4	Forde 2014
Q32LE5	Forde 2014
Q32LF5	Forde 2014
Q32LP2	Forde 2014
Q32PA1	Forde 2014
Q32PF2	Forde 2014
Q32S38	Forde 2014
Q32T06	Forde 2014
Q32XW6	Forde 2014
Q3B7N2	Forde 2014
Q3HWE8	Forde 2014
Q3HWF0	Forde 2014
Q3MHJ2	Forde 2014
Q3MHK0	Forde 2014
Q3MHL4	Forde 2014
Q3MHN7	Forde 2014
Q3MHR0	Forde 2014
Q3MHW0	Forde 2014
Q3MHY0	Forde 2014
Q3MI05	Forde 2014
Q3SWX7	Forde 2014
Q3SWY8	Forde 2014
Q3SX14	Forde 2014

Q3SX44	Forde 2014
Q3SX45	Forde 2014
Q3SYS1	Forde 2014
Q3SYT7	Forde 2014
Q3SYU0	Forde 2014
Q3SYU2	Forde 2014
Q3SYU9	Forde 2014
Q3SYV4	Forde 2014
Q3SYW9	Forde 2014
Q3SYZ9	Forde 2014
Q3SZ46	Forde 2014
Q3SZ57	Forde 2014
Q3SZ62	Forde 2014
Q3SZA2	Forde 2014
Q3SZA6	Forde 2014
Q3SZC4	Forde 2014
Q3SZF3	Forde 2014
Q3SZH5	Forde 2014
Q3SZH7	Forde 2014
Q3SZJ7	Forde 2014
Q3SZK3	Forde 2014
Q3SZL4	Forde 2014
Q3SZN1	Forde 2014
Q3SZN8	Forde 2014
Q3SZR3	Forde 2014
Q3SZT2	Forde 2014
Q3SZV3	Forde 2014
Q3SZV7	Forde 2014
Q3SZX8	Forde 2014
Q3T010	Forde 2014
Q3T052	Forde 2014
Q3T063	Forde 2014
Q3T0D9	Forde 2014
Q3T0L2	Forde 2014
Q3T0P6	Forde 2014
Q3T0Q4	Forde 2014
Q3T0T1	Forde 2014
Q3T0Z0	Forde 2014
Q3T0Z7	Forde 2014
Q3T101	Forde 2014
Q3T108	Forde 2014
Q3T113	Forde 2014
Q3T114	Forde 2014
Q3T141	Forde 2014
Q3T145	Forde 2014
Q3T166	Forde 2014
Q3T179	Forde 2014
Q3T2L0	Forde 2014
Q3T904	Forde 2014
Q3YJF7	Forde 2014
Q3YJG4	Forde 2014
Q3YJG5	Forde 2014
Q3YJG7	Forde 2014
Q3YJH0	Forde 2014
Q3YJH8	Forde 2014
Q3YJK3	Forde 2014
Q3ZBD7	Forde 2014
Q3ZBE4	Forde 2014
Q3ZBG9	Forde 2014
Q3ZBH2	Forde 2014
Q3ZBP1	Forde 2014
Q3ZBQ2	Forde 2014
Q3ZBQ3	Forde 2014
Q3ZBV8	Forde 2014
Q3ZBX5	Forde 2014
Q3ZBY4	Forde 2014
Q3ZC00	Forde 2014
Q3ZC09	Forde 2014
Q3ZC37	Forde 2014
Q3ZC42	Forde 2014
Q3ZC44	Forde 2014
Q3ZC50	Forde 2014
Q3ZC55	Forde 2014
Q3ZC84	Forde 2014
Q3ZC91	Forde 2014
Q3ZCH0	Forde 2014
Q3ZCH5	Forde 2014
Q3ZCH9	Forde 2014
Q3ZCI4	Forde 2014
Q3ZCJ2	Forde 2014
Q3ZCK1	Forde 2014
Q3ZCK3	Forde 2014
Q3ZEJ6	Forde 2014
Q45KX8	Forde 2014
Q45VK9	Forde 2014
Q4TVR5	Forde 2014
Q4ZJR8	Forde 2014
Q58CS3	Forde 2014
Q58CY6	Forde 2014
Q58D05	Forde 2014

Q58D34	Forde 2014
Q58D55	Forde 2014
Q58DC0	Forde 2014
Q58DC5	Forde 2014
Q58DD1	Forde 2014
Q58DK5	Forde 2014
Q58DN0	Forde 2014
Q58DR3	Forde 2014
Q58DR9	Forde 2014
Q58DU5	Forde 2014
Q58DW0	Forde 2014
Q58DW4	Forde 2014
Q5BIR5	Forde 2014
Q5DPW9	Forde 2014
Q5E946	Forde 2014
Q5E956	Forde 2014
Q5E963	Forde 2014
Q5E997	Forde 2014
Q5E998	Forde 2014
Q5E9A6	Forde 2014
Q5E9B7	Forde 2014
Q5E9F0	Forde 2014
Q5E9F5	Forde 2014
Q5E9G3	Forde 2014
Q5E9H3	Forde 2014
Q5E9J1	Forde 2014
Q5E9K0	Forde 2014
Q5E9L6	Forde 2014
Q5E9R2	Forde 2014
Q5EA46	Forde 2014

Q5EA56	Forde 2014
Q5EA67	Forde 2014
Q5EA79	Forde 2014
Q5EAC2	Forde 2014
Q5H9M7	Forde 2014
Q5J801	Forde 2014
Q5MB93	Forde 2014
Q5NTB3	Forde 2014
Q5XQN5	Forde 2014
Q687I9	Forde 2014
Q690N0	Forde 2014
Q6LBN7	Forde 2014
Q6PT94	Forde 2014
Q6PT98	Forde 2014
Q6VE48	Forde 2014
Q6VUQ8	Forde 2014
Q6YFP9	Forde 2014
Q704V6	Forde 2014
Q71SP7	Forde 2014
Q765P0	Forde 2014
Q76LV1	Forde 2014
Q76LV2	Forde 2014
Q7SIH1	Forde 2014
Q7YQK0	Forde 2014
Q7YRQ5	Forde 2014
Q861V2	Forde 2014
Q861V5	Forde 2014
Q862B8	Forde 2014
Q862L0	Forde 2014
Q862L1	Forde 2014

Q862Q3	Forde 2014
Q862S0	Forde 2014
Q863K6	Forde 2014
Q864S3	Forde 2014
Q865A3	Forde 2014
Q865V6	Forde 2014
Q8HXQ5	Forde 2014
Q8MJ29	Forde 2014
Q8SQB5	Forde 2014
Q8WMX8	Forde 2014
Q8WMY2	Forde 2014
Q8WN39	Forde 2014
Q8WN55	Forde 2014
Q95135	Forde 2014
Q95393	Forde 2014
Q95394	Forde 2014
Q95L54	Forde 2014
Q95M12	Forde 2014
Q95M18	Forde 2014
Q9BE39	Forde 2014
Q9BE45	Forde 2014
Q9BEG8	Forde 2014
Q9BGI1	Forde 2014
Q9BGI2	Forde 2014
Q9BGI3	Forde 2014
Q9BGI4	Forde 2014
Q9BGU5	Forde 2014
Q9GK13	Forde 2014
Q9GLC9	Forde 2014
Q9GMS5	Forde 2014

Q9MYK6	Forde 2014
Q9MYM4	Forde 2014
Q9MYW0	Forde 2014
Q9MZ08	Forde 2014
Q9N0V4	Forde 2014
Q9N0X7	Forde 2014
Q9N287	Forde 2014
Q9N2I2	Forde 2014
Q9TRE3	Forde 2014
Q9TRQ0	Forde 2014
Q9TRY0	Forde 2014
Q9TTE1	Forde 2014
Q9TTK8	Forde 2014
Q9TUQ0	Forde 2014
Q9XSC6	Forde 2014
Q9XSC9	Forde 2014
Q9XSG3	Forde 2014
Q9XSJ4	Forde 2014
Q9XTA2	Forde 2014
V6F7X8	Forde 2014
Z4YHD9	Forde 2014
A0A024R324	Forde 2015
A0A024RAE4	Forde 2015
A0A140T853	Forde 2015
A0A140T897	Forde 2015
A0A140T8A5	Forde 2015
A0JN59	Forde 2015
A0JNL5	Forde 2015
A1A4L5	Forde 2015
A1L5C0	Forde 2015

A2VE41	Forde 2015
A3KLR9	Forde 2015
A3KMV5	Forde 2015
A4D7S3	Forde 2015
A4IF68	Forde 2015
A4IF70	Forde 2015
A4IFQ7	Forde 2015
A5D7D1	Forde 2015
A5D9D1	Forde 2015
A5PJN2	Forde 2015
A5PK49	Forde 2015
A6BMK7	Forde 2015
A6H742	Forde 2015
A6H754	Forde 2015
A6QLF1	Forde 2015
A6QLL8	Forde 2015
A6QM09	Forde 2015
A6QNX2	Forde 2015
A6QPF3	Forde 2015
A6QPR9	Forde 2015
A6QPY4	Forde 2015
A6QQ07	Forde 2015
A6QQN6	Forde 2015
A6QQS9	Forde 2015
A6QR28	Forde 2015
A7E3S8	Forde 2015
A7E3W2	Forde 2015
A7E3W4	Forde 2015
A7YWF3	Forde 2015
A7YWG4	Forde 2015

A7YY28	Forde 2015
B0JYN6	Forde 2015
D4QBB4	Forde 2015
E1B7B4	Forde 2015
E1B9Y0	Forde 2015
E1BB16	Forde 2015
E1BB46	Forde 2015
E1BB52	Forde 2015
E1BCK4	Forde 2015
E1BEK2	Forde 2015
E1BFU2	Forde 2015
E1BI28	Forde 2015
E1BJ10	Forde 2015
E1BJT7	Forde 2015
E1BKK2	Forde 2015
F1MME5	Forde 2015
F1MNS5	Forde 2015
F1MWU9	Forde 2015
F1N0Q2	Forde 2015
F1N2I5	Forde 2015
F1N3H0	Forde 2015
G8CY11	Forde 2015
G8CY14	Forde 2015
M5FJZ9	Forde 2015
O02675	Forde 2015
O02739	Forde 2015
O18836	Forde 2015
O46375	Forde 2015
O46414	Forde 2015
O46728	Forde 2015

O77642	Forde 2015
O77834	Forde 2015
P00921	Forde 2015
P01035	Forde 2015
P01966	Forde 2015
P02070	Forde 2015
P02769	Forde 2015
P04272	Forde 2015
P04346	Forde 2015
P05689	Forde 2015
P07107	Forde 2015
P07688	Forde 2015
P08166	Forde 2015
P08728	Forde 2015
P09487	Forde 2015
P0CB32	Forde 2015
P10668	Forde 2015
P12763	Forde 2015
P13696	Forde 2015
P15497	Forde 2015
P16116	Forde 2015
P17697	Forde 2015
P18902	Forde 2015
P19803	Forde 2015
P19858	Forde 2015
P24591	Forde 2015
P25326	Forde 2015
P26779	Forde 2015
P28800	Forde 2015
P28801	Forde 2015

P30932	Forde 2015
P31976	Forde 2015
P32592	Forde 2015
P33097	Forde 2015
P34955	Forde 2015
P41361	Forde 2015
P45478	Forde 2015
P49951	Forde 2015
P50397	Forde 2015
P55203	Forde 2015
P55859	Forde 2015
P56541	Forde 2015
P60712	Forde 2015
P60901	Forde 2015
P60953	Forde 2015
P61011	Forde 2015
P61586	Forde 2015
P62258	Forde 2015
P68133	Forde 2015
P68510	Forde 2015
P69678	Forde 2015
P79345	Forde 2015
P80209	Forde 2015
P81187	Forde 2015
P81265	Forde 2015
Q03247	Forde 2015
Q08DD1	Forde 2015
Q08DN0	Forde 2015
Q08DU0	Forde 2015
Q08E20	Forde 2015

Q0III9	Forde 2015
Q0P597	Forde 2015
Q0V8R6	Forde 2015
Q0VBY1	Forde 2015
Q0VCX2	Forde 2015
Q0VD27	Forde 2015
Q17QB3	Forde 2015
Q1JPB0	Forde 2015
Q1LZ95	Forde 2015
Q1LZH9	Forde 2015
Q1RMM9	Forde 2015
Q1RMN0	Forde 2015
Q27965	Forde 2015
Q28017	Forde 2015
Q29443	Forde 2015
Q29RT6	Forde 2015
Q2HJ28	Forde 2015
Q2HJ57	Forde 2015
Q2HJ86	Forde 2015
Q2HJF0	Forde 2015
Q2KHU0	Forde 2015
Q2KHZ6	Forde 2015
Q2KI90	Forde 2015
Q2KII3	Forde 2015
Q2KIM0	Forde 2015
Q2KIT0	Forde 2015
Q2KIU3	Forde 2015
Q2KIY5	Forde 2015
Q2KJ75	Forde 2015
Q2KJF1	Forde 2015

Q2KJH7	Forde 2015
Q2KJJ0	Forde 2015
Q2TBI4	Forde 2015
Q2TBU5	Forde 2015
Q2UVX4	Forde 2015
Q32KX2	Forde 2015
Q32LE5	Forde 2015
Q32LP2	Forde 2015
Q32PA1	Forde 2015
Q32S38	Forde 2015
Q3MHL4	Forde 2015
Q3MI05	Forde 2015
Q3SWY8	Forde 2015
Q3SX02	Forde 2015
Q3SX14	Forde 2015
Q3SX44	Forde 2015
Q3SYS1	Forde 2015
Q3SYT7	Forde 2015
Q3SYV4	Forde 2015
Q3SYW9	Forde 2015
Q3SZ57	Forde 2015
Q3SZ62	Forde 2015
Q3SZA2	Forde 2015
Q3SZH5	Forde 2015
Q3SZN8	Forde 2015
Q3SZR3	Forde 2015
Q3SZV7	Forde 2015
Q3T010	Forde 2015
Q3T063	Forde 2015
Q3T0P6	Forde 2015
Q3T0Q4	Forde 2015
Q3T0Z0	Forde 2015
Q3T114	Forde 2015
Q3T145	Forde 2015
Q3UPK6	Forde 2015
Q3ZBD7	Forde 2015
Q3ZBG9	Forde 2015
Q3ZBY4	Forde 2015
Q3ZC00	Forde 2015
Q3ZC09	Forde 2015
Q3ZC55	Forde 2015
Q3ZC84	Forde 2015
Q3ZC91	Forde 2015
Q3ZCH5	Forde 2015
Q3ZCI4	Forde 2015
Q3ZCJ2	Forde 2015
Q3ZEJ6	Forde 2015
Q58CS3	Forde 2015
Q58DD1	Forde 2015
Q58DK5	Forde 2015
Q5DPW9	Forde 2015
Q5E946	Forde 2015
Q5E956	Forde 2015
Q5E998	Forde 2015
Q5E9B7	Forde 2015
Q5EA67	Forde 2015
Q5EAC2	Forde 2015
Q5J801	Forde 2015
Q6LBN7	Forde 2015
Q76LV1	Forde 2015
Q76LV2	Forde 2015
Q862Q3	Forde 2015
Q865A3	Forde 2015
Q8SQB5	Forde 2015
Q8WMY2	Forde 2015
Q95135	Forde 2015
Q95M12	Forde 2015
Q9BGI1	Forde 2015
Q9BGI2	Forde 2015
Q9BGI3	Forde 2015
Q9BGU5	Forde 2015
Q9BVT0	Forde 2015
Q9JKY0	Forde 2015
Q9MYM4	Forde 2015
Q9MZ08	Forde 2015
Q9N0V4	Forde 2015
Q9TTE1	Forde 2015
Q9XSC6	Forde 2015
Q9XSG3	Forde 2015
Q9XSJ4	Forde 2015
Q9Z2U1	Forde 2015
V9HW98	Forde 2015
Z4YHD9	Forde 2015
A0A068JLG7	Gegenfurtner 2020
A0A0A0MPA4	Gegenfurtner 2020
A0A140T831	Gegenfurtner 2020
A0A140T846	Gegenfurtner 2020
A0A140T861	Gegenfurtner 2020
A0A140T869	Gegenfurtner 2020
A0A140T871	Gegenfurtner 2020

A0A140T894	Gegenfurtner 2020
A0A140T8A5	Gegenfurtner 2020
A0A140T8C6	Gegenfurtner 2020
A0A1B3B5V9	Gegenfurtner 2020
A0JN39	Gegenfurtner 2020
A0JN52	Gegenfurtner 2020
A0JND7	Gegenfurtner 2020
A0JNE9	Gegenfurtner 2020
A0JNL5	Gegenfurtner 2020
A0JNP2	Gegenfurtner 2020
A0JNP8	Gegenfurtner 2020
A1A4I8	Gegenfurtner 2020
A1A4J1	Gegenfurtner 2020
A1A4K2	Gegenfurtner 2020
A1A4K3	Gegenfurtner 2020
A1A4K5	Gegenfurtner 2020
A1A4L1	Gegenfurtner 2020
A1A4L7	Gegenfurtner 2020
A1A4M0	Gegenfurtner 2020
A1L543	Gegenfurtner 2020
A1L555	Gegenfurtner 2020
A1L570	Gegenfurtner 2020
A1L588	Gegenfurtner 2020
A1L5B1	Gegenfurtner 2020
A1L5B6	Gegenfurtner 2020
A1L5B7	Gegenfurtner 2020
A1XED1	Gegenfurtner 2020
A2I7N2	Gegenfurtner 2020
A2T1U6	Gegenfurtner 2020
A2VDN6	Gegenfurtner 2020
A2VDN7	Gegenfurtner 2020
A2VDN8	Gegenfurtner 2020
A2VDU0	Gegenfurtner 2020
A2VDW0	Gegenfurtner 2020
A2VDX0	Gegenfurtner 2020
A2VE14	Gegenfurtner 2020
A2VE41	Gegenfurtner 2020
A2VE99	Gegenfurtner 2020
A3KLR9	Gegenfurtner 2020
A3KMV5	Gegenfurtner 2020
A3KMY4	Gegenfurtner 2020
A3KMY8	Gegenfurtner 2020
A3KN22	Gegenfurtner 2020
A4FUA8	Gegenfurtner 2020
A4FUC8	Gegenfurtner 2020
A4FUD0	Gegenfurtner 2020
A4FUG5	Gegenfurtner 2020
A4FUI2	Gegenfurtner 2020
A4FUZ1	Gegenfurtner 2020
A4FV08	Gegenfurtner 2020
A4FV12	Gegenfurtner 2020
A4FV54	Gegenfurtner 2020
A4FV69	Gegenfurtner 2020
A4FV74	Gegenfurtner 2020
A4FV90	Gegenfurtner 2020
A4IF78	Gegenfurtner 2020
A4IF97	Gegenfurtner 2020
A4IFC3	Gegenfurtner 2020
A4IFE6	Gegenfurtner 2020
A4IFQ6	Gegenfurtner 2020
A4IFQ7	Gegenfurtner 2020
A4IFS7	Gegenfurtner 2020
A4IFV2	Gegenfurtner 2020
A5D7A0	Gegenfurtner 2020
A5D7A2	Gegenfurtner 2020
A5D7D1	Gegenfurtner 2020
A5D7K0	Gegenfurtner 2020
A5D7P1	Gegenfurtner 2020
A5D7Q2	Gegenfurtner 2020
A5D7V3	Gegenfurtner 2020
A5D984	Gegenfurtner 2020
A5D9E9	Gegenfurtner 2020
A5D9F0	Gegenfurtner 2020
A5D9G1	Gegenfurtner 2020
A5D9G3	Gegenfurtner 2020
A5D9H5	Gegenfurtner 2020
A5PJH7	Gegenfurtner 2020
A5PJN2	Gegenfurtner 2020
A5PJY9	Gegenfurtner 2020
A5PK51	Gegenfurtner 2020
A5PK63	Gegenfurtner 2020
A5PK70	Gegenfurtner 2020
A5PK77	Gegenfurtner 2020
A5PKI0	Gegenfurtner 2020
A5PKI3	Gegenfurtner 2020
A6BMK7	Gegenfurtner 2020
A6H709	Gegenfurtner 2020
A6H722	Gegenfurtner 2020
A6H742	Gegenfurtner 2020
A6H744	Gegenfurtner 2020

A6H749	Gegenfurtner 2020
A6H767	Gegenfurtner 2020
A6H769	Gegenfurtner 2020
A6H772	Gegenfurtner 2020
A6H788	Gegenfurtner 2020
A6H7B5	Gegenfurtner 2020
A6H7C4	Gegenfurtner 2020
A6H7D7	Gegenfurtner 2020
A6H7E3	Gegenfurtner 2020
A6H7G2	Gegenfurtner 2020
A6H7H3	Gegenfurtner 2020
A6H7H6	Gegenfurtner 2020
A6H7I5	Gegenfurtner 2020
A6H7J6	Gegenfurtner 2020
A6QL85	Gegenfurtner 2020
A6QLA4	Gegenfurtner 2020
A6QLA8	Gegenfurtner 2020
A6QLB7	Gegenfurtner 2020
A6QLD6	Gegenfurtner 2020
A6QLG5	Gegenfurtner 2020
A6QLL8	Gegenfurtner 2020
A6QLN6	Gegenfurtner 2020
A6QLR2	Gegenfurtner 2020
A6QLR8	Gegenfurtner 2020
A6QLS9	Gegenfurtner 2020
A6QLT5	Gegenfurtner 2020
A6QLT9	Gegenfurtner 2020
A6QLU8	Gegenfurtner 2020
A6QLY4	Gegenfurtner 2020
A6QLZ0	Gegenfurtner 2020
A6QLZ3	Gegenfurtner 2020
A6QM01	Gegenfurtner 2020
A6QM09	Gegenfurtner 2020
A6QNL5	Gegenfurtner 2020
A6QNM0	Gegenfurtner 2020
A6QNS6	Gegenfurtner 2020
A6QNX2	Gegenfurtner 2020
A6QP36	Gegenfurtner 2020
A6QP39	Gegenfurtner 2020
A6QP79	Gegenfurtner 2020
A6QPB5	Gegenfurtner 2020
A6QPC5	Gegenfurtner 2020
A6QPH7	Gegenfurtner 2020
A6QPK0	Gegenfurtner 2020
A6QPN6	Gegenfurtner 2020
A6QPP7	Gegenfurtner 2020
A6QPQ2	Gegenfurtner 2020
A6QPS1	Gegenfurtner 2020
A6QPT4	Gegenfurtner 2020
A6QPT7	Gegenfurtner 2020
A6QPZ4	Gegenfurtner 2020
A6QQ11	Gegenfurtner 2020
A6QQA8	Gegenfurtner 2020
A6QQC9	Gegenfurtner 2020
A6QQL4	Gegenfurtner 2020
A6QQL9	Gegenfurtner 2020
A6QQN6	Gegenfurtner 2020
A6QQR7	Gegenfurtner 2020
A6QQT4	Gegenfurtner 2020
A6QQV3	Gegenfurtner 2020
A6QQZ8	Gegenfurtner 2020
A6QR15	Gegenfurtner 2020
A6QR28	Gegenfurtner 2020
A6QR32	Gegenfurtner 2020
A6QR56	Gegenfurtner 2020
A7E306	Gegenfurtner 2020
A7E307	Gegenfurtner 2020
A7E355	Gegenfurtner 2020
A7E392	Gegenfurtner 2020
A7E3C7	Gegenfurtner 2020
A7E3D5	Gegenfurtner 2020
A7E3Q8	Gegenfurtner 2020
A7E3S8	Gegenfurtner 2020
A7E3T7	Gegenfurtner 2020
A7E3W2	Gegenfurtner 2020
A7MAZ5	Gegenfurtner 2020
A7MB16	Gegenfurtner 2020
A7MB21	Gegenfurtner 2020
A7MB35	Gegenfurtner 2020
A7MB62	Gegenfurtner 2020
A7MB81	Gegenfurtner 2020
A7MBA2	Gegenfurtner 2020
A7MBC2	Gegenfurtner 2020
A7MBC5	Gegenfurtner 2020
A7MBD4	Gegenfurtner 2020
A7MBD9	Gegenfurtner 2020
A7MBG0	Gegenfurtner 2020
A7MBG8	Gegenfurtner 2020
A7MBG9	Gegenfurtner 2020
A7MBH9	Gegenfurtner 2020

A7MBI5	Gegenfurtner 2020
A7MBI7	Gegenfurtner 2020
A7MBI9	Gegenfurtner 2020
A7MBJ4	Gegenfurtner 2020
A7MBJ5	Gegenfurtner 2020
A7YW37	Gegenfurtner 2020
A7YW98	Gegenfurtner 2020
A7YWC6	Gegenfurtner 2020
A7YWF1	Gegenfurtner 2020
A7YY28	Gegenfurtner 2020
A7YY55	Gegenfurtner 2020
A7Z014	Gegenfurtner 2020
A7Z035	Gegenfurtner 2020
A7Z051	Gegenfurtner 2020
A7Z055	Gegenfurtner 2020
A7Z066	Gegenfurtner 2020
A8E4P2	Gegenfurtner 2020
A8E645	Gegenfurtner 2020
A8E646	Gegenfurtner 2020
A8E651	Gegenfurtner 2020
A8E654	Gegenfurtner 2020
A8YXY1	Gegenfurtner 2020
A8YXY3	Gegenfurtner 2020
A8YXY9	Gegenfurtner 2020
B0JYQ0	Gegenfurtner 2020
B1PK18	Gegenfurtner 2020
B3VTM3	Gegenfurtner 2020
B5AAU9	Gegenfurtner 2020
B8Y7I4	Gegenfurtner 2020
B8Y9S9	Gegenfurtner 2020

B8YB77	Gegenfurtner 2020
C0KTL1	Gegenfurtner 2020
C1JZ67	Gegenfurtner 2020
C7DU20	Gegenfurtner 2020
C7FE01	Gegenfurtner 2020
D3DMC3	Gegenfurtner 2020
D3JUI8	Gegenfurtner 2020
D4QBB3	Gegenfurtner 2020
E1B6Z6	Gegenfurtner 2020
E1B725	Gegenfurtner 2020
E1B726	Gegenfurtner 2020
E1B748	Gegenfurtner 2020
E1B772	Gegenfurtner 2020
E1B7B4	Gegenfurtner 2020
E1B7E9	Gegenfurtner 2020
E1B7Q0	Gegenfurtner 2020
E1B7R4	Gegenfurtner 2020
E1B7S3	Gegenfurtner 2020
E1B7W1	Gegenfurtner 2020
E1B8H8	Gegenfurtner 2020
E1B8K6	Gegenfurtner 2020
E1B8X4	Gegenfurtner 2020
E1B9A5	Gegenfurtner 2020
E1B9E8	Gegenfurtner 2020
E1B9H1	Gegenfurtner 2020
E1B9H3	Gegenfurtner 2020
E1B9K8	Gegenfurtner 2020
E1B9R3	Gegenfurtner 2020
E1B9S8	Gegenfurtner 2020
E1B9T9	Gegenfurtner 2020

E1BA10	Gegenfurtner 2020
E1BA29	Gegenfurtner 2020
E1BAK6	Gegenfurtner 2020
E1BAN2	Gegenfurtner 2020
E1BAQ3	Gegenfurtner 2020
E1BAT3	Gegenfurtner 2020
E1BAY3	Gegenfurtner 2020
E1BB08	Gegenfurtner 2020
E1BB36	Gegenfurtner 2020
E1BBG4	Gegenfurtner 2020
E1BBK6	Gegenfurtner 2020
E1BBM1	Gegenfurtner 2020
E1BBT0	Gegenfurtner 2020
E1BBT9	Gegenfurtner 2020
E1BBY7	Gegenfurtner 2020
E1BCP3	Gegenfurtner 2020
E1BCU6	Gegenfurtner 2020
E1BCX9	Gegenfurtner 2020
E1BD04	Gegenfurtner 2020
E1BDE6	Gegenfurtner 2020
E1BDP3	Gegenfurtner 2020
E1BDX8	Gegenfurtner 2020
E1BE25	Gegenfurtner 2020
E1BE60	Gegenfurtner 2020
E1BE98	Gegenfurtner 2020
E1BEB4	Gegenfurtner 2020
E1BEG2	Gegenfurtner 2020
E1BEI0	Gegenfurtner 2020
E1BEI7	Gegenfurtner 2020
E1BEM3	Gegenfurtner 2020

E1BEN4	Gegenfurtner 2020
E1BEQ4	Gegenfurtner 2020
E1BEX4	Gegenfurtner 2020
E1BF20	Gegenfurtner 2020
E1BF40	Gegenfurtner 2020
E1BF48	Gegenfurtner 2020
E1BF59	Gegenfurtner 2020
E1BF95	Gegenfurtner 2020
E1BFB0	Gegenfurtner 2020
E1BFB9	Gegenfurtner 2020
E1BFG0	Gegenfurtner 2020
E1BFN9	Gegenfurtner 2020
E1BFP1	Gegenfurtner 2020
E1BFQ6	Gegenfurtner 2020
E1BFV0	Gegenfurtner 2020
E1BFZ1	Gegenfurtner 2020
E1BG76	Gegenfurtner 2020
E1BGB0	Gegenfurtner 2020
E1BGE5	Gegenfurtner 2020
E1BGJ4	Gegenfurtner 2020
E1BGU4	Gegenfurtner 2020
E1BH02	Gegenfurtner 2020
E1BH17	Gegenfurtner 2020
E1BH89	Gegenfurtner 2020
E1BHK2	Gegenfurtner 2020
E1BHT5	Gegenfurtner 2020
E1BI28	Gegenfurtner 2020
E1BI82	Gegenfurtner 2020
E1BIA7	Gegenfurtner 2020
E1BIB4	Gegenfurtner 2020
E1BIM1	Gegenfurtner 2020
E1BIM8	Gegenfurtner 2020
E1BIN5	Gegenfurtner 2020
E1BIU0	Gegenfurtner 2020
E1BIU3	Gegenfurtner 2020
E1BJA2	Gegenfurtner 2020
E1BJB1	Gegenfurtner 2020
E1BJD2	Gegenfurtner 2020
E1BJG5	Gegenfurtner 2020
E1BJH6	Gegenfurtner 2020
E1BJL8	Gegenfurtner 2020
E1BK52	Gegenfurtner 2020
E1BKJ7	Gegenfurtner 2020
E1BKM4	Gegenfurtner 2020
E1BKW5	Gegenfurtner 2020
E1BKX7	Gegenfurtner 2020
E1BKZ1	Gegenfurtner 2020
E1BKZ9	Gegenfurtner 2020
E1BL29	Gegenfurtner 2020
E1BLA8	Gegenfurtner 2020
E1BLF0	Gegenfurtner 2020
E1BLI9	Gegenfurtner 2020
E1BLR9	Gegenfurtner 2020
E1BLV1	Gegenfurtner 2020
E1BLV6	Gegenfurtner 2020
E1BLZ8	Gegenfurtner 2020
E1BM12	Gegenfurtner 2020
E1BM20	Gegenfurtner 2020
E1BM26	Gegenfurtner 2020
E1BM57	Gegenfurtner 2020
E1BM92	Gegenfurtner 2020
E1BMD6	Gegenfurtner 2020
E1BME2	Gegenfurtner 2020
E1BMG1	Gegenfurtner 2020
E1BMP2	Gegenfurtner 2020
E1BMW9	Gegenfurtner 2020
E1BN47	Gegenfurtner 2020
E1BNB0	Gegenfurtner 2020
E1BND6	Gegenfurtner 2020
E1BNQ4	Gegenfurtner 2020
E1BNY9	Gegenfurtner 2020
E1BP41	Gegenfurtner 2020
E1BP50	Gegenfurtner 2020
E1BP91	Gegenfurtner 2020
E1BPK6	Gegenfurtner 2020
E1BPQ9	Gegenfurtner 2020
E1BPW1	Gegenfurtner 2020
E1BQ11	Gegenfurtner 2020
E1BQ16	Gegenfurtner 2020
E1BQ21	Gegenfurtner 2020
E1BQ32	Gegenfurtner 2020
E1BQ37	Gegenfurtner 2020
E3SAZ8	Gegenfurtner 2020
F1MAU3	Gegenfurtner 2020
F1MAV2	Gegenfurtner 2020
F1MB04	Gegenfurtner 2020
F1MB84	Gegenfurtner 2020
F1MBC5	Gegenfurtner 2020
F1MBF0	Gegenfurtner 2020
F1MBF6	Gegenfurtner 2020

F1MBG0	Gegenfurtner 2020
F1MBN2	Gegenfurtner 2020
F1MBP8	Gegenfurtner 2020
F1MBQ0	Gegenfurtner 2020
F1MBV2	Gegenfurtner 2020
F1MBV6	Gegenfurtner 2020
F1MC48	Gegenfurtner 2020
F1MC72	Gegenfurtner 2020
F1MC76	Gegenfurtner 2020
F1MC86	Gegenfurtner 2020
F1MCF1	Gegenfurtner 2020
F1MCK2	Gegenfurtner 2020
F1MCZ0	Gegenfurtner 2020
F1MD34	Gegenfurtner 2020
F1MD58	Gegenfurtner 2020
F1MD73	Gegenfurtner 2020
F1MD74	Gegenfurtner 2020
F1MD77	Gegenfurtner 2020
F1MDC1	Gegenfurtner 2020
F1MDD0	Gegenfurtner 2020
F1MDD6	Gegenfurtner 2020
F1MDF2	Gegenfurtner 2020
F1MDH3	Gegenfurtner 2020
F1MDM6	Gegenfurtner 2020
F1ME02	Gegenfurtner 2020
F1ME38	Gegenfurtner 2020
F1MEA1	Gegenfurtner 2020
F1MER7	Gegenfurtner 2020
F1MF68	Gegenfurtner 2020
F1MFD1	Gegenfurtner 2020
F1MFD5	Gegenfurtner 2020
F1MFK7	Gegenfurtner 2020
F1MFY6	Gegenfurtner 2020
F1MG10	Gegenfurtner 2020
F1MG56	Gegenfurtner 2020
F1MGS8	Gegenfurtner 2020
F1MHB8	Gegenfurtner 2020
F1MHC2	Gegenfurtner 2020
F1MHJ5	Gegenfurtner 2020
F1MHM5	Gegenfurtner 2020
F1MHP6	Gegenfurtner 2020
F1MHQ5	Gegenfurtner 2020
F1MHR4	Gegenfurtner 2020
F1MHR6	Gegenfurtner 2020
F1MI18	Gegenfurtner 2020
F1MI27	Gegenfurtner 2020
F1MI39	Gegenfurtner 2020
F1MI92	Gegenfurtner 2020
F1MIC9	Gegenfurtner 2020
F1MIF2	Gegenfurtner 2020
F1MIH9	Gegenfurtner 2020
F1MIM3	Gegenfurtner 2020
F1MIQ2	Gegenfurtner 2020
F1MIY5	Gegenfurtner 2020
F1MJ49	Gegenfurtner 2020
F1MJM4	Gegenfurtner 2020
F1MJQ1	Gegenfurtner 2020
F1MK03	Gegenfurtner 2020
F1MK52	Gegenfurtner 2020
F1MK69	Gegenfurtner 2020
F1MKB7	Gegenfurtner 2020
F1MKI5	Gegenfurtner 2020
F1MKM4	Gegenfurtner 2020
F1MKS3	Gegenfurtner 2020
F1ML12	Gegenfurtner 2020
F1ML49	Gegenfurtner 2020
F1MLD8	Gegenfurtner 2020
F1MLU7	Gegenfurtner 2020
F1MLV1	Gegenfurtner 2020
F1MLW7	Gegenfurtner 2020
F1MLW8	Gegenfurtner 2020
F1MLX9	Gegenfurtner 2020
F1MM14	Gegenfurtner 2020
F1MM34	Gegenfurtner 2020
F1MM57	Gegenfurtner 2020
F1MM83	Gegenfurtner 2020
F1MMA0	Gegenfurtner 2020
F1MME1	Gegenfurtner 2020
F1MMJ6	Gegenfurtner 2020
F1MMK2	Gegenfurtner 2020
F1MMK8	Gegenfurtner 2020
F1MMR6	Gegenfurtner 2020
F1MMV6	Gegenfurtner 2020
F1MMY6	Gegenfurtner 2020
F1MN61	Gegenfurtner 2020
F1MN84	Gegenfurtner 2020
F1MN93	Gegenfurtner 2020
F1MNC0	Gegenfurtner 2020
F1MNG7	Gegenfurtner 2020
F1MNM2	Gegenfurtner 2020

F1MNS5	Gegenfurtner 2020
F1MNS8	Gegenfurtner 2020
F1MNT4	Gegenfurtner 2020
F1MP10	Gegenfurtner 2020
F1MPE1	Gegenfurtner 2020
F1MPE5	Gegenfurtner 2020
F1MPE9	Gegenfurtner 2020
F1MPJ7	Gegenfurtner 2020
F1MPJ8	Gegenfurtner 2020
F1MQ37	Gegenfurtner 2020
F1MQ57	Gegenfurtner 2020
F1MQV8	Gegenfurtner 2020
F1MR07	Gegenfurtner 2020
F1MR08	Gegenfurtner 2020
F1MRR1	Gegenfurtner 2020
F1MRS1	Gegenfurtner 2020
F1MS94	Gegenfurtner 2020
F1MSF1	Gegenfurtner 2020
F1MSI2	Gegenfurtner 2020
F1MT39	Gegenfurtner 2020
F1MTR1	Gegenfurtner 2020
F1MTY9	Gegenfurtner 2020
F1MTZ0	Gegenfurtner 2020
F1MTZ1	Gegenfurtner 2020
F1MU12	Gegenfurtner 2020
F1MU34	Gegenfurtner 2020
F1MU80	Gegenfurtner 2020
F1MU84	Gegenfurtner 2020
F1MUA7	Gegenfurtner 2020
F1MUH4	Gegenfurtner 2020
F1MUP9	Gegenfurtner 2020
F1MUR6	Gegenfurtner 2020
F1MUZ9	Gegenfurtner 2020
F1MV07	Gegenfurtner 2020
F1MV22	Gegenfurtner 2020
F1MV66	Gegenfurtner 2020
F1MV90	Gegenfurtner 2020
F1MVK1	Gegenfurtner 2020
F1MVT7	Gegenfurtner 2020
F1MW03	Gegenfurtner 2020
F1MW68	Gegenfurtner 2020
F1MWD3	Gegenfurtner 2020
F1MWN1	Gegenfurtner 2020
F1MWQ2	Gegenfurtner 2020
F1MWR3	Gegenfurtner 2020
F1MWR8	Gegenfurtner 2020
F1MWU9	Gegenfurtner 2020
F1MWY9	Gegenfurtner 2020
F1MX04	Gegenfurtner 2020
F1MX50	Gegenfurtner 2020
F1MX51	Gegenfurtner 2020
F1MX83	Gegenfurtner 2020
F1MXD4	Gegenfurtner 2020
F1MXU5	Gegenfurtner 2020
F1MXX8	Gegenfurtner 2020
F1MY28	Gegenfurtner 2020
F1MY44	Gegenfurtner 2020
F1MY62	Gegenfurtner 2020
F1MYC9	Gegenfurtner 2020
F1MYD0	Gegenfurtner 2020
F1MYH6	Gegenfurtner 2020
F1MYN0	Gegenfurtner 2020
F1MYN1	Gegenfurtner 2020
F1MYN2	Gegenfurtner 2020
F1MYQ4	Gegenfurtner 2020
F1MYV9	Gegenfurtner 2020
F1MYX5	Gegenfurtner 2020
F1MYZ4	Gegenfurtner 2020
F1MZ00	Gegenfurtner 2020
F1MZ22	Gegenfurtner 2020
F1MZ33	Gegenfurtner 2020
F1MZ40	Gegenfurtner 2020
F1MZF2	Gegenfurtner 2020
F1MZK4	Gegenfurtner 2020
F1MZL6	Gegenfurtner 2020
F1MZR1	Gegenfurtner 2020
F1MZT6	Gegenfurtner 2020
F1N076	Gegenfurtner 2020
F1N091	Gegenfurtner 2020
F1N0E5	Gegenfurtner 2020
F1N0F2	Gegenfurtner 2020
F1N0F7	Gegenfurtner 2020
F1N0H3	Gegenfurtner 2020
F1N0M0	Gegenfurtner 2020
F1N0M5	Gegenfurtner 2020
F1N0W1	Gegenfurtner 2020
F1N0Z0	Gegenfurtner 2020
F1N152	Gegenfurtner 2020
F1N169	Gegenfurtner 2020
F1N1G7	Gegenfurtner 2020

F1N1K6	Gegenfurtner 2020
F1N1R8	Gegenfurtner 2020
F1N206	Gegenfurtner 2020
F1N214	Gegenfurtner 2020
F1N226	Gegenfurtner 2020
F1N2A1	Gegenfurtner 2020
F1N2A2	Gegenfurtner 2020
F1N2B5	Gegenfurtner 2020
F1N2F1	Gegenfurtner 2020
F1N2I5	Gegenfurtner 2020
F1N2P8	Gegenfurtner 2020
F1N2W0	Gegenfurtner 2020
F1N301	Gegenfurtner 2020
F1N327	Gegenfurtner 2020
F1N371	Gegenfurtner 2020
F1N3I4	Gegenfurtner 2020
F1N3L1	Gegenfurtner 2020
F1N3P2	Gegenfurtner 2020
F1N3S4	Gegenfurtner 2020
F1N3U5	Gegenfurtner 2020
F1N3Y1	Gegenfurtner 2020
F1N430	Gegenfurtner 2020
F1N443	Gegenfurtner 2020
F1N4E4	Gegenfurtner 2020
F1N4K1	Gegenfurtner 2020
F1N4N6	Gegenfurtner 2020
F1N4V5	Gegenfurtner 2020
F1N4Y6	Gegenfurtner 2020
F1N506	Gegenfurtner 2020
F1N521	Gegenfurtner 2020
F1N5H2	Gegenfurtner 2020
F1N5K2	Gegenfurtner 2020
F1N5S6	Gegenfurtner 2020
F1N5W4	Gegenfurtner 2020
F1N605	Gegenfurtner 2020
F1N619	Gegenfurtner 2020
F1N647	Gegenfurtner 2020
F1N6H1	Gegenfurtner 2020
F1N6U4	Gegenfurtner 2020
F1N6W6	Gegenfurtner 2020
F1N6Y1	Gegenfurtner 2020
F1N6Y7	Gegenfurtner 2020
F1N789	Gegenfurtner 2020
F1N7D7	Gegenfurtner 2020
F1N7F9	Gegenfurtner 2020
F1N7H5	Gegenfurtner 2020
F1N7I5	Gegenfurtner 2020
F1N7I6	Gegenfurtner 2020
F1N7U2	Gegenfurtner 2020
F2FB38	Gegenfurtner 2020
F2FB42	Gegenfurtner 2020
F2Y8C5	Gegenfurtner 2020
F2Z4E7	Gegenfurtner 2020
F2Z4F0	Gegenfurtner 2020
F2Z4F5	Gegenfurtner 2020
F2Z4H3	Gegenfurtner 2020
F6PW02	Gegenfurtner 2020
F6Q087	Gegenfurtner 2020
F6Q0C0	Gegenfurtner 2020
F6Q234	Gegenfurtner 2020
F6QD94	Gegenfurtner 2020
F6QHN4	Gegenfurtner 2020
F6QS88	Gegenfurtner 2020
F6QVC9	Gegenfurtner 2020
F6RPT3	Gegenfurtner 2020
F6RWK1	Gegenfurtner 2020
F6S1Q0	Gegenfurtner 2020
G1K1Q2	Gegenfurtner 2020
G1K1R6	Gegenfurtner 2020
G1K208	Gegenfurtner 2020
G3MWH3	Gegenfurtner 2020
G3MWX4	Gegenfurtner 2020
G3MXC8	Gegenfurtner 2020
G3MXD1	Gegenfurtner 2020
G3MXK8	Gegenfurtner 2020
G3MXR2	Gegenfurtner 2020
G3MXZ0	Gegenfurtner 2020
G3MY03	Gegenfurtner 2020
G3MY15	Gegenfurtner 2020
G3MY19	Gegenfurtner 2020
G3MY50	Gegenfurtner 2020
G3MYE8	Gegenfurtner 2020
G3MYW7	Gegenfurtner 2020
G3MZ83	Gegenfurtner 2020
G3MZ95	Gegenfurtner 2020
G3MZC0	Gegenfurtner 2020
G3MZC1	Gegenfurtner 2020
G3MZD8	Gegenfurtner 2020
G3MZE2	Gegenfurtner 2020
G3MZG5	Gegenfurtner 2020

G3MZH0	Gegenfurtner 2020
G3MZM3	Gegenfurtner 2020
G3N0B6	Gegenfurtner 2020
G3N0I4	Gegenfurtner 2020
G3N0Q8	Gegenfurtner 2020
G3N0V0	Gegenfurtner 2020
G3N0X4	Gegenfurtner 2020
G3N0Z6	Gegenfurtner 2020
G3N1H5	Gegenfurtner 2020
G3N1Q0	Gegenfurtner 2020
G3N2F0	Gegenfurtner 2020
G3N2G7	Gegenfurtner 2020
G3N2H8	Gegenfurtner 2020
G3N2K4	Gegenfurtner 2020
G3N337	Gegenfurtner 2020
G3N3D0	Gegenfurtner 2020
G3N3N1	Gegenfurtner 2020
G3X696	Gegenfurtner 2020
G3X6B1	Gegenfurtner 2020
G3X6D7	Gegenfurtner 2020
G3X6I0	Gegenfurtner 2020
G3X6L9	Gegenfurtner 2020
G3X6N3	Gegenfurtner 2020
G3X6P5	Gegenfurtner 2020
G3X6V0	Gegenfurtner 2020
G3X6Z3	Gegenfurtner 2020
G3X745	Gegenfurtner 2020
G3X7D5	Gegenfurtner 2020
G3X807	Gegenfurtner 2020
G5E531	Gegenfurtner 2020
G5E536	Gegenfurtner 2020
G5E567	Gegenfurtner 2020
G5E5A7	Gegenfurtner 2020
G5E5C3	Gegenfurtner 2020
G5E5C8	Gegenfurtner 2020
G5E5H2	Gegenfurtner 2020
G5E5Q6	Gegenfurtner 2020
G5E5T1	Gegenfurtner 2020
G5E604	Gegenfurtner 2020
G5E631	Gegenfurtner 2020
G5E6K6	Gegenfurtner 2020
G5E6N7	Gegenfurtner 2020
G8JKV2	Gegenfurtner 2020
G8JKV5	Gegenfurtner 2020
G8JKV6	Gegenfurtner 2020
G8JKV8	Gegenfurtner 2020
G8JKW7	Gegenfurtner 2020
G8JKX6	Gegenfurtner 2020
G8JKY0	Gegenfurtner 2020
G8JKZ8	Gegenfurtner 2020
G8JL00	Gegenfurtner 2020
H6ULC6	Gegenfurtner 2020
H6V5E5	Gegenfurtner 2020
H7BWW0	Gegenfurtner 2020
H7BWW2	Gegenfurtner 2020
J7JXJ4	Gegenfurtner 2020
K4JDR8	Gegenfurtner 2020
K4JF16	Gegenfurtner 2020
K8FK38	Gegenfurtner 2020
L7R5X3	Gegenfurtner 2020
M0QVZ0	Gegenfurtner 2020
M5FI38	Gegenfurtner 2020
M5FJX5	Gegenfurtner 2020
M5FK76	Gegenfurtner 2020
M5FKI8	Gegenfurtner 2020
N0E6I4	Gegenfurtner 2020
O02675	Gegenfurtner 2020
O02691	Gegenfurtner 2020
O02703	Gegenfurtner 2020
O02717	Gegenfurtner 2020
O02741	Gegenfurtner 2020
O02751	Gegenfurtner 2020
O02853	Gegenfurtner 2020
O18739	Gegenfurtner 2020
O18789	Gegenfurtner 2020
O18836	Gegenfurtner 2020
O18883	Gegenfurtner 2020
O19094	Gegenfurtner 2020
O46415	Gegenfurtner 2020
O46500	Gegenfurtner 2020
O46721	Gegenfurtner 2020
O46738	Gegenfurtner 2020
O62652	Gegenfurtner 2020
O62830	Gegenfurtner 2020
O77834	Gegenfurtner 2020
O97764	Gegenfurtner 2020
P00126	Gegenfurtner 2020
P00376	Gegenfurtner 2020
P00429	Gegenfurtner 2020
P00432	Gegenfurtner 2020

P00435	Gegenfurtner 2020
P00442	Gegenfurtner 2020
P00515	Gegenfurtner 2020
P00517	Gegenfurtner 2020
P00586	Gegenfurtner 2020
P00829	Gegenfurtner 2020
P00921	Gegenfurtner 2020
P00974	Gegenfurtner 2020
P01035	Gegenfurtner 2020
P01251	Gegenfurtner 2020
P01252	Gegenfurtner 2020
P02253	Gegenfurtner 2020
P02633	Gegenfurtner 2020
P02702	Gegenfurtner 2020
P04272	Gegenfurtner 2020
P04467	Gegenfurtner 2020
P04975	Gegenfurtner 2020
P05059	Gegenfurtner 2020
P05786	Gegenfurtner 2020
P06504	Gegenfurtner 2020
P06623	Gegenfurtner 2020
P07107	Gegenfurtner 2020
P07688	Gegenfurtner 2020
P07857	Gegenfurtner 2020
P08037	Gegenfurtner 2020
P08166	Gegenfurtner 2020
P08728	Gegenfurtner 2020
P08760	Gegenfurtner 2020
P08814	Gegenfurtner 2020
P09487	Gegenfurtner 2020
P09867	Gegenfurtner 2020
P10096	Gegenfurtner 2020
P10103	Gegenfurtner 2020
P10462	Gegenfurtner 2020
P10575	Gegenfurtner 2020
P10790	Gegenfurtner 2020
P10881	Gegenfurtner 2020
P10948	Gegenfurtner 2020
P11017	Gegenfurtner 2020
P11023	Gegenfurtner 2020
P11116	Gegenfurtner 2020
P11179	Gegenfurtner 2020
P12234	Gegenfurtner 2020
P12344	Gegenfurtner 2020
P12378	Gegenfurtner 2020
P13135	Gegenfurtner 2020
P13213	Gegenfurtner 2020
P13214	Gegenfurtner 2020
P13619	Gegenfurtner 2020
P13696	Gegenfurtner 2020
P14568	Gegenfurtner 2020
P15103	Gegenfurtner 2020
P15246	Gegenfurtner 2020
P15696	Gegenfurtner 2020
P16116	Gegenfurtner 2020
P17248	Gegenfurtner 2020
P18203	Gegenfurtner 2020
P18493	Gegenfurtner 2020
P18902	Gegenfurtner 2020
P19120	Gegenfurtner 2020
P19427	Gegenfurtner 2020
P19483	Gegenfurtner 2020
P19660	Gegenfurtner 2020
P19661	Gegenfurtner 2020
P19803	Gegenfurtner 2020
P19858	Gegenfurtner 2020
P20000	Gegenfurtner 2020
P20004	Gegenfurtner 2020
P20072	Gegenfurtner 2020
P20414	Gegenfurtner 2020
P20456	Gegenfurtner 2020
P20821	Gegenfurtner 2020
P21282	Gegenfurtner 2020
P21793	Gegenfurtner 2020
P21856	Gegenfurtner 2020
P22226	Gegenfurtner 2020
P23004	Gegenfurtner 2020
P23727	Gegenfurtner 2020
P24591	Gegenfurtner 2020
P25326	Gegenfurtner 2020
P26452	Gegenfurtner 2020
P26779	Gegenfurtner 2020
P26882	Gegenfurtner 2020
P26884	Gegenfurtner 2020
P27214	Gegenfurtner 2020
P27595	Gegenfurtner 2020
P28782	Gegenfurtner 2020
P28783	Gegenfurtner 2020
P28801	Gegenfurtner 2020
P29702	Gegenfurtner 2020

P30922	Gegenfurtner 2020
P31404	Gegenfurtner 2020
P31408	Gegenfurtner 2020
P31754	Gegenfurtner 2020
P31976	Gegenfurtner 2020
P33046	Gegenfurtner 2020
P33097	Gegenfurtner 2020
P33672	Gegenfurtner 2020
P35466	Gegenfurtner 2020
P35604	Gegenfurtner 2020
P35605	Gegenfurtner 2020
P35705	Gegenfurtner 2020
P37980	Gegenfurtner 2020
P38657	Gegenfurtner 2020
P39872	Gegenfurtner 2020
P40673	Gegenfurtner 2020
P41500	Gegenfurtner 2020
P41541	Gegenfurtner 2020
P41976	Gegenfurtner 2020
P42899	Gegenfurtner 2020
P43033	Gegenfurtner 2020
P45478	Gegenfurtner 2020
P46162	Gegenfurtner 2020
P46164	Gegenfurtner 2020
P46193	Gegenfurtner 2020
P46195	Gegenfurtner 2020
P48034	Gegenfurtner 2020
P48427	Gegenfurtner 2020
P48616	Gegenfurtner 2020
P48644	Gegenfurtner 2020
P48734	Gegenfurtner 2020
P48818	Gegenfurtner 2020
P49410	Gegenfurtner 2020
P49951	Gegenfurtner 2020
P50291	Gegenfurtner 2020
P50397	Gegenfurtner 2020
P51122	Gegenfurtner 2020
P52174	Gegenfurtner 2020
P52193	Gegenfurtner 2020
P52556	Gegenfurtner 2020
P53619	Gegenfurtner 2020
P53620	Gegenfurtner 2020
P54149	Gegenfurtner 2020
P54228	Gegenfurtner 2020
P55052	Gegenfurtner 2020
P55859	Gegenfurtner 2020
P55918	Gegenfurtner 2020
P56425	Gegenfurtner 2020
P56658	Gegenfurtner 2020
P56701	Gegenfurtner 2020
P56830	Gegenfurtner 2020
P60661	Gegenfurtner 2020
P60712	Gegenfurtner 2020
P60984	Gegenfurtner 2020
P61085	Gegenfurtner 2020
P61157	Gegenfurtner 2020
P61223	Gegenfurtner 2020
P61284	Gegenfurtner 2020
P61286	Gegenfurtner 2020
P61287	Gegenfurtner 2020
P61356	Gegenfurtner 2020
P61585	Gegenfurtner 2020
P61603	Gegenfurtner 2020
P61955	Gegenfurtner 2020
P62157	Gegenfurtner 2020
P62194	Gegenfurtner 2020
P62248	Gegenfurtner 2020
P62261	Gegenfurtner 2020
P62276	Gegenfurtner 2020
P62326	Gegenfurtner 2020
P62739	Gegenfurtner 2020
P62833	Gegenfurtner 2020
P62871	Gegenfurtner 2020
P62935	Gegenfurtner 2020
P62958	Gegenfurtner 2020
P62992	Gegenfurtner 2020
P62998	Gegenfurtner 2020
P63009	Gegenfurtner 2020
P63103	Gegenfurtner 2020
P63243	Gegenfurtner 2020
P63258	Gegenfurtner 2020
P67808	Gegenfurtner 2020
P68002	Gegenfurtner 2020
P68102	Gegenfurtner 2020
P68103	Gegenfurtner 2020
P68252	Gegenfurtner 2020
P68399	Gegenfurtner 2020
P68432	Gegenfurtner 2020
P68509	Gegenfurtner 2020
P79103	Gegenfurtner 2020

P79105	Gegenfurtner 2020
P79126	Gegenfurtner 2020
P79134	Gegenfurtner 2020
P79135	Gegenfurtner 2020
P79136	Gegenfurtner 2020
P79251	Gegenfurtner 2020
P79345	Gegenfurtner 2020
P80109	Gegenfurtner 2020
P80177	Gegenfurtner 2020
P80189	Gegenfurtner 2020
P80227	Gegenfurtner 2020
P80311	Gegenfurtner 2020
P80513	Gegenfurtner 2020
P80724	Gegenfurtner 2020
P81265	Gegenfurtner 2020
P81287	Gegenfurtner 2020
P81425	Gegenfurtner 2020
P81623	Gegenfurtner 2020
P81947	Gegenfurtner 2020
P81948	Gegenfurtner 2020
P83107	Gegenfurtner 2020
P84080	Gegenfurtner 2020
P84227	Gegenfurtner 2020
P85100	Gegenfurtner 2020
Q04467	Gegenfurtner 2020
Q05718	Gegenfurtner 2020
Q05B85	Gegenfurtner 2020
Q05B89	Gegenfurtner 2020
Q05FF2	Gegenfurtner 2020
Q05KI5	Gegenfurtner 2020
Q06285	Gegenfurtner 2020
Q07130	Gegenfurtner 2020
Q08DA1	Gegenfurtner 2020
Q08DB4	Gegenfurtner 2020
Q08DD1	Gegenfurtner 2020
Q08DD6	Gegenfurtner 2020
Q08DI3	Gegenfurtner 2020
Q08DM8	Gegenfurtner 2020
Q08DP0	Gegenfurtner 2020
Q08DQ4	Gegenfurtner 2020
Q08DQ6	Gegenfurtner 2020
Q08DR7	Gegenfurtner 2020
Q08DU0	Gegenfurtner 2020
Q08DU4	Gegenfurtner 2020
Q08DU9	Gegenfurtner 2020
Q08DV2	Gegenfurtner 2020
Q08DW2	Gegenfurtner 2020
Q08E18	Gegenfurtner 2020
Q08E20	Gegenfurtner 2020
Q08E32	Gegenfurtner 2020
Q08E38	Gegenfurtner 2020
Q08E52	Gegenfurtner 2020
Q08E58	Gegenfurtner 2020
Q09430	Gegenfurtner 2020
Q0II26	Gegenfurtner 2020
Q0II43	Gegenfurtner 2020
Q0II59	Gegenfurtner 2020
Q0IIA4	Gegenfurtner 2020
Q0IIF7	Gegenfurtner 2020
Q0IIG8	Gegenfurtner 2020
Q0IIH7	Gegenfurtner 2020
Q0III3	Gegenfurtner 2020
Q0III8	Gegenfurtner 2020
Q0IIJ0	Gegenfurtner 2020
Q0IIJ8	Gegenfurtner 2020
Q0IIK5	Gegenfurtner 2020
Q0IIL6	Gegenfurtner 2020
Q0IIM3	Gegenfurtner 2020
Q0P568	Gegenfurtner 2020
Q0P569	Gegenfurtner 2020
Q0P570	Gegenfurtner 2020
Q0P597	Gegenfurtner 2020
Q0P5A1	Gegenfurtner 2020
Q0P5A6	Gegenfurtner 2020
Q0P5D6	Gegenfurtner 2020
Q0P5F2	Gegenfurtner 2020
Q0P5F6	Gegenfurtner 2020
Q0P5G4	Gegenfurtner 2020
Q0P5I7	Gegenfurtner 2020
Q0P5K3	Gegenfurtner 2020
Q0P5N1	Gegenfurtner 2020
Q0PW28	Gegenfurtner 2020
Q0QEV5	Gegenfurtner 2020
Q0QF04	Gegenfurtner 2020
Q0V7N1	Gegenfurtner 2020
Q0V8B6	Gegenfurtner 2020
Q0V8D5	Gegenfurtner 2020
Q0V8F1	Gegenfurtner 2020
Q0V8L5	Gegenfurtner 2020
Q0V8N4	Gegenfurtner 2020

Q0V8P6	Gegenfurtner 2020
Q0V8R6	Gegenfurtner 2020
Q0VBZ9	Gegenfurtner 2020
Q0VC08	Gegenfurtner 2020
Q0VC36	Gegenfurtner 2020
Q0VC37	Gegenfurtner 2020
Q0VC64	Gegenfurtner 2020
Q0VC88	Gegenfurtner 2020
Q0VCC0	Gegenfurtner 2020
Q0VCE1	Gegenfurtner 2020
Q0VCH9	Gegenfurtner 2020
Q0VCI7	Gegenfurtner 2020
Q0VCK0	Gegenfurtner 2020
Q0VCK2	Gegenfurtner 2020
Q0VCK5	Gegenfurtner 2020
Q0VCL3	Gegenfurtner 2020
Q0VCM4	Gegenfurtner 2020
Q0VCN1	Gegenfurtner 2020
Q0VCP4	Gegenfurtner 2020
Q0VCQ6	Gegenfurtner 2020
Q0VCS3	Gegenfurtner 2020
Q0VCU1	Gegenfurtner 2020
Q0VCW4	Gegenfurtner 2020
Q0VCX2	Gegenfurtner 2020
Q0VCX4	Gegenfurtner 2020
Q0VCX5	Gegenfurtner 2020
Q0VCY7	Gegenfurtner 2020
Q0VCY8	Gegenfurtner 2020
Q0VD18	Gegenfurtner 2020
Q0VD19	Gegenfurtner 2020
Q0VD27	Gegenfurtner 2020
Q0VD48	Gegenfurtner 2020
Q0VD53	Gegenfurtner 2020
Q0VFX8	Gegenfurtner 2020
Q148C4	Gegenfurtner 2020
Q148C9	Gegenfurtner 2020
Q148D3	Gegenfurtner 2020
Q148G9	Gegenfurtner 2020
Q148I4	Gegenfurtner 2020
Q148I9	Gegenfurtner 2020
Q148J4	Gegenfurtner 2020
Q148J6	Gegenfurtner 2020
Q148J7	Gegenfurtner 2020
Q148N0	Gegenfurtner 2020
Q148N1	Gegenfurtner 2020
Q17Q89	Gegenfurtner 2020
Q17QB3	Gegenfurtner 2020
Q17QC0	Gegenfurtner 2020
Q17QC7	Gegenfurtner 2020
Q17QG2	Gegenfurtner 2020
Q17QI3	Gegenfurtner 2020
Q17QK8	Gegenfurtner 2020
Q17QN6	Gegenfurtner 2020
Q17QP9	Gegenfurtner 2020
Q17QQ2	Gegenfurtner 2020
Q17QX0	Gegenfurtner 2020
Q17R07	Gegenfurtner 2020
Q17R18	Gegenfurtner 2020
Q1ECT2	Gegenfurtner 2020
Q1JP79	Gegenfurtner 2020
Q1JP95	Gegenfurtner 2020
Q1JPA2	Gegenfurtner 2020
Q1JPB0	Gegenfurtner 2020
Q1JPD0	Gegenfurtner 2020
Q1JPJ2	Gegenfurtner 2020
Q1JQA7	Gegenfurtner 2020
Q1JQB2	Gegenfurtner 2020
Q1JQD0	Gegenfurtner 2020
Q1JQD2	Gegenfurtner 2020
Q1JQD4	Gegenfurtner 2020
Q1LZ72	Gegenfurtner 2020
Q1LZ74	Gegenfurtner 2020
Q1LZ81	Gegenfurtner 2020
Q1LZ90	Gegenfurtner 2020
Q1LZ95	Gegenfurtner 2020
Q1LZB6	Gegenfurtner 2020
Q1LZD9	Gegenfurtner 2020
Q1LZH8	Gegenfurtner 2020
Q1LZH9	Gegenfurtner 2020
Q1RMH0	Gegenfurtner 2020
Q1RMI2	Gegenfurtner 2020
Q1RMJ6	Gegenfurtner 2020
Q1RML6	Gegenfurtner 2020
Q1RMM2	Gegenfurtner 2020
Q1RMM9	Gegenfurtner 2020
Q1RMN0	Gegenfurtner 2020
Q1RMP3	Gegenfurtner 2020
Q1RMR3	Gegenfurtner 2020
Q1RMR8	Gegenfurtner 2020
Q1RMR9	Gegenfurtner 2020

Q1RMX7	Gegenfurtner 2020
Q1ZYR0	Gegenfurtner 2020
Q24JY1	Gegenfurtner 2020
Q24JZ7	Gegenfurtner 2020
Q24JZ8	Gegenfurtner 2020
Q24K02	Gegenfurtner 2020
Q24K03	Gegenfurtner 2020
Q24K04	Gegenfurtner 2020
Q24K11	Gegenfurtner 2020
Q24K13	Gegenfurtner 2020
Q27954	Gegenfurtner 2020
Q27970	Gegenfurtner 2020
Q29RM3	Gegenfurtner 2020
Q29RP4	Gegenfurtner 2020
Q29RQ2	Gegenfurtner 2020
Q29RT7	Gegenfurtner 2020
Q29RU4	Gegenfurtner 2020
Q29RV1	Gegenfurtner 2020
Q29RY9	Gegenfurtner 2020
Q29RZ0	Gegenfurtner 2020
Q29S11	Gegenfurtner 2020
Q29S21	Gegenfurtner 2020
Q2F6J9	Gegenfurtner 2020
Q2HJ26	Gegenfurtner 2020
Q2HJ28	Gegenfurtner 2020
Q2HJ33	Gegenfurtner 2020
Q2HJ49	Gegenfurtner 2020
Q2HJ54	Gegenfurtner 2020
Q2HJ57	Gegenfurtner 2020
Q2HJ58	Gegenfurtner 2020

Q27971	Gegenfurtner 2020
Q27975	Gegenfurtner 2020
Q28017	Gegenfurtner 2020
Q28034	Gegenfurtner 2020
Q28042	Gegenfurtner 2020
Q28046	Gegenfurtner 2020
Q28104	Gegenfurtner 2020
Q28141	Gegenfurtner 2020
Q28193	Gegenfurtner 2020
Q28201	Gegenfurtner 2020
Q28824	Gegenfurtner 2020
Q28869	Gegenfurtner 2020
Q2HJ60	Gegenfurtner 2020
Q2HJ65	Gegenfurtner 2020
Q2HJ73	Gegenfurtner 2020
Q2HJ74	Gegenfurtner 2020
Q2HJ86	Gegenfurtner 2020
Q2HJ97	Gegenfurtner 2020
Q2HJD7	Gegenfurtner 2020
Q2HJE4	Gegenfurtner 2020
Q2HJG2	Gegenfurtner 2020
Q2HJG5	Gegenfurtner 2020
Q2HJH0	Gegenfurtner 2020
Q2HJH1	Gegenfurtner 2020
Q2HJH3	Gegenfurtner 2020
Q2HJH9	Gegenfurtner 2020
Q2HJI6	Gegenfurtner 2020
Q2HJI9	Gegenfurtner 2020
Q2KHU0	Gegenfurtner 2020
Q2KHU8	Gegenfurtner 2020

Q28908	Gegenfurtner 2020
Q28910	Gegenfurtner 2020
Q29437	Gegenfurtner 2020
Q29448	Gegenfurtner 2020
Q29451	Gegenfurtner 2020
Q29460	Gegenfurtner 2020
Q29RI6	Gegenfurtner 2020
Q29RK1	Gegenfurtner 2020
Q29RK4	Gegenfurtner 2020
Q29RL2	Gegenfurtner 2020
Q2KHX6	Gegenfurtner 2020
Q2KHZ6	Gegenfurtner 2020
Q2KHZ8	Gegenfurtner 2020
Q2KI07	Gegenfurtner 2020
Q2KI42	Gegenfurtner 2020
Q2KI56	Gegenfurtner 2020
Q2KI59	Gegenfurtner 2020
Q2KI84	Gegenfurtner 2020
Q2KI86	Gegenfurtner 2020
Q2KIA2	Gegenfurtner 2020
Q2KIA5	Gegenfurtner 2020
Q2KIB0	Gegenfurtner 2020
Q2KIC5	Gegenfurtner 2020
Q2KIC7	Gegenfurtner 2020
Q2KII4	Gegenfurtner 2020
Q2KII9	Gegenfurtner 2020
Q2KIK0	Gegenfurtner 2020
Q2KIM0	Gegenfurtner 2020

Q2KIN5	Gegenfurtner 2020
Q2KIQ1	Gegenfurtner 2020
Q2KIT5	Gegenfurtner 2020
Q2KIT8	Gegenfurtner 2020
Q2KIV7	Gegenfurtner 2020
Q2KIV8	Gegenfurtner 2020
Q2KIW9	Gegenfurtner 2020
Q2KIX7	Gegenfurtner 2020
Q2KIY7	Gegenfurtner 2020
Q2KJ23	Gegenfurtner 2020
Q2KJ25	Gegenfurtner 2020
Q2KJ32	Gegenfurtner 2020
Q2KJ44	Gegenfurtner 2020
Q2KJ46	Gegenfurtner 2020
Q2KJ77	Gegenfurtner 2020
Q2KJ86	Gegenfurtner 2020
Q2KJ93	Gegenfurtner 2020
Q2KJ97	Gegenfurtner 2020
Q2KJA3	Gegenfurtner 2020
Q2KJC5	Gegenfurtner 2020
Q2KJD0	Gegenfurtner 2020
Q2KJE7	Gegenfurtner 2020
Q2KJG2	Gegenfurtner 2020
Q2KJG3	Gegenfurtner 2020
Q2KJH4	Gegenfurtner 2020
Q2KJH6	Gegenfurtner 2020
Q2KJH9	Gegenfurtner 2020
Q2KJJ7	Gegenfurtner 2020
Q2LGB2	Gegenfurtner 2020
Q2LGB5	Gegenfurtner 2020
Q2LGB8	Gegenfurtner 2020
Q2NKU1	Gegenfurtner 2020
Q2NKU4	Gegenfurtner 2020
Q2NKU6	Gegenfurtner 2020
Q2NKY7	Gegenfurtner 2020
Q2NL09	Gegenfurtner 2020
Q2NL22	Gegenfurtner 2020
Q2NL29	Gegenfurtner 2020
Q2NL31	Gegenfurtner 2020
Q2NL37	Gegenfurtner 2020
Q2NL38	Gegenfurtner 2020
Q2PS14	Gegenfurtner 2020
Q2T9L8	Gegenfurtner 2020
Q2T9M8	Gegenfurtner 2020
Q2T9P4	Gegenfurtner 2020
Q2T9R6	Gegenfurtner 2020
Q2T9S4	Gegenfurtner 2020
Q2T9Y6	Gegenfurtner 2020
Q2TA04	Gegenfurtner 2020
Q2TA23	Gegenfurtner 2020
Q2TA40	Gegenfurtner 2020
Q2TA49	Gegenfurtner 2020
Q2TBG2	Gegenfurtner 2020
Q2TBG8	Gegenfurtner 2020
Q2TBL2	Gegenfurtner 2020
Q2TBN1	Gegenfurtner 2020
Q2TBN5	Gegenfurtner 2020
Q2TBP0	Gegenfurtner 2020
Q2TBP7	Gegenfurtner 2020
Q2TBQ5	Gegenfurtner 2020
Q2TBR0	Gegenfurtner 2020
Q2TBU0	Gegenfurtner 2020
Q2TBU5	Gegenfurtner 2020
Q2TBU9	Gegenfurtner 2020
Q2TBV3	Gegenfurtner 2020
Q2TBW0	Gegenfurtner 2020
Q2TBW7	Gegenfurtner 2020
Q2TBX1	Gegenfurtner 2020
Q2TBX2	Gegenfurtner 2020
Q2TBX6	Gegenfurtner 2020
Q2WFX3	Gegenfurtner 2020
Q2YDE7	Gegenfurtner 2020
Q2YDE9	Gegenfurtner 2020
Q32KL2	Gegenfurtner 2020
Q32KP9	Gegenfurtner 2020
Q32KW2	Gegenfurtner 2020
Q32KX0	Gegenfurtner 2020
Q32L21	Gegenfurtner 2020
Q32L63	Gegenfurtner 2020
Q32L92	Gegenfurtner 2020
Q32L99	Gegenfurtner 2020
Q32LC7	Gegenfurtner 2020
Q32LE4	Gegenfurtner 2020
Q32LE5	Gegenfurtner 2020
Q32LE9	Gegenfurtner 2020
Q32LG3	Gegenfurtner 2020
Q32LJ9	Gegenfurtner 2020
Q32LM2	Gegenfurtner 2020
Q32LN7	Gegenfurtner 2020
Q32LP2	Gegenfurtner 2020

Q32P66	Gegenfurtner 2020
Q32PA1	Gegenfurtner 2020
Q32PA4	Gegenfurtner 2020
Q32PA5	Gegenfurtner 2020
Q32PA9	Gegenfurtner 2020
Q32PB0	Gegenfurtner 2020
Q32PB8	Gegenfurtner 2020
Q32PB9	Gegenfurtner 2020
Q32PD5	Gegenfurtner 2020
Q32PD7	Gegenfurtner 2020
Q32PE9	Gegenfurtner 2020
Q32PF2	Gegenfurtner 2020
Q32PF3	Gegenfurtner 2020
Q32PG1	Gegenfurtner 2020
Q32PI5	Gegenfurtner 2020
Q32PJ6	Gegenfurtner 2020
Q32PJ9	Gegenfurtner 2020
Q32S29	Gegenfurtner 2020
Q32S38	Gegenfurtner 2020
Q3B7M5	Gegenfurtner 2020
Q3B7M9	Gegenfurtner 2020
Q3B7N2	Gegenfurtner 2020
Q3B7N3	Gegenfurtner 2020
Q3MHE4	Gegenfurtner 2020
Q3MHF7	Gegenfurtner 2020
Q3MHG3	Gegenfurtner 2020
Q3MHH4	Gegenfurtner 2020
Q3MHK9	Gegenfurtner 2020
Q3MHL3	Gegenfurtner 2020
Q3MHL4	Gegenfurtner 2020
Q3MHL7	Gegenfurtner 2020
Q3MHM5	Gegenfurtner 2020
Q3MHM7	Gegenfurtner 2020
Q3MHN0	Gegenfurtner 2020
Q3MHP2	Gegenfurtner 2020
Q3MHP3	Gegenfurtner 2020
Q3MHP6	Gegenfurtner 2020
Q3MHQ6	Gegenfurtner 2020
Q3MHR0	Gegenfurtner 2020
Q3MHR3	Gegenfurtner 2020
Q3MHR7	Gegenfurtner 2020
Q3MHX5	Gegenfurtner 2020
Q3MHY1	Gegenfurtner 2020
Q3MHZ3	Gegenfurtner 2020
Q3MI02	Gegenfurtner 2020
Q3MI05	Gegenfurtner 2020
Q3SWW9	Gegenfurtner 2020
Q3SWY3	Gegenfurtner 2020
Q3SWZ6	Gegenfurtner 2020
Q3SX14	Gegenfurtner 2020
Q3SX24	Gegenfurtner 2020
Q3SX30	Gegenfurtner 2020
Q3SX32	Gegenfurtner 2020
Q3SX33	Gegenfurtner 2020
Q3SX44	Gegenfurtner 2020
Q3SX47	Gegenfurtner 2020
Q3SYR8	Gegenfurtner 2020
Q3SYT7	Gegenfurtner 2020
Q3SYT9	Gegenfurtner 2020
Q3SYU2	Gegenfurtner 2020
Q3SYU6	Gegenfurtner 2020
Q3SYU9	Gegenfurtner 2020
Q3SYV4	Gegenfurtner 2020
Q3SYV6	Gegenfurtner 2020
Q3SYW1	Gegenfurtner 2020
Q3SYW2	Gegenfurtner 2020
Q3SYW6	Gegenfurtner 2020
Q3SYX0	Gegenfurtner 2020
Q3SYZ4	Gegenfurtner 2020
Q3SZ15	Gegenfurtner 2020
Q3SZ16	Gegenfurtner 2020
Q3SZ18	Gegenfurtner 2020
Q3SZ19	Gegenfurtner 2020
Q3SZ32	Gegenfurtner 2020
Q3SZ43	Gegenfurtner 2020
Q3SZ52	Gegenfurtner 2020
Q3SZ54	Gegenfurtner 2020
Q3SZ62	Gegenfurtner 2020
Q3SZ65	Gegenfurtner 2020
Q3SZ71	Gegenfurtner 2020
Q3SZ73	Gegenfurtner 2020
Q3SZ76	Gegenfurtner 2020
Q3SZ94	Gegenfurtner 2020
Q3SZ96	Gegenfurtner 2020
Q3SZA0	Gegenfurtner 2020
Q3SZA6	Gegenfurtner 2020
Q3SZB7	Gegenfurtner 2020
Q3SZC0	Gegenfurtner 2020
Q3SZC1	Gegenfurtner 2020
Q3SZC2	Gegenfurtner 2020

Q3SZC4	Gegenfurtner 2020
Q3SZC6	Gegenfurtner 2020
Q3SZD7	Gegenfurtner 2020
Q3SZE2	Gegenfurtner 2020
Q3SZE9	Gegenfurtner 2020
Q3SZF2	Gegenfurtner 2020
Q3SZH7	Gegenfurtner 2020
Q3SZI2	Gegenfurtner 2020
Q3SZI4	Gegenfurtner 2020
Q3SZI8	Gegenfurtner 2020
Q3SZJ0	Gegenfurtner 2020
Q3SZJ7	Gegenfurtner 2020
Q3SZJ9	Gegenfurtner 2020
Q3SZK8	Gegenfurtner 2020
Q3SZM9	Gegenfurtner 2020
Q3SZN2	Gegenfurtner 2020
Q3SZN8	Gegenfurtner 2020
Q3SZP5	Gegenfurtner 2020
Q3SZQ6	Gegenfurtner 2020
Q3SZR8	Gegenfurtner 2020
Q3SZT2	Gegenfurtner 2020
Q3SZV7	Gegenfurtner 2020
Q3SZZ9	Gegenfurtner 2020
Q3T000	Gegenfurtner 2020
Q3T002	Gegenfurtner 2020
Q3T010	Gegenfurtner 2020
Q3T030	Gegenfurtner 2020
Q3T035	Gegenfurtner 2020
Q3T054	Gegenfurtner 2020
Q3T087	Gegenfurtner 2020

Q3T090	Gegenfurtner 2020
Q3T094	Gegenfurtner 2020
Q3T0A9	Gegenfurtner 2020
Q3T0B2	Gegenfurtner 2020
Q3T0B6	Gegenfurtner 2020
Q3T0D0	Gegenfurtner 2020
Q3T0D5	Gegenfurtner 2020
Q3T0E0	Gegenfurtner 2020
Q3T0E7	Gegenfurtner 2020
Q3T0F4	Gegenfurtner 2020
Q3T0F7	Gegenfurtner 2020
Q3T0F9	Gegenfurtner 2020
Q3T0G3	Gegenfurtner 2020
Q3T0G5	Gegenfurtner 2020
Q3T0I2	Gegenfurtner 2020
Q3T0I4	Gegenfurtner 2020
Q3T0J2	Gegenfurtner 2020
Q3T0K2	Gegenfurtner 2020
Q3T0L2	Gegenfurtner 2020
Q3T0L5	Gegenfurtner 2020
Q3T0L7	Gegenfurtner 2020
Q3T0M7	Gegenfurtner 2020
Q3T0P5	Gegenfurtner 2020
Q3T0P6	Gegenfurtner 2020
Q3T0Q4	Gegenfurtner 2020
Q3T0Q6	Gegenfurtner 2020
Q3T0R7	Gegenfurtner 2020
Q3T0S6	Gegenfurtner 2020
Q3T0S7	Gegenfurtner 2020
Q3T0T5	Gegenfurtner 2020

Q3T0U1	Gegenfurtner 2020
Q3T0U3	Gegenfurtner 2020
Q3T0V2	Gegenfurtner 2020
Q3T0V3	Gegenfurtner 2020
Q3T0V4	Gegenfurtner 2020
Q3T0V7	Gegenfurtner 2020
Q3T0W3	Gegenfurtner 2020
Q3T0W4	Gegenfurtner 2020
Q3T0W9	Gegenfurtner 2020
Q3T0X5	Gegenfurtner 2020
Q3T0X6	Gegenfurtner 2020
Q3T0Y1	Gegenfurtner 2020
Q3T0Y5	Gegenfurtner 2020
Q3T0Z0	Gegenfurtner 2020
Q3T0Z7	Gegenfurtner 2020
Q3T0Z8	Gegenfurtner 2020
Q3T101	Gegenfurtner 2020
Q3T102	Gegenfurtner 2020
Q3T105	Gegenfurtner 2020
Q3T108	Gegenfurtner 2020
Q3T112	Gegenfurtner 2020
Q3T114	Gegenfurtner 2020
Q3T122	Gegenfurtner 2020
Q3T140	Gegenfurtner 2020
Q3T145	Gegenfurtner 2020
Q3T147	Gegenfurtner 2020
Q3T148	Gegenfurtner 2020
Q3T149	Gegenfurtner 2020
Q3T165	Gegenfurtner 2020
Q3T168	Gegenfurtner 2020

Q3T169	Gegenfurtner 2020
Q3T171	Gegenfurtner 2020
Q3YFG6	Gegenfurtner 2020
Q3YJH2	Gegenfurtner 2020
Q3ZBD1	Gegenfurtner 2020
Q3ZBD9	Gegenfurtner 2020
Q3ZBE2	Gegenfurtner 2020
Q3ZBF7	Gegenfurtner 2020
Q3ZBG1	Gegenfurtner 2020
Q3ZBG9	Gegenfurtner 2020
Q3ZBH0	Gegenfurtner 2020
Q3ZBH2	Gegenfurtner 2020
Q3ZBH5	Gegenfurtner 2020
Q3ZBH8	Gegenfurtner 2020
Q3ZBH9	Gegenfurtner 2020
Q3ZBK2	Gegenfurtner 2020
Q3ZBL1	Gegenfurtner 2020
Q3ZBM5	Gegenfurtner 2020
Q3ZBN0	Gegenfurtner 2020
Q3ZBS8	Gegenfurtner 2020
Q3ZBT1	Gegenfurtner 2020
Q3ZBU7	Gegenfurtner 2020
Q3ZBV3	Gegenfurtner 2020
Q3ZBV8	Gegenfurtner 2020
Q3ZBV9	Gegenfurtner 2020
Q3ZBW4	Gegenfurtner 2020
Q3ZBX5	Gegenfurtner 2020
Q3ZBX9	Gegenfurtner 2020
Q3ZBY4	Gegenfurtner 2020
Q3ZBY8	Gegenfurtner 2020
Q3ZBZ8	Gegenfurtner 2020
Q3ZC07	Gegenfurtner 2020
Q3ZC09	Gegenfurtner 2020
Q3ZC10	Gegenfurtner 2020
Q3ZC12	Gegenfurtner 2020
Q3ZC13	Gegenfurtner 2020
Q3ZC20	Gegenfurtner 2020
Q3ZC41	Gegenfurtner 2020
Q3ZC42	Gegenfurtner 2020
Q3ZC44	Gegenfurtner 2020
Q3ZC64	Gegenfurtner 2020
Q3ZC79	Gegenfurtner 2020
Q3ZC84	Gegenfurtner 2020
Q3ZC89	Gegenfurtner 2020
Q3ZC91	Gegenfurtner 2020
Q3ZCA2	Gegenfurtner 2020
Q3ZCA7	Gegenfurtner 2020
Q3ZCC8	Gegenfurtner 2020
Q3ZCC9	Gegenfurtner 2020
Q3ZCD3	Gegenfurtner 2020
Q3ZCE0	Gegenfurtner 2020
Q3ZCE2	Gegenfurtner 2020
Q3ZCE8	Gegenfurtner 2020
Q3ZCF0	Gegenfurtner 2020
Q3ZCF3	Gegenfurtner 2020
Q3ZCF7	Gegenfurtner 2020
Q3ZCH0	Gegenfurtner 2020
Q3ZCH5	Gegenfurtner 2020
Q3ZCH9	Gegenfurtner 2020
Q3ZCI0	Gegenfurtner 2020
Q3ZCI4	Gegenfurtner 2020
Q3ZCI9	Gegenfurtner 2020
Q3ZCJ2	Gegenfurtner 2020
Q3ZCJ7	Gegenfurtner 2020
Q3ZCK1	Gegenfurtner 2020
Q3ZCK3	Gegenfurtner 2020
Q3ZCK9	Gegenfurtner 2020
Q3ZCL8	Gegenfurtner 2020
Q45VK8	Gegenfurtner 2020
Q4ZJS0	Gegenfurtner 2020
Q52UL2	Gegenfurtner 2020
Q56J78	Gegenfurtner 2020
Q56JU9	Gegenfurtner 2020
Q56JV1	Gegenfurtner 2020
Q56JV6	Gegenfurtner 2020
Q56JV9	Gegenfurtner 2020
Q56JW4	Gegenfurtner 2020
Q56JX3	Gegenfurtner 2020
Q56JX6	Gegenfurtner 2020
Q56JX8	Gegenfurtner 2020
Q56JY8	Gegenfurtner 2020
Q56JZ1	Gegenfurtner 2020
Q56JZ5	Gegenfurtner 2020
Q56K11	Gegenfurtner 2020
Q56K14	Gegenfurtner 2020
Q58CQ2	Gegenfurtner 2020
Q58CQ9	Gegenfurtner 2020
Q58CW7	Gegenfurtner 2020
Q58CX0	Gegenfurtner 2020
Q58CX1	Gegenfurtner 2020

Q58D08	Gegenfurtner 2020
Q58D10	Gegenfurtner 2020
Q58D31	Gegenfurtner 2020
Q58D55	Gegenfurtner 2020
Q58D70	Gegenfurtner 2020
Q58DC0	Gegenfurtner 2020
Q58DG1	Gegenfurtner 2020
Q58DI2	Gegenfurtner 2020
Q58DK4	Gegenfurtner 2020
Q58DK5	Gegenfurtner 2020
Q58DL4	Gegenfurtner 2020
Q58DM9	Gegenfurtner 2020
Q58DN4	Gegenfurtner 2020
Q58DQ0	Gegenfurtner 2020
Q58DQ3	Gegenfurtner 2020
Q58DR1	Gegenfurtner 2020
Q58DR7	Gegenfurtner 2020
Q58DR8	Gegenfurtner 2020
Q58DS9	Gegenfurtner 2020
Q58DU5	Gegenfurtner 2020
Q58DW0	Gegenfurtner 2020
Q58DW2	Gegenfurtner 2020
Q58DW5	Gegenfurtner 2020
Q58DW6	Gegenfurtner 2020
Q59A32	Gegenfurtner 2020
Q59HJ6	Gegenfurtner 2020
Q5BIN5	Gegenfurtner 2020
Q5BIP4	Gegenfurtner 2020
Q5DPW9	Gegenfurtner 2020
Q5E938	Gegenfurtner 2020
Q5E946	Gegenfurtner 2020
Q5E947	Gegenfurtner 2020
Q5E949	Gegenfurtner 2020
Q5E951	Gegenfurtner 2020
Q5E953	Gegenfurtner 2020
Q5E956	Gegenfurtner 2020
Q5E959	Gegenfurtner 2020
Q5E962	Gegenfurtner 2020
Q5E963	Gegenfurtner 2020
Q5E966	Gegenfurtner 2020
Q5E970	Gegenfurtner 2020
Q5E983	Gegenfurtner 2020
Q5E984	Gegenfurtner 2020
Q5E987	Gegenfurtner 2020
Q5E988	Gegenfurtner 2020
Q5E992	Gegenfurtner 2020
Q5E995	Gegenfurtner 2020
Q5E997	Gegenfurtner 2020
Q5E998	Gegenfurtner 2020
Q5E9A1	Gegenfurtner 2020
Q5E9A3	Gegenfurtner 2020
Q5E9A6	Gegenfurtner 2020
Q5E9B1	Gegenfurtner 2020
Q5E9B7	Gegenfurtner 2020
Q5E9C0	Gegenfurtner 2020
Q5E9D0	Gegenfurtner 2020
Q5E9D1	Gegenfurtner 2020
Q5E9D5	Gegenfurtner 2020
Q5E9D7	Gegenfurtner 2020
Q5E9E6	Gegenfurtner 2020
Q5E9F2	Gegenfurtner 2020
Q5E9F5	Gegenfurtner 2020
Q5E9F7	Gegenfurtner 2020
Q5E9F8	Gegenfurtner 2020
Q5E9F9	Gegenfurtner 2020
Q5E9G3	Gegenfurtner 2020
Q5E9I7	Gegenfurtner 2020
Q5E9J1	Gegenfurtner 2020
Q5E9K0	Gegenfurtner 2020
Q5E9Q4	Gegenfurtner 2020
Q5E9R3	Gegenfurtner 2020
Q5E9T4	Gegenfurtner 2020
Q5E9T9	Gegenfurtner 2020
Q5E9X4	Gegenfurtner 2020
Q5EA01	Gegenfurtner 2020
Q5EA50	Gegenfurtner 2020
Q5EA61	Gegenfurtner 2020
Q5EA62	Gegenfurtner 2020
Q5EA75	Gegenfurtner 2020
Q5EA79	Gegenfurtner 2020
Q5EA80	Gegenfurtner 2020
Q5EAC2	Gegenfurtner 2020
Q5EAC6	Gegenfurtner 2020
Q5EAC7	Gegenfurtner 2020
Q5EAD0	Gegenfurtner 2020
Q5EAD2	Gegenfurtner 2020
Q5EBY8	Gegenfurtner 2020
Q5GF34	Gegenfurtner 2020
Q5KR47	Gegenfurtner 2020
Q5KR49	Gegenfurtner 2020

Q5U7H2	Gegenfurtner 2020
Q5W5H1	Gegenfurtner 2020
Q5W5U3	Gegenfurtner 2020
Q645M6	Gegenfurtner 2020
Q6B411	Gegenfurtner 2020
Q6B855	Gegenfurtner 2020
Q6EWQ7	Gegenfurtner 2020
Q6H320	Gegenfurtner 2020
Q6IE76	Gegenfurtner 2020
Q6PTA0	Gegenfurtner 2020
Q6PZ03	Gegenfurtner 2020
Q6QRN6	Gegenfurtner 2020
Q6QRN7	Gegenfurtner 2020
Q6WQW9	Gegenfurtner 2020
Q6Y1E2	Gegenfurtner 2020
Q762I5	Gegenfurtner 2020
Q76I81	Gegenfurtner 2020
Q76I82	Gegenfurtner 2020
Q76LV1	Gegenfurtner 2020
Q76LV2	Gegenfurtner 2020
Q7M2Y2	Gegenfurtner 2020
Q7M365	Gegenfurtner 2020
Q7YRQ8	Gegenfurtner 2020
Q861U5	Gegenfurtner 2020
Q862B7	Gegenfurtner 2020
Q862B8	Gegenfurtner 2020
Q862I1	Gegenfurtner 2020
Q862J3	Gegenfurtner 2020
Q862K6	Gegenfurtner 2020
Q862K7	Gegenfurtner 2020
Q862M6	Gegenfurtner 2020
Q862N4	Gegenfurtner 2020
Q862Q3	Gegenfurtner 2020
Q862R3	Gegenfurtner 2020
Q863B3	Gegenfurtner 2020
Q863C3	Gegenfurtner 2020
Q864S1	Gegenfurtner 2020
Q865V6	Gegenfurtner 2020
Q8HXM1	Gegenfurtner 2020
Q8HYI9	Gegenfurtner 2020
Q8HYX0	Gegenfurtner 2020
Q8MII0	Gegenfurtner 2020
Q8MJ29	Gegenfurtner 2020
Q8MJ50	Gegenfurtner 2020
Q8MJJ7	Gegenfurtner 2020
Q8MKB7	Gegenfurtner 2020
Q8MKE3	Gegenfurtner 2020
Q8SPF8	Gegenfurtner 2020
Q8SPJ1	Gegenfurtner 2020
Q8SPP7	Gegenfurtner 2020
Q8SPU8	Gegenfurtner 2020
Q8SPX7	Gegenfurtner 2020
Q8SQ21	Gegenfurtner 2020
Q8SQB5	Gegenfurtner 2020
Q8SQG8	Gegenfurtner 2020
Q8SQH5	Gegenfurtner 2020
Q8WML4	Gegenfurtner 2020
Q8WMP9	Gegenfurtner 2020
Q8WMQ6	Gegenfurtner 2020
Q8WMV3	Gegenfurtner 2020
Q8WMY2	Gegenfurtner 2020
Q8WN55	Gegenfurtner 2020
Q92176	Gegenfurtner 2020
Q95135	Gegenfurtner 2020
Q95140	Gegenfurtner 2020
Q95KZ6	Gegenfurtner 2020
Q95L54	Gegenfurtner 2020
Q95M12	Gegenfurtner 2020
Q95M18	Gegenfurtner 2020
Q95M40	Gegenfurtner 2020
Q9BEA3	Gegenfurtner 2020
Q9BEG5	Gegenfurtner 2020
Q9BGI1	Gegenfurtner 2020
Q9BGI2	Gegenfurtner 2020
Q9BGI3	Gegenfurtner 2020
Q9BGU1	Gegenfurtner 2020
Q9GKI7	Gegenfurtner 2020
Q9GL30	Gegenfurtner 2020
Q9GL63	Gegenfurtner 2020
Q9GLC9	Gegenfurtner 2020
Q9GLE5	Gegenfurtner 2020
Q9GMB8	Gegenfurtner 2020
Q9MYM4	Gegenfurtner 2020
Q9MZ08	Gegenfurtner 2020
Q9N0E7	Gegenfurtner 2020
Q9N0T1	Gegenfurtner 2020
Q9N0T5	Gegenfurtner 2020
Q9N0X7	Gegenfurtner 2020
Q9TR36	Gegenfurtner 2020
Q9TRK0	Gegenfurtner 2020

Q9TRY0	Gegenfurtner 2020
Q9TS70	Gegenfurtner 2020
Q9TS85	Gegenfurtner 2020
Q9TTG6	Gegenfurtner 2020
Q9TTJ5	Gegenfurtner 2020
Q9TTK8	Gegenfurtner 2020
Q9TTS3	Gegenfurtner 2020
Q9TTW1	Gegenfurtner 2020
Q9TU03	Gegenfurtner 2020
Q9TU25	Gegenfurtner 2020
Q9TU47	Gegenfurtner 2020
Q9XSA7	Gegenfurtner 2020
Q9XSI3	Gegenfurtner 2020
Q9XSJ4	Gegenfurtner 2020
Q9XT56	Gegenfurtner 2020
V6F7P3	Gegenfurtner 2020
V6F7S3	Gegenfurtner 2020
V6F7X8	Gegenfurtner 2020
V6F953	Gegenfurtner 2020
V6F957	Gegenfurtner 2020
V6F9A3	Gegenfurtner 2020
Z4YHD9	Gegenfurtner 2020
A0A0A0MP88	Harlow 2015
A0A0A0MP89	Harlow 2015
A0A0N4STN0	Harlow 2015
A0A140T832	Harlow 2015
A0A140T841	Harlow 2015
A0A140T842	Harlow 2015
A0A140T846	Harlow 2015
A0A140T850	Harlow 2015
A0A140T853	Harlow 2015
A0A140T856	Harlow 2015
A0A140T860	Harlow 2015
A0A140T861	Harlow 2015
A0A140T862	Harlow 2015
A0A140T866	Harlow 2015
A0A140T867	Harlow 2015
A0A140T869	Harlow 2015
A0A140T871	Harlow 2015
A0A140T872	Harlow 2015
A0A140T881	Harlow 2015
A0A140T886	Harlow 2015
A0A140T887	Harlow 2015
A0A140T891	Harlow 2015
A0A140T892	Harlow 2015
A0A140T894	Harlow 2015
A0A140T897	Harlow 2015
A0A140T899	Harlow 2015
A0A140T8A1	Harlow 2015
A0A140T8A4	Harlow 2015
A0A140T8A5	Harlow 2015
A0A140T8A9	Harlow 2015
A0A140T8B1	Harlow 2015
A0A140T8C4	Harlow 2015
A0A140T8C6	Harlow 2015
A0A140T8D4	Harlow 2015
A0A3Q1LF34	Harlow 2015
A0A3Q1LF77	Harlow 2015
A0A3Q1LF87	Harlow 2015
A0A3Q1LFC5	Harlow 2015
A0A3Q1LFG8	Harlow 2015
A0A3Q1LFQ5	Harlow 2015
A0A3Q1LG04	Harlow 2015
A0A3Q1LGA6	Harlow 2015
A0A3Q1LGC4	Harlow 2015
A0A3Q1LGH8	Harlow 2015
A0A3Q1LGJ2	Harlow 2015
A0A3Q1LGM4	Harlow 2015
A0A3Q1LGS4	Harlow 2015
A0A3Q1LGS8	Harlow 2015
A0A3Q1LGY1	Harlow 2015
A0A3Q1LH48	Harlow 2015
A0A3Q1LH52	Harlow 2015
A0A3Q1LHA3	Harlow 2015
A0A3Q1LHB1	Harlow 2015
A0A3Q1LHD8	Harlow 2015
A0A3Q1LHE1	Harlow 2015
A0A3Q1LHM2	Harlow 2015
A0A3Q1LHR9	Harlow 2015
A0A3Q1LHX4	Harlow 2015
A0A3Q1LHZ0	Harlow 2015
A0A3Q1LI18	Harlow 2015
A0A3Q1LI39	Harlow 2015
A0A3Q1LI40	Harlow 2015
A0A3Q1LI46	Harlow 2015
A0A3Q1LI72	Harlow 2015
A0A3Q1LI93	Harlow 2015
A0A3Q1LIB4	Harlow 2015
A0A3Q1LIG1	Harlow 2015
A0A3Q1LIG8	Harlow 2015

A0A3Q1LIJ0	Harlow 2015
A0A3Q1LIQ9	Harlow 2015
A0A3Q1LIR5	Harlow 2015
A0A3Q1LIW2	Harlow 2015
A0A3Q1LIW3	Harlow 2015
A0A3Q1LIX4	Harlow 2015
A0A3Q1LIY9	Harlow 2015
A0A3Q1LJ52	Harlow 2015
A0A3Q1LJ64	Harlow 2015
A0A3Q1LJ93	Harlow 2015
A0A3Q1LJA4	Harlow 2015
A0A3Q1LJG6	Harlow 2015
A0A3Q1LJK1	Harlow 2015
A0A3Q1LJL3	Harlow 2015
A0A3Q1LJL4	Harlow 2015
A0A3Q1LJL6	Harlow 2015
A0A3Q1LJP5	Harlow 2015
A0A3Q1LJT3	Harlow 2015
A0A3Q1LJU0	Harlow 2015
A0A3Q1LJU5	Harlow 2015
A0A3Q1LJW6	Harlow 2015
A0A3Q1LK04	Harlow 2015
A0A3Q1LK06	Harlow 2015
A0A3Q1LK49	Harlow 2015
A0A3Q1LK61	Harlow 2015
A0A3Q1LK80	Harlow 2015
A0A3Q1LK90	Harlow 2015
A0A3Q1LKA4	Harlow 2015
A0A3Q1LKB0	Harlow 2015
A0A3Q1LKE5	Harlow 2015
A0A3Q1LKF1	Harlow 2015
A0A3Q1LKL2	Harlow 2015
A0A3Q1LKL3	Harlow 2015
A0A3Q1LKR8	Harlow 2015
A0A3Q1LKS3	Harlow 2015
A0A3Q1LKV8	Harlow 2015
A0A3Q1LL01	Harlow 2015
A0A3Q1LL06	Harlow 2015
A0A3Q1LL63	Harlow 2015
A0A3Q1LL67	Harlow 2015
A0A3Q1LL74	Harlow 2015
A0A3Q1LL86	Harlow 2015
A0A3Q1LLB2	Harlow 2015
A0A3Q1LLD4	Harlow 2015
A0A3Q1LLF1	Harlow 2015
A0A3Q1LLF2	Harlow 2015
A0A3Q1LLH4	Harlow 2015
A0A3Q1LLL1	Harlow 2015
A0A3Q1LLM4	Harlow 2015
A0A3Q1LLN4	Harlow 2015
A0A3Q1LLS1	Harlow 2015
A0A3Q1LLV8	Harlow 2015
A0A3Q1LLZ3	Harlow 2015
A0A3Q1LM31	Harlow 2015
A0A3Q1LM32	Harlow 2015
A0A3Q1LM43	Harlow 2015
A0A3Q1LM46	Harlow 2015
A0A3Q1LM63	Harlow 2015
A0A3Q1LMA3	Harlow 2015
A0A3Q1LMB5	Harlow 2015
A0A3Q1LMC1	Harlow 2015
A0A3Q1LMG1	Harlow 2015
A0A3Q1LMG9	Harlow 2015
A0A3Q1LMJ1	Harlow 2015
A0A3Q1LMJ5	Harlow 2015
A0A3Q1LMK8	Harlow 2015
A0A3Q1LML6	Harlow 2015
A0A3Q1LMM6	Harlow 2015
A0A3Q1LMP2	Harlow 2015
A0A3Q1LMP7	Harlow 2015
A0A3Q1LMQ9	Harlow 2015
A0A3Q1LMS5	Harlow 2015
A0A3Q1LMU9	Harlow 2015
A0A3Q1LMV3	Harlow 2015
A0A3Q1LMX0	Harlow 2015
A0A3Q1LN12	Harlow 2015
A0A3Q1LN22	Harlow 2015
A0A3Q1LN44	Harlow 2015
A0A3Q1LN63	Harlow 2015
A0A3Q1LN74	Harlow 2015
A0A3Q1LN78	Harlow 2015
A0A3Q1LN79	Harlow 2015
A0A3Q1LN81	Harlow 2015
A0A3Q1LNB7	Harlow 2015
A0A3Q1LNC8	Harlow 2015
A0A3Q1LNE7	Harlow 2015
A0A3Q1LNE9	Harlow 2015
A0A3Q1LNF7	Harlow 2015
A0A3Q1LNG7	Harlow 2015
A0A3Q1LNH8	Harlow 2015

A0A3Q1LNI1	Harlow 2015
A0A3Q1LNM0	Harlow 2015
A0A3Q1LNN7	Harlow 2015
A0A3Q1LNT7	Harlow 2015
A0A3Q1LNW7	Harlow 2015
A0A3Q1LNY5	Harlow 2015
A0A3Q1LNZ3	Harlow 2015
A0A3Q1LNZ7	Harlow 2015
A0A3Q1LP28	Harlow 2015
A0A3Q1LP76	Harlow 2015
A0A3Q1LP83	Harlow 2015
A0A3Q1LPB5	Harlow 2015
A0A3Q1LPB6	Harlow 2015
A0A3Q1LPC8	Harlow 2015
A0A3Q1LPE3	Harlow 2015
A0A3Q1LPF0	Harlow 2015
A0A3Q1LPF4	Harlow 2015
A0A3Q1LPH9	Harlow 2015
A0A3Q1LPK1	Harlow 2015
A0A3Q1LPL0	Harlow 2015
A0A3Q1LPN6	Harlow 2015
A0A3Q1LPP7	Harlow 2015
A0A3Q1LPQ0	Harlow 2015
A0A3Q1LPS9	Harlow 2015
A0A3Q1LPT1	Harlow 2015
A0A3Q1LPX4	Harlow 2015
A0A3Q1LPX6	Harlow 2015
A0A3Q1LPY4	Harlow 2015
A0A3Q1LPZ4	Harlow 2015
A0A3Q1LPZ8	Harlow 2015

A0A3Q1LQ01	Harlow 2015
A0A3Q1LQ34	Harlow 2015
A0A3Q1LQ36	Harlow 2015
A0A3Q1LQ51	Harlow 2015
A0A3Q1LQ76	Harlow 2015
A0A3Q1LQ81	Harlow 2015
A0A3Q1LQ85	Harlow 2015
A0A3Q1LQ87	Harlow 2015
A0A3Q1LQ97	Harlow 2015
A0A3Q1LQ98	Harlow 2015
A0A3Q1LQB6	Harlow 2015
A0A3Q1LQB9	Harlow 2015
A0A3Q1LQC4	Harlow 2015
A0A3Q1LQE2	Harlow 2015
A0A3Q1LQF0	Harlow 2015
A0A3Q1LQG2	Harlow 2015
A0A3Q1LQG8	Harlow 2015
A0A3Q1LQH0	Harlow 2015
A0A3Q1LQI0	Harlow 2015
A0A3Q1LQI3	Harlow 2015
A0A3Q1LQI5	Harlow 2015
A0A3Q1LQK2	Harlow 2015
A0A3Q1LQM4	Harlow 2015
A0A3Q1LQQ5	Harlow 2015
A0A3Q1LQS3	Harlow 2015
A0A3Q1LQT4	Harlow 2015
A0A3Q1LQU4	Harlow 2015
A0A3Q1LQV8	Harlow 2015
A0A3Q1LQX9	Harlow 2015
A0A3Q1LQY9	Harlow 2015

A0A3Q1LR19	Harlow 2015
A0A3Q1LR60	Harlow 2015
A0A3Q1LR62	Harlow 2015
A0A3Q1LR88	Harlow 2015
A0A3Q1LR93	Harlow 2015
A0A3Q1LRA9	Harlow 2015
A0A3Q1LRD1	Harlow 2015
A0A3Q1LRD6	Harlow 2015
A0A3Q1LRG2	Harlow 2015
A0A3Q1LRN7	Harlow 2015
A0A3Q1LRP4	Harlow 2015
A0A3Q1LRQ5	Harlow 2015
A0A3Q1LRR7	Harlow 2015
A0A3Q1LRW8	Harlow 2015
A0A3Q1LRX5	Harlow 2015
A0A3Q1LRY6	Harlow 2015
A0A3Q1LRZ2	Harlow 2015
A0A3Q1LRZ4	Harlow 2015
A0A3Q1LRZ7	Harlow 2015
A0A3Q1LS09	Harlow 2015
A0A3Q1LS46	Harlow 2015
A0A3Q1LS55	Harlow 2015
A0A3Q1LS67	Harlow 2015
A0A3Q1LSA9	Harlow 2015
A0A3Q1LSB2	Harlow 2015
A0A3Q1LSB6	Harlow 2015
A0A3Q1LSE5	Harlow 2015
A0A3Q1LSF9	Harlow 2015
A0A3Q1LSG3	Harlow 2015
A0A3Q1LSJ0	Harlow 2015

A0A3Q1LSJ7	Harlow 2015
A0A3Q1LSK2	Harlow 2015
A0A3Q1LSL4	Harlow 2015
A0A3Q1LSM9	Harlow 2015
A0A3Q1LSN0	Harlow 2015
A0A3Q1LSN6	Harlow 2015
A0A3Q1LSP2	Harlow 2015
A0A3Q1LSQ6	Harlow 2015
A0A3Q1LSS3	Harlow 2015
A0A3Q1LSW9	Harlow 2015
A0A3Q1LSZ3	Harlow 2015
A0A3Q1LSZ6	Harlow 2015
A0A3Q1LT30	Harlow 2015
A0A3Q1LT32	Harlow 2015
A0A3Q1LT48	Harlow 2015
A0A3Q1LT49	Harlow 2015
A0A3Q1LT59	Harlow 2015
A0A3Q1LTA0	Harlow 2015
A0A3Q1LTA2	Harlow 2015
A0A3Q1LTA7	Harlow 2015
A0A3Q1LTB0	Harlow 2015
A0A3Q1LTF1	Harlow 2015
A0A3Q1LTF4	Harlow 2015
A0A3Q1LTG0	Harlow 2015
A0A3Q1LTK9	Harlow 2015
A0A3Q1LTP0	Harlow 2015
A0A3Q1LTP5	Harlow 2015
A0A3Q1LTP9	Harlow 2015
A0A3Q1LTS2	Harlow 2015
A0A3Q1LTT0	Harlow 2015
A0A3Q1LTT1	Harlow 2015
A0A3Q1LTT9	Harlow 2015
A0A3Q1LTX7	Harlow 2015
A0A3Q1LTY7	Harlow 2015
A0A3Q1LTZ5	Harlow 2015
A0A3Q1LTZ6	Harlow 2015
A0A3Q1LU13	Harlow 2015
A0A3Q1LU21	Harlow 2015
A0A3Q1LU31	Harlow 2015
A0A3Q1LU64	Harlow 2015
A0A3Q1LU71	Harlow 2015
A0A3Q1LU77	Harlow 2015
A0A3Q1LU83	Harlow 2015
A0A3Q1LU90	Harlow 2015
A0A3Q1LU91	Harlow 2015
A0A3Q1LU97	Harlow 2015
A0A3Q1LU98	Harlow 2015
A0A3Q1LUA4	Harlow 2015
A0A3Q1LUB7	Harlow 2015
A0A3Q1LUC8	Harlow 2015
A0A3Q1LUE5	Harlow 2015
A0A3Q1LUF1	Harlow 2015
A0A3Q1LUF4	Harlow 2015
A0A3Q1LUG2	Harlow 2015
A0A3Q1LUG5	Harlow 2015
A0A3Q1LUJ8	Harlow 2015
A0A3Q1LUK7	Harlow 2015
A0A3Q1LUM6	Harlow 2015
A0A3Q1LUM9	Harlow 2015
A0A3Q1LUN2	Harlow 2015
A0A3Q1LUN4	Harlow 2015
A0A3Q1LUN6	Harlow 2015
A0A3Q1LUP0	Harlow 2015
A0A3Q1LUP8	Harlow 2015
A0A3Q1LUQ4	Harlow 2015
A0A3Q1LUR2	Harlow 2015
A0A3Q1LUR4	Harlow 2015
A0A3Q1LUS2	Harlow 2015
A0A3Q1LUT2	Harlow 2015
A0A3Q1LUU1	Harlow 2015
A0A3Q1LUU2	Harlow 2015
A0A3Q1LUW4	Harlow 2015
A0A3Q1LUY6	Harlow 2015
A0A3Q1LUZ1	Harlow 2015
A0A3Q1LUZ7	Harlow 2015
A0A3Q1LV18	Harlow 2015
A0A3Q1LV21	Harlow 2015
A0A3Q1LV32	Harlow 2015
A0A3Q1LV36	Harlow 2015
A0A3Q1LV39	Harlow 2015
A0A3Q1LV44	Harlow 2015
A0A3Q1LV72	Harlow 2015
A0A3Q1LV94	Harlow 2015
A0A3Q1LVA2	Harlow 2015
A0A3Q1LVA4	Harlow 2015
A0A3Q1LVA8	Harlow 2015
A0A3Q1LVA9	Harlow 2015
A0A3Q1LVC7	Harlow 2015
A0A3Q1LVC8	Harlow 2015
A0A3Q1LVD0	Harlow 2015

A0A3Q1LVE7	Harlow 2015
A0A3Q1LVF9	Harlow 2015
A0A3Q1LVG3	Harlow 2015
A0A3Q1LVH9	Harlow 2015
A0A3Q1LVI5	Harlow 2015
A0A3Q1LVJ8	Harlow 2015
A0A3Q1LVL2	Harlow 2015
A0A3Q1LVM5	Harlow 2015
A0A3Q1LVS2	Harlow 2015
A0A3Q1LVS3	Harlow 2015
A0A3Q1LVT9	Harlow 2015
A0A3Q1LVU1	Harlow 2015
A0A3Q1LVV7	Harlow 2015
A0A3Q1LVW2	Harlow 2015
A0A3Q1LVX4	Harlow 2015
A0A3Q1LVY5	Harlow 2015
A0A3Q1LVY9	Harlow 2015
A0A3Q1LW01	Harlow 2015
A0A3Q1LW10	Harlow 2015
A0A3Q1LW11	Harlow 2015
A0A3Q1LW23	Harlow 2015
A0A3Q1LW25	Harlow 2015
A0A3Q1LW27	Harlow 2015
A0A3Q1LW66	Harlow 2015
A0A3Q1LW69	Harlow 2015
A0A3Q1LW78	Harlow 2015
A0A3Q1LW79	Harlow 2015
A0A3Q1LW84	Harlow 2015
A0A3Q1LW91	Harlow 2015
A0A3Q1LW96	Harlow 2015

A0A3Q1LWB9	Harlow 2015
A0A3Q1LWC1	Harlow 2015
A0A3Q1LWF7	Harlow 2015
A0A3Q1LWG4	Harlow 2015
A0A3Q1LWG5	Harlow 2015
A0A3Q1LWI0	Harlow 2015
A0A3Q1LWK7	Harlow 2015
A0A3Q1LWL5	Harlow 2015
A0A3Q1LWL6	Harlow 2015
A0A3Q1LWL8	Harlow 2015
A0A3Q1LWN4	Harlow 2015
A0A3Q1LWU2	Harlow 2015
A0A3Q1LWU8	Harlow 2015
A0A3Q1LWY0	Harlow 2015
A0A3Q1LWZ4	Harlow 2015
A0A3Q1LX10	Harlow 2015
A0A3Q1LX34	Harlow 2015
A0A3Q1LX66	Harlow 2015
A0A3Q1LX89	Harlow 2015
A0A3Q1LXA1	Harlow 2015
A0A3Q1LXA8	Harlow 2015
A0A3Q1LXB1	Harlow 2015
A0A3Q1LXG3	Harlow 2015
A0A3Q1LXH1	Harlow 2015
A0A3Q1LXK9	Harlow 2015
A0A3Q1LXR9	Harlow 2015
A0A3Q1LXS8	Harlow 2015
A0A3Q1LXT8	Harlow 2015
A0A3Q1LXU9	Harlow 2015
A0A3Q1LXW9	Harlow 2015

A0A3Q1LXX0	Harlow 2015
A0A3Q1LXX9	Harlow 2015
A0A3Q1LXY5	Harlow 2015
A0A3Q1LY00	Harlow 2015
A0A3Q1LY05	Harlow 2015
A0A3Q1LY08	Harlow 2015
A0A3Q1LY09	Harlow 2015
A0A3Q1LY20	Harlow 2015
A0A3Q1LY56	Harlow 2015
A0A3Q1LY87	Harlow 2015
A0A3Q1LYA7	Harlow 2015
A0A3Q1LYE7	Harlow 2015
A0A3Q1LYH2	Harlow 2015
A0A3Q1LYH7	Harlow 2015
A0A3Q1LYI5	Harlow 2015
A0A3Q1LYI6	Harlow 2015
A0A3Q1LYJ9	Harlow 2015
A0A3Q1LYS7	Harlow 2015
A0A3Q1LYS8	Harlow 2015
A0A3Q1LYU3	Harlow 2015
A0A3Q1LZ07	Harlow 2015
A0A3Q1LZ09	Harlow 2015
A0A3Q1LZ10	Harlow 2015
A0A3Q1LZ18	Harlow 2015
A0A3Q1LZ24	Harlow 2015
A0A3Q1LZ25	Harlow 2015
A0A3Q1LZ29	Harlow 2015
A0A3Q1LZ31	Harlow 2015
A0A3Q1LZ47	Harlow 2015
A0A3Q1LZ53	Harlow 2015

A0A3Q1LZ54	Harlow 2015
A0A3Q1LZ55	Harlow 2015
A0A3Q1LZ83	Harlow 2015
A0A3Q1LZ84	Harlow 2015
A0A3Q1LZB8	Harlow 2015
A0A3Q1LZC9	Harlow 2015
A0A3Q1LZD7	Harlow 2015
A0A3Q1LZD9	Harlow 2015
A0A3Q1LZF5	Harlow 2015
A0A3Q1LZG6	Harlow 2015
A0A3Q1LZJ2	Harlow 2015
A0A3Q1LZN8	Harlow 2015
A0A3Q1LZP7	Harlow 2015
A0A3Q1LZQ5	Harlow 2015
A0A3Q1LZS5	Harlow 2015
A0A3Q1LZT9	Harlow 2015
A0A3Q1LZU8	Harlow 2015
A0A3Q1LZZ0	Harlow 2015
A0A3Q1M010	Harlow 2015
A0A3Q1M013	Harlow 2015
A0A3Q1M023	Harlow 2015
A0A3Q1M026	Harlow 2015
A0A3Q1M028	Harlow 2015
A0A3Q1M037	Harlow 2015
A0A3Q1M057	Harlow 2015
A0A3Q1M079	Harlow 2015
A0A3Q1M083	Harlow 2015
A0A3Q1M0C0	Harlow 2015
A0A3Q1M0C2	Harlow 2015
A0A3Q1M0D3	Harlow 2015

A0A3Q1M0D7	Harlow 2015
A0A3Q1M0F0	Harlow 2015
A0A3Q1M0G3	Harlow 2015
A0A3Q1M0G8	Harlow 2015
A0A3Q1M0H5	Harlow 2015
A0A3Q1M0H8	Harlow 2015
A0A3Q1M0K2	Harlow 2015
A0A3Q1M0L3	Harlow 2015
A0A3Q1M0R9	Harlow 2015
A0A3Q1M0T4	Harlow 2015
A0A3Q1M0U9	Harlow 2015
A0A3Q1M0V1	Harlow 2015
A0A3Q1M0V8	Harlow 2015
A0A3Q1M0Y7	Harlow 2015
A0A3Q1M119	Harlow 2015
A0A3Q1M124	Harlow 2015
A0A3Q1M143	Harlow 2015
A0A3Q1M165	Harlow 2015
A0A3Q1M168	Harlow 2015
A0A3Q1M193	Harlow 2015
A0A3Q1M1A9	Harlow 2015
A0A3Q1M1B1	Harlow 2015
A0A3Q1M1B2	Harlow 2015
A0A3Q1M1D3	Harlow 2015
A0A3Q1M1D5	Harlow 2015
A0A3Q1M1I0	Harlow 2015
A0A3Q1M1I6	Harlow 2015
A0A3Q1M1K1	Harlow 2015
A0A3Q1M1L4	Harlow 2015
A0A3Q1M1M5	Harlow 2015

A0A3Q1M1M7	Harlow 2015
A0A3Q1M1N7	Harlow 2015
A0A3Q1M1Q2	Harlow 2015
A0A3Q1M1Q3	Harlow 2015
A0A3Q1M1U2	Harlow 2015
A0A3Q1M1W9	Harlow 2015
A0A3Q1M1X0	Harlow 2015
A0A3Q1M1X1	Harlow 2015
A0A3Q1M1X4	Harlow 2015
A0A3Q1M1Z2	Harlow 2015
A0A3Q1M208	Harlow 2015
A0A3Q1M241	Harlow 2015
A0A3Q1M251	Harlow 2015
A0A3Q1M273	Harlow 2015
A0A3Q1M278	Harlow 2015
A0A3Q1M299	Harlow 2015
A0A3Q1M2A1	Harlow 2015
A0A3Q1M2A8	Harlow 2015
A0A3Q1M2B2	Harlow 2015
A0A3Q1M2B7	Harlow 2015
A0A3Q1M2D1	Harlow 2015
A0A3Q1M2E2	Harlow 2015
A0A3Q1M2E4	Harlow 2015
A0A3Q1M2F0	Harlow 2015
A0A3Q1M2H2	Harlow 2015
A0A3Q1M2H4	Harlow 2015
A0A3Q1M2I1	Harlow 2015
A0A3Q1M2I8	Harlow 2015
A0A3Q1M2J3	Harlow 2015
A0A3Q1M2L8	Harlow 2015

A0A3Q1M2M4	Harlow 2015
A0A3Q1M2P3	Harlow 2015
A0A3Q1M2P8	Harlow 2015
A0A3Q1M2P9	Harlow 2015
A0A3Q1M2U3	Harlow 2015
A0A3Q1M2U9	Harlow 2015
A0A3Q1M2W0	Harlow 2015
A0A3Q1M2Y4	Harlow 2015
A0A3Q1M2Z7	Harlow 2015
A0A3Q1M300	Harlow 2015
A0A3Q1M318	Harlow 2015
A0A3Q1M320	Harlow 2015
A0A3Q1M326	Harlow 2015
A0A3Q1M338	Harlow 2015
A0A3Q1M352	Harlow 2015
A0A3Q1M3B1	Harlow 2015
A0A3Q1M3F1	Harlow 2015
A0A3Q1M3I3	Harlow 2015
A0A3Q1M3I6	Harlow 2015
A0A3Q1M3K7	Harlow 2015
A0A3Q1M3N0	Harlow 2015
A0A3Q1M3N4	Harlow 2015
A0A3Q1M3Q7	Harlow 2015
A0A3Q1M3S4	Harlow 2015
A0A3Q1M3W4	Harlow 2015
A0A3Q1M3X9	Harlow 2015
A0A3Q1M3Y3	Harlow 2015
A0A3Q1M3Z5	Harlow 2015
A0A3Q1M3Z8	Harlow 2015
A0A3Q1M471	Harlow 2015

A0A3Q1M478	Harlow 2015
A0A3Q1M481	Harlow 2015
A0A3Q1M489	Harlow 2015
A0A3Q1M4B5	Harlow 2015
A0A3Q1M4D8	Harlow 2015
A0A3Q1M4E5	Harlow 2015
A0A3Q1M4E9	Harlow 2015
A0A3Q1M4F5	Harlow 2015
A0A3Q1M4I4	Harlow 2015
A0A3Q1M4K6	Harlow 2015
A0A3Q1M4M4	Harlow 2015
A0A3Q1M4T2	Harlow 2015
A0A3Q1M4X0	Harlow 2015
A0A3Q1M4Z2	Harlow 2015
A0A3Q1M517	Harlow 2015
A0A3Q1M524	Harlow 2015
A0A3Q1M529	Harlow 2015
A0A3Q1M537	Harlow 2015
A0A3Q1M558	Harlow 2015
A0A3Q1M5A0	Harlow 2015
A0A3Q1M5B4	Harlow 2015
A0A3Q1M5F6	Harlow 2015
A0A3Q1M5M9	Harlow 2015
A0A3Q1M5N3	Harlow 2015
A0A3Q1M5Q1	Harlow 2015
A0A3Q1M5Q7	Harlow 2015
A0A3Q1M5R4	Harlow 2015
A0A3Q1M5T0	Harlow 2015
A0A3Q1M5U2	Harlow 2015
A0A3Q1M5U9	Harlow 2015

A0A3Q1M5V8	Harlow 2015
A0A3Q1M5Y3	Harlow 2015
A0A3Q1M5Z8	Harlow 2015
A0A3Q1M633	Harlow 2015
A0A3Q1M656	Harlow 2015
A0A3Q1M657	Harlow 2015
A0A3Q1M671	Harlow 2015
A0A3Q1M698	Harlow 2015
A0A3Q1M6A2	Harlow 2015
A0A3Q1M6D9	Harlow 2015
A0A3Q1M6F0	Harlow 2015
A0A3Q1M6G4	Harlow 2015
A0A3Q1M6H3	Harlow 2015
A0A3Q1M6I5	Harlow 2015
A0A3Q1M6K2	Harlow 2015
A0A3Q1M6K6	Harlow 2015
A0A3Q1M6N3	Harlow 2015
A0A3Q1M6N7	Harlow 2015
A0A3Q1M6P7	Harlow 2015
A0A3Q1M6Q7	Harlow 2015
A0A3Q1M6R8	Harlow 2015
A0A3Q1M6S0	Harlow 2015
A0A3Q1M6S3	Harlow 2015
A0A3Q1M6T5	Harlow 2015
A0A3Q1M6V0	Harlow 2015
A0A3Q1M6V4	Harlow 2015
A0A3Q1M6X6	Harlow 2015
A0A3Q1M6X7	Harlow 2015
A0A3Q1M712	Harlow 2015
A0A3Q1M720	Harlow 2015

A0A3Q1M722	Harlow 2015
A0A3Q1M739	Harlow 2015
A0A3Q1M762	Harlow 2015
A0A3Q1M769	Harlow 2015
A0A3Q1M799	Harlow 2015
A0A3Q1M7B5	Harlow 2015
A0A3Q1M7H7	Harlow 2015
A0A3Q1M7J1	Harlow 2015
A0A3Q1M7J2	Harlow 2015
A0A3Q1M7M0	Harlow 2015
A0A3Q1M7Q5	Harlow 2015
A0A3Q1M7R4	Harlow 2015
A0A3Q1M7S5	Harlow 2015
A0A3Q1M7U0	Harlow 2015
A0A3Q1M7W0	Harlow 2015
A0A3Q1M7W5	Harlow 2015
A0A3Q1M7W9	Harlow 2015
A0A3Q1M7Y8	Harlow 2015
A0A3Q1M808	Harlow 2015
A0A3Q1M849	Harlow 2015
A0A3Q1M875	Harlow 2015
A0A3Q1M8B0	Harlow 2015
A0A3Q1M8B4	Harlow 2015
A0A3Q1M8D9	Harlow 2015
A0A3Q1M8H8	Harlow 2015
A0A3Q1M8H9	Harlow 2015
A0A3Q1M8I0	Harlow 2015
A0A3Q1M8I4	Harlow 2015
A0A3Q1M8I6	Harlow 2015
A0A3Q1M8J9	Harlow 2015
A0A3Q1M8K4	Harlow 2015
A0A3Q1M8L3	Harlow 2015
A0A3Q1M8L6	Harlow 2015
A0A3Q1M8S2	Harlow 2015
A0A3Q1M8V6	Harlow 2015
A0A3Q1M8Y4	Harlow 2015
A0A3Q1M909	Harlow 2015
A0A3Q1M913	Harlow 2015
A0A3Q1M917	Harlow 2015
A0A3Q1M922	Harlow 2015
A0A3Q1M930	Harlow 2015
A0A3Q1M952	Harlow 2015
A0A3Q1M978	Harlow 2015
A0A3Q1M993	Harlow 2015
A0A3Q1M994	Harlow 2015
A0A3Q1M9B3	Harlow 2015
A0A3Q1M9B5	Harlow 2015
A0A3Q1M9D2	Harlow 2015
A0A3Q1M9D9	Harlow 2015
A0A3Q1M9I5	Harlow 2015
A0A3Q1M9I9	Harlow 2015
A0A3Q1M9J2	Harlow 2015
A0A3Q1M9K4	Harlow 2015
A0A3Q1M9M0	Harlow 2015
A0A3Q1M9M6	Harlow 2015
A0A3Q1M9P3	Harlow 2015
A0A3Q1M9P9	Harlow 2015
A0A3Q1M9Q2	Harlow 2015
A0A3Q1M9V2	Harlow 2015
A0A3Q1M9W1	Harlow 2015
A0A3Q1M9W2	Harlow 2015
A0A3Q1M9W4	Harlow 2015
A0A3Q1MA03	Harlow 2015
A0A3Q1MA07	Harlow 2015
A0A3Q1MA31	Harlow 2015
A0A3Q1MA46	Harlow 2015
A0A3Q1MA60	Harlow 2015
A0A3Q1MA81	Harlow 2015
A0A3Q1MAA6	Harlow 2015
A0A3Q1MAB7	Harlow 2015
A0A3Q1MAG5	Harlow 2015
A0A3Q1MAI4	Harlow 2015
A0A3Q1MAJ0	Harlow 2015
A0A3Q1MAJ8	Harlow 2015
A0A3Q1MAL1	Harlow 2015
A0A3Q1MAM8	Harlow 2015
A0A3Q1MAQ1	Harlow 2015
A0A3Q1MAQ6	Harlow 2015
A0A3Q1MAQ8	Harlow 2015
A0A3Q1MAS2	Harlow 2015
A0A3Q1MAS9	Harlow 2015
A0A3Q1MAT9	Harlow 2015
A0A3Q1MAU7	Harlow 2015
A0A3Q1MAU9	Harlow 2015
A0A3Q1MB09	Harlow 2015
A0A3Q1MB35	Harlow 2015
A0A3Q1MB37	Harlow 2015
A0A3Q1MB39	Harlow 2015
A0A3Q1MB48	Harlow 2015
A0A3Q1MB56	Harlow 2015

A0A3Q1MB68	Harlow 2015
A0A3Q1MB98	Harlow 2015
A0A3Q1MB99	Harlow 2015
A0A3Q1MBD4	Harlow 2015
A0A3Q1MBJ7	Harlow 2015
A0A3Q1MBJ9	Harlow 2015
A0A3Q1MBM9	Harlow 2015
A0A3Q1MBN7	Harlow 2015
A0A3Q1MBP1	Harlow 2015
A0A3Q1MBP4	Harlow 2015
A0A3Q1MBQ7	Harlow 2015
A0A3Q1MBS5	Harlow 2015
A0A3Q1MBS7	Harlow 2015
A0A3Q1MBW4	Harlow 2015
A0A3Q1MBW7	Harlow 2015
A0A3Q1MBX5	Harlow 2015
A0A3Q1MBY6	Harlow 2015
A0A3Q1MC76	Harlow 2015
A0A3Q1MC90	Harlow 2015
A0A3Q1MCA4	Harlow 2015
A0A3Q1MCB6	Harlow 2015
A0A3Q1MCC2	Harlow 2015
A0A3Q1MCE0	Harlow 2015
A0A3Q1MCE5	Harlow 2015
A0A3Q1MCE8	Harlow 2015
A0A3Q1MCF4	Harlow 2015
A0A3Q1MCH3	Harlow 2015
A0A3Q1MCH6	Harlow 2015
A0A3Q1MCT2	Harlow 2015
A0A3Q1MCU7	Harlow 2015
A0A3Q1MCV5	Harlow 2015
A0A3Q1MCX0	Harlow 2015
A0A3Q1MD01	Harlow 2015
A0A3Q1MD28	Harlow 2015
A0A3Q1MD85	Harlow 2015
A0A3Q1MD87	Harlow 2015
A0A3Q1MDA4	Harlow 2015
A0A3Q1MDA5	Harlow 2015
A0A3Q1MDB1	Harlow 2015
A0A3Q1MDD4	Harlow 2015
A0A3Q1MDG7	Harlow 2015
A0A3Q1MDH5	Harlow 2015
A0A3Q1MDI3	Harlow 2015
A0A3Q1MDJ3	Harlow 2015
A0A3Q1MDL1	Harlow 2015
A0A3Q1MDM5	Harlow 2015
A0A3Q1MDR0	Harlow 2015
A0A3Q1MDR4	Harlow 2015
A0A3Q1MDR9	Harlow 2015
A0A3Q1MDS0	Harlow 2015
A0A3Q1MDS1	Harlow 2015
A0A3Q1MDS4	Harlow 2015
A0A3Q1MDT8	Harlow 2015
A0A3Q1MDV9	Harlow 2015
A0A3Q1MDW2	Harlow 2015
A0A3Q1MDW5	Harlow 2015
A0A3Q1ME13	Harlow 2015
A0A3Q1ME14	Harlow 2015
A0A3Q1ME19	Harlow 2015
A0A3Q1ME43	Harlow 2015
A0A3Q1ME65	Harlow 2015
A0A3Q1ME81	Harlow 2015
A0A3Q1ME85	Harlow 2015
A0A3Q1ME94	Harlow 2015
A0A3Q1MEA2	Harlow 2015
A0A3Q1MEC9	Harlow 2015
A0A3Q1MEF0	Harlow 2015
A0A3Q1MEF8	Harlow 2015
A0A3Q1MEH9	Harlow 2015
A0A3Q1MEI8	Harlow 2015
A0A3Q1MEK5	Harlow 2015
A0A3Q1MEM9	Harlow 2015
A0A3Q1MEN7	Harlow 2015
A0A3Q1MEY4	Harlow 2015
A0A3Q1MEZ2	Harlow 2015
A0A3Q1MF01	Harlow 2015
A0A3Q1MF04	Harlow 2015
A0A3Q1MF13	Harlow 2015
A0A3Q1MF14	Harlow 2015
A0A3Q1MF55	Harlow 2015
A0A3Q1MF67	Harlow 2015
A0A3Q1MF86	Harlow 2015
A0A3Q1MF90	Harlow 2015
A0A3Q1MFB6	Harlow 2015
A0A3Q1MFC3	Harlow 2015
A0A3Q1MFD0	Harlow 2015
A0A3Q1MFD6	Harlow 2015
A0A3Q1MFE3	Harlow 2015
A0A3Q1MFE4	Harlow 2015
A0A3Q1MFF3	Harlow 2015

A0A3Q1MFG3	Harlow 2015
A0A3Q1MFG5	Harlow 2015
A0A3Q1MFI2	Harlow 2015
A0A3Q1MFI5	Harlow 2015
A0A3Q1MFJ1	Harlow 2015
A0A3Q1MFJ3	Harlow 2015
A0A3Q1MFL7	Harlow 2015
A0A3Q1MFP5	Harlow 2015
A0A3Q1MFQ7	Harlow 2015
A0A3Q1MFR4	Harlow 2015
A0A3Q1MFR6	Harlow 2015
A0A3Q1MFS2	Harlow 2015
A0A3Q1MFU7	Harlow 2015
A0A3Q1MFV2	Harlow 2015
A0A3Q1MFY4	Harlow 2015
A0A3Q1MFY6	Harlow 2015
A0A3Q1MFZ4	Harlow 2015
A0A3Q1MG04	Harlow 2015
A0A3Q1MG13	Harlow 2015
A0A3Q1MG31	Harlow 2015
A0A3Q1MG83	Harlow 2015
A0A3Q1MG98	Harlow 2015
A0A3Q1MGD3	Harlow 2015
A0A3Q1MGE4	Harlow 2015
A0A3Q1MGE6	Harlow 2015
A0A3Q1MGI2	Harlow 2015
A0A3Q1MGI8	Harlow 2015
A0A3Q1MGJ4	Harlow 2015
A0A3Q1MGJ5	Harlow 2015
A0A3Q1MGL4	Harlow 2015

A0A3Q1MGQ5	Harlow 2015
A0A3Q1MGQ6	Harlow 2015
A0A3Q1MGS1	Harlow 2015
A0A3Q1MGT0	Harlow 2015
A0A3Q1MGZ4	Harlow 2015
A0A3Q1MH25	Harlow 2015
A0A3Q1MH27	Harlow 2015
A0A3Q1MH36	Harlow 2015
A0A3Q1MH41	Harlow 2015
A0A3Q1MH44	Harlow 2015
A0A3Q1MH46	Harlow 2015
A0A3Q1MH47	Harlow 2015
A0A3Q1MH57	Harlow 2015
A0A3Q1MH84	Harlow 2015
A0A3Q1MHA1	Harlow 2015
A0A3Q1MHC4	Harlow 2015
A0A3Q1MHD3	Harlow 2015
A0A3Q1MHE5	Harlow 2015
A0A3Q1MHG7	Harlow 2015
A0A3Q1MHI5	Harlow 2015
A0A3Q1MHJ2	Harlow 2015
A0A3Q1MHP5	Harlow 2015
A0A3Q1MHS3	Harlow 2015
A0A3Q1MHT0	Harlow 2015
A0A3Q1MHV1	Harlow 2015
A0A3Q1MHV3	Harlow 2015
A0A3Q1MHV6	Harlow 2015
A0A3Q1MHW9	Harlow 2015
A0A3Q1MHX1	Harlow 2015
A0A3Q1MHX8	Harlow 2015

A0A3Q1MI01	Harlow 2015
A0A3Q1MI08	Harlow 2015
A0A3Q1MI13	Harlow 2015
A0A3Q1MI22	Harlow 2015
A0A3Q1MI24	Harlow 2015
A0A3Q1MI26	Harlow 2015
A0A3Q1MI56	Harlow 2015
A0A3Q1MI86	Harlow 2015
A0A3Q1MI90	Harlow 2015
A0A3Q1MI98	Harlow 2015
A0A3Q1MIA4	Harlow 2015
A0A3Q1MIB0	Harlow 2015
A0A3Q1MIC2	Harlow 2015
A0A3Q1MID4	Harlow 2015
A0A3Q1MIE7	Harlow 2015
A0A3Q1MIF1	Harlow 2015
A0A3Q1MIF2	Harlow 2015
A0A3Q1MIF4	Harlow 2015
A0A3Q1MIG2	Harlow 2015
A0A3Q1MIG4	Harlow 2015
A0A3Q1MII4	Harlow 2015
A0A3Q1MIM4	Harlow 2015
A0A3Q1MIS1	Harlow 2015
A0A3Q1MIU1	Harlow 2015
A0A3Q1MIU3	Harlow 2015
A0A3Q1MIW2	Harlow 2015
A0A3Q1MIX4	Harlow 2015
A0A3Q1MIY3	Harlow 2015
A0A3Q1MIY6	Harlow 2015
A0A3Q1MJ12	Harlow 2015

A0A3Q1MJ34	Harlow 2015
A0A3Q1MJ68	Harlow 2015
A0A3Q1MJ74	Harlow 2015
A0A3Q1MJA9	Harlow 2015
A0A3Q1MJC4	Harlow 2015
A0A3Q1MJD5	Harlow 2015
A0A3Q1MJD9	Harlow 2015
A0A3Q1MJE6	Harlow 2015
A0A3Q1MJF5	Harlow 2015
A0A3Q1MJJ4	Harlow 2015
A0A3Q1MJM1	Harlow 2015
A0A3Q1MJQ7	Harlow 2015
A0A3Q1MJR0	Harlow 2015
A0A3Q1MJT2	Harlow 2015
A0A3Q1MJU0	Harlow 2015
A0A3Q1MJV7	Harlow 2015
A0A3Q1MJY0	Harlow 2015
A0A3Q1MJY5	Harlow 2015
A0A3Q1MK01	Harlow 2015
A0A3Q1MK02	Harlow 2015
A0A3Q1MK32	Harlow 2015
A0A3Q1MK42	Harlow 2015
A0A3Q1MK57	Harlow 2015
A0A3Q1MK58	Harlow 2015
A0A3Q1MK64	Harlow 2015
A0A3Q1MK68	Harlow 2015
A0A3Q1MK72	Harlow 2015
A0A3Q1MK76	Harlow 2015
A0A3Q1MK96	Harlow 2015
A0A3Q1MK99	Harlow 2015

A0A3Q1MKB2	Harlow 2015
A0A3Q1MKC8	Harlow 2015
A0A3Q1MKD0	Harlow 2015
A0A3Q1MKE9	Harlow 2015
A0A3Q1MKF2	Harlow 2015
A0A3Q1MKK4	Harlow 2015
A0A3Q1MKK7	Harlow 2015
A0A3Q1MKM2	Harlow 2015
A0A3Q1MKQ7	Harlow 2015
A0A3Q1MKR0	Harlow 2015
A0A3Q1MKR2	Harlow 2015
A0A3Q1MKT0	Harlow 2015
A0A3Q1MKT5	Harlow 2015
A0A3Q1MKU4	Harlow 2015
A0A3Q1MKU5	Harlow 2015
A0A3Q1ML00	Harlow 2015
A0A3Q1ML02	Harlow 2015
A0A3Q1ML09	Harlow 2015
A0A3Q1ML30	Harlow 2015
A0A3Q1ML66	Harlow 2015
A0A3Q1ML78	Harlow 2015
A0A3Q1MLC3	Harlow 2015
A0A3Q1MLC6	Harlow 2015
A0A3Q1MLH0	Harlow 2015
A0A3Q1MLH4	Harlow 2015
A0A3Q1MLJ3	Harlow 2015
A0A3Q1MLK0	Harlow 2015
A0A3Q1MLK2	Harlow 2015
A0A3Q1MLL4	Harlow 2015
A0A3Q1MLN1	Harlow 2015

A0A3Q1MLN6	Harlow 2015
A0A3Q1MLP3	Harlow 2015
A0A3Q1MLQ2	Harlow 2015
A0A3Q1MLQ6	Harlow 2015
A0A3Q1MLQ7	Harlow 2015
A0A3Q1MLR1	Harlow 2015
A0A3Q1MLU4	Harlow 2015
A0A3Q1MLV0	Harlow 2015
A0A3Q1MLV3	Harlow 2015
A0A3Q1MLW1	Harlow 2015
A0A3Q1MM18	Harlow 2015
A0A3Q1MM26	Harlow 2015
A0A3Q1MM44	Harlow 2015
A0A3Q1MM52	Harlow 2015
A0A3Q1MM55	Harlow 2015
A0A3Q1MM65	Harlow 2015
A0A3Q1MM92	Harlow 2015
A0A3Q1MMA1	Harlow 2015
A0A3Q1MMD7	Harlow 2015
A0A3Q1MME4	Harlow 2015
A0A3Q1MMI4	Harlow 2015
A0A3Q1MMI6	Harlow 2015
A0A3Q1MMJ3	Harlow 2015
A0A3Q1MMQ9	Harlow 2015
A0A3Q1MMR9	Harlow 2015
A0A3Q1MMS8	Harlow 2015
A0A3Q1MMV0	Harlow 2015
A0A3Q1MMW5	Harlow 2015
A0A3Q1MN10	Harlow 2015
A0A3Q1MN33	Harlow 2015

A0A3Q1MN40	Harlow 2015
A0A3Q1MN64	Harlow 2015
A0A3Q1MN70	Harlow 2015
A0A3Q1MN97	Harlow 2015
A0A3Q1MNC1	Harlow 2015
A0A3Q1MNG0	Harlow 2015
A0A3Q1MNG1	Harlow 2015
A0A3Q1MNL9	Harlow 2015
A0A3Q1MNM3	Harlow 2015
A0A3Q1MNM7	Harlow 2015
A0A3Q1MNN7	Harlow 2015
A0A3Q1MNP8	Harlow 2015
A0A3Q1MP13	Harlow 2015
A0A3Q1MP40	Harlow 2015
A0A3Q1MP67	Harlow 2015
A0A3Q1MP69	Harlow 2015
A0A3Q1MP70	Harlow 2015
A0A3Q1MPB3	Harlow 2015
A0A3Q1MPD2	Harlow 2015
A0A3Q1MPF1	Harlow 2015
A0A3Q1MPG5	Harlow 2015
A0A3Q1MPJ4	Harlow 2015
A0A3Q1MPJ7	Harlow 2015
A0A3Q1MPQ0	Harlow 2015
A0A3Q1MPS4	Harlow 2015
A0A3Q1MPV5	Harlow 2015
A0A3Q1MPW4	Harlow 2015
A0A3Q1MPY8	Harlow 2015
A0A3Q1MPZ9	Harlow 2015
A0A3Q1MQ27	Harlow 2015
A0A3Q1MQ34	Harlow 2015
A0A3Q1MQ51	Harlow 2015
A0A3Q1MQ59	Harlow 2015
A0A3Q1MQ68	Harlow 2015
A0A3Q1MQ69	Harlow 2015
A0A3Q1MQ74	Harlow 2015
A0A3Q1MQ83	Harlow 2015
A0A3Q1MQ92	Harlow 2015
A0A3Q1MQA8	Harlow 2015
A0A3Q1MQD5	Harlow 2015
A0A3Q1MQD7	Harlow 2015
A0A3Q1MQE0	Harlow 2015
A0A3Q1MQF2	Harlow 2015
A0A3Q1MQF7	Harlow 2015
A0A3Q1MQG2	Harlow 2015
A0A3Q1MQH2	Harlow 2015
A0A3Q1MQJ1	Harlow 2015
A0A3Q1MQK6	Harlow 2015
A0A3Q1MQM1	Harlow 2015
A0A3Q1MQM3	Harlow 2015
A0A3Q1MQP3	Harlow 2015
A0A3Q1MQR5	Harlow 2015
A0A3Q1MQS3	Harlow 2015
A0A3Q1MQT6	Harlow 2015
A0A3Q1MQX7	Harlow 2015
A0A3Q1MQZ2	Harlow 2015
A0A3Q1MR04	Harlow 2015
A0A3Q1MR22	Harlow 2015
A0A3Q1MR38	Harlow 2015
A0A3Q1MR52	Harlow 2015
A0A3Q1MR68	Harlow 2015
A0A3Q1MR86	Harlow 2015
A0A3Q1MR92	Harlow 2015
A0A3Q1MR95	Harlow 2015
A0A3Q1MRD9	Harlow 2015
A0A3Q1MRE3	Harlow 2015
A0A3Q1MRF3	Harlow 2015
A0A3Q1MRG1	Harlow 2015
A0A3Q1MRJ4	Harlow 2015
A0A3Q1MRK2	Harlow 2015
A0A3Q1MRL1	Harlow 2015
A0A3Q1MRM2	Harlow 2015
A0A3Q1MRM3	Harlow 2015
A0A3Q1MRM9	Harlow 2015
A0A3Q1MRN4	Harlow 2015
A0A3Q1MRN5	Harlow 2015
A0A3Q1MRN9	Harlow 2015
A0A3Q1MRS3	Harlow 2015
A0A3Q1MRU0	Harlow 2015
A0A3Q1MRW2	Harlow 2015
A0A3Q1MS04	Harlow 2015
A0A3Q1MS19	Harlow 2015
A0A3Q1MS21	Harlow 2015
A0A3Q1MS33	Harlow 2015
A0A3Q1MS55	Harlow 2015
A0A3Q1MS82	Harlow 2015
A0A3Q1MS92	Harlow 2015
A0A3Q1MSA1	Harlow 2015
A0A3Q1MSB9	Harlow 2015
A0A3Q1MSE0	Harlow 2015

A0A3Q1MSI5	Harlow 2015
A0A3Q1MSL5	Harlow 2015
A0A3Q1MSN7	Harlow 2015
A0A3Q1MSP0	Harlow 2015
A0A3Q1MSP7	Harlow 2015
A0A3Q1MSS6	Harlow 2015
A0A3Q1MSW9	Harlow 2015
A0A3Q1MT05	Harlow 2015
A0A3Q1MT60	Harlow 2015
A0A3Q1MT78	Harlow 2015
A0A3Q1MT80	Harlow 2015
A0A3Q1MT88	Harlow 2015
A0A3Q1MTA5	Harlow 2015
A0A3Q1MTD4	Harlow 2015
A0A3Q1MTD5	Harlow 2015
A0A3Q1MTE4	Harlow 2015
A0A3Q1MTF8	Harlow 2015
A0A3Q1MTI5	Harlow 2015
A0A3Q1MTK9	Harlow 2015
A0A3Q1MTL6	Harlow 2015
A0A3Q1MTL8	Harlow 2015
A0A3Q1MTN6	Harlow 2015
A0A3Q1MTT6	Harlow 2015
A0A3Q1MTV4	Harlow 2015
A0A3Q1MTX8	Harlow 2015
A0A3Q1MTZ0	Harlow 2015
A0A3Q1MTZ5	Harlow 2015
A0A3Q1MU19	Harlow 2015
A0A3Q1MU31	Harlow 2015
A0A3Q1MU33	Harlow 2015
A0A3Q1MU45	Harlow 2015
A0A3Q1MU95	Harlow 2015
A0A3Q1MU98	Harlow 2015
A0A3Q1MUD4	Harlow 2015
A0A3Q1MUH4	Harlow 2015
A0A3Q1MUH7	Harlow 2015
A0A3Q1MUI0	Harlow 2015
A0A3Q1MUJ8	Harlow 2015
A0A3Q1MUM9	Harlow 2015
A0A3Q1MUN6	Harlow 2015
A0A3Q1MUQ8	Harlow 2015
A0A3Q1MUT5	Harlow 2015
A0A3Q1MUU9	Harlow 2015
A0A3Q1MUX4	Harlow 2015
A0A3Q1MV21	Harlow 2015
A0A3Q1MV91	Harlow 2015
A0A3Q1MVE5	Harlow 2015
A0A3Q1MVE8	Harlow 2015
A0A3Q1MVG1	Harlow 2015
A0A3Q1MVH8	Harlow 2015
A0A3Q1MVI8	Harlow 2015
A0A3Q1MVJ5	Harlow 2015
A0A3Q1MVL5	Harlow 2015
A0A3Q1MVM8	Harlow 2015
A0A3Q1MVQ3	Harlow 2015
A0A3Q1MVS3	Harlow 2015
A0A3Q1MVT2	Harlow 2015
A0A3Q1MVV4	Harlow 2015
A0A3Q1MVZ1	Harlow 2015
A0A3Q1MW26	Harlow 2015
A0A3Q1MW92	Harlow 2015
A0A3Q1MWA3	Harlow 2015
A0A3Q1MWC7	Harlow 2015
A0A3Q1MWD4	Harlow 2015
A0A3Q1MWG7	Harlow 2015
A0A3Q1MWH0	Harlow 2015
A0A3Q1MWK8	Harlow 2015
A0A3Q1MWL3	Harlow 2015
A0A3Q1MWL9	Harlow 2015
A0A3Q1MWN1	Harlow 2015
A0A3Q1MWX6	Harlow 2015
A0A3Q1MX25	Harlow 2015
A0A3Q1MX54	Harlow 2015
A0A3Q1MXB7	Harlow 2015
A0A3Q1MXK6	Harlow 2015
A0A3Q1MXL6	Harlow 2015
A0A3Q1MXM4	Harlow 2015
A0A3Q1MXQ0	Harlow 2015
A0A3Q1MXU7	Harlow 2015
A0A3Q1MY28	Harlow 2015
A0A3Q1MYB4	Harlow 2015
A0A3Q1MYD5	Harlow 2015
A0A3Q1MYD8	Harlow 2015
A0A3Q1MYG1	Harlow 2015
A0A3Q1MYL9	Harlow 2015
A0A3Q1MYM6	Harlow 2015
A0A3Q1MZ37	Harlow 2015
A0A3Q1MZ77	Harlow 2015
A0A3Q1MZC5	Harlow 2015
A0A3Q1MZI6	Harlow 2015

A0A3Q1MZJ9	Harlow 2015
A0A3Q1MZP8	Harlow 2015
A0A3Q1MZU3	Harlow 2015
A0A3Q1N008	Harlow 2015
A0A3Q1N064	Harlow 2015
A0A3Q1N077	Harlow 2015
A0A3Q1N0A8	Harlow 2015
A0A3Q1N0B0	Harlow 2015
A0A3Q1N0N9	Harlow 2015
A0A3Q1N0S0	Harlow 2015
A0A3Q1N0S5	Harlow 2015
A0A3Q1N0V7	Harlow 2015
A0A3Q1N108	Harlow 2015
A0A3Q1N116	Harlow 2015
A0A3Q1N134	Harlow 2015
A0A3Q1N140	Harlow 2015
A0A3Q1N147	Harlow 2015
A0A3Q1N178	Harlow 2015
A0A3Q1N191	Harlow 2015
A0A3Q1N1C0	Harlow 2015
A0A3Q1N1C2	Harlow 2015
A0A3Q1N1J5	Harlow 2015
A0A3Q1N1N6	Harlow 2015
A0A3Q1N1R3	Harlow 2015
A0A3Q1N1T6	Harlow 2015
A0A3Q1N203	Harlow 2015
A0A3Q1N238	Harlow 2015
A0A3Q1N2D0	Harlow 2015
A0A3Q1N2E0	Harlow 2015
A0A3Q1N2J5	Harlow 2015
A0A3Q1N2K5	Harlow 2015
A0A3Q1N2L3	Harlow 2015
A0A3Q1N2Q9	Harlow 2015
A0A3Q1N308	Harlow 2015
A0A3Q1N348	Harlow 2015
A0A3Q1N357	Harlow 2015
A0A3Q1N369	Harlow 2015
A0A3Q1N3A8	Harlow 2015
A0A3Q1N3C1	Harlow 2015
A0A3Q1N3C7	Harlow 2015
A0A3Q1N3D9	Harlow 2015
A0A3Q1N3F6	Harlow 2015
A0A3Q1N3K4	Harlow 2015
A0A3Q1N3Q0	Harlow 2015
A0A3Q1N3Q6	Harlow 2015
A0A3Q1N443	Harlow 2015
A0A3Q1N453	Harlow 2015
A0A3Q1N461	Harlow 2015
A0A3Q1N471	Harlow 2015
A0A3Q1N4F3	Harlow 2015
A0A3Q1N4H7	Harlow 2015
A0A3Q1N4K8	Harlow 2015
A0A3Q1N4L8	Harlow 2015
A0A3Q1N4X8	Harlow 2015
A0A3Q1N4Z6	Harlow 2015
A0A3Q1N4Z7	Harlow 2015
A0A3Q1N522	Harlow 2015
A0A3Q1N535	Harlow 2015
A0A3Q1N541	Harlow 2015
A0A3Q1N557	Harlow 2015
A0A3Q1N568	Harlow 2015
A0A3Q1N5A9	Harlow 2015
A0A3Q1N5D7	Harlow 2015
A0A3Q1N5F9	Harlow 2015
A0A3Q1N5G3	Harlow 2015
A0A3Q1N5G5	Harlow 2015
A0A3Q1N5P3	Harlow 2015
A0A3Q1N5S3	Harlow 2015
A0A3Q1N5T2	Harlow 2015
A0A3Q1N5Y6	Harlow 2015
A0A3Q1N6B9	Harlow 2015
A0A3Q1N6D1	Harlow 2015
A0A3Q1N6E2	Harlow 2015
A0A3Q1N6J6	Harlow 2015
A0A3Q1N6L6	Harlow 2015
A0A3Q1N6S6	Harlow 2015
A0A3Q1N6S7	Harlow 2015
A0A3Q1N6T1	Harlow 2015
A0A3Q1N6W8	Harlow 2015
A0A3Q1N703	Harlow 2015
A0A3Q1N7H1	Harlow 2015
A0A3Q1N7L1	Harlow 2015
A0A3Q1N7L7	Harlow 2015
A0A3Q1N7Q5	Harlow 2015
A0A3Q1N7R1	Harlow 2015
A0A3Q1N7X1	Harlow 2015
A0A3Q1N827	Harlow 2015
A0A3Q1N839	Harlow 2015
A0A3Q1N842	Harlow 2015
A0A3Q1N855	Harlow 2015

A0A3Q1N894	Harlow 2015
A0A3Q1N8A3	Harlow 2015
A0A3Q1N8C9	Harlow 2015
A0A3Q1N8E3	Harlow 2015
A0A3Q1N8F8	Harlow 2015
A0A3Q1N8I6	Harlow 2015
A0A3Q1N8K4	Harlow 2015
A0A3Q1N8P4	Harlow 2015
A0A3Q1N8Q5	Harlow 2015
A0A3Q1N8Y0	Harlow 2015
A0A3Q1N960	Harlow 2015
A0A3Q1N9B4	Harlow 2015
A0A3Q1N9L4	Harlow 2015
A0A3Q1N9S1	Harlow 2015
A0A3Q1N9S5	Harlow 2015
A0A3Q1N9V7	Harlow 2015
A0A3Q1N9Y5	Harlow 2015
A0A3Q1NA32	Harlow 2015
A0A3Q1NA44	Harlow 2015
A0A3Q1NA92	Harlow 2015
A0A3Q1NAE3	Harlow 2015
A0A3Q1NAI5	Harlow 2015
A0A3Q1NAY9	Harlow 2015
A0A3Q1NB13	Harlow 2015
A0A3Q1NB30	Harlow 2015
A0A3Q1NB36	Harlow 2015
A0A3Q1NB40	Harlow 2015
A0A3Q1NBB0	Harlow 2015
A0A3Q1NBC4	Harlow 2015
A0A3Q1NBQ6	Harlow 2015
A0A3Q1NC41	Harlow 2015
A0A3Q1NC75	Harlow 2015
A0A3Q1NCF4	Harlow 2015
A0A3Q1NCP7	Harlow 2015
A0A3Q1NCT6	Harlow 2015
A0A3Q1ND22	Harlow 2015
A0A3Q1ND53	Harlow 2015
A0A3Q1NDD3	Harlow 2015
A0A3Q1NDE1	Harlow 2015
A0A3Q1NDH3	Harlow 2015
A0A3Q1NDM7	Harlow 2015
A0A3Q1NDQ7	Harlow 2015
A0A3Q1NDR1	Harlow 2015
A0A3Q1NDY6	Harlow 2015
A0A3Q1NE05	Harlow 2015
A0A3Q1NE22	Harlow 2015
A0A3Q1NE82	Harlow 2015
A0A3Q1NE99	Harlow 2015
A0A3Q1NEG9	Harlow 2015
A0A3Q1NEI6	Harlow 2015
A0A3Q1NEN2	Harlow 2015
A0A3Q1NES2	Harlow 2015
A0A3Q1NES9	Harlow 2015
A0A3Q1NEU9	Harlow 2015
A0A3Q1NF78	Harlow 2015
A0A3Q1NFD1	Harlow 2015
A0A3Q1NG06	Harlow 2015
A0A3Q1NG34	Harlow 2015
A0A3Q1NGC5	Harlow 2015
A0A3Q1NGD2	Harlow 2015
A0A3Q1NGJ6	Harlow 2015
A0A3Q1NGM8	Harlow 2015
A0A3Q1NGN7	Harlow 2015
A0A3Q1NGS3	Harlow 2015
A0A3Q1NGX5	Harlow 2015
A0A3Q1NGY7	Harlow 2015
A0A3Q1NH02	Harlow 2015
A0A3Q1NH87	Harlow 2015
A0A3Q1NHD7	Harlow 2015
A0A3Q1NHQ0	Harlow 2015
A0A3Q1NHX1	Harlow 2015
A0A3Q1NHX4	Harlow 2015
A0A3Q1NHX9	Harlow 2015
A0A3Q1NI32	Harlow 2015
A0A3Q1NIA2	Harlow 2015
A0A3Q1NIC2	Harlow 2015
A0A3Q1NIF0	Harlow 2015
A0A3Q1NIK5	Harlow 2015
A0A3Q1NIP5	Harlow 2015
A0A3Q1NIR2	Harlow 2015
A0A3Q1NIT1	Harlow 2015
A0A3Q1NJB1	Harlow 2015
A0A3Q1NJR8	Harlow 2015
A0A3Q1NJS2	Harlow 2015
A0A3Q1NJS7	Harlow 2015
A0A3Q1NJT2	Harlow 2015
A0A3Q1NJU0	Harlow 2015
A0A3Q1NJX5	Harlow 2015
A0A3Q1NK91	Harlow 2015
A0A3Q1NKA6	Harlow 2015

A0A3Q1NKL1	Harlow 2015
A0A3Q1NKN6	Harlow 2015
A0A3Q1NKS6	Harlow 2015
A0A3Q1NLJ5	Harlow 2015
A0A3Q1NLL5	Harlow 2015
A0A3Q1NLN3	Harlow 2015
A0A3Q1NLQ2	Harlow 2015
A0A3Q1NLS8	Harlow 2015
A0A3Q1NLT3	Harlow 2015
A0A3Q1NLY8	Harlow 2015
A0A3Q1NM72	Harlow 2015
A0A3Q1NM85	Harlow 2015
A0A3Q1NMC5	Harlow 2015
A0A3Q1NMJ7	Harlow 2015
A0A3Q1NMV9	Harlow 2015
A0A3Q1NN69	Harlow 2015
A0A3Q1NNJ3	Harlow 2015
A0A3Q1NNP6	Harlow 2015
A0A3S5ZP34	Harlow 2015
A0A3S5ZP35	Harlow 2015
A0A3S5ZP47	Harlow 2015
A0A3S5ZP75	Harlow 2015
A0A3S5ZP82	Harlow 2015
A0A3S5ZP87	Harlow 2015
A0A3S5ZP98	Harlow 2015
A0A3S5ZPA1	Harlow 2015
A0A3S5ZPB0	Harlow 2015
A0A3S5ZPB1	Harlow 2015
A0A3S5ZPC6	Harlow 2015
A0A3S5ZPD5	Harlow 2015
A0A3S5ZPD7	Harlow 2015
A0A3S5ZPE0	Harlow 2015
A0A3S5ZPF0	Harlow 2015
A0A3S5ZPF7	Harlow 2015
A0A3S5ZPG2	Harlow 2015
A0A3S5ZPI7	Harlow 2015
A0A3S5ZPJ4	Harlow 2015
A0A3S5ZPJ6	Harlow 2015
A0A3S5ZPJ7	Harlow 2015
A0A3S5ZPM3	Harlow 2015
A0A3S5ZPN6	Harlow 2015
A0A3S5ZPT9	Harlow 2015
A0A3S5ZPU9	Harlow 2015
A0A3S5ZPW7	Harlow 2015
A0A3S5ZPX3	Harlow 2015
A0A452DHL8	Harlow 2015
A0A452DHT5	Harlow 2015
A0A452DHU0	Harlow 2015
A0A452DHV9	Harlow 2015
A0A452DHW3	Harlow 2015
A0A452DHW8	Harlow 2015
A0A452DHX0	Harlow 2015
A0A452DHY4	Harlow 2015
A0A452DHY5	Harlow 2015
A0A452DHZ1	Harlow 2015
A0A452DHZ3	Harlow 2015
A0A452DHZ5	Harlow 2015
A0A452DHZ7	Harlow 2015
A0A452DI00	Harlow 2015
A0A452DI02	Harlow 2015
A0A452DI03	Harlow 2015
A0A452DI08	Harlow 2015
A0A452DI13	Harlow 2015
A0A452DI24	Harlow 2015
A0A452DI25	Harlow 2015
A0A452DI27	Harlow 2015
A0A452DI40	Harlow 2015
A0A452DI43	Harlow 2015
A0A452DI44	Harlow 2015
A0A452DI45	Harlow 2015
A0A452DI53	Harlow 2015
A0A452DI55	Harlow 2015
A0A452DI64	Harlow 2015
A0A452DI66	Harlow 2015
A0A452DI72	Harlow 2015
A0A452DI79	Harlow 2015
A0A452DI85	Harlow 2015
A0A452DI87	Harlow 2015
A0A452DI93	Harlow 2015
A0A452DI96	Harlow 2015
A0A452DI97	Harlow 2015
A0A452DIA6	Harlow 2015
A0A452DIA7	Harlow 2015
A0A452DIB1	Harlow 2015
A0A452DIB4	Harlow 2015
A0A452DIB6	Harlow 2015
A0A452DIC6	Harlow 2015
A0A452DIC8	Harlow 2015
A0A452DID1	Harlow 2015
A0A452DID6	Harlow 2015

A0A452DID7	Harlow 2015
A0A452DID9	Harlow 2015
A0A452DIE1	Harlow 2015
A0A452DIE3	Harlow 2015
A0A452DIE5	Harlow 2015
A0A452DIE7	Harlow 2015
A0A452DIE9	Harlow 2015
A0A452DIF2	Harlow 2015
A0A452DIF4	Harlow 2015
A0A452DIF5	Harlow 2015
A0A452DIF8	Harlow 2015
A0A452DIG0	Harlow 2015
A0A452DIG6	Harlow 2015
A0A452DIG7	Harlow 2015
A0A452DIH2	Harlow 2015
A0A452DIH3	Harlow 2015
A0A452DIH7	Harlow 2015
A0A452DII8	Harlow 2015
A0A452DIJ4	Harlow 2015
A0A452DIK0	Harlow 2015
A0A452DIK3	Harlow 2015
A0A452DIL1	Harlow 2015
A0A452DIL3	Harlow 2015
A0A452DIL6	Harlow 2015
A0A452DIM2	Harlow 2015
A0A452DIM3	Harlow 2015
A0A452DIM5	Harlow 2015
A0A452DIM7	Harlow 2015
A0A452DIP2	Harlow 2015
A0A452DIP9	Harlow 2015

A0A452DIR0	Harlow 2015
A0A452DIR2	Harlow 2015
A0A452DIS6	Harlow 2015
A0A452DIT0	Harlow 2015
A0A452DIT4	Harlow 2015
A0A452DIU2	Harlow 2015
A0A452DIU3	Harlow 2015
A0A452DIU4	Harlow 2015
A0A452DIU9	Harlow 2015
A0A452DIW1	Harlow 2015
A0A452DIW4	Harlow 2015
A0A452DIW7	Harlow 2015
A0A452DIX3	Harlow 2015
A0A452DIX4	Harlow 2015
A0A452DIX8	Harlow 2015
A0A452DIZ2	Harlow 2015
A0A452DIZ9	Harlow 2015
A0A452DJ01	Harlow 2015
A0A452DJ09	Harlow 2015
A0A452DJ17	Harlow 2015
A0A452DJ21	Harlow 2015
A0A452DJ34	Harlow 2015
A0A452DJ42	Harlow 2015
A0A452DJ46	Harlow 2015
A0A452DJ57	Harlow 2015
A0A452DJ66	Harlow 2015
A0A452DJ80	Harlow 2015
A0A452DJ82	Harlow 2015
A0A452DJ87	Harlow 2015
A0A452DJ91	Harlow 2015

A0A452DJ95	Harlow 2015
A0A452DJA8	Harlow 2015
A0A452DJF3	Harlow 2015
A0A452DJF8	Harlow 2015
A0A452DJG1	Harlow 2015
A0A452DJG2	Harlow 2015
A0A452DJG7	Harlow 2015
A0A452DJH4	Harlow 2015
A0A452DJK6	Harlow 2015
A0A452DJL3	Harlow 2015
A0A452DJL6	Harlow 2015
A0A452DJM0	Harlow 2015
A0A452DJS3	Harlow 2015
A0A452DJS8	Harlow 2015
A0A452DJU4	Harlow 2015
A0A452DJX3	Harlow 2015
A0A452DJY5	Harlow 2015
A0A452DK30	Harlow 2015
A0A452DK44	Harlow 2015
A0A452DKH0	Harlow 2015
A0A452DKI9	Harlow 2015
A0A493UA87	Harlow 2015
A0A498UZ20	Harlow 2015
A0JN39	Harlow 2015
A0JN43	Harlow 2015
A0JN52	Harlow 2015
A0JN77	Harlow 2015
A0JNE6	Harlow 2015
A1A4J1	Harlow 2015
A1A4K5	Harlow 2015

A1A4L7	Harlow 2015
A1A4M0	Harlow 2015
A1A4M6	Harlow 2015
A1A4N6	Harlow 2015
A1A4Q9	Harlow 2015
A1L528	Harlow 2015
A1L5A6	Harlow 2015
A1L5A7	Harlow 2015
A1L5B7	Harlow 2015
A1XG22	Harlow 2015
A2VDK6	Harlow 2015
A2VDM7	Harlow 2015
A2VDN6	Harlow 2015
A2VDN7	Harlow 2015
A2VDP5	Harlow 2015
A2VDS1	Harlow 2015
A2VDY3	Harlow 2015
A2VDZ9	Harlow 2015
A2VE07	Harlow 2015
A2VE10	Harlow 2015
A2VE14	Harlow 2015
A2VE17	Harlow 2015
A2VE21	Harlow 2015
A2VE41	Harlow 2015
A2VE99	Harlow 2015
A3KMV2	Harlow 2015
A3KMV5	Harlow 2015
A3KMV6	Harlow 2015
A3KMY4	Harlow 2015
A3KMY8	Harlow 2015

A3KN04	Harlow 2015
A3KN22	Harlow 2015
A4FUA8	Harlow 2015
A4FUC6	Harlow 2015
A4FUC8	Harlow 2015
A4FUC9	Harlow 2015
A4FUD0	Harlow 2015
A4FUG8	Harlow 2015
A4FUZ1	Harlow 2015
A4FUZ3	Harlow 2015
A4FV08	Harlow 2015
A4FV12	Harlow 2015
A4FV54	Harlow 2015
A4FV69	Harlow 2015
A4FV74	Harlow 2015
A4IF69	Harlow 2015
A4IF78	Harlow 2015
A4IFB1	Harlow 2015
A4IFB8	Harlow 2015
A4IFC3	Harlow 2015
A4IFD1	Harlow 2015
A4IFE3	Harlow 2015
A4IFE6	Harlow 2015
A4IFF4	Harlow 2015
A4IFJ8	Harlow 2015
A4IFK5	Harlow 2015
A4IFN6	Harlow 2015
A4IFP2	Harlow 2015
A4IFQ7	Harlow 2015
A5D7A0	Harlow 2015

A5D7A2	Harlow 2015
A5D7C4	Harlow 2015
A5D7C6	Harlow 2015
A5D7D1	Harlow 2015
A5D7D9	Harlow 2015
A5D7E1	Harlow 2015
A5D7E8	Harlow 2015
A5D7J6	Harlow 2015
A5D7K0	Harlow 2015
A5D7M6	Harlow 2015
A5D7P3	Harlow 2015
A5D7R6	Harlow 2015
A5D973	Harlow 2015
A5D980	Harlow 2015
A5D984	Harlow 2015
A5D9H5	Harlow 2015
A5PJA6	Harlow 2015
A5PJD6	Harlow 2015
A5PJI5	Harlow 2015
A5PJK0	Harlow 2015
A5PJL4	Harlow 2015
A5PJN2	Harlow 2015
A5PJP2	Harlow 2015
A5PJQ1	Harlow 2015
A5PJU8	Harlow 2015
A5PJY9	Harlow 2015
A5PJZ1	Harlow 2015
A5PK65	Harlow 2015
A5PK70	Harlow 2015
A5PK71	Harlow 2015

A5PK88	Harlow 2015
A5PK96	Harlow 2015
A5PKC2	Harlow 2015
A5PKI0	Harlow 2015
A5PKI3	Harlow 2015
A5PKK0	Harlow 2015
A5PKL2	Harlow 2015
A6H6Y0	Harlow 2015
A6H6Z5	Harlow 2015
A6H722	Harlow 2015
A6H742	Harlow 2015
A6H744	Harlow 2015
A6H749	Harlow 2015
A6H768	Harlow 2015
A6H769	Harlow 2015
A6H783	Harlow 2015
A6H788	Harlow 2015
A6H797	Harlow 2015
A6H7A2	Harlow 2015
A6H7B5	Harlow 2015
A6H7E3	Harlow 2015
A6H7H3	Harlow 2015
A6H7H6	Harlow 2015
A6QL85	Harlow 2015
A6QL99	Harlow 2015
A6QLA4	Harlow 2015
A6QLA8	Harlow 2015
A6QLB7	Harlow 2015
A6QLD6	Harlow 2015
A6QLG5	Harlow 2015

A6QLG6	Harlow 2015
A6QLL2	Harlow 2015
A6QLL8	Harlow 2015
A6QLP7	Harlow 2015
A6QLS9	Harlow 2015
A6QLT5	Harlow 2015
A6QLT9	Harlow 2015
A6QLU1	Harlow 2015
A6QLU8	Harlow 2015
A6QLW3	Harlow 2015
A6QLY4	Harlow 2015
A6QLZ3	Harlow 2015
A6QM01	Harlow 2015
A6QNN9	Harlow 2015
A6QNP1	Harlow 2015
A6QNW7	Harlow 2015
A6QNX2	Harlow 2015
A6QNZ5	Harlow 2015
A6QNZ7	Harlow 2015
A6QP36	Harlow 2015
A6QP39	Harlow 2015
A6QP44	Harlow 2015
A6QPC1	Harlow 2015
A6QPC5	Harlow 2015
A6QPG6	Harlow 2015
A6QPH1	Harlow 2015
A6QPN6	Harlow 2015
A6QPT4	Harlow 2015
A6QPT7	Harlow 2015
A6QPZ0	Harlow 2015

A6QPZ6	Harlow 2015
A6QQ28	Harlow 2015
A6QQ92	Harlow 2015
A6QQL4	Harlow 2015
A6QQN6	Harlow 2015
A6QQR5	Harlow 2015
A6QQR7	Harlow 2015
A6QQT4	Harlow 2015
A6QQT5	Harlow 2015
A6QQT9	Harlow 2015
A6QQV3	Harlow 2015
A6QR40	Harlow 2015
A6QR55	Harlow 2015
A6QR57	Harlow 2015
A6QR61	Harlow 2015
A7E307	Harlow 2015
A7E350	Harlow 2015
A7E3Q8	Harlow 2015
A7E3S8	Harlow 2015
A7E3T1	Harlow 2015
A7E3T7	Harlow 2015
A7E3W2	Harlow 2015
A7E3W7	Harlow 2015
A7MB16	Harlow 2015
A7MB23	Harlow 2015
A7MB30	Harlow 2015
A7MB45	Harlow 2015
A7MB57	Harlow 2015
A7MB62	Harlow 2015
A7MB78	Harlow 2015

A7MBA2	Harlow 2015
A7MBC0	Harlow 2015
A7MBC2	Harlow 2015
A7MBC5	Harlow 2015
A7MBD4	Harlow 2015
A7MBG0	Harlow 2015
A7MBG8	Harlow 2015
A7MBH9	Harlow 2015
A7MBI5	Harlow 2015
A7MBI6	Harlow 2015
A7MBI8	Harlow 2015
A7MBI9	Harlow 2015
A7MBJ5	Harlow 2015
A7YW98	Harlow 2015
A7YWC6	Harlow 2015
A7YWF1	Harlow 2015
A7YWH5	Harlow 2015
A7YY24	Harlow 2015
A7YY28	Harlow 2015
A7YY47	Harlow 2015
A7YY55	Harlow 2015
A7YY64	Harlow 2015
A7Z014	Harlow 2015
A7Z018	Harlow 2015
A7Z025	Harlow 2015
A7Z035	Harlow 2015
A7Z051	Harlow 2015
A7Z055	Harlow 2015
A7Z057	Harlow 2015
A7Z066	Harlow 2015

A7Z085	Harlow 2015
A7Z090	Harlow 2015
A8E4P2	Harlow 2015
A8E4P3	Harlow 2015
A8E654	Harlow 2015
A8YXY4	Harlow 2015
A8YXY5	Harlow 2015
C3V9V7	Harlow 2015
C7FFR6	Harlow 2015
D3JUI8	Harlow 2015
E1B6Z6	Harlow 2015
E1B717	Harlow 2015
E1B726	Harlow 2015
E1B748	Harlow 2015
E1B7G3	Harlow 2015
E1B7K5	Harlow 2015
E1B7R4	Harlow 2015
E1B7S3	Harlow 2015
E1B7U1	Harlow 2015
E1B7W1	Harlow 2015
E1B7Y2	Harlow 2015
E1B864	Harlow 2015
E1B885	Harlow 2015
E1B8A0	Harlow 2015
E1B8I3	Harlow 2015
E1B8K6	Harlow 2015
E1B8N6	Harlow 2015
E1B8P9	Harlow 2015
E1B8Q6	Harlow 2015
E1B8X4	Harlow 2015

E1B9G4	Harlow 2015
E1B9H3	Harlow 2015
E1B9N6	Harlow 2015
E1B9R3	Harlow 2015
E1BA29	Harlow 2015
E1BAK6	Harlow 2015
E1BAU7	Harlow 2015
E1BB08	Harlow 2015
E1BB17	Harlow 2015
E1BB36	Harlow 2015
E1BB38	Harlow 2015
E1BB91	Harlow 2015
E1BBC4	Harlow 2015
E1BBG4	Harlow 2015
E1BBY7	Harlow 2015
E1BCU6	Harlow 2015
E1BCX9	Harlow 2015
E1BD36	Harlow 2015
E1BDF5	Harlow 2015
E1BDJ1	Harlow 2015
E1BDM8	Harlow 2015
E1BDN9	Harlow 2015
E1BDP3	Harlow 2015
E1BDU8	Harlow 2015
E1BDV5	Harlow 2015
E1BDX8	Harlow 2015
E1BDY3	Harlow 2015
E1BE76	Harlow 2015
E1BE86	Harlow 2015
E1BE98	Harlow 2015

E1BEG2	Harlow 2015
E1BEI0	Harlow 2015
E1BEK9	Harlow 2015
E1BEL9	Harlow 2015
E1BEN4	Harlow 2015
E1BEX4	Harlow 2015
E1BF20	Harlow 2015
E1BF59	Harlow 2015
E1BF81	Harlow 2015
E1BFB0	Harlow 2015
E1BFG0	Harlow 2015
E1BFL8	Harlow 2015
E1BFN2	Harlow 2015
E1BFQ6	Harlow 2015
E1BFV0	Harlow 2015
E1BG25	Harlow 2015
E1BG26	Harlow 2015
E1BG38	Harlow 2015
E1BG76	Harlow 2015
E1BGB0	Harlow 2015
E1BGC1	Harlow 2015
E1BGE5	Harlow 2015
E1BGG1	Harlow 2015
E1BGH0	Harlow 2015
E1BGJ4	Harlow 2015
E1BGL5	Harlow 2015
E1BGX4	Harlow 2015
E1BH15	Harlow 2015
E1BH78	Harlow 2015
E1BHK2	Harlow 2015
E1BHT5	Harlow 2015
E1BI28	Harlow 2015
E1BI98	Harlow 2015
E1BIB4	Harlow 2015
E1BIB8	Harlow 2015
E1BIM8	Harlow 2015
E1BIN5	Harlow 2015
E1BIP8	Harlow 2015
E1BIQ8	Harlow 2015
E1BIS6	Harlow 2015
E1BIU0	Harlow 2015
E1BJ59	Harlow 2015
E1BJA2	Harlow 2015
E1BJG5	Harlow 2015
E1BJH7	Harlow 2015
E1BJP2	Harlow 2015
E1BJV0	Harlow 2015
E1BKH1	Harlow 2015
E1BKH6	Harlow 2015
E1BKM4	Harlow 2015
E1BKQ2	Harlow 2015
E1BKS0	Harlow 2015
E1BKT9	Harlow 2015
E1BKW5	Harlow 2015
E1BKX3	Harlow 2015
E1BKX7	Harlow 2015
E1BKY3	Harlow 2015
E1BKY9	Harlow 2015
E1BKZ1	Harlow 2015
E1BL29	Harlow 2015
E1BLA8	Harlow 2015
E1BLF0	Harlow 2015
E1BLF7	Harlow 2015
E1BLR9	Harlow 2015
E1BLV6	Harlow 2015
E1BLZ8	Harlow 2015
E1BM12	Harlow 2015
E1BM26	Harlow 2015
E1BM28	Harlow 2015
E1BM92	Harlow 2015
E1BMD6	Harlow 2015
E1BME9	Harlow 2015
E1BMG2	Harlow 2015
E1BMI5	Harlow 2015
E1BMN5	Harlow 2015
E1BMP2	Harlow 2015
E1BMS0	Harlow 2015
E1BMW2	Harlow 2015
E1BMW9	Harlow 2015
E1BMX0	Harlow 2015
E1BN47	Harlow 2015
E1BNC9	Harlow 2015
E1BND6	Harlow 2015
E1BNG8	Harlow 2015
E1BNQ4	Harlow 2015
E1BNQ9	Harlow 2015
E1BNR0	Harlow 2015
E1BNY9	Harlow 2015
E1BP50	Harlow 2015
E1BP91	Harlow 2015

E1BPE2	Harlow 2015
E1BPI3	Harlow 2015
E1BPL8	Harlow 2015
E1BPP6	Harlow 2015
E1BPP7	Harlow 2015
E1BPQ9	Harlow 2015
E1BPW1	Harlow 2015
E1BPX9	Harlow 2015
E1BQ11	Harlow 2015
E1BQ16	Harlow 2015
E1BQ32	Harlow 2015
E1BQ37	Harlow 2015
F1MAV0	Harlow 2015
F1MAV2	Harlow 2015
F1MAZ1	Harlow 2015
F1MAZ3	Harlow 2015
F1MB04	Harlow 2015
F1MB08	Harlow 2015
F1MB60	Harlow 2015
F1MB84	Harlow 2015
F1MBF0	Harlow 2015
F1MBF6	Harlow 2015
F1MBI1	Harlow 2015
F1MBJ7	Harlow 2015
F1MBM5	Harlow 2015
F1MBN2	Harlow 2015
F1MBP4	Harlow 2015
F1MBP8	Harlow 2015
F1MBQ0	Harlow 2015
F1MBS3	Harlow 2015

F1MBT8	Harlow 2015
F1MBV6	Harlow 2015
F1MBW3	Harlow 2015
F1MC48	Harlow 2015
F1MC76	Harlow 2015
F1MC86	Harlow 2015
F1MCA8	Harlow 2015
F1MCK2	Harlow 2015
F1MCN8	Harlow 2015
F1MCT8	Harlow 2015
F1MCU4	Harlow 2015
F1MCZ0	Harlow 2015
F1MCZ3	Harlow 2015
F1MD34	Harlow 2015
F1MD66	Harlow 2015
F1MD74	Harlow 2015
F1MDD0	Harlow 2015
F1MDH3	Harlow 2015
F1MDM6	Harlow 2015
F1MDN4	Harlow 2015
F1MDS3	Harlow 2015
F1MDW1	Harlow 2015
F1ME02	Harlow 2015
F1ME38	Harlow 2015
F1ME46	Harlow 2015
F1ME65	Harlow 2015
F1MEC0	Harlow 2015
F1MEN8	Harlow 2015
F1MEP6	Harlow 2015
F1MEQ3	Harlow 2015

F1MER7	Harlow 2015
F1MF68	Harlow 2015
F1MFC2	Harlow 2015
F1MFC6	Harlow 2015
F1MFD1	Harlow 2015
F1MFD9	Harlow 2015
F1MFG7	Harlow 2015
F1MFJ3	Harlow 2015
F1MG02	Harlow 2015
F1MG05	Harlow 2015
F1MG07	Harlow 2015
F1MG56	Harlow 2015
F1MGC0	Harlow 2015
F1MGK8	Harlow 2015
F1MGK9	Harlow 2015
F1MGN7	Harlow 2015
F1MGU7	Harlow 2015
F1MGX0	Harlow 2015
F1MGY9	Harlow 2015
F1MGZ5	Harlow 2015
F1MH20	Harlow 2015
F1MH61	Harlow 2015
F1MHB8	Harlow 2015
F1MHC2	Harlow 2015
F1MHJ5	Harlow 2015
F1MHM5	Harlow 2015
F1MHP6	Harlow 2015
F1MHR6	Harlow 2015
F1MHS5	Harlow 2015
F1MI32	Harlow 2015

F1MI43	Harlow 2015
F1MI54	Harlow 2015
F1MIC5	Harlow 2015
F1MIC9	Harlow 2015
F1MIF2	Harlow 2015
F1MIH2	Harlow 2015
F1MIH4	Harlow 2015
F1MIH9	Harlow 2015
F1MIT2	Harlow 2015
F1MIU2	Harlow 2015
F1MJ12	Harlow 2015
F1MJ56	Harlow 2015
F1MJ80	Harlow 2015
F1MJH1	Harlow 2015
F1MJI7	Harlow 2015
F1MJM4	Harlow 2015
F1MJN4	Harlow 2015
F1MJP7	Harlow 2015
F1MJQ1	Harlow 2015
F1MJS4	Harlow 2015
F1MK08	Harlow 2015
F1MK30	Harlow 2015
F1MK36	Harlow 2015
F1MKE9	Harlow 2015
F1MKH6	Harlow 2015
F1MKH8	Harlow 2015
F1MKI5	Harlow 2015
F1MKS5	Harlow 2015
F1MKU3	Harlow 2015
F1MKW9	Harlow 2015

F1ML12	Harlow 2015
F1ML72	Harlow 2015
F1MLA4	Harlow 2015
F1MLB8	Harlow 2015
F1MLD8	Harlow 2015
F1MLE8	Harlow 2015
F1MLG1	Harlow 2015
F1MLU7	Harlow 2015
F1MLV1	Harlow 2015
F1MLV3	Harlow 2015
F1MLW2	Harlow 2015
F1MLX0	Harlow 2015
F1MLX9	Harlow 2015
F1MM13	Harlow 2015
F1MM14	Harlow 2015
F1MM32	Harlow 2015
F1MM34	Harlow 2015
F1MM57	Harlow 2015
F1MM59	Harlow 2015
F1MM83	Harlow 2015
F1MM86	Harlow 2015
F1MMA0	Harlow 2015
F1MMB0	Harlow 2015
F1MMD5	Harlow 2015
F1MMD7	Harlow 2015
F1MMK1	Harlow 2015
F1MMK2	Harlow 2015
F1MMK8	Harlow 2015
F1MMQ6	Harlow 2015
F1MMQ8	Harlow 2015

F1MMR6	Harlow 2015
F1MMR8	Harlow 2015
F1MMU4	Harlow 2015
F1MN04	Harlow 2015
F1MN23	Harlow 2015
F1MN84	Harlow 2015
F1MN93	Harlow 2015
F1MNI4	Harlow 2015
F1MNN6	Harlow 2015
F1MNN7	Harlow 2015
F1MNQ3	Harlow 2015
F1MNS2	Harlow 2015
F1MNS5	Harlow 2015
F1MNS8	Harlow 2015
F1MNV8	Harlow 2015
F1MP10	Harlow 2015
F1MPE1	Harlow 2015
F1MPE5	Harlow 2015
F1MPG6	Harlow 2015
F1MPK4	Harlow 2015
F1MPU0	Harlow 2015
F1MPZ9	Harlow 2015
F1MQ37	Harlow 2015
F1MQ43	Harlow 2015
F1MQ57	Harlow 2015
F1MQ65	Harlow 2015
F1MQD1	Harlow 2015
F1MQF6	Harlow 2015
F1MQG6	Harlow 2015
F1MQH8	Harlow 2015

F1MR07	Harlow 2015
F1MR22	Harlow 2015
F1MR63	Harlow 2015
F1MR96	Harlow 2015
F1MRE5	Harlow 2015
F1MRG0	Harlow 2015
F1MRS1	Harlow 2015
F1MRY9	Harlow 2015
F1MRZ5	Harlow 2015
F1MRZ6	Harlow 2015
F1MS05	Harlow 2015
F1MS25	Harlow 2015
F1MS32	Harlow 2015
F1MS40	Harlow 2015
F1MS56	Harlow 2015
F1MS62	Harlow 2015
F1MSB7	Harlow 2015
F1MSD2	Harlow 2015
F1MSE4	Harlow 2015
F1MSE7	Harlow 2015
F1MSF1	Harlow 2015
F1MSI2	Harlow 2015
F1MSN2	Harlow 2015
F1MSQ9	Harlow 2015
F1MSS2	Harlow 2015
F1MSZ6	Harlow 2015
F1MT25	Harlow 2015
F1MT69	Harlow 2015
F1MTI7	Harlow 2015
F1MTK7	Harlow 2015
F1MTP5	Harlow 2015
F1MTP9	Harlow 2015
F1MTR1	Harlow 2015
F1MTV9	Harlow 2015
F1MTX7	Harlow 2015
F1MTY3	Harlow 2015
F1MTY9	Harlow 2015
F1MTZ0	Harlow 2015
F1MTZ1	Harlow 2015
F1MU08	Harlow 2015
F1MU12	Harlow 2015
F1MU18	Harlow 2015
F1MU19	Harlow 2015
F1MU24	Harlow 2015
F1MU34	Harlow 2015
F1MU48	Harlow 2015
F1MU79	Harlow 2015
F1MU85	Harlow 2015
F1MUA8	Harlow 2015
F1MUB9	Harlow 2015
F1MUF4	Harlow 2015
F1MUK3	Harlow 2015
F1MUK8	Harlow 2015
F1MUN7	Harlow 2015
F1MUP9	Harlow 2015
F1MUR6	Harlow 2015
F1MUT3	Harlow 2015
F1MUZ9	Harlow 2015
F1MV74	Harlow 2015
F1MVL2	Harlow 2015
F1MVT7	Harlow 2015
F1MVW5	Harlow 2015
F1MVX2	Harlow 2015
F1MVY8	Harlow 2015
F1MW03	Harlow 2015
F1MW06	Harlow 2015
F1MW39	Harlow 2015
F1MW91	Harlow 2015
F1MWD3	Harlow 2015
F1MWE0	Harlow 2015
F1MWH2	Harlow 2015
F1MWJ3	Harlow 2015
F1MWN1	Harlow 2015
F1MWQ2	Harlow 2015
F1MWR3	Harlow 2015
F1MWR7	Harlow 2015
F1MWY9	Harlow 2015
F1MX04	Harlow 2015
F1MX05	Harlow 2015
F1MX38	Harlow 2015
F1MX61	Harlow 2015
F1MX83	Harlow 2015
F1MX88	Harlow 2015
F1MXE4	Harlow 2015
F1MXI4	Harlow 2015
F1MXJ5	Harlow 2015
F1MXP8	Harlow 2015
F1MXR0	Harlow 2015
F1MXU5	Harlow 2015
F1MXX0	Harlow 2015

F1MXX6	Harlow 2015
F1MXY8	Harlow 2015
F1MXY9	Harlow 2015
F1MXZ0	Harlow 2015
F1MY16	Harlow 2015
F1MY28	Harlow 2015
F1MY44	Harlow 2015
F1MY84	Harlow 2015
F1MY85	Harlow 2015
F1MYB8	Harlow 2015
F1MYC9	Harlow 2015
F1MYF9	Harlow 2015
F1MYG5	Harlow 2015
F1MYH6	Harlow 2015
F1MYH8	Harlow 2015
F1MYI2	Harlow 2015
F1MYN2	Harlow 2015
F1MYS7	Harlow 2015
F1MYV9	Harlow 2015
F1MYX5	Harlow 2015
F1MYZ7	Harlow 2015
F1MZ00	Harlow 2015
F1MZ33	Harlow 2015
F1MZ38	Harlow 2015
F1MZ40	Harlow 2015
F1MZ46	Harlow 2015
F1MZ83	Harlow 2015
F1MZ85	Harlow 2015
F1MZD5	Harlow 2015
F1MZE4	Harlow 2015

F1MZF2	Harlow 2015
F1MZK0	Harlow 2015
F1MZK4	Harlow 2015
F1MZL6	Harlow 2015
F1MZL8	Harlow 2015
F1MZN7	Harlow 2015
F1MZR1	Harlow 2015
F1MZT7	Harlow 2015
F1MZU1	Harlow 2015
F1MZU2	Harlow 2015
F1MZV1	Harlow 2015
F1MZV2	Harlow 2015
F1MZY2	Harlow 2015
F1N036	Harlow 2015
F1N045	Harlow 2015
F1N049	Harlow 2015
F1N076	Harlow 2015
F1N081	Harlow 2015
F1N091	Harlow 2015
F1N0E5	Harlow 2015
F1N0F2	Harlow 2015
F1N0F7	Harlow 2015
F1N0H3	Harlow 2015
F1N0I3	Harlow 2015
F1N0J2	Harlow 2015
F1N0R8	Harlow 2015
F1N102	Harlow 2015
F1N120	Harlow 2015
F1N161	Harlow 2015
F1N169	Harlow 2015

F1N1A3	Harlow 2015
F1N1D5	Harlow 2015
F1N1F7	Harlow 2015
F1N1F9	Harlow 2015
F1N1G7	Harlow 2015
F1N1I6	Harlow 2015
F1N1M7	Harlow 2015
F1N1R8	Harlow 2015
F1N1S0	Harlow 2015
F1N1S3	Harlow 2015
F1N1S8	Harlow 2015
F1N206	Harlow 2015
F1N214	Harlow 2015
F1N218	Harlow 2015
F1N238	Harlow 2015
F1N2B5	Harlow 2015
F1N2D3	Harlow 2015
F1N2E5	Harlow 2015
F1N2F1	Harlow 2015
F1N2I5	Harlow 2015
F1N2K1	Harlow 2015
F1N2K8	Harlow 2015
F1N2L9	Harlow 2015
F1N2W0	Harlow 2015
F1N318	Harlow 2015
F1N338	Harlow 2015
F1N339	Harlow 2015
F1N365	Harlow 2015
F1N399	Harlow 2015
F1N3B0	Harlow 2015

F1N3H1	Harlow 2015
F1N3I4	Harlow 2015
F1N3J0	Harlow 2015
F1N3J3	Harlow 2015
F1N3J9	Harlow 2015
F1N3P2	Harlow 2015
F1N3Q7	Harlow 2015
F1N3R4	Harlow 2015
F1N3U5	Harlow 2015
F1N3V0	Harlow 2015
F1N3Y1	Harlow 2015
F1N3Z3	Harlow 2015
F1N401	Harlow 2015
F1N405	Harlow 2015
F1N412	Harlow 2015
F1N430	Harlow 2015
F1N441	Harlow 2015
F1N443	Harlow 2015
F1N468	Harlow 2015
F1N4K1	Harlow 2015
F1N4M7	Harlow 2015
F1N4M9	Harlow 2015
F1N4N6	Harlow 2015
F1N4Q3	Harlow 2015
F1N4X7	Harlow 2015
F1N556	Harlow 2015
F1N5F7	Harlow 2015
F1N5H2	Harlow 2015
F1N5H8	Harlow 2015
F1N5J8	Harlow 2015
F1N5P8	Harlow 2015
F1N5S6	Harlow 2015
F1N5T0	Harlow 2015
F1N5W4	Harlow 2015
F1N605	Harlow 2015
F1N619	Harlow 2015
F1N622	Harlow 2015
F1N632	Harlow 2015
F1N647	Harlow 2015
F1N650	Harlow 2015
F1N690	Harlow 2015
F1N6A0	Harlow 2015
F1N6C2	Harlow 2015
F1N6C4	Harlow 2015
F1N6D4	Harlow 2015
F1N6D5	Harlow 2015
F1N6H1	Harlow 2015
F1N6I5	Harlow 2015
F1N6N3	Harlow 2015
F1N6T3	Harlow 2015
F1N6U4	Harlow 2015
F1N6W6	Harlow 2015
F1N6W9	Harlow 2015
F1N6Y1	Harlow 2015
F1N6Y7	Harlow 2015
F1N6Z0	Harlow 2015
F1N726	Harlow 2015
F1N789	Harlow 2015
F1N7D7	Harlow 2015
F1N7F9	Harlow 2015
F1N7H5	Harlow 2015
F1N7H7	Harlow 2015
F1N7I5	Harlow 2015
F1N7I6	Harlow 2015
F1N7K1	Harlow 2015
F1N7K8	Harlow 2015
F1N7T1	Harlow 2015
F1N7U2	Harlow 2015
F1N7V7	Harlow 2015
F1N7X3	Harlow 2015
F2Z4C6	Harlow 2015
F2Z4E7	Harlow 2015
F2Z4E9	Harlow 2015
F2Z4F0	Harlow 2015
F2Z4F5	Harlow 2015
F2Z4H3	Harlow 2015
F2Z4I5	Harlow 2015
F2Z4I6	Harlow 2015
F2Z4J5	Harlow 2015
F6PRB5	Harlow 2015
F6PRQ6	Harlow 2015
F6PS38	Harlow 2015
F6PSK5	Harlow 2015
F6PTQ9	Harlow 2015
F6PTX8	Harlow 2015
F6PU21	Harlow 2015
F6PWM7	Harlow 2015
F6PZJ9	Harlow 2015
F6Q087	Harlow 2015
F6Q234	Harlow 2015

F6Q334	Harlow 2015
F6Q8A8	Harlow 2015
F6Q9Q9	Harlow 2015
F6Q9S4	Harlow 2015
F6QAM6	Harlow 2015
F6QBF9	Harlow 2015
F6QEU6	Harlow 2015
F6QGM3	Harlow 2015
F6QH17	Harlow 2015
F6QH94	Harlow 2015
F6QHN4	Harlow 2015
F6QIA5	Harlow 2015
F6QIB4	Harlow 2015
F6QIP7	Harlow 2015
F6QIT9	Harlow 2015
F6QJE8	Harlow 2015
F6QLM5	Harlow 2015
F6QMF3	Harlow 2015
F6QND5	Harlow 2015
F6QNX4	Harlow 2015
F6QP30	Harlow 2015
F6QQ46	Harlow 2015
F6QQ60	Harlow 2015
F6QQE8	Harlow 2015
F6QQY9	Harlow 2015
F6QS28	Harlow 2015
F6QS88	Harlow 2015
F6QT01	Harlow 2015
F6QTA8	Harlow 2015
F6QVC9	Harlow 2015
F6QVN4	Harlow 2015
F6R0H3	Harlow 2015
F6R695	Harlow 2015
F6R9E0	Harlow 2015
F6R9I4	Harlow 2015
F6RAL2	Harlow 2015
F6RBQ9	Harlow 2015
F6RBS0	Harlow 2015
F6RFE5	Harlow 2015
F6RH18	Harlow 2015
F6RJ80	Harlow 2015
F6RJG0	Harlow 2015
F6RMV5	Harlow 2015
F6RPB7	Harlow 2015
F6RPS1	Harlow 2015
F6RQ58	Harlow 2015
F6RQK3	Harlow 2015
F6RWK1	Harlow 2015
F6S1D0	Harlow 2015
F6S1Q0	Harlow 2015
G1K122	Harlow 2015
G1K134	Harlow 2015
G1K192	Harlow 2015
G1K1B4	Harlow 2015
G1K1P8	Harlow 2015
G1K1S1	Harlow 2015
G1K1X0	Harlow 2015
G3MW01	Harlow 2015
G3MWH1	Harlow 2015
G3MWJ8	Harlow 2015
G3MWR4	Harlow 2015
G3MX65	Harlow 2015
G3MX91	Harlow 2015
G3MXC8	Harlow 2015
G3MXI7	Harlow 2015
G3MXJ5	Harlow 2015
G3MXK6	Harlow 2015
G3MXN0	Harlow 2015
G3MXS7	Harlow 2015
G3MXV0	Harlow 2015
G3MXW7	Harlow 2015
G3MY03	Harlow 2015
G3MY19	Harlow 2015
G3MY44	Harlow 2015
G3MY67	Harlow 2015
G3MY87	Harlow 2015
G3MYN4	Harlow 2015
G3MYW7	Harlow 2015
G3MYZ3	Harlow 2015
G3MZ54	Harlow 2015
G3MZ71	Harlow 2015
G3MZE2	Harlow 2015
G3MZF7	Harlow 2015
G3MZH4	Harlow 2015
G3MZZ6	Harlow 2015
G3N016	Harlow 2015
G3N0L3	Harlow 2015
G3N0Q8	Harlow 2015
G3N132	Harlow 2015
G3N178	Harlow 2015

G3N1D8	Harlow 2015
G3N1E7	Harlow 2015
G3N1Q0	Harlow 2015
G3N2G7	Harlow 2015
G3N2H4	Harlow 2015
G3N2K4	Harlow 2015
G3N2L2	Harlow 2015
G3N2N7	Harlow 2015
G3N2P6	Harlow 2015
G3N2U8	Harlow 2015
G3N361	Harlow 2015
G3N371	Harlow 2015
G3N3D4	Harlow 2015
G3N3N1	Harlow 2015
G3N3S2	Harlow 2015
G3X696	Harlow 2015
G3X6K8	Harlow 2015
G3X6L8	Harlow 2015
G3X6L9	Harlow 2015
G3X6P5	Harlow 2015
G3X702	Harlow 2015
G3X736	Harlow 2015
G3X743	Harlow 2015
G3X755	Harlow 2015
G3X757	Harlow 2015
G3X7G4	Harlow 2015
G3X7N4	Harlow 2015
G3X7P5	Harlow 2015
G3X8E8	Harlow 2015
G5E531	Harlow 2015

G5E532	Harlow 2015
G5E535	Harlow 2015
G5E543	Harlow 2015
G5E567	Harlow 2015
G5E589	Harlow 2015
G5E5A8	Harlow 2015
G5E5A9	Harlow 2015
G5E5B0	Harlow 2015
G5E5C8	Harlow 2015
G5E5J2	Harlow 2015
G5E5K1	Harlow 2015
G5E5M5	Harlow 2015
G5E5R3	Harlow 2015
G5E5T1	Harlow 2015
G5E619	Harlow 2015
G5E631	Harlow 2015
G5E643	Harlow 2015
G5E675	Harlow 2015
G5E6M1	Harlow 2015
G5E6M7	Harlow 2015
G5E6P3	Harlow 2015
G8JKV5	Harlow 2015
G8JKV7	Harlow 2015
G8JKX7	Harlow 2015
G8JKX8	Harlow 2015
H7BWW0	Harlow 2015
H7BWW2	Harlow 2015
M0QVZ6	Harlow 2015
O02675	Harlow 2015
O02691	Harlow 2015

O02703	Harlow 2015
O18836	Harlow 2015
O19094	Harlow 2015
O41515	Harlow 2015
O46375	Harlow 2015
O46414	Harlow 2015
O46415	Harlow 2015
O46629	Harlow 2015
O62768	Harlow 2015
O77784	Harlow 2015
O77834	Harlow 2015
O97680	Harlow 2015
O97764	Harlow 2015
P00125	Harlow 2015
P00129	Harlow 2015
P00171	Harlow 2015
P00257	Harlow 2015
P00423	Harlow 2015
P00426	Harlow 2015
P00432	Harlow 2015
P00442	Harlow 2015
P00515	Harlow 2015
P00517	Harlow 2015
P00570	Harlow 2015
P00727	Harlow 2015
P00847	Harlow 2015
P01017	Harlow 2015
P01035	Harlow 2015
P01156	Harlow 2015
P01252	Harlow 2015

P02081	Harlow 2015
P02465	Harlow 2015
P02510	Harlow 2015
P02584	Harlow 2015
P02633	Harlow 2015
P02638	Harlow 2015
P02721	Harlow 2015
P04272	Harlow 2015
P04394	Harlow 2015
P04467	Harlow 2015
P04975	Harlow 2015
P05631	Harlow 2015
P06504	Harlow 2015
P06623	Harlow 2015
P07107	Harlow 2015
P07514	Harlow 2015
P07688	Harlow 2015
P08037	Harlow 2015
P08166	Harlow 2015
P08728	Harlow 2015
P08760	Harlow 2015
P09487	Harlow 2015
P09867	Harlow 2015
P10096	Harlow 2015
P10103	Harlow 2015
P10462	Harlow 2015
P10568	Harlow 2015
P10575	Harlow 2015
P10790	Harlow 2015
P10881	Harlow 2015

P11017	Harlow 2015
P11019	Harlow 2015
P11024	Harlow 2015
P11064	Harlow 2015
P11116	Harlow 2015
P11242	Harlow 2015
P11966	Harlow 2015
P12234	Harlow 2015
P12344	Harlow 2015
P12378	Harlow 2015
P12624	Harlow 2015
P12763	Harlow 2015
P13135	Harlow 2015
P13182	Harlow 2015
P13213	Harlow 2015
P13214	Harlow 2015
P13272	Harlow 2015
P13619	Harlow 2015
P13620	Harlow 2015
P13621	Harlow 2015
P13696	Harlow 2015
P14568	Harlow 2015
P14769	Harlow 2015
P15396	Harlow 2015
P15497	Harlow 2015
P15690	Harlow 2015
P17248	Harlow 2015
P17694	Harlow 2015
P17697	Harlow 2015
P17870	Harlow 2015

P18203	Harlow 2015
P19035	Harlow 2015
P19120	Harlow 2015
P19660	Harlow 2015
P19661	Harlow 2015
P19858	Harlow 2015
P20000	Harlow 2015
P20004	Harlow 2015
P20072	Harlow 2015
P20456	Harlow 2015
P20821	Harlow 2015
P21282	Harlow 2015
P21327	Harlow 2015
P21752	Harlow 2015
P21856	Harlow 2015
P22226	Harlow 2015
P22292	Harlow 2015
P23004	Harlow 2015
P23356	Harlow 2015
P23934	Harlow 2015
P23935	Harlow 2015
P25326	Harlow 2015
P25975	Harlow 2015
P26285	Harlow 2015
P26452	Harlow 2015
P26882	Harlow 2015
P26884	Harlow 2015
P28782	Harlow 2015
P28800	Harlow 2015
P31404	Harlow 2015

P31408	Harlow 2015
P31976	Harlow 2015
P32007	Harlow 2015
P33097	Harlow 2015
P33672	Harlow 2015
P34943	Harlow 2015
P34955	Harlow 2015
P35466	Harlow 2015
P35604	Harlow 2015
P35605	Harlow 2015
P35705	Harlow 2015
P37980	Harlow 2015
P38409	Harlow 2015
P39872	Harlow 2015
P40673	Harlow 2015
P40682	Harlow 2015
P41500	Harlow 2015
P41541	Harlow 2015
P42028	Harlow 2015
P42899	Harlow 2015
P45879	Harlow 2015
P46195	Harlow 2015
P46196	Harlow 2015
P48427	Harlow 2015
P48616	Harlow 2015
P48644	Harlow 2015
P48818	Harlow 2015
P49410	Harlow 2015
P49951	Harlow 2015
P50227	Harlow 2015

P51122	Harlow 2015
P52556	Harlow 2015
P53619	Harlow 2015
P54149	Harlow 2015
P55052	Harlow 2015
P55906	Harlow 2015
P56701	Harlow 2015
P56965	Harlow 2015
P60661	Harlow 2015
P60902	Harlow 2015
P61085	Harlow 2015
P61157	Harlow 2015
P61223	Harlow 2015
P61282	Harlow 2015
P61283	Harlow 2015
P61284	Harlow 2015
P61286	Harlow 2015
P61356	Harlow 2015
P61585	Harlow 2015
P61603	Harlow 2015
P61763	Harlow 2015
P62157	Harlow 2015
P62194	Harlow 2015
P62248	Harlow 2015
P62261	Harlow 2015
P62871	Harlow 2015
P62894	Harlow 2015
P62935	Harlow 2015
P62992	Harlow 2015
P63009	Harlow 2015

P63103	Harlow 2015
P63243	Harlow 2015
P63258	Harlow 2015
P67774	Harlow 2015
P67808	Harlow 2015
P68002	Harlow 2015
P68102	Harlow 2015
P68103	Harlow 2015
P68399	Harlow 2015
P68401	Harlow 2015
P79103	Harlow 2015
P79105	Harlow 2015
P79126	Harlow 2015
P79134	Harlow 2015
P79135	Harlow 2015
P79251	Harlow 2015
P79342	Harlow 2015
P79345	Harlow 2015
P80177	Harlow 2015
P80227	Harlow 2015
P80311	Harlow 2015
P80513	Harlow 2015
P81134	Harlow 2015
P81282	Harlow 2015
P81623	Harlow 2015
P81644	Harlow 2015
P81948	Harlow 2015
P82908	Harlow 2015
P83939	Harlow 2015
P84080	Harlow 2015

Q00361	Harlow 2015
Q01321	Harlow 2015
Q02369	Harlow 2015
Q02373	Harlow 2015
Q02375	Harlow 2015
Q04467	Harlow 2015
Q05443	Harlow 2015
Q05B89	Harlow 2015
Q07130	Harlow 2015
Q08DA1	Harlow 2015
Q08DB4	Harlow 2015
Q08DD1	Harlow 2015
Q08DJ3	Harlow 2015
Q08DK2	Harlow 2015
Q08DL0	Harlow 2015
Q08DM3	Harlow 2015
Q08DM8	Harlow 2015
Q08DS7	Harlow 2015
Q08DU9	Harlow 2015
Q08DV2	Harlow 2015
Q08DW2	Harlow 2015
Q08DY5	Harlow 2015
Q08E01	Harlow 2015
Q08E18	Harlow 2015
Q08E20	Harlow 2015
Q08E32	Harlow 2015
Q08E34	Harlow 2015
Q08E38	Harlow 2015
Q08E52	Harlow 2015
Q08E54	Harlow 2015
Q08E58	Harlow 2015
Q09430	Harlow 2015
Q09TE3	Harlow 2015
Q0II26	Harlow 2015
Q0II59	Harlow 2015
Q0IIA3	Harlow 2015
Q0IIF7	Harlow 2015
Q0IIK5	Harlow 2015
Q0IIL6	Harlow 2015
Q0IIM3	Harlow 2015
Q0P570	Harlow 2015
Q0P592	Harlow 2015
Q0P5A3	Harlow 2015
Q0P5D0	Harlow 2015
Q0P5D6	Harlow 2015
Q0P5F2	Harlow 2015
Q0P5F6	Harlow 2015
Q0P5F7	Harlow 2015
Q0P5K3	Harlow 2015
Q0P5L6	Harlow 2015
Q0P5M8	Harlow 2015
Q0P5N1	Harlow 2015
Q0R345	Harlow 2015
Q0R346	Harlow 2015
Q0V7N7	Harlow 2015
Q0V8F2	Harlow 2015
Q0V8H6	Harlow 2015
Q0V8R6	Harlow 2015
Q0V8S0	Harlow 2015
Q0VBW6	Harlow 2015
Q0VBX6	Harlow 2015
Q0VC27	Harlow 2015
Q0VC36	Harlow 2015
Q0VC37	Harlow 2015
Q0VC53	Harlow 2015
Q0VC82	Harlow 2015
Q0VC87	Harlow 2015
Q0VCA5	Harlow 2015
Q0VCC0	Harlow 2015
Q0VCH0	Harlow 2015
Q0VCH9	Harlow 2015
Q0VCK0	Harlow 2015
Q0VCK5	Harlow 2015
Q0VCL3	Harlow 2015
Q0VCM4	Harlow 2015
Q0VCM5	Harlow 2015
Q0VCN1	Harlow 2015
Q0VCP4	Harlow 2015
Q0VCQ6	Harlow 2015
Q0VCQ9	Harlow 2015
Q0VCU8	Harlow 2015
Q0VCV0	Harlow 2015
Q0VCW2	Harlow 2015
Q0VCX4	Harlow 2015
Q0VCX5	Harlow 2015
Q0VCY1	Harlow 2015
Q0VCY7	Harlow 2015
Q0VCY8	Harlow 2015
Q0VD16	Harlow 2015
Q0VD18	Harlow 2015

Q0VD27	Harlow 2015
Q0VD48	Harlow 2015
Q0VD49	Harlow 2015
Q0VD53	Harlow 2015
Q0VFX9	Harlow 2015
Q148C8	Harlow 2015
Q148C9	Harlow 2015
Q148D3	Harlow 2015
Q148E6	Harlow 2015
Q148G4	Harlow 2015
Q148G9	Harlow 2015
Q148J4	Harlow 2015
Q148J6	Harlow 2015
Q148J8	Harlow 2015
Q148K7	Harlow 2015
Q148M1	Harlow 2015
Q148N0	Harlow 2015
Q17Q89	Harlow 2015
Q17QB3	Harlow 2015
Q17QG2	Harlow 2015
Q17QH2	Harlow 2015
Q17QH5	Harlow 2015
Q17QI3	Harlow 2015
Q17QJ1	Harlow 2015
Q17QK3	Harlow 2015
Q17QL4	Harlow 2015
Q17QL7	Harlow 2015
Q17QL8	Harlow 2015
Q17QP9	Harlow 2015
Q17QQ1	Harlow 2015
Q17QQ2	Harlow 2015
Q17QR2	Harlow 2015
Q17QU3	Harlow 2015
Q17QZ9	Harlow 2015
Q1JP79	Harlow 2015
Q1JPA0	Harlow 2015
Q1JPB0	Harlow 2015
Q1JPK7	Harlow 2015
Q1JQ98	Harlow 2015
Q1JQB2	Harlow 2015
Q1JQB5	Harlow 2015
Q1JQD4	Harlow 2015
Q1LZ72	Harlow 2015
Q1LZ81	Harlow 2015
Q1LZA3	Harlow 2015
Q1LZB6	Harlow 2015
Q1LZD9	Harlow 2015
Q1LZF9	Harlow 2015
Q1LZH1	Harlow 2015
Q1RMI2	Harlow 2015
Q1RMJ6	Harlow 2015
Q1RML6	Harlow 2015
Q1RML9	Harlow 2015
Q1RMM9	Harlow 2015
Q1RMR3	Harlow 2015
Q1RMR8	Harlow 2015
Q1RMR9	Harlow 2015
Q1RMS2	Harlow 2015
Q1RMU4	Harlow 2015
Q1RMW9	Harlow 2015
Q1RMX7	Harlow 2015
Q24JZ7	Harlow 2015
Q24JZ8	Harlow 2015
Q24K02	Harlow 2015
Q24K03	Harlow 2015
Q27966	Harlow 2015
Q27971	Harlow 2015
Q27975	Harlow 2015
Q27991	Harlow 2015
Q28050	Harlow 2015
Q28056	Harlow 2015
Q28104	Harlow 2015
Q28141	Harlow 2015
Q28205	Harlow 2015
Q28851	Harlow 2015
Q29460	Harlow 2015
Q29RH3	Harlow 2015
Q29RI6	Harlow 2015
Q29RI9	Harlow 2015
Q29RK1	Harlow 2015
Q29RK2	Harlow 2015
Q29RK4	Harlow 2015
Q29RL2	Harlow 2015
Q29RL9	Harlow 2015
Q29RN2	Harlow 2015
Q29RQ2	Harlow 2015
Q29RR2	Harlow 2015
Q29RT7	Harlow 2015
Q29RZ0	Harlow 2015
Q29S00	Harlow 2015

Q29S11	Harlow 2015
Q29S21	Harlow 2015
Q2HJ26	Harlow 2015
Q2HJ33	Harlow 2015
Q2HJ49	Harlow 2015
Q2HJ54	Harlow 2015
Q2HJ57	Harlow 2015
Q2HJ58	Harlow 2015
Q2HJ60	Harlow 2015
Q2HJ65	Harlow 2015
Q2HJ74	Harlow 2015
Q2HJ81	Harlow 2015
Q2HJ86	Harlow 2015
Q2HJ94	Harlow 2015
Q2HJ97	Harlow 2015
Q2HJD7	Harlow 2015
Q2HJF6	Harlow 2015
Q2HJG5	Harlow 2015
Q2HJH0	Harlow 2015
Q2HJH1	Harlow 2015
Q2HJH9	Harlow 2015
Q2KHT7	Harlow 2015
Q2KHU8	Harlow 2015
Q2KHZ6	Harlow 2015
Q2KI35	Harlow 2015
Q2KI42	Harlow 2015
Q2KI56	Harlow 2015
Q2KI57	Harlow 2015
Q2KI84	Harlow 2015
Q2KI86	Harlow 2015
Q2KIA2	Harlow 2015
Q2KIA5	Harlow 2015
Q2KIC5	Harlow 2015
Q2KIC7	Harlow 2015
Q2KII9	Harlow 2015
Q2KIK0	Harlow 2015
Q2KIL5	Harlow 2015
Q2KIM0	Harlow 2015
Q2KIM6	Harlow 2015
Q2KIN5	Harlow 2015
Q2KIR1	Harlow 2015
Q2KIU7	Harlow 2015
Q2KIV7	Harlow 2015
Q2KIV8	Harlow 2015
Q2KIW1	Harlow 2015
Q2KJ17	Harlow 2015
Q2KJ25	Harlow 2015
Q2KJ32	Harlow 2015
Q2KJ42	Harlow 2015
Q2KJ45	Harlow 2015
Q2KJ46	Harlow 2015
Q2KJ86	Harlow 2015
Q2KJA1	Harlow 2015
Q2KJC8	Harlow 2015
Q2KJD0	Harlow 2015
Q2KJD1	Harlow 2015
Q2KJD7	Harlow 2015
Q2KJE7	Harlow 2015
Q2KJF1	Harlow 2015
Q2KJH6	Harlow 2015
Q2KJH7	Harlow 2015
Q2KJI2	Harlow 2015
Q2KJI3	Harlow 2015
Q2LGB5	Harlow 2015
Q2LGB8	Harlow 2015
Q2NKR5	Harlow 2015
Q2NKU6	Harlow 2015
Q2NKY7	Harlow 2015
Q2NKZ1	Harlow 2015
Q2NKZ9	Harlow 2015
Q2NL00	Harlow 2015
Q2NL04	Harlow 2015
Q2NL22	Harlow 2015
Q2NL24	Harlow 2015
Q2NL29	Harlow 2015
Q2T9M8	Harlow 2015
Q2T9P4	Harlow 2015
Q2T9S0	Harlow 2015
Q2T9S4	Harlow 2015
Q2T9Y6	Harlow 2015
Q2TA37	Harlow 2015
Q2TA49	Harlow 2015
Q2TBG8	Harlow 2015
Q2TBN3	Harlow 2015
Q2TBQ5	Harlow 2015
Q2TBU5	Harlow 2015
Q2TBX1	Harlow 2015
Q2TBX5	Harlow 2015
Q2TBX9	Harlow 2015
Q2UVX4	Harlow 2015

Q2YDE4	Harlow 2015
Q2YDE9	Harlow 2015
Q2YDM1	Harlow 2015
Q32KP9	Harlow 2015
Q32KW2	Harlow 2015
Q32KY3	Harlow 2015
Q32L41	Harlow 2015
Q32L54	Harlow 2015
Q32L92	Harlow 2015
Q32L99	Harlow 2015
Q32LA7	Harlow 2015
Q32LC3	Harlow 2015
Q32LC7	Harlow 2015
Q32LE4	Harlow 2015
Q32LE5	Harlow 2015
Q32LG3	Harlow 2015
Q32LM0	Harlow 2015
Q32LM2	Harlow 2015
Q32LN7	Harlow 2015
Q32LP2	Harlow 2015
Q32P77	Harlow 2015
Q32P85	Harlow 2015
Q32PA8	Harlow 2015
Q32PB8	Harlow 2015
Q32PB9	Harlow 2015
Q32PD5	Harlow 2015
Q32PF2	Harlow 2015
Q32PG1	Harlow 2015
Q32PJ8	Harlow 2015
Q32S38	Harlow 2015

Q3B7M2	Harlow 2015
Q3B7M5	Harlow 2015
Q3B7N2	Harlow 2015
Q3B7N3	Harlow 2015
Q3B8S0	Harlow 2015
Q3MHE8	Harlow 2015
Q3MHF5	Harlow 2015
Q3MHH4	Harlow 2015
Q3MHK9	Harlow 2015
Q3MHL3	Harlow 2015
Q3MHL4	Harlow 2015
Q3MHL7	Harlow 2015
Q3MHL8	Harlow 2015
Q3MHM7	Harlow 2015
Q3MHN0	Harlow 2015
Q3MHN2	Harlow 2015
Q3MHP1	Harlow 2015
Q3MHP2	Harlow 2015
Q3MHR3	Harlow 2015
Q3MHR5	Harlow 2015
Q3MHR7	Harlow 2015
Q3MHX5	Harlow 2015
Q3MHY1	Harlow 2015
Q3MI00	Harlow 2015
Q3SWW9	Harlow 2015
Q3SWX1	Harlow 2015
Q3SWX3	Harlow 2015
Q3SWX8	Harlow 2015
Q3SWY3	Harlow 2015
Q3SWZ6	Harlow 2015

Q3SX29	Harlow 2015
Q3SX30	Harlow 2015
Q3SX32	Harlow 2015
Q3SX36	Harlow 2015
Q3SX40	Harlow 2015
Q3SX41	Harlow 2015
Q3SX44	Harlow 2015
Q3SX47	Harlow 2015
Q3SYR0	Harlow 2015
Q3SYR7	Harlow 2015
Q3SYR8	Harlow 2015
Q3SYT9	Harlow 2015
Q3SYU2	Harlow 2015
Q3SYU6	Harlow 2015
Q3SYU7	Harlow 2015
Q3SYU8	Harlow 2015
Q3SYW1	Harlow 2015
Q3SYW2	Harlow 2015
Q3SYW6	Harlow 2015
Q3SZ00	Harlow 2015
Q3SZ07	Harlow 2015
Q3SZ11	Harlow 2015
Q3SZ15	Harlow 2015
Q3SZ16	Harlow 2015
Q3SZ18	Harlow 2015
Q3SZ19	Harlow 2015
Q3SZ20	Harlow 2015
Q3SZ32	Harlow 2015
Q3SZ54	Harlow 2015
Q3SZ62	Harlow 2015

Q3SZ65	Harlow 2015
Q3SZ73	Harlow 2015
Q3SZA0	Harlow 2015
Q3SZA5	Harlow 2015
Q3SZB7	Harlow 2015
Q3SZC0	Harlow 2015
Q3SZC2	Harlow 2015
Q3SZC4	Harlow 2015
Q3SZC6	Harlow 2015
Q3SZD1	Harlow 2015
Q3SZF2	Harlow 2015
Q3SZF8	Harlow 2015
Q3SZH5	Harlow 2015
Q3SZH7	Harlow 2015
Q3SZI0	Harlow 2015
Q3SZI4	Harlow 2015
Q3SZJ0	Harlow 2015
Q3SZJ7	Harlow 2015
Q3SZJ9	Harlow 2015
Q3SZK8	Harlow 2015
Q3SZM5	Harlow 2015
Q3SZN2	Harlow 2015
Q3SZN4	Harlow 2015
Q3SZP5	Harlow 2015
Q3SZQ6	Harlow 2015
Q3SZR8	Harlow 2015
Q3SZT2	Harlow 2015
Q3SZW9	Harlow 2015
Q3SZZ9	Harlow 2015
Q3T000	Harlow 2015

Q3T004	Harlow 2015
Q3T005	Harlow 2015
Q3T010	Harlow 2015
Q3T030	Harlow 2015
Q3T035	Harlow 2015
Q3T057	Harlow 2015
Q3T094	Harlow 2015
Q3T0A3	Harlow 2015
Q3T0B6	Harlow 2015
Q3T0C7	Harlow 2015
Q3T0D0	Harlow 2015
Q3T0D5	Harlow 2015
Q3T0E0	Harlow 2015
Q3T0F4	Harlow 2015
Q3T0F7	Harlow 2015
Q3T0F9	Harlow 2015
Q3T0G3	Harlow 2015
Q3T0I4	Harlow 2015
Q3T0I5	Harlow 2015
Q3T0K2	Harlow 2015
Q3T0L2	Harlow 2015
Q3T0M0	Harlow 2015
Q3T0P6	Harlow 2015
Q3T0R7	Harlow 2015
Q3T0S6	Harlow 2015
Q3T0S7	Harlow 2015
Q3T0T1	Harlow 2015
Q3T0U1	Harlow 2015
Q3T0U3	Harlow 2015
Q3T0U5	Harlow 2015

Q3T0V2	Harlow 2015
Q3T0V3	Harlow 2015
Q3T0V4	Harlow 2015
Q3T0V7	Harlow 2015
Q3T0V9	Harlow 2015
Q3T0W4	Harlow 2015
Q3T0W9	Harlow 2015
Q3T0X5	Harlow 2015
Q3T0X6	Harlow 2015
Q3T0Y1	Harlow 2015
Q3T0Y5	Harlow 2015
Q3T0Z0	Harlow 2015
Q3T0Z7	Harlow 2015
Q3T102	Harlow 2015
Q3T106	Harlow 2015
Q3T108	Harlow 2015
Q3T112	Harlow 2015
Q3T122	Harlow 2015
Q3T132	Harlow 2015
Q3T133	Harlow 2015
Q3T140	Harlow 2015
Q3T145	Harlow 2015
Q3T147	Harlow 2015
Q3T149	Harlow 2015
Q3T165	Harlow 2015
Q3T168	Harlow 2015
Q3T169	Harlow 2015
Q3T178	Harlow 2015
Q3ZBA4	Harlow 2015
Q3ZBA8	Harlow 2015

Q3ZBD0	Harlow 2015
Q3ZBD1	Harlow 2015
Q3ZBD3	Harlow 2015
Q3ZBD7	Harlow 2015
Q3ZBD9	Harlow 2015
Q3ZBE9	Harlow 2015
Q3ZBG0	Harlow 2015
Q3ZBG1	Harlow 2015
Q3ZBH0	Harlow 2015
Q3ZBH2	Harlow 2015
Q3ZBH5	Harlow 2015
Q3ZBH8	Harlow 2015
Q3ZBK2	Harlow 2015
Q3ZBL0	Harlow 2015
Q3ZBL1	Harlow 2015
Q3ZBL4	Harlow 2015
Q3ZBN0	Harlow 2015
Q3ZBS7	Harlow 2015
Q3ZBT5	Harlow 2015
Q3ZBT6	Harlow 2015
Q3ZBU0	Harlow 2015
Q3ZBU2	Harlow 2015
Q3ZBU5	Harlow 2015
Q3ZBU7	Harlow 2015
Q3ZBV8	Harlow 2015
Q3ZBW4	Harlow 2015
Q3ZBZ8	Harlow 2015
Q3ZC07	Harlow 2015
Q3ZC10	Harlow 2015
Q3ZC13	Harlow 2015
Q3ZC41	Harlow 2015
Q3ZC42	Harlow 2015
Q3ZC44	Harlow 2015
Q3ZC50	Harlow 2015
Q3ZC57	Harlow 2015
Q3ZC64	Harlow 2015
Q3ZC84	Harlow 2015
Q3ZCA2	Harlow 2015
Q3ZCA7	Harlow 2015
Q3ZCA8	Harlow 2015
Q3ZCC9	Harlow 2015
Q3ZCD3	Harlow 2015
Q3ZCE0	Harlow 2015
Q3ZCE1	Harlow 2015
Q3ZCE2	Harlow 2015
Q3ZCF0	Harlow 2015
Q3ZCF3	Harlow 2015
Q3ZCH0	Harlow 2015
Q3ZCI9	Harlow 2015
Q3ZCJ2	Harlow 2015
Q3ZCJ6	Harlow 2015
Q3ZCJ7	Harlow 2015
Q3ZCK1	Harlow 2015
Q3ZCK2	Harlow 2015
Q3ZCK3	Harlow 2015
Q3ZCK9	Harlow 2015
Q3ZCL8	Harlow 2015
Q56JU9	Harlow 2015
Q56JV1	Harlow 2015
Q56JV9	Harlow 2015
Q56JX6	Harlow 2015
Q56JX8	Harlow 2015
Q56JY1	Harlow 2015
Q56JY2	Harlow 2015
Q56JY8	Harlow 2015
Q56JZ5	Harlow 2015
Q56K03	Harlow 2015
Q56K10	Harlow 2015
Q56K14	Harlow 2015
Q58CQ2	Harlow 2015
Q58CS7	Harlow 2015
Q58CX1	Harlow 2015
Q58D57	Harlow 2015
Q58D84	Harlow 2015
Q58DK5	Harlow 2015
Q58DL9	Harlow 2015
Q58DM8	Harlow 2015
Q58DQ3	Harlow 2015
Q58DS9	Harlow 2015
Q58DT1	Harlow 2015
Q58DU5	Harlow 2015
Q58DU7	Harlow 2015
Q58DW0	Harlow 2015
Q58DW5	Harlow 2015
Q58DW6	Harlow 2015
Q59A32	Harlow 2015
Q5BIP4	Harlow 2015
Q5BIR5	Harlow 2015
Q5E936	Harlow 2015
Q5E938	Harlow 2015

Q5E946	Harlow 2015
Q5E947	Harlow 2015
Q5E951	Harlow 2015
Q5E952	Harlow 2015
Q5E954	Harlow 2015
Q5E958	Harlow 2015
Q5E959	Harlow 2015
Q5E963	Harlow 2015
Q5E964	Harlow 2015
Q5E966	Harlow 2015
Q5E971	Harlow 2015
Q5E973	Harlow 2015
Q5E983	Harlow 2015
Q5E987	Harlow 2015
Q5E988	Harlow 2015
Q5E992	Harlow 2015
Q5E997	Harlow 2015
Q5E9A1	Harlow 2015
Q5E9A6	Harlow 2015
Q5E9B1	Harlow 2015
Q5E9B7	Harlow 2015
Q5E9C0	Harlow 2015
Q5E9D5	Harlow 2015
Q5E9E6	Harlow 2015
Q5E9F1	Harlow 2015
Q5E9F2	Harlow 2015
Q5E9F5	Harlow 2015
Q5E9F7	Harlow 2015
Q5E9F8	Harlow 2015
Q5E9F9	Harlow 2015

Q5E9G3	Harlow 2015
Q5E9H9	Harlow 2015
Q5E9I7	Harlow 2015
Q5E9J1	Harlow 2015
Q5E9K0	Harlow 2015
Q5E9K3	Harlow 2015
Q5E9M1	Harlow 2015
Q5E9T9	Harlow 2015
Q5E9X4	Harlow 2015
Q5EA01	Harlow 2015
Q5EA50	Harlow 2015
Q5EA61	Harlow 2015
Q5EA79	Harlow 2015
Q5EAB4	Harlow 2015
Q5EAC6	Harlow 2015
Q5EAC7	Harlow 2015
Q5EAD0	Harlow 2015
Q5EAD4	Harlow 2015
Q5GN72	Harlow 2015
Q5KR47	Harlow 2015
Q5KR48	Harlow 2015
Q645M6	Harlow 2015
Q6B857	Harlow 2015
Q6EWQ7	Harlow 2015
Q76I81	Harlow 2015
Q76I82	Harlow 2015
Q76LV2	Harlow 2015
Q7YQE1	Harlow 2015
Q7YRE6	Harlow 2015
Q7YRE7	Harlow 2015

Q7YRW9	Harlow 2015
Q861S4	Harlow 2015
Q862I1	Harlow 2015
Q863B3	Harlow 2015
Q863C3	Harlow 2015
Q865S1	Harlow 2015
Q865V6	Harlow 2015
Q8HYI9	Harlow 2015
Q8HZJ5	Harlow 2015
Q8HZY1	Harlow 2015
Q8MHZ9	Harlow 2015
Q8MJ50	Harlow 2015
Q8MJG1	Harlow 2015
Q8SPJ1	Harlow 2015
Q8SPP7	Harlow 2015
Q8SQ21	Harlow 2015
Q8SQH5	Harlow 2015
Q8WN55	Harlow 2015
Q92176	Harlow 2015
Q95107	Harlow 2015
Q95108	Harlow 2015
Q95121	Harlow 2015
Q95L54	Harlow 2015
Q95M18	Harlow 2015
Q9BGI1	Harlow 2015
Q9BGI3	Harlow 2015
Q9GLX9	Harlow 2015
Q9GMB8	Harlow 2015
Q9MYM4	Harlow 2015
Q9MZ08	Harlow 2015

Q9N179	Harlow 2015
Q9TR36	Harlow 2015
Q9TS87	Harlow 2015
Q9TTK8	Harlow 2015
Q9TU47	Harlow 2015
Q9XSA7	Harlow 2015
Q9XSK7	Harlow 2015
Z4YHD9	Harlow 2015
A0A059UMC6	Helfrich 2020
A0A075TEJ1	Helfrich 2020
A0A077S1J7	Helfrich 2020
A0A077S9Q3	Helfrich 2020
A0A077SA06	Helfrich 2020
A0A0A0MP88	Helfrich 2020
A0A0A0MP89	Helfrich 2020
A0A0A0MP90	Helfrich 2020
A0A0A0MP92	Helfrich 2020
A0A0A0MP99	Helfrich 2020
A0A0A0MPA0	Helfrich 2020
A0A0F6QMJ3	Helfrich 2020
A0A0K1L4Y6	Helfrich 2020
A0A0N4STN1	Helfrich 2020
A0A140T832	Helfrich 2020
A0A140T841	Helfrich 2020
A0A140T843	Helfrich 2020
A0A140T846	Helfrich 2020
A0A140T850	Helfrich 2020
A0A140T851	Helfrich 2020
A0A140T853	Helfrich 2020
A0A140T854	Helfrich 2020
A0A140T856	Helfrich 2020
A0A140T862	Helfrich 2020
A0A140T866	Helfrich 2020
A0A140T871	Helfrich 2020
A0A140T872	Helfrich 2020
A0A140T879	Helfrich 2020
A0A140T881	Helfrich 2020
A0A140T886	Helfrich 2020
A0A140T887	Helfrich 2020
A0A140T892	Helfrich 2020
A0A140T894	Helfrich 2020
A0A140T897	Helfrich 2020
A0A140T8A1	Helfrich 2020
A0A140T8A4	Helfrich 2020
A0A140T8A5	Helfrich 2020
A0A140T8B1	Helfrich 2020
A0A140T8D2	Helfrich 2020
A0A140T8D4	Helfrich 2020
A0A173FDL1	Helfrich 2020
A0FDH2	Helfrich 2020
A0JBZ9	Helfrich 2020
A0JN39	Helfrich 2020
A0JN47	Helfrich 2020
A0JN52	Helfrich 2020
A0JN53	Helfrich 2020
A0JN60	Helfrich 2020
A0JN77	Helfrich 2020
A0JN82	Helfrich 2020
A0JN96	Helfrich 2020
A0JN97	Helfrich 2020
A0JND7	Helfrich 2020
A0JNE6	Helfrich 2020
A0JNE9	Helfrich 2020
A0JNJ5	Helfrich 2020
A0JNL5	Helfrich 2020
A1A4I4	Helfrich 2020
A1A4I8	Helfrich 2020
A1A4I9	Helfrich 2020
A1A4J1	Helfrich 2020
A1A4K3	Helfrich 2020
A1A4K5	Helfrich 2020
A1A4L7	Helfrich 2020
A1A4M6	Helfrich 2020
A1A4N6	Helfrich 2020
A1A4N9	Helfrich 2020
A1A4P5	Helfrich 2020
A1A4Q2	Helfrich 2020
A1A4Q9	Helfrich 2020
A1L520	Helfrich 2020
A1L528	Helfrich 2020
A1L5A6	Helfrich 2020
A1L5B3	Helfrich 2020
A1L5B6	Helfrich 2020
A1XEA0	Helfrich 2020
A1XG22	Helfrich 2020
A2T1U6	Helfrich 2020
A2VDK6	Helfrich 2020
A2VDL8	Helfrich 2020
A2VDM7	Helfrich 2020
A2VDN7	Helfrich 2020

A2VDP5	Helfrich 2020
A2VDS0	Helfrich 2020
A2VDS1	Helfrich 2020
A2VDU0	Helfrich 2020
A2VDV2	Helfrich 2020
A2VDW0	Helfrich 2020
A2VDX0	Helfrich 2020
A2VDY3	Helfrich 2020
A2VE06	Helfrich 2020
A2VE07	Helfrich 2020
A2VE08	Helfrich 2020
A2VE14	Helfrich 2020
A2VE17	Helfrich 2020
A2VE21	Helfrich 2020
A2VE39	Helfrich 2020
A2VE41	Helfrich 2020
A2VE46	Helfrich 2020
A2VE51	Helfrich 2020
A2VE52	Helfrich 2020
A2VE69	Helfrich 2020
A2VE70	Helfrich 2020
A2VE83	Helfrich 2020
A2VE99	Helfrich 2020
A2VEA3	Helfrich 2020
A3KLR9	Helfrich 2020
A3KMV2	Helfrich 2020
A3KMV5	Helfrich 2020
A3KMV6	Helfrich 2020
A3KMX4	Helfrich 2020
A3KMX8	Helfrich 2020

A3KMY4	Helfrich 2020
A3KMY8	Helfrich 2020
A3KN12	Helfrich 2020
A3KN22	Helfrich 2020
A3KN51	Helfrich 2020
A4FUA8	Helfrich 2020
A4FUC2	Helfrich 2020
A4FUC5	Helfrich 2020
A4FUC6	Helfrich 2020
A4FUC8	Helfrich 2020
A4FUC9	Helfrich 2020
A4FUD0	Helfrich 2020
A4FUD3	Helfrich 2020
A4FUE5	Helfrich 2020
A4FUG8	Helfrich 2020
A4FUI1	Helfrich 2020
A4FUI2	Helfrich 2020
A4FUX9	Helfrich 2020
A4FUZ1	Helfrich 2020
A4FUZ3	Helfrich 2020
A4FV00	Helfrich 2020
A4FV05	Helfrich 2020
A4FV09	Helfrich 2020
A4FV10	Helfrich 2020
A4FV12	Helfrich 2020
A4FV50	Helfrich 2020
A4FV54	Helfrich 2020
A4FV56	Helfrich 2020
A4FV58	Helfrich 2020
A4FV68	Helfrich 2020

A4FV69	Helfrich 2020
A4FV72	Helfrich 2020
A4FV74	Helfrich 2020
A4FV94	Helfrich 2020
A4IF69	Helfrich 2020
A4IF78	Helfrich 2020
A4IF81	Helfrich 2020
A4IF82	Helfrich 2020
A4IF88	Helfrich 2020
A4IF89	Helfrich 2020
A4IFA5	Helfrich 2020
A4IFB1	Helfrich 2020
A4IFB8	Helfrich 2020
A4IFC0	Helfrich 2020
A4IFC3	Helfrich 2020
A4IFC4	Helfrich 2020
A4IFD1	Helfrich 2020
A4IFE0	Helfrich 2020
A4IFE6	Helfrich 2020
A4IFF4	Helfrich 2020
A4IFI0	Helfrich 2020
A4IFJ5	Helfrich 2020
A4IFJ8	Helfrich 2020
A4IFK5	Helfrich 2020
A4IFK6	Helfrich 2020
A4IFN6	Helfrich 2020
A4IFN7	Helfrich 2020
A4IFP7	Helfrich 2020
A4IFQ7	Helfrich 2020
A4IFV2	Helfrich 2020

A5D785	Helfrich 2020
A5D792	Helfrich 2020
A5D794	Helfrich 2020
A5D7A0	Helfrich 2020
A5D7A2	Helfrich 2020
A5D7B9	Helfrich 2020
A5D7C4	Helfrich 2020
A5D7C6	Helfrich 2020
A5D7D1	Helfrich 2020
A5D7D3	Helfrich 2020
A5D7D9	Helfrich 2020
A5D7E1	Helfrich 2020
A5D7E4	Helfrich 2020
A5D7E8	Helfrich 2020
A5D7G1	Helfrich 2020
A5D7H6	Helfrich 2020
A5D7J6	Helfrich 2020
A5D7K0	Helfrich 2020
A5D7N8	Helfrich 2020
A5D7P1	Helfrich 2020
A5D7P3	Helfrich 2020
A5D7Q2	Helfrich 2020
A5D7Q4	Helfrich 2020
A5D7R6	Helfrich 2020
A5D7S0	Helfrich 2020
A5D7U5	Helfrich 2020
A5D7U9	Helfrich 2020
A5D973	Helfrich 2020
A5D980	Helfrich 2020
A5D986	Helfrich 2020

A5D987	Helfrich 2020
A5D9B6	Helfrich 2020
A5D9D1	Helfrich 2020
A5D9D2	Helfrich 2020
A5D9E9	Helfrich 2020
A5D9F7	Helfrich 2020
A5D9H1	Helfrich 2020
A5H027	Helfrich 2020
A5PJ69	Helfrich 2020
A5PJ77	Helfrich 2020
A5PJA4	Helfrich 2020
A5PJD6	Helfrich 2020
A5PJE3	Helfrich 2020
A5PJF9	Helfrich 2020
A5PJH9	Helfrich 2020
A5PJI5	Helfrich 2020
A5PJJ9	Helfrich 2020
A5PJK0	Helfrich 2020
A5PJL4	Helfrich 2020
A5PJL8	Helfrich 2020
A5PJN2	Helfrich 2020
A5PJP2	Helfrich 2020
A5PJP6-1	Helfrich 2020
A5PJP8	Helfrich 2020
A5PJQ1	Helfrich 2020
A5PJQ6	Helfrich 2020
A5PJR3	Helfrich 2020
A5PJR4	Helfrich 2020
A5PJR9	Helfrich 2020
A5PJS6	Helfrich 2020

A5PJT7	Helfrich 2020
A5PJV5	Helfrich 2020
A5PJX0	Helfrich 2020
A5PJY9	Helfrich 2020
A5PJZ5	Helfrich 2020
A5PJZ7	Helfrich 2020
A5PJZ8	Helfrich 2020
A5PK07	Helfrich 2020
A5PK19	Helfrich 2020
A5PK33	Helfrich 2020
A5PK39	Helfrich 2020
A5PK49	Helfrich 2020
A5PK51-1	Helfrich 2020
A5PK55	Helfrich 2020
A5PK61	Helfrich 2020
A5PK65	Helfrich 2020
A5PK70	Helfrich 2020
A5PK72	Helfrich 2020
A5PK76	Helfrich 2020
A5PK77	Helfrich 2020
A5PK80	Helfrich 2020
A5PK88	Helfrich 2020
A5PK96	Helfrich 2020
A5PKC2	Helfrich 2020
A5PKD2	Helfrich 2020
A5PKE2	Helfrich 2020
A5PKG2	Helfrich 2020
A5PKG6	Helfrich 2020
A5PKH3	Helfrich 2020
A5PKH8	Helfrich 2020

A5PKI0	Helfrich 2020
A5PKI3	Helfrich 2020
A5PKI6	Helfrich 2020
A5PKJ3	Helfrich 2020
A5PKJ5	Helfrich 2020
A5PKK0	Helfrich 2020
A5PKK6	Helfrich 2020
A5PKM0	Helfrich 2020
A6BMK7	Helfrich 2020
A6BML7	Helfrich 2020
A6H6Y0	Helfrich 2020
A6H6Z5	Helfrich 2020
A6H709	Helfrich 2020
A6H722	Helfrich 2020
A6H742	Helfrich 2020
A6H744	Helfrich 2020
A6H761	Helfrich 2020
A6H767	Helfrich 2020
A6H768	Helfrich 2020
A6H769	Helfrich 2020
A6H772	Helfrich 2020
A6H785	Helfrich 2020
A6H788	Helfrich 2020
A6H7A2	Helfrich 2020
A6H7B5	Helfrich 2020
A6H7C4	Helfrich 2020
A6H7D3	Helfrich 2020
A6H7D7	Helfrich 2020
A6H7E3	Helfrich 2020
A6H7F6	Helfrich 2020

A6H7G2	Helfrich 2020
A6H7H1	Helfrich 2020
A6H7H2	Helfrich 2020
A6H7H6	Helfrich 2020
A6H7I2	Helfrich 2020
A6H7I5	Helfrich 2020
A6H7J6	Helfrich 2020
A6H7J7	Helfrich 2020
A6QL72	Helfrich 2020
A6QL75	Helfrich 2020
A6QL81	Helfrich 2020
A6QL85	Helfrich 2020
A6QLA4	Helfrich 2020
A6QLA8	Helfrich 2020
A6QLB0	Helfrich 2020
A6QLB5	Helfrich 2020
A6QLB7	Helfrich 2020
A6QLB8	Helfrich 2020
A6QLC4	Helfrich 2020
A6QLD1	Helfrich 2020
A6QLD6	Helfrich 2020
A6QLG1	Helfrich 2020
A6QLG5	Helfrich 2020
A6QLJ8	Helfrich 2020
A6QLL8	Helfrich 2020
A6QLN8	Helfrich 2020
A6QLN9	Helfrich 2020
A6QLP9	Helfrich 2020
A6QLR1	Helfrich 2020
A6QLR2	Helfrich 2020

A6QLR7	Helfrich 2020
A6QLR8	Helfrich 2020
A6QLR9	Helfrich 2020
A6QLS8	Helfrich 2020
A6QLS9	Helfrich 2020
A6QLT9	Helfrich 2020
A6QLU7	Helfrich 2020
A6QLU8	Helfrich 2020
A6QLV3	Helfrich 2020
A6QLW3	Helfrich 2020
A6QLW5	Helfrich 2020
A6QLY4	Helfrich 2020
A6QLY8	Helfrich 2020
A6QLZ0	Helfrich 2020
A6QLZ3	Helfrich 2020
A6QLZ6	Helfrich 2020
A6QM01	Helfrich 2020
A6QM09	Helfrich 2020
A6QNJ7	Helfrich 2020
A6QNL0	Helfrich 2020
A6QNL5	Helfrich 2020
A6QNN7	Helfrich 2020
A6QNS2	Helfrich 2020
A6QNS3	Helfrich 2020
A6QNS6	Helfrich 2020
A6QNT8	Helfrich 2020
A6QNX2	Helfrich 2020
A6QNZ5	Helfrich 2020
A6QNZ7	Helfrich 2020
A6QP30	Helfrich 2020

A6QP36	Helfrich 2020
A6QP39	Helfrich 2020
A6QP44	Helfrich 2020
A6QPB5	Helfrich 2020
A6QPC5	Helfrich 2020
A6QPG6	Helfrich 2020
A6QPH7	Helfrich 2020
A6QPK7	Helfrich 2020
A6QPN5	Helfrich 2020
A6QPN6	Helfrich 2020
A6QPP2	Helfrich 2020
A6QPS1	Helfrich 2020
A6QPT7	Helfrich 2020
A6QPX6	Helfrich 2020
A6QQ07	Helfrich 2020
A6QQ11	Helfrich 2020
A6QQ47	Helfrich 2020
A6QQ70	Helfrich 2020
A6QQ85	Helfrich 2020
A6QQA8	Helfrich 2020
A6QQF5	Helfrich 2020
A6QQH1	Helfrich 2020
A6QQL4	Helfrich 2020
A6QQN6	Helfrich 2020
A6QQR7	Helfrich 2020
A6QQS1	Helfrich 2020
A6QQS5	Helfrich 2020
A6QQT4	Helfrich 2020
A6QQV3	Helfrich 2020
A6QQW3	Helfrich 2020
A6QQW8	Helfrich 2020
A6QR01	Helfrich 2020
A6QR08	Helfrich 2020
A6QR15	Helfrich 2020
A6QR28	Helfrich 2020
A6QR35	Helfrich 2020
A6QR40	Helfrich 2020
A6QR46	Helfrich 2020
A6QR55	Helfrich 2020
A6QR56	Helfrich 2020
A6QR61	Helfrich 2020
A7E307	Helfrich 2020
A7E3C7	Helfrich 2020
A7E3Q2	Helfrich 2020
A7E3S8	Helfrich 2020
A7E3T7	Helfrich 2020
A7E3V0	Helfrich 2020
A7E3W2	Helfrich 2020
A7E3W7	Helfrich 2020
A7MAZ3	Helfrich 2020
A7MAZ5	Helfrich 2020
A7MB01	Helfrich 2020
A7MB16	Helfrich 2020
A7MB21	Helfrich 2020
A7MB23	Helfrich 2020
A7MB24	Helfrich 2020
A7MB28	Helfrich 2020
A7MB30	Helfrich 2020
A7MB31	Helfrich 2020
A7MB32	Helfrich 2020
A7MB33	Helfrich 2020
A7MB45	Helfrich 2020
A7MB47	Helfrich 2020
A7MB48	Helfrich 2020
A7MB62	Helfrich 2020
A7MB70	Helfrich 2020
A7MB78	Helfrich 2020
A7MBA2	Helfrich 2020
A7MBA6	Helfrich 2020
A7MBA7	Helfrich 2020
A7MBC0	Helfrich 2020
A7MBC2	Helfrich 2020
A7MBC5	Helfrich 2020
A7MBD4	Helfrich 2020
A7MBF8	Helfrich 2020
A7MBG0	Helfrich 2020
A7MBG8	Helfrich 2020
A7MBH9	Helfrich 2020
A7MBI5	Helfrich 2020
A7MBI6	Helfrich 2020
A7MBI7	Helfrich 2020
A7MBI8	Helfrich 2020
A7MBJ4	Helfrich 2020
A7MBJ5	Helfrich 2020
A7YW37	Helfrich 2020
A7YW40	Helfrich 2020
A7YW98	Helfrich 2020
A7YWC6	Helfrich 2020
A7YWF1	Helfrich 2020
A7YWL9	Helfrich 2020

A7YWM8	Helfrich 2020
A7YWP6	Helfrich 2020
A7YY24	Helfrich 2020
A7YY28	Helfrich 2020
A7Z014	Helfrich 2020
A7Z025	Helfrich 2020
A7Z034	Helfrich 2020
A7Z035	Helfrich 2020
A7Z051	Helfrich 2020
A7Z054	Helfrich 2020
A7Z055	Helfrich 2020
A7Z057	Helfrich 2020
A7Z066	Helfrich 2020
A7Z090	Helfrich 2020
A8E4N0	Helfrich 2020
A8E4P2	Helfrich 2020
A8E4P3	Helfrich 2020
A8E4R4	Helfrich 2020
A8E645	Helfrich 2020
A8E651	Helfrich 2020
A8E662	Helfrich 2020
A8YXX7	Helfrich 2020
A8YXY3	Helfrich 2020
A8YXZ2	Helfrich 2020
A9UIB1	Helfrich 2020
B0JYK4	Helfrich 2020
B0JYL2	Helfrich 2020
B0JYP5	Helfrich 2020
B0JYQ0	Helfrich 2020
B0JYR3	Helfrich 2020

B1H0W8	Helfrich 2020
B1PK18	Helfrich 2020
B2CZT3	Helfrich 2020
B3IVN4	Helfrich 2020
B3VTM3	Helfrich 2020
B8Y898	Helfrich 2020
B8Y9S9	Helfrich 2020
B8Y9T0	Helfrich 2020
B9UKL8	Helfrich 2020
C1JZ67	Helfrich 2020
C4T7Z1	Helfrich 2020
C4T8B4	Helfrich 2020
D3JUI8	Helfrich 2020
D3U796	Helfrich 2020
D4QBB3	Helfrich 2020
E0AE18	Helfrich 2020
E1B6Z6	Helfrich 2020
E1B725	Helfrich 2020
E1B726	Helfrich 2020
E1B748	Helfrich 2020
E1B7A3	Helfrich 2020
E1B7B4	Helfrich 2020
E1B7G3	Helfrich 2020
E1B7K5	Helfrich 2020
E1B7R0	Helfrich 2020
E1B7R4	Helfrich 2020
E1B7S3	Helfrich 2020
E1B7Z4	Helfrich 2020
E1B805	Helfrich 2020
E1B818	Helfrich 2020

E1B864	Helfrich 2020
E1B885	Helfrich 2020
E1B888	Helfrich 2020
E1B891	Helfrich 2020
E1B8B5	Helfrich 2020
E1B8E7	Helfrich 2020
E1B8G9	Helfrich 2020
E1B8H8	Helfrich 2020
E1B8K6	Helfrich 2020
E1B8P9	Helfrich 2020
E1B8Q8	Helfrich 2020
E1B8X4	Helfrich 2020
E1B937	Helfrich 2020
E1B953	Helfrich 2020
E1B9D1	Helfrich 2020
E1B9E8	Helfrich 2020
E1B9G4	Helfrich 2020
E1B9H3	Helfrich 2020
E1B9H4	Helfrich 2020
E1B9H5	Helfrich 2020
E1B9R3	Helfrich 2020
E1B9R8	Helfrich 2020
E1B9S7	Helfrich 2020
E1B9S8	Helfrich 2020
E1B9T9	Helfrich 2020
E1B9V7	Helfrich 2020
E1B9W3	Helfrich 2020
E1BA10	Helfrich 2020
E1BA24	Helfrich 2020
E1BA27	Helfrich 2020

E1BA29	Helfrich 2020
E1BAA2	Helfrich 2020
E1BAB9	Helfrich 2020
E1BAI4	Helfrich 2020
E1BAL7	Helfrich 2020
E1BAU7	Helfrich 2020
E1BAV2	Helfrich 2020
E1BAZ4	Helfrich 2020
E1BB08	Helfrich 2020
E1BB17	Helfrich 2020
E1BB36	Helfrich 2020
E1BB38	Helfrich 2020
E1BB73	Helfrich 2020
E1BB91	Helfrich 2020
E1BB97	Helfrich 2020
E1BBG4	Helfrich 2020
E1BBI8	Helfrich 2020
E1BBJ7	Helfrich 2020
E1BBQ3	Helfrich 2020
E1BBT9	Helfrich 2020
E1BBY7	Helfrich 2020
E1BC59	Helfrich 2020
E1BCE0	Helfrich 2020
E1BCL3	Helfrich 2020
E1BCU6	Helfrich 2020
E1BCU8	Helfrich 2020
E1BCW0	Helfrich 2020
E1BCW3	Helfrich 2020
E1BCX9	Helfrich 2020
E1BD36	Helfrich 2020
E1BD65	Helfrich 2020
E1BDE6	Helfrich 2020
E1BDF3	Helfrich 2020
E1BDF5	Helfrich 2020
E1BDM8	Helfrich 2020
E1BDP3	Helfrich 2020
E1BDR2	Helfrich 2020
E1BDU8	Helfrich 2020
E1BDV7	Helfrich 2020
E1BDW7	Helfrich 2020
E1BDX8	Helfrich 2020
E1BDY3	Helfrich 2020
E1BDZ2	Helfrich 2020
E1BE13	Helfrich 2020
E1BE76	Helfrich 2020
E1BE92	Helfrich 2020
E1BE98	Helfrich 2020
E1BEB4	Helfrich 2020
E1BED8	Helfrich 2020
E1BEG2	Helfrich 2020
E1BEI0	Helfrich 2020
E1BEI7	Helfrich 2020
E1BEK9	Helfrich 2020
E1BEL8	Helfrich 2020
E1BEL9	Helfrich 2020
E1BEM3	Helfrich 2020
E1BEN4	Helfrich 2020
E1BEP7	Helfrich 2020
E1BEQ3	Helfrich 2020
E1BEW3	Helfrich 2020
E1BEX4	Helfrich 2020
E1BF20	Helfrich 2020
E1BF59	Helfrich 2020
E1BF68	Helfrich 2020
E1BF81	Helfrich 2020
E1BF95	Helfrich 2020
E1BFB0	Helfrich 2020
E1BFB4	Helfrich 2020
E1BFB9	Helfrich 2020
E1BFD5	Helfrich 2020
E1BFE9	Helfrich 2020
E1BFG0	Helfrich 2020
E1BFI4	Helfrich 2020
E1BFL8	Helfrich 2020
E1BFN6	Helfrich 2020
E1BFP1	Helfrich 2020
E1BFV0	Helfrich 2020
E1BFX4	Helfrich 2020
E1BG07	Helfrich 2020
E1BG08	Helfrich 2020
E1BG38	Helfrich 2020
E1BG62	Helfrich 2020
E1BG76	Helfrich 2020
E1BGB0	Helfrich 2020
E1BGE5	Helfrich 2020
E1BGH0	Helfrich 2020
E1BGH6	Helfrich 2020
E1BGJ0	Helfrich 2020
E1BGJ4	Helfrich 2020
E1BGL5	Helfrich 2020

E1BGU4	Helfrich 2020
E1BGX4	Helfrich 2020
E1BH06	Helfrich 2020
E1BH78	Helfrich 2020
E1BH79	Helfrich 2020
E1BH94	Helfrich 2020
E1BHE5	Helfrich 2020
E1BHK2	Helfrich 2020
E1BHM9	Helfrich 2020
E1BHN4	Helfrich 2020
E1BHT5	Helfrich 2020
E1BHX7	Helfrich 2020
E1BHY6	Helfrich 2020
E1BI28	Helfrich 2020
E1BI31	Helfrich 2020
E1BI60	Helfrich 2020
E1BI82	Helfrich 2020
E1BI98	Helfrich 2020
E1BIA7	Helfrich 2020
E1BIB4	Helfrich 2020
E1BIC8	Helfrich 2020
E1BIE5	Helfrich 2020
E1BIM8	Helfrich 2020
E1BIN5	Helfrich 2020
E1BIP8	Helfrich 2020
E1BIU0	Helfrich 2020
E1BIU7	Helfrich 2020
E1BIU8	Helfrich 2020
E1BIW0	Helfrich 2020
E1BIZ3	Helfrich 2020

E1BJ08	Helfrich 2020
E1BJ49	Helfrich 2020
E1BJ78	Helfrich 2020
E1BJB1	Helfrich 2020
E1BJF9	Helfrich 2020
E1BJG5	Helfrich 2020
E1BJH7	Helfrich 2020
E1BJL8	Helfrich 2020
E1BJM1	Helfrich 2020
E1BJN3	Helfrich 2020
E1BJP1	Helfrich 2020
E1BJQ7	Helfrich 2020
E1BJV0	Helfrich 2020
E1BJY4	Helfrich 2020
E1BK29	Helfrich 2020
E1BK63	Helfrich 2020
E1BKC9	Helfrich 2020
E1BKI3	Helfrich 2020
E1BKI9	Helfrich 2020
E1BKM4	Helfrich 2020
E1BKQ9	Helfrich 2020
E1BKS0	Helfrich 2020
E1BKT9	Helfrich 2020
E1BKW5	Helfrich 2020
E1BKX3	Helfrich 2020
E1BKX7	Helfrich 2020
E1BKZ1	Helfrich 2020
E1BKZ9	Helfrich 2020
E1BL26	Helfrich 2020
E1BL29	Helfrich 2020

E1BL56	Helfrich 2020
E1BLA8	Helfrich 2020
E1BLB4	Helfrich 2020
E1BLC8	Helfrich 2020
E1BLF0	Helfrich 2020
E1BLF7	Helfrich 2020
E1BLL9	Helfrich 2020
E1BLR9	Helfrich 2020
E1BLV6	Helfrich 2020
E1BLZ8	Helfrich 2020
E1BM12	Helfrich 2020
E1BM26	Helfrich 2020
E1BM28	Helfrich 2020
E1BM48	Helfrich 2020
E1BM57	Helfrich 2020
E1BM92	Helfrich 2020
E1BMD6	Helfrich 2020
E1BMF5	Helfrich 2020
E1BMG1	Helfrich 2020
E1BMG7	Helfrich 2020
E1BMH6	Helfrich 2020
E1BMJ0	Helfrich 2020
E1BMK3	Helfrich 2020
E1BMK7	Helfrich 2020
E1BMM0	Helfrich 2020
E1BMM4	Helfrich 2020
E1BMN5	Helfrich 2020
E1BMP2	Helfrich 2020
E1BMS0	Helfrich 2020
E1BMW2	Helfrich 2020

E1BMW9	Helfrich 2020
E1BMX8	Helfrich 2020
E1BN47	Helfrich 2020
E1BN61	Helfrich 2020
E1BN63	Helfrich 2020
E1BN75	Helfrich 2020
E1BNC9	Helfrich 2020
E1BND0	Helfrich 2020
E1BND6	Helfrich 2020
E1BNF8	Helfrich 2020
E1BNG2	Helfrich 2020
E1BNG8	Helfrich 2020
E1BNH5	Helfrich 2020
E1BNJ0	Helfrich 2020
E1BNJ9	Helfrich 2020
E1BNN7	Helfrich 2020
E1BNP8	Helfrich 2020
E1BNQ4	Helfrich 2020
E1BNQ9	Helfrich 2020
E1BNR0	Helfrich 2020
E1BNR9	Helfrich 2020
E1BNU2	Helfrich 2020
E1BNX1	Helfrich 2020
E1BNY1	Helfrich 2020
E1BNY9	Helfrich 2020
E1BP20	Helfrich 2020
E1BP30	Helfrich 2020
E1BP42	Helfrich 2020
E1BP50	Helfrich 2020
E1BP87	Helfrich 2020

E1BP90	Helfrich 2020
E1BP91	Helfrich 2020
E1BPA9	Helfrich 2020
E1BPB3	Helfrich 2020
E1BPK6	Helfrich 2020
E1BPP6	Helfrich 2020
E1BPP7	Helfrich 2020
E1BPQ9	Helfrich 2020
E1BPW1	Helfrich 2020
E1BQ11	Helfrich 2020
E1BQ16	Helfrich 2020
E1BQ21	Helfrich 2020
E1BQ32	Helfrich 2020
E1BQ37	Helfrich 2020
E9LZ03	Helfrich 2020
F1MAU6	Helfrich 2020
F1MAV0	Helfrich 2020
F1MB04	Helfrich 2020
F1MB08	Helfrich 2020
F1MB60	Helfrich 2020
F1MB84	Helfrich 2020
F1MB85	Helfrich 2020
F1MBG5	Helfrich 2020
F1MBG6	Helfrich 2020
F1MBI1	Helfrich 2020
F1MBJ7	Helfrich 2020
F1MBM9	Helfrich 2020
F1MBN2	Helfrich 2020
F1MBP8	Helfrich 2020
F1MBQ0	Helfrich 2020

F1MBU5	Helfrich 2020
F1MBX4	Helfrich 2020
F1MC11	Helfrich 2020
F1MC22	Helfrich 2020
F1MC45	Helfrich 2020
F1MC48	Helfrich 2020
F1MCF8	Helfrich 2020
F1MCK2	Helfrich 2020
F1MCN8	Helfrich 2020
F1MCT8	Helfrich 2020
F1MCU6	Helfrich 2020
F1MCX5	Helfrich 2020
F1MD34	Helfrich 2020
F1MD44	Helfrich 2020
F1MD58	Helfrich 2020
F1MD73	Helfrich 2020
F1MD79	Helfrich 2020
F1MDA7	Helfrich 2020
F1MDD5	Helfrich 2020
F1MDD6	Helfrich 2020
F1MDH3	Helfrich 2020
F1MDM4	Helfrich 2020
F1MDM6	Helfrich 2020
F1MDR7	Helfrich 2020
F1MDW1	Helfrich 2020
F1ME38	Helfrich 2020
F1ME97	Helfrich 2020
F1MED7	Helfrich 2020
F1MEM8	Helfrich 2020
F1MEN8	Helfrich 2020

F1MEP1	Helfrich 2020
F1MER7	Helfrich 2020
F1MER9	Helfrich 2020
F1MES6	Helfrich 2020
F1MEW3	Helfrich 2020
F1MEY2	Helfrich 2020
F1MF38	Helfrich 2020
F1MF50	Helfrich 2020
F1MF78	Helfrich 2020
F1MF86	Helfrich 2020
F1MFC2	Helfrich 2020
F1MFC6	Helfrich 2020
F1MFD6	Helfrich 2020
F1MFJ6	Helfrich 2020
F1MFJ9	Helfrich 2020
F1MFK7	Helfrich 2020
F1MFR9	Helfrich 2020
F1MFT1	Helfrich 2020
F1MFW9	Helfrich 2020
F1MFZ6	Helfrich 2020
F1MFZ7	Helfrich 2020
F1MG10	Helfrich 2020
F1MG56	Helfrich 2020
F1MGJ4	Helfrich 2020
F1MGK8	Helfrich 2020
F1MGK9	Helfrich 2020
F1MGP5	Helfrich 2020
F1MGR8	Helfrich 2020
F1MGS9	Helfrich 2020
F1MGU7	Helfrich 2020

F1MGY9	Helfrich 2020
F1MGZ5	Helfrich 2020
F1MH20	Helfrich 2020
F1MH24	Helfrich 2020
F1MH40	Helfrich 2020
F1MH48	Helfrich 2020
F1MH61	Helfrich 2020
F1MHB8	Helfrich 2020
F1MHC2	Helfrich 2020
F1MHE7	Helfrich 2020
F1MHF1	Helfrich 2020
F1MHF7	Helfrich 2020
F1MHM5	Helfrich 2020
F1MHR3	Helfrich 2020
F1MHR6	Helfrich 2020
F1MHS5	Helfrich 2020
F1MHT1	Helfrich 2020
F1MHU2	Helfrich 2020
F1MHU9	Helfrich 2020
F1MI32	Helfrich 2020
F1MIF2	Helfrich 2020
F1MIH2	Helfrich 2020
F1MIH4	Helfrich 2020
F1MIH9	Helfrich 2020
F1MIL9	Helfrich 2020
F1MIX6	Helfrich 2020
F1MIZ7	Helfrich 2020
F1MIZ9	Helfrich 2020
F1MJ09	Helfrich 2020
F1MJ12	Helfrich 2020

F1MJ56	Helfrich 2020
F1MJ59	Helfrich 2020
F1MJ73	Helfrich 2020
F1MJ80	Helfrich 2020
F1MJ96	Helfrich 2020
F1MJJ8	Helfrich 2020
F1MJK3	Helfrich 2020
F1MJP7	Helfrich 2020
F1MJQ1	Helfrich 2020
F1MJQ3	Helfrich 2020
F1MJV5	Helfrich 2020
F1MJZ9	Helfrich 2020
F1MK08	Helfrich 2020
F1MK38	Helfrich 2020
F1MK61	Helfrich 2020
F1MKB7	Helfrich 2020
F1MKH6	Helfrich 2020
F1MKJ5	Helfrich 2020
F1MKM4	Helfrich 2020
F1MKS3	Helfrich 2020
F1MKS5	Helfrich 2020
F1MKX4	Helfrich 2020
F1MKX7	Helfrich 2020
F1MKZ5	Helfrich 2020
F1ML12	Helfrich 2020
F1ML72	Helfrich 2020
F1ML89	Helfrich 2020
F1MLA4	Helfrich 2020
F1MLB8	Helfrich 2020
F1MLE1	Helfrich 2020

F1MLE3	Helfrich 2020
F1MLE8	Helfrich 2020
F1MLJ5	Helfrich 2020
F1MLQ1	Helfrich 2020
F1MLV1	Helfrich 2020
F1MLV3	Helfrich 2020
F1MLW0	Helfrich 2020
F1MLW2	Helfrich 2020
F1MLW8	Helfrich 2020
F1MLX0	Helfrich 2020
F1MLX9	Helfrich 2020
F1MM13	Helfrich 2020
F1MM14	Helfrich 2020
F1MM23	Helfrich 2020
F1MM34	Helfrich 2020
F1MM52	Helfrich 2020
F1MM57	Helfrich 2020
F1MM83	Helfrich 2020
F1MM86	Helfrich 2020
F1MM88	Helfrich 2020
F1MMA0	Helfrich 2020
F1MMB0	Helfrich 2020
F1MMC8	Helfrich 2020
F1MMD5	Helfrich 2020
F1MMD7	Helfrich 2020
F1MMG3	Helfrich 2020
F1MMJ6	Helfrich 2020
F1MMK2	Helfrich 2020
F1MMK8	Helfrich 2020
F1MMK9	Helfrich 2020

F1MMP5	Helfrich 2020
F1MMQ5	Helfrich 2020
F1MMR6	Helfrich 2020
F1MMR8	Helfrich 2020
F1MMS9	Helfrich 2020
F1MMV6	Helfrich 2020
F1MMW8	Helfrich 2020
F1MN29	Helfrich 2020
F1MN78	Helfrich 2020
F1MN84	Helfrich 2020
F1MND5	Helfrich 2020
F1MNF8	Helfrich 2020
F1MNG6	Helfrich 2020
F1MNI4	Helfrich 2020
F1MNK0	Helfrich 2020
F1MNL4	Helfrich 2020
F1MNN6	Helfrich 2020
F1MNN7	Helfrich 2020
F1MNQ3	Helfrich 2020
F1MNQ4	Helfrich 2020
F1MNS5	Helfrich 2020
F1MNS8	Helfrich 2020
F1MNV5	Helfrich 2020
F1MNV8	Helfrich 2020
F1MPA1	Helfrich 2020
F1MPD1	Helfrich 2020
F1MPE1	Helfrich 2020
F1MPE5	Helfrich 2020
F1MPG6	Helfrich 2020
F1MPH9	Helfrich 2020

F1MPS5	Helfrich 2020
F1MPZ9	Helfrich 2020
F1MQ37	Helfrich 2020
F1MQ56	Helfrich 2020
F1MQ57	Helfrich 2020
F1MQ65	Helfrich 2020
F1MQ83	Helfrich 2020
F1MQ96	Helfrich 2020
F1MQD1	Helfrich 2020
F1MQH8	Helfrich 2020
F1MQI1	Helfrich 2020
F1MQJ0	Helfrich 2020
F1MQJ8	Helfrich 2020
F1MQT9	Helfrich 2020
F1MQX0	Helfrich 2020
F1MR07	Helfrich 2020
F1MR22	Helfrich 2020
F1MR63	Helfrich 2020
F1MR86	Helfrich 2020
F1MRE5	Helfrich 2020
F1MRM8	Helfrich 2020
F1MRR1	Helfrich 2020
F1MRS1	Helfrich 2020
F1MRZ6	Helfrich 2020
F1MS05	Helfrich 2020
F1MS08	Helfrich 2020
F1MS32	Helfrich 2020
F1MS38	Helfrich 2020
F1MS40	Helfrich 2020
F1MS56	Helfrich 2020

F1MS62	Helfrich 2020
F1MSA1	Helfrich 2020
F1MSB5	Helfrich 2020
F1MSB7	Helfrich 2020
F1MSD2	Helfrich 2020
F1MSE4	Helfrich 2020
F1MSE7	Helfrich 2020
F1MSF1	Helfrich 2020
F1MSI2	Helfrich 2020
F1MSJ9	Helfrich 2020
F1MSM4	Helfrich 2020
F1MSM9	Helfrich 2020
F1MSN2	Helfrich 2020
F1MSW9	Helfrich 2020
F1MSZ6	Helfrich 2020
F1MT25	Helfrich 2020
F1MT69	Helfrich 2020
F1MTG3	Helfrich 2020
F1MTK0	Helfrich 2020
F1MTK2	Helfrich 2020
F1MTP8	Helfrich 2020
F1MTR1	Helfrich 2020
F1MTT3	Helfrich 2020
F1MTV7	Helfrich 2020
F1MTX7	Helfrich 2020
F1MTZ0	Helfrich 2020
F1MU08	Helfrich 2020
F1MU19	Helfrich 2020
F1MU34	Helfrich 2020
F1MU39	Helfrich 2020

F1MU56	Helfrich 2020
F1MU80	Helfrich 2020
F1MU84	Helfrich 2020
F1MU85	Helfrich 2020
F1MUA7	Helfrich 2020
F1MUA8	Helfrich 2020
F1MUB9	Helfrich 2020
F1MUC5	Helfrich 2020
F1MUD4	Helfrich 2020
F1MUF1	Helfrich 2020
F1MUI0	Helfrich 2020
F1MUI5	Helfrich 2020
F1MUK3	Helfrich 2020
F1MUP9	Helfrich 2020
F1MUR6	Helfrich 2020
F1MUT3	Helfrich 2020
F1MUT6	Helfrich 2020
F1MUW4	Helfrich 2020
F1MUZ8	Helfrich 2020
F1MUZ9	Helfrich 2020
F1MV07	Helfrich 2020
F1MV66	Helfrich 2020
F1MV74	Helfrich 2020
F1MV85	Helfrich 2020
F1MVC0	Helfrich 2020
F1MVI9	Helfrich 2020
F1MVJ8	Helfrich 2020
F1MVK1	Helfrich 2020
F1MVT7	Helfrich 2020
F1MVW4	Helfrich 2020

F1MVX2	Helfrich 2020
F1MW27	Helfrich 2020
F1MW38	Helfrich 2020
F1MW39	Helfrich 2020
F1MW44	Helfrich 2020
F1MW60	Helfrich 2020
F1MW68	Helfrich 2020
F1MW79	Helfrich 2020
F1MWD3	Helfrich 2020
F1MWE7	Helfrich 2020
F1MWG9	Helfrich 2020
F1MWI1	Helfrich 2020
F1MWJ3	Helfrich 2020
F1MWK8	Helfrich 2020
F1MWQ2	Helfrich 2020
F1MWR3	Helfrich 2020
F1MWS3	Helfrich 2020
F1MWT0	Helfrich 2020
F1MWU9	Helfrich 2020
F1MWY9	Helfrich 2020
F1MX04	Helfrich 2020
F1MX09	Helfrich 2020
F1MX38	Helfrich 2020
F1MX50	Helfrich 2020
F1MX59	Helfrich 2020
F1MX61	Helfrich 2020
F1MX69	Helfrich 2020
F1MX87	Helfrich 2020
F1MXD4	Helfrich 2020
F1MXE4	Helfrich 2020

F1MXF5	Helfrich 2020
F1MXR0	Helfrich 2020
F1MXS8	Helfrich 2020
F1MXU5	Helfrich 2020
F1MXX2	Helfrich 2020
F1MXX5	Helfrich 2020
F1MXX6	Helfrich 2020
F1MXY9	Helfrich 2020
F1MXZ0	Helfrich 2020
F1MY26	Helfrich 2020
F1MY28	Helfrich 2020
F1MY44	Helfrich 2020
F1MY58	Helfrich 2020
F1MY62	Helfrich 2020
F1MY84	Helfrich 2020
F1MY85	Helfrich 2020
F1MYB8	Helfrich 2020
F1MYC9	Helfrich 2020
F1MYD0	Helfrich 2020
F1MYE4	Helfrich 2020
F1MYG5	Helfrich 2020
F1MYH8	Helfrich 2020
F1MYM3	Helfrich 2020
F1MYM9	Helfrich 2020
F1MYN0	Helfrich 2020
F1MYN2	Helfrich 2020
F1MYN5	Helfrich 2020
F1MYP4	Helfrich 2020
F1MYS2	Helfrich 2020
F1MYS7	Helfrich 2020

F1MYU1	Helfrich 2020
F1MYV9	Helfrich 2020
F1MYX5	Helfrich 2020
F1MYZ4	Helfrich 2020
F1MZ00	Helfrich 2020
F1MZ22	Helfrich 2020
F1MZ33	Helfrich 2020
F1MZ38	Helfrich 2020
F1MZ40	Helfrich 2020
F1MZ69	Helfrich 2020
F1MZ92	Helfrich 2020
F1MZ96	Helfrich 2020
F1MZB4	Helfrich 2020
F1MZD5	Helfrich 2020
F1MZF2	Helfrich 2020
F1MZK0	Helfrich 2020
F1MZK4	Helfrich 2020
F1MZL8	Helfrich 2020
F1MZN7	Helfrich 2020
F1MZP0	Helfrich 2020
F1MZT7	Helfrich 2020
F1MZU2	Helfrich 2020
F1MZV1	Helfrich 2020
F1N027	Helfrich 2020
F1N036	Helfrich 2020
F1N045	Helfrich 2020
F1N076	Helfrich 2020
F1N081	Helfrich 2020
F1N090	Helfrich 2020
F1N091	Helfrich 2020

F1N0E5	Helfrich 2020
F1N0F7	Helfrich 2020
F1N0H3	Helfrich 2020
F1N0L0	Helfrich 2020
F1N0N6	Helfrich 2020
F1N0N7	Helfrich 2020
F1N0R5	Helfrich 2020
F1N0R8	Helfrich 2020
F1N0T3	Helfrich 2020
F1N0V7	Helfrich 2020
F1N0W1	Helfrich 2020
F1N102	Helfrich 2020
F1N120	Helfrich 2020
F1N124	Helfrich 2020
F1N152	Helfrich 2020
F1N169	Helfrich 2020
F1N196	Helfrich 2020
F1N1C7	Helfrich 2020
F1N1D5	Helfrich 2020
F1N1D8	Helfrich 2020
F1N1F7	Helfrich 2020
F1N1G7	Helfrich 2020
F1N1I1	Helfrich 2020
F1N1I6	Helfrich 2020
F1N1R4	Helfrich 2020
F1N1R8	Helfrich 2020
F1N1S8	Helfrich 2020
F1N1S9	Helfrich 2020
F1N1U1	Helfrich 2020
F1N1W5	Helfrich 2020

F1N1X8	Helfrich 2020
F1N1Z2	Helfrich 2020
F1N206	Helfrich 2020
F1N214	Helfrich 2020
F1N226	Helfrich 2020
F1N238	Helfrich 2020
F1N2A2	Helfrich 2020
F1N2D3	Helfrich 2020
F1N2D5	Helfrich 2020
F1N2F1	Helfrich 2020
F1N2G9	Helfrich 2020
F1N2I5	Helfrich 2020
F1N2K0	Helfrich 2020
F1N2L9	Helfrich 2020
F1N2W0	Helfrich 2020
F1N2X7	Helfrich 2020
F1N301	Helfrich 2020
F1N308	Helfrich 2020
F1N318	Helfrich 2020
F1N322	Helfrich 2020
F1N338	Helfrich 2020
F1N339	Helfrich 2020
F1N365	Helfrich 2020
F1N399	Helfrich 2020
F1N3A1	Helfrich 2020
F1N3H1	Helfrich 2020
F1N3I3	Helfrich 2020
F1N3I4	Helfrich 2020
F1N3J3	Helfrich 2020
F1N3K8	Helfrich 2020

F1N3P2	Helfrich 2020
F1N3Q7	Helfrich 2020
F1N3S4	Helfrich 2020
F1N401	Helfrich 2020
F1N405	Helfrich 2020
F1N412	Helfrich 2020
F1N430	Helfrich 2020
F1N431	Helfrich 2020
F1N443	Helfrich 2020
F1N455	Helfrich 2020
F1N458	Helfrich 2020
F1N468	Helfrich 2020
F1N474	Helfrich 2020
F1N4C7	Helfrich 2020
F1N4E4	Helfrich 2020
F1N4F8	Helfrich 2020
F1N4K1	Helfrich 2020
F1N4M7	Helfrich 2020
F1N4N6	Helfrich 2020
F1N4Q2	Helfrich 2020
F1N4Q3	Helfrich 2020
F1N4V5	Helfrich 2020
F1N4Y6	Helfrich 2020
F1N514	Helfrich 2020
F1N545	Helfrich 2020
F1N549	Helfrich 2020
F1N556	Helfrich 2020
F1N579	Helfrich 2020
F1N5H2	Helfrich 2020
F1N5H8	Helfrich 2020

F1N5I2	Helfrich 2020
F1N5J8	Helfrich 2020
F1N5K2	Helfrich 2020
F1N5M2	Helfrich 2020
F1N5P8	Helfrich 2020
F1N5T0	Helfrich 2020
F1N5W4	Helfrich 2020
F1N611	Helfrich 2020
F1N647	Helfrich 2020
F1N650	Helfrich 2020
F1N6A0	Helfrich 2020
F1N6C0	Helfrich 2020
F1N6D4	Helfrich 2020
F1N6G5	Helfrich 2020
F1N6H1	Helfrich 2020
F1N6I5	Helfrich 2020
F1N6T3	Helfrich 2020
F1N6U4	Helfrich 2020
F1N6Y1	Helfrich 2020
F1N6Y7	Helfrich 2020
F1N6Z0	Helfrich 2020
F1N719	Helfrich 2020
F1N726	Helfrich 2020
F1N746	Helfrich 2020
F1N775	Helfrich 2020
F1N789	Helfrich 2020
F1N7B5	Helfrich 2020
F1N7D7	Helfrich 2020
F1N7F9	Helfrich 2020
F1N7H5	Helfrich 2020

F1N7I5	Helfrich 2020
F1N7N8	Helfrich 2020
F1N7R4	Helfrich 2020
F1N7T1	Helfrich 2020
F1N7U2	Helfrich 2020
F1N7V7	Helfrich 2020
F1N7X3	Helfrich 2020
F2FB38	Helfrich 2020
F2FB41	Helfrich 2020
F2FB42	Helfrich 2020
F2Z4C1	Helfrich 2020
F2Z4C6	Helfrich 2020
F2Z4D5	Helfrich 2020
F2Z4E7	Helfrich 2020
F2Z4E9	Helfrich 2020
F2Z4F0	Helfrich 2020
F2Z4F5	Helfrich 2020
F2Z4H3	Helfrich 2020
F2Z4I1	Helfrich 2020
F2Z4I2	Helfrich 2020
F2Z4I5	Helfrich 2020
F2Z4J5	Helfrich 2020
F2Z4J7	Helfrich 2020
F6PWD5	Helfrich 2020
F6Q234	Helfrich 2020
F6Q9X9	Helfrich 2020
F6QE33	Helfrich 2020
F6QK33	Helfrich 2020
F6QNX4	Helfrich 2020
F6QS88	Helfrich 2020
F6R0H3	Helfrich 2020
F6R2J7	Helfrich 2020
F6R6Q1	Helfrich 2020
F6RAG5	Helfrich 2020
F6RJG0	Helfrich 2020
F6RSR1	Helfrich 2020
F6RWK1	Helfrich 2020
F6RYN2	Helfrich 2020
G1K122	Helfrich 2020
G1K192	Helfrich 2020
G1K1P8	Helfrich 2020
G1K1R6	Helfrich 2020
G1K1S1	Helfrich 2020
G1K1X9	Helfrich 2020
G1K231	Helfrich 2020
G3M8V1	Helfrich 2020
G3MWH1	Helfrich 2020
G3MWI5	Helfrich 2020
G3MWR4	Helfrich 2020
G3MWU8	Helfrich 2020
G3MX65	Helfrich 2020
G3MX66	Helfrich 2020
G3MX91	Helfrich 2020
G3MXB5	Helfrich 2020
G3MXC8	Helfrich 2020
G3MXG6	Helfrich 2020
G3MXJ5	Helfrich 2020
G3MXK6	Helfrich 2020
G3MXL3	Helfrich 2020
G3MXR2	Helfrich 2020
G3MXS7	Helfrich 2020
G3MXV0	Helfrich 2020
G3MXV7	Helfrich 2020
G3MY01	Helfrich 2020
G3MY03	Helfrich 2020
G3MY19	Helfrich 2020
G3MY87	Helfrich 2020
G3MYK9	Helfrich 2020
G3MYP1	Helfrich 2020
G3MYT1	Helfrich 2020
G3MYU2	Helfrich 2020
G3MYZ3	Helfrich 2020
G3MZ05	Helfrich 2020
G3MZ44	Helfrich 2020
G3MZ54	Helfrich 2020
G3MZ71	Helfrich 2020
G3MZC1	Helfrich 2020
G3MZD8	Helfrich 2020
G3MZE2	Helfrich 2020
G3MZH4	Helfrich 2020
G3MZI7	Helfrich 2020
G3MZT9	Helfrich 2020
G3MZZ0	Helfrich 2020
G3MZZ6	Helfrich 2020
G3N016	Helfrich 2020
G3N048	Helfrich 2020
G3N088	Helfrich 2020
G3N0P5	Helfrich 2020
G3N0S9	Helfrich 2020
G3N0T0	Helfrich 2020

G3N0V0	Helfrich 2020
G3N0V2	Helfrich 2020
G3N0W8	Helfrich 2020
G3N0X4	Helfrich 2020
G3N132	Helfrich 2020
G3N157	Helfrich 2020
G3N188	Helfrich 2020
G3N1D8	Helfrich 2020
G3N1R1	Helfrich 2020
G3N1U2	Helfrich 2020
G3N1U7	Helfrich 2020
G3N1Y3	Helfrich 2020
G3N252	Helfrich 2020
G3N277	Helfrich 2020
G3N2D7	Helfrich 2020
G3N2D8	Helfrich 2020
G3N2H4	Helfrich 2020
G3N2H5	Helfrich 2020
G3N337	Helfrich 2020
G3N342	Helfrich 2020
G3N361	Helfrich 2020
G3N3B7	Helfrich 2020
G3N3D0	Helfrich 2020
G3N3D4	Helfrich 2020
G3N3N1	Helfrich 2020
G3N3P0	Helfrich 2020
G3N3Q3	Helfrich 2020
G3X696	Helfrich 2020
G3X6I0	Helfrich 2020
G3X6K1	Helfrich 2020
G3X6K8	Helfrich 2020
G3X6L8	Helfrich 2020
G3X6L9	Helfrich 2020
G3X6M2	Helfrich 2020
G3X6N3	Helfrich 2020
G3X6S5	Helfrich 2020
G3X6U1	Helfrich 2020
G3X702	Helfrich 2020
G3X736	Helfrich 2020
G3X745	Helfrich 2020
G3X755	Helfrich 2020
G3X757	Helfrich 2020
G3X782	Helfrich 2020
G3X7A8	Helfrich 2020
G3X7D2	Helfrich 2020
G3X7D7	Helfrich 2020
G3X894	Helfrich 2020
G5E505	Helfrich 2020
G5E513	Helfrich 2020
G5E531	Helfrich 2020
G5E537	Helfrich 2020
G5E567	Helfrich 2020
G5E589	Helfrich 2020
G5E5A7	Helfrich 2020
G5E5C8	Helfrich 2020
G5E5H0	Helfrich 2020
G5E5H2	Helfrich 2020
G5E5K1	Helfrich 2020
G5E5N3	Helfrich 2020
G5E5R3	Helfrich 2020
G5E5T1	Helfrich 2020
G5E5T5	Helfrich 2020
G5E5V1	Helfrich 2020
G5E5Y0	Helfrich 2020
G5E600	Helfrich 2020
G5E604	Helfrich 2020
G5E630	Helfrich 2020
G5E631	Helfrich 2020
G5E6M8	Helfrich 2020
G5E6N7	Helfrich 2020
G8JKW7	Helfrich 2020
G8JKX7	Helfrich 2020
G8JKY4	Helfrich 2020
G8JKY6	Helfrich 2020
G8JKZ1	Helfrich 2020
H2XJF0	Helfrich 2020
H7BWV5	Helfrich 2020
H7BWW0	Helfrich 2020
H7BWW2	Helfrich 2020
J7JXJ4	Helfrich 2020
K4JB97	Helfrich 2020
K4JDT2	Helfrich 2020
K7DXW6	Helfrich 2020
K7QEP0	Helfrich 2020
L7R4Y6	Helfrich 2020
M0QW25	Helfrich 2020
M1ZMP2	Helfrich 2020
M5FKH8	Helfrich 2020
M5FKI8	Helfrich 2020
M5FMV7	Helfrich 2020

O02659	Helfrich 2020
O02675	Helfrich 2020
O02691	Helfrich 2020
O02703	Helfrich 2020
O02717	Helfrich 2020
O02739	Helfrich 2020
O02751	Helfrich 2020
O18739	Helfrich 2020
O18789	Helfrich 2020
O18836	Helfrich 2020
O18879	Helfrich 2020
O18964	Helfrich 2020
O18973	Helfrich 2020
O46375	Helfrich 2020
O46411	Helfrich 2020
O46414	Helfrich 2020
O46415	Helfrich 2020
O62768	Helfrich 2020
O62829	Helfrich 2020
O62830-1	Helfrich 2020
O77482	Helfrich 2020
O77588	Helfrich 2020
O77834	Helfrich 2020
O77977	Helfrich 2020
O97680	Helfrich 2020
O97764	Helfrich 2020
O97941	Helfrich 2020
P00432	Helfrich 2020
P00435	Helfrich 2020
P00442	Helfrich 2020
P00514	Helfrich 2020
P00515	Helfrich 2020
P00517	Helfrich 2020
P00570	Helfrich 2020
P00586	Helfrich 2020
P00727	Helfrich 2020
P00735	Helfrich 2020
P00741	Helfrich 2020
P00743	Helfrich 2020
P00829	Helfrich 2020
P00921	Helfrich 2020
P00974	Helfrich 2020
P00975	Helfrich 2020
P01030	Helfrich 2020
P01035	Helfrich 2020
P01045-2	Helfrich 2020
P01156	Helfrich 2020
P01888	Helfrich 2020
P01966	Helfrich 2020
P02070	Helfrich 2020
P02453	Helfrich 2020
P02465	Helfrich 2020
P02510	Helfrich 2020
P02584	Helfrich 2020
P02633	Helfrich 2020
P02638	Helfrich 2020
P02694	Helfrich 2020
P02702	Helfrich 2020
P04272	Helfrich 2020
P04467	Helfrich 2020
P04836	Helfrich 2020
P04896	Helfrich 2020
P04973-1	Helfrich 2020
P05131-2	Helfrich 2020
P05786	Helfrich 2020
P06504	Helfrich 2020
P06623	Helfrich 2020
P06868	Helfrich 2020
P07107	Helfrich 2020
P07224	Helfrich 2020
P07456	Helfrich 2020
P07688	Helfrich 2020
P08037-1	Helfrich 2020
P08166-1	Helfrich 2020
P08487	Helfrich 2020
P08728	Helfrich 2020
P09487	Helfrich 2020
P09867	Helfrich 2020
P0C0T1	Helfrich 2020
P0CB32	Helfrich 2020
P10096	Helfrich 2020
P10103	Helfrich 2020
P10152	Helfrich 2020
P10462	Helfrich 2020
P10568	Helfrich 2020
P10575	Helfrich 2020
P10790	Helfrich 2020
P10881	Helfrich 2020
P10895	Helfrich 2020
P10948	Helfrich 2020

P11017	Helfrich 2020
P11019	Helfrich 2020
P11116	Helfrich 2020
P11179	Helfrich 2020
P12344	Helfrich 2020
P12378	Helfrich 2020
P12763	Helfrich 2020
P13135	Helfrich 2020
P13213	Helfrich 2020
P13214	Helfrich 2020
P13384	Helfrich 2020
P13696	Helfrich 2020
P14568	Helfrich 2020
P14769	Helfrich 2020
P15103	Helfrich 2020
P15497	Helfrich 2020
P16116	Helfrich 2020
P17248	Helfrich 2020
P17697	Helfrich 2020
P19035	Helfrich 2020
P19120	Helfrich 2020
P19660	Helfrich 2020
P19661	Helfrich 2020
P19803	Helfrich 2020
P19858	Helfrich 2020
P20000	Helfrich 2020
P20004	Helfrich 2020
P20072	Helfrich 2020
P20414	Helfrich 2020
P20427	Helfrich 2020

P20811	Helfrich 2020
P20959	Helfrich 2020
P21146	Helfrich 2020
P21282	Helfrich 2020
P21327	Helfrich 2020
P21793	Helfrich 2020
P21809	Helfrich 2020
P21856	Helfrich 2020
P23356	Helfrich 2020
P23727	Helfrich 2020
P24591	Helfrich 2020
P24627	Helfrich 2020
P25326	Helfrich 2020
P25417	Helfrich 2020
P25975	Helfrich 2020
P26285	Helfrich 2020
P26452	Helfrich 2020
P26779-2	Helfrich 2020
P26882	Helfrich 2020
P26884	Helfrich 2020
P27214-2	Helfrich 2020
P28782	Helfrich 2020
P28800	Helfrich 2020
P28801	Helfrich 2020
P30932	Helfrich 2020
P31404	Helfrich 2020
P31408	Helfrich 2020
P31754	Helfrich 2020
P31976	Helfrich 2020
P33046	Helfrich 2020

P33097	Helfrich 2020
P33672	Helfrich 2020
P34955	Helfrich 2020
P35466	Helfrich 2020
P35604	Helfrich 2020
P35605	Helfrich 2020
P35705	Helfrich 2020
P36225-3	Helfrich 2020
P37141	Helfrich 2020
P37980	Helfrich 2020
P38409	Helfrich 2020
P38447	Helfrich 2020
P40673	Helfrich 2020
P40682	Helfrich 2020
P41500-1	Helfrich 2020
P41541	Helfrich 2020
P41976	Helfrich 2020
P42899	Helfrich 2020
P43033	Helfrich 2020
P46196	Helfrich 2020
P46201	Helfrich 2020
P48034	Helfrich 2020
P48427	Helfrich 2020
P48452-1	Helfrich 2020
P48616	Helfrich 2020
P48644	Helfrich 2020
P48818	Helfrich 2020
P49355	Helfrich 2020
P49410	Helfrich 2020
P49907	Helfrich 2020

P49951	Helfrich 2020
P50227	Helfrich 2020
P50397	Helfrich 2020
P50448	Helfrich 2020
P51122	Helfrich 2020
P52174	Helfrich 2020
P52556	Helfrich 2020
P52898	Helfrich 2020
P53619	Helfrich 2020
P54149	Helfrich 2020
P55052	Helfrich 2020
P55859	Helfrich 2020
P55906	Helfrich 2020
P55918	Helfrich 2020
P56449	Helfrich 2020
P56652	Helfrich 2020
P56701	Helfrich 2020
P56965	Helfrich 2020
P56966	Helfrich 2020
P60519	Helfrich 2020
P60661-1	Helfrich 2020
P60712	Helfrich 2020
P60902	Helfrich 2020
P60984	Helfrich 2020
P60986	Helfrich 2020
P61085	Helfrich 2020
P61157	Helfrich 2020
P61257	Helfrich 2020
P61282	Helfrich 2020
P61284	Helfrich 2020
P61286	Helfrich 2020
P61287	Helfrich 2020
P61356	Helfrich 2020
P61585	Helfrich 2020
P61603	Helfrich 2020
P62194	Helfrich 2020
P62248	Helfrich 2020
P62261	Helfrich 2020
P62739	Helfrich 2020
P62833	Helfrich 2020
P62871	Helfrich 2020
P62894	Helfrich 2020
P62935	Helfrich 2020
P62958	Helfrich 2020
P62964	Helfrich 2020
P62992	Helfrich 2020
P62998	Helfrich 2020
P63097	Helfrich 2020
P63103	Helfrich 2020
P63243	Helfrich 2020
P67774	Helfrich 2020
P67868	Helfrich 2020
P68102	Helfrich 2020
P68103	Helfrich 2020
P68399	Helfrich 2020
P68401	Helfrich 2020
P68509	Helfrich 2020
P79126	Helfrich 2020
P79134	Helfrich 2020
P79135-2	Helfrich 2020
P79136	Helfrich 2020
P79251	Helfrich 2020
P79345	Helfrich 2020
P79465	Helfrich 2020
P80109	Helfrich 2020
P80227	Helfrich 2020
P80311	Helfrich 2020
P80513	Helfrich 2020
P80724	Helfrich 2020
P81187	Helfrich 2020
P81265	Helfrich 2020
P81287	Helfrich 2020
P81425	Helfrich 2020
P81623	Helfrich 2020
P81644	Helfrich 2020
P81948	Helfrich 2020
P83939	Helfrich 2020
P84080	Helfrich 2020
P84081	Helfrich 2020
P85100	Helfrich 2020
Q01314	Helfrich 2020
Q02399	Helfrich 2020
Q04173	Helfrich 2020
Q04467	Helfrich 2020
Q05443	Helfrich 2020
Q05927	Helfrich 2020
Q05B55	Helfrich 2020
Q05B60	Helfrich 2020
Q05B89	Helfrich 2020
Q07130	Helfrich 2020

Q07537	Helfrich 2020
Q08D83-2	Helfrich 2020
Q08D91	Helfrich 2020
Q08DB4	Helfrich 2020
Q08DD1	Helfrich 2020
Q08DD6	Helfrich 2020
Q08DE9	Helfrich 2020
Q08DJ3	Helfrich 2020
Q08DK5	Helfrich 2020
Q08DL0	Helfrich 2020
Q08DL9	Helfrich 2020
Q08DM8	Helfrich 2020
Q08DN7	Helfrich 2020
Q08DP0	Helfrich 2020
Q08DQ1	Helfrich 2020
Q08DQ6	Helfrich 2020
Q08DR7	Helfrich 2020
Q08DS7	Helfrich 2020
Q08DU4	Helfrich 2020
Q08DV2	Helfrich 2020
Q08DW2	Helfrich 2020
Q08DY1	Helfrich 2020
Q08DY5	Helfrich 2020
Q08E01	Helfrich 2020
Q08E11	Helfrich 2020
Q08E20	Helfrich 2020
Q08E32	Helfrich 2020
Q08E38	Helfrich 2020
Q08E52	Helfrich 2020
Q08E54	Helfrich 2020

Q08E58	Helfrich 2020
Q08E64	Helfrich 2020
Q09430	Helfrich 2020
Q09TE3	Helfrich 2020
Q0II26	Helfrich 2020
Q0II27	Helfrich 2020
Q0II31	Helfrich 2020
Q0II49	Helfrich 2020
Q0II59	Helfrich 2020
Q0IIF0	Helfrich 2020
Q0IIF2	Helfrich 2020
Q0IIF6	Helfrich 2020
Q0IIG7	Helfrich 2020
Q0IIG8	Helfrich 2020
Q0IIH5	Helfrich 2020
Q0IIH7	Helfrich 2020
Q0III3	Helfrich 2020
Q0III8	Helfrich 2020
Q0IIJ0	Helfrich 2020
Q0IIL6	Helfrich 2020
Q0IIM2	Helfrich 2020
Q0IIM3	Helfrich 2020
Q0IIM6	Helfrich 2020
Q0P568	Helfrich 2020
Q0P569	Helfrich 2020
Q0P570	Helfrich 2020
Q0P580	Helfrich 2020
Q0P592	Helfrich 2020
Q0P594	Helfrich 2020
Q0P5A1	Helfrich 2020

Q0P5B0	Helfrich 2020
Q0P5D0	Helfrich 2020
Q0P5D4	Helfrich 2020
Q0P5D6	Helfrich 2020
Q0P5F2	Helfrich 2020
Q0P5F3	Helfrich 2020
Q0P5F6	Helfrich 2020
Q0P5F7	Helfrich 2020
Q0P5G4	Helfrich 2020
Q0P5H9	Helfrich 2020
Q0P5I7	Helfrich 2020
Q0P5J8	Helfrich 2020
Q0P5M8	Helfrich 2020
Q0V7L6	Helfrich 2020
Q0V7M0	Helfrich 2020
Q0V7N2	Helfrich 2020
Q0V8A3	Helfrich 2020
Q0V8D5	Helfrich 2020
Q0V8F7	Helfrich 2020
Q0V8H6	Helfrich 2020
Q0V8J4	Helfrich 2020
Q0V8R6	Helfrich 2020
Q0V8S0	Helfrich 2020
Q0VBZ0	Helfrich 2020
Q0VBZ2	Helfrich 2020
Q0VC24	Helfrich 2020
Q0VC36	Helfrich 2020
Q0VC37	Helfrich 2020
Q0VC53	Helfrich 2020
Q0VC55	Helfrich 2020

Q0VC68	Helfrich 2020
Q0VC82	Helfrich 2020
Q0VC92	Helfrich 2020
Q0VC96	Helfrich 2020
Q0VCA5	Helfrich 2020
Q0VCC0	Helfrich 2020
Q0VCH0	Helfrich 2020
Q0VCH9	Helfrich 2020
Q0VCI1	Helfrich 2020
Q0VCI3	Helfrich 2020
Q0VCJ2	Helfrich 2020
Q0VCK0	Helfrich 2020
Q0VCK5	Helfrich 2020
Q0VCL3	Helfrich 2020
Q0VCM4	Helfrich 2020
Q0VCN1	Helfrich 2020
Q0VCP3	Helfrich 2020
Q0VCP4	Helfrich 2020
Q0VCQ0	Helfrich 2020
Q0VCQ6	Helfrich 2020
Q0VCQ9	Helfrich 2020
Q0VCS8	Helfrich 2020
Q0VCS9	Helfrich 2020
Q0VCU1	Helfrich 2020
Q0VCU3	Helfrich 2020
Q0VCU8	Helfrich 2020
Q0VCV0	Helfrich 2020
Q0VCW2	Helfrich 2020
Q0VCW8	Helfrich 2020
Q0VCX2	Helfrich 2020
Q0VCX4	Helfrich 2020
Q0VCX5	Helfrich 2020
Q0VCY7	Helfrich 2020
Q0VCY8	Helfrich 2020
Q0VCZ4	Helfrich 2020
Q0VD16	Helfrich 2020
Q0VD18	Helfrich 2020
Q0VD19	Helfrich 2020
Q0VD22	Helfrich 2020
Q0VD27	Helfrich 2020
Q0VD29	Helfrich 2020
Q0VD48	Helfrich 2020
Q0VD49	Helfrich 2020
Q0VD53	Helfrich 2020
Q0VFX8	Helfrich 2020
Q0VFX9	Helfrich 2020
Q10741	Helfrich 2020
Q148C9	Helfrich 2020
Q148D3	Helfrich 2020
Q148E9	Helfrich 2020
Q148F1	Helfrich 2020
Q148G4	Helfrich 2020
Q148G9	Helfrich 2020
Q148I1	Helfrich 2020
Q148J4	Helfrich 2020
Q148J6	Helfrich 2020
Q148L6	Helfrich 2020
Q148N0	Helfrich 2020
Q17QB3	Helfrich 2020
Q17QC7	Helfrich 2020
Q17QE2	Helfrich 2020
Q17QG2	Helfrich 2020
Q17QH2	Helfrich 2020
Q17QH5	Helfrich 2020
Q17QI3	Helfrich 2020
Q17QJ1	Helfrich 2020
Q17QK3	Helfrich 2020
Q17QL1	Helfrich 2020
Q17QL7	Helfrich 2020
Q17QL8	Helfrich 2020
Q17QM6	Helfrich 2020
Q17QN3	Helfrich 2020
Q17QN6	Helfrich 2020
Q17QP9	Helfrich 2020
Q17QQ1	Helfrich 2020
Q17QQ2	Helfrich 2020
Q17QR2	Helfrich 2020
Q17QT7	Helfrich 2020
Q17QU3	Helfrich 2020
Q17QZ9	Helfrich 2020
Q17R06	Helfrich 2020
Q17R07	Helfrich 2020
Q17R10	Helfrich 2020
Q1JP79	Helfrich 2020
Q1JPA0	Helfrich 2020
Q1JPA2	Helfrich 2020
Q1JPA6	Helfrich 2020
Q1JPB0	Helfrich 2020
Q1JPB6	Helfrich 2020
Q1JPD3	Helfrich 2020

Q1JPE3	Helfrich 2020
Q1JPG7	Helfrich 2020
Q1JPH6	Helfrich 2020
Q1JPJ2	Helfrich 2020
Q1JQ98	Helfrich 2020
Q1JQA5	Helfrich 2020
Q1JQA7	Helfrich 2020
Q1JQB2	Helfrich 2020
Q1JQD2	Helfrich 2020
Q1JQD4	Helfrich 2020
Q1LZ72	Helfrich 2020
Q1LZ74	Helfrich 2020
Q1LZ81	Helfrich 2020
Q1LZA1	Helfrich 2020
Q1LZA3	Helfrich 2020
Q1LZB2	Helfrich 2020
Q1LZD9	Helfrich 2020
Q1RMH4	Helfrich 2020
Q1RMH5	Helfrich 2020
Q1RMH8	Helfrich 2020
Q1RMI2	Helfrich 2020
Q1RMI4	Helfrich 2020
Q1RMI8	Helfrich 2020
Q1RMJ6	Helfrich 2020
Q1RML6	Helfrich 2020
Q1RML9	Helfrich 2020
Q1RMM1	Helfrich 2020
Q1RMM9	Helfrich 2020
Q1RMN8	Helfrich 2020
Q1RMQ7	Helfrich 2020

Q1RMR2	Helfrich 2020
Q1RMR3	Helfrich 2020
Q1RMR9	Helfrich 2020
Q1RMS2	Helfrich 2020
Q1RMT6	Helfrich 2020
Q1RMW4	Helfrich 2020
Q1RMW9	Helfrich 2020
Q1RMX2	Helfrich 2020
Q1RMX7	Helfrich 2020
Q1ZYR0	Helfrich 2020
Q24JZ6	Helfrich 2020
Q24JZ7	Helfrich 2020
Q24JZ8	Helfrich 2020
Q24K00	Helfrich 2020
Q24K01	Helfrich 2020
Q24K02	Helfrich 2020
Q24K03	Helfrich 2020
Q24K04	Helfrich 2020
Q24K21	Helfrich 2020
Q27965	Helfrich 2020
Q27966	Helfrich 2020
Q27970	Helfrich 2020
Q27971	Helfrich 2020
Q27975	Helfrich 2020
Q27991	Helfrich 2020
Q28007	Helfrich 2020
Q28009	Helfrich 2020
Q28021	Helfrich 2020
Q28029	Helfrich 2020
Q28034	Helfrich 2020

Q28042	Helfrich 2020
Q28085	Helfrich 2020
Q28104	Helfrich 2020
Q28107	Helfrich 2020
Q28133	Helfrich 2020
Q28150	Helfrich 2020
Q28153	Helfrich 2020
Q28194	Helfrich 2020
Q28205	Helfrich 2020
Q28908	Helfrich 2020
Q28910	Helfrich 2020
Q29437	Helfrich 2020
Q29443	Helfrich 2020
Q29448	Helfrich 2020
Q29451	Helfrich 2020
Q29460	Helfrich 2020
Q29626	Helfrich 2020
Q29RH3	Helfrich 2020
Q29RI6	Helfrich 2020
Q29RI9	Helfrich 2020
Q29RJ1	Helfrich 2020
Q29RK1	Helfrich 2020
Q29RK4	Helfrich 2020
Q29RL2	Helfrich 2020
Q29RL9	Helfrich 2020
Q29RN2	Helfrich 2020
Q29RQ1	Helfrich 2020
Q29RQ2	Helfrich 2020
Q29RS5	Helfrich 2020
Q29RT7	Helfrich 2020

Q29RY9	Helfrich 2020
Q29RZ0	Helfrich 2020
Q29RZ1	Helfrich 2020
Q29RZ5	Helfrich 2020
Q29S00	Helfrich 2020
Q29S21	Helfrich 2020
Q2HJ26	Helfrich 2020
Q2HJ33	Helfrich 2020
Q2HJ47	Helfrich 2020
Q2HJ49	Helfrich 2020
Q2HJ54	Helfrich 2020
Q2HJ56	Helfrich 2020
Q2HJ57	Helfrich 2020
Q2HJ58	Helfrich 2020
Q2HJ60	Helfrich 2020
Q2HJ73	Helfrich 2020
Q2HJ81	Helfrich 2020
Q2HJ86	Helfrich 2020
Q2HJ88	Helfrich 2020
Q2HJ94	Helfrich 2020
Q2HJB6	Helfrich 2020
Q2HJD3	Helfrich 2020
Q2HJD7	Helfrich 2020
Q2HJD8	Helfrich 2020
Q2HJE4	Helfrich 2020
Q2HJF0	Helfrich 2020
Q2HJG5	Helfrich 2020
Q2HJH1	Helfrich 2020
Q2HJH2	Helfrich 2020
Q2HJH3	Helfrich 2020

Q2HJH7	Helfrich 2020
Q2HJH9	Helfrich 2020
Q2HJI1	Helfrich 2020
Q2HJJ0	Helfrich 2020
Q2KHT7	Helfrich 2020
Q2KHU0	Helfrich 2020
Q2KHU5	Helfrich 2020
Q2KHU8	Helfrich 2020
Q2KHX6	Helfrich 2020
Q2KHZ6	Helfrich 2020
Q2KI42-1	Helfrich 2020
Q2KI56	Helfrich 2020
Q2KI84	Helfrich 2020
Q2KI86	Helfrich 2020
Q2KI95	Helfrich 2020
Q2KIA2	Helfrich 2020
Q2KIA5	Helfrich 2020
Q2KIA9	Helfrich 2020
Q2KIC3	Helfrich 2020
Q2KIC5	Helfrich 2020
Q2KIC7	Helfrich 2020
Q2KID6	Helfrich 2020
Q2KIF2	Helfrich 2020
Q2KIG2	Helfrich 2020
Q2KIG3	Helfrich 2020
Q2KII4	Helfrich 2020
Q2KII9	Helfrich 2020
Q2KIK0	Helfrich 2020
Q2KIK6	Helfrich 2020
Q2KIM0	Helfrich 2020

Q2KIN5	Helfrich 2020
Q2KIQ3	Helfrich 2020
Q2KIS7	Helfrich 2020
Q2KIT0	Helfrich 2020
Q2KIT5	Helfrich 2020
Q2KIT8	Helfrich 2020
Q2KIU3	Helfrich 2020
Q2KIV7	Helfrich 2020
Q2KIV8	Helfrich 2020
Q2KIV9	Helfrich 2020
Q2KIW9	Helfrich 2020
Q2KIX6	Helfrich 2020
Q2KIX7	Helfrich 2020
Q2KJ19	Helfrich 2020
Q2KJ25	Helfrich 2020
Q2KJ30	Helfrich 2020
Q2KJ32	Helfrich 2020
Q2KJ39	Helfrich 2020
Q2KJ41	Helfrich 2020
Q2KJ44	Helfrich 2020
Q2KJ46	Helfrich 2020
Q2KJ63	Helfrich 2020
Q2KJ77	Helfrich 2020
Q2KJ81	Helfrich 2020
Q2KJ86	Helfrich 2020
Q2KJ93	Helfrich 2020
Q2KJ97-1	Helfrich 2020
Q2KJA1	Helfrich 2020
Q2KJB1	Helfrich 2020
Q2KJD0	Helfrich 2020

Q2KJD7	Helfrich 2020
Q2KJE5	Helfrich 2020
Q2KJE7	Helfrich 2020
Q2KJF1	Helfrich 2020
Q2KJG2	Helfrich 2020
Q2KJH0	Helfrich 2020
Q2KJH4	Helfrich 2020
Q2KJH6	Helfrich 2020
Q2KJH7	Helfrich 2020
Q2KJI3	Helfrich 2020
Q2KJJ4	Helfrich 2020
Q2KJJ7	Helfrich 2020
Q2KJJ8	Helfrich 2020
Q2KJJ9	Helfrich 2020
Q2LGB5	Helfrich 2020
Q2LGB8	Helfrich 2020
Q2NKS3	Helfrich 2020
Q2NKU4	Helfrich 2020
Q2NKY7	Helfrich 2020
Q2NKZ1	Helfrich 2020
Q2NKZ9	Helfrich 2020
Q2NL00	Helfrich 2020
Q2NL22	Helfrich 2020
Q2NL24	Helfrich 2020
Q2NL29	Helfrich 2020
Q2NL31	Helfrich 2020
Q2NL36	Helfrich 2020
Q2NL37	Helfrich 2020
Q2T9P4	Helfrich 2020
Q2T9S0	Helfrich 2020

Q2T9S4	Helfrich 2020
Q2T9T7	Helfrich 2020
Q2T9U0	Helfrich 2020
Q2T9U1	Helfrich 2020
Q2T9V8	Helfrich 2020
Q2T9X7	Helfrich 2020
Q2T9Y6	Helfrich 2020
Q2TA08	Helfrich 2020
Q2TA49	Helfrich 2020
Q2TBG8	Helfrich 2020
Q2TBI4	Helfrich 2020
Q2TBL9	Helfrich 2020
Q2TBM6	Helfrich 2020
Q2TBQ1	Helfrich 2020
Q2TBQ5	Helfrich 2020
Q2TBR0	Helfrich 2020
Q2TBR3	Helfrich 2020
Q2TBU5	Helfrich 2020
Q2TBV3	Helfrich 2020
Q2TBW8	Helfrich 2020
Q2TBX0	Helfrich 2020
Q2TBX1	Helfrich 2020
Q2TBX4	Helfrich 2020
Q2UVX4	Helfrich 2020
Q2YDE4	Helfrich 2020
Q2YDE9	Helfrich 2020
Q2YDG3	Helfrich 2020
Q2YDM1	Helfrich 2020
Q2YDP3	Helfrich 2020
Q32KL2	Helfrich 2020

Q32KP9	Helfrich 2020
Q32KR8	Helfrich 2020
Q32KS0	Helfrich 2020
Q32KV6	Helfrich 2020
Q32KW2	Helfrich 2020
Q32KX8	Helfrich 2020
Q32KX9	Helfrich 2020
Q32KY4	Helfrich 2020
Q32L31	Helfrich 2020
Q32L41	Helfrich 2020
Q32L46	Helfrich 2020
Q32L76	Helfrich 2020
Q32L92	Helfrich 2020
Q32L93	Helfrich 2020
Q32L99	Helfrich 2020
Q32LC3	Helfrich 2020
Q32LC7	Helfrich 2020
Q32LE4	Helfrich 2020
Q32LE5	Helfrich 2020
Q32LE9	Helfrich 2020
Q32LF7	Helfrich 2020
Q32LG3	Helfrich 2020
Q32LM0	Helfrich 2020
Q32LM2	Helfrich 2020
Q32LN7	Helfrich 2020
Q32LP0	Helfrich 2020
Q32P72	Helfrich 2020
Q32PA4	Helfrich 2020
Q32PB8	Helfrich 2020
Q32PB9	Helfrich 2020

Q32PC9-1	Helfrich 2020
Q32PD5	Helfrich 2020
Q32PF2	Helfrich 2020
Q32PF3	Helfrich 2020
Q32PG1	Helfrich 2020
Q32PH8	Helfrich 2020
Q32PJ6	Helfrich 2020
Q32PK0	Helfrich 2020
Q32S38	Helfrich 2020
Q32T06	Helfrich 2020
Q3B7M2	Helfrich 2020
Q3B7M5	Helfrich 2020
Q3B7M9	Helfrich 2020
Q3B7N2	Helfrich 2020
Q3MHE2	Helfrich 2020
Q3MHE4	Helfrich 2020
Q3MHF7	Helfrich 2020
Q3MHG3	Helfrich 2020
Q3MHH4	Helfrich 2020
Q3MHH9	Helfrich 2020
Q3MHK9	Helfrich 2020
Q3MHL3	Helfrich 2020
Q3MHL4	Helfrich 2020
Q3MHL7	Helfrich 2020
Q3MHM5	Helfrich 2020
Q3MHN0	Helfrich 2020
Q3MHN2	Helfrich 2020
Q3MHN5	Helfrich 2020
Q3MHP1	Helfrich 2020
Q3MHP2	Helfrich 2020
Q3MHP5	Helfrich 2020
Q3MHR0	Helfrich 2020
Q3MHR7	Helfrich 2020
Q3MHW8	Helfrich 2020
Q3MHX3	Helfrich 2020
Q3MHX5	Helfrich 2020
Q3MHY1	Helfrich 2020
Q3MHY6	Helfrich 2020
Q3MI00	Helfrich 2020
Q3MI06	Helfrich 2020
Q3SWW9	Helfrich 2020
Q3SWX3	Helfrich 2020
Q3SWX8	Helfrich 2020
Q3SWY3	Helfrich 2020
Q3SWY7	Helfrich 2020
Q3SWZ6	Helfrich 2020
Q3SX04	Helfrich 2020
Q3SX29	Helfrich 2020
Q3SX43	Helfrich 2020
Q3SX44	Helfrich 2020
Q3SX46	Helfrich 2020
Q3SX47	Helfrich 2020
Q3SYR0	Helfrich 2020
Q3SYR8	Helfrich 2020
Q3SYT9	Helfrich 2020
Q3SYU2	Helfrich 2020
Q3SYU6	Helfrich 2020
Q3SYU7	Helfrich 2020
Q3SYV4	Helfrich 2020
Q3SYW1	Helfrich 2020
Q3SYW6	Helfrich 2020
Q3SYZ2	Helfrich 2020
Q3SYZ4	Helfrich 2020
Q3SYZ5	Helfrich 2020
Q3SYZ6	Helfrich 2020
Q3SZ07	Helfrich 2020
Q3SZ15	Helfrich 2020
Q3SZ16	Helfrich 2020
Q3SZ18	Helfrich 2020
Q3SZ19	Helfrich 2020
Q3SZ20	Helfrich 2020
Q3SZ32	Helfrich 2020
Q3SZ43	Helfrich 2020
Q3SZ52	Helfrich 2020
Q3SZ54	Helfrich 2020
Q3SZ62	Helfrich 2020
Q3SZ65	Helfrich 2020
Q3SZ73	Helfrich 2020
Q3SZ76	Helfrich 2020
Q3SZ81	Helfrich 2020
Q3SZ85	Helfrich 2020
Q3SZ96	Helfrich 2020
Q3SZA0	Helfrich 2020
Q3SZA5	Helfrich 2020
Q3SZB1	Helfrich 2020
Q3SZB6	Helfrich 2020
Q3SZB7	Helfrich 2020
Q3SZC2	Helfrich 2020
Q3SZC4	Helfrich 2020
Q3SZC6	Helfrich 2020

Q3SZE9	Helfrich 2020
Q3SZF2	Helfrich 2020
Q3SZF8	Helfrich 2020
Q3SZG7	Helfrich 2020
Q3SZH5	Helfrich 2020
Q3SZH7	Helfrich 2020
Q3SZI0	Helfrich 2020
Q3SZI4	Helfrich 2020
Q3SZI8	Helfrich 2020
Q3SZJ9	Helfrich 2020
Q3SZK6	Helfrich 2020
Q3SZK8	Helfrich 2020
Q3SZM9	Helfrich 2020
Q3SZN0	Helfrich 2020
Q3SZN2	Helfrich 2020
Q3SZN4	Helfrich 2020
Q3SZN8	Helfrich 2020
Q3SZR3	Helfrich 2020
Q3SZR8	Helfrich 2020
Q3SZT2	Helfrich 2020
Q3SZT5	Helfrich 2020
Q3SZV7	Helfrich 2020
Q3T000	Helfrich 2020
Q3T003	Helfrich 2020
Q3T004	Helfrich 2020
Q3T005	Helfrich 2020
Q3T010	Helfrich 2020
Q3T015	Helfrich 2020
Q3T018	Helfrich 2020
Q3T030	Helfrich 2020
Q3T035	Helfrich 2020
Q3T054	Helfrich 2020
Q3T057	Helfrich 2020
Q3T076	Helfrich 2020
Q3T087	Helfrich 2020
Q3T093	Helfrich 2020
Q3T0A3	Helfrich 2020
Q3T0B6	Helfrich 2020
Q3T0B7	Helfrich 2020
Q3T0C7	Helfrich 2020
Q3T0D0	Helfrich 2020
Q3T0D5	Helfrich 2020
Q3T0D7	Helfrich 2020
Q3T0E0	Helfrich 2020
Q3T0E5	Helfrich 2020
Q3T0E7	Helfrich 2020
Q3T0F7	Helfrich 2020
Q3T0F9	Helfrich 2020
Q3T0G3	Helfrich 2020
Q3T0G5	Helfrich 2020
Q3T0I2	Helfrich 2020
Q3T0I4	Helfrich 2020
Q3T0I5	Helfrich 2020
Q3T0J0	Helfrich 2020
Q3T0K2	Helfrich 2020
Q3T0L2	Helfrich 2020
Q3T0L5	Helfrich 2020
Q3T0L7	Helfrich 2020
Q3T0M0	Helfrich 2020
Q3T0M7	Helfrich 2020
Q3T0N1	Helfrich 2020
Q3T0N5	Helfrich 2020
Q3T0P6	Helfrich 2020
Q3T0Q3	Helfrich 2020
Q3T0Q4	Helfrich 2020
Q3T0Q6	Helfrich 2020
Q3T0R1	Helfrich 2020
Q3T0R7	Helfrich 2020
Q3T0S6	Helfrich 2020
Q3T0S7	Helfrich 2020
Q3T0T1	Helfrich 2020
Q3T0T7	Helfrich 2020
Q3T0U1	Helfrich 2020
Q3T0U2	Helfrich 2020
Q3T0U3	Helfrich 2020
Q3T0U5	Helfrich 2020
Q3T0V3	Helfrich 2020
Q3T0V4	Helfrich 2020
Q3T0V7	Helfrich 2020
Q3T0V9	Helfrich 2020
Q3T0W4	Helfrich 2020
Q3T0X5	Helfrich 2020
Q3T0X6	Helfrich 2020
Q3T0X8	Helfrich 2020
Q3T0Y1	Helfrich 2020
Q3T0Y5	Helfrich 2020
Q3T0Z7	Helfrich 2020
Q3T0Z8	Helfrich 2020
Q3T101	Helfrich 2020
Q3T102	Helfrich 2020

Q3T105	Helfrich 2020
Q3T106	Helfrich 2020
Q3T108	Helfrich 2020
Q3T112	Helfrich 2020
Q3T114	Helfrich 2020
Q3T122	Helfrich 2020
Q3T140	Helfrich 2020
Q3T145	Helfrich 2020
Q3T147	Helfrich 2020
Q3T148	Helfrich 2020
Q3T149	Helfrich 2020
Q3T168	Helfrich 2020
Q3T169	Helfrich 2020
Q3T171	Helfrich 2020
Q3T172	Helfrich 2020
Q3Y5Z3	Helfrich 2020
Q3YJF3	Helfrich 2020
Q3YJF7	Helfrich 2020
Q3YJJ7	Helfrich 2020
Q3ZBA6	Helfrich 2020
Q3ZBA8	Helfrich 2020
Q3ZBD0	Helfrich 2020
Q3ZBD2	Helfrich 2020
Q3ZBD3	Helfrich 2020
Q3ZBD7	Helfrich 2020
Q3ZBD9	Helfrich 2020
Q3ZBE9	Helfrich 2020
Q3ZBF0	Helfrich 2020
Q3ZBF7	Helfrich 2020
Q3ZBG0	Helfrich 2020
Q3ZBG1	Helfrich 2020
Q3ZBG2	Helfrich 2020
Q3ZBG9	Helfrich 2020
Q3ZBH0	Helfrich 2020
Q3ZBH2	Helfrich 2020
Q3ZBH5	Helfrich 2020
Q3ZBH8	Helfrich 2020
Q3ZBH9	Helfrich 2020
Q3ZBK2	Helfrich 2020
Q3ZBL1	Helfrich 2020
Q3ZBL4	Helfrich 2020
Q3ZBM5	Helfrich 2020
Q3ZBN0	Helfrich 2020
Q3ZBQ0	Helfrich 2020
Q3ZBQ2	Helfrich 2020
Q3ZBS3	Helfrich 2020
Q3ZBS7	Helfrich 2020
Q3ZBU0	Helfrich 2020
Q3ZBU7	Helfrich 2020
Q3ZBV1	Helfrich 2020
Q3ZBV8	Helfrich 2020
Q3ZBV9	Helfrich 2020
Q3ZBW4	Helfrich 2020
Q3ZBW5	Helfrich 2020
Q3ZBX5	Helfrich 2020
Q3ZBY4	Helfrich 2020
Q3ZBY8	Helfrich 2020
Q3ZBZ1	Helfrich 2020
Q3ZBZ8	Helfrich 2020
Q3ZC09	Helfrich 2020
Q3ZC10	Helfrich 2020
Q3ZC13	Helfrich 2020
Q3ZC32	Helfrich 2020
Q3ZC41	Helfrich 2020
Q3ZC42	Helfrich 2020
Q3ZC44	Helfrich 2020
Q3ZC53	Helfrich 2020
Q3ZC64	Helfrich 2020
Q3ZC84	Helfrich 2020
Q3ZC87	Helfrich 2020
Q3ZCA2	Helfrich 2020
Q3ZCA7	Helfrich 2020
Q3ZCC8	Helfrich 2020
Q3ZCC9	Helfrich 2020
Q3ZCE0	Helfrich 2020
Q3ZCE1	Helfrich 2020
Q3ZCE2	Helfrich 2020
Q3ZCE8	Helfrich 2020
Q3ZCF0	Helfrich 2020
Q3ZCF3	Helfrich 2020
Q3ZCG6	Helfrich 2020
Q3ZCH0	Helfrich 2020
Q3ZCH5	Helfrich 2020
Q3ZCH9	Helfrich 2020
Q3ZCI4	Helfrich 2020
Q3ZCI9	Helfrich 2020
Q3ZCJ2	Helfrich 2020
Q3ZCJ6	Helfrich 2020
Q3ZCK1	Helfrich 2020
Q3ZCK3	Helfrich 2020

Q3ZCK9	Helfrich 2020
Q3ZCL5	Helfrich 2020
Q3ZEJ6	Helfrich 2020
Q4JF28	Helfrich 2020
Q4U5R4	Helfrich 2020
Q56JU9	Helfrich 2020
Q56JV6	Helfrich 2020
Q56JV9	Helfrich 2020
Q56JW4	Helfrich 2020
Q56JX3	Helfrich 2020
Q56JX5	Helfrich 2020
Q56JX6	Helfrich 2020
Q56JX8	Helfrich 2020
Q56JY0	Helfrich 2020
Q56JZ5	Helfrich 2020
Q56JZ9	Helfrich 2020
Q56K10	Helfrich 2020
Q56K14	Helfrich 2020
Q58CQ2	Helfrich 2020
Q58CQ9	Helfrich 2020
Q58CS7	Helfrich 2020
Q58CS8	Helfrich 2020
Q58CX1	Helfrich 2020
Q58D08	Helfrich 2020
Q58D31	Helfrich 2020
Q58D43	Helfrich 2020
Q58D56	Helfrich 2020
Q58D62	Helfrich 2020
Q58D84	Helfrich 2020
Q58DA0	Helfrich 2020
Q58DC0	Helfrich 2020
Q58DG1	Helfrich 2020
Q58DJ9	Helfrich 2020
Q58DK5	Helfrich 2020
Q58DL9	Helfrich 2020
Q58DM8	Helfrich 2020
Q58DN4	Helfrich 2020
Q58DP6	Helfrich 2020
Q58DQ0	Helfrich 2020
Q58DQ3	Helfrich 2020
Q58DS9	Helfrich 2020
Q58DT1	Helfrich 2020
Q58DU5	Helfrich 2020
Q58DU7	Helfrich 2020
Q58DV7	Helfrich 2020
Q58DW0	Helfrich 2020
Q58DW5	Helfrich 2020
Q58DW6	Helfrich 2020
Q59A28	Helfrich 2020
Q59A32	Helfrich 2020
Q5BIP4	Helfrich 2020
Q5BIR5	Helfrich 2020
Q5BIS9	Helfrich 2020
Q5DPW9	Helfrich 2020
Q5E938	Helfrich 2020
Q5E946	Helfrich 2020
Q5E947	Helfrich 2020
Q5E949	Helfrich 2020
Q5E951	Helfrich 2020
Q5E952	Helfrich 2020
Q5E953	Helfrich 2020
Q5E954	Helfrich 2020
Q5E956	Helfrich 2020
Q5E958	Helfrich 2020
Q5E959	Helfrich 2020
Q5E963	Helfrich 2020
Q5E964	Helfrich 2020
Q5E966	Helfrich 2020
Q5E970	Helfrich 2020
Q5E973	Helfrich 2020
Q5E983	Helfrich 2020
Q5E984	Helfrich 2020
Q5E987	Helfrich 2020
Q5E988	Helfrich 2020
Q5E992	Helfrich 2020
Q5E997	Helfrich 2020
Q5E9A1	Helfrich 2020
Q5E9A3	Helfrich 2020
Q5E9A6	Helfrich 2020
Q5E9B1	Helfrich 2020
Q5E9B4	Helfrich 2020
Q5E9B7	Helfrich 2020
Q5E9C0	Helfrich 2020
Q5E9D5	Helfrich 2020
Q5E9D6	Helfrich 2020
Q5E9E2	Helfrich 2020
Q5E9E3	Helfrich 2020
Q5E9E6	Helfrich 2020
Q5E9F5	Helfrich 2020
Q5E9F7	Helfrich 2020

Q5E9F9	Helfrich 2020
Q5E9H9	Helfrich 2020
Q5E9I4	Helfrich 2020
Q5E9I6	Helfrich 2020
Q5E9J1	Helfrich 2020
Q5E9J8	Helfrich 2020
Q5E9K0	Helfrich 2020
Q5E9K1	Helfrich 2020
Q5E9K3	Helfrich 2020
Q5E9R3	Helfrich 2020
Q5E9T1	Helfrich 2020
Q5E9T4	Helfrich 2020
Q5E9T9	Helfrich 2020
Q5E9V6	Helfrich 2020
Q5E9X4	Helfrich 2020
Q5E9Y6	Helfrich 2020
Q5E9Z2	Helfrich 2020
Q5E9Z8	Helfrich 2020
Q5EA01	Helfrich 2020
Q5EA50	Helfrich 2020
Q5EA61	Helfrich 2020
Q5EA67	Helfrich 2020
Q5EA75	Helfrich 2020
Q5EA77	Helfrich 2020
Q5EA79	Helfrich 2020
Q5EA80	Helfrich 2020
Q5EAB0	Helfrich 2020
Q5EAB2	Helfrich 2020
Q5EAC6	Helfrich 2020
Q5EAC7	Helfrich 2020

Q5EAD2	Helfrich 2020
Q5GF34	Helfrich 2020
Q5KR47	Helfrich 2020
Q5KR47-2	Helfrich 2020
Q5KR49	Helfrich 2020
Q5NDF9	Helfrich 2020
Q5XQN5	Helfrich 2020
Q645M6	Helfrich 2020
Q66LN0	Helfrich 2020
Q68RU0	Helfrich 2020
Q693V9	Helfrich 2020
Q6B856	Helfrich 2020
Q6B857	Helfrich 2020
Q6BBL6	Helfrich 2020
Q6EWQ7	Helfrich 2020
Q6Q0I7	Helfrich 2020
Q6QRN6	Helfrich 2020
Q6VUQ8	Helfrich 2020
Q6Y1E2	Helfrich 2020
Q70IB2	Helfrich 2020
Q71SP7	Helfrich 2020
Q765N9	Helfrich 2020
Q769I5	Helfrich 2020
Q76I81	Helfrich 2020
Q76I82	Helfrich 2020
Q76LV1	Helfrich 2020
Q76LV2	Helfrich 2020
Q7M2V3	Helfrich 2020
Q7M2Y2	Helfrich 2020
Q7SIH1	Helfrich 2020

Q7YQE1	Helfrich 2020
Q7YRE7	Helfrich 2020
Q7YRZ7	Helfrich 2020
Q861S4	Helfrich 2020
Q862F5	Helfrich 2020
Q862H7	Helfrich 2020
Q862I1	Helfrich 2020
Q862S5	Helfrich 2020
Q863B3	Helfrich 2020
Q863C3	Helfrich 2020
Q865A2	Helfrich 2020
Q865S1	Helfrich 2020
Q865V6	Helfrich 2020
Q8HXK9	Helfrich 2020
Q8HYI9	Helfrich 2020
Q8HZJ5	Helfrich 2020
Q8HZY1	Helfrich 2020
Q8MII0	Helfrich 2020
Q8MJ16	Helfrich 2020
Q8MJ50	Helfrich 2020
Q8MKF1	Helfrich 2020
Q8SPJ1	Helfrich 2020
Q8SPP7	Helfrich 2020
Q8SPX7	Helfrich 2020
Q8SQ28	Helfrich 2020
Q8WML4	Helfrich 2020
Q8WMP9	Helfrich 2020
Q8WMQ6	Helfrich 2020
Q8WN55	Helfrich 2020
Q92176	Helfrich 2020

Q95121	Helfrich 2020
Q95140	Helfrich 2020
Q95KV0	Helfrich 2020
Q95L54	Helfrich 2020
Q95M17	Helfrich 2020
Q95M18	Helfrich 2020
Q95M57	Helfrich 2020
Q9BDG1	Helfrich 2020
Q9BE39	Helfrich 2020
Q9BE40	Helfrich 2020
Q9BEG5-1	Helfrich 2020
Q9BGI1-1	Helfrich 2020
Q9BGI2	Helfrich 2020
Q9BGI3	Helfrich 2020
Q9GJW7	Helfrich 2020
Q9GKI7-1	Helfrich 2020
Q9GLX9	Helfrich 2020
Q9GMB8	Helfrich 2020
Q9MYM4	Helfrich 2020
Q9MZ08	Helfrich 2020
Q9N0E7-1	Helfrich 2020
Q9N0T1	Helfrich 2020
Q9N0T5	Helfrich 2020
Q9N0V4	Helfrich 2020
Q9N2I2	Helfrich 2020
Q9N2I8	Helfrich 2020
Q9N2J2-1	Helfrich 2020
Q9TR36	Helfrich 2020
Q9TRY0	Helfrich 2020
Q9TS85	Helfrich 2020

Q9TS87	Helfrich 2020
Q9TTE1	Helfrich 2020
Q9TTK8	Helfrich 2020
Q9TU03	Helfrich 2020
Q9TU25	Helfrich 2020
Q9TU47	Helfrich 2020
Q9TU73	Helfrich 2020
Q9XSA7	Helfrich 2020
Q9XSC6	Helfrich 2020
Q9XSC9	Helfrich 2020
Q9XSJ0	Helfrich 2020
Q9XSK7	Helfrich 2020
Q9XSW5	Helfrich 2020
Q9XT56	Helfrich 2020
S5G966	Helfrich 2020
V6F9B4	Helfrich 2020
38596	Mullen 2012
39326	Mullen 2012
1433B	Mullen 2012
1433Z	Mullen 2012
A0FJZ6	Mullen 2012
A0JN34	Mullen 2012
A0JNJ8	Mullen 2012
A0PDJ3	Mullen 2012
A1A4N9	Mullen 2012
A1A4Q6	Mullen 2012
A1AG	Mullen 2012
A1AT	Mullen 2012
A1BG	Mullen 2012
A1L528	Mullen 2012

A1L555	Mullen 2012
A1L568	Mullen 2012
A1L5B6	Mullen 2012
A1L5B7	Mullen 2012
A1XEB1	Mullen 2012
A2AP	Mullen 2012
A2I7M9	Mullen 2012
A2I7N0	Mullen 2012
A2I7N3	Mullen 2012
A2VDM7	Mullen 2012
A2VDN7	Mullen 2012
A2VDW0	Mullen 2012
A2VE41	Mullen 2012
A2VE92	Mullen 2012
A3KLR9	Mullen 2012
A3KMY8	Mullen 2012
A4FUG9	Mullen 2012
A4FUZ1	Mullen 2012
A4IFC8	Mullen 2012
A4IFJ2	Mullen 2012
A4IFP2	Mullen 2012
A5D7C6	Mullen 2012
A5D7D8	Mullen 2012
A5D7E0	Mullen 2012
A5D7Q2	Mullen 2012
A5D7R6	Mullen 2012
A5D986	Mullen 2012
A5D9D1	Mullen 2012
A5PJ79	Mullen 2012
A5PK12	Mullen 2012

A5PK49	Mullen 2012
A5PKI3	Mullen 2012
A6H749	Mullen 2012
A6H7C4	Mullen 2012
A6H7J7	Mullen 2012
A6QL85	Mullen 2012
A6QLA8	Mullen 2012
A6QLL8	Mullen 2012
A6QLR7	Mullen 2012
A6QLS4	Mullen 2012
A6QLT7	Mullen 2012
A6QLZ0	Mullen 2012
A6QM09	Mullen 2012
A6QNM1	Mullen 2012
A6QNU3	Mullen 2012
A6QNW7	Mullen 2012
A6QNX2	Mullen 2012
A6QP39	Mullen 2012
A6QPN6	Mullen 2012
A6QPZ0	Mullen 2012
A6QPZ4	Mullen 2012
A6QQ02	Mullen 2012
A6QQ11	Mullen 2012
A6QQ20	Mullen 2012
A6QQA8	Mullen 2012
A6QQN6	Mullen 2012
A6QR28	Mullen 2012
A7E350	Mullen 2012
A7E394	Mullen 2012
A7E3C7	Mullen 2012

A7E3D5	Mullen 2012
A7E3E1	Mullen 2012
A7MBD7	Mullen 2012
A7MBI5	Mullen 2012
A7YWC6	Mullen 2012
A7YWF1	Mullen 2012
A7YY47	Mullen 2012
A8E647	Mullen 2012
AATC	Mullen 2012
AATM	Mullen 2012
ABHEB	Mullen 2012
ACBP	Mullen 2012
ACOC	Mullen 2012
ACTA	Mullen 2012
ACTB	Mullen 2012
ACTN4	Mullen 2012
ADCY7	Mullen 2012
ADIPO	Mullen 2012
ADO	Mullen 2012
AK1A1	Mullen 2012
AL7A1	Mullen 2012
AL9A1	Mullen 2012
ALBU	Mullen 2012
ALDR	Mullen 2012
ALL2	Mullen 2012
AMBP	Mullen 2012
AMPM1	Mullen 2012
AMPN	Mullen 2012
AN32A	Mullen 2012
AN32B	Mullen 2012

ANT3	Mullen 2012
ANXA1	Mullen 2012
ANXA2	Mullen 2012
ANXA3	Mullen 2012
ANXA4	Mullen 2012
ANXA5	Mullen 2012
AOCX	Mullen 2012
APEX1	Mullen 2012
APOA1	Mullen 2012
APOA2	Mullen 2012
APOA4	Mullen 2012
APOC3	Mullen 2012
APOH	Mullen 2012
APT	Mullen 2012
ARF1	Mullen 2012
ARMET	Mullen 2012
ARNT	Mullen 2012
ARP3	Mullen 2012
ARPC2	Mullen 2012
ARSA	Mullen 2012
ASAH1	Mullen 2012
ASGL1	Mullen 2012
ASM3A	Mullen 2012
ATIF1	Mullen 2012
ATOX1	Mullen 2012
AZO1	Mullen 2012
B0JYL8	Mullen 2012
B0JYM7	Mullen 2012
B0JYN1	Mullen 2012
B0JYN3	Mullen 2012

B0JYN6	Mullen 2012
B0JYN8	Mullen 2012
B0JYP6	Mullen 2012
B0JYQ0	Mullen 2012
B0JYQ1	Mullen 2012
B0LJ56	Mullen 2012
B2BX69	Mullen 2012
B2MG	Mullen 2012
B3GN1	Mullen 2012
B3VTM3	Mullen 2012
B6VAP8	Mullen 2012
B8Y7I4	Mullen 2012
B9DUI1	Mullen 2012
B9DVF7	Mullen 2012
B9TUC3	Mullen 2012
BASP	Mullen 2012
BASP1	Mullen 2012
BCAM	Mullen 2012
BCTN5	Mullen 2012
BDH2	Mullen 2012
BHMT1	Mullen 2012
BLVRB	Mullen 2012
BMA34	Mullen 2012
BPT1	Mullen 2012
BPT2	Mullen 2012
BRE1A	Mullen 2012
C0LQJ5	Mullen 2012
C1K3N7	Mullen 2012
C4BPA	Mullen 2012
CA123	Mullen 2012

CADH1	Mullen 2012
CAH2	Mullen 2012
CALM	Mullen 2012
CALR	Mullen 2012
CAN1	Mullen 2012
CAP1	Mullen 2012
CASA1	Mullen 2012
CASB	Mullen 2012
CASC4	Mullen 2012
CATA	Mullen 2012
CATB	Mullen 2012
CATD	Mullen 2012
CATH	Mullen 2012
CATL	Mullen 2012
CATS	Mullen 2012
CATZ	Mullen 2012
CBPB2	Mullen 2012
CCD72	Mullen 2012
CD44	Mullen 2012
CENPN	Mullen 2012
CFAB	Mullen 2012
CFAH	Mullen 2012
CFDP2	Mullen 2012
CG024	Mullen 2012
CH10	Mullen 2012
CHM1B	Mullen 2012
CHM2B	Mullen 2012
CHRD1	Mullen 2012
CK054	Mullen 2012
CLIC1	Mullen 2012

CLIC4	Mullen 2012
CLUS	Mullen 2012
CMGA	Mullen 2012
CNDP2	Mullen 2012
CNPD	Mullen 2012
CNPY3	Mullen 2012
CO041	Mullen 2012
CO3	Mullen 2012
CO4	Mullen 2012
CO4A1	Mullen 2012
CO6	Mullen 2012
CO7	Mullen 2012
CO9	Mullen 2012
COA1	Mullen 2012
COF1	Mullen 2012
CONG	Mullen 2012
COPB2	Mullen 2012
CS010	Mullen 2012
CSPG2	Mullen 2012
CT195	Mullen 2012
CTHL1	Mullen 2012
CTHL2	Mullen 2012
CTHL3	Mullen 2012
CTHL4	Mullen 2012
CTHL5	Mullen 2012
CTHL6	Mullen 2012
CTHL7	Mullen 2012
CUTA	Mullen 2012
CX7A2	Mullen 2012
CXA1	Mullen 2012

CYB5	Mullen 2012
CYBP	Mullen 2012
CYC	Mullen 2012
CYC2	Mullen 2012
CYTB	Mullen 2012
CYTC	Mullen 2012
D0VD68	Mullen 2012
DAG1	Mullen 2012
DAP1	Mullen 2012
DCOR	Mullen 2012
DDAH2	Mullen 2012
DHPR	Mullen 2012
DLRB1	Mullen 2012
DNS2A	Mullen 2012
DOPD	Mullen 2012
DPOL	Mullen 2012
DPYL2	Mullen 2012
DYL1	Mullen 2012
DYL2	Mullen 2012
EDF1	Mullen 2012
EF1A1	Mullen 2012
EF2	Mullen 2012
EFCB3	Mullen 2012
EFHD2	Mullen 2012
EFNA1	Mullen 2012
EFTU	Mullen 2012
ENDP1	Mullen 2012
ENOA	Mullen 2012
ENOB	Mullen 2012
ENSA	Mullen 2012

ERGI3	Mullen 2012
ESTD	Mullen 2012
EZRI	Mullen 2012
F107B	Mullen 2012
F12AI	Mullen 2012
F92A1	Mullen 2012
FA5	Mullen 2012
FA53C	Mullen 2012
FABPB	Mullen 2012
FABPE	Mullen 2012
FETA	Mullen 2012
FETUA	Mullen 2012
FETUB	Mullen 2012
FGL2	Mullen 2012
FIBA	Mullen 2012
FIBB	Mullen 2012
FIBG	Mullen 2012
FINC	Mullen 2012
FKB1A	Mullen 2012
FKBP2	Mullen 2012
FKBP3	Mullen 2012
FKBP4	Mullen 2012
FOLR1	Mullen 2012
G3P	Mullen 2012
G6PI	Mullen 2012
G6PI	Mullen 2012
GBG2	Mullen 2012
GCSH	Mullen 2012
GDF8	Mullen 2012
GDIA	Mullen 2012

GDIB	Mullen 2012
GDIR	Mullen 2012
GDIR1	Mullen 2012
GDIR2	Mullen 2012
GDIS	Mullen 2012
GELS	Mullen 2012
GGCT	Mullen 2012
GGH	Mullen 2012
GIPC2	Mullen 2012
GLPD	Mullen 2012
GLRX1	Mullen 2012
GNAT1	Mullen 2012
GNS	Mullen 2012
GPBAR	Mullen 2012
GPX1	Mullen 2012
GRB2	Mullen 2012
GRP	Mullen 2012
GRP78	Mullen 2012
GSTM1	Mullen 2012
GSTP1	Mullen 2012
H2B1K	Mullen 2012
H4	Mullen 2012
HBA	Mullen 2012
HBB	Mullen 2012
HBBA	Mullen 2012
HDGF	Mullen 2012
HEM2	Mullen 2012
HEM3	Mullen 2012
HEMO	Mullen 2012
HEXA	Mullen 2012

HINT1	Mullen 2012
HMGB1	Mullen 2012
HMGB2	Mullen 2012
HMGN1	Mullen 2012
HMGN2	Mullen 2012
HMGN3	Mullen 2012
HMGN4	Mullen 2012
HNRH2	Mullen 2012
HPRT	Mullen 2012
HPT	Mullen 2012
HRG	Mullen 2012
HS71A	Mullen 2012
HS71L	Mullen 2012
HS90A	Mullen 2012
HS90B	Mullen 2012
HSP7C	Mullen 2012
HSPB1	Mullen 2012
IBP1	Mullen 2012
IBP5	Mullen 2012
IBP6	Mullen 2012
IBPS	Mullen 2012
IDHC	Mullen 2012
IF4A1	Mullen 2012
IF5A1	Mullen 2012
IF6	Mullen 2012
IGF2	Mullen 2012
ILEU	Mullen 2012
IMPA1	Mullen 2012
ISCA1	Mullen 2012
ITIH1	Mullen 2012

ITIH4	Mullen 2012
ITPR1	Mullen 2012
JAM1	Mullen 2012
K1C10	Mullen 2012
K1C14	Mullen 2012
K1C17	Mullen 2012
K2C5	Mullen 2012
K2C7	Mullen 2012
K2C75	Mullen 2012
K2C8	Mullen 2012
KAD2	Mullen 2012
KCAB1	Mullen 2012
KCRB	Mullen 2012
KNG1	Mullen 2012
KNG1	Mullen 2012
KNG2	Mullen 2012
KRIT1	Mullen 2012
LACB	Mullen 2012
LALBA	Mullen 2012
LASP1	Mullen 2012
LDH6B	Mullen 2012
LEG1	Mullen 2012
LG3BP	Mullen 2012
LGMN	Mullen 2012
LKA2B	Mullen 2012
LPLC1	Mullen 2012
LUM	Mullen 2012
LY66C	Mullen 2012
LYAG	Mullen 2012
MA2B1	Mullen 2012

MAP4	Mullen 2012
MARE1	Mullen 2012
MDHC	Mullen 2012
MDHM	Mullen 2012
MESD2	Mullen 2012
MET	Mullen 2012
METK	Mullen 2012
MIF	Mullen 2012
MNME	Mullen 2012
MOES	Mullen 2012
MT1A	Mullen 2012
MTP	Mullen 2012
MYC	Mullen 2012
MYH10	Mullen 2012
NACA	Mullen 2012
NADC	Mullen 2012
NCPR	Mullen 2012
NDKA1	Mullen 2012
NDKA2	Mullen 2012
NDKB	Mullen 2012
NDUBA	Mullen 2012
NDUS1	Mullen 2012
NEDD8	Mullen 2012
NHRF3	Mullen 2012
NPC2	Mullen 2012
NPM	Mullen 2012
NT5D1	Mullen 2012
NU5M	Mullen 2012
NUCB1	Mullen 2012
NUCKS	Mullen 2012

NUDC	Mullen 2012
O02717	Mullen 2012
O11993	Mullen 2012
O46626	Mullen 2012
OSTK	Mullen 2012
OSTP	Mullen 2012
PA1B2	Mullen 2012
PA1B3	Mullen 2012
PABP1	Mullen 2012
PARK7	Mullen 2012
PCBP1	Mullen 2012
PCNP	Mullen 2012
PCY2	Mullen 2012
PDCD5	Mullen 2012
PDIA1	Mullen 2012
PDIA3	Mullen 2012
PDLI1	Mullen 2012
PDXK	Mullen 2012
PDZD1	Mullen 2012
PEBP1	Mullen 2012
PEDF	Mullen 2012
PERL	Mullen 2012
PGAM1	Mullen 2012
PGK1	Mullen 2012
PGRP	Mullen 2012
PGRP1	Mullen 2012
PGRP1	Mullen 2012
PIGR	Mullen 2012
PIPNA	Mullen 2012
PIPNB	Mullen 2012

PLBL2	Mullen 2012
PLMN	Mullen 2012
PNPH	Mullen 2012
PNPO	Mullen 2012
POLG	Mullen 2012
POLG	Mullen 2012
POP7	Mullen 2012
PP1A	Mullen 2012
PPAC	Mullen 2012
PPBT	Mullen 2012
PPCE	Mullen 2012
PPGB	Mullen 2012
PPIA	Mullen 2012
PPIB	Mullen 2012
PRDX1	Mullen 2012
PRDX2	Mullen 2012
PRDX4	Mullen 2012
PRDX5	Mullen 2012
PRDX6	Mullen 2012
PROF1	Mullen 2012
PROF2	Mullen 2012
PRS7	Mullen 2012
PRS8	Mullen 2012
PSA1	Mullen 2012
PSA2	Mullen 2012
PSA3	Mullen 2012
PSA4	Mullen 2012
PSA5	Mullen 2012
PSA6	Mullen 2012
PSA7	Mullen 2012

PSB1	Mullen 2012
PSB10	Mullen 2012
PSB2	Mullen 2012
PSB4	Mullen 2012
PSB5	Mullen 2012
PSB6	Mullen 2012
PSB7	Mullen 2012
PSB8	Mullen 2012
PSB9	Mullen 2012
PSME2	Mullen 2012
PTGDS	Mullen 2012
PTGR1	Mullen 2012
PTMA	Mullen 2012
PTMS	Mullen 2012
PYGM	Mullen 2012
Q05B85	Mullen 2012
Q08DU0	Mullen 2012
Q08DV2	Mullen 2012
Q08E32	Mullen 2012
Q0IIA4	Mullen 2012
Q0IIH5	Mullen 2012
Q0III8	Mullen 2012
Q0QEQ4	Mullen 2012
Q0QES8	Mullen 2012
Q0V8E1	Mullen 2012
Q0VCS8	Mullen 2012
Q0VCZ4	Mullen 2012
Q17QC8	Mullen 2012
Q17QX0	Mullen 2012
Q1JPB6	Mullen 2012

Q1JPD0	Mullen 2012
Q1RMN0	Mullen 2012
Q1RMN8	Mullen 2012
Q1RMP3	Mullen 2012
Q1RMS9	Mullen 2012
Q29RL4	Mullen 2012
Q2HJF0	Mullen 2012
Q2HJI6	Mullen 2012
Q2KHZ6	Mullen 2012
Q2KI90	Mullen 2012
Q2KIF2	Mullen 2012
Q2KIT0	Mullen 2012
Q2KIU3	Mullen 2012
Q2KIX7	Mullen 2012
Q2KJH7	Mullen 2012
Q2TBR3	Mullen 2012
Q2YDL0	Mullen 2012
Q2YTM1	Mullen 2012
Q2YUX7	Mullen 2012
Q2YVQ3	Mullen 2012
Q2YWU7	Mullen 2012
Q2YYA4	Mullen 2012
Q32KV1	Mullen 2012
Q32P72	Mullen 2012
Q32PA1	Mullen 2012
Q32PI4	Mullen 2012
Q32T06	Mullen 2012
Q3MHF7	Mullen 2012
Q3MHH8	Mullen 2012
Q3MHP6	Mullen 2012

Q3SX33	Mullen 2012
Q3SYR8	Mullen 2012
Q3SYU8	Mullen 2012
Q3SZN8	Mullen 2012
Q3SZQ1	Mullen 2012
Q3SZZ9	Mullen 2012
Q3T010	Mullen 2012
Q3T0Z0	Mullen 2012
Q3T101	Mullen 2012
Q3ZBH2	Mullen 2012
Q3ZBH5	Mullen 2012
Q3ZBR2	Mullen 2012
Q3ZC00	Mullen 2012
Q3ZC20	Mullen 2012
Q3ZC44	Mullen 2012
Q3ZC81	Mullen 2012
Q3ZC87	Mullen 2012
Q3ZCA8	Mullen 2012
Q3ZCD3	Mullen 2012
Q4N0A3	Mullen 2012
Q4N1Z0	Mullen 2012
Q4N263	Mullen 2012
Q4N293	Mullen 2012
Q4N4F3	Mullen 2012
Q4N5L2	Mullen 2012
Q4N708	Mullen 2012
Q4N783	Mullen 2012
Q4N7P6	Mullen 2012
Q4N8M2	Mullen 2012
Q4N9Q6	Mullen 2012

Q56J78	Mullen 2012
Q58DR3	Mullen 2012
Q5BIS8	Mullen 2012
Q5DPW9	Mullen 2012
Q5E970	Mullen 2012
Q5EM56	Mullen 2012
Q6MSD0	Mullen 2012
Q6MSS8	Mullen 2012
Q6MSW9	Mullen 2012
Q6PT94	Mullen 2012
Q6TVT4	Mullen 2012
Q7M312	Mullen 2012
Q861V9	Mullen 2012
Q862E0	Mullen 2012
Q862H7	Mullen 2012
Q8HYX0	Mullen 2012
Q8SQ31	Mullen 2012
Q8SQB5	Mullen 2012
Q91E89	Mullen 2012
Q95ND8	Mullen 2012
Q9BGU1	Mullen 2012
Q9BGU5	Mullen 2012
Q9TS74	Mullen 2012
Q9TSB1	Mullen 2012
R1AB	Mullen 2012
RADI	Mullen 2012
RECA	Mullen 2012
RET4	Mullen 2012
RGS9	Mullen 2012
RHG15	Mullen 2012

RL10A	Mullen 2012
RL11	Mullen 2012
RL12	Mullen 2012
RL2	Mullen 2012
RL35	Mullen 2012
RL38	Mullen 2012
RL5	Mullen 2012
RL9	Mullen 2012
RLP24	Mullen 2012
RN128	Mullen 2012
RNH2B	Mullen 2012
ROA1	Mullen 2012
ROA2	Mullen 2012
RPB5	Mullen 2012
RS15A	Mullen 2012
RS16	Mullen 2012
RS17	Mullen 2012
RS19	Mullen 2012
RS21	Mullen 2012
RS28	Mullen 2012
RS30	Mullen 2012
RSSA	Mullen 2012
S100G	Mullen 2012
S10A2	Mullen 2012
S10A4	Mullen 2012
S10A7	Mullen 2012
S10A8	Mullen 2012
S10A9	Mullen 2012
S10AA	Mullen 2012
S10AC	Mullen 2012

S10AD	Mullen 2012
SAA	Mullen 2012
SAHH	Mullen 2012
SAMP	Mullen 2012
SAP	Mullen 2012
SBP1	Mullen 2012
SDHL	Mullen 2012
SERA	Mullen 2012
SERB	Mullen 2012
SERC2	Mullen 2012
SFRP1	Mullen 2012
SFRP5	Mullen 2012
SFRS1	Mullen 2012
SFRS2	Mullen 2012
SFRS7	Mullen 2012
SH3L1	Mullen 2012
SH3L3	Mullen 2012
SMD1	Mullen 2012
SMD2	Mullen 2012
SODC	Mullen 2012
SPA31	Mullen 2012
SPB6	Mullen 2012
ST1A1	Mullen 2012
STIP1	Mullen 2012
STMN1	Mullen 2012
STRN3	Mullen 2012
STX19	Mullen 2012
SUMO2	Mullen 2012
SUMO3	Mullen 2012
SYE	Mullen 2012

SYSC	Mullen 2012
SYWC	Mullen 2012
TALDO	Mullen 2012
TBA1B	Mullen 2012
TBA1D	Mullen 2012
TBB2B	Mullen 2012
TBB2C	Mullen 2012
TBB5	Mullen 2012
TBCA	Mullen 2012
TBCB	Mullen 2012
TCPG	Mullen 2012
TEBP	Mullen 2012
TERA	Mullen 2012
TES	Mullen 2012
TETN	Mullen 2012
THAP1	Mullen 2012
THBG	Mullen 2012
THIO	Mullen 2012
THRB	Mullen 2012
THTR	Mullen 2012
TIMP2	Mullen 2012
TKT	Mullen 2012
TPIS	Mullen 2012
TPM1	Mullen 2012
TPM2	Mullen 2012
TPM3	Mullen 2012
TPMT	Mullen 2012
TPP1	Mullen 2012
TPPP3	Mullen 2012
TPST2	Mullen 2012

TRFE	Mullen 2012
TRFL	Mullen 2012
TRFL	Mullen 2012
TRXR1	Mullen 2012
TRYP	Mullen 2012
TSN	Mullen 2012
TSP1	Mullen 2012
TUFT1	Mullen 2012
TYB10	Mullen 2012
TYB4	Mullen 2012
TYB9	Mullen 2012
UACA	Mullen 2012
UB2V2	Mullen 2012
UBA1	Mullen 2012
UBE2N	Mullen 2012
UBIQ	Mullen 2012
UCHL1	Mullen 2012
UK114	Mullen 2012
VGLN	Mullen 2012
VIME	Mullen 2012
VNN1	Mullen 2012
VNS1	Mullen 2012
VP4	Mullen 2012
VTDB	Mullen 2012
XDH	Mullen 2012
XYLB	Mullen 2012
Y724	Mullen 2012
Y807	Mullen 2012
YBOX1	Mullen 2012
ZA2G	Mullen 2012

ZFX	Mullen 2012
ZMAT4	Mullen 2012
ZN668	Mullen 2012
A2VE14	Munoz 2014
A7MB62	Munoz 2014
O60506	Munoz 2014
O97680	Munoz 2014
P00570	Munoz 2014
P02676	Munoz 2014
P02769	Munoz 2014
P08728	Munoz 2014
P10096	Munoz 2014
P10881	Munoz 2014
P11974	Munoz 2014
P12799	Munoz 2014
P13214	Munoz 2014
P13696	Munoz 2014
P14568	Munoz 2014
P19803	Munoz 2014
P24627	Munoz 2014
P26452	Munoz 2014
P31976	Munoz 2014
P48818	Munoz 2014
P62935	Munoz 2014
P62935	Munoz 2014
P79136	Munoz 2014
P79136	Munoz 2014
P81187	Munoz 2014
Q0P5A6	Munoz 2014
Q0VCK0	Munoz 2014

Q0VCX2	Munoz 2014
Q0VD48	Munoz 2014
Q2T9X2	Munoz 2014
Q3SX14	Munoz 2014
Q3ZC84	Munoz 2014
Q3ZCK3	Munoz 2014
Q56JV6	Munoz 2014
Q5E956	Munoz 2014
Q9BGI3	Munoz 2014
Q9CPV4	Munoz 2014
Q9XSJ4	Munoz 2014
Q9XSK7	Munoz 2014
P62261	Moraes 2020
B0JYM5	Moraes 2020
Q3SZI4	Moraes 2020
P06623	Moraes 2020
O02691	Moraes 2020
Q0VCK0	Moraes 2020
Q3ZCI4	Moraes 2020
Q5EAD6	Moraes 2020
Q7SIH1	Moraes 2020
A7YY28	Moraes 2020
Q29RZ0	Moraes 2020
Q1JPB6	Moraes 2020
Q0VCU1	Moraes 2020
P20004	Moraes 2020
P68138	Moraes 2020
Q3B7N2	Moraes 2020
A5D7D1	Moraes 2020
P48818	Moraes 2020

Q08DS7	Moraes 2020
Q5E9I6	Moraes 2020
B0JYQ0	Moraes 2020
Q3ZCJ2	Moraes 2020
P48644	Moraes 2020
Q1JPA0	Moraes 2020
P20000	Moraes 2020
A6QLL8	Moraes 2020
P09487	Moraes 2020
P34955	Moraes 2020
Q2KJF1	Moraes 2020
K4JF16	Moraes 2020
P00978	Moraes 2020
Q3SZH5	Moraes 2020
P20072	Moraes 2020
Q95L54	Moraes 2020
Q6QRN6	Moraes 2020
A7YWR0	Moraes 2020
A0A140T843	Moraes 2020
Q08DD1	Moraes 2020
Q17QB3	Moraes 2020
Q8MJ16	Moraes 2020
A4IFK5	Moraes 2020
Q5EAD0	Moraes 2020
Q9MZ08	Moraes 2020
A4IFQ7	Moraes 2020
H7BWW2	Moraes 2020
P80724	Moraes 2020
Q5EA61	Moraes 2020
A6QQ07	Moraes 2020

A5D7U1	Moraes 2020
P62157	Moraes 2020
A5D7J6	Moraes 2020
A7MBJ5	Moraes 2020
A7Z066	Moraes 2020
Q27970	Moraes 2020
A4FUA8	Moraes 2020
P00921	Moraes 2020
Q0VCX4	Moraes 2020
P33046	Moraes 2020
P19660	Moraes 2020
P05689	Moraes 2020
Q2KHZ6	Moraes 2020
A2VE92	Moraes 2020
A6QNW7	Moraes 2020
P30932	Moraes 2020
A6QLC4	Moraes 2020
A6H7H6	Moraes 2020
Q2KJ93	Moraes 2020
Q148D9	Moraes 2020
Q1ZYR0	Moraes 2020
P63103	Moraes 2020
P19483	Moraes 2020
P00727	Moraes 2020
P55859	Moraes 2020
Q32L40	Moraes 2020
P60712	Moraes 2020
P07688	Moraes 2020
P61157	Moraes 2020
P01888	Moraes 2020

P79345	Moraes 2020
Q29437	Moraes 2020
P19120	Moraes 2020
P08037	Moraes 2020
Q08DA1	Moraes 2020
P02584	Moraes 2020
P21856	Moraes 2020
F2Z4C1	Moraes 2020
Q2UVX4	Moraes 2020
P18902	Moraes 2020
P81947	Moraes 2020
P00366	Moraes 2020
P49951	Moraes 2020
A7MB62	Moraes 2020
P00442	Moraes 2020
Q2KJD0	Moraes 2020
P35705	Moraes 2020
Q6B856	Moraes 2020
Q3SZN8	Moraes 2020
P00432	Moraes 2020
P01966	Moraes 2020
P04896	Moraes 2020
P52175	Moraes 2020
P00829	Moraes 2020
P02070	Moraes 2020
Q3MHR7	Moraes 2020
Q148J6	Moraes 2020
Q7SIB2	Moraes 2020
Q5E9K0	Moraes 2020
Q3T101	Moraes 2020

P10096	Moraes 2020
Q5E9B7	Moraes 2020
P35526	Moraes 2020
P17697	Moraes 2020
P35605	Moraes 2020
B0JYL8	Moraes 2020
A4FV05	Moraes 2020
E1BI98	Moraes 2020
Q0V7N2	Moraes 2020
Q29RU4	Moraes 2020
Q29RQ1	Moraes 2020
Q2KIH5	Moraes 2020
P81187	Moraes 2020
P23805	Moraes 2020
A0A140T856	Moraes 2020
P61603	Moraes 2020
O97764	Moraes 2020
P67808	Moraes 2020
P22226	Moraes 2020
A6H722	Moraes 2020
Q5DPW9	Moraes 2020
Q3MHY1	Moraes 2020
P08728	Moraes 2020
A5D986	Moraes 2020
A1A4K3	Moraes 2020
P21793	Moraes 2020
P56541	Moraes 2020
F1MZF2	Moraes 2020
Q3T0Z7	Moraes 2020
O02675	Moraes 2020

Q58CS3	Moraes 2020
P81425	Moraes 2020
A6QNX2	Moraes 2020
F1N7D7	Moraes 2020
A1A4K5	Moraes 2020
P15396	Moraes 2020
A2VE41	Moraes 2020
P68103	Moraes 2020
Q3SYU2	Moraes 2020
Q3SZQ8	Moraes 2020
Q17QK4	Moraes 2020
A6QPT7	Moraes 2020
Q08E20	Moraes 2020
Q1JQD0	Moraes 2020
A3KLR9	Moraes 2020
P31976	Moraes 2020
Q28107	Moraes 2020
A5PKI3	Moraes 2020
P55052	Moraes 2020
A5D7S8	Moraes 2020
Q0VCD7	Moraes 2020
B0JYQ1	Moraes 2020
A5PJE3	Moraes 2020
A6QPX7	Moraes 2020
F1MAV0	Moraes 2020
P50291	Moraes 2020
F1MR86	Moraes 2020
Q3ZBY4	Moraes 2020
Q148D3	Moraes 2020
Q28024	Moraes 2020

A5D7U5	Moraes 2020
P11116	Moraes 2020
A6QNJ8	Moraes 2020
A5D7A2	Moraes 2020
A7YWG4	Moraes 2020
A7MBI6	Moraes 2020
Q95M18	Moraes 2020
Q32S38	Moraes 2020
A1A4L7	Moraes 2020
G3X745	Moraes 2020
P63243	Moraes 2020
A4IF70	Moraes 2020
Q2HJI6	Moraes 2020
Q863C3	Moraes 2020
A5PKM0	Moraes 2020
A7MBH9	Moraes 2020
P62871	Moraes 2020
P11017	Moraes 2020
E1BA29	Moraes 2020
A3KMY8	Moraes 2020
Q08E18	Moraes 2020
E1BBY7	Moraes 2020
A7E3S8	Moraes 2020
Q0VCX2	Moraes 2020
Q76LV2	Moraes 2020
Q76LV1	Moraes 2020
A5D9H5	Moraes 2020
Q5E9J1	Moraes 2020
Q0V8R6	Moraes 2020
Q8SQ21	Moraes 2020

Q9BGU1	Moraes 2020
Q3ZBX9	Moraes 2020
Q8SQG8	Moraes 2020
Q2KJC5	Moraes 2020
Q0IIL6	Moraes 2020
Q9GJT9	Moraes 2020
A6QPN6	Moraes 2020
Q3SYR8	Moraes 2020
Q2HJF0	Moraes 2020
Q0VCM5	Moraes 2020
Q28125	Moraes 2020
Q9GLL5	Moraes 2020
P56831	Moraes 2020
Q0VC51	Moraes 2020
Q0V8D5	Moraes 2020
Q32LE5	Moraes 2020
A0A140T853	Moraes 2020
Q1LZ95	Moraes 2020
A5D7R6	Moraes 2020
Q0VCZ4	Moraes 2020
A4FV94	Moraes 2020
A0A140T867	Moraes 2020
A1L595	Moraes 2020
F6S1Q0	Moraes 2020
Q5XQN5	Moraes 2020
Q29S21	Moraes 2020
Q2KHX6	Moraes 2020
P01044	Moraes 2020
P01045	Moraes 2020
P05786	Moraes 2020

P24627	Moraes 2020
Q95M12	Moraes 2020
Q2KIF2	Moraes 2020
P62803	Moraes 2020
A6QQ85	Moraes 2020
Q05443	Moraes 2020
A0JNL5	Moraes 2020
Q9MYM4	Moraes 2020
Q8WMP9	Moraes 2020
G3MXJ5	Moraes 2020
Q6B411	Moraes 2020
Q56J78	Moraes 2020
A6QLB0	Moraes 2020
A0A060IHZ1	Moraes 2020
E1B7B4	Moraes 2020
Z4YHD9	Moraes 2020
Q5E9I4	Moraes 2020
O46738	Moraes 2020
P55918	Moraes 2020
Q9N0E6	Moraes 2020
Q3ZC41	Moraes 2020
A6QP39	Moraes 2020
Q28910	Moraes 2020
Q8WML4	Moraes 2020
A6QLD6	Moraes 2020
Q27966	Moraes 2020
P85100	Moraes 2020
Q5E9E2	Moraes 2020
C6KEF7	Moraes 2020
O18836	Moraes 2020

M5FJT7	Moraes 2020
Q1LZH9	Moraes 2020
A6QPY4	Moraes 2020
E1BFX4	Moraes 2020
Q1RMN0	Moraes 2020
Q28030	Moraes 2020
Q3SZK8	Moraes 2020
A6QM01	Moraes 2020
A6BMK7	Moraes 2020
Q05B89	Moraes 2020
Q0P569	Moraes 2020
Q17QX0	Moraes 2020
A1L579	Moraes 2020
P13214	Moraes 2020
F1N726	Moraes 2020
Q95114	Moraes 2020
A5D7E8	Moraes 2020
A6QNL5	Moraes 2020
Q8SPP7	Moraes 2020
Q5E947	Moraes 2020
Q9BGI3	Moraes 2020
Q9BGI1	Moraes 2020
O77834	Moraes 2020
A6QQ11	Moraes 2020
Q2KIW4	Moraes 2020
P80109	Moraes 2020
A1A4J1	Moraes 2020
Q08DP0	Moraes 2020
Q2HJ26	Moraes 2020
Q95121	Moraes 2020

Q1RML9	Moraes 2020
Q2KJD1	Moraes 2020
Q2KJ75	Moraes 2020
F1MYX5	Moraes 2020
Q17QC7	Moraes 2020
Q5E9A3	Moraes 2020
A7MAZ5	Moraes 2020
G3N0V2	Moraes 2020
P60661	Moraes 2020
F1MU80	Moraes 2020
G8JKW7	Moraes 2020
O46499	Moraes 2020
Q28057	Moraes 2020
A5D7C6	Moraes 2020
P60986	Moraes 2020
Q08DU0	Moraes 2020
Q2YDE4	Moraes 2020
Q1RMP3	Moraes 2020
Q2KIT0	Moraes 2020
Q2KIX7	Moraes 2020
Q2KIU3	Moraes 2020
P28782	Moraes 2020
P02702	Moraes 2020
A6QR28	Moraes 2020
A8YXY5	Moraes 2020
A7MBJ4	Moraes 2020
Q2KIY5	Moraes 2020
Q0II59	Moraes 2020
Q58D08	Moraes 2020
A5D984	Moraes 2020

A6QQA8	Moraes 2020
P50397	Moraes 2020
P62833	Moraes 2020
A6QLS9	Moraes 2020
Q2HJH2	Moraes 2020
Q1KZG2	Moraes 2020
Q3T0R7	Moraes 2020
Q3ZCK3	Moraes 2020
Q2KJH9	Moraes 2020
Q3T0V4	Moraes 2020
Q3ZBZ1	Moraes 2020
Q95140	Moraes 2020
P42899	Moraes 2020
Q3ZC91	Moraes 2020
P07107	Moraes 2020
P41500	Moraes 2020
Q3MHL4	Moraes 2020
P08166	Moraes 2020
Q3SYV4	Moraes 2020
Q3Y5Z3	Moraes 2020
P16116	Moraes 2020
Q3SZR3	Moraes 2020
P28800	Moraes 2020
P12763	Moraes 2020
Q9XSJ4	Moraes 2020
P79098	Moraes 2020
P04272	Moraes 2020
Q3SWX7	Moraes 2020
P81287	Moraes 2020
Q3SYW1	Moraes 2020

P15497	Moraes 2020
Q3SZJ0	Moraes 2020
P33097	Moraes 2020
P12344	Moraes 2020
Q5EA01	Moraes 2020
P06504	Moraes 2020
Q3T168	Moraes 2020
P25975	Moraes 2020
P25326	Moraes 2020
Q9XSK2	Moraes 2020
Q9XSA7	Moraes 2020
P05059	Moraes 2020
Q29RK1	Moraes 2020
Q2HJ57	Moraes 2020
Q28104	Moraes 2020
Q3T0B6	Moraes 2020
Q28085	Moraes 2020
Q9TTK8	Moraes 2020
P25417	Moraes 2020
Q3ZC84	Moraes 2020
Q3ZCJ8	Moraes 2020
Q3MHR3	Moraes 2020
Q3SZV3	Moraes 2020
Q3T0L2	Moraes 2020
Q3T0L5	Moraes 2020
P79136	Moraes 2020
P10790	Moraes 2020
Q3SZZ9	Moraes 2020
P07589	Moraes 2020
Q2KIB0	Moraes 2020

Q2YDG0	Moraes 2020
P15103	Moraes 2020
P10575	Moraes 2020
P28801	Moraes 2020
Q3T054	Moraes 2020
P38409	Moraes 2020
Q3ZCH9	Moraes 2020
Q27975	Moraes 2020
Q3SZV7	Moraes 2020
P09867	Moraes 2020
Q3T0D0	Moraes 2020
P10103	Moraes 2020
Q2M2T1	Moraes 2020
P24591	Moraes 2020
Q05718	Moraes 2020
Q3T052	Moraes 2020
Q04467	Moraes 2020
Q9XT56	Moraes 2020
P06394	Moraes 2020
P19858	Moraes 2020
Q5E9B1	Moraes 2020
Q1JPB0	Moraes 2020
Q3SZH7	Moraes 2020
Q3MI05	Moraes 2020
Q3SYU9	Moraes 2020
Q32LG3	Moraes 2020
P12624	Moraes 2020
Q3SX44	Moraes 2020
Q3T063	Moraes 2020
Q3T0Q4	Moraes 2020

P45478	Moraes 2020
Q1JQD4	Moraes 2020
P10731	Moraes 2020
P62935	Moraes 2020
P80311	Moraes 2020
P13696	Moraes 2020
Q3T0P6	Moraes 2020
Q3SZ62	Moraes 2020
Q3ZBG9	Moraes 2020
Q2KHU0	Moraes 2020
Q3T0I2	Moraes 2020
Q2TBR0	Moraes 2020
P26779	Moraes 2020
Q3T0X5	Moraes 2020
Q3ZCK9	Moraes 2020
Q3ZBG0	Moraes 2020
Q2TBX6	Moraes 2020
Q3T108	Moraes 2020
Q3T112	Moraes 2020
Q29RV1	Moraes 2020
P05307	Moraes 2020
Q2HJE5	Moraes 2020
P51176	Moraes 2020
P00735	Moraes 2020
Q3MHP2	Moraes 2020
Q3ZBK2	Moraes 2020
P19803	Moraes 2020
Q9TU03	Moraes 2020
Q3T114	Moraes 2020
Q3MHF7	Moraes 2020

P02769	Moraes 2020
Q3T147	Moraes 2020
Q9N0T1	Moraes 2020
Q3ZCH0	Moraes 2020
Q3ZBZ8	Moraes 2020
Q3T0K2	Moraes 2020
Q3MHL7	Moraes 2020
Q2KIS7	Moraes 2020
O62768	Moraes 2020
P00586	Moraes 2020
Q3ZBV8	Moraes 2020
Q9TS87	Moraes 2020
Q3ZBT1	Moraes 2020
P17248	Moraes 2020
Q3ZCC8	Moraes 2020
P46201	Moraes 2020
Q9MZ13	Moraes 2020
Q0P5D6	Moraes 2020
Q2NKZ9	Moraes 2020
P61585	Moraes 2020
Q58DQ3	Moraes 2020
Q0III8	Moraes 2020
A6QLG5	Moraes 2020
A2VE17	Moraes 2020
Q2KJ32	Moraes 2020
Q9N2I2	Moraes 2020
F1N152	Moraes 2020
Q29443	Moraes 2020
A2I7N1	Moraes 2020
Q32T06	Moraes 2020

Q2KJH6	Moraes 2020
O02739	Moraes 2020
A5PK77	Moraes 2020
Q9TTE1	Moraes 2020
Q3ZEJ6	Moraes 2020
A6QPQ2	Moraes 2020
A6QPZ4	Moraes 2020
A6QPP2	Moraes 2020
Q2TBR3	Moraes 2020
A5PKC2	Moraes 2020
Q862Q2	Moraes 2020
A7MB31	Moraes 2020
Q08DL0	Moraes 2020
A3KMY4	Moraes 2020
A6QQN6	Moraes 2020
Q27960	Moraes 2020
Q0VD19	Moraes 2020
C4T8T2	Moraes 2020
A8E4P3	Moraes 2020
A7YWC6	Moraes 2020
Q24JZ7	Moraes 2020
Q0V7N1	Moraes 2020
Q3SZA6	Moraes 2020
A8YXX7	Moraes 2020
O97680	Moraes 2020
Q2KIM0	Moraes 2020
A7MBA6	Moraes 2020
Q5EAD2	Moraes 2020
Q3T149	Moraes 2020
Q3ZC44	Moraes 2020

E9LZ03	Moraes 2020
E1BM92	Moraes 2020
Q56K14	Moraes 2020
G3MZJ9	Moraes 2020
O46375	Moraes 2020
P15696	Moraes 2020
Q3ZBU7	Moraes 2020
A0A140T894	Moraes 2020
P68250	Moraes 2020
A3KMV5	Moraes 2020
O02741	Moraes 2020
Q0P568	Moraes 2020
P63048	Moraes 2020
A8E4P0	Moraes 2020
A5D7Q2	Moraes 2020
A6QM09	Moraes 2020
P01035	Moraes 2020
P04836	Moraes 2020
P40682	Moraes 2020
Q58CQ9	Moraes 2020
A5D9D1	Moraes 2020
Q3ZBS7	Moraes 2020
Q8SPF8	Moraes 2020
Q3T0Z0	Moraes 2020
Q2KJH4	Moraes 2020
Q0III5	Moraes 2020
Q3ZCH5	Moraes 2020
P02662	Moraes 2020
P02668	Moraes 2020
P12234	Moraes 2020

P08169	Moraes 2020
P10568	Moraes 2020
P10279	Moraes 2020
P20414	Moraes 2020
Q28193	Moraes 2020
Q28017	Moraes 2020
P42201	Moraes 2020
P41541	Moraes 2020
Q28150	Moraes 2020
P50448	Moraes 2020
P54229	Moraes 2020
O02703	Moraes 2020
Q28065	Moraes 2020
Q28046	Moraes 2020
O02717	Moraes 2020
Q9TTW1	Moraes 2020
Q9TT36	Moraes 2020
Q9N0K1	Moraes 2020
Q9GLC9	Moraes 2020
Q9GKI7	Moraes 2020
Q9BGI2	Moraes 2020
P80209	Moraes 2020
A0A0P0QLR2	Moraes 2020
Q8WN55	Moraes 2020
Q8SPU8	Moraes 2020
P81282	Moraes 2020
Q8MKB7	Moraes 2020
Q58DU5	Moraes 2020
Q862I1	Moraes 2020
P62998	Moraes 2020

Q8MJ05	Moraes 2020
Q27991	Moraes 2020
P54228	Moraes 2020
O46415	Moraes 2020
Q9BEA3	Moraes 2020
P62992	Moraes 2020
Q03763	Moraes 2020
P62958	Moraes 2020
Q865V6	Moraes 2020
A0A140T897	Moraes 2020
Q07130	Moraes 2020
P61286	Moraes 2020
Q6B855	Moraes 2020
Q68V19	Moraes 2020
P68002	Moraes 2020
Q5E987	Moraes 2020
P69678	Moraes 2020
Q58DK5	Moraes 2020
Q58DT1	Moraes 2020
Q3YJH8	Moraes 2020
Q3SZG7	Moraes 2020
Q3SZ43	Moraes 2020
P50227	Moraes 2020
A0A140T8A5	Moraes 2020
Q5E946	Moraes 2020
Q58DS5	Moraes 2020
Q58DW5	Moraes 2020
Q3ZCM0	Moraes 2020
Q3SZB7	Moraes 2020
Q3T2L0	Moraes 2020

Q3SZF2	Moraes 2020
Q3T145	Moraes 2020
Q3MHM5	Moraes 2020
Q3ZCA7	Moraes 2020
A0A0M4MD57	Moraes 2020
Q2TBW8	Moraes 2020
Q2TBV8	Moraes 2020
Q2QDE9	Moraes 2020
Q32PB8	Moraes 2020
Q3T0Y5	Moraes 2020
Q3T0T1	Moraes 2020
Q3MHN0	Moraes 2020
Q3SZC2	Moraes 2020
Q3T087	Moraes 2020
Q3T0U2	Moraes 2020
Q3T0L7	Moraes 2020
Q3T0S6	Moraes 2020
Q3ZBH8	Moraes 2020
O18789	Moraes 2020
Q17R18	Moraes 2020
Q8SPJ1	Moraes 2020
Q17QK3	Moraes 2020
Q17QC8	Moraes 2020
Q58DS9	Moraes 2020
Q17QI3	Moraes 2020
Q17R14	Moraes 2020
P20456	Moraes 2020
Q3SZ54	Moraes 2020
Q148N0	Moraes 2020
Q148I9	Moraes 2020

Q148H5	Moraes 2020
P80177	Moraes 2020
Q3MHR5	Moraes 2020
P11179	Moraes 2020
Q0V8I2	Moraes 2020
Q0V8B6	Moraes 2020
Q32KP9	Moraes 2020
Q0VC27	Moraes 2020
Q0VCH9	Moraes 2020
Q0VCC0	Moraes 2020
Q0VCK1	Moraes 2020
Q0VFX8	Moraes 2020
Q0P5J6	Moraes 2020
Q0IIA4	Moraes 2020
Q2HJ49	Moraes 2020
Q1RMX7	Moraes 2020
Q2NL19	Moraes 2020
Q2KIT8	Moraes 2020
Q2KI48	Moraes 2020
Q2LGB2	Moraes 2020
Q2HJH1	Moraes 2020
Q29S11	Moraes 2020
Q58DH9	Moraes 2020
Q08E55	Moraes 2020
Q08DJ3	Moraes 2020
Q08DX9	Moraes 2020
Q3ZCI9	Moraes 2020
Q2T9X2	Moraes 2020
Q3ZBA8	Moraes 2020
Q32LE4	Moraes 2020

Q148I8	Moraes 2020
Q0VD04	Moraes 2020
Q32PA4	Moraes 2020
Q32L99	Moraes 2020
Q9TR36	Moraes 2020
A0JND7	Moraes 2020
P79103	Moraes 2020
P46193	Moraes 2020
A1A4I4	Moraes 2020
Q5E958	Moraes 2020
E1BJW3	Moraes 2020
A1L5B1	Moraes 2020
Q32PF2	Moraes 2020
P26452	Moraes 2020
Q3SZC4	Moraes 2020
Q3SZJ4	Moraes 2020
Q3T0E5	Moraes 2020
Q3ZBW4	Moraes 2020
Q3ZC42	Moraes 2020
Q3SZR8	Moraes 2020
Q3T106	Moraes 2020
Q0P5B0	Moraes 2020
Q1RMI2	Moraes 2020
P31404	Moraes 2020
A2VDN8	Moraes 2020
B1H0W7	Moraes 2020
A2VDN7	Moraes 2020
Q32L48	Moraes 2020
Q9BEG5	Moraes 2020
A3KN04	Moraes 2020

A4FUD0	Moraes 2020
A4FV56	Moraes 2020
P80227	Moraes 2020
A4FUZ7	Moraes 2020
P31408	Moraes 2020
A4FUZ0	Moraes 2020
A3KN26	Moraes 2020
A5D7N6	Moraes 2020
A5D7R9	Moraes 2020
A5D7H3	Moraes 2020
P81134	Moraes 2020
A5D977	Moraes 2020
Q9TRY0	Moraes 2020
A5D9B6	Moraes 2020
A2VE07	Moraes 2020
P35071	Moraes 2020
A4IFP2	Moraes 2020
A5PJY0	Moraes 2020
P61284	Moraes 2020
Q3T0W9	Moraes 2020
A5PJJ1	Moraes 2020
A0A0F7RQ40	Moraes 2020
Q862H7	Moraes 2020
A5PKJ3	Moraes 2020
A6H730	Moraes 2020
A6H742	Moraes 2020
A6H769	Moraes 2020
A6H7G2	Moraes 2020
A6H768	Moraes 2020
A6QLN9	Moraes 2020

A6QNS6	Moraes 2020
A6QLY4	Moraes 2020
A6QLZ0	Moraes 2020
A6QLU7	Moraes 2020
A6QPP7	Moraes 2020
A6QL85	Moraes 2020
A6QLZ3	Moraes 2020
A0A140T891	Moraes 2020
A6QQR7	Moraes 2020
P00435	Moraes 2020
P56701	Moraes 2020
A7E3T7	Moraes 2020
A7E3V1	Moraes 2020
A7E3W2	Moraes 2020
A7YY47	Moraes 2020
B0JYN3	Moraes 2020
A8E4P2	Moraes 2020
A7MB45	Moraes 2020
A7MBG8	Moraes 2020
A7MBI5	Moraes 2020
Q56JV9	Moraes 2020
O18736	Moraes 2020
A7E306	Moraes 2020
A6QLN6	Moraes 2020
A7YW37	Moraes 2020
A7YWN0	Moraes 2020
A7Z014	Moraes 2020
A4FV54	Moraes 2020
P02754	Moraes 2020
Q29460	Moraes 2020

P18203	Moraes 2020
Q0P5F6	Moraes 2020
Q3SYR7	Moraes 2020
G5E5C8	Moraes 2020
Q2TBL6	Moraes 2020
F1N1I6	Moraes 2020
C4T8B4	Moraes 2020
A2I7M9	Moraes 2020
Q5H9M6	Moraes 2020
F1MWD3	Moraes 2020
Q3ZBH0	Moraes 2020
Q2NKZ1	Moraes 2020
F1N3I4	Moraes 2020
F2Z4F0	Moraes 2020
F1MI98	Moraes 2020
F1MYC9	Moraes 2020
E1B898	Moraes 2020
F1MN49	Moraes 2020
E1BI28	Moraes 2020
E1B7W1	Moraes 2020
F1MNS5	Moraes 2020
A6QNU3	Moraes 2020
F6K7I7	Moraes 2020
G3X6L9	Moraes 2020
E1BFE9	Moraes 2020
P31800	Moraes 2020
P23004	Moraes 2020
E1BJT7	Moraes 2020
P02253	Moraes 2020
K4JDR8	Moraes 2020

K4JDT2	Moraes 2020
L7R4Y6	Moraes 2020
F1MHS5	Moraes 2020
A0A0A0MP92	Moraes 2020
C1ITJ8	Moraes 2020
A6QLT9	Moraes 2020
E1B9T2	Moraes 2020

Table S5-4 proteins identified as containing *Sec* signal peptides and thus putatively secreted through the classical secretion path as determined by SignalP analysis. Protein ID is in FASTA format. SP= probability of having a signal peptide. CS position: cleavage site position. Pr: probability of the signal peptide sequence being 100% accurate.

Protein ID	SP	CS Position
tr_F1MDS0_F1MDS0_BOVIN	0.999857	CS pos: 23-24. ASS-QD. Pr: 0.9702
sp_A0JNL5_LY66C_BOVIN	0.999795	CS pos: 18-19. VSA-DI. Pr: 0.9147
tr_EQ3T0Z0_EQ3T0Z0_BOVIN	0.999712	CS pos: 26-27. VTG-SI. Pr: 0.7706
tr_A0A3EQ1LEQ34_A0A3EQ1LEQ34_BOVIN	0.999712	CS pos: 26-27. VTG-SI. Pr: 0.7706
tr_G3MX65_G3MX65_BOVIN	0.999712	CS pos: 26-27. VTG-SI. Pr: 0.7706
sp_Q0VCX2_BIP_BOVIN	0.999595	CS pos: 19-20. ARA-EE. Pr: 0.9836
tr_A0A3EQ1NJB1_A0A3EQ1NJB1_BOVIN	0.999585	CS pos: 19-20. AWA-KD. Pr: 0.9459
tr_F1N076_F1N076_BOVIN	0.999585	CS pos: 19-20. AWA-KD. Pr: 0.9459
tr_A2VE41_A2VE41_BOVIN	0.99955	CS pos: 17-18. VKS-QD. Pr: 0.9219
tr_F1MIA9_F1MIA9_BOVIN	0.999462	CS pos: 20-21. AQA-DV. Pr: 0.9826
tr_E1BNR0_E1BNR0_BOVIN	0.999423	CS pos: 22-23. ANA-QA. Pr: 0.5942
tr_B0JYN6_B0JYN6_BOVIN	0.999422	CS pos: 18-19. CHS-IP. Pr: 0.9728
sp_P12763_FETUA_BOVIN	0.999422	CS pos: 18-19. CHS-IP. Pr: 0.9728
tr_A4IFI0_A4IFI0_BOVIN	0.9993	CS pos: 19-20. SWA-QA. Pr: 0.7011
tr_A0A3EQ1MFR4_A0A3EQ1MFR4_BOVIN	0.999284	CS pos: 22-23. ANA-QA. Pr: 0.5580
sp_A8YXX7_TFF3_BOVIN	0.999268	CS pos: 23-24. STG-QY. Pr: 0.4884
sp_P00978_AMBP_BOVIN	0.999247	CS pos: 19-20. VNA-SS. Pr: 0.7151
tr_F1MM86_F1MM86_BOVIN	0.999217	CS pos: 21-22. SQA-CF. Pr: 0.9878
tr_F1MZ96_F1MZ96_BOVIN	0.999108	CS pos: 20-21. SSG-DV. Pr: 0.8459
tr_A5D7S8_A5D7S8_BOVIN	0.999103	CS pos: 29-30. AGA-DV. Pr: 0.8354
tr_F1MAV0_F1MAV0_BOVIN	0.999091	CS pos: 16-17. VQA-QF. Pr: 0.9701
sp_P17697_CLUS_BOVIN	0.99909	CS pos: 19-20. GWA-IS. Pr: 0.9421
tr_A0A3EQ1LXG6_A0A3EQ1LXG6_BOVIN	0.99898	CS pos: 19-20. SWA-QA. Pr: 0.6887

tr_B0JYP6_B0JYP6_BOVIN	0.998946	CS pos: 20-21. SSG-DV. Pr: 0.8461
sp_Q863C3_GRP_BOVIN	0.998939	CS pos: 23-24. GWA-AP. Pr: 0.9839
tr_EQ1RMN8_EQ1RMN8_BOVIN	0.998936	CS pos: 19-20. SWA-QA. Pr: 0.7045
tr_E1BJP1_E1BJP1_BOVIN	0.998843	CS pos: 15-16. VCA-QE. Pr: 0.8173
sp_P01888_B2MG_BOVIN	0.998792	CS pos: 20-21. LDA-IQ. Pr: 0.8371
tr_A0A3EQ1MIF4_A0A3EQ1MIF4_BOVIN	0.998732	CS pos: 20-21. CEA-HH. Pr: 0.9015
sp_EQ29RU4_CO6_BOVIN	0.998718	CS pos: 21-22. SQA-CF. Pr: 0.9860
tr_A0A3EQ1LUE9_A0A3EQ1LUE9_BOVIN	0.998647	CS pos: 22-23. SWA-QA. Pr: 0.7345
tr_A0A3EQ1LTY4_A0A3EQ1LTY4_BOVIN	0.998638	CS pos: 24-25. LQA-AV. Pr: 0.8696
tr_A5PK72_A5PK72_BOVIN	0.998626	CS pos: 19-20. SWA-QA. Pr: 0.6963
sp_Q95M18_ENPL_BOVIN	0.998426	CS pos: 21-22. VRA-DD. Pr: 0.9497
tr_Q5DPW9_Q5DPW9_BOVIN	0.998413	CS pos: 28-29. ARA-RP. Pr: 0.8568
sp_O46375_TTHY_BOVIN	0.998381	CS pos: 20-21. SEA-GS. Pr: 0.7141
tr_G5E5H2_G5E5H2_BOVIN	0.99823	CS pos: 19-20. SWA-QA. Pr: 0.7064
sp_P50448_F12AI_BOVIN	0.998151	CS pos: 23-24. VTS-DM. Pr: 0.9450
tr_A0A3EQ1LWV8_A0A3EQ1LWV8_BOVIN	0.998137	CS pos: 19-20. SWA-QA. Pr: 0.6669
tr_A0A3EQ1M1Z4_A0A3EQ1M1Z4_BOVIN	0.998079	CS pos: 19-20. SWA-QA. Pr: 0.5952
tr_A0A3EQ1LSF0_A0A3EQ1LSF0_BOVIN	0.998079	CS pos: 19-20. SWA-QA. Pr: 0.5952
tr_A0A3EQ1MNN6_A0A3EQ1MNN6_BOVIN	0.998026	CS pos: 24-25. ASA-TS. Pr: 0.9338
tr_F1MJK3_F1MJK3_BOVIN	0.998026	CS pos: 24-25. ASA-TS. Pr: 0.9338
tr_F1MKS5_F1MKS5_BOVIN	0.997944	CS pos: 20-21. CSC-AV. Pr: 0.6483
tr_Q9BGU1_Q9BGU1_BOVIN	0.997944	CS pos: 20-21. CSC-AV. Pr: 0.6483
tr_G3MZE0_G3MZE0_BOVIN	0.997911	CS pos: 19-20. SWA-QA. Pr: 0.7080
sp_P19035_APOC3_BOVIN	0.9979	CS pos: 23-24. TKA-EE. Pr: 0.8450
tr_V6F9A3_V6F9A3_BOVIN	0.9979	CS pos: 23-24. TKA-EE. Pr: 0.8450
sp_P02702_FOLR1_BOVIN	0.997892	CS pos: 19-20. AWG-AQ. Pr: 0.5668
tr_G3MZU3_G3MZU3_BOVIN	0.997871	CS pos: 15-16. VCA-QE. Pr: 0.8116
sp_Q8SPP7_PGRP1_BOVIN	0.997818	CS pos: 21-22. GAA-QD. Pr: 0.8671

tr_H2CNR1_H2CNR1_BOVIN	0.997818	CS pos: 21-22. GAA-QD. Pr: 0.8671
tr_F1MY85_F1MY85_BOVIN	0.997773	CS pos: 18-19. SWG-QE. Pr: 0.9763
tr_G3X6N3_G3X6N3_BOVIN	0.997717	CS pos: 19-20. CLA-DP. Pr: 0.8990
sp_EQ29443_TRFE_BOVIN	0.997717	CS pos: 19-20. CLA-DP. Pr: 0.8990
sp_P15497_APOA1_BOVIN	0.997708	CS pos: 18-19. SQA-RH. Pr: 0.9851
tr_V6F9A2_V6F9A2_BOVIN	0.997708	CS pos: 18-19. SQA-RH. Pr: 0.9851
tr_A0A3EQ1NG86_A0A3EQ1NG86_BOVIN	0.997679	CS pos: 15-16. ALA-RP. Pr: 0.8906
tr_B5B3R8_B5B3R8_BOVIN	0.997679	CS pos: 15-16. ALA-RP. Pr: 0.8906
sp_P02662_CASA1_BOVIN	0.997679	CS pos: 15-16. ALA-RP. Pr: 0.8906
sp_P02453_CO1A1_BOVIN	0.997677	CS pos: 22-23. THG-QE. Pr: 0.9195
tr_V6F7X3_V6F7X3_BOVIN	0.997642	CS pos: 20-21. AEA-EV. Pr: 0.7403
sp_Q7SIH1_A2MG_BOVIN	0.997579	CS pos: 23-24. TDA-SV. Pr: 0.7099
tr_K4JBR5_K4JBR5_BOVIN	0.997579	CS pos: 23-24. TDA-SV. Pr: 0.7099
tr_A5D7J6_A5D7J6_BOVIN	0.997545	CS pos: 17-18. AAA-DR. Pr: 0.9452
tr_F1MLW8_F1MLW8_BOVIN	0.997439	CS pos: 21-22. ASS-QL. Pr: 0.7709
sp_Q0VCM5_ITIH1_BOVIN	0.997395	CS pos: 22-23. VAA-QG. Pr: 0.3482
tr_A5D7R6_A5D7R6_BOVIN	0.997383	CS pos: 18-19. SRG-FE. Pr: 0.9261
tr_A0A3EQ1LJT1_A0A3EQ1LJT1_BOVIN	0.997359	CS pos: 20-21. VVS-YE. Pr: 0.8633
sp_P28800_A2AP_BOVIN	0.997351	CS pos: 21-22. CSA-QF. Pr: 0.8684
tr_Q5GN72_Q5GN72_BOVIN	0.997175	CS pos: 18-19. LDA-QS. Pr: 0.9037
tr_Q95ND9_Q95ND9_BOVIN	0.996984	CS pos: 22-23. THG-QE. Pr: 0.9209
tr_F1N3J3_F1N3J3_BOVIN	0.996844	CS pos: 20-21. TLA-KD. Pr: 0.9529
tr_EQ2HJF0_EQ2HJF0_BOVIN	0.996778	CS pos: 19-20. CLA-VP. Pr: 0.8481
tr_A0A452DI25_A0A452DI25_BOVIN	0.996775	CS pos: 23-24. AKA-HP. Pr: 0.8565
sp_EQ3MHN5_VTDB_BOVIN	0.996767	CS pos: 16-17. VHA-LE. Pr: 0.9495
tr_A0A3EQ1MGT0_A0A3EQ1MGT0_BOVIN	0.996641	CS pos: 22-23. ALG-NP. Pr: 0.9592
tr_EQ3T101_EQ3T101_BOVIN	0.996299	CS pos: 19-20. SWA-QA. Pr: 0.7279
sp_EQ3ZCH5_ZA2G_BOVIN	0.995871	CS pos: 17-18. AVS-EE. Pr: 0.7426

tr_A0A452DK44_A0A452DK44_BOVIN	0.995871	CS pos: 17-18. AVS-EE. Pr: 0.7426
tr_A6QNX2_A6QNX2_BOVIN	0.995777	CS pos: 26-27. LEA-RA. Pr: 0.5934
sp_EQ2KJH6_SERPH_BOVIN	0.995635	CS pos: 18-19. ALA-AE. Pr: 0.9031
sp_P81265_PIGR_BOVIN	0.99555	CS pos: 17-18. VVS-MK. Pr: 0.4296
tr_B3VTM3_B3VTM3_BOVIN	0.995394	CS pos: 19-20. CLA-AP. Pr: 0.9374
tr_G3X6K8_G3X6K8_BOVIN	0.995265	CS pos: 25-26. SEA-TA. Pr: 0.3054
sp_EQ2TBU0_HPT_BOVIN	0.995265	CS pos: 25-26. SEA-TA. Pr: 0.3054
tr_A0A0M4MD57_A0A0M4MD57_BOVIN	0.995265	CS pos: 25-26. SEA-TA. Pr: 0.3054
tr_F2FB42_F2FB42_BOVIN	0.994941	CS pos: 23-24. GTA-DT. Pr: 0.4840
sp_P81644_APOA2_BOVIN	0.994938	CS pos: 18-19. LEG-AL. Pr: 0.7387
tr_A0A3EQ1MA31_A0A3EQ1MA31_BOVIN	0.994909	CS pos: 27-28. SKA-QK. Pr: 0.9597
tr_Q5EA67_Q5EA67_BOVIN	0.994909	CS pos: 27-28. SKA-QK. Pr: 0.9597
sp_P38657_PDIA3_BOVIN	0.994643	CS pos: 24-25. AAA-SD. Pr: 0.7666
tr_A5D7E8_A5D7E8_BOVIN	0.994643	CS pos: 24-25. AAA-SD. Pr: 0.7666
tr_EQ3SYR8_EQ3SYR8_BOVIN	0.994132	CS pos: 22-23. VTA-QD. Pr: 0.9059
tr_B8Y9T0_B8Y9T0_BOVIN	0.993492	CS pos: 27-28. AGA-SK. Pr: 0.3492
tr_A0A3EQ1NHX9_A0A3EQ1NHX9_BOVIN	0.993492	CS pos: 27-28. AGA-SK. Pr: 0.3492
tr_B8Y9S9_B8Y9S9_BOVIN	0.993492	CS pos: 27-28. AGA-SK. Pr: 0.3492
sp_P07589_FINC_BOVIN	0.993492	CS pos: 27-28. AGA-SK. Pr: 0.3492
tr_A6H7J7_A6H7J7_BOVIN	0.993254	CS pos: 19-20. SWA-LA. Pr: 0.6170
tr_A6QM09_A6QM09_BOVIN	0.992805	CS pos: 20-21. VVS-YK. Pr: 0.7769
sp_Q08DD1_ARSA_BOVIN	0.99147	CS pos: 18-19. AAA-SP. Pr: 0.7940
tr_A0A3EQ1M471_A0A3EQ1M471_BOVIN	0.99147	CS pos: 18-19. AAA-SP. Pr: 0.7940
sp_P81187_CFAB_BOVIN	0.991105	CS pos: 25-26. VGM-TP. Pr: 0.4070
sp_Q95121_PEDF_BOVIN	0.990579	CS pos: 19-20. GRC-QN. Pr: 0.7169
tr_B0JYQ0_B0JYQ0_BOVIN	0.989765	CS pos: 18-19. AYS-RG. Pr: 0.7603
sp_P34955_A1AT_BOVIN	0.98954	CS pos: 24-25. SLA-GV. Pr: 0.8586
sp_G3MYZ3_AFAM_BOVIN	0.989477	CS pos: 21-22. SLT-LP. Pr: 0.5642

tr_A0A3EQ1LGM4_A0A3EQ1LGM4_BOVIN	0.989301	CS pos: 18-19. SFC-ED. Pr: 0.8860
tr_F1N4M7_F1N4M7_BOVIN	0.989301	CS pos: 18-19. SFC-ED. Pr: 0.8860
tr_EQ32PI4_EQ32PI4_BOVIN	0.989301	CS pos: 18-19. SFC-ED. Pr: 0.8860
tr_A0A3EQ1MF14_A0A3EQ1MF14_BOVIN	0.989301	CS pos: 18-19. SFC-ED. Pr: 0.8860
tr_A0A3EQ1M2A8_A0A3EQ1M2A8_BOVIN	0.989301	CS pos: 18-19. SFC-ED. Pr: 0.8860
tr_A5D7EQ2_A5D7EQ2_BOVIN	0.989301	CS pos: 19-20. VLS-QV. Pr: 0.8885
tr_A0A452DHX8_A0A452DHX8_BOVIN	0.988933	CS pos: 16-17. AMG-RE. Pr: 0.6640
tr_E1BE11_E1BE11_BOVIN	0.988441	CS pos: 21-22. SRA-QD. Pr: 0.9189
sp_A7E3W2_LG3BP_BOVIN	0.98815	CS pos: 18-19. TRG-VK. Pr: 0.8984
tr_E1BI28_E1BI28_BOVIN	0.987815	CS pos: 23-24. ALP-AR. Pr: 0.7955
tr_A6QQA8_A6QQA8_BOVIN	0.987162	CS pos: 30-31. AGA-AP. Pr: 0.8227
sp_EQ3T0U1_MESD_BOVIN	0.986983	CS pos: 31-32. AFA-TE. Pr: 0.9478
sp_EQ2KJF1_A1BG_BOVIN	0.985782	CS pos: 21-22. TEQ-AT. Pr: 0.6990
sp_EQ29437_AOCX_BOVIN	0.985416	CS pos: 16-17. VMG-RE. Pr: 0.6743
tr_EQ3SZZ9_EQ3SZZ9_BOVIN	0.984901	CS pos: 24-25. CLA-YV. Pr: 0.7933
tr_A6QQN6_A6QQN6_BOVIN	0.984277	CS pos: 18-19. ARA-VP. Pr: 0.9105
sp_P19660_CTHL2_BOVIN	0.983956	CS pos: 29-30. ASA-QA. Pr: 0.6715
sp_EQ3SZR3_A1AG_BOVIN	0.983368	CS pos: 18-19. LDA-QS. Pr: 0.9028
sp_P22226_CTHL1_BOVIN	0.983131	CS pos: 29-30. ASA-QA. Pr: 0.6743
tr_A0A3EQ1N0C4_A0A3EQ1N0C4_BOVIN	0.982411	CS pos: 18-19. TES-GL. Pr: 0.6920
tr_F6QH94_F6QH94_BOVIN	0.981621	CS pos: 19-20. VNG-LY. Pr: 0.7405
sp_P33046_CTHL4_BOVIN	0.981136	CS pos: 29-30. ASA-QA. Pr: 0.6778
tr_A6QPP2_A6QPP2_BOVIN	0.980914	CS pos: 20-21. CRT-LG. Pr: 0.6016
sp_A6QQ85_UPK3L_BOVIN	0.979813	CS pos: 26-27. GMS-LE. Pr: 0.8444
tr_G3N3EQ3_G3N3EQ3_BOVIN	0.979522	CS pos: 26-27. VLS-QV. Pr: 0.8740
tr_A0A3EQ1M9I5_A0A3EQ1M9I5_BOVIN	0.979386	CS pos: 26-27. GHM-AN. Pr: 0.4934
tr_A0A3EQ1MRM3_A0A3EQ1MRM3_BOVIN	0.979386	CS pos: 26-27. GHM-AN. Pr: 0.4934
tr_E1B864_E1B864_BOVIN	0.979386	CS pos: 26-27. GHM-AN. Pr: 0.4934

sp_P09487_PPBT_BOVIN	0.978646	CS pos: 17-18. ASS-LV. Pr: 0.4388
tr_G3N148_G3N148_BOVIN	0.978434	CS pos: 26-27. VLS-QV. Pr: 0.8727
tr_A0A3EQ1MDA5_A0A3EQ1MDA5_BOVIN	0.975879	CS pos: 38-39. AQA-AD. Pr: 0.7951
tr_A6QP39_A6QP39_BOVIN	0.975879	CS pos: 38-39. AQA-AD. Pr: 0.7951
tr_F1MNV5_F1MNV5_BOVIN	0.975812	CS pos: 18-19. SLT-QE. Pr: 0.7490
sp_P01045_KNG2_BOVIN	0.975812	CS pos: 18-19. SLT-QE. Pr: 0.7490
tr_A0A3EQ1LSS0_A0A3EQ1LSS0_BOVIN	0.975286	CS pos: 37-38. ASA-SD. Pr: 0.6590
tr_F1MET0_F1MET0_BOVIN	0.975286	CS pos: 37-38. ASA-SD. Pr: 0.6590
tr_A5D9D7_A5D9D7_BOVIN	0.975286	CS pos: 37-38. ASA-SD. Pr: 0.6590
sp_EQ2KIU3_HP252_BOVIN	0.973409	CS pos: 30-31. ADA-TS. Pr: 0.4920
tr_A0A3EQ1MUR2_A0A3EQ1MUR2_BOVIN	0.973121	CS pos: 26-27. VLS-QV. Pr: 0.8595
tr_A5D986_A5D986_BOVIN	0.973028	CS pos: 22-23. VSA-GG. Pr: 0.8361
tr_A0A3EQ1M0K3_A0A3EQ1M0K3_BOVIN	0.972978	CS pos: 26-27. VLS-QV. Pr: 0.8591
tr_G3MWT1_G3MWT1_BOVIN	0.972096	CS pos: 26-27. VLS-KV. Pr: 0.8451
tr_A0A3EQ1MBP6_A0A3EQ1MBP6_BOVIN	0.971938	CS pos: 23-24. VGG-QV. Pr: 0.8777
tr_A0A3EQ1MZY9_A0A3EQ1MZY9_BOVIN	0.971938	CS pos: 23-24. VGG-QV. Pr: 0.8777
tr_E3W9A0_E3W9A0_BOVIN	0.971938	CS pos: 23-24. VGG-QV. Pr: 0.8777
tr_A0A3EQ1N0Z7_A0A3EQ1N0Z7_BOVIN	0.971938	CS pos: 23-24. VGG-QV. Pr: 0.8777
tr_A0A3EQ1MI29_A0A3EQ1MI29_BOVIN	0.97024	CS pos: 26-27. VLS-QV. Pr: 0.8565
tr_G3N1U4_G3N1U4_BOVIN	0.96835	CS pos: 24-25. VHC-LP. Pr: 0.7415
tr_G3N1H5_G3N1H5_BOVIN	0.967645	CS pos: 26-27. VLS-QV. Pr: 0.8539
tr_A0A3EQ1MFI7_A0A3EQ1MFI7_BOVIN	0.966937	CS pos: 26-27. VLS-QV. Pr: 0.8534
tr_EQ32PB7_EQ32PB7_BOVIN	0.963594	CS pos: 18-19. VSS-QR. Pr: 0.8634
tr_Q0IIA4_Q0IIA4_BOVIN	0.961539	CS pos: 26-27. SST-EQ. Pr: 0.3310
tr_A0A3EQ1M193_A0A3EQ1M193_BOVIN	0.961539	CS pos: 26-27. SST-EQ. Pr: 0.3310
tr_F1N726_F1N726_BOVIN	0.961539	CS pos: 26-27. SST-EQ. Pr: 0.3310
tr_E1B726_E1B726_BOVIN	0.952875	CS pos: 26-27. GLG-DL. Pr: 0.9093
sp_O18836_GDF8_BOVIN	0.952142	CS pos: 18-19. IVA-GP. Pr: 0.2308

tr_C6KEF7_C6KEF7_BOVIN	0.952142	CS pos: 18-19. IVA-GP. Pr: 0.2308
tr_Q0P5D6_Q0P5D6_BOVIN	0.951882	CS pos: 38-39. AAA-SG. Pr: 0.5163
tr_G3X6I0_G3X6I0_BOVIN	0.951538	CS pos: 24-25. QEA-SV. Pr: 0.2476
tr_A4ZVC5_A4ZVC5_BOVIN	0.943421	CS pos: 23-24. VDL-NE. Pr: 0.2328
tr_A0A3EQ1LQU4_A0A3EQ1LQU4_BOVIN	0.937515	CS pos: 29-30. TQS-HW. Pr: 0.6158
tr_F2FB38_F2FB38_BOVIN	0.935466	CS pos: 34-35. SVA-TT. Pr: 0.6452
tr_A6H7H6_A6H7H6_BOVIN	0.933153	CS pos: 22-23. GYG-QE. Pr: 0.8682
sp_O18738_DAG1_BOVIN	0.926522	CS pos: 29-30. TQS-HW. Pr: 0.6044
tr_F1MGZ5_F1MGZ5_BOVIN	0.926382	CS pos: 21-22. ALS-DS. Pr: 0.8187
tr_A0A3EQ1MIL5_A0A3EQ1MIL5_BOVIN	0.904803	CS pos: 22-23. VLS-QV. Pr: 0.7571
sp_P00735_THRB_BOVIN	0.876908	CS pos: 24-25. VHS-QH. Pr: 0.7859
tr_A0A452DI66_A0A452DI66_BOVIN	0.876908	CS pos: 24-25. VHS-QH. Pr: 0.7859
sp_EQ2KIX7_HP251_BOVIN	0.868945	CS pos: 34-35. SSA-DS. Pr: 0.4685
tr_A0A3EQ1N1N6_A0A3EQ1N1N6_BOVIN	0.867339	CS pos: 21-22. ALA-AV. Pr: 0.6189
tr_A0A3EQ1LTK9_A0A3EQ1LTK9_BOVIN	0.867339	CS pos: 21-22. ALA-AV. Pr: 0.6189
tr_A0A3EQ1M6A2_A0A3EQ1M6A2_BOVIN	0.867339	CS pos: 21-22. ALA-AV. Pr: 0.6189
tr_A0A3EQ1M299_A0A3EQ1M299_BOVIN	0.867339	CS pos: 21-22. ALA-AV. Pr: 0.6189
tr_A0A3EQ1LI93_A0A3EQ1LI93_BOVIN	0.867339	CS pos: 21-22. ALA-AV. Pr: 0.6189
sp_Q58CQ9_VNN1_BOVIN	0.851877	CS pos: 22-23. ASS-LD. Pr: 0.5561
tr_EQ2KIF2_EQ2KIF2_BOVIN	0.846455	CS pos: 34-35. AQG-LT. Pr: 0.6356
tr_A0A3EQ1MBP1_A0A3EQ1MBP1_BOVIN	0.836941	CS pos: 30-31. ALS-DT. Pr: 0.4228
tr_A0A3EQ1M930_A0A3EQ1M930_BOVIN	0.836941	CS pos: 30-31. ALS-DT. Pr: 0.4228
sp_EQ3MHN2_CO9_BOVIN	0.833904	CS pos: 21-22. LRA-GP. Pr: 0.5508
tr_F1MUC5_F1MUC5_BOVIN	0.83041	CS pos: 30-31. TRS-AT. Pr: 0.2187
tr_A0A3EQ1MUA3_A0A3EQ1MUA3_BOVIN	0.83041	CS pos: 30-31. TRS-AT. Pr: 0.2187
tr_F1MVK1_F1MVK1_BOVIN	0.825893	CS pos: 17-18. ALS-LQ. Pr: 0.4098
tr_E1BH06_E1BH06_BOVIN	0.825893	CS pos: 17-18. ALS-LQ. Pr: 0.4098
tr_E1B748_E1B748_BOVIN	0.812407	CS pos: 30-31. ALS-DT. Pr: 0.4103

tr_E1BI72_E1BI72_BOVIN	0.812233	CS pos: 20-21. AEM-GS. Pr: 0.3983
tr_A0A3EQ1MG04_A0A3EQ1MG04_BOVIN	0.790749	CS pos: 36-37. VQA-QF. Pr: 0.7598
tr_A0A3EQ1M1A9_A0A3EQ1M1A9_BOVIN	0.79051	CS pos: 35-36. SQA-LL. Pr: 0.2895
tr_E1B9H0_E1B9H0_BOVIN	0.788252	CS pos: 25-26. VQA-AL. Pr: 0.4165
tr_E1B9E8_E1B9E8_BOVIN	0.788252	CS pos: 25-26. VQA-AL. Pr: 0.4165
tr_F1MPE1_F1MPE1_BOVIN	0.782109	CS pos: 21-22. ALA-AV. Pr: 0.4713
tr_A0A3EQ1LWV4_A0A3EQ1LWV4_BOVIN	0.782061	CS pos: 37-38. AHG-LL. Pr: 0.4996
sp_EQ2KIT0_HP20_BOVIN	0.753053	CS pos: 23-24. GGC-TG. Pr: 0.2734
tr_F6RMV5_F6RMV5_BOVIN	0.719747	CS pos: 41-42. AQG-LT. Pr: 0.5350
sp_P80311_PPIB_BOVIN	0.717989	CS pos: 33-34. SAA-DE. Pr: 0.6327
tr_A6QNJ8_A6QNJ8_BOVIN	0.663636	CS pos: 28-29. TFA-VD. Pr: 0.5160
tr_F1N0F2_F1N0F2_BOVIN	0.653929	CS pos: 22-23. VSA-GG. Pr: 0.5277
tr_EQ2KI90_EQ2KI90_BOVIN	0.653929	CS pos: 22-23. VSA-GG. Pr: 0.5277
tr_G3MYC9_G3MYC9_BOVIN	0.612735	CS pos: 17-18. SRA-LE. Pr: 0.2653
tr_Q58D57_Q58D57_BOVIN	0.602769	CS pos: 17-18. SRA-LE. Pr: 0.2623
tr_A6QNL5_A6QNL5_BOVIN	0.551335	CS pos: 32-33. VNG-LY. Pr: 0.4709
tr_E1BH94_E1BH94_BOVIN	0.544842	CS pos: 31-32. GTA-TL. Pr: 0.3593
sp_P42899_RLA2_BOVIN	0.50869	CS pos: 16-17. GNS-SP. Pr: 0.3016

Table S5-5 General linear model analysis of protein abundance (Exp. P3) across dpp and OC.

Col-umn1	p_Q	p_Oestrus	p_inter	Molecule	Q_FDRcorr	Oest_FDRcorr	inter_FDRcorr
239	8.03E-05	0.035031622	0.001386	A6H7J7_BOVIN	0.003676911	0.701306609	0.063452081
641	0.001478	0.251659406	0.018578	G3N1F5_BOVIN	0.063180168	0.990714556	0.524156036
427	0.004931	0.017793415	0.007187	Q56JV4_BOVIN	0.197554632	0.49589474	0.287922297
209	0.007645	0.088358798	0.020123	AOCX_BOVIN	0.288258047	0.858055202	0.524156036
178	0.010978	0.066430485	0.019124	ITIH1_BOVIN	0.357583809	0.858055202	0.524156036
471	0.011157	0.161012129	0.05448	A0A3Q1LKJ1_BOVIN	0.357583809	0.979315877	0.851397162
234	0.010813	0.356880786	0.053982	A0A3Q1N3Q6_BOVIN	0.357583809	0.990714556	0.851397162
106	0.012073	0.025437199	0.015569	CO9_BOVIN	0.368524138	0.582330163	0.501500583
144	0.014405	0.001547463	0.003038	A2AP_BOVIN	0.403278759	0.070851715	0.129833931
410	0.014611	0.081049574	0.025505	A0A3Q1M0K3_BOVIN	0.403278759	0.858055202	0.605513873
275	0.015099	0.600517594	0.127158	CFDP2_BOVIN	0.403278759	0.990714556	0.964775773
309	0.017596	0.283550297	0.092676	F1MY85_BOVIN	0.451167347	0.990714556	0.964775773
301	0.021293	0.036104708	0.021071	F1MHB8_BOVIN	0.524949434	0.701306609	0.524156036
95	0.025124	0.731224731	0.180795	HNRPK_BOVIN	0.536812666	0.990714556	0.964775773
350	0.024652	0.470807661	0.155207	Q3MHG9_BOVIN	0.536812666	0.990714556	0.964775773
453	0.024439	0.667061287	0.184064	A0A3Q1M8H9_BOVIN	0.536812666	0.990714556	0.964775773
137	0.023749	0.653098794	0.200709	A0A3Q1MM55_BOVIN	0.536812666	0.990714556	0.98209708
291	0.027602	0.029958308	0.021261	A6QM09_BOVIN	0.552905567	0.640109174	0.524156036
623	0.027225	0.092097339	0.059624	RAN_BOVIN	0.552905567	0.858055202	0.851397162
45	0.814501	0.011	0.902992	A0A452DI25_BOVIN	0.55430884	0.035124564	0.851397162
289	0.030266	0.051454758	0.028626	A0A3Q1M478_BOVIN	0.55430884	0.789938111	0.655336063
345	0.030196	0.102770353	0.049737	A0A3Q1MTF0_BOVIN	0.55430884	0.861265483	0.851397162
336	0.029182	0.349866019	0.115479	A0A3Q1M2A1_BOVIN	0.55430884	0.990714556	0.964775773
142	0.464058	0.007	0.251329	PRDX5_BOVIN	0.624235749	0.048244654	0.851397162
97	0.042295	0.008090475	0.015647	F6R4P6_BOVIN	0.624235749	0.305058511	0.501500583
526	0.037948	0.097719235	0.039698	DHE3_BOVIN	0.624235749	0.858055202	0.820843466
394	0.040353	0.096067315	0.072157	GDF8_BOVIN	0.624235749	0.858055202	0.911965137

134	0.040723	0.196956504	0.071758	A0A3Q1MJ46_BOVIN	0.624235749	0.984775119	0.911965137
204	0.038065	0.348312072	0.135871	FABPH_BOVIN	0.624235749	0.990714556	0.964775773
482	0.036903	0.262423864	0.097281	A7Z055_BOVIN	0.624235749	0.990714556	0.964775773
650	0.040693	0.505345825	0.172571	PSA6_BOVIN	0.624235749	0.990714556	0.964775773
652	0.042849	0.384580726	0.130261	EFHD2_BOVIN	0.624235749	0.990714556	0.964775773
374	0.04148	0.612859836	0.213967	E1BMD1_BOVIN	0.624235749	0.990714556	0.984318014
487	0.047519	0.239052039	0.105619	G3MXL6_BOVIN	0.662172356	0.990714556	0.964775773
200	0.046788	0.500554812	0.263942	F1N619_BOVIN	0.662172356	0.990714556	0.994543987
143	0.05103	0.1768248	0.117081	PURA2_BOVIN	0.666529411	0.984775119	0.964775773
352	0.050721	0.530622368	0.169103	A0A3Q1LUW6_BOVIN	0.666529411	0.990714556	0.964775773
418	0.051991	0.3775401	0.212994	F1MHL1_BOVIN	0.666529411	0.990714556	0.984318014
373	0.050665	0.631704969	0.247687	G5E569_BOVIN	0.666529411	0.990714556	0.994543987
130	0.471352	0.603213936	0.509952	G3X6I0_BOVIN	0.696436291	0.780714556	0.064543987
614	0.064354	0.227790081	0.14768	RS28_BOVIN	0.808839841	0.990714556	0.964775773
264	0.068663	0.025025622	0.018605	A0A3Q1LMV9_BOVIN	0.816449273	0.582330163	0.524156036
567	0.080535	0.104802976	0.04259	A0A3Q1LUP1_BOVIN	0.816449273	0.861265483	0.827272132
602	0.081282	0.091442425	0.097429	F1MC40_BOVIN	0.816449273	0.858055202	0.964775773
625	0.082791	0.131392205	0.129989	F2FB38_BOVIN	0.816449273	0.919683065	0.964775773
91	0.075247	0.249181826	0.121767	A0A3Q1LVA2_BOVIN	0.816449273	0.990714556	0.964775773
122	0.072161	0.350704238	0.140539	PCP4_BOVIN	0.816449273	0.990714556	0.964775773
304	0.077882	0.290871061	0.180905	HMGB1_BOVIN	0.816449273	0.990714556	0.964775773
339	0.082363	0.463326717	0.171472	SYNC_BOVIN	0.816449273	0.990714556	0.964775773
415	0.078085	0.293066083	0.182435	A0A3Q1M1Z4_BOVIN	0.816449273	0.990714556	0.964775773
489	0.067766	0.226580249	0.103732	F1N1C9_BOVIN	0.816449273	0.990714556	0.964775773
574	0.078132	0.492210783	0.175423	A2VDX0_BOVIN	0.816449273	0.990714556	0.964775773
105	0.071659	0.496374824	0.270185	NACA_BOVIN	0.816449273	0.990714556	0.994543987
520	0.078118	0.378601638	0.310041	F6QQ60_BOVIN	0.816449273	0.990714556	0.994543987
622	0.072465	0.58215903	0.307217	F6QND5_BOVIN	0.816449273	0.990714556	0.994543987
595	0.08623	0.076853692	0.08536	G5E5H2_BOVIN	0.825379534	0.858055202	0.964775773
592	0.086272	0.458784345	0.198787	A0A3Q1LJB2_BOVIN	0.825379534	0.990714556	0.98209708

60	0.091876	0.583488689	0.330882	F6Q9Q9_BOVIN	0.866068051	0.990714556	0.994543987
507	0.100102	0.007675207	0.007646	KCRU_BOVIN	0.873440845	0.305058511	0.288281874
493	0.096143	0.039289574	0.036446	A0A3Q1MK01_BOVIN	0.873440845	0.740724019	0.805586197
490	0.09945	0.382297091	0.183278	DDAH2_BOVIN	0.873440845	0.990714556	0.964775773
497	0.097193	0.644100442	0.616735	CZIB_BOVIN	0.873440845	0.990714556	0.994543987
517	0.100834	0.67882282	0.235249	F1MKU4_BOVIN	0.873440845	0.990714556	0.994543987
528	0.096632	0.226926427	0.225782	A0A3Q1LQR2_BOVIN	0.873440845	0.990714556	0.994543987
211	0.104841	0.361390483	0.287584	F1MWU9_BOVIN	0.895133384	0.990714556	0.994543987
359	0.106131	0.713861995	0.34819	DX39B_BOVIN	0.895133384	0.990714556	0.994543987
183	0.11101	0.459461858	0.230231	PSA5_BOVIN	0.92412292	0.990714556	0.994543987
71	0.112667	0.047211187	0.057528	Q3SYR8_BOVIN	0.92589524	0.781636274	0.851397162
93	0.11644	0.367355525	0.170236	APOC3_BOVIN	0.927914382	0.990714556	0.964775773
171	0.117256	0.599415293	0.306974	A0A3Q1N4K8_BOVIN	0.927914382	0.990714556	0.994543987
408	0.114439	0.52676939	0.255806	E1BI72_BOVIN	0.927914382	0.990714556	0.994543987
585	0.121283	0.091426527	0.113266	A5D7J6_BOVIN	0.936658134	0.858055202	0.964775773
220	0.120297	0.836971811	0.34994	A6H7E3_BOVIN	0.936658134	0.990714556	0.994543987
323	0.129295	0.855955497	0.421966	A7MBI5_BOVIN	0.986641871	0.990714556	0.994543987
203	0.134202	0.093379716	0.04916	E1BKX7_BOVIN	0.991368295	0.858055202	0.851397162
378	0.133705	0.173470071	0.10036	O62652_BOVIN	0.991368295	0.984775119	0.964775773
361	0.134554	0.355744254	0.309424	UPK3L_BOVIN	0.991368295	0.990714556	0.994543987
432	0.268203	0.004681947	0.013342	MESD_BOVIN	0.996436291	0.200075189	0.475136946
401	0.226318	0.021605411	0.038979	E1BLV6_BOVIN	0.996436291	0.532656478	0.820843466
406	0.315356	0.01372719	0.041987	TM214_BOVIN	0.996436291	0.472981997	0.827272132
170	0.231752	0.014322099	0.059676	HP252_BOVIN	0.996436291	0.472981997	0.851397162
17	0.220219	0.016675585	0.059902	APOA1_BOVIN	0.996436291	0.485865903	0.851397162
485	0.522242	0.015960625	0.056453	E1BP41_BOVIN	0.996436291	0.485865903	0.851397162
534	0.317073	0.044378772	0.052622	RLA0_BOVIN	0.996436291	0.781636274	0.851397162
407	0.199105	0.052991168	0.054916	A5D7Q2_BOVIN	0.996436291	0.789938111	0.851397162
654	0.169575	0.052073107	0.061099	S100G_BOVIN	0.996436291	0.789938111	0.851397162
238	0.14716	0.065381241	0.059615	G3N1H5_BOVIN	0.996436291	0.858055202	0.851397162

445	0.182194	0.046067642	0.072559	G3MZE0_BOVIN	0.996436291	0.781636274	0.911965137
368	0.250774	0.055350438	0.067705	COMT_BOVIN	0.996436291	0.806355243	0.911965137
250	0.14937	0.060374736	0.068466	A0A3Q1ML26_BOVIN	0.996436291	0.858055202	0.911965137
308	0.597402	0.014757629	0.079868	D2U6Q4_BOVIN	0.996436291	0.472981997	0.964775773
498	0.59294	0.019231812	0.103912	F1MMK9_BOVIN	0.996436291	0.513649633	0.964775773
14	0.496968	0.020464205	0.115238	B0JYQ0_BOVIN	0.996436291	0.524702204	0.964775773
547	0.492698	0.029259744	0.105795	A0A3Q1MBT3_BOVIN	0.996436291	0.640109174	0.964775773
518	0.536923	0.034935261	0.085909	F1MTR1_BOVIN	0.996436291	0.701306609	0.964775773
389	0.609234	0.047556653	0.136723	PSA3_BOVIN	0.996436291	0.781636274	0.964775773
642	0.596168	0.04302621	0.183544	A0A3Q1LP76_BOVIN	0.996436291	0.781636274	0.964775773
360	0.287321	0.052241062	0.10251	Q2KJ57_BOVIN	0.996436291	0.789938111	0.964775773
36	0.374024	0.075583582	0.182445	B0JYN6_BOVIN	0.996436291	0.858055202	0.964775773
40	0.154621	0.072779191	0.120382	A1BG_BOVIN	0.996436291	0.858055202	0.964775773
221	0.478133	0.070029238	0.1639	A0A3Q1LWV8_BOVIN	0.996436291	0.858055202	0.964775773
223	0.85947	0.073940795	0.149898	MVP_BOVIN	0.996436291	0.858055202	0.964775773
281	0.453483	0.069475166	0.123857	A6QLZ0_BOVIN	0.996436291	0.858055202	0.964775773
338	0.508588	0.073308363	0.14441	A0A3Q1M8L6_BOVIN	0.996436291	0.858055202	0.964775773
365	0.271803	0.096460952	0.162621	F1N694_BOVIN	0.996436291	0.858055202	0.964775773
385	0.325628	0.076116928	0.137883	Q5H9M6_BOVIN	0.996436291	0.858055202	0.964775773
474	0.365027	0.071950844	0.129319	TBB5_BOVIN	0.996436291	0.858055202	0.964775773
511	0.472509	0.095415667	0.171329	M5FMU4_BOVIN	0.996436291	0.858055202	0.964775773
540	0.423131	0.070049855	0.150985	AFAM_BOVIN	0.996436291	0.858055202	0.964775773
551	0.523184	0.089679336	0.185036	A0A3Q1MBP6_BOVIN	0.996436291	0.858055202	0.964775773
552	0.425587	0.0863586	0.149719	G3N1E4_BOVIN	0.996436291	0.858055202	0.964775773
78	0.334923	0.102843494	0.08524	K1C19_BOVIN	0.996436291	0.861265483	0.964775773
327	0.213769	0.102253213	0.185129	A0A3Q1M9I5_BOVIN	0.996436291	0.861265483	0.964775773
384	0.273741	0.104206627	0.126151	F1N169_BOVIN	0.996436291	0.861265483	0.964775773
62	0.276692	0.116375566	0.1518	PDIA3_BOVIN	0.996436291	0.919683065	0.964775773
69	0.230125	0.136784171	0.139614	HP20_BOVIN	0.996436291	0.919683065	0.964775773
157	0.288062	0.124040407	0.161139	PSMD2_BOVIN	0.996436291	0.919683065	0.964775773

248	0.218555	0.127689087	0.180796	RLA2_BOVIN	0.996436291	0.919683065	0.964775773
294	0.478339	0.113367855	0.148592	E1BLZ8_BOVIN	0.996436291	0.919683065	0.964775773
324	0.636282	0.122475687	0.147977	Q32PB7_BOVIN	0.996436291	0.919683065	0.964775773
399	0.342392	0.118252708	0.152294	E1BEX4_BOVIN	0.996436291	0.919683065	0.964775773
404	0.169021	0.13515889	0.121334	A0A452DHY4_BOVIN	0.996436291	0.919683065	0.964775773
530	0.314013	0.131718865	0.119218	A0A3Q1NJM8_BOVIN	0.996436291	0.919683065	0.964775773
594	0.292811	0.127620664	0.168932	F1N3Q7_BOVIN	0.996436291	0.919683065	0.964775773
231	0.49319	0.14070669	0.164738	Q2TBR3_BOVIN	0.996436291	0.922052917	0.964775773
557	0.895878	0.142773819	0.181559	A0A3Q1MF86_BOVIN	0.996436291	0.924424424	0.964775773
129	0.171336	0.183438743	0.098179	SYWC_BOVIN	0.996436291	0.984775119	0.964775773
267	0.144553	0.17965262	0.089385	MOES_BOVIN	0.996436291	0.984775119	0.964775773
303	0.194228	0.177157324	0.106104	E1BFV0_BOVIN	0.996436291	0.984775119	0.964775773
332	0.529266	0.214982964	0.172312	F1MJ95_BOVIN	0.996436291	0.984775119	0.964775773
500	0.316027	0.209879484	0.166099	F2FB42_BOVIN	0.996436291	0.984775119	0.964775773
635	0.194042	0.190970193	0.176594	A4IFV2_BOVIN	0.996436291	0.984775119	0.964775773
70	0.243716	0.226768939	0.150956	LKHA4_BOVIN	0.996436291	0.990714556	0.964775773
259	0.326859	0.243613738	0.153512	PGAM1_BOVIN	0.996436291	0.990714556	0.964775773
391	0.825428	0.078855085	0.190728	F2Z4D5_BOVIN	0.996436291	0.858055202	0.97892464
375	0.437479	0.156048091	0.192116	E1BKQ7_BOVIN	0.996436291	0.974458659	0.97892464
226	0.252205	0.408863887	0.192425	ENPL_BOVIN	0.996436291	0.990714556	0.97892464
577	0.976029	0.091366527	0.195505	F1MWD3_BOVIN	0.996436291	0.858055202	0.979054762
227	0.182553	0.155092517	0.195318	AK1A1_BOVIN	0.996436291	0.974458659	0.979054762
495	0.285652	0.202004055	0.200207	A0A140T846_BOVIN	0.996436291	0.984775119	0.98209708
572	0.689052	0.115200879	0.210941	E1B748_BOVIN	0.996436291	0.919683065	0.984318014
126	0.424565	0.193133802	0.214984	AMPL_BOVIN	0.996436291	0.984775119	0.984318014
181	0.71001	0.193848214	0.206194	F2Z4C1_BOVIN	0.996436291	0.984775119	0.984318014
195	0.158174	0.212821043	0.209043	F1MU19_BOVIN	0.996436291	0.984775119	0.984318014
619	0.552288	0.179973332	0.212258	USO1_BOVIN	0.996436291	0.984775119	0.984318014
523	0.16933	0.473368981	0.207271	CLP1_BOVIN	0.996436291	0.990714556	0.984318014
649	0.185619	0.331596143	0.2109	A0A3Q1M6K6_BOVIN	0.996436291	0.990714556	0.984318014

117	0.414482	0.09145192	0.423321	A0A452DIM3_BOVIN	0.996436291	0.858055202	0.994543987
645	0.646523	0.083496772	0.280674	F1MQH8_BOVIN	0.996436291	0.858055202	0.994543987
174	0.732554	0.135271975	0.298717	A0A3Q1LVC8_BOVIN	0.996436291	0.919683065	0.994543987
266	0.984651	0.121173899	0.314679	A0A3Q1MJ74_BOVIN	0.996436291	0.919683065	0.994543987
351	0.834779	0.129133075	0.315348	F1MLM2_BOVIN	0.996436291	0.919683065	0.994543987
456	0.527966	0.120061012	0.245734	E1BM96_BOVIN	0.996436291	0.919683065	0.994543987
571	0.626249	0.137737245	0.323926	A0A3Q1MFI7_BOVIN	0.996436291	0.919683065	0.994543987
662	0.96369	0.13771266	0.305402	A0A452DI85_BOVIN	0.996436291	0.919683065	0.994543987
632	0.663266	0.140969089	0.464763	E1BNG8_BOVIN	0.996436291	0.922052917	0.994543987
455	0.738553	0.14791416	0.363347	A0A3Q1LV73_BOVIN	0.996436291	0.948129765	0.994543987
509	0.611729	0.156582281	0.33903	A0A3Q1MDA5_BOVIN	0.996436291	0.974458659	0.994543987
33	0.516676	0.166529533	0.246246	PRDX6_BOVIN	0.996436291	0.979315877	0.994543987
307	0.250251	0.166372583	0.238962	A6H7A2_BOVIN	0.996436291	0.979315877	0.994543987
331	0.713737	0.160024205	0.220101	Q2KJ75_BOVIN	0.996436291	0.979315877	0.994543987
412	0.490326	0.163491087	0.303497	A0A3Q1N1K0_BOVIN	0.996436291	0.979315877	0.994543987
640	0.733379	0.164654026	0.488985	A1A4N9_BOVIN	0.996436291	0.979315877	0.994543987
34	0.652572	0.20618374	0.442941	VTDB_BOVIN	0.996436291	0.984775119	0.994543987
94	0.468502	0.206531206	0.399105	ASGL1_BOVIN	0.996436291	0.984775119	0.994543987
110	0.716891	0.194707261	0.231188	A0A3Q1LN63_BOVIN	0.996436291	0.984775119	0.994543987
233	0.34348	0.210947812	0.314638	ACLY_BOVIN	0.996436291	0.984775119	0.994543987
240	0.6487	0.209948616	0.479195	C1QBP_BOVIN	0.996436291	0.984775119	0.994543987
276	0.86946	0.206128567	0.508393	A0A3Q1MIN7_BOVIN	0.996436291	0.984775119	0.994543987
280	0.534283	0.209251546	0.322738	B8Y9T0_BOVIN	0.996436291	0.984775119	0.994543987
296	0.309379	0.210624473	0.275715	F1MW03_BOVIN	0.996436291	0.984775119	0.994543987
376	0.941836	0.198582089	0.461555	A5PJV5_BOVIN	0.996436291	0.984775119	0.994543987
382	0.938168	0.211841654	0.47609	F193B_BOVIN	0.996436291	0.984775119	0.994543987
403	0.703142	0.215083489	0.388326	Q0VD52_BOVIN	0.996436291	0.984775119	0.994543987
423	0.721084	0.204145113	0.338921	G3MYM8_BOVIN	0.996436291	0.984775119	0.994543987
496	0.794895	0.209954477	0.424436	G3MX65_BOVIN	0.996436291	0.984775119	0.994543987
501	0.697264	0.210872606	0.399456	ABRAL_BOVIN	0.996436291	0.984775119	0.994543987

531	0.865612	0.18521478	0.261587	EF1B_BOVIN	0.996436291	0.984775119	0.994543987
575	0.462516	0.196847797	0.23306	A0A3Q1LY31_BOVIN	0.996436291	0.984775119	0.994543987
603	0.157407	0.203241039	0.252394	A0A3Q1LHZ0_BOVIN	0.996436291	0.984775119	0.994543987
15	0.723433	0.80072163	0.890098	HBB_BOVIN	0.996436291	0.990714556	0.994543987
16	0.378154	0.26301801	0.243661	HBA_BOVIN	0.996436291	0.990714556	0.994543987
19	0.681659	0.535614671	0.636644	ANXA1_BOVIN	0.996436291	0.990714556	0.994543987
20	0.189908	0.817346386	0.308922	FOLR1_BOVIN	0.996436291	0.990714556	0.994543987
21	0.704588	0.574759805	0.803247	ANXA2_BOVIN	0.996436291	0.990714556	0.994543987
23	0.528609	0.384260109	0.511703	E1BI28_BOVIN	0.996436291	0.990714556	0.994543987
24	0.819388	0.702126854	0.71177	HSPB1_BOVIN	0.996436291	0.990714556	0.994543987
25	0.760551	0.691414784	0.891144	KCRB_BOVIN	0.996436291	0.990714556	0.994543987
26	0.146224	0.96874577	0.491049	A6QLL8_BOVIN	0.996436291	0.990714556	0.994543987
28	0.730206	0.732515477	0.658286	EZRI_BOVIN	0.996436291	0.990714556	0.994543987
29	0.407301	0.343646542	0.286354	PIGR_BOVIN	0.996436291	0.990714556	0.994543987
30	0.706238	0.527172004	0.718603	A1AG_BOVIN	0.996436291	0.990714556	0.994543987
31	0.963066	0.633982313	0.514856	Q3ZC87_BOVIN	0.996436291	0.990714556	0.994543987
32	0.608507	0.473309301	0.649614	CFAB_BOVIN	0.996436291	0.990714556	0.994543987
35	0.390745	0.890161377	0.852026	TPIS_BOVIN	0.996436291	0.990714556	0.994543987
37	0.743357	0.367085302	0.444899	PPIA_BOVIN	0.996436291	0.990714556	0.994543987
38	0.174803	0.502714617	0.23225	GSTP1_BOVIN	0.996436291	0.990714556	0.994543987
41	0.895979	0.776994219	0.835888	A7Z014_BOVIN	0.996436291	0.990714556	0.994543987
42	0.207064	0.492368317	0.397656	NDKB_BOVIN	0.996436291	0.990714556	0.994543987
43	0.894252	0.880010325	0.948764	THIO_BOVIN	0.996436291	0.990714556	0.994543987
44	0.979303	0.668298822	0.870054	F1MAV0_BOVIN	0.996436291	0.990714556	0.994543987
46	0.821358	0.656276121	0.897613	PROF1_BOVIN	0.996436291	0.990714556	0.994543987
47	0.515452	0.384780466	0.272359	GDIB_BOVIN	0.996436291	0.990714556	0.994543987
48	0.897718	0.406262473	0.411169	Q3ZCI4_BOVIN	0.996436291	0.990714556	0.994543987
49	0.584368	0.424667677	0.654742	MIF_BOVIN	0.996436291	0.990714556	0.994543987
50	0.505988	0.935073276	0.872726	A7Z057_BOVIN	0.996436291	0.990714556	0.994543987
51	0.506192	0.693073256	0.907242	GRP_BOVIN	0.996436291	0.990714556	0.994543987

53	0.689963	0.924942	0.830559	ABHEB_BOVIN	0.996436291	0.990714556	0.994543987
54	0.477788	0.5749247	0.614507	Q5DPW9_BOVIN	0.996436291	0.990714556	0.994543987
55	0.589724	0.935988731	0.877385	A0A452DIW4_BOVIN	0.996436291	0.990714556	0.994543987
56	0.232708	0.668022429	0.507549	BIP_BOVIN	0.996436291	0.990714556	0.994543987
57	0.713249	0.750601685	0.826317	PEBP1_BOVIN	0.996436291	0.990714556	0.994543987
58	0.942888	0.632730535	0.949091	PARK7_BOVIN	0.996436291	0.990714556	0.994543987
59	0.80761	0.334006638	0.318622	A0A3Q1M5R4_BOVIN	0.996436291	0.990714556	0.994543987
63	0.585049	0.871431216	0.903818	G3X757_BOVIN	0.996436291	0.990714556	0.994543987
65	0.559229	0.390354201	0.626239	A0A140T831_BOVIN	0.996436291	0.990714556	0.994543987
66	0.206282	0.361913596	0.302885	S10A4_BOVIN	0.996436291	0.990714556	0.994543987
67	0.510407	0.708377722	0.860085	A0A3Q1LKR8_BOVIN	0.996436291	0.990714556	0.994543987
68	0.720969	0.7325528	0.867002	AMPN_BOVIN	0.996436291	0.990714556	0.994543987
72	0.829751	0.770045678	0.775164	AN32A_BOVIN	0.996436291	0.990714556	0.994543987
73	0.986005	0.869428089	0.845349	G5E5C8_BOVIN	0.996436291	0.990714556	0.994543987
74	0.681199	0.797149865	0.913719	ACTN4_BOVIN	0.996436291	0.990714556	0.994543987
75	0.673507	0.532919572	0.746809	SAHH_BOVIN	0.996436291	0.990714556	0.994543987
76	0.747467	0.822061365	0.822333	A0A3Q1LJT1_BOVIN	0.996436291	0.990714556	0.994543987
79	0.638393	0.565568532	0.837065	F1MQ37_BOVIN	0.996436291	0.990714556	0.994543987
80	0.968668	0.859804838	0.932401	F1N2I5_BOVIN	0.996436291	0.990714556	0.994543987
81	0.777826	0.590428406	0.798545	F1N0E5_BOVIN	0.996436291	0.990714556	0.994543987
82	0.64067	0.866036222	0.950515	GLRX1_BOVIN	0.996436291	0.990714556	0.994543987
84	0.490298	0.374442631	0.31081	F1N3J3_BOVIN	0.996436291	0.990714556	0.994543987
86	0.743766	0.887701266	0.928412	F1MM83_BOVIN	0.996436291	0.990714556	0.994543987
87	0.466255	0.751928853	0.642402	ATOX1_BOVIN	0.996436291	0.990714556	0.994543987
88	0.946111	0.747775769	0.727485	LG3BP_BOVIN	0.996436291	0.990714556	0.994543987
89	0.794357	0.790459208	0.881808	CAH2_BOVIN	0.996436291	0.990714556	0.994543987
90	0.205307	0.600660156	0.38462	A0A452DII8_BOVIN	0.996436291	0.990714556	0.994543987
92	0.489925	0.303290229	0.368187	F1MP31_BOVIN	0.996436291	0.990714556	0.994543987
96	0.427229	0.523397268	0.832965	A7E3D5_BOVIN	0.996436291	0.990714556	0.994543987
98	0.755595	0.888701288	0.949335	STIP1_BOVIN	0.996436291	0.990714556	0.994543987

99	0.145585	0.582897316	0.441809	VNN1_BOVIN	0.996436291	0.990714556	0.994543987
100	0.906368	0.903204687	0.856701	F1N4K1_BOVIN	0.996436291	0.990714556	0.994543987
101	0.604591	0.31930205	0.413172	A0A3Q1MFI5_BOVIN	0.996436291	0.990714556	0.994543987
102	0.891594	0.756329387	0.685218	ANXA8_BOVIN	0.996436291	0.990714556	0.994543987
103	0.852107	0.79402138	0.592029	ARF1_BOVIN	0.996436291	0.990714556	0.994543987
104	0.687229	0.563657779	0.702181	A0A3Q1NNJ3_BOVIN	0.996436291	0.990714556	0.994543987
107	0.601672	0.789707862	0.605064	F1MYN5_BOVIN	0.996436291	0.990714556	0.994543987
108	0.447802	0.465301896	0.393042	Q17QX0_BOVIN	0.996436291	0.990714556	0.994543987
109	0.921923	0.282627374	0.488444	TCPD_BOVIN	0.996436291	0.990714556	0.994543987
111	0.652943	0.829620299	0.55549	Q1RMP3_BOVIN	0.996436291	0.990714556	0.994543987
112	0.490775	0.948370894	0.760365	A0A3Q1M352_BOVIN	0.996436291	0.990714556	0.994543987
113	0.86404	0.847842934	0.768784	ACBP_BOVIN	0.996436291	0.990714556	0.994543987
114	0.832611	0.635768806	0.736783	FKB1A_BOVIN	0.996436291	0.990714556	0.994543987
115	0.34087	0.332862901	0.344703	Q58CS3_BOVIN	0.996436291	0.990714556	0.994543987
116	0.729833	0.286585679	0.486887	B3VTM3_BOVIN	0.996436291	0.990714556	0.994543987
119	0.532251	0.410997354	0.92352	A0A3Q1NJB1_BOVIN	0.996436291	0.990714556	0.994543987
120	0.185927	0.451922157	0.233191	SERA_BOVIN	0.996436291	0.990714556	0.994543987
121	0.659861	0.818799038	0.613161	ARSA_BOVIN	0.996436291	0.990714556	0.994543987
123	0.845791	0.818301495	0.805382	PSME1_BOVIN	0.996436291	0.990714556	0.994543987
125	0.356951	0.584220447	0.635727	PTMA_BOVIN	0.996436291	0.990714556	0.994543987
127	0.909141	0.795093632	0.601269	LDHA_BOVIN	0.996436291	0.990714556	0.994543987
128	0.586323	0.711849251	0.670576	A0A3Q1MKY2_BOVIN	0.996436291	0.990714556	0.994543987
131	0.489072	0.648789217	0.529004	TAGL2_BOVIN	0.996436291	0.990714556	0.994543987
132	0.964567	0.81980148	0.958158	CAPG_BOVIN	0.996436291	0.990714556	0.994543987
133	0.31123	0.595007691	0.550055	TCPZ_BOVIN	0.996436291	0.990714556	0.994543987
135	0.884675	0.749680819	0.837488	F1MUZ9_BOVIN	0.996436291	0.990714556	0.994543987
136	0.915957	0.522082528	0.552453	ENOPH_BOVIN	0.996436291	0.990714556	0.994543987
138	0.532206	0.892004619	0.795274	COF1_BOVIN	0.996436291	0.990714556	0.994543987
139	0.552898	0.533632062	0.345062	RL40_BOVIN	0.996436291	0.990714556	0.994543987
140	0.892232	0.78967138	0.850402	PCBP1_BOVIN	0.996436291	0.990714556	0.994543987

141	0.955429	0.384287218	0.450221	F1MYX5_BOVIN	0.996436291	0.990714556	0.994543987
145	0.390105	0.679246057	0.722635	A0A3Q1LX83_BOVIN	0.996436291	0.990714556	0.994543987
146	0.302953	0.709247337	0.526501	ST1A1_BOVIN	0.996436291	0.990714556	0.994543987
147	0.732723	0.774870663	0.900625	MYL9_BOVIN	0.996436291	0.990714556	0.994543987
148	0.501743	0.960874196	0.610959	TTHY_BOVIN	0.996436291	0.990714556	0.994543987
149	0.823127	0.786383399	0.939311	HSP7C_BOVIN	0.996436291	0.990714556	0.994543987
150	0.443636	0.779872182	0.622464	A0A3Q1MEU1_BOVIN	0.996436291	0.990714556	0.994543987
151	0.749388	0.482675382	0.636173	THRB_BOVIN	0.996436291	0.990714556	0.994543987
152	0.200396	0.93798794	0.575028	F6QEU6_BOVIN	0.996436291	0.990714556	0.994543987
153	0.269047	0.886809486	0.912737	A0A3Q1LU13_BOVIN	0.996436291	0.990714556	0.994543987
154	0.691878	0.310484282	0.427153	APOA2_BOVIN	0.996436291	0.990714556	0.994543987
156	0.355443	0.364709552	0.302073	CALM_BOVIN	0.996436291	0.990714556	0.994543987
158	0.855188	0.715538701	0.914199	F1N647_BOVIN	0.996436291	0.990714556	0.994543987
159	0.454118	0.860971087	0.942195	PNCB_BOVIN	0.996436291	0.990714556	0.994543987
160	0.892044	0.375461984	0.404461	APT_BOVIN	0.996436291	0.990714556	0.994543987
161	0.851103	0.606722933	0.642206	1433T_BOVIN	0.996436291	0.990714556	0.994543987
162	0.593467	0.274749581	0.471964	TFF3_BOVIN	0.996436291	0.990714556	0.994543987
163	0.633587	0.793315315	0.719335	PSA1_BOVIN	0.996436291	0.990714556	0.994543987
164	0.493923	0.744546549	0.922239	CLIC1_BOVIN	0.996436291	0.990714556	0.994543987
165	0.309016	0.691578587	0.810531	F1MWR8_BOVIN	0.996436291	0.990714556	0.994543987
166	0.89203	0.736906471	0.798966	1433E_BOVIN	0.996436291	0.990714556	0.994543987
167	0.427105	0.76452395	0.937412	A1AT_BOVIN	0.996436291	0.990714556	0.994543987
168	0.946131	0.73522139	0.671586	A0A3Q1MFC3_BOVIN	0.996436291	0.990714556	0.994543987
169	0.757135	0.92555209	0.867264	G3X6S5_BOVIN	0.996436291	0.990714556	0.994543987
172	0.35127	0.83791452	0.660112	H9KUV2_BOVIN	0.996436291	0.990714556	0.994543987
173	0.437201	0.375669612	0.467071	A0A3Q1LPG0_BOVIN	0.996436291	0.990714556	0.994543987
175	0.449012	0.821423775	0.682826	A6QNL5_BOVIN	0.996436291	0.990714556	0.994543987
176	0.444478	0.301771079	0.384479	G3P_BOVIN	0.996436291	0.990714556	0.994543987
177	0.87423	0.445324525	0.522709	GALK1_BOVIN	0.996436291	0.990714556	0.994543987
179	0.848071	0.274405284	0.279527	F1MCK2_BOVIN	0.996436291	0.990714556	0.994543987

180	0.779933	0.686143982	0.948804	ESTD_BOVIN	0.996436291	0.990714556	0.994543987
182	0.934569	0.555397539	0.590936	A0A3Q1MN33_BOVIN	0.996436291	0.990714556	0.994543987
186	0.51714	0.870745619	0.791412	A4FV56_BOVIN	0.996436291	0.990714556	0.994543987
187	0.685247	0.482735432	0.806838	STMN1_BOVIN	0.996436291	0.990714556	0.994543987
188	0.733705	0.582627213	0.571739	GDIA_BOVIN	0.996436291	0.990714556	0.994543987
189	0.964624	0.589265784	0.758072	PRDX1_BOVIN	0.996436291	0.990714556	0.994543987
191	0.984067	0.63486794	0.717318	TBB2B_BOVIN	0.996436291	0.990714556	0.994543987
192	0.34331	0.219015403	0.337027	Q0IIA4_BOVIN	0.996436291	0.990714556	0.994543987
193	0.409387	0.727194355	0.871887	G6PI_BOVIN	0.996436291	0.990714556	0.994543987
196	0.199245	0.347396321	0.220741	EF2_BOVIN	0.996436291	0.990714556	0.994543987
197	0.785559	0.707314969	0.583176	MVD1_BOVIN	0.996436291	0.990714556	0.994543987
198	0.713439	0.277132513	0.289379	A0A3Q1LGM4_BOVIN	0.996436291	0.990714556	0.994543987
199	0.829828	0.27445828	0.534442	AN32B_BOVIN	0.996436291	0.990714556	0.994543987
201	0.508841	0.660267178	0.478981	A5D9D1_BOVIN	0.996436291	0.990714556	0.994543987
202	0.210206	0.798112926	0.666175	G5E5Y5_BOVIN	0.996436291	0.990714556	0.994543987
205	0.883598	0.471230092	0.54915	RANG_BOVIN	0.996436291	0.990714556	0.994543987
206	0.827692	0.794344893	0.568038	Q3SZN8_BOVIN	0.996436291	0.990714556	0.994543987
207	0.279779	0.480512171	0.340466	GPX1_BOVIN	0.996436291	0.990714556	0.994543987
208	0.509392	0.297687855	0.382712	PGK1_BOVIN	0.996436291	0.990714556	0.994543987
210	0.838588	0.842076627	0.869927	Q28908_BOVIN	0.996436291	0.990714556	0.994543987
212	0.798973	0.855566119	0.832082	LY66C_BOVIN	0.996436291	0.990714556	0.994543987
213	0.544252	0.695878655	0.460556	BPNT1_BOVIN	0.996436291	0.990714556	0.994543987
214	0.308363	0.359383888	0.304334	LEG1_BOVIN	0.996436291	0.990714556	0.994543987
215	0.600387	0.254775638	0.356735	NHRF3_BOVIN	0.996436291	0.990714556	0.994543987
216	0.669451	0.667756034	0.67294	A0A3Q1N1N6_BOVIN	0.996436291	0.990714556	0.994543987
217	0.978126	0.718212959	0.859351	CAH1_BOVIN	0.996436291	0.990714556	0.994543987
218	0.564664	0.904248605	0.718867	SPSY_BOVIN	0.996436291	0.990714556	0.994543987
219	0.912617	0.68343065	0.685061	A0A3Q1LTP0_BOVIN	0.996436291	0.990714556	0.994543987
222	0.501214	0.862001438	0.903154	GRP75_BOVIN	0.996436291	0.990714556	0.994543987
224	0.645407	0.841726277	0.858136	ADHX_BOVIN	0.996436291	0.990714556	0.994543987

225	0.839588	0.73363831	0.540378	PTGR1_BOVIN	0.996436291	0.990714556	0.994543987
228	0.94433	0.427248107	0.442156	A0A3Q1LQ34_BOVIN	0.996436291	0.990714556	0.994543987
229	0.805087	0.273654119	0.530383	DBNL_BOVIN	0.996436291	0.990714556	0.994543987
230	0.25919	0.600456774	0.300705	F1MKS5_BOVIN	0.996436291	0.990714556	0.994543987
232	0.688226	0.333307141	0.36379	A0A3Q1LU36_BOVIN	0.996436291	0.990714556	0.994543987
235	0.585255	0.844395454	0.828028	A0A3Q1MM86_BOVIN	0.996436291	0.990714556	0.994543987
237	0.565739	0.492116433	0.481949	A6QLT9_BOVIN	0.996436291	0.990714556	0.994543987
241	0.325185	0.650536707	0.533835	A0A3Q1MDA4_BOVIN	0.996436291	0.990714556	0.994543987
242	0.900468	0.438404643	0.601973	A0A3Q1MFJ2_BOVIN	0.996436291	0.990714556	0.994543987
243	0.428455	0.275961018	0.420285	TPMT_BOVIN	0.996436291	0.990714556	0.994543987
244	0.866451	0.813123135	0.804926	F1N3P2_BOVIN	0.996436291	0.990714556	0.994543987
245	0.377452	0.42675055	0.753205	A0A452DHV9_BOVIN	0.996436291	0.990714556	0.994543987
246	0.936633	0.723633891	0.835789	F1MM57_BOVIN	0.996436291	0.990714556	0.994543987
249	0.613434	0.422741581	0.621289	A0A3Q1LXR9_BOVIN	0.996436291	0.990714556	0.994543987
251	0.803928	0.258537541	0.246364	PSA4_BOVIN	0.996436291	0.990714556	0.994543987
253	0.230121	0.436684446	0.437274	TBCA_BOVIN	0.996436291	0.990714556	0.994543987
254	0.945511	0.49874335	0.639142	ANXA4_BOVIN	0.996436291	0.990714556	0.994543987
255	0.189832	0.536807879	0.309894	TYB10_BOVIN	0.996436291	0.990714556	0.994543987
256	0.464883	0.301982209	0.456643	IF5A1_BOVIN	0.996436291	0.990714556	0.994543987
257	0.773805	0.665656933	0.782986	F1MLX9_BOVIN	0.996436291	0.990714556	0.994543987
258	0.761543	0.672540592	0.761839	HP251_BOVIN	0.996436291	0.990714556	0.994543987
260	0.915938	0.56974245	0.833215	A2VE41_BOVIN	0.996436291	0.990714556	0.994543987
261	0.919921	0.412766421	0.6975	Q0P5D6_BOVIN	0.996436291	0.990714556	0.994543987
262	0.530028	0.259504611	0.302038	A0A498UZ20_BOVIN	0.996436291	0.990714556	0.994543987
265	0.16946	0.434920294	0.24864	F1MDH3_BOVIN	0.996436291	0.990714556	0.994543987
268	0.855502	0.619501812	0.662927	F1MPU0_BOVIN	0.996436291	0.990714556	0.994543987
269	0.158601	0.523317116	0.420653	WDR1_BOVIN	0.996436291	0.990714556	0.994543987
270	0.751288	0.59574723	0.589419	B2MG_BOVIN	0.996436291	0.990714556	0.994543987
272	0.383514	0.696963447	0.521744	SERPH_BOVIN	0.996436291	0.990714556	0.994543987
273	0.853153	0.680874973	0.835537	E1BDF5_BOVIN	0.996436291	0.990714556	0.994543987

274	0.650077	0.663010507	0.748937	Q2KIF2_BOVIN	0.996436291	0.990714556	0.994543987
277	0.949602	0.435473933	0.813008	A0A140T894_BOVIN	0.996436291	0.990714556	0.994543987
279	0.641343	0.310402833	0.471535	A0A3Q1LKU1_BOVIN	0.996436291	0.990714556	0.994543987
282	0.958834	0.651496052	0.890244	A0A3Q1LTS9_BOVIN	0.996436291	0.990714556	0.994543987
283	0.696724	0.461721509	0.591877	PEDF_BOVIN	0.996436291	0.990714556	0.994543987
285	0.572606	0.352607271	0.511205	Q3T0Z0_BOVIN	0.996436291	0.990714556	0.994543987
286	0.349002	0.613755964	0.481253	E1BJG5_BOVIN	0.996436291	0.990714556	0.994543987
287	0.901261	0.797167443	0.91126	SODC_BOVIN	0.996436291	0.990714556	0.994543987
290	0.81928	0.609643509	0.737224	E1BBY7_BOVIN	0.996436291	0.990714556	0.994543987
292	0.642805	0.405147859	0.823138	E1BJP1_BOVIN	0.996436291	0.990714556	0.994543987
293	0.168468	0.264040387	0.275723	A0A3Q1M4L0_BOVIN	0.996436291	0.990714556	0.994543987
295	0.54478	0.296115952	0.494229	A0A3Q1LQQ0_BOVIN	0.996436291	0.990714556	0.994543987
297	0.481761	0.360695572	0.339698	A0A3Q1MNN6_BOVIN	0.996436291	0.990714556	0.994543987
298	0.555997	0.436948529	0.885015	A4IFI0_BOVIN	0.996436291	0.990714556	0.994543987
299	0.611851	0.890212679	0.574796	A6QQA8_BOVIN	0.996436291	0.990714556	0.994543987
300	0.929572	0.92489998	0.744646	A0A140T8A5_BOVIN	0.996436291	0.990714556	0.994543987
302	0.399383	0.24786613	0.277843	FRIL_BOVIN	0.996436291	0.990714556	0.994543987
305	0.475513	0.726645797	0.622393	V6F9B4_BOVIN	0.996436291	0.990714556	0.994543987
306	0.786112	0.864826844	0.875057	RL4_BOVIN	0.996436291	0.990714556	0.994543987
310	0.191953	0.323611895	0.281837	G5E580_BOVIN	0.996436291	0.990714556	0.994543987
312	0.783997	0.812911518	0.919079	IF4A2_BOVIN	0.996436291	0.990714556	0.994543987
313	0.981184	0.382644078	0.657354	A0A3Q1NE05_BOVIN	0.996436291	0.990714556	0.994543987
314	0.846447	0.476341846	0.660698	A0A3Q1MA31_BOVIN	0.996436291	0.990714556	0.994543987
315	0.5414	0.898553846	0.859655	A5PK72_BOVIN	0.996436291	0.990714556	0.994543987
316	0.534114	0.336469652	0.326854	A0A3S5ZPB2_BOVIN	0.996436291	0.990714556	0.994543987
317	0.794221	0.579560403	0.941403	A0A3Q1LTY4_BOVIN	0.996436291	0.990714556	0.994543987
318	0.724781	0.831791734	0.92641	PUR2_BOVIN	0.996436291	0.990714556	0.994543987
319	0.966021	0.565383568	0.711619	CAYP1_BOVIN	0.996436291	0.990714556	0.994543987
320	0.951379	0.389998302	0.631039	G8JKV3_BOVIN	0.996436291	0.990714556	0.994543987
321	0.443126	0.480917194	0.432693	KAP2_BOVIN	0.996436291	0.990714556	0.994543987

322	0.938205	0.614098204	0.675822	TCPQ_BOVIN	0.996436291	0.990714556	0.994543987
325	0.656954	0.904009757	0.848827	TPPP3_BOVIN	0.996436291	0.990714556	0.994543987
326	0.974359	0.784689335	0.788533	AL9A1_BOVIN	0.996436291	0.990714556	0.994543987
328	0.692127	0.393534202	0.570686	Q2HJF0_BOVIN	0.996436291	0.990714556	0.994543987
329	0.925337	0.24930069	0.55547	A0A3Q1LFQ2_BOVIN	0.996436291	0.990714556	0.994543987
330	0.449621	0.955774448	0.617769	A0A3Q1M9W4_BOVIN	0.996436291	0.990714556	0.994543987
334	0.517696	0.543208874	0.437409	A6QQN6_BOVIN	0.996436291	0.990714556	0.994543987
335	0.203309	0.75762044	0.531531	A0A3Q1LRY6_BOVIN	0.996436291	0.990714556	0.994543987
337	0.64685	0.262999447	0.55175	TCPB_BOVIN	0.996436291	0.990714556	0.994543987
340	0.271581	0.764362225	0.437944	A0A3Q1NH43_BOVIN	0.996436291	0.990714556	0.994543987
342	0.707278	0.76224524	0.924633	Q8MII0_BOVIN	0.996436291	0.990714556	0.994543987
344	0.33389	0.624098192	0.36478	A0A3Q1NG86_BOVIN	0.996436291	0.990714556	0.994543987
346	0.977851	0.947183776	0.884651	A0A3Q1MBL5_BOVIN	0.996436291	0.990714556	0.994543987
347	0.943509	0.861152568	0.918811	A0A3Q1MAJ2_BOVIN	0.996436291	0.990714556	0.994543987
348	0.313585	0.323493306	0.346605	E1BPP3_BOVIN	0.996436291	0.990714556	0.994543987
349	0.586377	0.556092629	0.951402	A0A3Q1MHJ3_BOVIN	0.996436291	0.990714556	0.994543987
353	0.283334	0.905484905	0.697608	A0A3Q1MWF7_BOVIN	0.996436291	0.990714556	0.994543987
355	0.439375	0.844917442	0.6884	A0A3Q1MSF7_BOVIN	0.996436291	0.990714556	0.994543987
356	0.834829	0.38396983	0.789315	A0A3Q1N147_BOVIN	0.996436291	0.990714556	0.994543987
357	0.580845	0.778895121	0.625384	TRAP1_BOVIN	0.996436291	0.990714556	0.994543987
358	0.904172	0.780485571	0.924304	E1BKB7_BOVIN	0.996436291	0.990714556	0.994543987
362	0.560192	0.282506182	0.254569	F1MIA9_BOVIN	0.996436291	0.990714556	0.994543987
363	0.60712	0.961653011	0.661818	A0A3Q1NND6_BOVIN	0.996436291	0.990714556	0.994543987
364	0.909796	0.578867296	0.714411	A0A3Q1M0U8_BOVIN	0.996436291	0.990714556	0.994543987
366	0.711608	0.412397808	0.402608	A5PJZ8_BOVIN	0.996436291	0.990714556	0.994543987
367	0.560012	0.520737753	0.543237	TKT_BOVIN	0.996436291	0.990714556	0.994543987
369	0.555301	0.485511579	0.631722	G3N1U4_BOVIN	0.996436291	0.990714556	0.994543987
370	0.639257	0.636967482	0.957926	E1BE11_BOVIN	0.996436291	0.990714556	0.994543987
371	0.474605	0.86906578	0.514072	G3N022_BOVIN	0.996436291	0.990714556	0.994543987
372	0.815724	0.344292521	0.523099	A0A3Q1MKT5_BOVIN	0.996436291	0.990714556	0.994543987

377	0.469478	0.962977931	0.71154	A0A3Q1MBX2_BOVIN	0.996436291	0.990714556	0.994543987
379	0.88015	0.507687227	0.670467	A0A3Q1NEW0_BOVIN	0.996436291	0.990714556	0.994543987
380	0.249058	0.533756809	0.457475	G3N3Q3_BOVIN	0.996436291	0.990714556	0.994543987
383	0.926215	0.566311848	0.561679	Q862F3_BOVIN	0.996436291	0.990714556	0.994543987
386	0.718982	0.511197415	0.79321	F1N469_BOVIN	0.996436291	0.990714556	0.994543987
387	0.745247	0.315761549	0.331482	V6F869_BOVIN	0.996436291	0.990714556	0.994543987
390	0.799832	0.274326691	0.358145	G5E6N4_BOVIN	0.996436291	0.990714556	0.994543987
392	0.956231	0.912866871	0.958858	HS71B_BOVIN	0.996436291	0.990714556	0.994543987
393	0.943979	0.911039331	0.8734	F1MD63_BOVIN	0.996436291	0.990714556	0.994543987
395	0.491462	0.623395491	0.507281	TBB6_BOVIN	0.996436291	0.990714556	0.994543987
396	0.206458	0.914796252	0.463649	A0A3Q1LPD2_BOVIN	0.996436291	0.990714556	0.994543987
398	0.732872	0.660513296	0.733583	VATB2_BOVIN	0.996436291	0.990714556	0.994543987
402	0.980702	0.704238726	0.716057	ALDH2_BOVIN	0.996436291	0.990714556	0.994543987
405	0.984087	0.73688078	0.818833	F1MGZ5_BOVIN	0.996436291	0.990714556	0.994543987
409	0.798598	0.557333511	0.611437	K4JBR5_BOVIN	0.996436291	0.990714556	0.994543987
411	0.677948	0.258937319	0.583418	E1BAR2_BOVIN	0.996436291	0.990714556	0.994543987
414	0.242944	0.731610543	0.583315	A0A3Q1N0C4_BOVIN	0.996436291	0.990714556	0.994543987
416	0.685878	0.629627018	0.536967	A5D986_BOVIN	0.996436291	0.990714556	0.994543987
420	0.686496	0.949346635	0.756653	PPID_BOVIN	0.996436291	0.990714556	0.994543987
422	0.478901	0.532542282	0.521513	F1ML12_BOVIN	0.996436291	0.990714556	0.994543987
425	0.849375	0.939300043	0.739934	A0A452DI72_BOVIN	0.996436291	0.990714556	0.994543987
426	0.801456	0.488301301	0.711117	F1N091_BOVIN	0.996436291	0.990714556	0.994543987
429	0.637939	0.668499669	0.768946	DDX1_BOVIN	0.996436291	0.990714556	0.994543987
430	0.949671	0.736902402	0.853575	A0A3Q1MMY7_BOVIN	0.996436291	0.990714556	0.994543987
434	0.713837	0.53803092	0.464725	E1BKU2_BOVIN	0.996436291	0.990714556	0.994543987
435	0.765542	0.419169934	0.592182	A7E3Q2_BOVIN	0.996436291	0.990714556	0.994543987
437	0.649433	0.450140396	0.543526	NP1L4_BOVIN	0.996436291	0.990714556	0.994543987
439	0.744682	0.45014361	0.46079	E1BP73_BOVIN	0.996436291	0.990714556	0.994543987
441	0.308678	0.836132521	0.783474	A6H7D3_BOVIN	0.996436291	0.990714556	0.994543987
442	0.558956	0.416937222	0.40748	A16A1_BOVIN	0.996436291	0.990714556	0.994543987

447	0.727324	0.650192672	0.599709	A0A3Q1LKS8_BOVIN	0.996436291	0.990714556	0.994543987
449	0.849193	0.759517468	0.666461	RL8_BOVIN	0.996436291	0.990714556	0.994543987
451	0.339821	0.24606558	0.231666	F1MNW5_BOVIN	0.996436291	0.990714556	0.994543987
454	0.296525	0.739903088	0.54977	CNN3_BOVIN	0.996436291	0.990714556	0.994543987
457	0.166513	0.725067955	0.421	FKBP4_BOVIN	0.996436291	0.990714556	0.994543987
458	0.339006	0.445802998	0.378417	SERB_BOVIN	0.996436291	0.990714556	0.994543987
459	0.40768	0.533004728	0.553522	G3MYC9_BOVIN	0.996436291	0.990714556	0.994543987
460	0.749256	0.957907166	0.745446	F1MWI1_BOVIN	0.996436291	0.990714556	0.994543987
461	0.730171	0.931592671	0.771707	F1MB19_BOVIN	0.996436291	0.990714556	0.994543987
462	0.773683	0.681793663	0.935264	G5E5V1_BOVIN	0.996436291	0.990714556	0.994543987
463	0.910543	0.969076485	0.775811	PSB1_BOVIN	0.996436291	0.990714556	0.994543987
465	0.139739	0.669036609	0.331713	F1MZR1_BOVIN	0.996436291	0.990714556	0.994543987
466	0.201766	0.57855612	0.466058	S10A2_BOVIN	0.996436291	0.990714556	0.994543987
467	0.471859	0.547257582	0.895887	A0A3Q1LL25_BOVIN	0.996436291	0.990714556	0.994543987
468	0.733491	0.94824558	0.70054	A0A3Q1M0V5_BOVIN	0.996436291	0.990714556	0.994543987
469	0.215155	0.858675619	0.429073	A5D9H5_BOVIN	0.996436291	0.990714556	0.994543987
470	0.529974	0.497878949	0.520741	A0A3Q1LSS0_BOVIN	0.996436291	0.990714556	0.994543987
473	0.731661	0.929517183	0.764911	F1MIJ5_BOVIN	0.996436291	0.990714556	0.994543987
475	0.260491	0.711350347	0.488625	F1MNV5_BOVIN	0.996436291	0.990714556	0.994543987
476	0.852884	0.837518956	0.957732	CAZA1_BOVIN	0.996436291	0.990714556	0.994543987
477	0.511373	0.680386391	0.454931	DOPD_BOVIN	0.996436291	0.990714556	0.994543987
478	0.588291	0.94558492	0.868532	A0A3Q1N522_BOVIN	0.996436291	0.990714556	0.994543987
480	0.934448	0.452576986	0.789769	A0A3Q1NKD1_BOVIN	0.996436291	0.990714556	0.994543987
483	0.920107	0.941738804	0.918838	CAN2_BOVIN	0.996436291	0.990714556	0.994543987
486	0.170138	0.289340939	0.302024	A0A3Q1MKI2_BOVIN	0.996436291	0.990714556	0.994543987
488	0.399373	0.366858311	0.28671	1433B_BOVIN	0.996436291	0.990714556	0.994543987
491	0.924	0.677971558	0.87449	E1BCL3_BOVIN	0.996436291	0.990714556	0.994543987
492	0.591431	0.852259164	0.792639	K2C8_BOVIN	0.996436291	0.990714556	0.994543987
494	0.914718	0.343877812	0.648057	B0JYP6_BOVIN	0.996436291	0.990714556	0.994543987
499	0.448278	0.943150766	0.604741	E1B8Y9_BOVIN	0.996436291	0.990714556	0.994543987

502	0.555656	0.498335136	0.750143	F1MJI7_BOVIN	0.996436291	0.990714556	0.994543987
503	0.752	0.404608416	0.760341	CO1A1_BOVIN	0.996436291	0.990714556	0.994543987
504	0.450928	0.389499258	0.311803	E1B726_BOVIN	0.996436291	0.990714556	0.994543987
505	0.327107	0.877212529	0.826384	HEM2_BOVIN	0.996436291	0.990714556	0.994543987
506	0.905082	0.475648722	0.517775	A0A3Q1N2B9_BOVIN	0.996436291	0.990714556	0.994543987
508	0.405107	0.337729399	0.452542	A0A140T887_BOVIN	0.996436291	0.990714556	0.994543987
510	0.580791	0.43937381	0.490889	A0A3S5ZPB0_BOVIN	0.996436291	0.990714556	0.994543987
512	0.563159	0.931801111	0.7715	A0A3Q1M2Q2_BOVIN	0.996436291	0.990714556	0.994543987
513	0.404788	0.731948492	0.412785	A0A3Q1LWV4_BOVIN	0.996436291	0.990714556	0.994543987
514	0.866396	0.58753631	0.804612	MDHM_BOVIN	0.996436291	0.990714556	0.994543987
515	0.306819	0.957657302	0.577333	KCNB2_BOVIN	0.996436291	0.990714556	0.994543987
516	0.306819	0.957657302	0.577333	G3X8A0_BOVIN	0.996436291	0.990714556	0.994543987
519	0.701126	0.791560236	0.866119	RLA1_BOVIN	0.996436291	0.990714556	0.994543987
521	0.19367	0.850657766	0.720303	F1N712_BOVIN	0.996436291	0.990714556	0.994543987
522	0.805802	0.845346691	0.863197	A0A3Q1LI44_BOVIN	0.996436291	0.990714556	0.994543987
524	0.7446	0.336067585	0.811158	F1MXF5_BOVIN	0.996436291	0.990714556	0.994543987
525	0.810704	0.968750576	0.815311	Q862L2_BOVIN	0.996436291	0.990714556	0.994543987
527	0.464757	0.45013281	0.502722	HBBF_BOVIN	0.996436291	0.990714556	0.994543987
532	0.746164	0.96473863	0.957026	AOXA_BOVIN	0.996436291	0.990714556	0.994543987
533	0.789313	0.656197795	0.543025	EF1A1_BOVIN	0.996436291	0.990714556	0.994543987
535	0.725203	0.952504372	0.673965	G3X7I5_BOVIN	0.996436291	0.990714556	0.994543987
536	0.242062	0.541700379	0.325695	ACTS_BOVIN	0.996436291	0.990714556	0.994543987
537	0.629444	0.392335661	0.578408	G3MXG6_BOVIN	0.996436291	0.990714556	0.994543987
538	0.200154	0.581661213	0.432238	Q687I9_BOVIN	0.996436291	0.990714556	0.994543987
539	0.767672	0.756151255	0.851542	F1N1I6_BOVIN	0.996436291	0.990714556	0.994543987
541	0.202742	0.911064817	0.604251	A0A3Q1LZ35_BOVIN	0.996436291	0.990714556	0.994543987
542	0.480391	0.946692827	0.765216	A0A3Q1LN27_BOVIN	0.996436291	0.990714556	0.994543987
543	0.714299	0.784266132	0.86119	A0A3Q1LR88_BOVIN	0.996436291	0.990714556	0.994543987
544	0.563877	0.65146102	0.518836	E1B9H0_BOVIN	0.996436291	0.990714556	0.994543987
545	0.901429	0.670674484	0.699211	CRIP2_BOVIN	0.996436291	0.990714556	0.994543987

546	0.669159	0.346053445	0.796656	M5FJW2_BOVIN	0.996436291	0.990714556	0.994543987
548	0.792513	0.618651538	0.715149	NSF1C_BOVIN	0.996436291	0.990714556	0.994543987
549	0.429379	0.431063598	0.772473	G3MZU3_BOVIN	0.996436291	0.990714556	0.994543987
550	0.690326	0.513002732	0.713715	A0A3Q1LL35_BOVIN	0.996436291	0.990714556	0.994543987
553	0.716935	0.348178192	0.401638	G3X6K8_BOVIN	0.996436291	0.990714556	0.994543987
554	0.250234	0.407156917	0.898705	A0A3Q1MLP4_BOVIN	0.996436291	0.990714556	0.994543987
555	0.569305	0.235998541	0.319941	A0A3Q1N8C6_BOVIN	0.996436291	0.990714556	0.994543987
556	0.773201	0.917391168	0.794829	A0A452DHX8_BOVIN	0.996436291	0.990714556	0.994543987
560	0.978305	0.828976976	0.767022	A0A3Q1MG31_BOVIN	0.996436291	0.990714556	0.994543987
561	0.680164	0.677659438	0.782033	UBE2N_BOVIN	0.996436291	0.990714556	0.994543987
562	0.285458	0.549587168	0.454188	IRF6_BOVIN	0.996436291	0.990714556	0.994543987
563	0.935827	0.844375432	0.810324	A0A3Q1LU85_BOVIN	0.996436291	0.990714556	0.994543987
564	0.815946	0.793171068	0.821009	CSRP1_BOVIN	0.996436291	0.990714556	0.994543987
565	0.172988	0.373516739	0.368291	A1L5B6_BOVIN	0.996436291	0.990714556	0.994543987
566	0.813442	0.665899669	0.788463	A0A3Q1ML30_BOVIN	0.996436291	0.990714556	0.994543987
568	0.819289	0.436499426	0.453767	F1N160_BOVIN	0.996436291	0.990714556	0.994543987
569	0.969904	0.367200819	0.610665	A0A452DJE9_BOVIN	0.996436291	0.990714556	0.994543987
570	0.319703	0.81741894	0.451378	A0A3Q1N5N9_BOVIN	0.996436291	0.990714556	0.994543987
573	0.322963	0.876679857	0.59433	F1MUP9_BOVIN	0.996436291	0.990714556	0.994543987
576	0.685684	0.406929441	0.792253	CLIC4_BOVIN	0.996436291	0.990714556	0.994543987
578	0.524754	0.728012317	0.750387	1433F_BOVIN	0.996436291	0.990714556	0.994543987
579	0.804248	0.261831931	0.456347	F1MLH6_BOVIN	0.996436291	0.990714556	0.994543987
580	0.647202	0.468547131	0.824704	SYQ_BOVIN	0.996436291	0.990714556	0.994543987
581	0.477916	0.940583148	0.865135	S10AA_BOVIN	0.996436291	0.990714556	0.994543987
582	0.854039	0.887126294	0.876348	LDH6B_BOVIN	0.996436291	0.990714556	0.994543987
583	0.67919	0.963171077	0.81711	A5D7R6_BOVIN	0.996436291	0.990714556	0.994543987
584	0.545497	0.807473207	0.802795	E1BH06_BOVIN	0.996436291	0.990714556	0.994543987
586	0.775173	0.400914346	0.508362	A0A452DIS6_BOVIN	0.996436291	0.990714556	0.994543987
588	0.513262	0.964642513	0.720979	ANXA5_BOVIN	0.996436291	0.990714556	0.994543987
589	0.380246	0.510977877	0.370043	Q1JPA2_BOVIN	0.996436291	0.990714556	0.994543987

590	0.394464	0.727119144	0.93274	A6QNM1_BOVIN	0.996436291	0.990714556	0.994543987
591	0.625312	0.731761797	0.639505	A0A3Q1MJD9_BOVIN	0.996436291	0.990714556	0.994543987
593	0.746587	0.765582909	0.842712	SKP1_BOVIN	0.996436291	0.990714556	0.994543987
596	0.443458	0.402045636	0.29996	CO6_BOVIN	0.996436291	0.990714556	0.994543987
597	0.534562	0.702573863	0.661414	G5E531_BOVIN	0.996436291	0.990714556	0.994543987
598	0.535519	0.565030885	0.53679	A0A3Q1MA07_BOVIN	0.996436291	0.990714556	0.994543987
600	0.826444	0.950022722	0.903888	E1BCC9_BOVIN	0.996436291	0.990714556	0.994543987
601	0.904306	0.820983862	0.761305	F1MYQ7_BOVIN	0.996436291	0.990714556	0.994543987
604	0.779905	0.616670423	0.909258	PPM1G_BOVIN	0.996436291	0.990714556	0.994543987
605	0.554351	0.861487139	0.934739	G5E6J5_BOVIN	0.996436291	0.990714556	0.994543987
606	0.817039	0.69422036	0.814123	G3X6N3_BOVIN	0.996436291	0.990714556	0.994543987
607	0.59572	0.930111861	0.796601	A0A452DJ53_BOVIN	0.996436291	0.990714556	0.994543987
608	0.248156	0.609095791	0.430732	F1MUC5_BOVIN	0.996436291	0.990714556	0.994543987
609	0.34765	0.236163483	0.224158	A0A3Q1M970_BOVIN	0.996436291	0.990714556	0.994543987
610	0.769996	0.482749607	0.687289	A0A3Q1MTT6_BOVIN	0.996436291	0.990714556	0.994543987
611	0.419883	0.502757684	0.458005	RSSA_BOVIN	0.996436291	0.990714556	0.994543987
612	0.759324	0.879488788	0.937669	A0A3Q1M2E4_BOVIN	0.996436291	0.990714556	0.994543987
613	0.852869	0.628811351	0.757649	A6QNJ7_BOVIN	0.996436291	0.990714556	0.994543987
615	0.315446	0.413983065	0.352124	RS6_BOVIN	0.996436291	0.990714556	0.994543987
616	0.714702	0.849350844	0.774288	PA1B3_BOVIN	0.996436291	0.990714556	0.994543987
617	0.420985	0.766371211	0.774458	A0A3Q1N7K2_BOVIN	0.996436291	0.990714556	0.994543987
618	0.714887	0.4299707	0.444159	E1B8H0_BOVIN	0.996436291	0.990714556	0.994543987
620	0.987109	0.714584459	0.66116	A0A3Q1MTI5_BOVIN	0.996436291	0.990714556	0.994543987
621	0.520529	0.899251177	0.855326	TCPG_BOVIN	0.996436291	0.990714556	0.994543987
624	0.414531	0.813181459	0.80941	A0A3Q1M053_BOVIN	0.996436291	0.990714556	0.994543987
626	0.610261	0.824359714	0.697161	A0A3Q1LQQ5_BOVIN	0.996436291	0.990714556	0.994543987
627	0.544412	0.596406391	0.403191	XPO2_BOVIN	0.996436291	0.990714556	0.994543987
629	0.673336	0.529986689	0.639487	A0A3Q1NLD8_BOVIN	0.996436291	0.990714556	0.994543987
630	0.529682	0.609284262	0.941779	H2A2C_BOVIN	0.996436291	0.990714556	0.994543987
631	0.143332	0.645666637	0.685458	A0A3Q1MGT0_BOVIN	0.996436291	0.990714556	0.994543987

633	0.218308	0.881883399	0.777138	KNG2_BOVIN	0.996436291	0.990714556	0.994543987
634	0.905802	0.845784226	0.802337	CDC42_BOVIN	0.996436291	0.990714556	0.994543987
636	0.538815	0.846426795	0.665616	PLSI_BOVIN	0.996436291	0.990714556	0.994543987
637	0.79827	0.95667617	0.745131	A0A3Q1LYV7_BOVIN	0.996436291	0.990714556	0.994543987
638	0.526038	0.498597364	0.612603	Q2KIV8_BOVIN	0.996436291	0.990714556	0.994543987
639	0.598456	0.827495136	0.926044	F12AI_BOVIN	0.996436291	0.990714556	0.994543987
644	0.563115	0.581456931	0.518538	E1BMG2_BOVIN	0.996436291	0.990714556	0.994543987
646	0.611479	0.387618201	0.530279	A0A3Q1MI98_BOVIN	0.996436291	0.990714556	0.994543987
647	0.458698	0.378084927	0.41501	F1MLW8_BOVIN	0.996436291	0.990714556	0.994543987
648	0.40269	0.383886761	0.255175	G3X7K5_BOVIN	0.996436291	0.990714556	0.994543987
651	0.899402	0.587786786	0.775196	CTHL2_BOVIN	0.996436291	0.990714556	0.994543987
653	0.639418	0.715155903	0.9245	MSRA_BOVIN	0.996436291	0.990714556	0.994543987
655	0.299155	0.249270167	0.245763	Q17QL7_BOVIN	0.996436291	0.990714556	0.994543987
656	0.655111	0.671178302	0.947239	CTHL1_BOVIN	0.996436291	0.990714556	0.994543987
657	0.612157	0.82391494	0.903644	A0A3Q1MR74_BOVIN	0.996436291	0.990714556	0.994543987
658	0.266694	0.721012379	0.746554	A0A3Q1MFR4_BOVIN	0.996436291	0.990714556	0.994543987
660	0.478504	0.404209979	0.486819	A0A3Q1NNP6_BOVIN	0.996436291	0.990714556	0.994543987
661	0.968732	0.906269006	0.868895	A0A3Q1LSF9_BOVIN	0.996436291	0.990714556	0.994543987
663	0.172657	0.300286522	0.380408	A0A3Q1M2E0_BOVIN	0.996436291	0.990714556	0.994543987
664	0.725034	0.872890817	0.756693	LASP1_BOVIN	0.996436291	0.990714556	0.994543987
665	0.964232	0.33531165	0.752187	E1BGV8_BOVIN	0.996436291	0.990714556	0.994543987
666	0.743349	0.2303851	0.323893	Q3T0Y1_BOVIN	0.996436291	0.990714556	0.994543987
83	0.473293	0.978614608	0.629695	PPBT_BOVIN	0.996436291	0.990983109	0.994543987
236	0.971478	0.971543316	0.765644	A0A3Q1M0D3_BOVIN	0.996436291	0.990983109	0.994543987
343	0.969324	0.97713434	0.894482	LYST_BOVIN	0.996436291	0.990983109	0.994543987
424	0.425641	0.973762599	0.72165	A0A3Q1NNJ8_BOVIN	0.996436291	0.990983109	0.994543987
61	0.769483	0.98647114	0.955347	A0A452DJ82_BOVIN	0.996436291	0.992789658	0.994543987
64	0.538447	0.987522784	0.957295	PDXK_BOVIN	0.996436291	0.992789658	0.994543987
190	0.978443	0.98969203	0.823588	A2MG_BOVIN	0.996436291	0.992789658	0.994543987
529	0.885574	0.986939179	0.952566	F1MUR6_BOVIN	0.996436291	0.992789658	0.994543987

271	0.432422	0.995479009	0.83852	A0A3Q1NKP5_BOVIN	0.996436291	0.997034445	0.994543987
464	0.834342	0.997882259	0.919953	ACOC_BOVIN	0.996436291	0.997882259	0.994543987
85	0.770052	0.943675912	0.96542	A6QNX2_BOVIN	0.996436291	0.990714556	0.99651208
118	0.562395	0.641867346	0.962795	TBB4B_BOVIN	0.996436291	0.990714556	0.99651208
263	0.939621	0.753071945	0.964104	CPNE1_BOVIN	0.996436291	0.990714556	0.99651208
341	0.759977	0.844100614	0.969005	A0A3Q1MGU4_BOVIN	0.996436291	0.990714556	0.998604421
22	0.571604	0.843981761	0.974272	HS90B_BOVIN	0.996436291	0.990714556	0.998796294
333	0.85421	0.961797274	0.973256	PPIB_BOVIN	0.996436291	0.990714556	0.998796294
599	0.574612	0.73370591	0.975424	PGRP1_BOVIN	0.996436291	0.990714556	0.998796294
643	0.887674	0.982149987	0.97178	A0A3Q1N3K8_BOVIN	0.996436291	0.992789658	0.998796294
18	0.962713	0.742260662	0.980136	ACTG_BOVIN	0.996436291	0.990714556	0.998835126
52	0.789603	0.677181255	0.977494	Q3SZZ9_BOVIN	0.996436291	0.990714556	0.998835126
194	0.965885	0.978615145	0.97873	A0A3Q1MRN4_BOVIN	0.996436291	0.990983109	0.998835126
27	0.798139	0.864651848	0.991795	ZA2G_BOVIN	0.996436291	0.990714556	0.999141681
77	0.462679	0.845869618	0.996823	A0A452DID9_BOVIN	0.996436291	0.990714556	0.999141681
184	0.774534	0.589510219	0.993441	PUR9_BOVIN	0.996436291	0.990714556	0.999141681
185	0.889479	0.82770429	0.996837	F1N049_BOVIN	0.996436291	0.990714556	0.999141681
247	0.385808	0.679847308	0.996357	CNDP2_BOVIN	0.996436291	0.990714556	0.999141681
311	0.904442	0.947633114	0.99712	TRFE_BOVIN	0.996436291	0.990714556	0.999141681
417	0.770272	0.915935106	0.997751	RS18_BOVIN	0.996436291	0.990714556	0.999141681
481	0.878528	0.887387804	0.986493	ITPA_BOVIN	0.996436291	0.990714556	0.999141681
587	0.623767	0.75019022	0.98866	CTHL4_BOVIN	0.996436291	0.990714556	0.999141681
659	0.586882	0.77835884	0.991784	LHPP_BOVIN	0.996436291	0.990714556	0.999141681
39	0.673528	0.978289946	0.997287	PRDX2_BOVIN	0.996436291	0.990983109	0.999141681
559	0.826165	0.989150414	0.999142	G3MWT1_BOVIN	0.996436291	0.992789658	0.999141681
628	0.98929	0.494290105	0.764734	HS71L_BOVIN	0.997067449	0.990714556	0.994543987
354	0.991962	0.459051892	0.576532	BRX1_BOVIN	0.998190877	0.990714556	0.994543987
124	0.993699	0.891061686	0.939565	CAN1_BOVIN	0.998371215	0.990714556	0.994543987
155	0.997382	0.381531115	0.440183	F1MC48_BOVIN	0.998973199	0.990714556	0.994543987
284	0.997415	0.79405157	0.930936	A0A3Q1LPY0_BOVIN	0.998973199	0.990714556	0.994543987

558	0.999753	0.502634152	0.878465	A0A3Q1MUR2_BOVIN	0.999752698	0.990714556	0.994543987
252	NA	NA	NA	F1MVK1_BOVIN	NA	NA	NA
278	NA	NA	NA	A0A3Q1MI29_BOVIN	NA	NA	NA
288	NA	NA	NA	A0A3Q1M032_BOVIN	NA	NA	NA
381	NA	NA	NA	A0JN68_BOVIN	NA	NA	NA
388	NA	NA	NA	G5E5T5_BOVIN	NA	NA	NA
397	NA	NA	NA	F1MZ96_BOVIN	NA	NA	NA
400	NA	NA	NA	A0A3Q1MV83_BOVIN	NA	NA	NA
413	NA	NA	NA	A0A3Q1MU51_BOVIN	NA	NA	NA
419	NA	NA	NA	Q0VCY8_BOVIN	NA	NA	NA
421	NA	NA	NA	F1MD34_BOVIN	NA	NA	NA
428	NA	NA	NA	A0A3Q1N8Q5_BOVIN	NA	NA	NA
431	NA	NA	NA	G3MWV5_BOVIN	NA	NA	NA
433	NA	NA	NA	Q3ZBG1_BOVIN	NA	NA	NA
436	NA	NA	NA	F1MR60_BOVIN	NA	NA	NA
438	NA	NA	NA	A0A3Q1LSF0_BOVIN	NA	NA	NA
440	NA	NA	NA	Q3ZBH5_BOVIN	NA	NA	NA
443	NA	NA	NA	ARPC3_BOVIN	NA	NA	NA
444	NA	NA	NA	F1MZ92_BOVIN	NA	NA	NA
446	NA	NA	NA	IF4A1_BOVIN	NA	NA	NA
448	NA	NA	NA	A0A3Q1MCX8_BOVIN	NA	NA	NA
450	NA	NA	NA	MARE1_BOVIN	NA	NA	NA
452	NA	NA	NA	A7MBA2_BOVIN	NA	NA	NA
472	NA	NA	NA	Q3T101_BOVIN	NA	NA	NA
479	NA	NA	NA	A0A3S5ZP98_BOVIN	NA	NA	NA
484	NA	NA	NA	Q5EA67_BOVIN	NA	NA	NA

Table S6-1 Compounds detected in this study using broadly targeted or untargeted approaches, or both. Underlined, those not previously reported in bovine ULF.

Targeted	Both	Untargeted
1-Hexadecanol	D-Xylose	2-Hydroxypyridine
2-Deoxy-glucose	Fructose	2-Methyl-2-butanol
3-Methylcrotonylglycine	Hydroxylamine	4-Hydroxypyridine
5-Methoxytryptamine	Maltose	Alpha-Lactose
Allose	myo-Inositol	Beta-D-Glucose
Arabitol	N-Acetylmannosamine	beta-Lactose
Cadaverine	Trehalose	D-Galactose
Cholesterol	Benzoic acid	Dihydroxyacetone phosphate acyl ester
Cystamine	3-Hydroxybutyric acid	Gamma-valeronolactone
D-Xylulose	Beta-Alanine	Glycyl-glycine
Epinephrine	Citric acid	Hexamethyldisiloxane
Fucose	Creatinine	L-Fucose
Galactitol	D-Glucose	L-Iditol
Galactose	D-Mannose	Methylamine
Glucosamine	D-Ribose	N-Methylalanine
Glyceraldehyde	D-Ribulose	Tyrosol
Isomaltose	Ethanolamine	2-Pentenoic acid
Lactitol	Glucose 6-phosphate	3-Phosphoglyceric acid
Lactose	Glyceric acid	Allantoin
L-Arabinose	Glycerol	conduritol-beta-epoxide
L-Erythrulose	Glycine	D-Galacturonic acid
Levoglucosan	Glycolic acid	Dihydroxyacetone (dimer)
Lyxose	Hypotaurine	D-Maltose
Maltitol	Hypoxanthine	L-Malic acid
Metoprolol	Inosine	L-Serine

N6-Acetyl-L-lysine	L-Alanine	Methylmalonic acid
Norvaline	L-Asparagine	Pyrophosphate
Octadecanol	L-Aspartic acid	Tartaric acid
Phosphoserine	L-Glutamic acid	
p-Octopamine	L-Isoleucine	
Psicose	L-Lactic acid	
Rhamnose	L-Leucine	
Ribonolactone	L-Lysine	
Serine	L-Methionine	
Sorbitol	L-Phenylalanine	
Sorbose	L-Proline	
Threitol	L-Threonine	
Thymine	L-Tyrosine	
Tryptamine	L-Valine	
Xylitol	Nicotinic acid	
(S)-3-Hydroxyisobutyric acid	O-Phosphoethanolamine	
2-Aminobutyric acid	Ornithine	
2-Aminoheptanedioic acid	Oxalic acid	
2-Aminoisobutyric acid	Palmitic acid	
2-Hydroxy-3-methylbutyric acid	Putrescine	
2-Hydroxybutyric acid	Pyroglutamic acid	
2-Keto-isovaleric acid	Ribitol	
3-Aminoglutaric acid	Sarcosine	
3-Aminoisobutanoic acid	Stearic acid	
3-Dehydroquinate	Succinic acid	
3-Hydroxyisovaleric acid	Sucrose	
3-Hydroxyphenylacetic acid	Taurine	
3-Methyl-2-oxovaleric acid	Threonic acid	

4-Aminobutyric acid
4-Hydroxybenzoic acid
4-Hydroxyproline
5-Aminopentanoic acid
5'-Methylthioadenosine
Acetoacetic acid
Acetylglycine
Adenine
Adenosine
Adipic acid
Alkylresorcinol C17
Alkylresorcinol C19
Alpha-Hydroxyisobutyric acid
alpha-Tocopherol succinate
Arachidonic acid
Asymmetric dimethylarginine
Azelaic acid
Capric acid
Caproic acid
Caprylic acid
cis-Aconitic acid
Citramalic acid
Cytosine
D-2-Hydroxyglutaric acid
Deoxyuridine
D-Erythrose 4-phosphate
D-Fructose
Dihydroxyacetone

Dihydroxyacetone phosphate
Docosahexaenoic acid
Dodecanoic acid
Dopamine
D-Ribose 5-phosphate
D-Ribulose 5-phosphate
Eicosapentaenoic acid
Elaidic acid
Erythrityl Tetranitrate
Ethylmalonic acid
Fructose 1-phosphate
Fumaric acid
Galacturonic acid
Glucaric acid
Gluconic acid
Glucono-1,5-lactone
Glucuronic acid
Glutaric acid
Glycerol 2-phosphate
Glycerol 3-phosphate
Glyoxylic acid
Guanosine
Heptadecanoic acid
Hippuric acid
Histamine
Hydroxyphenyllactic acid
Hydroxypropionic acid
Indoleacetic acid

Isocitric acid
Ketoleucine
L-Arginine
L-Cysteine
L-Glutamine
L-Histidine
Linoleic acid
L-Kynurenine
L-Tryptophan
Maleic acid
Malic acid
Malonic acid
Mannitol
Mannose 6-phosphate
Mesaconic acid
Methoprene acid
Methylsuccinic acid
MG (18:0e/0:0/0:0)
Myristic acid
N-Acetylglutamine
N-Acetylneuraminic acid
N-Acetylornithine
Niacinamide
Norepinephrine
Oleic acid
Oxoadipic acid
Oxoglutaric acid
Palmitoleic acid

Pantothenic acid
Pelargonic acid
Phenylacetic acid
Phosphoenolpyruvic acid
Phosphoric acid
Pyruvic acid
Sebacic acid
Spermidine
Spermine
Suberic acid
Threo-b-hydroxyaspartic acid
Triethanolamine
Tyramine
Uracil
Urea
Uric acid
Uridine
Urocanic acid
Vanillic acid

Table S6-2 Pathways to which metabolites detected in this study were mapped, as per Metaboanalyst overrepresentation analysis against the bovine metabolome. Colour on the left indicates significance, i.e. p-value (red= highly significant; white=non-significant)

	Metabolite Set	Total	Hits	Expect	P value	Holm P	FDR
	Aminoacyl-tRNA biosynthesis	48	20	6.94	2.73E-06	2.29E-04	2.29E-04
	Arginine biosynthesis	14	9	2.02	2.45E-05	0.00203	0.00103
	Galactose metabolism	27	12	3.9	1.45E-04	0.0119	0.00391
	D-Glutamine and D-glutamate metabolism	6	5	0.867	3.21E-04	0.0257	0.00539
	Alanine, aspartate and glutamate metabolism	28	11	4.05	0.001	0.0792	0.014
	Glyoxylate and dicarboxylate metabolism	32	11	4.63	0.00352	0.275	0.0412
	Citrate cycle (TCA cycle)	20	8	2.89	0.00442	0.34	0.0412
	Fructose and mannose metabolism	20	8	2.89	0.00442	0.34	0.0412
	Starch and sucrose metabolism	18	7	2.6	0.00925	0.693	0.0777
	Arginine and proline metabolism	38	11	5.49	0.0148	1	0.104
	Glycerolipid metabolism	16	6	2.31	0.0193	1	0.124
	beta-Alanine metabolism	21	7	3.04	0.023	1	0.129
	Glycine, serine and threonine metabolism	33	9	4.77	0.0386	1	0.191

	Taurine and hypotaurine metabolism	8	3	1.16	0.0957	1	0.335
	Phenylalanine, tyrosine and tryptophan biosynthesis	4	2	0.578	0.102	1	0.344
	Valine, leucine and isoleucine degradation	40	8	5.78	0.211	1	0.632
	Tyrosine metabolism	42	8	6.07	0.253	1	0.694
	Pentose and glucuronate interconversions	18	4	2.6	0.256	1	0.694
	Biosynthesis of unsaturated fatty acids	36	7	5.2	0.256	1	0.694
	Ascorbate and aldarate metabolism	8	2	1.16	0.326	1	0.848
	Nicotinate and nicotinamide metabolism	15	3	2.17	0.372	1	0.919
	Pyruvate metabolism	22	4	3.18	0.396	1	0.95
	Linoleic acid metabolism	5	1	0.723	0.542	1	1
	Tryptophan metabolism	41	6	5.93	0.556	1	1
	Thiamine metabolism	7	1	1.01	0.666	1	1
	Ubiquinone and other terpenoid-quinone biosynthesis	9	1	1.3	0.756	1	1
	Sphingolipid metabolism	21	2	3.04	0.831	1	1
	Inositol phosphate metabolism	30	3	4.34	0.832	1	1

	Lysine degradation	25	2	3.61	0.897	1	1
	Porphyrin and chlorophyll metabolism	30	2	4.34	0.946	1	1
	Selenocompound metabolism	20	1	2.89	0.957	1	1
	Ether lipid metabolism	20	1	2.89	0.957	1	1
	Phosphatidylinositol signaling system	28	1	4.05	0.988	1	1

Table S6-3 Univariate analysis of ULF metabolomics data, according to EQ1 (a), EQ2 (b) and EQ3 (c) embryo classification systems.

a

p_dpp	p_EQ1	p_inter_dpp_EQ1	Molecule	q_EQ1	q_dpp	q_interaction
7.21E-05	0.326971	0.998115665	Glycolic acid	0.652466836	0.000913466	0.998115665
0.0009	0.923617	0.645579742	3-Hydroxypropionic acid	0.968112837	0.010254491	0.8975133
0.014534	0.191198	0.242429168	Xylitol	0.597344489	0.150625496	0.658022027
0.017523	0.214834	0.218631206	Arabinose	0.597344489	0.16510987	0.607901402
0.018828	0.376209	0.156519571	Lyxose	0.693810023	0.16510987	0.511154922
0.024384	0.22879	0.338793319	Ribose	0.603942451	0.19855173	0.671872639
0.089748	0.18683	0.31950061	Acetylglycine	0.597344489	0.447585971	0.671872639
0.077901	0.259589	0.85730901	Allose	0.603942451	0.447585971	0.960070845
0.075048	0.247629	0.47442457	Galactose	0.603942451	0.447585971	0.845068766
0.063001	0.275369	0.909540801	Glucono-1,5-lactone	0.627842302	0.447585971	0.960070845
0.090302	0.21455	0.571417676	Glucose	0.597344489	0.447585971	0.857061834
0.089127	0.482234	0.624142126	Mannose	0.792744196	0.447585971	0.8975133
0.059121	0.041611	0.530809615	Monostearin	0.388831319	0.447585971	0.849432595
0.068856	0.374185	0.153233807	Ribonolactone	0.693810023	0.447585971	0.511154922
0.084915	0.571488	0.147201981	Tyrosine	0.831390079	0.447585971	0.511154922
0.103941	0.214741	0.280931589	Sorbose	0.597344489	0.493718368	0.667212524
0.132146	0.015113	0.117812302	2-Hydroxyisovaleric acid	0.191433364	0.557950868	0.511154922
0.127175	0.530685	0.881777077	Malic acid	0.822157584	0.557950868	0.960070845
0.132138	0.152498	0.62592041	Ribulose	0.579492146	0.557950868	0.8975133
0.148959	0.194464	0.398319145	Mannitol	0.597344489	0.569361909	0.751306001
0.151	0.919149	0.216772205	Ribitol	0.968112837	0.569361909	0.607901402
0.154826	0.331957	0.685760811	Sarcosine	0.652466836	0.569361909	0.909031773
0.149322	0.19506	0.634951378	D-Xylulose	0.597344489	0.569361909	0.8975133
0.161797	0.510703	0.00128084	Glutamic acid	0.820002322	0.576402447	0.016223967
0.17666	0.923043	0.005484824	Cystathionine	0.968112837	0.610278837	0.052105825

0.188173	0.430765	0.6824326	Stearic acid	0.767299405	0.630931967	0.909031773
0.197459	0.595766	0.974463022	Fumaric acid	0.838485125	0.641715701	0.983086589
0.208276	0.986776	0.905326016	Palmitic acid	0.986775626	0.641715701	0.960070845
0.207296	0.286905	0.498066191	Suberic acid	0.640160167	0.641715701	0.849432595
0.216002	0.074993	0.87857049	3-Hydroxyisobutyric acid	0.500088479	0.648007143	0.960070845
0.226216	0.111131	0.907508643	Isoleucine	0.500088479	0.661246831	0.960070845
0.237265	0.920986	0.148781368	Alanine	0.968112837	0.676204006	0.511154922
0.248195	0.668266	0.296638746	Ribose 5-phosphate	0.865708327	0.690104416	0.671872639
0.256316	0.113176	0.864416074	3-Hydroxybutyric acid	0.500088479	0.695714971	0.960070845
0.269518	0.321997	0.27318076	Fructose	0.652466836	0.713087769	0.662608652
0.281482	0.175868	0.836118979	Leucine	0.597344489	0.713087769	0.960070845
0.275535	0.706888	0.216272124	Phosphoric acid	0.879640574	0.713087769	0.607901402
0.293222	0.302049	0.684710974	Hydroxylamine	0.640160167	0.726680507	0.909031773
0.304158	0.973756	0.523528983	Azelaic acid	0.982373277	0.737744538	0.849432595
0.34289	0.319658	0.331609691	3-methoxy-4-hydroxybenzoic acid	0.652466836	0.798586483	0.671872639
0.343252	0.682749	0.543934907	Glycerol	0.867444151	0.798586483	0.849432595
0.369986	0.127498	0.135880278	2-Aminobutyric acid	0.519098778	0.799171288	0.511154922
0.356955	0.89895	0.161081006	Glutaric acid	0.968112837	0.799171288	0.511154922
0.362567	0.39138	0.127177835	Lactic acid	0.708211714	0.799171288	0.511154922
0.371545	0.11376	0.856867823	Nonanoic acid	0.500088479	0.799171288	0.960070845
0.386802	0.255026	0.341829939	Glycine	0.603942451	0.801734094	0.671872639
0.384874	0.912703	0.098616981	Inositol	0.968112837	0.801734094	0.46843066
0.401889	0.212149	0.962700341	Valine	0.597344489	0.81813078	0.983086589
0.436083	0.063503	0.131228485	2-Hydroxybutyric acid	0.452460338	0.82880145	0.511154922
0.431646	0.90787	0.089902394	Guanosine	0.968112837	0.82880145	0.461724257
0.429194	0.486773	0.081744198	Metoprolol	0.792744196	0.82880145	0.44375422
0.436211	0.709885	0.507569133	Octadecanol	0.879640574	0.82880145	0.849432595
0.447711	0.841737	0.518474095	2-Hydroxyisocaproic acid	0.968112837	0.836705816	0.849432595
0.482469	0.092491	0.047316997	2-Hydroxyisobutyric acid	0.500088479	0.851781992	0.296510243

0.545417	0.94797	0.417059415	2-Ketoglutaric acid	0.968112837	0.851781992	0.766851183
0.540483	0.450641	0.402014615	5-Oxoproline	0.781623692	0.851781992	0.751306001
0.523051	0.879736	0.313307426	Hypotaurine	0.968112837	0.851781992	0.671872639
0.49221	0.452519	0.004576291	Mannose 6-phosphate	0.781623692	0.851781992	0.047427019
0.525983	0.923761	0.093154894	N-Acetylmannosamine	0.968112837	0.851781992	0.461724257
0.503597	0.767912	0.814976382	Norepinephrine	0.931297195	0.851781992	0.960070845
0.545439	0.121357	0.307304842	Octanoic acid	0.51239648	0.851781992	0.671872639
0.534642	0.114055	0.002444235	O-Phosphoethanolamine	0.500088479	0.851781992	0.027864281
0.496113	0.145351	0.159873818	Pyruvic acid	0.571378979	0.851781992	0.511154922
0.515713	0.951128	0.73117277	Sebacic acid	0.968112837	0.851781992	0.915974678
0.487996	0.028771	0.109166729	Tagatose	0.298168152	0.851781992	0.497800286
0.55887	0.461309	0.642342259	Lauric acid	0.784913433	0.860962639	0.8975133
0.616981	0.296092	0.956862804	2-Aminopimelic acid	0.640160167	0.879738133	0.983086589
0.640511	0.100965	0.838102219	Batyl alcohol	0.500088479	0.879738133	0.960070845
0.584721	0.907921	0.183371526	Beta alanine	0.968112837	0.879738133	0.550114579
0.625627	0.045675	0.049418374	Caproic acid	0.388831319	0.879738133	0.296510243
0.592227	0.197113	0.540954247	Glyoxylic acid	0.597344489	0.879738133	0.849432595
0.596929	0.533681	0.805902304	Maltose	0.822157584	0.879738133	0.960070845
0.611588	0.107798	0.031071759	Psicose	0.500088479	0.879738133	0.251576441
0.638125	0.051162	0.569147463	Rhamnose	0.388831319	0.879738133	0.857061834
0.629382	0.620808	0.073590187	Uridine	0.852675876	0.879738133	0.419464063
0.655888	0.785888	0.578892642	Benzoic acid	0.943065234	0.890133375	0.857061834
0.693503	0.303234	0.463490699	Gluconic acid	0.640160167	0.930110237	0.838697455
0.741644	0.557227	0.017736663	3-Aminoglutaric acid	0.831390079	0.939415537	0.155536892
0.738296	0.684824	0.355076307	5-Aminovaleric acid	0.867444151	0.939415537	0.686079644
0.735923	0.639603	0.17997055	Serine	0.857820036	0.939415537	0.550114579
0.723675	0.834421	0.341418748	Succinic acid	0.968112837	0.939415537	0.671872639
0.738852	0.638001	0.570480155	Trehalose	0.857820036	0.939415537	0.857061834
0.768155	0.648228	0.527132685	Lactitol	0.859279599	0.962304228	0.849432595
0.793545	0.08448	0.700803401	Catechol	0.500088479	0.962384712	0.915812392

0.787405	0.929768	0.661064156	Ethylmalonic acid	0.968112837	0.962384712	0.907967636
0.778661	0.17255	0.264487044	Urea	0.597344489	0.962384712	0.662608652
0.935108	0.469556	0.257462725	2-Aminoethanol	0.787196457	0.990668204	0.662608652
0.972986	0.668214	0.161417344	3-Aminopropanoic acid	0.865708327	0.990668204	0.511154922
0.893606	0.237204	0.813104946	3-Hydroxyphenylacetic acid	0.603942451	0.990668204	0.960070845
0.947626	0.377335	0.037587782	Aspartic acid	0.693810023	0.990668204	0.253977363
0.854456	0.736381	0.332090199	Cadaverine	0.902660044	0.990668204	0.671872639
0.869517	0.226247	0.897556587	Citric acid	0.603942451	0.990668204	0.960070845
0.862816	0.94173	0.037873817	Cysteine	0.968112837	0.990668204	0.253977363
0.876172	0.250522	0.973390587	Cytidine	0.603942451	0.990668204	0.983086589
0.945656	0.098448	0.941382291	Glucuronic acid	0.500088479	0.990668204	0.983086589
0.879493	0.251175	0.861335535	Glyceric acid	0.603942451	0.990668204	0.960070845
0.942966	0.567603	0.327302692	Inosine	0.831390079	0.990668204	0.671872639
0.960475	0.019014	0.723009783	Lactose	0.216758948	0.990668204	0.915812392
0.927359	0.570798	0.270407658	Ornithine	0.831390079	0.990668204	0.662608652
0.874358	0.365458	0.716616313	Putrescine	0.693810023	0.990668204	0.915812392
0.973288	0.615424	0.264208939	Sucrose	0.852675876	0.990668204	0.662608652
0.948	0.591861	0.033102163	Threonic acid	0.838485125	0.990668204	0.251576441
0.960991	0.531681	0.492848932	Threonine	0.822157584	0.990668204	0.849432595
0.847964	0.942464	0.851678378	Uracil	0.968112837	0.990668204	0.960070845
0.992158	0.049785	0.721448319	Galacturonic acid	0.388831319	0.992157906	0.915812392
0.989058	0.576139	0.862640347	Myristic acid	0.831390079	0.992157906	0.960070845

b

p_EQ2	Metabolites	q_EQ2
0.019951	Succinic acid	0.159607
0.024891	Mannose 6-phosphate	0.186681
0.051084	Cystathionine	0.360593
0.071874	Threonic acid	0.479163

0.091343	3-Hydroxypropionic acid	0.498233
0.087774	Glutamic acid	0.498233
0.088309	Myristic acid	0.498233
0.087288	O-Phosphoethanolamine	0.498233
0.112701	2-Hydroxybutyric acid	0.588006
0.204875	2-Hydroxyisovaleric acid	0.742221
0.17619	3-Aminoglutaric acid	0.742221
0.210296	5-Aminovaleric acid	0.742221
0.182402	Cysteine	0.742221
0.192877	Cytidine	0.742221
0.206521	Glutaric acid	0.742221
0.187636	Glycine	0.742221
0.19762	Inositol	0.742221
0.181368	N-Acetylmannosamine	0.742221
0.191025	Phosphoric acid	0.742221
0.154946	Uridine	0.742221
0.222227	Cadaverine	0.761921
0.233179	Metoprolol	0.777263
0.261365	Caproic acid	0.825363
0.254974	Lauric acid	0.825363
0.296047	Hypotaurine	0.905214
0.301738	Norepinephrine	0.905214
0.331225	Octadecanol	0.969438
0.854885	2-Aminobutyric acid	0.980764
0.600631	2-Aminoethanol	0.980764
0.9249	2-Aminopimelic acid	0.980764
0.781824	2-Hydroxyisobutyric acid	0.980764
0.660449	2-Hydroxyisocaproic acid	0.980764
0.642219	2-Ketoglutaric acid	0.980764
0.86116	3-Aminopropanoic acid	0.980764

0.400041	3-Hydroxybutyric acid	0.980764
0.585359	3-Hydroxyisobutyric acid	0.980764
0.665109	3-Hydroxyphenylacetic acid	0.980764
0.381898	3-methoxy-4-hydroxybenzoic acid	0.980764
0.515318	5-Oxoproline	0.980764
0.604696	Acetylglycine	0.980764
0.527574	Alanine	0.980764
0.836107	Allose	0.980764
0.956261	Arabinose	0.980764
0.541688	Aspartic acid	0.980764
0.693997	Azelaic acid	0.980764
0.504911	Benzoic acid	0.980764
0.919353	Beta alanine	0.980764
0.608064	Catechol	0.980764
0.85018	Citric acid	0.980764
0.423678	Ethylmalonic acid	0.980764
0.735502	Fructose	0.980764
0.720583	Fumaric acid	0.980764
0.786235	Galactose	0.980764
0.964418	Galacturonic acid	0.980764
0.348107	Gluconic acid	0.980764
0.837074	Glucono-1,5-lactone	0.980764
0.816494	Glucose	0.980764
0.753348	Glucuronic acid	0.980764
0.945298	Glyceric acid	0.980764
0.396408	Glycerol	0.980764
0.404778	Glycolic acid	0.980764
0.786594	Glyoxylic acid	0.980764
0.93946	Guanosine	0.980764

0.396171	Hydroxylamine	0.980764
0.450495	Inosine	0.980764
0.700857	Isoleucine	0.980764
0.399172	Lactic acid	0.980764
0.587961	Lactitol	0.980764
0.948323	Lactose	0.980764
0.938772	Leucine	0.980764
0.934026	Lyxose	0.980764
0.956545	Malic acid	0.980764
0.786838	Maltose	0.980764
0.82404	Mannitol	0.980764
0.794763	Mannose	0.980764
0.669764	Monostearin	0.980764
0.49535	Nonanoic acid	0.980764
0.947794	Octanoic acid	0.980764
0.510059	Ornithine	0.980764
0.46516	Palmitic acid	0.980764
0.519927	Psicose	0.980764
0.385903	Putrescine	0.980764
0.887397	Pyruvic acid	0.980764
0.518494	Rhamnose	0.980764
0.714263	Ribitol	0.980764
0.813239	Ribonolactone	0.980764
0.701158	Ribose 5-phosphate	0.980764
0.729859	Ribulose	0.980764
0.705627	Sarcosine	0.980764
0.472759	Sebacic acid	0.980764
0.575973	Serine	0.980764
0.744084	Sorbose	0.980764
0.92126	Stearic acid	0.980764

0.805663	Suberic acid	0.980764
0.860586	Sucrose	0.980764
0.860743	Tagatose	0.980764
0.473324	Threonine	0.980764
0.800212	Trehalose	0.980764
0.877133	Tyrosine	0.980764
0.959654	Uracil	0.980764
0.921475	Urea	0.980764
0.9004	Valine	0.980764
0.948389	Xylitol	0.980764
0.695401	Xylulose	0.980764
0.997606	Batyl alcohol	0.997606
0.994067	Ribose	0.997606

c

p_EQ3	Metabolites	q_EQ3
0.055577	Monostearin	0.444617
0.062092	Sarcosine	0.445926
0.063173	Maltose	0.445926
0.070936	Lactitol	0.472906
0.088214	Valine	0.557141
0.093599	Trehalose	0.561596
0.119911	Acetylglycine	0.685204
0.140561	Nonanoic acid	0.766698
0.16618	Ribitol	0.855363
0.183143	Cytidine	0.855363
0.186614	Phosphoric acid	0.855363
0.199383	2-Aminoethanol	0.855363
0.202345	Mannose 6-phosphate	0.855363

0.20318	Isoleucine	0.855363
0.206713	Batyl alcohol	0.855363
0.216144	Inosine	0.864575
0.241796	Leucine	0.890597
0.248291	Norepinephrine	0.890597
0.262931	2-Hydroxyisovaleric acid	0.890597
0.265699	Psicose	0.890597
0.267952	2-Ketoglutaric acid	0.890597
0.276277	3-Hydroxypropionic acid	0.890597
0.329325	Mannitol	0.890597
0.341206	Glucose	0.890597
0.345925	Sebacic acid	0.890597
0.346132	Citric acid	0.890597
0.364917	Uridine	0.890597
0.372982	Glycolic acid	0.890597
0.376315	Galactose	0.890597
0.392139	Glutamic acid	0.890597
0.393467	Glucono-1,5-lactone	0.890597
0.402542	2-Hydroxyisobutyric acid	0.890597
0.402597	Urea	0.890597
0.406675	Rhamnose	0.890597
0.41106	Aspartic acid	0.890597
0.43091	2-Aminobutyric acid	0.890597
0.431718	Octanoic acid	0.890597
0.438629	Allose	0.890597
0.440765	Tagatose	0.890597
0.445571	3-Hydroxyphenylacetic acid	0.890597
0.451366	Fructose	0.890597
0.479829	Cystathionine	0.890597
0.487795	Ornithine	0.890597

0.489355	Glutaric acid	0.890597
0.494609	Glyoxylic acid	0.890597
0.520309	Catechol	0.890597
0.52603	Myristic acid	0.890597
0.545416	Beta alanine	0.890597
0.545573	Guanosine	0.890597
0.554615	2-Aminopimelic acid	0.890597
0.558679	Inositol	0.890597
0.573546	Suberic acid	0.890597
0.577466	O-Phosphoethanolamine	0.890597
0.583944	Cadaverine	0.890597
0.596999	3-Aminopropanoic acid	0.890597
0.600376	3-Hydroxybutyric acid	0.890597
0.602748	Ribose 5-phosphate	0.890597
0.612249	Threonic acid	0.890597
0.624954	Hypotaurine	0.890597
0.627515	Xylitol	0.890597
0.63838	Putrescine	0.890597
0.640731	Malic acid	0.890597
0.642507	Benzoic acid	0.890597
0.648781	Mannose	0.890597
0.651241	Lactose	0.890597
0.652961	2-Hydroxybutyric acid	0.890597
0.661961	N-Acetylmannosamine	0.890597
0.668431	5-Aminovaleric acid	0.890597
0.668894	Glycine	0.890597
0.668986	Glycerol	0.890597
0.671006	Alanine	0.890597
0.672923	Azelaic acid	0.890597
0.679631	Serine	0.890597

0.6851	Hydroxylamine	0.890597
0.688301	Galacturonic acid	0.890597
0.707951	Octadecanol	0.890597
0.710925	Sorbose	0.890597
0.715646	Caproic acid	0.890597
0.725609	Palmitic acid	0.890597
0.730631	3-Hydroxyisobutyric acid	0.890597
0.731405	Ribose	0.890597
0.732614	Glucuronic acid	0.890597
0.737878	Sucrose	0.890597
0.744543	Lyxose	0.890597
0.745802	Tyrosine	0.890597
0.751146	Glyceric acid	0.890597
0.756627	Ethylmalonic acid	0.890597
0.757007	Ribonolactone	0.890597
0.778645	5-Oxoproline	0.893515
0.779015	Arabinose	0.893515
0.785954	Cysteine	0.893515
0.789271	Lauric acid	0.893515
0.798414	Uracil	0.895417
0.806656	2-Hydroxyisocaproic acid	0.896285
0.828542	Fumaric acid	0.912157
0.840824	Stearic acid	0.917263
0.849354	Xylulose	0.918221
0.880274	Threonine	0.94315
0.903902	Gluconic acid	0.959896
0.924991	3-methoxy-4-hydroxybenzoic acid	0.973675
0.937814	Succinic acid	0.973966
0.942246	Metoprolol	0.973966

0.949617	Ribulose	0.973966
0.969929	3-Aminoglutaric acid	0.976228
0.971253	Lactic acid	0.976228
0.976228	Pyruvic acid	0.976228

Table S6-4 differentially regulated pathways across oestrus after calving (OC) by Metaboanalyst - metabolites only

	Total Cmpd	Hits	Raw p	mi-nuslog(p)	FDR	Impact	p (OC)	q (OC)
Pyrimidine metabolism	**10**	**3**	**9.70E-06**	**5.0134**	**0.000427**	**0.11416**	**0.000102**	**0.001497**
Galactose metabolism	**9**	**7**	**6.42E-05**	**4.1925**	**0.001329**	**0.23707**	**2.43E-07**	**1.07E-05**
Thiamine metabolism	**1**	**1**	**9.06E-05**	**4.0427**	**0.001329**	**0**	**0.001593**	**0.010016**
Glycerophospholipid metabolism	**3**	**2**	**0.000325**	**3.4884**	**0.003052**	**0.03747**	**0.002254**	**0.012396**
Glycerolipid metabolism	**4**	**2**	**0.000441**	**3.3556**	**0.003052**	**0.33022**	**6.51E-07**	**1.43E-05**
Ascorbate and aldarate metabolism	**2**	**2**	**0.000555**	**3.2559**	**0.003052**	**0.25**	**0.005665**	**0.021098**
Inositol phosphate metabolism	**4**	**2**	**0.000555**	**3.2559**	**0.003052**	**0.12939**	**0.005665**	**0.021098**
Phosphatidylinositol signaling system	**2**	**1**	**0.000555**	**3.2558**	**0.003052**	**0.03736**	**0.005665**	**0.021098**
Propanoate metabolism	**5**	**4**	**0.001365**	**2.8648**	**0.006674**	**0**	**0.000762**	**0.006707**
Pentose phosphate pathway	**9**	**4**	**0.002551**	**2.5932**	**0.011226**	**0.22059**	**0.005754**	**0.021098**
beta-Alanine metabolism	**8**	**4**	**0.003782**	**2.4222**	**0.015129**	**0.39925**	**0.000655**	**0.006707**
Pentose and glucuronate interconversions	**5**	**3**	**0.004472**	**2.3495**	**0.016396**	**0.42188**	**0.009716**	**0.032885**
Cysteine and methionine metabolism	**10**	**5**	**0.006581**	**2.1817**	**0.022275**	**0.33809**	**0.007872**	**0.045775**
Butanoate metabolism	5	2	0.009067	2.0425	0.028497	0		
Citrate cycle (TCA cycle)	9	5	0.00975	2.011	0.028601	0.25782		
Pyruvate metabolism	5	3	0.013891	1.8573	0.037046	0.29082		
Glutathione metabolism	6	4	0.017988	1.745	0.037046	0.09925		
Glyoxylate and dicarboxylate metabolism	10	5	0.018501	1.7328	0.037046	0.25927		
Glycine, serine and threonine metabolism	11	7	0.018502	1.7328	0.037046	0.58693		
Primary bile acid biosynthesis	2	1	0.018503	1.7328	0.037046	0.02239		
Porphyrin and chlorophyll metabolism	2	1	0.018503	1.7328	0.037046	0		
Aminoacyl-tRNA biosynthesis	15	8	0.018523	1.7323	0.037046	0.16667		
Starch and sucrose metabolism	4	3	0.13603	0.86638	0.25024	0.54399		
Neomycin, kanamycin and gentamicin biosyn-thesis	1	1	0.13649	0.86489	0.25024	0		
Amino sugar and nucleotide sugar metabolism	8	5	0.1836	0.73612	0.32314	0.15882		
Pantothenate and CoA biosynthesis	8	5	0.21405	0.66948	0.36225	0.02143		
Histidine metabolism	3	1	0.27928	0.55396	0.45512	0		

Taurine and hypotaurine metabolism	3	2	0.30157	0.52061	0.46877	0.28571
Sphingolipid metabolism	2	2	0.30896	0.51009	0.46877	0.0142
Valine, leucine and isoleucine degradation	7	4	0.32884	0.48302	0.48143	0.02837
Valine, leucine and isoleucine biosynthesis	5	3	0.33919	0.46956	0.48143	0
Arginine and proline metabolism	8	2	0.42087	0.37586	0.57869	0.11063
Tyrosine metabolism	10	3	0.45274	0.34415	0.60365	0.11335
Glycolysis / Gluconeogenesis	5	1	0.56539	0.24765	0.69884	0.10044
Purine metabolism	14	3	0.57175	0.2428	0.69884	0.01583
Arginine biosynthesis	9	5	0.57178	0.24277	0.69884	0.06091
Alanine, aspartate and glutamate metabolism	12	7	0.72801	0.13786	0.83473	0.27404
D-Glutamine and D-glutamate metabolism	2	1	0.74798	0.12611	0.83473	0
Fatty acid biosynthesis	5	3	0.77542	0.11046	0.83473	0.01473
Selenocompound metabolism	1	1	0.77798	0.10903	0.83473	0
Fatty acid elongation	1	1	0.79679	0.098656	0.83473	0
Fatty acid degradation	1	1	0.79679	0.098656	0.83473	0
Fructose and mannose metabolism	6	2	0.82941	0.081233	0.8487	0.15735
Biosynthesis of unsaturated fatty acids	6	2	0.89188	0.049696	0.89188	0

Table S6-5 enrichment results IMPaLA OC joint analysis

pathway_name	P_genes	Q_genes	P_metabolites	Q_metabolites	P_joint	Q_joint
Metabolism	7.03E-15	3.23E-11	0.00441	1	1.21E-15	1.22E-12
Immune System	1.51E-07	0.000347	1	1	2.52E-06	0.000846
TCR (T cell antigen receptor)	3.58E-07	0.000547	1	1	3.58E-07	0.000547
Innate Immune System	9.90E-07	0.00114	1	1	1.47E-05	0.00295
Neutrophil degranulation	1.32E-06	0.00121	1	1	1.32E-06	0.00121
Metabolism of lipids	3.81E-06	0.00292	0.0122	1	8.33E-07	0.000419
Metabolism of amino acids and derivatives	9.15E-06	0.006	0.406	1	5.02E-05	0.00841
Gene and protein expression by JAK-STAT signaling after Interleukin-12 stimulation	3.05E-05	0.0175	1	1	3.05E-05	0.0175
Gene expression (Transcription)	3.76E-05	0.0192	0.25	1	0.000118	0.017
Biological oxidations	6.10E-05	0.028	0.0156	1	1.42E-05	0.00295
RNA Polymerase II Transcription	7.50E-05	0.0313	0.5	1	0.000042	0.0384
EGFR1	9.18E-05	0.0351	1	1	9.18E-05	0.0351
Glycolysis / Gluconeogenesis	0.000107	0.0377	0.25	1	0.000308	0.0344
Metabolism of proteins	0.000145	0.0474	0.38	1	0.000595	0.046

Generic Transcription Pathway	**0.000215**	**0.0657**	**0.5**	**1**	**0.00109**	**0.073**
Cellular responses to stress	**0.000242**	**0.0694**	**0.5**	**1**	**0.00121**	**0.0762**
Glycolysis and Gluconeogenesis	0.00061	0.165	0.312	1	0.00182	0.102
Cellular responses to external stimuli	0.00073	0.186		1	0.00325	0.156
Signal Transduction	**0.00092**	**0.204**	**0.025**	**1**	**0.000268**	**0.0337**
Phase II - Conjugation of compounds	**0.000977**	**0.204**	**0.0313**	**1**	**0.000348**	**0.035**
G2/M Transition	0.000977	0.204	1	1	0.00775	0.278
Mitotic G2-G2/M phases	0.000977	0.204	1	1	0.00775	0.278
Metabolic reprogramming in colon cancer	**0.00134**	**0.237**	**0.0391**	**1**	**0.000569**	**0.046**
Metabolism of carbohydrates	**0.00126**	**0.237**	**0.0507**	**1**	**0.000681**	**0.049**
Cell Cycle	0.00129	0.237	0.5	1	0.00538	0.235
Peptide chain elongation	0.00122	0.237	1	1	0.00941	0.291
Selenoamino acid metabolism	0.00146	0.249	0.812	1	0.0092	0.291
Eukaryotic Translation Elongation	0.00153	0.25	1	1	0.0114	0.291
Cellular response to heat stress	0.00168	0.266	1	1	0.0124	0.291
Focal Adhesion	0.00195	0.299	1	1	0.00195	0.299

Sudden Infant Death Syndrome (SIDS) Susceptibility Pathways	0.00244	0.32	1	1	0.0171	0.319
Formation of a pool of free 40S subunits	0.00244	0.32	1	1	0.00244	0.32
Nuclear Receptors Meta-Pathway	0.00248	0.32	1	1	0.00248	0.32
Pathways in clear cell renal cell carcinoma	0.00269	0.32	1	1	0.00269	0.32
Cytoplasmic Ribosomal Proteins	0.00293	0.32	1	1	0.00293	0.32
SRP-dependent cotranslational protein targeting to membrane	0.00293	0.32	1	1	0.00293	0.32
Nonsense-Mediated Decay (NMD)	0.00293	0.32	1	1	0.00293	0.32
Ribosome - Homo sapiens (human)	0.00293	0.32	1	1	0.00293	0.32
Nonsense Mediated Decay (NMD) independent of the Exon Junction Complex (EJC)	0.00293	0.32	1	1	0.00293	0.32
Nonsense Mediated Decay (NMD) enhanced by the Exon Junction Complex (EJC)	0.00293	0.32	1	1	0.00293	0.32
Eukaryotic Translation Termination	0.00293	0.32	1	1	0.02	0.343
Selenocysteine synthesis	0.00293	0.32	1	1	0.02	0.343
Trans-sulfuration pathway	0.00391	0.345	0.0625	1	0.00227	0.12
Glutathione metabolism - Homo sapiens (human)	0.00391	0.345	0.438	1	0.0126	0.291
RHO GTPases activate PKNs	0.00391	0.345	0.5	1	0.0141	0.291
Cysteine and methionine metabolism - Homo sapiens (human)	0.00391	0.345	0.625	1	0.0171	0.319
Deubiquitination	0.00336	0.345	1	1	0.00336	0.345

Validated targets of C-MYC transcriptional activation	0.00391	0.345	1	1	0.00391	0.345
Organelle biogenesis and maintenance	0.00385	0.345	1	1	0.0252	0.373
Cytokine Signaling in Immune system	0.00391	0.345	1	1	0.0256	0.373
Regulation of PLK1 Activity at G2/M Transition	0.00391	0.345	1	1	0.0256	0.373
Semaphorin interactions	0.00391	0.345	1	1	0.0256	0.373
Transcriptional Regulation by TP53	0.00403	0.349	0.5	1	0.0145	0.291
Transport of small molecules	0.00471	0.386	0.0385	1	0.00175	0.102
Gluconeogenesis	0.00488	0.386	0.156	1	0.00624	0.262
gluconeogenesis	0.00488	0.386	0.5	1	0.0171	0.319
Regulation of actin cytoskeleton - Homo sapiens (human)	0.00464	0.386	1	1	0.00464	0.386
Focal adhesion - Homo sapiens (human)	0.00488	0.386	1	1	0.00488	0.386
miR-targeted genes in epithelium - TarBase	0.00528	0.41	1	1	0.00528	0.41
RHO GTPase Effectors	0.00554	0.424	0.5	1	0.0191	0.343
Signaling by Rho GTPases	0.00613	0.461	0.5	1	0.0208	0.343
Fatty acid metabolism	0.00781	0.478	0.0391	1	0.00278	0.14
Urea cycle and metabolism of arginine_ proline_ glutamate_ aspartate and asparagine	0.00781	0.478	0.241	1	0.0137	0.291

Cori Cycle	0.00781	0.478	0.5	1	0.0256	0.373
superpathway of purine nucleotide salvage	0.00781	0.478	0.625	1	0.0309	0.42
purine nucleotides de novo biosynthesis	0.00781	0.478	0.625	1	0.0309	0.42
Translation	0.00714	0.478	0.734	1	0.0328	0.434
Role of Calcineurin-dependent NFAT signaling in lymphocytes	0.00781	0.478	1	1	0.00781	0.478
Cell Cycle Checkpoints	0.00781	0.478	1	1	0.00781	0.478
Oocyte meiosis - Homo sapiens (human)	0.00781	0.478	1	1	0.00781	0.478
Hippo signaling pathway - Homo sapiens (human)	0.00781	0.478	1	1	0.00781	0.478
Thiopurine Pathway_ Pharmacokinetics/Pharmacodynamics	0.00781	0.478	1	1	0.00781	0.478
Host Interactions of HIV factors	0.00781	0.478	1	1	0.0457	0.554
HIV Infection	0.00781	0.478	1	1	0.0457	0.554
Mitotic Prometaphase	0.00781	0.478	1	1	0.0457	0.554
NRF2 pathway	0.00854	0.516	1	1	0.00854	0.516
Metabolism of nucleotides	0.00919	0.548	0.322	1	0.0202	0.343
Protein processing in endoplasmic reticulum - Homo sapiens (human)	0.00944	0.555	1	1	0.00944	0.555
Post-translational protein modification	0.0098	0.562	0.313	1	0.0208	0.343

Glycolysis Pathway D (2)	0.00977	0.562	0.5	1	0.0309	0.42
Hemostasis	0.01	0.567	0.5	1	0.0315	0.423
Cell Cycle_ Mitotic	0.0107	0.567	0.5	1	0.0334	0.437
L13a-mediated translational silencing of Ceruloplasmin expression	0.0107	0.567	1	1	0.0107	0.567
Cilium Assembly	0.0103	0.567	1	1	0.0572	0.634
GTP hydrolysis and joining of the 60S ribosomal subunit	0.0107	0.567	1	1	0.0594	0.636
Cap-dependent Translation Initiation	0.0107	0.567	1	1	0.0594	0.636
Eukaryotic Translation Initiation	0.0107	0.567	1	1	0.0594	0.636
Regulation of HSF1-mediated heat shock response	0.0122	0.637	1	1	0.066	0.684
Pyruvate metabolism - Homo sapiens (human)	0.0156	0.67	0.25	1	0.0256	0.373
Arginine Proline metabolism	0.0156	0.67	0.432	1	0.0405	0.522
Ub-specific processing proteases	0.0134	0.67	1	1	0.0134	0.67
insulin	0.0137	0.67	1	1	0.0137	0.67
insulin Mam	0.0137	0.67	1	1	0.0137	0.67
Regulation of nuclear beta catenin signaling and target gene transcription	0.0156	0.67	1	1	0.0156	0.67
a6b1 and a6b4 Integrin signaling	0.0156	0.67	1	1	0.0156	0.67

RhoA signaling pathway	0.0156	0.67	1	1	0.0156	0.67
LKB1 signaling events	0.0156	0.67	1	1	0.0156	0.67
Leukocyte transendothelial migration - Homo sapiens (human)	0.0156	0.67	1	1	0.0156	0.67
Alpha6Beta4Integrin	0.0156	0.67	1	1	0.0156	0.67
Recruitment of mitotic centrosome proteins and complexes	0.0156	0.67	1	1	0.0156	0.67
Loss of Nlp from mitotic centrosomes	0.0156	0.67	1	1	0.0156	0.67
Loss of proteins required for interphase microtubule organization from the centrosome	0.0156	0.67	1	1	0.0156	0.67
Centrosome maturation	0.0156	0.67	1	1	0.0156	0.67
AURKA Activation by TPX2	0.0156	0.67	1	1	0.0156	0.67
Recruitment of NuMA to mitotic centrosomes	0.0156	0.67	1	1	0.0156	0.67
Vesicle-mediated transport	0.0139	0.67	1	1	0.0734	0.724
Ibuprofen Action Pathway	0.0156	0.67	1	1	0.0806	0.765
TNFalpha	0.0181	0.768	1	1	0.0181	0.768
Amino Acid metabolism	0.0186	0.781	0.177	1	0.022	0.358
Iron uptake and transport	0.0195	0.786	0.5	1	0.055	0.621
glycolysis	0.0195	0.786	0.5	1	0.055	0.621

Apoptosis	0.0195	0.786	1	1	0.0964	0.851
Programmed Cell Death	0.0195	0.786	1	1	0.0964	0.851
Pathways in cancer - Homo sapiens (human)	0.0195	0.786	1	1	0.0964	0.851
Disease	0.0206	0.822	0.5	1	0.0574	0.634
Tight junction - Homo sapiens (human)	0.0208	0.824	1	1	0.0208	0.824
Necroptosis - Homo sapiens (human)	0.0234	0.912	1	1	0.0234	0.912
Myometrial Relaxation and Contraction Pathways	0.0234	0.912	1	1	0.0234	0.912
Signaling by GPCR	0.0256	0.938	0.0353	1	0.00723	0.278
GPCR downstream signalling	0.0256	0.938	0.0353	1	0.00723	0.278
Glycolysis and Gluconeogenesis	0.0313	0.938	0.125	1	0.0256	0.373
Folate metabolism	0.0313	0.938	0.25	1	0.0457	0.554
Arginine and proline metabolism - Homo sapiens (human)	0.0313	0.938	0.375	1	0.0638	0.674
M Phase	0.0269	0.938	0.5	1	0.0713	0.717
Signaling by Nuclear Receptors	0.0313	0.938	0.5	1	0.0806	0.765
Neddylation	0.0256	0.938	1	1	0.0256	0.938
AndrogenReceptor	0.0266	0.938	1	1	0.0266	0.938

UCH proteinases	0.0266	0.938	1	1	0.0266	0.938
PI3K-Akt signaling pathway - Homo sapiens (human)	0.0295	0.938	1	1	0.0295	0.938
Metapathway biotransformation Phase I and II	0.0313	0.938	1	1	0.0313	0.938
Drug metabolism - other enzymes - Homo sapiens (human)	0.0313	0.938	1	1	0.0313	0.938
Association of TriC/CCT with target proteins during biosynthesis	0.0313	0.938	1	1	0.0313	0.938
Rap1 signaling pathway - Homo sapiens (human)	0.0313	0.938	1	1	0.0313	0.938
Fluid shear stress and atherosclerosis - Homo sapiens (human)	0.0313	0.938	1	1	0.0313	0.938
Spinal Cord Injury	0.0313	0.938	1	1	0.0313	0.938
p38 signaling mediated by MAPKAP kinases	0.0313	0.938	1	1	0.0313	0.938
FoxO family signaling	0.0313	0.938	1	1	0.0313	0.938
Class I PI3K signaling events mediated by Akt	0.0313	0.938	1	1	0.0313	0.938
Trk receptor signaling mediated by PI3K and PLC-gamma	0.0313	0.938	1	1	0.0313	0.938
G2/M DNA damage checkpoint	0.0313	0.938	1	1	0.0313	0.938
Signaling events mediated by VEGFR1 and VEGFR2	0.0313	0.938	1	1	0.0313	0.938
G2/M Checkpoints	0.0313	0.938	1	1	0.0313	0.938
Cell cycle - Homo sapiens (human)	0.0313	0.938	1	1	0.0313	0.938

Hepatitis C - Homo sapiens (human)	0.0313	0.938	1	1	0.0313	0.938
Apoptosis - Homo sapiens (human)	0.0313	0.938	1	1	0.0313	0.938
Cell Cycle	0.0313	0.938	1	1	0.0313	0.938
Cooperation of PDCL (PhLP1) and TRiC/CCT in G-protein beta folding	0.0313	0.938	1	1	0.14	0.982
Ion channel transport	0.0313	0.938	1	1	0.14	0.982
Folding of actin by CCT/TriC	0.0313	0.938	1	1	0.14	0.982
Cargo trafficking to the periciliary membrane	0.0313	0.938	1	1	0.14	0.982
Metabolism of steroids	0.0313	0.938	1	1	0.14	0.982
Sterol Regulatory Element-Binding Proteins (SREBP) signalling	0.0313	0.938	1	1	0.14	0.982
ESR-mediated signaling	0.0313	0.938	1	1	0.14	0.982
TP53 Regulates Metabolic Genes	0.0322	0.961	0.5	1	0.0826	0.777
superpathway of conversion of glucose to acetyl CoA and entry into the TCA cycle	0.0327	0.968	0.0625	1	0.0147	0.291
Purine metabolism - Homo sapiens (human)	0.0342	0.968	0.625	1	0.104	0.906
Mercaptopurine Action Pathway	0.0342	0.968	0.844	1	0.131	0.982
Azathioprine Action Pathway	0.0342	0.968	0.844	1	0.131	0.982
Thioguanine Action Pathway	0.0342	0.968	0.844	1	0.131	0.982

Chaperonin-mediated protein folding	0.0342	0.968	1	1	0.15	1
Cooperation of Prefoldin and TriC/CCT in actin and tubulin folding	0.0342	0.968	1	1	0.15	1
Formation of tubulin folding intermediates by CCT/TriC	0.0342	0.968	1	1	0.15	1
Warburg Effect	0.0353	0.993	0.0137	1	0.00417	0.19
The citric acid (TCA) cycle and respiratory electron transport	0.0781	1	0.0156	1	0.00941	0.291
Transmission across Chemical Synapses	0.0625	1	0.021	1	0.01	0.291
Glycolysis Gluconeogenesis	0.064	1	0.0244	1	0.0117	0.291
G alpha (i) signalling events	0.0923	1	0.0195	1	0.0132	0.291
Glucagon signaling pathway - Homo sapiens (human)	0.0625	1	0.0313	1	0.0141	0.291
Phosphoenolpyruvate carboxykinase deficiency 1 (PEPCK1)	0.0625	1	0.0313	1	0.0141	0.291
Gluconeogenesis	0.0625	1	0.0313	1	0.0141	0.291
Glycogenosis_ Type IA. Von gierke disease	0.0625	1	0.0313	1	0.0141	0.291
Glycogenosis_ Type IC	0.0625	1	0.0313	1	0.0141	0.291
Glycogen Storage Disease Type 1A (GSD1A) or Von Gierke Disease	0.0625	1	0.0313	1	0.0141	0.291
Triosephosphate isomerase	0.0625	1	0.0313	1	0.0141	0.291
Fructose-1_6-diphosphatase deficiency	0.0625	1	0.0313	1	0.0141	0.291
Glycogenosis_ Type IB	0.0625	1	0.0313	1	0.0141	0.291

Neuronal System	0.0977	1	0.021	1	0.0147	0.291
Pyruvate metabolism and Citric Acid (TCA) cycle	0.188	1	0.0156	1	0.02	0.343
Class A/1 (Rhodopsin-like receptors)	0.156	1	0.0273	1	0.0276	0.396
Glucose metabolism	0.0398	1	0.109	1	0.028	0.397
Glutathione conjugation	0.0625	1	0.125	1	0.0457	0.554
GPCR ligand binding	0.156	1	0.0574	1	0.0512	0.614
Tyrosine metabolism - Homo sapiens (human)	0.0625	1	0.156	1	0.055	0.621
Methionine Cysteine metabolism	0.0625	1	0.156	1	0.055	0.621
Citrate cycle	0.156	1	0.0625	1	0.055	0.621
Central carbon metabolism in cancer - Homo sapiens (human)	0.125	1	0.0946	1	0.0643	0.674
Glycolysis	0.102	1	0.125	1	0.0681	0.699
Purine nucleotides nucleosides metabolism	0.0537	1	0.25	1	0.0713	0.717
Metabolism of vitamins and cofactors	0.211	1	0.0645	1	0.0722	0.719
Pyruvate metabolism	0.0625	1	0.25	1	0.0806	0.765
Glutathione metabolism	0.0625	1	0.25	1	0.0806	0.765
HIF-1 signaling pathway - Homo sapiens (human)	0.156	1	0.125	1	0.0964	0.851
The oncogenic action of L-2-hydroxyglutarate in Hydroxyguaricaciduria	0.625	1	0.0313	1	0.0964	0.851

The oncogenic action of D-2-hydroxyglutarate in Hydroxygluaricaciduria	0.625	1	0.0313	1	0.0964	0.851
fig-met-1-last-solution	0.312	1	0.0625	1	0.0964	0.851
Pentose and glucuronate interconversions - Homo sapiens (human)	1	1	0.0223	1	0.107	0.927
Metabolism of RNA	0.09	1	0.25	1	0.108	0.928
Platelet activation_ signaling and aggregation	0.0528	1	0.5	1	0.122	0.982
Neurotransmitter release cycle	1	1	0.0273	1	0.126	0.982
The oncogenic action of Fumarate	0.875	1	0.0313	1	0.126	0.982
The oncogenic action of 2-hydroxyglutarate	0.875	1	0.0313	1	0.126	0.982
Developmental Biology	0.113	1	0.25	1	0.129	0.982
Purine metabolism	0.0625	1	0.461	1	0.131	0.982
Axon guidance	0.12	1	0.25	1	0.135	0.982
Pyruvate metabolism	0.25	1	0.125	1	0.14	0.982
Pyrimidine metabolism - Homo sapiens (human)	0.25	1	0.125	1	0.14	0.982
TCA Cycle and Deficiency of Pyruvate Dehydrogenase complex (PDHc)	0.25	1	0.125	1	0.14	0.982
superpathway of methionine degradation	1	1	0.0313	1	0.14	0.982
Glycolysis	0.125	1	0.25	1	0.14	0.982
Glycogenosis_ Type VII. Tarui disease	0.125	1	0.25	1	0.14	0.982
Fanconi-bickel syndrome	0.125	1	0.25	1	0.14	0.982
Histidine metabolism	0.25	1	0.125	1	0.14	0.982
Phenylalanine metabolism - Homo sapiens (human)	0.5	1	0.0625	1	0.14	0.982

Glutaminolysis and Cancer	0.312	1	0.102	1	0.141	0.987
Digestion and absorption	1	1	0.00391	1	0.00391	1
Digestion	1	1	0.00391	1	0.00391	1
Digestion	1	1	0.0156	1	0.0156	1
The citric acid (TCA) cycle and respiratory electron transport	1	1	0.0156	1	0.0156	1
Digestion of dietary carbohydrate	1	1	0.0313	1	0.0313	1
HSF1 activation	0.0371	1	1	1	0.0371	1
Attenuation phase	0.0371	1	1	1	0.0371	1
HSF1-dependent transactivation	0.0371	1	1	1	0.0371	1
Human papillomavirus infection - Homo sapiens (human)	0.0469	1	1	1	0.0469	1
Measles - Homo sapiens (human)	0.0469	1	1	1	0.0469	1
TGF_beta_Receptor	0.0469	1	1	1	0.0469	1
Regulation of Actin Cytoskeleton	0.0488	1	1	1	0.0488	1
Post-translational protein phosphorylation	0.0502	1	1	1	0.0502	1
Prefoldin mediated transfer of substrate to CCT/TriC	0.0537	1	1	1	0.0537	1
Transport of bile salts and organic acids_ metal ions and amine compounds	1	1	0.0547	1	0.0547	1

miR-targeted genes in squamous cell - TarBase	0.0547	1	1	1	0.0547	1
Phase II - Conjugation of compounds	1	1	0.0579	1	0.0579	1
Regulation of Insulin-like Growth Factor (IGF) transport and uptake by Insulin-like Growth Factor Binding Proteins (IGFBPs)	0.0605	1	1	1	0.0605	1
Ciliary landscape	0.0625	1	1	1	0.0625	1
Chk1/Chk2(Cds1) mediated inactivation of Cyclin B:Cdk1 complex	0.0625	1	1	1	0.0625	1
Beta2 integrin cell surface interactions	0.0625	1	1	1	0.0625	1
Signaling events mediated by HDAC Class II	0.0625	1	1	1	0.0625	1
Insulin-mediated glucose transport	0.0625	1	1	1	0.0625	1
Validated transcriptional targets of TAp63 isoforms	0.0625	1	1	1	0.0625	1
Integrin-linked kinase signaling	0.0625	1	1	1	0.0625	1
EGF	0.0625	1	1	1	0.0625	1
FGF	0.0625	1	1	1	0.0625	1
Fas	0.0625	1	1	1	0.0625	1
integrin signaling pathway	0.0625	1	1	1	0.0625	1
Carbohydrate digestion and absorption - Homo sapiens (human)	1	1	0.0625	1	0.0625	1
Protein methylation	0.0625	1	1	1	0.0625	1

Abacavir Pathway_ Pharmacokinetics/Pharmacodynamics	0.0625	1	1	1	0.0625	1
Malonyl-coa decarboxylase deficiency	1	1	0.0625	1	0.0625	1
Malonic Aciduria	1	1	0.0625	1	0.0625	1
Propanoate Metabolism	1	1	0.0625	1	0.0625	1
Methylmalonic Aciduria Due to Cobalamin-Related Disorders	1	1	0.0625	1	0.0625	1
Glucose metabolism	1	1	0.0625	1	0.0625	1
EGF-EGFR Signaling Pathway	0.0625	1	1	1	0.0625	1
HIF-1-alpha transcription factor network	0.0625	1	1	1	0.0625	1
Taste transduction - Homo sapiens (human)	1	1	0.0625	1	0.0625	1
BBSome-mediated cargo-targeting to cilium	0.0625	1	1	1	0.0625	1
Parkin-Ubiquitin Proteasomal System pathway	0.0637	1	1	1	0.0637	1
Class A-1 (Rhodopsin-like receptors)	1	1	0.0645	1	0.0645	1
G13 Signaling Pathway	0.0781	1	1	1	0.0781	1
Formation of the ternary complex_ and subsequently_ the 43S complex	0.0781	1	1	1	0.0781	1
C-MYB transcription factor network	0.0781	1	1	1	0.0781	1
Galactose metabolism	1	1	0.0781	1	0.0781	1

Salmonella infection - Homo sapiens (human)	0.0781	1	1	1	0.0781	1
Integrin-mediated Cell Adhesion	0.0781	1	1	1	0.0781	1
mcalpain and friends in cell motility	0.0781	1	1	1	0.0781	1
Amoebiasis - Homo sapiens (human)	0.0781	1	1	1	0.0781	1
Antigen processing and presentation - Homo sapiens (human)	0.0785	1	1	1	0.0785	1
Biochemical Pathways Part I	1	1	0.0801	1	0.0801	1
Proteasome Degradation	0.0803	1	1	1	0.0803	1
Primary Focal Segmental Glomerulosclerosis FSGS	0.084	1	1	1	0.084	1
p73 transcription factor network	0.0938	1	1	1	0.0938	1
ucalpain and friends in cell spread	0.0938	1	1	1	0.0938	1
Peroxisome - Homo sapiens (human)	0.0938	1	1	1	0.0938	1
fibrinolysis pathway	0.0938	1	1	1	0.0938	1
downregulated of mta-3 in er-negative breast tumors	0.0938	1	1	1	0.0938	1
Phosphatidylinositol phosphate metabolism	1	1	0.0938	1	0.0938	1
Anchoring of the basal body to the plasma membrane	0.0977	1	1	1	0.0977	1
TLR NFkB	0.102	1	1	1	0.102	1

Proteasome - Homo sapiens (human)	0.102	1	1	1	0.102	1
IL-1 NFkB	0.102	1	1	1	0.102	1
MAPK signaling pathway - Homo sapiens (human)	0.105	1	1	1	0.105	1
MAPK Signaling Pathway	0.105	1	1	1	0.105	1
Integrin	0.109	1	1	1	0.109	1
VEGFA-VEGFR2 Signaling Pathway	0.119	1	1	1	0.119	1
Estrogen signaling pathway - Homo sapiens (human)	0.119	1	1	1	0.119	1
B cell receptor signaling	0.123	1	1	1	0.123	1
CD4 T cell receptor signaling-NFkB cascade	0.123	1	1	1	0.123	1
CD4 T cell receptor signaling	0.123	1	1	1	0.123	1
Tryptophan metabolism	0.125	1	1	1	0.125	1
T-Cell antigen Receptor (TCR) Signaling Pathway	0.125	1	1	1	0.125	1
Transcriptional regulation by RUNX2	0.125	1	1	1	0.125	1
Tyrosinemia Type 2 (or Richner-Hanhart syndrome)	1	1	0.125	1	0.125	1
tyrosine degradation	1	1	0.125	1	0.125	1
Glycerolipid Metabolism	1	1	0.125	1	0.125	1

Scavenging of heme from plasma	0.125	1	1	1	0.125	1
Familial lipoprotein lipase deficiency	1	1	0.125	1	0.125	1
Tyrosinemia Type 3 (TYRO3)	1	1	0.125	1	0.125	1
D-glyceric acidura	1	1	0.125	1	0.125	1
Signaling mediated by p38-alpha and p38-beta	0.125	1	1	1	0.125	1
Nectin adhesion pathway	0.125	1	1	1	0.125	1
FOXA2 and FOXA3 transcription factor networks	0.125	1	1	1	0.125	1
Lissencephaly gene (LIS1) in neuronal migration and development	0.125	1	1	1	0.125	1
Posttranslational regulation of adherens junction stability and dissassembly	0.125	1	1	1	0.125	1
E-cadherin signaling in the nascent adherens junction	0.125	1	1	1	0.125	1
Tryptophan metabolism - Homo sapiens (human)	0.125	1	1	1	0.125	1
Regulation of cholesterol biosynthesis by SREBP (SREBF)	0.125	1	1	1	0.125	1
EPHA-mediated growth cone collapse	0.125	1	1	1	0.125	1
Glycosphingolipid metabolism	1	1	0.125	1	0.125	1
Butanoate metabolism - Homo sapiens (human)	1	1	0.125	1	0.125	1
Organic anion transporters	1	1	0.125	1	0.125	1

Oxytocin signaling pathway - Homo sapiens (human)	0.125	1	1	1	0.125	1
Ubiquitin mediated proteolysis - Homo sapiens (human)	0.125	1	1	1	0.125	1
Alzheimer disease - Homo sapiens (human)	0.125	1	1	1	0.125	1
IL-17 signaling pathway - Homo sapiens (human)	0.125	1	1	1	0.125	1
Vibrio cholerae infection - Homo sapiens (human)	0.125	1	1	1	0.125	1
Free fatty acid receptors	1	1	0.125	1	0.125	1
RHO GTPases activate CIT	0.125	1	1	1	0.125	1
RHO GTPases activate IQGAPs	0.125	1	1	1	0.125	1
Sema4D induced cell migration and growth-cone collapse	0.125	1	1	1	0.125	1
L-cysteine degradation II	1	1	0.125	1	0.125	1
COPI-independent Golgi-to-ER retrograde traffic	0.125	1	1	1	0.125	1
L-cysteine degradation I	1	1	0.125	1	0.125	1
Sphingolipid de novo biosynthesis	1	1	0.125	1	0.125	1
Antimetabolite Pathway - Folate Cycle_ Pharmacodynamics	0.125	1	1	1	0.125	1
Methotrexate Pathway (Cancer Cell)_ Pharmacodynamics	0.125	1	1	1	0.125	1
Ibuprofen Metabolism Pathway	0.125	1	1	1	0.125	1

Phenylalanine and Tyrosine Metabolism	1	1	0.125	1	0.125	1
Morphine Metabolism Pathway	0.125	1	1	1	0.125	1
Sorafenib Metabolism Pathway	0.125	1	1	1	0.125	1
Glycerol Kinase Deficiency	1	1	0.125	1	0.125	1
Vitamin A Deficiency	0.125	1	1	1	0.125	1
Phenylketonuria	1	1	0.125	1	0.125	1
Retinol Metabolism	0.125	1	1	1	0.125	1
Gamma carboxylation_ hypusine formation and arylsulfatase activation	0.125	1	1	1	0.125	1
Fibroblast growth factor-1	0.125	1	1	1	0.125	1
4-hydroxyproline degradation	1	1	0.125	1	0.125	1
TNF alpha Signaling Pathway	0.125	1	1	1	0.125	1
Mesodermal Commitment Pathway	0.125	1	1	1	0.125	1
XBP1(S) activates chaperone genes	0.125	1	1	1	0.125	1
Histidine_ lysine_ phenylalanine_ tyrosine_ proline and tryptophan catabolism	1	1	0.125	1	0.125	1
TGF-beta Signaling Pathway	0.125	1	1	1	0.125	1
ATM Signaling Network in Development and Disease	0.125	1	1	1	0.125	1

Nucleobase catabolism	1	1	0.125	1	0.125	1
triacylglycerol degradation	1	1	0.148	1	0.148	1
Adherens junction - Homo sapiens (human)	0.148	1	1	1	0.148	1
Legionellosis - Homo sapiens (human)	0.151	1	1	1	0.151	1
G alpha (i) signalling events	1	1	0.156	1	0.156	1
RNA transport - Homo sapiens (human)	0.156	1	1	1	0.156	1
Peptide ligand-binding receptors	0.156	1	1	1	0.156	1
intrinsic prothrombin activation pathway	0.156	1	1	1	0.156	1
Longevity regulating pathway - multiple species - Homo sapiens (human)	0.156	1	1	1	0.156	1
Antigen processing: Ubiquitination & Proteasome degradation	0.156	1	1	1	0.156	1
Protein ubiquitination	0.156	1	1	1	0.156	1
Neurotransmitter release cycle	1	1	0.156	1	0.156	1
Pentose phosphate cycle	0.0645	1	0.563	1	0.157	1
Pyrimidine nucleotides nucleosides metabolism	0.125	1	0.297	1	0.159	1
Translation initiation complex formation	0.164	1	1	1	0.164	1
Activation of the mRNA upon binding of the cap-binding complex and eIFs_ and subsequent binding to 43S	0.164	1	1	1	0.164	1

Spliceosome - Homo sapiens (human)	0.164	1	1	1	0.164	1
Collagen formation	0.0391	1	1	1	0.166	1
Tyrosine metabolism	0.25	1	0.156	1	0.166	1
Integration of energy metabolism	0.125	1	0.312	1	0.166	1
Citrate cycle (TCA cycle) - Homo sapiens (human)	0.313	1	0.125	1	0.166	1
Lysine degradation	0.25	1	0.156	1	0.166	1
Visual phototransduction	0.156	1	0.25	1	0.166	1
Sulfur amino acid metabolism	0.25	1	0.156	1	0.166	1
Pathogenic Escherichia coli infection - Homo sapiens (human)	0.168	1	1	1	0.168	1
Pathogenic Escherichia coli infection	0.168	1	1	1	0.168	1
3-Phosphoglycerate dehydrogenase deficiency	0.75	1	0.0537	1	0.17	1
Non Ketotic Hyperglycinemia	0.75	1	0.0537	1	0.17	1
Glycine and Serine Metabolism	0.75	1	0.0537	1	0.17	1
Dimethylglycine Dehydrogenase Deficiency	0.75	1	0.0537	1	0.17	1
Hyperglycinemia_ non-ketotic	0.75	1	0.0537	1	0.17	1
Dimethylglycine Dehydrogenase Deficiency	0.75	1	0.0537	1	0.17	1
Sarcosinemia	0.75	1	0.0537	1	0.17	1
Dihydropyrimidine Dehydrogenase Deficiency (DHPD)	0.75	1	0.0537	1	0.17	1
SLC-mediated transmembrane transport	0.875	1	0.0463	1	0.17	1
Metabolism of polyamines	0.0625	1	0.688	1	0.178	1

Ferroptosis	0.188	1	1	1	0.188	1
Dissolution of Fibrin Clot	0.188	1	1	1	0.188	1
Pyrimidine catabolism	1	1	0.188	1	0.188	1
Toxoplasmosis - Homo sapiens (human)	0.188	1	1	1	0.188	1
Shigellosis - Homo sapiens (human)	0.188	1	1	1	0.188	1
pentose phosphate pathway	0.188	1	1	1	0.188	1
Glycerophospholipid biosynthesis	1	1	0.188	1	0.188	1
Glucose Alanine cycle	1	1	0.188	1	0.188	1
Human metabolism overview	1	1	0.191	1	0.191	1
Notch	0.193	1	1	1	0.193	1
TLR JNK	0.193	1	1	1	0.193	1
TLR p38	0.193	1	1	1	0.193	1
Wnt Canonical	0.193	1	1	1	0.193	1
DroToll-like	0.193	1	1	1	0.193	1
Wnt Mammals	0.193	1	1	1	0.193	1
IL-1 JNK	0.193	1	1	1	0.193	1

IL-1 p38	0.193	1	1	1	0.193	1
chondroitin sulfate degradation (metazoa)	1	1	0.195	1	0.195	1
dermatan sulfate degradation (metazoa)	1	1	0.195	1	0.195	1
Pentose phosphate pathway - Homo sapiens (human)	0.084	1	0.578	1	0.195	1
Infectious disease	0.0494	1	1	1	0.198	1
Membrane Trafficking	0.0504	1	1	1	0.201	1
Viral carcinogenesis - Homo sapiens (human)	0.206	1	1	1	0.206	1
Endocytosis - Homo sapiens (human)	0.207	1	1	1	0.207	1
miR-targeted genes in leukocytes - TarBase	0.208	1	1	1	0.208	1
sphingosine and sphingosine-1-phosphate metabolism	1	1	0.0547	1	0.214	1
The oncogenic action of Succinate	0.875	1	0.0625	1	0.214	1
Methionine De Novo and Salvage Pathway	0.125	1	0.438	1	0.214	1
Lysine degradation - Homo sapiens (human)	0.125	1	0.438	1	0.214	1
fatty acid β-oxidation	1	1	0.219	1	0.219	1
phospholipases	1	1	0.219	1	0.219	1
the visual cycle I (vertebrates)	1	1	0.219	1	0.219	1

acyl-CoA hydrolysis	1	1	0.219	1	0.219	1
sphingomyelin metabolism/ceramide salvage	1	1	0.219	1	0.219	1
fatty acid β-oxidation (peroxisome)	1	1	0.219	1	0.219	1
Pyruvate Carboxylase Deficiency	1	1	0.219	1	0.219	1
Primary Hyperoxaluria Type I	1	1	0.219	1	0.219	1
Lactic Acidemia	1	1	0.219	1	0.219	1
Alanine Metabolism	1	1	0.219	1	0.219	1
Chylomicron assembly	0.219	1	1	1	0.219	1
Blood Clotting Cascade	0.219	1	1	1	0.219	1
Dengue-2 Interactions with Blood Clotting Cascade	0.219	1	1	1	0.219	1
miR-targeted genes in muscle cell - TarBase	0.222	1	1	1	0.222	1
Adaptive Immune System	0.0602	1	1	1	0.229	1
One carbon metabolism and related pathways	0.312	1	0.195	1	0.232	1
Glutamate Glutamine metabolism	0.125	1	0.496	1	0.234	1
Starch and sucrose metabolism - Homo sapiens (human)	0.5	1	0.125	1	0.236	1
Glutathione synthesis and recycling	0.5	1	0.125	1	0.236	1

Interconversion of nucleotide di- and triphosphates	0.125	1	0.5	1	0.236	1
Activation of BAD and translocation to mitochondria	0.0625	1	1	1	0.236	1
Activation of BH3-only proteins	0.0625	1	1	1	0.236	1
Intrinsic Pathway for Apoptosis	0.0625	1	1	1	0.236	1
Cystinosis_ ocular nonnephropathic	1	1	0.0625	1	0.236	1
Signaling by Interleukins	0.0625	1	1	1	0.236	1
Proximal tubule bicarbonate reclamation - Homo sapiens (human)	0.125	1	0.5	1	0.236	1
RHO GTPases Activate ROCKs	0.0625	1	1	1	0.236	1
Beta-mercaptolactate-cysteine disulfiduria	1	1	0.0625	1	0.236	1
Thyroid hormone synthesis - Homo sapiens (human)	0.0625	1	1	1	0.236	1
Propanoate metabolism	0.0625	1	1	1	0.236	1
Phenytoin (Antiarrhythmic) Action Pathway	0.0625	1	1	1	0.236	1
Sphingolipid metabolism	0.5	1	0.125	1	0.236	1
Transfer of Acetyl Groups into Mitochondria	0.5	1	0.125	1	0.236	1
Translocation of GLUT4 to the plasma membrane	0.0625	1	1	1	0.236	1
Cysteine Metabolism	1	1	0.0625	1	0.236	1

Butanoate metabolism	0.5	1	0.125	1	0.236	1
G alpha (q) signalling events	0.25	1	0.25	1	0.236	1
Trans-sulfuration pathway	0.5	1	0.125	1	0.236	1
One Carbon Metabolism	0.0625	1	1	1	0.236	1
Interferon Signaling	0.0625	1	1	1	0.236	1
Pyruvate dehydrogenase deficiency (E2)	1	1	0.0625	1	0.236	1
Citric Acid Cycle	1	1	0.0625	1	0.236	1
2-ketoglutarate dehydrogenase complex deficiency	1	1	0.0625	1	0.236	1
Arachidonic acid metabolism	0.125	1	0.5	1	0.236	1
Citric acid cycle (TCA cycle)	1	1	0.0625	1	0.236	1
RHO GTPases activate PAKs	0.0625	1	1	1	0.236	1
Pyruvate dehydrogenase deficiency (E3)	1	1	0.0625	1	0.236	1
Mitochondrial complex II deficiency	1	1	0.0625	1	0.236	1
Fumarase deficiency	1	1	0.0625	1	0.236	1
Congenital lactic acidosis	1	1	0.0625	1	0.236	1
Acetaminophen Metabolism Pathway	0.0625	1	1	1	0.236	1

HIF1A and PPARG regulation of glycolysis	0.25	1	0.25	1	0.236	1
Propanoate metabolism - Homo sapiens (human)	0.25	1	0.25	1	0.236	1
Signaling by Receptor Tyrosine Kinases	0.064	1	1	1	0.24	1
Tyrosine metabolism	0.5	1	0.129	1	0.241	1
ErbB1 downstream signaling	0.244	1	1	1	0.244	1
Selenium Micronutrient Network	0.266	1	0.25	1	0.247	1
Integrin cell surface interactions	0.25	1	1	1	0.25	1
Bile salt and organic anion SLC transporters	1	1	0.25	1	0.25	1
Drug metabolism - cytochrome P450 - Homo sapiens (human)	0.25	1	1	1	0.25	1
Validated targets of C-MYC transcriptional repression	0.25	1	1	1	0.25	1
Signaling events mediated by Hepatocyte Growth Factor Receptor (c-Met)	0.25	1	1	1	0.25	1
GRB2:SOS provides linkage to MAPK signaling for Integrins	0.25	1	1	1	0.25	1
TCR signaling in naïve CD4+ T cells	0.25	1	1	1	0.25	1
p130Cas linkage to MAPK signaling for integrins	0.25	1	1	1	0.25	1
Synthesis of active ubiquitin: roles of E1 and E2 enzymes	0.25	1	1	1	0.25	1
Activation of C3 and C5	0.25	1	1	1	0.25	1
corticosteroids and cardioprotection	0.25	1	1	1	0.25	1
extrinsic prothrombin activation pathway	0.25	1	1	1	0.25	1
Chemical carcinogenesis - Homo sapiens (human)	0.25	1	1	1	0.25	1
Prostate cancer - Homo sapiens (human)	0.25	1	1	1	0.25	1
Prolactin	0.25	1	1	1	0.25	1
Ifosfamide Pathway_ Pharmacodynamics	0.25	1	1	1	0.25	1
Integration of energy metabolism	1	1	0.25	1	0.25	1
Liver steatosis AOP	0.25	1	1	1	0.25	1
Exercise-induced Circadian Regulation	0.25	1	1	1	0.25	1

PI3K-Akt Signaling Pathway	0.25	1	1	1	0.25	1
Serine biosynthesis	1	1	0.25	1	0.25	1
One carbon pool by folate - Homo sapiens (human)	0.25	1	1	1	0.25	1
Degradation of beta-catenin by the destruction complex	0.25	1	1	1	0.25	1
β-alanine degradation	1	1	0.25	1	0.25	1
Nucleotide-binding domain_ leucine rich repeat containing receptor (NLR) signaling pathways	0.25	1	1	1	0.25	1
Histidine catabolism	1	1	0.25	1	0.25	1
Regulation of pyruvate dehydrogenase (PDH) complex	1	1	0.25	1	0.25	1
Lysine catabolism	1	1	0.25	1	0.25	1
Signaling by the B Cell Receptor (BCR)	0.25	1	1	1	0.25	1
Arachidonic acid metabolism - Homo sapiens (human)	0.25	1	1	1	0.25	1
Interleukin-1 signaling	0.25	1	1	1	0.25	1
Stabilization and expansion of the E-cadherin adherens junction	0.25	1	1	1	0.25	1
FOXA1 transcription factor network	0.25	1	1	1	0.25	1
Arf6 downstream pathway	0.25	1	1	1	0.25	1
IL4-mediated signaling events	0.25	1	1	1	0.25	1
p53 pathway	0.25	1	1	1	0.25	1
Fatty acyl-CoA biosynthesis	1	1	0.25	1	0.25	1
Prostaglandin formation from arachidonate	1	1	0.25	1	0.25	1
Retrograde endocannabinoid signaling - Homo sapiens (human)	1	1	0.25	1	0.25	1
mechanism of protein import into the nucleus	0.25	1	1	1	0.25	1
role of ran in mitotic spindle regulation	0.25	1	1	1	0.25	1
T cell receptor signaling pathway - Homo sapiens (human)	0.25	1	1	1	0.25	1
RNA degradation - Homo sapiens (human)	0.25	1	1	1	0.25	1
mRNA surveillance pathway - Homo sapiens (human)	0.25	1	1	1	0.25	1
Axon guidance - Homo sapiens (human)	0.25	1	1	1	0.25	1
Signaling by NOTCH1	0.25	1	1	1	0.25	1
NOD-like receptor signaling pathway - Homo sapiens (human)	0.25	1	1	1	0.25	1
Collecting duct acid secretion - Homo sapiens (human)	0.25	1	1	1	0.25	1

Vitamin digestion and absorption - Homo sapiens (human)	0.25	1	1	1	0.25	1
Cellular senescence - Homo sapiens (human)	0.25	1	1	1	0.25	1
Influenza A - Homo sapiens (human)	0.25	1	1	1	0.25	1
Progesterone-mediated oocyte maturation - Homo sapiens (human)	0.25	1	1	1	0.25	1
Synthesis of PE	1	1	0.25	1	0.25	1
Signaling by NOTCH	0.25	1	1	1	0.25	1
Sphingolipid metabolism	1	1	0.25	1	0.25	1
Peroxisomal protein import	0.25	1	1	1	0.25	1
4-hydroxybenzoate biosynthesis	1	1	0.25	1	0.25	1
Sema3A PAK dependent Axon repulsion	0.25	1	1	1	0.25	1
Fat digestion and absorption - Homo sapiens (human)	0.25	1	1	1	0.25	1
Ovarian tumor domain proteases	0.25	1	1	1	0.25	1
Regulation of Telomerase	0.25	1	1	1	0.25	1
p75 NTR receptor-mediated signalling	0.25	1	1	1	0.25	1
Death Receptor Signalling	0.25	1	1	1	0.25	1
ATM pathway	0.25	1	1	1	0.25	1
Lamivudine Pathway_ Pharmacokinetics/Pharmacodynamics	0.25	1	1	1	0.25	1
Doxorubicin Pathway_ Pharmacokinetics	0.25	1	1	1	0.25	1
Glucocorticoid Pathway (Peripheral Tissue)_ Pharmacodynamics	0.25	1	1	1	0.25	1
Cyclophosphamide Pathway_ Pharmacodynamics	0.25	1	1	1	0.25	1
Plasmalogen Synthesis	1	1	0.25	1	0.25	1
Lactose Degradation	1	1	0.25	1	0.25	1
Lactose Intolerance	1	1	0.25	1	0.25	1
NOTCH-Ncore	0.25	1	1	1	0.25	1
Translation Factors	0.25	1	1	1	0.25	1
Cell-Cell communication	0.25	1	1	1	0.25	1
pyrimidine ribonucleosides degradation	1	1	0.25	1	0.25	1
(S)-reticuline biosynthesis	1	1	0.25	1	0.25	1
Alzheimers Disease	0.25	1	1	1	0.25	1
Aryl Hydrocarbon Receptor	0.25	1	1	1	0.25	1

ISG15 antiviral mechanism	0.25	1	1	1	0.25	1
Antiviral mechanism by IFN-stimulated genes	0.25	1	1	1	0.25	1
TCA Cycle Nutrient Utilization and Invasiveness of Ovarian Cancer	1	1	0.25	1	0.25	1
Constitutive Androstane Receptor Pathway	0.25	1	1	1	0.25	1
Copper homeostasis	0.25	1	1	1	0.25	1
NOTCH1 Intracellular Domain Regulates Transcription	0.25	1	1	1	0.25	1
Interleukin-1 family signaling	0.25	1	1	1	0.25	1
Prion disease pathway	0.25	1	1	1	0.25	1
Interleukin-4 and Interleukin-13 signaling	0.25	1	1	1	0.25	1
Oxidative Stress	0.25	1	1	1	0.25	1
Nicotinate metabolism	1	1	0.25	1	0.25	1
Disorders of the Krebs cycle	1	1	0.25	1	0.25	1
miR-targeted genes in lymphocytes - TarBase	0.252	1	1	1	0.252	1
Disulfiram Action Pathway	0.125	1	0.563	1	0.257	1
HSP90 chaperone cycle for steroid hormone receptors (SHR)	0.0742	1	1	1	0.267	1
Vitamin B12 Metabolism	0.297	1	0.25	1	0.267	1
Folate Metabolism	0.301	1	0.25	1	0.27	1
beta-Alanine metabolism - Homo sapiens (human)	0.125	1	0.625	1	0.277	1
Nucleobase biosynthesis	0.125	1	0.625	1	0.277	1
TCA cycle	0.625	1	0.125	1	0.277	1
Pantothenate and CoA biosynthesis - Homo sapiens (human)	0.25	1	0.312	1	0.277	1
Metabolism of fat-soluble vitamins	0.156	1	0.5	1	0.277	1

Retinoid metabolism and transport	0.156	1	0.5	1	0.277	1
Gamma-glutamyl-transpeptidase deficiency	0.25	1	0.313	1	0.277	1
5-oxoprolinase deficiency	0.25	1	0.313	1	0.277	1
Gamma-Glutamyltransferase Deficiency	0.25	1	0.313	1	0.277	1
Glutathione Metabolism	0.25	1	0.313	1	0.277	1
Glutathione Synthetase Deficiency	0.25	1	0.313	1	0.277	1
5-Oxoprolinuria	0.25	1	0.313	1	0.277	1
Hedgehog	0.278	1	1	1	0.278	1
erk and pi-3 kinase are necessary for collagen binding in corneal epithelia	0.297	1	1	1	0.297	1
Systemic lupus erythematosus - Homo sapiens (human)	0.297	1	1	1	0.297	1
Bacterial invasion of epithelial cells - Homo sapiens (human)	0.297	1	1	1	0.297	1
Platelet degranulation	0.0865	1	1	1	0.298	1
Response to elevated platelet cytosolic Ca2+	0.0865	1	1	1	0.298	1
Androgen receptor signaling pathway	0.301	1	1	1	0.301	1
Proteoglycans in cancer - Homo sapiens (human)	0.301	1	1	1	0.301	1
Statin Pathway	0.312	1	1	1	0.312	1

G alpha (q) signalling events	1	1	0.312	1	0.312	1
Transport of vitamins_ nucleosides_ and related molecules	1	1	0.312	1	0.312	1
Direct p53 effectors	0.312	1	1	1	0.312	1
Integrins in angiogenesis	0.312	1	1	1	0.312	1
Apoptotic execution phase	0.312	1	1	1	0.312	1
Cholesterol metabolism - Homo sapiens (human)	0.312	1	1	1	0.312	1
PPAR signaling pathway - Homo sapiens (human)	0.312	1	1	1	0.312	1
Sulfur amino acid metabolism	1	1	0.312	1	0.312	1
Chylomicron remodeling	0.312	1	1	1	0.312	1
Common Pathway of Fibrin Clot Formation	0.312	1	1	1	0.312	1
O-linked glycosylation	0.312	1	1	1	0.312	1
PPAR signaling pathway	0.312	1	1	1	0.312	1
Validated nuclear estrogen receptor alpha network	0.313	1	1	1	0.313	1
mechanism of gene regulation by peroxisome proliferators via ppara	0.313	1	1	1	0.313	1
AGE-RAGE pathway	0.313	1	1	1	0.313	1
Ascorbate and aldarate metabolism - Homo sapiens (human)	0.5	1	0.188	1	0.316	1

Ferroptosis - Homo sapiens (human)	0.188	1	0.5	1	0.316	1
Phospholipid metabolism	0.5	1	0.188	1	0.316	1
Signaling by WNT	0.0938	1	1	1	0.316	1
Pentose phosphate pathway (hexose monophosphate shunt)	0.0938	1	1	1	0.316	1
Porphyrin and chlorophyll metabolism - Homo sapiens (human)	0.125	1	0.75	1	0.316	1
Signaling events mediated by focal adhesion kinase	0.0938	1	1	1	0.316	1
Histidine_ lysine_ phenylalanine_ tyrosine_ proline and tryptophan catabolism	0.5	1	0.206	1	0.337	1
Transport of bile salts and organic acids_ metal ions and amine compounds	1	1	0.107	1	0.346	1
Purine Nucleoside Phosphorylase Deficiency	0.129	1	0.844	1	0.35	1
Xanthine Dehydrogenase Deficiency (Xanthinuria)	0.129	1	0.844	1	0.35	1
Adenylosuccinate Lyase Deficiency	0.129	1	0.844	1	0.35	1
Adenine phosphoribosyltransferase deficiency (APRT)	0.129	1	0.844	1	0.35	1
Mitochondrial DNA depletion syndrome	0.129	1	0.844	1	0.35	1
Myoadenylate deaminase deficiency	0.129	1	0.844	1	0.35	1
Purine Metabolism	0.129	1	0.844	1	0.35	1
Molybdenum Cofactor Deficiency	0.129	1	0.844	1	0.35	1
Adenosine Deaminase Deficiency	0.129	1	0.844	1	0.35	1
Gout or Kelley-Seegmiller Syndrome	0.129	1	0.844	1	0.35	1
Lesch-Nyhan Syndrome (LNS)	0.129	1	0.844	1	0.35	1
Xanthinuria type I	0.129	1	0.844	1	0.35	1
Xanthinuria type II	0.129	1	0.844	1	0.35	1
AICA-Ribosiduria	0.129	1	0.844	1	0.35	1

Galactose metabolism - Homo sapiens (human)	0.5	1	0.219	1	0.351	1
Pyrimidine metabolism	0.5	1	0.219	1	0.351	1
Valine_ leucine and isoleucine degradation	0.25	1	0.438	1	0.351	1
Binding and Uptake of Ligands by Scavenger Receptors	0.11	1	1	1	0.352	1
TNF	0.359	1	1	1	0.359	1
proteasome complex	0.359	1	1	1	0.359	1
Glycerophospholipid metabolism	0.25	1	0.461	1	0.364	1
Regulation of TLR by endogenous ligand	0.375	1	1	1	0.375	1
Assembly of collagen fibrils and other multimeric structures	0.375	1	1	1	0.375	1
Arf6 trafficking events	0.375	1	1	1	0.375	1
Plasma lipoprotein clearance	0.375	1	1	1	0.375	1
role of pi3k subunit p85 in regulation of actin organization and cell migration	0.375	1	1	1	0.375	1
Pertussis - Homo sapiens (human)	0.375	1	1	1	0.375	1
Neurotrophin signaling pathway - Homo sapiens (human)	0.375	1	1	1	0.375	1
how does salmonella hijack a cell	0.375	1	1	1	0.375	1
PCP/CE pathway	0.375	1	1	1	0.375	1

KitReceptor	0.375	1	1	1	0.375	1
Pentose Phosphate Pathway (Erythrocyte)	0.375	1	1	1	0.375	1
Statin Pathway_ Pharmacodynamics	0.375	1	1	1	0.375	1
Sialuria or French Type Sialuria	1	1	0.375	1	0.375	1
Sialuria or French Type Sialuria	1	1	0.375	1	0.375	1
G(M2)-Gangliosidosis: Variant B_ Tay-sachs disease	1	1	0.375	1	0.375	1
Tay-Sachs Disease	1	1	0.375	1	0.375	1
Amino Sugar Metabolism	1	1	0.375	1	0.375	1
Salla Disease/Infantile Sialic Acid Storage Disease	1	1	0.375	1	0.375	1
PPAR Alpha Pathway	0.375	1	1	1	0.375	1
Factors involved in megakaryocyte development and platelet production	0.375	1	1	1	0.375	1
Tryptophan catabolism	1	1	0.375	1	0.375	1
Urea cycle and metabolism of amino groups	0.125	1	1	1	0.385	1
TCA Cycle (aka Krebs or citric acid cycle)	1	1	0.125	1	0.385	1
Toll Like Receptor 5 (TLR5) Cascade	0.125	1	1	1	0.385	1
Serine biosynthesis	1	1	0.125	1	0.385	1

Interleukin-17 signaling	0.125	1	1	1	0.385	1
lactate fermentation (reoxidation of cytosolic NADH)	0.25	1	0.5	1	0.385	1
TRIF(TICAM1)-mediated TLR4 signaling	0.125	1	1	1	0.385	1
Toll Like Receptor 4 (TLR4) Cascade	0.125	1	1	1	0.385	1
Fatty acyl-CoA biosynthesis	0.5	1	0.25	1	0.385	1
Toll Like Receptor 9 (TLR9) Cascade	0.125	1	1	1	0.385	1
Late Phase of HIV Life Cycle	0.125	1	1	1	0.385	1
MyD88 cascade initiated on plasma membrane	0.125	1	1	1	0.385	1
Toll Like Receptor 10 (TLR10) Cascade	0.125	1	1	1	0.385	1
Toll Like Receptor 3 (TLR3) Cascade	0.125	1	1	1	0.385	1
Toll Like Receptor 7/8 (TLR7/8) Cascade	0.125	1	1	1	0.385	1
Glycogenosis_ Type III. Cori disease_ Debrancher glycogenosis	1	1	0.125	1	0.385	1
Glycogenosis_ Type VI. Hers disease	1	1	0.125	1	0.385	1
Fatty acid biosynthesis - Homo sapiens (human)	1	1	0.125	1	0.385	1
Phase I - Functionalization of compounds	0.125	1	1	1	0.385	1
TCA cycle	1	1	0.125	1	0.385	1

hypoxia-inducible factor in the cardivascular system	0.25	1	0.5	1	0.385	1
RHO GTPases Activate Formins	0.125	1	1	1	0.385	1
Nucleotide salvage	0.25	1	0.5	1	0.385	1
Sucrase-isomaltase deficiency	1	1	0.125	1	0.385	1
Signaling by Hedgehog	0.125	1	1	1	0.385	1
Nicotinate metabolism	1	1	0.125	1	0.385	1
MAP kinase activation	0.125	1	1	1	0.385	1
TRAF6 mediated induction of NFkB and MAP kinases upon TLR7/8 or 9 activation	0.125	1	1	1	0.385	1
Sema4D in semaphorin signaling	0.125	1	1	1	0.385	1
ABC-family proteins mediated transport	0.125	1	1	1	0.385	1
MyD88 dependent cascade initiated on endosome	0.125	1	1	1	0.385	1
leucine degradation	1	1	0.125	1	0.385	1
Negative regulation of MAPK pathway	0.125	1	1	1	0.385	1
Glycerolipid metabolism - Homo sapiens (human)	0.25	1	0.5	1	0.385	1
Glycogen synthetase deficiency	1	1	0.125	1	0.385	1
Mucopolysaccharidosis VI. Sly syndrome	1	1	0.125	1	0.385	1

Glycogenosis_ Type IV. Amylopectinosis_ Anderson disease	1	1	0.125	1	0.385	1
Pyruvate Dehydrogenase Complex Deficiency	0.5	1	0.25	1	0.385	1
Primary hyperoxaluria II_ PH2	0.5	1	0.25	1	0.385	1
Pyruvate kinase deficiency	0.5	1	0.25	1	0.385	1
Irinotecan Action Pathway	0.125	1	1	1	0.385	1
Starch and Sucrose Metabolism	1	1	0.125	1	0.385	1
Leigh Syndrome	0.5	1	0.25	1	0.385	1
Morphine Action Pathway	0.125	1	1	1	0.385	1
MyD88-independent TLR4 cascade	0.125	1	1	1	0.385	1
Etoposide Action Pathway	0.125	1	1	1	0.385	1
Lamivudine Metabolism Pathway	0.25	1	0.5	1	0.385	1
Pyruvate Metabolism	0.5	1	0.25	1	0.385	1
Pyruvate Decarboxylase E1 Component Deficiency (PDHE1 Deficiency)	0.5	1	0.25	1	0.385	1
Irinotecan Metabolism Pathway	0.125	1	1	1	0.385	1
Etoposide Metabolism Pathway	0.125	1	1	1	0.385	1
HIV Life Cycle	0.125	1	1	1	0.385	1

Fatty Acid Biosynthesis	1	1	0.125	1	0.385	1
Propanoate metabolism	0.5	1	0.25	1	0.385	1
De novo fatty acid biosynthesis	1	1	0.125	1	0.385	1
Toll Like Receptor TLR1:TLR2 Cascade	0.125	1	1	1	0.385	1
Toll Like Receptor TLR6:TLR2 Cascade	0.125	1	1	1	0.385	1
Toll Like Receptor 2 (TLR2) Cascade	0.125	1	1	1	0.385	1
Cellular response to heat stress	0.125	1	1	1	0.385	1
Pyrimidine metabolism	0.25	1	0.5	1	0.385	1
MyD88:Mal cascade initiated on plasma membrane	0.125	1	1	1	0.385	1
Hereditary leiomyomatosis and renal cell carcinoma pathway	1	1	0.125	1	0.385	1
Asparagine N-linked glycosylation	0.358	1	0.375	1	0.403	1
MAPK family signaling cascades	0.273	1	0.5	1	0.409	1
Ebola Virus Pathway on Host	0.413	1	1	1	0.413	1
Hawkinsinuria	0.25	1	0.563	1	0.416	1
Tyrosinemia_ transient_ of the newborn	0.25	1	0.563	1	0.416	1
Dopamine beta-hydroxylase deficiency	0.25	1	0.563	1	0.416	1

Tyrosine Metabolism	0.25	1	0.563	1	0.416	1
Alkaptonuria	0.25	1	0.563	1	0.416	1
Monoamine oxidase-a deficiency (MAO-A)	0.25	1	0.563	1	0.416	1
Tyrosinemia Type I	0.25	1	0.563	1	0.416	1
Hyperornithinemia with gyrate atrophy (HOGA)	0.25	1	0.57	1	0.42	1
Creatine deficiency_ guanidinoacetate methyltransferase deficiency	0.25	1	0.57	1	0.42	1
L-arginine:glycine amidinotransferase deficiency	0.25	1	0.57	1	0.42	1
Hyperornithinemia-hyperammonemia-homocitrullinuria [HHH-syndrome]	0.25	1	0.57	1	0.42	1
Guanidinoacetate Methyltransferase Deficiency (GAMT Deficiency)	0.25	1	0.57	1	0.42	1
Prolinemia Type II	0.25	1	0.57	1	0.42	1
Prolidase Deficiency (PD)	0.25	1	0.57	1	0.42	1
Arginine and Proline Metabolism	0.25	1	0.57	1	0.42	1
Hyperprolinemia Type I	0.25	1	0.57	1	0.42	1
Hyperprolinemia Type II	0.25	1	0.57	1	0.42	1
Ornithine Aminotransferase Deficiency (OAT Deficiency)	0.25	1	0.57	1	0.42	1
Arginine: Glycine Amidinotransferase Deficiency (AGAT Deficiency)	0.25	1	0.57	1	0.42	1
Complement and coagulation cascades - Homo sapiens (human)	0.431	1	1	1	0.431	1
Golgi-to-ER retrograde transport	0.148	1	1	1	0.432	1
Intra-Golgi and retrograde Golgi-to-ER traffic	0.148	1	1	1	0.432	1
Urokinase-type plasminogen activator (uPA) and uPAR-mediated signaling	0.438	1	1	1	0.438	1
Cell junction organization	0.438	1	1	1	0.438	1

Transport of inorganic cations-anions and amino acids-oligopeptides	1	1	0.438	1	0.438	1
Complement Activation	0.438	1	1	1	0.438	1
Prostaglandin Synthesis and Regulation	0.438	1	1	1	0.438	1
Prion diseases - Homo sapiens (human)	0.438	1	1	1	0.438	1
Herpes simplex infection - Homo sapiens (human)	0.438	1	1	1	0.438	1
Collagen biosynthesis and modifying enzymes	0.156	1	1	1	0.446	1
Plasma lipoprotein remodeling	0.156	1	1	1	0.446	1
mTOR signaling pathway	0.156	1	1	1	0.446	1
Amino sugar and nucleotide sugar metabolism - Homo sapiens (human)	0.25	1	0.625	1	0.446	1
Transport of vitamins_ nucleosides_ and related molecules	1	1	0.156	1	0.446	1
Carboxyterminal post-translational modifications of tubulin	0.625	1	0.25	1	0.446	1
Purine ribonucleoside monophosphate biosynthesis	0.25	1	0.625	1	0.446	1
Lysine metabolism	0.25	1	0.625	1	0.446	1
L1CAM interactions	0.313	1	0.5	1	0.446	1
Ammonia Recycling	0.5	1	0.313	1	0.446	1
Hypoacetylaspartia	0.5	1	0.313	1	0.446	1

Aspartate Metabolism	0.5	1	0.313	1	0.446	1
Canavan Disease	0.5	1	0.313	1	0.446	1
Ribosomal scanning and start codon recognition	0.164	1	1	1	0.461	1
Glyoxylate and dicarboxylate metabolism - Homo sapiens (human)	1	1	0.164	1	0.461	1
Formation of Fibrin Clot (Clotting Cascade)	0.461	1	1	1	0.461	1
Protein folding	0.168	1	1	1	0.467	1
Cell surface interactions at the vascular wall	0.469	1	1	1	0.469	1
mRNA Processing	0.469	1	1	1	0.469	1
Flavan-3-ols	1	1	0.174	1	0.478	1
Phagosome - Homo sapiens (human)	0.492	1	1	1	0.492	1
Vitamin D Receptor Pathway	0.492	1	1	1	0.492	1
JAK STAT pathway and regulation	0.492	1	1	1	0.492	1
Amine compound SLC transporters	1	1	0.496	1	0.496	1
Focal Adhesion-PI3K-Akt-mTOR-signaling pathway	0.496	1	1	1	0.496	1
fatty acid α-oxidation III	1	1	0.5	1	0.5	1
LncRNA involvement in canonical Wnt signaling and colorectal cancer	0.5	1	1	1	0.5	1
Breast cancer pathway	0.5	1	1	1	0.5	1
Pancreatic adenocarcinoma pathway	0.5	1	1	1	0.5	1

MTHFR deficiency	0.5	1	1	1	0.5	1
Transcriptional regulation by RUNX2	0.5	1	1	1	0.5	1
Passive transport by Aquaporins	1	1	0.5	1	0.5	1
creatine biosynthesis	1	1	0.5	1	0.5	1
Insulin Signaling	0.5	1	1	1	0.5	1
Interferon type I signaling pathways	0.5	1	1	1	0.5	1
Notch Signaling Pathway	0.5	1	1	1	0.5	1
Sulfation Biotransformation Reaction	0.5	1	1	1	0.5	1
Estrogen metabolism	0.5	1	1	1	0.5	1
Signaling by NOTCH1 in Cancer	0.5	1	1	1	0.5	1
FoxO signaling pathway - Homo sapiens (human)	1	1	0.5	1	0.5	1
uracil degradation	1	1	0.5	1	0.5	1
Biosynthesis of unsaturated fatty acids - Homo sapiens (human)	1	1	0.5	1	0.5	1
UTP and CTP dephosphorylation II	1	1	0.5	1	0.5	1
stearate biosynthesis	1	1	0.5	1	0.5	1
Intestinal absorption	1	1	0.5	1	0.5	1
VLDL assembly	0.5	1	1	1	0.5	1
VEGFA-VEGFR2 Pathway	0.5	1	1	1	0.5	1
Assembly Of The HIV Virion	0.5	1	1	1	0.5	1
Budding and maturation of HIV virion	0.5	1	1	1	0.5	1
The NLRP3 inflammasome	0.5	1	1	1	0.5	1
IL6	0.5	1	1	1	0.5	1
Neurotransmitter uptake and metabolism In glial cells	1	1	0.5	1	0.5	1
TICAM1_ RIP1-mediated IKK complex recruitment	0.5	1	1	1	0.5	1
pyrimidine deoxyribonucleotide phosphorylation	0.5	1	1	1	0.5	1
Senescence-Associated Secretory Phenotype (SASP)	0.5	1	1	1	0.5	1
Inflammasomes	0.5	1	1	1	0.5	1
Kinesins	0.5	1	1	1	0.5	1
guanosine deoxyribonucleotides de novo biosynthesis	0.5	1	1	1	0.5	1
Activation of NF-kappaB in B cells	0.5	1	1	1	0.5	1

adenosine deoxyribonucleotides de novo biosynthesis	0.5	1	1	1	0.5	1
Downstream signaling events of B Cell Receptor (BCR)	0.5	1	1	1	0.5	1
Vitamin B6 metabolism - Homo sapiens (human)	0.5	1	1	1	0.5	1
Import of palmitoyl-CoA into the mitochondrial matrix	1	1	0.5	1	0.5	1
Organic anion transport	1	1	0.5	1	0.5	1
Canonical NF-kappaB pathway	0.5	1	1	1	0.5	1
PAR1-mediated thrombin signaling events	0.5	1	1	1	0.5	1
CXCR4-mediated signaling events	0.5	1	1	1	0.5	1
Internalization of ErbB1	0.5	1	1	1	0.5	1
Class I PI3K signaling events	0.5	1	1	1	0.5	1
Validated transcriptional targets of deltaNp63 isoforms	0.5	1	1	1	0.5	1
FAS (CD95) signaling pathway	0.5	1	1	1	0.5	1
Alpha-synuclein signaling	0.5	1	1	1	0.5	1
IL1-mediated signaling events	0.5	1	1	1	0.5	1
Notch signaling pathway	0.5	1	1	1	0.5	1
E2F transcription factor network	0.5	1	1	1	0.5	1
TGF-beta receptor signaling	0.5	1	1	1	0.5	1
ROS_ RNS production in phagocytes	0.5	1	1	1	0.5	1
Cleavage of Growing Transcript in the Termination Region	0.5	1	1	1	0.5	1
RNA Polymerase II Transcription Termination	0.5	1	1	1	0.5	1
Ethanol oxidation	0.5	1	1	1	0.5	1
Notch	0.5	1	1	1	0.5	1
Choline catabolism	1	1	0.5	1	0.5	1
Retinol metabolism - Homo sapiens (human)	0.5	1	1	1	0.5	1
L-glutamine tRNA biosynthesis	1	1	0.5	1	0.5	1
Fatty Acids bound to GPR40 (FFAR1) regulate insulin secretion	1	1	0.5	1	0.5	1
Neomycin_ kanamycin and gentamicin biosynthesis - Homo sapiens (human)	1	1	0.5	1	0.5	1
Melanin biosynthesis	1	1	0.5	1	0.5	1
SCF(Skp2)-mediated degradation of p27/p21	0.5	1	1	1	0.5	1

Formation of xylulose-5-phosphate	1	1	0.5	1	0.5	1
Vitamins B6 activation to pyridoxal phosphate	0.5	1	1	1	0.5	1
regulators of bone mineralization	0.5	1	1	1	0.5	1
prion pathway	0.5	1	1	1	0.5	1
Primary immunodeficiency - Homo sapiens (human)	0.5	1	1	1	0.5	1
TGF-beta signaling pathway - Homo sapiens (human)	0.5	1	1	1	0.5	1
p38 mapk signaling pathway	0.5	1	1	1	0.5	1
akt signaling pathway	0.5	1	1	1	0.5	1
Th17 cell differentiation - Homo sapiens (human)	0.5	1	1	1	0.5	1
cycling of ran in nucleocytoplasmic transport	0.5	1	1	1	0.5	1
VEGF signaling pathway - Homo sapiens (human)	0.5	1	1	1	0.5	1
role of mal in rho-mediated activation of srf	0.5	1	1	1	0.5	1
stress induction of hsp regulation	0.5	1	1	1	0.5	1
Gastric acid secretion - Homo sapiens (human)	0.5	1	1	1	0.5	1
Rheumatoid arthritis - Homo sapiens (human)	0.5	1	1	1	0.5	1
Thyroid cancer - Homo sapiens (human)	0.5	1	1	1	0.5	1
Hepatitis B - Homo sapiens (human)	0.5	1	1	1	0.5	1
Prolactin signaling pathway - Homo sapiens (human)	1	1	0.5	1	0.5	1
Orc1 removal from chromatin	0.5	1	1	1	0.5	1
Switching of origins to a post-replicative state	0.5	1	1	1	0.5	1
Proton-coupled neutral amino acid transporters	1	1	0.5	1	0.5	1
Pyrimidine salvage	1	1	0.5	1	0.5	1
Cysteine formation from homocysteine	1	1	0.5	1	0.5	1
Synthesis of DNA	0.5	1	1	1	0.5	1
Separation of Sister Chromatids	0.5	1	1	1	0.5	1
GLI3 is processed to GLI3R by the proteasome	0.5	1	1	1	0.5	1
Degradation of GLI2 by the proteasome	0.5	1	1	1	0.5	1
tetrahydrofolate salvage from 5_10-methenyltetrahydrofolate	0.5	1	1	1	0.5	1
Degradation of GLI1 by the proteasome	0.5	1	1	1	0.5	1
CMP phosphorylation	0.5	1	1	1	0.5	1

superpathway of pyrimidine deoxyribonucleoside salvage	0.5	1	1	1	0.5	1
glutamine biosynthesis	1	1	0.5	1	0.5	1
Type II diabetes mellitus - Homo sapiens (human)	1	1	0.5	1	0.5	1
Insulin secretion - Homo sapiens (human)	1	1	0.5	1	0.5	1
NF-kappa B signaling pathway - Homo sapiens (human)	0.5	1	1	1	0.5	1
Sialic acid metabolism	1	1	0.5	1	0.5	1
Triglyceride biosynthesis	1	1	0.5	1	0.5	1
MAP3K8 (TPL2)-dependent MAPK1/3 activation	0.5	1	1	1	0.5	1
purine deoxyribonucleosides salvage	0.5	1	1	1	0.5	1
The role of GTSE1 in G2/M progression after G2 checkpoint	0.5	1	1	1	0.5	1
Vpu mediated degradation of CD4	0.5	1	1	1	0.5	1
FBXL7 down-regulates AURKA during mitotic entry and in early mitosis	0.5	1	1	1	0.5	1
pyrimidine deoxyribonucleosides degradation	1	1	0.5	1	0.5	1
Cell death signalling via NRAGE_ NRIF and NADE	0.5	1	1	1	0.5	1
The role of Nef in HIV-1 replication and disease pathogenesis	0.5	1	1	1	0.5	1
pyrimidine ribonucleosides degradation	1	1	0.5	1	0.5	1
Josephin domain DUBs	0.5	1	1	1	0.5	1
lysine degradation II (pipecolate pathway)	1	1	0.5	1	0.5	1
TCR signaling in naïve CD8+ T cells	0.5	1	1	1	0.5	1
Free fatty acids regulate insulin secretion	1	1	0.5	1	0.5	1
SCF-beta-TrCP mediated degradation of Emi1	0.5	1	1	1	0.5	1
hydrogen sulfide biosynthesis (trans-sulfuration)	1	1	0.5	1	0.5	1
Multifunctional anion exchangers	1	1	0.5	1	0.5	1
Intestinal hexose absorption	1	1	0.5	1	0.5	1
Astrocytic Glutamate-Glutamine Uptake And Metabolism	1	1	0.5	1	0.5	1
cysteine biosynthesis/homocysteine degradation (trans-sulfuration)	1	1	0.5	1	0.5	1
Regulation of TP53 Activity through Methylation	0.5	1	1	1	0.5	1
formaldehyde oxidation	0.5	1	1	1	0.5	1
Signaling by VEGF	0.5	1	1	1	0.5	1
Signaling events mediated by PTP1B	0.5	1	1	1	0.5	1

Signaling events mediated by HDAC Class I	0.5	1	1	1	0.5	1
Glycerophospholipid metabolism - Homo sapiens (human)	1	1	0.5	1	0.5	1
Reversible hydration of carbon dioxide	0.5	1	1	1	0.5	1
Sialic acid metabolism	1	1	0.5	1	0.5	1
Translesion Synthesis by POLH	0.5	1	1	1	0.5	1
Nuclear import of Rev protein	0.5	1	1	1	0.5	1
cardiac protection against ros	0.5	1	1	1	0.5	1
Proton-coupled monocarboxylate transport	1	1	0.5	1	0.5	1
Porphyrin metabolism	0.5	1	1	1	0.5	1
superoxide radicals degradation	0.5	1	1	1	0.5	1
Regulation of APC/C activators between G1/S and early anaphase	0.5	1	1	1	0.5	1
glycine betaine degradation	1	1	0.5	1	0.5	1
Estrogen Metabolism Pathway	0.5	1	1	1	0.5	1
Tenofovir/Adefovir Pathway_ Pharmacodynamics	0.5	1	1	1	0.5	1
Tenofovir/Adefovir Pathway_ Pharmacokinetics	0.5	1	1	1	0.5	1
Doxorubicin Pathway (Cancer Cell)_ Pharmacodynamics	0.5	1	1	1	0.5	1
Busulfan Pathway_ Pharmacodynamics	0.5	1	1	1	0.5	1
Zidovudine Pathway_ Pharmacokinetics/Pharmacodynamics	0.5	1	1	1	0.5	1
Estrogen-dependent gene expression	0.5	1	1	1	0.5	1
Oxidative Stress Pathway (Erythrocyte)	0.5	1	1	1	0.5	1
Pathway_PA165980337	0.5	1	1	1	0.5	1
Oxidative Stress Pathway (Erythrocyte)	0.5	1	1	1	0.5	1
Methylene Blue Pathway_ Pharmacodynamics	0.5	1	1	1	0.5	1
Tacrolimus/Cyclosporine Pathway_ Pharmacodynamics	0.5	1	1	1	0.5	1
Advanced glycosylation endproduct receptor signaling	0.5	1	1	1	0.5	1
Polythiazide Action Pathway	1	1	0.5	1	0.5	1
Methyclothiazide Action Pathway	1	1	0.5	1	0.5	1
Bumetanide Action Pathway	1	1	0.5	1	0.5	1
Transcriptional activation of mitochondrial biogenesis	0.5	1	1	1	0.5	1

Translesion synthesis by Y family DNA polymerases bypasses lesions on DNA template	0.5	1	1	1	0.5	1
Digestion of dietary lipid	1	1	0.5	1	0.5	1
Activation of gene expression by SREBF (SREBP)	0.5	1	1	1	0.5	1
pentose phosphate pathway (non-oxidative branch)	0.5	1	1	1	0.5	1
Mitochondrial biogenesis	0.5	1	1	1	0.5	1
Spironolactone Action Pathway	1	1	0.5	1	0.5	1
Eplerenone Action Pathway	1	1	0.5	1	0.5	1
Triamterene Action Pathway	1	1	0.5	1	0.5	1
Amiloride Action Pathway	1	1	0.5	1	0.5	1
Leucine Stimulation on Insulin Signaling	1	1	0.5	1	0.5	1
Signaling by Hippo	0.5	1	1	1	0.5	1
Hyperlysinemia I_ Familial	1	1	0.5	1	0.5	1
Signaling by ERBB4	0.5	1	1	1	0.5	1
Glycosphingolipid metabolism	0.5	1	1	1	0.5	1
UTP and CTP dephosphorylation I	1	1	0.5	1	0.5	1
APC/C-mediated degradation of cell cycle proteins	0.5	1	1	1	0.5	1
Regulation of mitotic cell cycle	0.5	1	1	1	0.5	1
Trehalose Degradation	1	1	0.5	1	0.5	1
Synthesis of PG	1	1	0.5	1	0.5	1
Passive transport by Aquaporins	1	1	0.5	1	0.5	1
lysine degradation I (saccharopine pathway)	1	1	0.5	1	0.5	1
2-aminoadipic 2-oxoadipic aciduria	1	1	0.5	1	0.5	1
Ethacrynic Acid Action Pathway	1	1	0.5	1	0.5	1
Quinethazone Action Pathway	1	1	0.5	1	0.5	1
Bendroflumethiazide Action Pathway	1	1	0.5	1	0.5	1
Constitutive Signaling by NOTCH1 PEST Domain Mutants	0.5	1	1	1	0.5	1
Adefovir Dipivoxil Metabolism Pathway	0.5	1	1	1	0.5	1
Chlorthalidone Action Pathway	1	1	0.5	1	0.5	1
Trichlormethiazide Action Pathway	1	1	0.5	1	0.5	1

Constitutive Signaling by NOTCH1 HD+PEST Domain Mutants	0.5	1	1	1	0.5	1
Signaling by NOTCH1 HD+PEST Domain Mutants in Cancer	0.5	1	1	1	0.5	1
Iminoglycinuria	1	1	0.5	1	0.5	1
Lysinuric Protein Intolerance	1	1	0.5	1	0.5	1
Insulin Signalling	1	1	0.5	1	0.5	1
Lysine Degradation	1	1	0.5	1	0.5	1
Blue diaper syndrome	1	1	0.5	1	0.5	1
Lysinuric protein intolerance (LPI)	1	1	0.5	1	0.5	1
Metoprolol Action Pathway	1	1	0.5	1	0.5	1
Pyridoxine dependency with seizures	1	1	0.5	1	0.5	1
IKK complex recruitment mediated by RIP1	0.5	1	1	1	0.5	1
Saccharopinuria/Hyperlysinemia II	1	1	0.5	1	0.5	1
Tenofovir Metabolism Pathway	0.5	1	1	1	0.5	1
Cystinuria	1	1	0.5	1	0.5	1
Indapamide Action Pathway	1	1	0.5	1	0.5	1
Furosemide Action Pathway	1	1	0.5	1	0.5	1
Torsemide Action Pathway	1	1	0.5	1	0.5	1
Scavenging by Class B Receptors	0.5	1	1	1	0.5	1
Hartnup Disorder	1	1	0.5	1	0.5	1
Glucose Transporter Defect (SGLT2)	1	1	0.5	1	0.5	1
Glutaric Aciduria Type I	1	1	0.5	1	0.5	1
IL1	0.5	1	1	1	0.5	1
Kidney Function	1	1	0.5	1	0.5	1
Type I hemidesmosome assembly	0.5	1	1	1	0.5	1
Kennedy pathway from Sphingolipids	1	1	0.5	1	0.5	1
Hyperlysinemia II or Saccharopinuria	1	1	0.5	1	0.5	1
Glucose Transporter Defect (SGLT2)	1	1	0.5	1	0.5	1
Homocysteine Degradation	1	1	0.5	1	0.5	1
Gamma-cystathionase deficiency (CTH)	1	1	0.5	1	0.5	1
Homocystinuria_ cystathionine beta-synthase deficiency	1	1	0.5	1	0.5	1

Metolazone Action Pathway	1	1	0.5	1	0.5	1
Hydrochlorothiazide Action Pathway	1	1	0.5	1	0.5	1
Cyclothiazide Action Pathway	1	1	0.5	1	0.5	1
Hydroflumethiazide Action Pathway	1	1	0.5	1	0.5	1
Chlorothiazide Action Pathway	1	1	0.5	1	0.5	1
tryptophan degradation X (mammalian_ via tryptamine)	0.5	1	1	1	0.5	1
Biopterin metabolism	1	1	0.5	1	0.5	1
Vitamin B3 (nicotinate and nicotinamide) metabolism	1	1	0.5	1	0.5	1
Platelet sensitization by LDL	0.5	1	1	1	0.5	1
Platelet homeostasis	0.5	1	1	1	0.5	1
Target Of Rapamycin (TOR) Signaling	0.5	1	1	1	0.5	1
Human Thyroid Stimulating Hormone (TSH) signaling pathway	0.5	1	1	1	0.5	1
L1CAM interactions	1	1	0.5	1	0.5	1
phosphatidylethanolamine biosynthesis II	1	1	0.5	1	0.5	1
superpathway of choline degradation to L-serine	1	1	0.5	1	0.5	1
carnosine biosynthesis	1	1	0.5	1	0.5	1
RAGE	0.5	1	1	1	0.5	1
B Cell Receptor Signaling Pathway	0.5	1	1	1	0.5	1
Corticotropin-releasing hormone signaling pathway	0.5	1	1	1	0.5	1
Adipogenesis	0.5	1	1	1	0.5	1
Histone Modifications	0.5	1	1	1	0.5	1
D-galactose degradation V (Leloir pathway)	0.5	1	1	1	0.5	1
Integrated Lung Cancer Pathway	0.5	1	1	1	0.5	1
Nef-mediates down modulation of cell surface receptors by recruiting them to clathrin adapters	0.5	1	1	1	0.5	1
Iron uptake and transport	1	1	0.5	1	0.5	1
Visual phototransduction	1	1	0.5	1	0.5	1
TCF dependent signaling in response to WNT	0.5	1	1	1	0.5	1
IL-3 Signaling Pathway	0.5	1	1	1	0.5	1
proline biosynthesis	1	1	0.5	1	0.5	1

mRNA 3_-end processing	0.5	1	1	1	0.5	1
TGF-beta receptor signaling in EMT (epithelial to mesenchymal transition)	0.5	1	1	1	0.5	1
Signaling by NOTCH1 PEST Domain Mutants in Cancer	0.5	1	1	1	0.5	1
Photodynamic therapy-induced HIF-1 survival signaling	0.5	1	1	1	0.5	1
Lung fibrosis	0.5	1	1	1	0.5	1
NAD+ metabolism	1	1	0.5	1	0.5	1
Wnt	0.5	1	1	1	0.5	1
Factors and pathways affecting insulin-like growth factor (IGF1)-Akt signaling	0.5	1	1	1	0.5	1
Oxidative Damage	0.5	1	1	1	0.5	1
Regulation of RUNX2 expression and activity	0.5	1	1	1	0.5	1
Wnt Signaling Pathway and Pluripotency	0.5	1	1	1	0.5	1
p38 MAPK Signaling Pathway	0.5	1	1	1	0.5	1
InlA-mediated entry of Listeria monocytogenes into host cells	0.5	1	1	1	0.5	1
Import of palmitoyl-CoA into the mitochondrial matrix	1	1	0.5	1	0.5	1
Nucleotide salvage	1	1	0.5	1	0.5	1
Triglyceride metabolism	1	1	0.5	1	0.5	1
Degradation pathway of sphingolipids_ including diseases	0.5	1	1	1	0.5	1
Listeria monocytogenes entry into host cells	0.5	1	1	1	0.5	1
Pyrimidine metabolism and related diseases	1	1	0.5	1	0.5	1
tRNA modification in the nucleus and cytosol	1	1	0.5	1	0.5	1
Synthesis of wybutosine at G37 of tRNA(Phe)	1	1	0.5	1	0.5	1
4-aminobutyrate degradation	1	1	0.5	1	0.5	1
Amino acid conjugation of benzoic acid	1	1	0.5	1	0.5	1
Metabolism of xenobiotics by cytochrome P450 - Homo sapiens (human)	0.5	1	1	1	0.5	1
Coregulation of Androgen receptor activity	0.5	1	1	1	0.5	1
Syndecan-1-mediated signaling events	0.5	1	1	1	0.5	1
EPHB forward signaling	0.5	1	1	1	0.5	1
Arf1 pathway	0.5	1	1	1	0.5	1

GABA synthesis_ release_ reuptake and degradation	1	1	0.5	1	0.5	1
mtor signaling pathway	0.5	1	1	1	0.5	1
endocytotic role of ndk phosphins and dynamin	0.5	1	1	1	0.5	1
cystic fibrosis transmembrane conductance regulator (cftr) and beta 2 adrenergic receptor (b2ar) pathway	0.5	1	1	1	0.5	1
ion channels and their functional role in vascular endothelium	0.5	1	1	1	0.5	1
vegf hypoxia and angiogenesis	0.5	1	1	1	0.5	1
Vasopressin-regulated water reabsorption - Homo sapiens (human)	0.5	1	1	1	0.5	1
Pancreatic secretion - Homo sapiens (human)	0.5	1	1	1	0.5	1
Hepatocellular carcinoma - Homo sapiens (human)	0.5	1	1	1	0.5	1
Tuberculosis - Homo sapiens (human)	0.5	1	1	1	0.5	1
Hedgehog _off_ state	0.5	1	1	1	0.5	1
Inositol phosphate metabolism	1	1	0.5	1	0.5	1
Organic cation/anion/zwitterion transport	1	1	0.5	1	0.5	1
GPCR Dopamine D1like receptor	0.5	1	1	1	0.5	1
Mitotic Prophase	1	1	0.5	1	0.5	1
Synthesis of IP2_ IP_ and Ins in the cytosol	1	1	0.5	1	0.5	1
Inositol phosphate metabolism	1	1	0.5	1	0.5	1
Degradation of GABA	1	1	0.5	1	0.5	1
Neurexins and neuroligins	0.5	1	1	1	0.5	1
Initial triggering of complement	0.5	1	1	1	0.5	1
Non-integrin membrane-ECM interactions	0.5	1	1	1	0.5	1
Synthesis of wybutosine at G37 of tRNA(Phe)	1	1	0.5	1	0.5	1
retinol biosynthesis	1	1	0.5	1	0.5	1
Doxorubicin Pathway (Cardiomyocyte Cell)_ Pharmacodynamics	0.5	1	1	1	0.5	1
Inositol Metabolism	1	1	0.5	1	0.5	1
N-Glycan biosynthesis	1	1	0.5	1	0.5	1
Nephrin family interactions	0.5	1	1	1	0.5	1
fatty acid activation	1	1	0.5	1	0.5	1
Incretin synthesis_ secretion_ and inactivation	1	1	0.5	1	0.5	1

Inositol phosphate metabolism	1	1	0.5	1	0.5	1
Regulation of Microtubule Cytoskeleton	0.5	1	1	1	0.5	1
JAK-STAT	0.5	1	1	1	0.5	1
Branched-chain amino acid catabolism	1	1	0.5	1	0.5	1
Selenoamino acid metabolism	1	1	0.5	1	0.5	1
superpathway of pyrimidine deoxyribonucleotides de novo bio-synthesis	0.25	1	0.75	1	0.501	1
superpathway of tryptophan utilization	0.188	1	1	1	0.501	1
Tryptophan degradation	0.188	1	1	1	0.501	1
adenosine ribonucleotides de novo biosynthesis	0.25	1	0.75	1	0.501	1
Nitrogen metabolism - Homo sapiens (human)	0.375	1	0.5	1	0.501	1
Glycerophospholipid biosynthesis	1	1	0.188	1	0.501	1
Pentose Phosphate Metabolism	0.188	1	1	1	0.501	1
superpathway of pyrimidine ribonucleotides de novo biosynthesis	0.25	1	0.75	1	0.501	1
Fas Ligand (FasL) pathway and Stress induction of Heat Shock Proteins (HSP) regulation	0.188	1	1	1	0.501	1
Oxidative phosphorylation - Homo sapiens (human)	0.375	1	0.5	1	0.501	1
Fatty acid degradation - Homo sapiens (human)	0.25	1	0.75	1	0.501	1
Nucleobase catabolism	0.875	1	0.219	1	0.508	1
Muscle contraction	0.195	1	1	1	0.514	1

DNA Repair	0.812	1	0.25	1	0.527	1
PDGFR-beta signaling pathway	0.206	1	1	1	0.532	1
RAF/MAP kinase cascade	0.413	1	0.5	1	0.532	1
MAPK1/MAPK3 signaling	0.413	1	0.5	1	0.532	1
Methionine and cysteine metabolism	0.5	1	0.413	1	0.532	1
Trans-sulfuration and one carbon metabolism	0.312	1	0.688	1	0.545	1
CDC42 signaling events	0.547	1	1	1	0.547	1
Diseases of signal transduction	0.217	1	1	1	0.548	1
Metabolism of water-soluble vitamins and cofactors	1	1	0.219	1	0.551	1
Cargo recognition for clathrin-mediated endocytosis	0.219	1	1	1	0.551	1
Phenprocoumon Action Pathway	0.563	1	1	1	0.563	1
Alteplase Action Pathway	0.563	1	1	1	0.563	1
Aminocaproic Acid Action Pathway	0.563	1	1	1	0.563	1
Tranexamic Acid Action Pathway	0.563	1	1	1	0.563	1
Urokinase Action Pathway	0.563	1	1	1	0.563	1
Reteplase Action Pathway	0.563	1	1	1	0.563	1

Streptokinase Action Pathway	0.563	1	1	1	0.563	1
Tenecteplase Action Pathway	0.563	1	1	1	0.563	1
Anistreplase Action Pathway	0.563	1	1	1	0.563	1
Aprotinin Action Pathway	0.563	1	1	1	0.563	1
Phenindione Action Pathway	0.563	1	1	1	0.563	1
Dicoumarol Action Pathway	0.563	1	1	1	0.563	1
Warfarin Action Pathway	0.563	1	1	1	0.563	1
Coagulation	0.563	1	1	1	0.563	1
Bivalirudin Action Pathway	0.563	1	1	1	0.563	1
Argatroban Action Pathway	0.563	1	1	1	0.563	1
Ardeparin Action Pathway	0.563	1	1	1	0.563	1
Heparin Action Pathway	0.563	1	1	1	0.563	1
Fondaparinux Action Pathway	0.563	1	1	1	0.563	1
Enoxaparin Action Pathway	0.563	1	1	1	0.563	1
Dicumarol Action Pathway	0.563	1	1	1	0.563	1
Ximelagatran Action Pathway	0.563	1	1	1	0.563	1

Lepirudin Action Pathway	0.563	1	1	1	0.563	1
Acenocoumarol Action Pathway	0.563	1	1	1	0.563	1
Alanine_ aspartate and glutamate metabolism - Homo sapiens (human)	0.5	1	0.461	1	0.569	1
Valine Leucine Isoleucine degradation	0.5	1	0.469	1	0.574	1
3-Methylglutaconic Aciduria Type IV	0.5	1	0.469	1	0.574	1
Beta-Ketothiolase Deficiency	0.5	1	0.469	1	0.574	1
3-Methylglutaconic Aciduria Type I	0.5	1	0.469	1	0.574	1
Valine_ Leucine and Isoleucine Degradation	0.5	1	0.469	1	0.574	1
2-Methyl-3-Hydroxybutryl CoA Dehydrogenase Deficiency	0.5	1	0.469	1	0.574	1
Isovaleric Aciduria	0.5	1	0.469	1	0.574	1
3-Methylcrotonyl Coa Carboxylase Deficiency Type I	0.5	1	0.469	1	0.574	1
Propionic Acidemia	0.5	1	0.469	1	0.574	1
Maple Syrup Urine Disease	0.5	1	0.469	1	0.574	1
3-Hydroxy-3-Methylglutaryl-CoA Lyase Deficiency	0.5	1	0.469	1	0.574	1
Isobutyryl-coa dehydrogenase deficiency	0.5	1	0.469	1	0.574	1
3-hydroxyisobutyric aciduria	0.5	1	0.469	1	0.574	1

3-hydroxyisobutyric acid dehydrogenase deficiency	0.5	1	0.469	1	0.574	1
Isovaleric acidemia	0.5	1	0.469	1	0.574	1
Methylmalonate Semialdehyde Dehydrogenase Deficiency	0.5	1	0.469	1	0.574	1
Methylmalonic Aciduria	0.5	1	0.469	1	0.574	1
3-Methylglutaconic Aciduria Type III	0.5	1	0.469	1	0.574	1
Glucose Homeostasis	1	1	0.578	1	0.578	1
Glyoxylate metabolism and glycine degradation	1	1	0.578	1	0.578	1
COPI-mediated anterograde transport	0.578	1	1	1	0.578	1
Mineral absorption - Homo sapiens (human)	0.625	1	0.383	1	0.581	1
Complement and Coagulation Cascades	0.583	1	1	1	0.583	1
Extracellular matrix organization	0.491	1	0.5	1	0.59	1
EPH-Ephrin signaling	0.492	1	0.5	1	0.591	1
2-Hydroxyglutric Aciduria (D And L Form)	0.5	1	0.496	1	0.594	1
Homocarnosinosis	0.5	1	0.496	1	0.594	1
Hyperinsulinism-Hyperammonemia Syndrome	0.5	1	0.496	1	0.594	1
Succinic semialdehyde dehydrogenase deficiency	0.5	1	0.496	1	0.594	1
4-Hydroxybutyric Aciduria/Succinic Semialdehyde Dehydrogenase Deficiency	0.5	1	0.496	1	0.594	1

Glutamate Metabolism	0.5	1	0.496	1	0.594	1
Glucuronidation	0.5	1	0.5	1	0.597	1
glutathione biosynthesis	1	1	0.25	1	0.597	1
Transport of fatty acids	1	1	0.25	1	0.597	1
Stimuli-sensing channels	0.25	1	1	1	0.597	1
Vitamin B6 metabolism	0.5	1	0.5	1	0.597	1
Thiamine metabolism - Homo sapiens (human)	1	1	0.25	1	0.597	1
serine and glycine biosynthesis	1	1	0.25	1	0.597	1
Integrin alphaIIb beta3 signaling	0.25	1	1	1	0.597	1
Valine_ leucine and isoleucine degradation - Homo sapiens (human)	0.25	1	1	1	0.597	1
Integrin signaling	0.25	1	1	1	0.597	1
Histidine degradation	0.5	1	0.5	1	0.597	1
tRNA processing	1	1	0.25	1	0.597	1
GABA synthesis_ release_ reuptake and degradation	1	1	0.25	1	0.597	1
Linoleate metabolism	0.5	1	0.5	1	0.597	1
UTP and CTP de novo biosynthesis	0.5	1	0.5	1	0.597	1

MECP2 and Associated Rett Syndrome	0.5	1	0.5	1	0.597	1
Glycogen Synthesis and Degradation	0.25	1	1	1	0.597	1
Biogenic Amine Synthesis	0.5	1	0.5	1	0.597	1
GLUT-1 deficiency syndrome	1	1	0.25	1	0.597	1
Magnesium salicylate Action Pathway	0.25	1	1	1	0.597	1
Congenital disorder of glycosylation CDG-IId	1	1	0.25	1	0.597	1
Cytosolic sulfonation of small molecules	0.25	1	1	1	0.597	1
Chromatin organization	0.25	1	1	1	0.597	1
Transferrin endocytosis and recycling	0.25	1	1	1	0.597	1
Globoid Cell Leukodystrophy	1	1	0.25	1	0.597	1
Lactose Synthesis	1	1	0.25	1	0.597	1
MAPK6/MAPK4 signaling	0.25	1	1	1	0.597	1
Histidine metabolism - Homo sapiens (human)	0.25	1	1	1	0.597	1
Metachromatic Leukodystrophy (MLD)	1	1	0.25	1	0.597	1
Cellular Senescence	0.25	1	1	1	0.597	1
cysteine biosynthesis	1	1	0.25	1	0.597	1

MNGIE (Mitochondrial Neurogastrointestinal Encephalopathy)	1	1	0.25	1	0.597	1
Metabolism of porphyrins	0.25	1	1	1	0.597	1
5-aminoimidazole ribonucleotide biosynthesis	0.5	1	0.5	1	0.597	1
Arachidonic Acid Metabolism	0.25	1	1	1	0.597	1
The canonical retinoid cycle in rods (twilight vision)	1	1	0.25	1	0.597	1
Sphingolipid Metabolism	1	1	0.25	1	0.597	1
Cyclin D associated events in G1	0.25	1	1	1	0.597	1
G1 Phase	0.25	1	1	1	0.597	1
Signaling by TGF-beta family members	0.25	1	1	1	0.597	1
Biosynthesis of specialized proresolving mediators (SPMs)	0.25	1	1	1	0.597	1
Dopaminergic synapse - Homo sapiens (human)	0.25	1	1	1	0.597	1
Epithelial cell signaling in Helicobacter pylori infection - Homo sapiens (human)	0.25	1	1	1	0.597	1
G1/S Transition	0.25	1	1	1	0.597	1
Hedgehog ligand biogenesis	0.25	1	1	1	0.597	1
Pyrimidine Metabolism	1	1	0.25	1	0.597	1
Purine salvage	0.25	1	1	1	0.597	1

Synthesis of substrates in N-glycan biosythesis	1	1	0.25	1	0.597	1
Biosynthesis of the N-glycan precursor (dolichol lipid-linked oligosaccharide_ LLO) and transfer to a nascent protein	1	1	0.25	1	0.597	1
Methylation	0.25	1	1	1	0.597	1
serine biosynthesis (phosphorylated route)	1	1	0.25	1	0.597	1
Galactose metabolism	1	1	0.25	1	0.597	1
Mitotic G1-G1/S phases	0.25	1	1	1	0.597	1
Beta Ureidopropionase Deficiency	1	1	0.25	1	0.597	1
Regulation of TP53 Activity	0.25	1	1	1	0.597	1
Neurotransmitter receptors and postsynaptic signal transmission	0.5	1	0.5	1	0.597	1
Interactions of Rev with host cellular proteins	0.25	1	1	1	0.597	1
Nicotinamide salvaging	1	1	0.25	1	0.597	1
Chromatin modifying enzymes	0.25	1	1	1	0.597	1
Etodolac Action Pathway	0.25	1	1	1	0.597	1
Ketoprofen Action Pathway	0.25	1	1	1	0.597	1
Rofecoxib Action Pathway	0.25	1	1	1	0.597	1
Acetylsalicylic Acid Action Pathway	0.25	1	1	1	0.597	1

Diflunisal Action Pathway	0.25	1	1	1	0.597	1
Leukotriene C4 Synthesis Deficiency	0.25	1	1	1	0.597	1
Mitochondrial Electron Transport Chain	0.5	1	0.5	1	0.597	1
Histidine Metabolism	1	1	0.25	1	0.597	1
Celecoxib Action Pathway	0.25	1	1	1	0.597	1
Sulindac Action Pathway	0.25	1	1	1	0.597	1
Diclofenac Action Pathway	0.25	1	1	1	0.597	1
Ketorolac Action Pathway	0.25	1	1	1	0.597	1
Gaucher Disease	1	1	0.25	1	0.597	1
Naproxen Action Pathway	0.25	1	1	1	0.597	1
Etoricoxib Action Pathway	0.25	1	1	1	0.597	1
Carprofen Action Pathway	0.25	1	1	1	0.597	1
Flurbiprofen Action Pathway	0.25	1	1	1	0.597	1
Fenoprofen Action Pathway	0.25	1	1	1	0.597	1
Antrafenine Action Pathway	0.25	1	1	1	0.597	1
Antipyrine Action Pathway	0.25	1	1	1	0.597	1

Lumiracoxib Action Pathway	0.25	1	1	1	0.597	1
UMP Synthase Deiciency (Orotic Aciduria)	1	1	0.25	1	0.597	1
Histidinemia	1	1	0.25	1	0.597	1
Trisalicylate-choline Action Pathway	0.25	1	1	1	0.597	1
Nepafenac Action Pathway	0.25	1	1	1	0.597	1
Phenylbutazone Action Pathway	0.25	1	1	1	0.597	1
Lornoxicam Action Pathway	0.25	1	1	1	0.597	1
Salsalate Action Pathway	0.25	1	1	1	0.597	1
Tenoxicam Action Pathway	0.25	1	1	1	0.597	1
Tiaprofenic Acid Action Pathway	0.25	1	1	1	0.597	1
Tolmetin Action Pathway	0.25	1	1	1	0.597	1
Salicylic Acid Action Pathway	0.25	1	1	1	0.597	1
Salicylate-sodium Action Pathway	0.25	1	1	1	0.597	1
Fabry disease	1	1	0.25	1	0.597	1
Oxaprozin Action Pathway	0.25	1	1	1	0.597	1
Valdecoxib Action Pathway	0.25	1	1	1	0.597	1

Nabumetone Action Pathway	0.25	1	1	1	0.597	1
Tryptophan Metabolism	0.25	1	1	1	0.597	1
Signaling by TGF-beta Receptor Complex	0.25	1	1	1	0.597	1
Mercaptopurine Metabolism Pathway	0.25	1	1	1	0.597	1
Krabbe disease	1	1	0.25	1	0.597	1
Indomethacin Action Pathway	0.25	1	1	1	0.597	1
Meloxicam Action Pathway	0.25	1	1	1	0.597	1
Suprofen Action Pathway	0.25	1	1	1	0.597	1
Bromfenac Action Pathway	0.25	1	1	1	0.597	1
Mefenamic Acid Action Pathway	0.25	1	1	1	0.597	1
Piroxicam Action Pathway	0.25	1	1	1	0.597	1
Dihydropyrimidinase Deficiency	1	1	0.25	1	0.597	1
Arachidonic acid metabolism	0.5	1	0.5	1	0.597	1
Bile acid biosynthesis	0.25	1	1	1	0.597	1
Dopamine metabolism	0.25	1	1	1	0.597	1
Transcriptional regulation by RUNX1	0.25	1	1	1	0.597	1

Acetaminophen Action Pathway	0.25	1	1	1	0.597	1
Lipid Metabolism Pathway	0.5	1	0.5	1	0.597	1
Purine metabolism	0.25	1	1	1	0.597	1
glutathione-mediated detoxification	0.5	1	0.5	1	0.597	1
Human Complement System	0.611	1	1	1	0.611	1
Aurora B signaling	0.625	1	1	1	0.625	1
Beta1 integrin cell surface interactions	0.625	1	1	1	0.625	1
Beta3 integrin cell surface interactions	0.625	1	1	1	0.625	1
Apoptotic cleavage of cellular proteins	0.625	1	1	1	0.625	1
ECM-receptor interaction - Homo sapiens (human)	0.625	1	1	1	0.625	1
Fc gamma R-mediated phagocytosis - Homo sapiens (human)	0.625	1	1	1	0.625	1
granzyme a mediated apoptosis pathway	0.625	1	1	1	0.625	1
rho cell motility signaling pathway	0.625	1	1	1	0.625	1
y branching of actin filaments	0.625	1	1	1	0.625	1
Human immunodeficiency virus 1 infection - Homo sapiens (human)	0.625	1	1	1	0.625	1
Human T-cell leukemia virus 1 infection - Homo sapiens (human)	0.625	1	1	1	0.625	1

alanine biosynthesis/degradation	1	1	0.625	1	0.625	1
Intrinsic Pathway of Fibrin Clot Formation	0.625	1	1	1	0.625	1
Integrated Breast Cancer Pathway	0.625	1	1	1	0.625	1
Prolactin Signaling Pathway	0.625	1	1	1	0.625	1
Arrhythmogenic Right Ventricular Cardiomyopathy	0.625	1	1	1	0.625	1
Allograft Rejection	0.625	1	1	1	0.625	1
E3 ubiquitin ligases ubiquitinate target proteins	0.625	1	1	1	0.625	1
Apoptosis-related network due to altered Notch3 in ovarian cancer	0.625	1	1	1	0.625	1
Striated Muscle Contraction Pathway	0.625	1	1	1	0.625	1
Pentose Phosphate Pathway	0.313	1	0.875	1	0.628	1
Glucose-6-phosphate dehydrogenase deficiency	0.313	1	0.875	1	0.628	1
Ribose-5-phosphate isomerase deficiency	0.313	1	0.875	1	0.628	1
Transaldolase deficiency	0.313	1	0.875	1	0.628	1
Alanine Aspartate Asparagine metabolism	1	1	0.275	1	0.631	1
Dengue-2 Interactions with Complement and Coagulation Cascades	0.639	1	1	1	0.639	1
Regulation of Complement cascade	0.641	1	1	1	0.641	1

Complement cascade	0.641	1	1	1	0.641	1
Argininemia	0.5	1	0.57	1	0.643	1
Citrullinemia Type I	0.5	1	0.57	1	0.643	1
Carbamoyl Phosphate Synthetase Deficiency	0.5	1	0.57	1	0.643	1
Argininosuccinic Aciduria	0.5	1	0.57	1	0.643	1
Urea Cycle	0.5	1	0.57	1	0.643	1
Ornithine Transcarbamylase Deficiency (OTC Deficiency)	0.5	1	0.57	1	0.643	1
Glycine Serine metabolism	0.75	1	0.38	1	0.643	1
Detoxification of Reactive Oxygen Species	0.652	1	1	1	0.652	1
Smooth Muscle Contraction	0.297	1	1	1	0.657	1
Branched-chain amino acid catabolism	1	1	0.297	1	0.657	1
Insulin signaling pathway - Homo sapiens (human)	0.312	1	1	1	0.676	1
Platelet Aggregation (Plug Formation)	0.312	1	1	1	0.676	1
S-Adenosylhomocysteine (SAH) Hydrolase Deficiency	1	1	0.312	1	0.676	1
Methionine Metabolism	1	1	0.312	1	0.676	1
Methionine Adenosyltransferase Deficiency	1	1	0.312	1	0.676	1

Glycine N-methyltransferase Deficiency	1	1	0.312	1	0.676	1
Hypermethioninemia	1	1	0.312	1	0.676	1
Methylenetetrahydrofolate Reductase Deficiency (MTHFRD)	1	1	0.312	1	0.676	1
Glucose-Alanine Cycle	1	1	0.312	1	0.676	1
Homocystinuria-megaloblastic anemia due to defect in cobalamin metabolism_ cblG complementation type	1	1	0.312	1	0.676	1
Cystathionine Beta-Synthase Deficiency	1	1	0.312	1	0.676	1
Calcium Regulation in the Cardiac Cell	0.313	1	1	1	0.676	1
Galactosemia	1	1	0.313	1	0.676	1
Huntington disease - Homo sapiens (human)	0.313	1	1	1	0.676	1
Galactose Metabolism	1	1	0.313	1	0.676	1
γ-glutamyl cycle	0.5	1	0.638	1	0.683	1
Glycine_ serine and threonine metabolism - Homo sapiens (human)	0.75	1	0.426	1	0.684	1
Class I MHC mediated antigen processing & presentation	0.322	1	1	1	0.687	1
Plasma lipoprotein assembly_ remodeling_ and clearance	0.322	1	1	1	0.687	1
RAC1 signaling pathway	0.688	1	1	1	0.688	1
Platelet Aggregation Inhibitor Pathway_ Pharmacodynamics	0.688	1	1	1	0.688	1

mRNA Splicing - Major Pathway	0.688	1	1	1	0.688	1
mRNA Splicing	0.688	1	1	1	0.688	1
TGF-beta super family signaling pathway canonical	0.695	1	1	1	0.695	1
S-methyl-5-thio-α-D-ribose 1-phosphate degradation	1	1	0.34	1	0.706	1
Phenylalanine and tyrosine catabolism	0.5	1	0.688	1	0.711	1
Urea cycle	0.5	1	0.688	1	0.711	1
Mitochondrial tRNA aminoacylation	1	1	0.734	1	0.734	1
Signaling by BRAF and RAF fusions	0.734	1	1	1	0.734	1
Oncogenic MAPK signaling	0.734	1	1	1	0.734	1
Glycine_ serine_ alanine and threonine metabolism	0.5	1	0.735	1	0.736	1
ABC transporters - Homo sapiens (human)	1	1	0.371	1	0.738	1
Post-translational modification: synthesis of GPI-anchored proteins	0.742	1	1	1	0.742	1
Aminosugars metabolism	1	1	0.375	1	0.743	1
Synaptic vesicle cycle - Homo sapiens (human)	0.375	1	1	1	0.743	1
Lysosome - Homo sapiens (human)	0.375	1	1	1	0.743	1
Fructose Mannose metabolism	1	1	0.375	1	0.743	1

Signaling by NTRK1 (TRKA)	0.375	1	1	1	0.743	1
Signaling by NTRKs	0.375	1	1	1	0.743	1
Beta-catenin independent WNT signaling	0.375	1	1	1	0.743	1
Mitochondrial protein import	0.375	1	1	1	0.743	1
Parkinson disease - Homo sapiens (human)	0.75	1	0.5	1	0.743	1
rRNA processing	0.75	1	1	1	0.75	1
iron-sulfur cluster biosynthesis	1	1	0.75	1	0.75	1
Chagas disease (American trypanosomiasis) - Homo sapiens (human)	0.75	1	1	1	0.75	1
rRNA modification in the nucleus and cytosol	0.75	1	1	1	0.75	1
rRNA processing in the nucleus and cytosol	0.75	1	1	1	0.75	1
Retinoblastoma Gene in Cancer	0.75	1	1	1	0.75	1
Metabolism of polyamines	1	1	0.75	1	0.75	1
Collagen chain trimerization	0.75	1	1	1	0.75	1
amb2 Integrin signaling	0.75	1	1	1	0.75	1
Caspase-mediated cleavage of cytoskeletal proteins	0.75	1	1	1	0.75	1
LDL clearance	0.75	1	1	1	0.75	1
Immunoregulatory interactions between a Lymphoid and a non-Lymphoid cell	0.75	1	1	1	0.75	1
Gap junction degradation	0.75	1	1	1	0.75	1
Arrhythmogenic right ventricular cardiomyopathy (ARVC) - Homo sapiens (human)	0.75	1	1	1	0.75	1
Endocrine and other factor-regulated calcium reabsorption - Homo sapiens (human)	0.75	1	1	1	0.75	1
pentose phosphate pathway (oxidative branch)	0.75	1	1	1	0.75	1
Netrin-1 signaling	0.75	1	1	1	0.75	1
Platinum Pathway_ Pharmacokinetics/Pharmacodynamics	0.75	1	1	1	0.75	1

Gap junction trafficking	0.75	1	1	1	0.75	1
Gap junction trafficking and regulation	0.75	1	1	1	0.75	1
Angiogenesis overview	0.75	1	1	1	0.75	1
Synaptic Vesicle Pathway	0.75	1	1	1	0.75	1
Recycling pathway of L1	0.438	1	1	1	0.799	1
Gap junction - Homo sapiens (human)	0.438	1	1	1	0.799	1
AMPK signaling pathway - Homo sapiens (human)	0.875	1	0.5	1	0.799	1
Carnosinuria_ carnosinemia	1	1	0.438	1	0.799	1
Ureidopropionase deficiency	1	1	0.438	1	0.799	1
GABA-Transaminase Deficiency	1	1	0.438	1	0.799	1
Beta-Alanine Metabolism	1	1	0.438	1	0.799	1
Mitotic Prophase	0.875	1	0.5	1	0.799	1
Caspase Cascade in Apoptosis	0.812	1	1	1	0.812	1
RHO GTPases Activate WASPs and WAVEs	0.812	1	1	1	0.812	1
Deregulated CDK5 triggers multiple neurodegenerative pathways in Alz-heimer_s disease models	0.813	1	1	1	0.813	1
Neurodegenerative Diseases	0.813	1	1	1	0.813	1
Staphylococcus aureus infection - Homo sapiens (human)	0.813	1	1	1	0.813	1
mRNA_ protein_ and metabolite induction pathway by cyclosporin A	1	1	0.813	1	0.813	1

Transport to the Golgi and subsequent modification	0.461	1	1	1	0.818	1
Alanine and aspartate metabolism	1	1	0.461	1	0.818	1
ER to Golgi Anterograde Transport	0.461	1	1	1	0.818	1
Plasma lipoprotein assembly	0.469	1	1	1	0.824	1
Glycerophospholipid Biosynthetic Pathway	1	1	0.829	1	0.829	1
Na+/Cl- dependent neurotransmitter transporters	1	1	0.844	1	0.844	1
Platelet activation - Homo sapiens (human)	0.844	1	1	1	0.844	1
GPCR signaling-G alpha s PKA and ERK	0.844	1	1	1	0.844	1
Amino acid synthesis and interconversion (transamination)	1	1	0.844	1	0.844	1
Transport of inorganic cations/anions and amino acids/oligopeptides	1	1	0.497	1	0.845	1
Amino acid and oligopeptide SLC transporters	1	1	0.497	1	0.845	1
RAF activation	0.5	1	1	1	0.847	1
ESR-mediated signaling	0.5	1	1	1	0.847	1
HDR through Homologous Recombination (HR) or Single Strand Annealing (SSA)	0.5	1	1	1	0.847	1
ABC transporter disorders	0.5	1	1	1	0.847	1
Disorders of transmembrane transporters	0.5	1	1	1	0.847	1

Heme Biosynthesis	0.5	1	1	1	0.847	1
Methylation Pathways	0.5	1	1	1	0.847	1
Folate Metabolism	1	1	0.5	1	0.847	1
Homology Directed Repair	0.5	1	1	1	0.847	1
serotonin degradation	0.5	1	1	1	0.847	1
Triglyceride catabolism	1	1	0.5	1	0.847	1
pyrimidine deoxyribonucleotides biosynthesis from CTP	0.5	1	1	1	0.847	1
DNA Double-Strand Break Repair	0.5	1	1	1	0.847	1
acetyl-CoA biosynthesis from citrate	1	1	0.5	1	0.847	1
glutamate biosynthesis/degradation	1	1	0.5	1	0.847	1
Defective CFTR causes cystic fibrosis	0.5	1	1	1	0.847	1
Fructose metabolism	1	1	0.5	1	0.847	1
Simvastatin Action Pathway	1	1	0.5	1	0.847	1
Amphetamine addiction - Homo sapiens (human)	1	1	0.5	1	0.847	1
Mevalonic aciduria	1	1	0.5	1	0.847	1
noradrenaline and adrenaline degradation	0.5	1	1	1	0.847	1

Rev-mediated nuclear export of HIV RNA	0.5	1	1	1	0.847	1
Insulin effects increased synthesis of Xylulose-5-Phosphate	0.5	1	1	1	0.847	1
Oxidative Stress Induced Senescence	0.5	1	1	1	0.847	1
palmitate biosynthesis	1	1	0.5	1	0.847	1
ABC transporters in lipid homeostasis	0.5	1	1	1	0.847	1
Smith-Lemli-Opitz Syndrome (SLOS)	1	1	0.5	1	0.847	1
Chondrodysplasia Punctata II_ X Linked Dominant (CDPX2)	1	1	0.5	1	0.847	1
Desmosterolosis	1	1	0.5	1	0.847	1
Downstream TCR signaling	0.5	1	1	1	0.847	1
TCR signaling	0.5	1	1	1	0.847	1
Synthesis of Leukotrienes (LT) and Eoxins (EX)	0.5	1	1	1	0.847	1
malate-aspartate shuttle	0.5	1	1	1	0.847	1
Sulfite oxidase deficiency	0.5	1	1	1	0.847	1
Hypercholesterolemia	1	1	0.5	1	0.847	1
Protein repair	0.5	1	1	1	0.847	1
Costimulation by the CD28 family	0.5	1	1	1	0.847	1

guanosine ribonucleotides de novo biosynthesis	0.5	1	1	1	0.847	1
guanosine nucleotides de novo biosynthesis	0.5	1	1	1	0.847	1
Insulin receptor recycling	0.5	1	1	1	0.847	1
Signaling by Insulin receptor	0.5	1	1	1	0.847	1
Heme biosynthesis	0.5	1	1	1	0.847	1
Rosuvastatin Action Pathway	1	1	0.5	1	0.847	1
heme biosynthesis	0.5	1	1	1	0.847	1
Methotrexate Action Pathway	1	1	0.5	1	0.847	1
Respiratory electron transport_ ATP synthesis by chemiosmotic coupling_ and heat production by uncoupling proteins.	0.5	1	1	1	0.847	1
eNOS activation	0.5	1	1	1	0.847	1
EPHB-mediated forward signaling	1	1	0.5	1	0.847	1
Aminosugars metabolism	1	1	0.5	1	0.847	1
Cyclin E associated events during G1/S transition	0.5	1	1	1	0.847	1
Type II diabetes mellitus	1	1	0.5	1	0.847	1
Arginine biosynthesis - Homo sapiens (human)	0.5	1	1	1	0.847	1
Biosynthesis of DHA-derived SPMs	0.5	1	1	1	0.847	1

Downregulation of SMAD2/3:SMAD4 transcriptional activity	0.5	1	1	1	0.847	1
Transcriptional activity of SMAD2/SMAD3:SMAD4 heterotrimer	0.5	1	1	1	0.847	1
pyrimidine deoxyribonucleotides de novo biosynthesis	0.5	1	1	1	0.847	1
Vascular smooth muscle contraction - Homo sapiens (human)	0.5	1	1	1	0.847	1
Bile secretion - Homo sapiens (human)	1	1	0.5	1	0.847	1
Alcoholism - Homo sapiens (human)	1	1	0.5	1	0.847	1
Cocaine addiction - Homo sapiens (human)	1	1	0.5	1	0.847	1
Cyclin A:Cdk2-associated events at S phase entry	0.5	1	1	1	0.847	1
DNA Replication	0.5	1	1	1	0.847	1
Folate-Alcohol and Cancer Pathway Hypotheses	1	1	0.5	1	0.847	1
Metabolism of cofactors	0.5	1	1	1	0.847	1
S Phase	0.5	1	1	1	0.847	1
EGFR downregulation	0.5	1	1	1	0.847	1
Signaling by EGFR	0.5	1	1	1	0.847	1
Base Excision Repair	1	1	0.5	1	0.847	1
purine ribonucleosides degradation to ribose-1-phosphate	0.5	1	1	1	0.847	1

Downregulation of ERBB2 signaling	0.5	1	1	1	0.847	1
Steroid Biosynthesis	1	1	0.5	1	0.847	1
Famotidine Action Pathway	1	1	0.5	1	0.847	1
D-Glutamine and D-glutamate metabolism - Homo sapiens (human)	1	1	0.5	1	0.847	1
Triglyceride metabolism	1	1	0.5	1	0.847	1
Amyotrophic lateral sclerosis (ALS) - Homo sapiens (human)	0.5	1	1	1	0.847	1
Aquaporin-mediated transport	1	1	0.5	1	0.847	1
Insulin resistance - Homo sapiens (human)	1	1	0.5	1	0.847	1
Regulation of TP53 Degradation	0.5	1	1	1	0.847	1
Regulation of TP53 Expression and Degradation	0.5	1	1	1	0.847	1
PIP3 activates AKT signaling	0.5	1	1	1	0.847	1
Neurotransmitter clearance	0.5	1	1	1	0.847	1
Signaling by PDGF	0.5	1	1	1	0.847	1
Interferon gamma signaling	0.5	1	1	1	0.847	1
Glutamate binding_ activation of AMPA receptors and synaptic plasticity	1	1	0.5	1	0.847	1
Methylenetetrahydrofolate Reductase Deficiency (MTHFRD)	1	1	0.5	1	0.847	1

Nicotinate Nicotinamide metabolism	1	1	0.5	1	0.847	1
Mitotic Anaphase	0.5	1	1	1	0.847	1
Mitotic Metaphase and Anaphase	0.5	1	1	1	0.847	1
Phenylalanine degradation	1	1	0.5	1	0.847	1
Fructose catabolism	1	1	0.5	1	0.847	1
Galactose catabolism	0.5	1	1	1	0.847	1
Signaling by ERBB2	0.5	1	1	1	0.847	1
Pravastatin Action Pathway	1	1	0.5	1	0.847	1
Atorvastatin Action Pathway	1	1	0.5	1	0.847	1
Folate malabsorption_ hereditary	1	1	0.5	1	0.847	1
Sulfate/Sulfite Metabolism	0.5	1	1	1	0.847	1
Hyper-IgD syndrome	1	1	0.5	1	0.847	1
Cholesteryl ester storage disease	1	1	0.5	1	0.847	1
Lysosomal Acid Lipase Deficiency (Wolman Disease)	1	1	0.5	1	0.847	1
Alendronate Action Pathway	1	1	0.5	1	0.847	1
Hereditary Coproporphyria (HCP)	0.5	1	1	1	0.847	1

Porphyria Variegata (PV)	0.5	1	1	1	0.847	1
Congenital Erythropoietic Porphyria (CEP) or Gunther Disease	0.5	1	1	1	0.847	1
Acute Intermittent Porphyria	0.5	1	1	1	0.847	1
Wolman disease	1	1	0.5	1	0.847	1
Oxidation of Branched Chain Fatty Acids	0.5	1	1	1	0.847	1
Risedronate Action Pathway	1	1	0.5	1	0.847	1
Cerivastatin Action Pathway	1	1	0.5	1	0.847	1
Fluvastatin Action Pathway	1	1	0.5	1	0.847	1
Hh mutants that don_t undergo autocatalytic processing are degraded by ERAD	0.5	1	1	1	0.847	1
Hh mutants abrogate ligand secretion	0.5	1	1	1	0.847	1
CHILD Syndrome	1	1	0.5	1	0.847	1
Porphyrin Metabolism	0.5	1	1	1	0.847	1
Formation of Incision Complex in GG-NER	0.5	1	1	1	0.847	1
Zoledronate Action Pathway	1	1	0.5	1	0.847	1
Ibandronate Action Pathway	1	1	0.5	1	0.847	1
Recruitment and ATM-mediated phosphorylation of repair and signaling proteins at DNA double strand breaks	0.5	1	1	1	0.847	1

DNA Double Strand Break Response	0.5	1	1	1	0.847	1
Leukotriene metabolism	0.5	1	1	1	0.847	1
Vitamin B5 - CoA biosynthesis from pantothenate	1	1	0.5	1	0.847	1
Ethanol effects on histone modifications	0.5	1	1	1	0.847	1
Global Genome Nucleotide Excision Repair (GG-NER)	0.5	1	1	1	0.847	1
AMP-activated Protein Kinase (AMPK) Signaling	0.5	1	1	1	0.847	1
Catabolism of glucuronate to xylulose-5-phosphate	1	1	0.5	1	0.847	1
L-dopa degradation	1	1	0.5	1	0.847	1
TGF-beta receptor signaling activates SMADs	0.5	1	1	1	0.847	1
Activation of gene expression by SREBF (SREBP)	0.5	1	1	1	0.847	1
Amyotrophic lateral sclerosis (ALS)	0.5	1	1	1	0.847	1
Nicotinate and Nicotinamide Metabolism	1	1	0.5	1	0.847	1
Regulation of lipid metabolism by Peroxisome proliferator-activated receptor alpha (PPARalpha)	0.5	1	1	1	0.847	1
Processing of DNA double-strand break ends	0.5	1	1	1	0.847	1
Pamidronate Action Pathway	1	1	0.5	1	0.847	1
Fatty Acid Biosynthesis	0.5	1	1	1	0.847	1

Lovastatin Action Pathway	1	1	0.5	1	0.847	1
Angiopoietin Like Protein 8 Regulatory Pathway	0.5	1	1	1	0.847	1
Nucleotide Excision Repair	0.5	1	1	1	0.847	1
NO-cGMP-PKG mediated Neuroprotection	0.5	1	1	1	0.847	1
Nucleotide Metabolism	1	1	0.5	1	0.847	1
Glycogen breakdown (glycogenolysis)	0.5	1	1	1	0.847	1
Glycogen metabolism	0.5	1	1	1	0.847	1
Thiamine metabolic pathways	1	1	0.5	1	0.847	1
folate polyglutamylation	1	1	0.5	1	0.847	1
Regulation of insulin secretion	1	1	0.5	1	0.847	1
Metabolism of nitric oxide	0.5	1	1	1	0.847	1
GABAergic synapse - Homo sapiens (human)	1	1	0.5	1	0.847	1
Vitamin B9 (folate) metabolism	1	1	0.5	1	0.847	1
Metabolism of folate and pterines	1	1	0.5	1	0.847	1
eNOS activation and regulation	0.5	1	1	1	0.847	1
Porphyrin metabolism	1	1	0.5	1	0.847	1

Vitamin B5 (pantothenate) metabolism	0.5	1	1	1	0.847	1
Intracellular signaling by second messengers	0.5	1	1	1	0.847	1
Protein-protein interactions at synapses	0.5	1	1	1	0.847	1
HDL remodeling	0.5	1	1	1	0.847	1
Fructose and mannose metabolism	1	1	0.5	1	0.847	1
Parkinsons Disease Pathway	0.5	1	1	1	0.847	1
GABA shunt	1	1	0.5	1	0.847	1
Fructose and mannose metabolism - Homo sapiens (human)	0.844	1	0.625	1	0.865	1
Tigecycline Action Pathway	1	1	0.875	1	0.875	1
RAB GEFs exchange GTP for GDP on RABs	0.875	1	1	1	0.875	1
Tobramycin Action Pathway	1	1	0.875	1	0.875	1
Troleandomycin Action Pathway	1	1	0.875	1	0.875	1
Clarithromycin Action Pathway	1	1	0.875	1	0.875	1
Clindamycin Action Pathway	1	1	0.875	1	0.875	1
Azithromycin Action Pathway	1	1	0.875	1	0.875	1
C-type lectin receptors (CLRs)	0.875	1	1	1	0.875	1

Dilated cardiomyopathy (DCM) - Homo sapiens (human)	0.875	1	1	1	0.875	1
Methacycline Action Pathway	1	1	0.875	1	0.875	1
Rolitetracycline Action Pathway	1	1	0.875	1	0.875	1
Minocycline Action Pathway	1	1	0.875	1	0.875	1
glycine biosynthesis	1	1	0.875	1	0.875	1
Erythromycin Action Pathway	1	1	0.875	1	0.875	1
Telithromycin Action Pathway	1	1	0.875	1	0.875	1
Streptomycin Action Pathway	1	1	0.875	1	0.875	1
Spectinomycin Action Pathway	1	1	0.875	1	0.875	1
Hypertrophic cardiomyopathy (HCM) - Homo sapiens (human)	0.875	1	1	1	0.875	1
Oxidative Stress Regulatory Pathway (Erythrocyte)	0.875	1	1	1	0.875	1
Josamycin Action Pathway	1	1	0.875	1	0.875	1
Kanamycin Action Pathway	1	1	0.875	1	0.875	1
Gentamicin Action Pathway	1	1	0.875	1	0.875	1
Netilmicin Action Pathway	1	1	0.875	1	0.875	1
Neomycin Action Pathway	1	1	0.875	1	0.875	1

Roxithromycin Action Pathway	1	1	0.875	1	0.875	1
Amikacin Action Pathway	1	1	0.875	1	0.875	1
Doxycycline Action Pathway	1	1	0.875	1	0.875	1
Demeclocycline Action Pathway	1	1	0.875	1	0.875	1
Oxytetracycline Action Pathway	1	1	0.875	1	0.875	1
Clomocycline Action Pathway	1	1	0.875	1	0.875	1
Lincomycin Action Pathway	1	1	0.875	1	0.875	1
Chloramphenicol Action Pathway	1	1	0.875	1	0.875	1
Scavenging by Class F Receptors	0.875	1	1	1	0.875	1
Arbekacin Action Pathway	1	1	0.875	1	0.875	1
Paromomycin Action Pathway	1	1	0.875	1	0.875	1
Glyoxylate metabolism and glycine degradation	1	1	0.875	1	0.875	1
Lymecycline Action Pathway	1	1	0.875	1	0.875	1
Tetracycline Action Pathway	1	1	0.875	1	0.875	1
Rho GTPase cycle	0.563	1	1	1	0.886	1
Scavenging by Class A Receptors	0.563	1	1	1	0.886	1

Protein digestion and absorption - Homo sapiens (human)	0.75	1	0.765	1	0.892	1
Processing of Capped Intron-Containing Pre-mRNA	0.578	1	1	1	0.895	1
Lysosome Vesicle Biogenesis	0.625	1	1	1	0.919	1
ornithine de novo biosynthesis	1	1	0.625	1	0.919	1
sucrose degradation	0.625	1	1	1	0.919	1
Degradation of cysteine and homocysteine	1	1	0.625	1	0.919	1
Valine_ leucine and isoleucine biosynthesis - Homo sapiens (human)	1	1	0.625	1	0.919	1
COPI-dependent Golgi-to-ER retrograde traffic	0.625	1	1	1	0.919	1
COPII-mediated vesicle transport	0.625	1	1	1	0.919	1
Tryptophan metabolism	1	1	0.625	1	0.919	1
tRNA charging	1	1	0.652	1	0.931	1
Aminoacyl-tRNA biosynthesis - Homo sapiens (human)	1	1	0.652	1	0.931	1
leukotriene biosynthesis	1	1	0.652	1	0.931	1
Nicotinate and nicotinamide metabolism - Homo sapiens (human)	0.75	1	0.875	1	0.933	1
Keratinization	0.938	1	1	1	0.938	1
Regulation of mRNA stability by proteins that bind AU-rich elements	0.938	1	1	1	0.938	1

Amino acid synthesis and interconversion (transamination)	0.75	1	0.91	1	0.943	1
Golgi Associated Vesicle Biogenesis	0.688	1	1	1	0.945	1
Clathrin derived vesicle budding	0.688	1	1	1	0.945	1
trans-Golgi Network Vesicle Budding	0.688	1	1	1	0.945	1
MAP2K and MAPK activation	0.945	1	1	1	0.945	1
Signaling by RAS mutants	0.945	1	1	1	0.945	1
Signaling by high-kinase activity BRAF mutants	0.945	1	1	1	0.945	1
Signaling by moderate kinase activity BRAF mutants	0.945	1	1	1	0.945	1
Paradoxical activation of RAF signaling by kinase inactive BRAF	0.945	1	1	1	0.945	1
Toll-Like Receptors Cascades	0.734	1	1	1	0.961	1
tRNA Aminoacylation	1	1	0.734	1	0.961	1
Cytosolic tRNA aminoacylation	1	1	0.734	1	0.961	1
Regulation of actin dynamics for phagocytic cup formation	0.742	1	1	1	0.963	1
Fcgamma receptor (FCGR) dependent phagocytosis	0.742	1	1	1	0.963	1
isoleucine degradation	1	1	0.75	1	0.966	1
inosine-5_-phosphate biosynthesis	1	1	0.75	1	0.966	1

Pyrimidine biosynthesis	1	1	0.75	1	0.966	1
UMP biosynthesis	1	1	0.75	1	0.966	1
MHC class II antigen presentation	0.75	1	1	1	0.966	1
hemoglobins chaperone	0.75	1	1	1	0.966	1
AGE-RAGE signaling pathway in diabetic complications - Homo sapiens (human)	0.75	1	1	1	0.966	1
Neuroactive ligand-receptor interaction - Homo sapiens (human)	0.75	1	1	1	0.966	1
Amine-derived hormones	1	1	0.75	1	0.966	1
Metabolism of ingested SeMet_ Sec_ MeSec into H2Se	1	1	0.812	1	0.981	1
urea cycle	1	1	0.812	1	0.981	1
Influenza Life Cycle	0.844	1	1	1	0.987	1
Influenza Infection	0.844	1	1	1	0.987	1
Signaling by ROBO receptors	0.844	1	1	1	0.987	1
Inositol phosphate metabolism - Homo sapiens (human)	1	1	0.85	1	0.988	1
N-glycan trimming in the ER and Calnexin/Calreticulin cycle	0.875	1	1	1	0.992	1
Fructosuria	0.875	1	1	1	0.992	1
Regulation of CDC42 activity	0.875	1	1	1	0.992	1

Antigen Presentation: Folding_ assembly and peptide loading of class I MHC	0.875	1	1	1	0.992	1
mTOR signaling pathway - Homo sapiens (human)	0.875	1	1	1	0.992	1
Purine catabolism	0.875	1	1	1	0.992	1
Fructose intolerance_ hereditary	0.875	1	1	1	0.992	1
Malate-Aspartate Shuttle	1	1	0.875	1	0.992	1
Fructose and Mannose Degradation	0.875	1	1	1	0.992	1
Degradation of the extracellular matrix	0.945	1	1	1	0.998	1
Clathrin-mediated endocytosis	0.966	1	1	1	0.999	1
Brain-Derived Neurotrophic Factor (BDNF) signaling pathway	1	1	1	1	1	1
Epithelial to mesenchymal transition in colorectal cancer	1	1	1	1	1	1
POLB-Dependent Long Patch Base Excision Repair	1	1	1	1	1	1
phosphatidylserine biosynthesis II	1	1	1	1	1	1
Wnt Signaling	1	1	1	1	1	1
Cholesterol biosynthesis_ regulation and transport	1	1	1	1	1	1
Genotoxicity pathway	1	1	1	1	1	1
Methionine metabolism and related disorders	1	1	1	1	1	1
Extracellular vesicles in the crosstalk of cardiac cells	1	1	1	1	1	1
Rett syndrome causing genes	1	1	1	1	1	1
Malate-aspartate shuttle	1	1	1	1	1	1
Vindesine Action Pathway	1	1	1	1	1	1
Nonalcoholic fatty liver disease	1	1	1	1	1	1
tryptophan degradation to 2-amino-3-carboxymuconate semialdehyde	1	1	1	1	1	1
tryptophan degradation	1	1	1	1	1	1

glycine/serine biosynthesis	1	1	1	1	1	1
G alpha (z) signalling events	1	1	1	1	1	1
G alpha (s) signalling events	1	1	1	1	1	1
COPII-mediated vesicle transport	1	1	1	1	1	1
Negative regulation of FGFR2 signaling	1	1	1	1	1	1
Signaling by FGFR2	1	1	1	1	1	1
Signaling by PTK6	1	1	1	1	1	1
ATF6 (ATF6-alpha) activates chaperones	1	1	1	1	1	1
Leptin	1	1	1	1	1	1
AOP CYP2E1 Activation Leading To Neurodegeneration	1	1	1	1	1	1
Signaling by NTRK3 (TRKC)	1	1	1	1	1	1
GABA receptor activation	1	1	1	1	1	1
Glutamate binding_ activation of AMPA receptors and synaptic plasticity	1	1	1	1	1	1
DNA Replication Pre-Initiation	1	1	1	1	1	1
Inflammatory Response Pathway	1	1	1	1	1	1
DNA Replication	1	1	1	1	1	1
Endochondral Ossification	1	1	1	1	1	1
Hypertrophy Model	1	1	1	1	1	1
Acetylcholine Synthesis	1	1	1	1	1	1
TGF-beta Receptor Signaling	1	1	1	1	1	1
Monoamine GPCRs	1	1	1	1	1	1
Senescence and Autophagy in Cancer	1	1	1	1	1	1
Oxidative phosphorylation	1	1	1	1	1	1
TET1_2_3 and TDG demethylate DNA	1	1	1	1	1	1
Arachidonate Epoxygenase - Epoxide Hydrolase	1	1	1	1	1	1
Polyol Pathway	1	1	1	1	1	1
Tamoxifen metabolism	1	1	1	1	1	1
Role of phospholipids in phagocytosis	1	1	1	1	1	1
Amino acid conjugation	1	1	1	1	1	1
glutamate removal from folates	1	1	1	1	1	1

thio-molybdenum cofactor biosynthesis	1	1	1	1	1	1
NADE modulates death signalling	1	1	1	1	1	1
agrin in postsynaptic differentiation	1	1	1	1	1	1
RUNX2 regulates genes involved in differentiation of myeloid cells	1	1	1	1	1	1
Steroids metabolism	1	1	1	1	1	1
BCR	1	1	1	1	1	1
VxPx cargo-targeting to cilium	1	1	1	1	1	1
UDP-N-acetyl-D-galactosamine biosynthesis II	1	1	1	1	1	1
Resolution of Sister Chromatid Cohesion	1	1	1	1	1	1
Antigen activates B Cell Receptor (BCR) leading to generation of second messengers	1	1	1	1	1	1
glutathione redox reactions I	1	1	1	1	1	1
p53-Independent DNA Damage Response	1	1	1	1	1	1
Pink/Parkin Mediated Mitophagy	1	1	1	1	1	1
Endometrial cancer	1	1	1	1	1	1
activation of camp-dependent protein kinase pka	1	1	1	1	1	1
NRF2-ARE regulation	1	1	1	1	1	1
Integrin alphaIIb beta3 signaling	1	1	1	1	1	1
Mepivacaine Action Pathway	1	1	1	1	1	1
Activation of APC/C and APC/C:Cdc20 mediated degradation of mitotic proteins	1	1	1	1	1	1
PERK regulates gene expression	1	1	1	1	1	1
Acebutolol Action Pathway	1	1	1	1	1	1
Syndecan-2-mediated signaling events	1	1	1	1	1	1
Glucagon-like Peptide-1 (GLP1) regulates insulin secretion	1	1	1	1	1	1
Negative regulation of FGFR3 signaling	1	1	1	1	1	1
Signaling by FGFR3	1	1	1	1	1	1
thyroid hormone metabolism II (via conjugation and/or degradation)	1	1	1	1	1	1
Benzocaine Action Pathway	1	1	1	1	1	1
G1/S DNA Damage Checkpoints	1	1	1	1	1	1

adenine and adenosine salvage I	1	1	1	1	1	1
Calcineurin-regulated NFAT-dependent transcription in lymphocytes	1	1	1	1	1	1
Joubert syndrome	1	1	1	1	1	1
Ca-dependent events	1	1	1	1	1	1
Bladder cancer - Homo sapiens (human)	1	1	1	1	1	1
G alpha (12-13) signalling events	1	1	1	1	1	1
Thermogenesis	1	1	1	1	1	1
adenine and adenosine salvage II	1	1	1	1	1	1
Oxprenolol Action Pathway	1	1	1	1	1	1
folate transformations	1	1	1	1	1	1
mRNA capping	1	1	1	1	1	1
Glucuronidation	1	1	1	1	1	1
Esmolol Action Pathway	1	1	1	1	1	1
methylglyoxal degradation VI	1	1	1	1	1	1
Epigenetic regulation of gene expression	1	1	1	1	1	1
Bisoprolol Action Pathway	1	1	1	1	1	1
Amino acid transport across the plasma membrane	1	1	1	1	1	1
Tamoxifen Action Pathway	1	1	1	1	1	1
CREB phosphorylation through the activation of CaMKII	1	1	1	1	1	1
DCC mediated attractive signaling	1	1	1	1	1	1
COPI-mediated anterograde transport	1	1	1	1	1	1
Nonhomologous End-Joining (NHEJ)	1	1	1	1	1	1
Post NMDA receptor activation events	1	1	1	1	1	1
signal dependent regulation of myogenesis by corepressor mitr	1	1	1	1	1	1
DNA Damage Recognition in GG-NER	1	1	1	1	1	1
Pancreatic cancer - Homo sapiens (human)	1	1	1	1	1	1
Activation of NMDA receptor and postsynaptic events	1	1	1	1	1	1
Synthesis of PIPs in the nucleus	1	1	1	1	1	1
GDP-glucose biosynthesis II	1	1	1	1	1	1
Coenzyme A biosynthesis	1	1	1	1	1	1

asparagine biosynthesis	1	1	1	1	1	1
glutamate dependent acid resistance	1	1	1	1	1	1
DAP12 signaling	1	1	1	1	1	1
Negative regulation of FGFR4 signaling	1	1	1	1	1	1
Signaling by FGFR4	1	1	1	1	1	1
induction of apoptosis through dr3 and dr4/5 death receptors	1	1	1	1	1	1
Anileridine Action Pathway	1	1	1	1	1	1
Mitochondrial translation	1	1	1	1	1	1
p75NTR signals via NF-kB	1	1	1	1	1	1
thioredoxin pathway	1	1	1	1	1	1
Transcriptional regulation by RUNX3	1	1	1	1	1	1
Differentiation Pathway	1	1	1	1	1	1
L-carnitine biosynthesis	1	1	1	1	1	1
Cimetidine Action Pathway	1	1	1	1	1	1
NAD biosynthesis from 2-amino-3-carboxymuconate semialdehyde	1	1	1	1	1	1
cardiolipin biosynthesis	1	1	1	1	1	1
Degradation of beta catenin	1	1	1	1	1	1
trehalose degradation	1	1	1	1	1	1
Endometrial cancer - Homo sapiens (human)	1	1	1	1	1	1
Hematopoietic cell lineage - Homo sapiens (human)	1	1	1	1	1	1
regulation of bad phosphorylation	1	1	1	1	1	1
Oxybuprocaine Action Pathway	1	1	1	1	1	1
citrulline-nitric oxide cycle	1	1	1	1	1	1
Aryl hydrocarbon receptor signalling	1	1	1	1	1	1
Sulfur metabolism - Homo sapiens (human)	1	1	1	1	1	1
Butyrate Response Factor 1 (BRF1) binds and destabilizes mRNA	1	1	1	1	1	1
Peroxisomal lipid metabolism	1	1	1	1	1	1
L-serine degradation	1	1	1	1	1	1
APC/C:Cdc20 mediated degradation of mitotic proteins	1	1	1	1	1	1
4-hydroxy-2-nonenal detoxification	1	1	1	1	1	1

ccr3 signaling in eosinophils	1	1	1	1	1	1
aspartate biosynthesis	1	1	1	1	1	1
HDL assembly	1	1	1	1	1	1
Nuclear Envelope Breakdown	1	1	1	1	1	1
asparagine degradation	1	1	1	1	1	1
Growth hormone receptor signaling	1	1	1	1	1	1
TCR signaling	1	1	1	1	1	1
spermine biosynthesis	1	1	1	1	1	1
IL-2 Signaling Pathway	1	1	1	1	1	1
Vitamin A and Carotenoid Metabolism	1	1	1	1	1	1
Mitochondrial biogenesis	1	1	1	1	1	1
IL-7 signaling	1	1	1	1	1	1
Post-chaperonin tubulin folding pathway	1	1	1	1	1	1
Termination of translesion DNA synthesis	1	1	1	1	1	1
Tristetraprolin (TTP_ ZFP36) binds and destabilizes mRNA	1	1	1	1	1	1
glycogen biosynthesis	1	1	1	1	1	1
arsenate detoxification I (glutaredoxin)	1	1	1	1	1	1
Smooth Muscle Contraction	1	1	1	1	1	1
Regulation of PTEN localization	1	1	1	1	1	1
transcription regulation by methyltransferase of carm1	1	1	1	1	1	1
CMP-N-acetylneuraminate biosynthesis I (eukaryotes)	1	1	1	1	1	1
DNA Damage Bypass	1	1	1	1	1	1
Fructose biosynthesis	1	1	1	1	1	1
Gamma-carboxylation of protein precursors	1	1	1	1	1	1
TGFBR1 KD Mutants in Cancer	1	1	1	1	1	1
Prolactin receptor signaling	1	1	1	1	1	1
Loss of Function of TGFBR1 in Cancer	1	1	1	1	1	1
Hyaluronan uptake and degradation	1	1	1	1	1	1
Hyaluronan metabolism	1	1	1	1	1	1
Signaling by TGF-beta Receptor Complex in Cancer	1	1	1	1	1	1

TBC/RABGAPs	1	1	1	1	1	1
Rab regulation of trafficking	1	1	1	1	1	1
signal transduction through il1r	1	1	1	1	1	1
glutathione redox reactions II	1	1	1	1	1	1
Transcriptional Regulation by E2F6	1	1	1	1	1	1
Oxygen-dependent proline hydroxylation of Hypoxia-inducible Factor Alpha	1	1	1	1	1	1
Constitutive Signaling by Ligand-Responsive EGFR Cancer Variants	1	1	1	1	1	1
Pentose phosphate pathway	1	1	1	1	1	1
TSH	1	1	1	1	1	1
hiv-1 nef: negative effector of fas and tnf	1	1	1	1	1	1
Transcription of the HIV genome	1	1	1	1	1	1
ErbB Signaling Pathway	1	1	1	1	1	1
Intracellular Signalling Through FSH Receptor and Follicle Stimulating Hormone	1	1	1	1	1	1
LDL remodeling	1	1	1	1	1	1
cAMP signaling pathway - Homo sapiens (human)	1	1	1	1	1	1
sumoylation by ranbp2 regulates transcriptional repression	1	1	1	1	1	1
Transport of Ribonucleoproteins into the Host Nucleus	1	1	1	1	1	1
SALM protein interactions at the synapse	1	1	1	1	1	1
Choline metabolism in cancer - Homo sapiens (human)	1	1	1	1	1	1
Cellular response to hypoxia	1	1	1	1	1	1
GDP-L-fucose biosynthesis I (from GDP-D-mannose)	1	1	1	1	1	1
p53-Independent G1/S DNA damage checkpoint	1	1	1	1	1	1
Flecainide Action Pathway	1	1	1	1	1	1
Lysosomal oligosaccharide catabolism	1	1	1	1	1	1
ncRNAs involved in Wnt signaling in hepatocellular carcinoma	1	1	1	1	1	1
toll-like receptor pathway	1	1	1	1	1	1
IRE1alpha activates chaperones	1	1	1	1	1	1
Adherens junctions interactions	1	1	1	1	1	1

Oncogene Induced Senescence	1	1	1	1	1	1
Unfolded Protein Response (UPR)	1	1	1	1	1	1
Conjugation of benzoate with glycine	1	1	1	1	1	1
NIK-->noncanonical NF-kB signaling	1	1	1	1	1	1
Verapamil Action Pathway	1	1	1	1	1	1
Glucagon signaling in metabolic regulation	1	1	1	1	1	1
Synthesis of very long-chain fatty acyl-CoAs	1	1	1	1	1	1
MicroRNA (miRNA) biogenesis	1	1	1	1	1	1
b cell survival pathway	1	1	1	1	1	1
Conjugation of salicylate with glycine	1	1	1	1	1	1
Conjugation of carboxylic acids	1	1	1	1	1	1
Amino Acid conjugation	1	1	1	1	1	1
SUMO is transferred from E1 to E2 (UBE2I_ UBC9)	1	1	1	1	1	1
Synthesis_ secretion_ and deacylation of Ghrelin	1	1	1	1	1	1
HIF-2-alpha transcription factor network	1	1	1	1	1	1
Spermidine and Spermine Biosynthesis	1	1	1	1	1	1
ER Quality Control Compartment (ERQC)	1	1	1	1	1	1
Calnexin/calreticulin cycle	1	1	1	1	1	1
Thyroid hormone signaling pathway - Homo sapiens (human)	1	1	1	1	1	1
Phase 3 - rapid repolarisation	1	1	1	1	1	1
Cardiac conduction	1	1	1	1	1	1
Phosphorylation of CD3 and TCR zeta chains	1	1	1	1	1	1
selenocysteine biosynthesis	1	1	1	1	1	1
PP2A-mediated dephosphorylation of key metabolic factors	1	1	1	1	1	1
BMP2 signaling TGF-beta MV	1	1	1	1	1	1
snRNP Assembly	1	1	1	1	1	1
Translocation of ZAP-70 to Immunological synapse	1	1	1	1	1	1
Glutamatergic synapse - Homo sapiens (human)	1	1	1	1	1	1
Renin secretion - Homo sapiens (human)	1	1	1	1	1	1
tetrapyrrole biosynthesis	1	1	1	1	1	1

GDP-mannose biosynthesis	1	1	1	1	1	1
Serotonergic synapse - Homo sapiens (human)	1	1	1	1	1	1
Escitalopram Action Pathway	1	1	1	1	1	1
Autodegradation of Cdh1 by Cdh1:APC/C	1	1	1	1	1	1
Entry of Influenza Virion into Host Cell via Endocytosis	1	1	1	1	1	1
ACE Inhibitor Pathway	1	1	1	1	1	1
pyridoxal 5_-phosphate salvage	1	1	1	1	1	1
Plus-strand DNA synthesis	1	1	1	1	1	1
Vitamin A (retinol) metabolism	1	1	1	1	1	1
HS-GAG degradation	1	1	1	1	1	1
Heparan sulfate/heparin (HS-GAG) metabolism	1	1	1	1	1	1
eicosanoid metabolism	1	1	1	1	1	1
fatty acid elongation -- saturated	1	1	1	1	1	1
p75NTR regulates axonogenesis	1	1	1	1	1	1
Ion transport by P-type ATPases	1	1	1	1	1	1
Retinoid metabolism and transport	1	1	1	1	1	1
rho-selective guanine exchange factor akap13 mediates stress fiber for-mation	1	1	1	1	1	1
Thrombin signalling through proteinase activated receptors (PARs)	1	1	1	1	1	1
GP1b-IX-V activation signalling	1	1	1	1	1	1
ER-Phagosome pathway	1	1	1	1	1	1
p75(NTR)-mediated signaling	1	1	1	1	1	1
NOTCH3 Activation and Transmission of Signal to the Nucleus	1	1	1	1	1	1
Ion influx/efflux at host-pathogen interface	1	1	1	1	1	1
NAD de novo biosynthesis	1	1	1	1	1	1
TYROBP Causal Network	1	1	1	1	1	1
Trafficking and processing of endosomal TLR	1	1	1	1	1	1
RNA Polymerase II Transcription Initiation And Promoter Clearance	1	1	1	1	1	1
Other types of O-glycan biosynthesis - Homo sapiens (human)	1	1	1	1	1	1
Regulation of IFNA signaling	1	1	1	1	1	1

Glycosaminoglycan metabolism	1	1	1	1	1	1
Interferon alpha/beta signaling	1	1	1	1	1	1
Nuclear Receptors	1	1	1	1	1	1
bupropion degradation	1	1	1	1	1	1
Loss of Function of TGFBR2 in Cancer	1	1	1	1	1	1
nfat and hypertrophy of the heart	1	1	1	1	1	1
DDX1 as a regulatory component of the Drosha microprocessor	1	1	1	1	1	1
Docetaxel Action Pathway	1	1	1	1	1	1
APC-Cdc20 mediated degradation of Nek2A	1	1	1	1	1	1
vRNP Assembly	1	1	1	1	1	1
Regulation of RUNX3 expression and activity	1	1	1	1	1	1
signaling pathway from g-protein families	1	1	1	1	1	1
Glycine degradation	1	1	1	1	1	1
APC:Cdc20 mediated degradation of cell cycle proteins prior to satisfation of the cell cycle checkpoint	1	1	1	1	1	1
Segawa syndrome	1	1	1	1	1	1
NF-kB is activated and signals survival	1	1	1	1	1	1
NOD1/2 Signaling Pathway	1	1	1	1	1	1
Synthesis of 5-eicosatetraenoic acids	1	1	1	1	1	1
Hyperphenylalaniemia due to guanosine triphosphate cyclohydrolase deficiency	1	1	1	1	1	1
Tyrosine hydroxylase deficiency	1	1	1	1	1	1
Hyperphenylalaninemia due to dhpr-deficiency	1	1	1	1	1	1
Human cytomegalovirus infection - Homo sapiens (human)	1	1	1	1	1	1
Transport of Mature mRNA derived from an Intron-Containing Transcript	1	1	1	1	1	1
Interleukin-12 family signaling	1	1	1	1	1	1
Signaling by MET	1	1	1	1	1	1
Constitutive Signaling by EGFRvIII	1	1	1	1	1	1
Synthesis of 15-eicosatetraenoic acid derivatives	1	1	1	1	1	1
Signal attenuation	1	1	1	1	1	1

Laminin interactions	1	1	1	1	1	1
Mitochondrial Fatty Acid Beta-Oxidation	1	1	1	1	1	1
Synthesis of 12-eicosatetraenoic acid derivatives	1	1	1	1	1	1
CDK-mediated phosphorylation and removal of Cdc6	1	1	1	1	1	1
AUF1 (hnRNP D0) binds and destabilizes mRNA	1	1	1	1	1	1
Pancreas Function	1	1	1	1	1	1
Succinyl CoA: 3-ketoacid CoA transferase deficiency	1	1	1	1	1	1
Influenza Viral RNA Transcription and Replication	1	1	1	1	1	1
Vitamin B1 (thiamin) metabolism	1	1	1	1	1	1
CD28 co-stimulation	1	1	1	1	1	1
methionine degradation	1	1	1	1	1	1
SUMOylation of RNA binding proteins	1	1	1	1	1	1
Cytosolic sensors of pathogen-associated DNA	1	1	1	1	1	1
Phosphatidylinositol signaling system - Homo sapiens (human)	1	1	1	1	1	1
Notch signaling pathway - Homo sapiens (human)	1	1	1	1	1	1
D-myo-inositol (1_4_5)-trisphosphate degradation	1	1	1	1	1	1
CTLA4 inhibitory signaling	1	1	1	1	1	1
Adefovir Dipivoxil Action Pathway	1	1	1	1	1	1
SUMO E3 ligases SUMOylate target proteins	1	1	1	1	1	1
Potassium Channels	1	1	1	1	1	1
Osteoblast Signaling	1	1	1	1	1	1
Export of Viral Ribonucleoproteins from Nucleus	1	1	1	1	1	1
VEGF	1	1	1	1	1	1
tRNA Aminoacylation	1	1	1	1	1	1
Insulin receptor signalling cascade	1	1	1	1	1	1
Carfentanil Action Pathway	1	1	1	1	1	1
Proline catabolism	1	1	1	1	1	1
Interconversion of 2-oxoglutarate and 2-hydroxyglutarate	1	1	1	1	1	1
NADPH regeneration	1	1	1	1	1	1
how progesterone initiates the oocyte maturation	1	1	1	1	1	1

Phospholipid Biosynthesis	1	1	1	1	1	1
Reactions specific to the complex N-glycan synthesis pathway	1	1	1	1	1	1
Adrenoleukodystrophy_ X-linked	1	1	1	1	1	1
er associated degradation (erad) pathway	1	1	1	1	1	1
HDACs deacetylate histones	1	1	1	1	1	1
HuR (ELAVL1) binds and stabilizes mRNA	1	1	1	1	1	1
Endosomal Sorting Complex Required For Transport (ESCRT)	1	1	1	1	1	1
Dectin-2 family	1	1	1	1	1	1
Gastrin	1	1	1	1	1	1
N-glycan antennae elongation in the medial/trans-Golgi	1	1	1	1	1	1
Folate biosynthesis - Homo sapiens (human)	1	1	1	1	1	1
ROBO receptors bind AKAP5	1	1	1	1	1	1
protein kinase a at the centrosome	1	1	1	1	1	1
Assembly of Viral Components at the Budding Site	1	1	1	1	1	1
BMP signaling Dro	1	1	1	1	1	1
alpha-linolenic acid (ALA) metabolism	1	1	1	1	1	1
IL-7	1	1	1	1	1	1
nuclear receptors coordinate the activities of chromatin remodeling complexes and coactivators to facilitate initiation of transcription in carcinoma cells	1	1	1	1	1	1
gata3 participate in activating the th2 cytokine genes expression	1	1	1	1	1	1
Metabolism of Angiotensinogen to Angiotensins	1	1	1	1	1	1
Doxorubicin Metabolism Pathway	1	1	1	1	1	1
Regulation of innate immune responses to cytosolic DNA	1	1	1	1	1	1
alpha-linolenic (omega3) and linoleic (omega6) acid metabolism	1	1	1	1	1	1
Heme degradation	1	1	1	1	1	1
Prostaglandin Leukotriene metabolism	1	1	1	1	1	1
O-linked glycosylation of mucins	1	1	1	1	1	1
Transport of organic anions	1	1	1	1	1	1
Gemcitabine Metabolism Pathway	1	1	1	1	1	1

Pathway_PA165986194 -need delete	1	1	1	1	1	1
HDMs demethylate histones	1	1	1	1	1	1
Signaling by PTK6	1	1	1	1	1	1
MASTL Facilitates Mitotic Progression	1	1	1	1	1	1
Terpenoid backbone biosynthesis - Homo sapiens (human)	1	1	1	1	1	1
RUNX1 regulates transcription of genes involved in differentiation of HSCs	1	1	1	1	1	1
Virus Assembly and Release	1	1	1	1	1	1
RANKL	1	1	1	1	1	1
Fatty acid elongation - Homo sapiens (human)	1	1	1	1	1	1
Dectin-1 mediated noncanonical NF-kB signaling	1	1	1	1	1	1
Signaling by NTRK1 (TRKA)	1	1	1	1	1	1
Activation of Ca-permeable Kainate Receptor	1	1	1	1	1	1
Ionotropic activity of kainate receptors	1	1	1	1	1	1
Taurine and hypotaurine metabolism - Homo sapiens (human)	1	1	1	1	1	1
morphine biosynthesis	1	1	1	1	1	1
wybutosine biosynthesis	1	1	1	1	1	1
Methionine salvage pathway	1	1	1	1	1	1
Osteopontin-mediated events	1	1	1	1	1	1
BMP receptor signaling	1	1	1	1	1	1
Notch-mediated HES/HEY network	1	1	1	1	1	1
Regulation of Ras family activation	1	1	1	1	1	1
Regulation of RAC1 activity	1	1	1	1	1	1
Glucocorticoid receptor regulatory network	1	1	1	1	1	1
ALK1 signaling events	1	1	1	1	1	1
Neurotrophic factor-mediated Trk receptor signaling	1	1	1	1	1	1
Oxygen-dependent asparagine hydroxylation of Hypoxia-inducible Factor Alpha	1	1	1	1	1	1
TNF receptor signaling pathway	1	1	1	1	1	1
Downstream signaling in naïve CD8+ T cells	1	1	1	1	1	1

Fc-epsilon receptor I signaling in mast cells	1	1	1	1	1	1
D-myo-inositol (1_3_4)-trisphosphate biosynthesis	1	1	1	1	1	1
Visual signal transduction: Rods	1	1	1	1	1	1
Netrin-mediated signaling events	1	1	1	1	1	1
N-cadherin signaling events	1	1	1	1	1	1
Fanconi anemia pathway	1	1	1	1	1	1
Endogenous TLR signaling	1	1	1	1	1	1
Signaling events mediated by TCPTP	1	1	1	1	1	1
Primary bile acid biosynthesis - Homo sapiens (human)	1	1	1	1	1	1
Thromboxane A2 receptor signaling	1	1	1	1	1	1
AP-1 transcription factor network	1	1	1	1	1	1
PLK1 signaling events	1	1	1	1	1	1
Noncanonical Wnt signaling pathway	1	1	1	1	1	1
Regulation of p38-alpha and p38-beta	1	1	1	1	1	1
VEGFR3 signaling in lymphatic endothelium	1	1	1	1	1	1
E-cadherin signaling in keratinocytes	1	1	1	1	1	1
Aromatic L-Aminoacid Decarboxylase Deficiency	1	1	1	1	1	1
p38 MAPK signaling pathway	1	1	1	1	1	1
IGF1 pathway	1	1	1	1	1	1
Regulation of Androgen receptor activity	1	1	1	1	1	1
Sumoylation by RanBP2 regulates transcriptional repression	1	1	1	1	1	1
Arf6 signaling events	1	1	1	1	1	1
Plasma membrane estrogen receptor signaling	1	1	1	1	1	1
Hypoxic and oxygen homeostasis regulation of HIF-1-alpha	1	1	1	1	1	1
ATF-2 transcription factor network	1	1	1	1	1	1
FOXM1 transcription factor network	1	1	1	1	1	1
Nongenotropic Androgen signaling	1	1	1	1	1	1
Alpha4 beta1 integrin signaling events	1	1	1	1	1	1
Lactose synthesis	1	1	1	1	1	1
Regulation of IFNG signaling	1	1	1	1	1	1

Validated transcriptional targets of AP1 family members Fra1 and Fra2	1	1	1	1	1	1
Trk receptor signaling mediated by the MAPK pathway	1	1	1	1	1	1
RXR and RAR heterodimerization with other nuclear receptor	1	1	1	1	1	1
Hedgehog signaling events mediated by Gli proteins	1	1	1	1	1	1
ErbB receptor signaling network	1	1	1	1	1	1
ATR signaling pathway	1	1	1	1	1	1
IL6-mediated signaling events	1	1	1	1	1	1
Angiopoietin receptor Tie2-mediated signaling	1	1	1	1	1	1
Endothelins	1	1	1	1	1	1
IL8- and CXCR2-mediated signaling events	1	1	1	1	1	1
FGF signaling pathway	1	1	1	1	1	1
Nephrin/Neph1 signaling in the kidney podocyte	1	1	1	1	1	1
IL3-mediated signaling events	1	1	1	1	1	1
Caffeine metabolism - Homo sapiens (human)	1	1	1	1	1	1
Signaling mediated by p38-gamma and p38-delta	1	1	1	1	1	1
lactose degradation III	1	1	1	1	1	1
Regulation of RhoA activity	1	1	1	1	1	1
Cellular roles of Anthrax toxin	1	1	1	1	1	1
Ubiquitin-dependent degradation of Cyclin D1	1	1	1	1	1	1
Basigin interactions	1	1	1	1	1	1
RMTs methylate histone arginines	1	1	1	1	1	1
M-G1 Transition	1	1	1	1	1	1
Removal of aminoterminal propeptides from gamma-carboxylated proteins	1	1	1	1	1	1
Gamma-carboxylation_ transport_ and amino-terminal cleavage of proteins	1	1	1	1	1	1
Vitamin B2 (riboflavin) metabolism	1	1	1	1	1	1
Collagen degradation	1	1	1	1	1	1
Processing of Intronless Pre-mRNAs	1	1	1	1	1	1
Processing of Capped Intronless Pre-mRNA	1	1	1	1	1	1

serotonin and melatonin biosynthesis	1	1	1	1	1	1
Notch Signaling	1	1	1	1	1	1
GABA receptor Signaling	1	1	1	1	1	1
Carnitine palmitoyl transferase deficiency (I)	1	1	1	1	1	1
Propionyl-CoA catabolism	1	1	1	1	1	1
Mitochondrial Fatty Acid Beta-Oxidation	1	1	1	1	1	1
Synthesis of diphthamide-EEF2	1	1	1	1	1	1
SUMO is conjugated to E1 (UBA2:SAE1)	1	1	1	1	1	1
#NAME?	1	1	1	1	1	1
Formation of ATP by chemiosmotic coupling	1	1	1	1	1	1
Cell adhesion molecules (CAMs) - Homo sapiens (human)	1	1	1	1	1	1
IGF-Core	1	1	1	1	1	1
Phosphate bond hydrolysis by NTPDase proteins	1	1	1	1	1	1
Fatty acids	1	1	1	1	1	1
Fc epsilon receptor (FCERI) signaling	1	1	1	1	1	1
The activation of arylsulfatases	1	1	1	1	1	1
RUNX2 regulates osteoblast differentiation	1	1	1	1	1	1
Collagen degradation	1	1	1	1	1	1
Splicing factor NOVA regulated synaptic proteins	1	1	1	1	1	1
Synthesis of epoxy (EET) and dihydroxyeicosatrienoic acids (DHET)	1	1	1	1	1	1
Riboflavin metabolism - Homo sapiens (human)	1	1	1	1	1	1
BCR signaling pathway	1	1	1	1	1	1
TGF-Core	1	1	1	1	1	1
Amplification of signal from unattached kinetochores via a MAD2 inhibitory signal	1	1	1	1	1	1
Amplification of signal from the kinetochores	1	1	1	1	1	1
EGF-Ncore	1	1	1	1	1	1
HDL clearance	1	1	1	1	1	1
NEP/NS2 Interacts with the Cellular Export Machinery	1	1	1	1	1	1
Chylomicron clearance	1	1	1	1	1	1

Acyl chain remodeling of DAG and TAG	1	1	1	1	1	1
Gastric cancer - Homo sapiens (human)	1	1	1	1	1	1
Alpha-oxidation of phytanate	1	1	1	1	1	1
Interleukin-12 signaling	1	1	1	1	1	1
Mitotic Spindle Checkpoint	1	1	1	1	1	1
Alternative complement activation	1	1	1	1	1	1
RAF-independent MAPK1/3 activation	1	1	1	1	1	1
Uptake and actions of bacterial toxins	1	1	1	1	1	1
Parathyroid hormone synthesis_ secretion and action - Homo sapiens (human)	1	1	1	1	1	1
Regulation of Hypoxia-inducible Factor (HIF) by oxygen	1	1	1	1	1	1
PCNA-Dependent Long Patch Base Excision Repair	1	1	1	1	1	1
TNFR2 non-canonical NF-kB pathway	1	1	1	1	1	1
Phosphonate and phosphinate metabolism - Homo sapiens (human)	1	1	1	1	1	1
Signaling by FGFR1	1	1	1	1	1	1
Sphingolipid metabolism - Homo sapiens (human)	1	1	1	1	1	1
NOSTRIN mediated eNOS trafficking	1	1	1	1	1	1
Relaxin signaling pathway - Homo sapiens (human)	1	1	1	1	1	1
sorbitol degradation I	1	1	1	1	1	1
Fluoxetine Action Pathway	1	1	1	1	1	1
Metabolism of nitric oxide	1	1	1	1	1	1
Apoptotic cleavage of cell adhesion proteins	1	1	1	1	1	1
phenylalanine degradation/tyrosine biosynthesis	1	1	1	1	1	1
Beta-oxidation of very long chain fatty acids	1	1	1	1	1	1
the igf-1 receptor and longevity	1	1	1	1	1	1
NAD+ biosynthetic pathways	1	1	1	1	1	1
Abacavir transmembrane transport	1	1	1	1	1	1
ARMS-mediated activation	1	1	1	1	1	1
Prolonged ERK activation events	1	1	1	1	1	1
Synthesis of Lipoxins (LX)	1	1	1	1	1	1

RHO GTPases activate PAKs	1	1	1	1	1	1
Dual Incision in GG-NER	1	1	1	1	1	1
African trypanosomiasis - Homo sapiens (human)	1	1	1	1	1	1
Antimicrobial peptides	1	1	1	1	1	1
Cobalamin (Cbl_ vitamin B12) transport and metabolism	1	1	1	1	1	1
Nuclear Receptor transcription pathway	1	1	1	1	1	1
Abacavir transport and metabolism	1	1	1	1	1	1
Pyrophosphate hydrolysis	1	1	1	1	1	1
O2/CO2 exchange in erythrocytes	1	1	1	1	1	1
Collagen biosynthesis and modifying enzymes	1	1	1	1	1	1
Regulation of cytoplasmic and nuclear SMAD2/3 signaling	1	1	1	1	1	1
Biosynthesis of E-series 18(S)-resolvins	1	1	1	1	1	1
Metabolism of water-soluble vitamins and cofactors	1	1	1	1	1	1
Vitamin B2 (riboflavin) metabolism	1	1	1	1	1	1
Activation of DNA fragmentation factor	1	1	1	1	1	1
Apoptosis induced DNA fragmentation	1	1	1	1	1	1
Inhibition of replication initiation of damaged DNA by RB1/E2F1	1	1	1	1	1	1
Retrograde neurotrophin signalling	1	1	1	1	1	1
Desipramine Action Pathway	1	1	1	1	1	1
Binding and entry of HIV virion	1	1	1	1	1	1
Biosynthesis of E-series 18(R)-resolvins	1	1	1	1	1	1
Biosynthesis of EPA-derived SPMs	1	1	1	1	1	1
Xenobiotics metabolism	1	1	1	1	1	1
Axonal growth inhibition (RHOA activation)	1	1	1	1	1	1
VLDL clearance	1	1	1	1	1	1
nicotine degradation IV	1	1	1	1	1	1
Regulation of RAS by GAPs	1	1	1	1	1	1
ras-independent pathway in nk cell-mediated cytotoxicity	1	1	1	1	1	1
Gastric acid production	1	1	1	1	1	1
glycine cleavage	1	1	1	1	1	1

Molecules associated with elastic fibres	1	1	1	1	1	1
PLC beta mediated events	1	1	1	1	1	1
creatine-phosphate biosynthesis	1	1	1	1	1	1
Apoptosis Modulation and Signaling	1	1	1	1	1	1
Epstein-Barr virus infection - Homo sapiens (human)	1	1	1	1	1	1
Trafficking of AMPA receptors	1	1	1	1	1	1
Biosynthesis of D-series resolvins	1	1	1	1	1	1
Signaling by FGFR	1	1	1	1	1	1
Cholesterol biosynthesis	1	1	1	1	1	1
RNA Polymerase II Transcription	1	1	1	1	1	1
Gap-filling DNA repair synthesis and ligation in GG-NER	1	1	1	1	1	1
Arylamine metabolism	1	1	1	1	1	1
Syndecan-4-mediated signaling events	1	1	1	1	1	1
Biosynthesis of aspirin-triggered D-series resolvins	1	1	1	1	1	1
pyruvate decarboxylation to acetyl CoA	1	1	1	1	1	1
Benzo(a)pyrene metabolism	1	1	1	1	1	1
Transcriptional regulation of white adipocyte differentiation	1	1	1	1	1	1
Monoamine Transport	1	1	1	1	1	1
adenosine nucleotides degradation	1	1	1	1	1	1
regulation of cell cycle progression by plk3	1	1	1	1	1	1
EPH-Ephrin signaling	1	1	1	1	1	1
Biosynthesis of protectins	1	1	1	1	1	1
Ion homeostasis	1	1	1	1	1	1
Fatty Acid Beta Oxidation	1	1	1	1	1	1
Elastic fibre formation	1	1	1	1	1	1
Nucleotide-binding Oligomerization Domain (NOD) pathway	1	1	1	1	1	1
APC/C:Cdc20 mediated degradation of Cyclin B	1	1	1	1	1	1
PKA activation	1	1	1	1	1	1
PKA-mediated phosphorylation of CREB	1	1	1	1	1	1
Syndecan interactions	1	1	1	1	1	1

Class C-3 (Metabotropic glutamate-pheromone receptors)	1	1	1	1	1	1
APC/C:Cdc20 mediated degradation of Securin	1	1	1	1	1	1
Vitamin D Metabolism	1	1	1	1	1	1
G alpha (s) signalling events	1	1	1	1	1	1
Fanconi Anemia Pathway	1	1	1	1	1	1
guanosine nucleotides degradation	1	1	1	1	1	1
Calmodulin induced events	1	1	1	1	1	1
CaM pathway	1	1	1	1	1	1
Presynaptic function of Kainate receptors	1	1	1	1	1	1
Activation of kainate receptors upon glutamate binding	1	1	1	1	1	1
Resolution of Abasic Sites (AP sites)	1	1	1	1	1	1
Hypothetical Craniofacial Development Pathway	1	1	1	1	1	1
Clathrin-mediated endocytosis	1	1	1	1	1	1
SMAD2/SMAD3:SMAD4 heterotrimer regulates transcription	1	1	1	1	1	1
role of nicotinic acetylcholine receptors in the regulation of apoptosis	1	1	1	1	1	1
Formation of TC-NER Pre-Incision Complex	1	1	1	1	1	1
Biosynthesis of maresin conjugates in tissue regeneration (MCTR)	1	1	1	1	1	1
Synthesis of bile acids and bile salts	1	1	1	1	1	1
Fluoropyrimidine Activity	1	1	1	1	1	1
Type 2 papillary renal cell carcinoma	1	1	1	1	1	1
purine nucleotides degradation	1	1	1	1	1	1
Biosynthesis of maresins	1	1	1	1	1	1
Biotin metabolism - Homo sapiens (human)	1	1	1	1	1	1
D-Arginine and D-ornithine metabolism - Homo sapiens (human)	1	1	1	1	1	1
Biosynthesis of protectin and resolvin conjugates in tissue regeneration (PCTR and RCTR)	1	1	1	1	1	1
Biosynthesis of DHA-derived sulfido conjugates	1	1	1	1	1	1
DAP12 interactions	1	1	1	1	1	1
ahr signal transduction pathway	1	1	1	1	1	1
mets affect on macrophage differentiation	1	1	1	1	1	1

phospholipase c-epsilon pathway	1	1	1	1	1	1
roles of arrestin dependent recruitment of src kinases in gpcr signaling	1	1	1	1	1	1
g-protein signaling through tubby proteins	1	1	1	1	1	1
activation of pkc through g-protein coupled receptors	1	1	1	1	1	1
Recycling of bile acids and salts	1	1	1	1	1	1
akap95 role in mitosis and chromosome dynamics	1	1	1	1	1	1
tnfr1 signaling pathway	1	1	1	1	1	1
alternative complement pathway	1	1	1	1	1	1
cyclin e destruction pathway	1	1	1	1	1	1
repression of pain sensation by the transcriptional regulator dream	1	1	1	1	1	1
Regulation of lipolysis in adipocytes - Homo sapiens (human)	1	1	1	1	1	1
B cell receptor signaling pathway - Homo sapiens (human)	1	1	1	1	1	1
Sulfur relay system - Homo sapiens (human)	1	1	1	1	1	1
Inositol transporters	1	1	1	1	1	1
p53 signaling pathway - Homo sapiens (human)	1	1	1	1	1	1
Circadian rhythm - Homo sapiens (human)	1	1	1	1	1	1
Penbutolol Action Pathway	1	1	1	1	1	1
thrombin signaling and protease-activated receptors	1	1	1	1	1	1
antigen processing and presentation	1	1	1	1	1	1
Leishmaniasis - Homo sapiens (human)	1	1	1	1	1	1
transcriptional activation of dbpb from mrna	1	1	1	1	1	1
Adrenaline_noradrenaline inhibits insulin secretion	1	1	1	1	1	1
rac1 cell motility signaling pathway	1	1	1	1	1	1
Surfactant metabolism	1	1	1	1	1	1
Melanogenesis - Homo sapiens (human)	1	1	1	1	1	1
Chemokine signaling pathway - Homo sapiens (human)	1	1	1	1	1	1
Intestinal immune network for IgA production - Homo sapiens (human)	1	1	1	1	1	1
Synthesis of PC	1	1	1	1	1	1
Melanoma - Homo sapiens (human)	1	1	1	1	1	1
Renal cell carcinoma - Homo sapiens (human)	1	1	1	1	1	1

Nicotine addiction - Homo sapiens (human)	1	1	1	1	1	1
GnRH signaling pathway - Homo sapiens (human)	1	1	1	1	1	1
Kaposi sarcoma-associated herpesvirus infection - Homo sapiens (human)	1	1	1	1	1	1
Amine ligand-binding receptors	1	1	1	1	1	1
Butanoate metabolism	1	1	1	1	1	1
RANKL-RANK (Receptor activator of NFKB (ligand)) Signaling Pathway	1	1	1	1	1	1
Nuclear Events (kinase and transcription factor activation)	1	1	1	1	1	1
S-methyl-5_-thioadenosine degradation	1	1	1	1	1	1
Inactivation of CDC42 and RAC1	1	1	1	1	1	1
Cleavage of the damaged pyrimidine	1	1	1	1	1	1
Depyrimidination	1	1	1	1	1	1
Base-Excision Repair_ AP Site Formation	1	1	1	1	1	1
Amyloid fiber formation	1	1	1	1	1	1
RUNX1 regulates genes involved in megakaryocyte differentiation and platelet function	1	1	1	1	1	1
Mitophagy	1	1	1	1	1	1
Processing and activation of SUMO	1	1	1	1	1	1
Buprenorphine Action Pathway	1	1	1	1	1	1
Nucleobase biosynthesis	1	1	1	1	1	1
Molybdenum cofactor biosynthesis	1	1	1	1	1	1
Degradation of DVL	1	1	1	1	1	1
NCAM signaling for neurite out-growth	1	1	1	1	1	1
Cargo concentration in the ER	1	1	1	1	1	1
ketolysis	1	1	1	1	1	1
Alvimopan Action Pathway	1	1	1	1	1	1
Downregulation of ERBB4 signaling	1	1	1	1	1	1
Gap-filling DNA repair synthesis and ligation in TC-NER	1	1	1	1	1	1
Hydroxycarboxylic acid-binding receptors	1	1	1	1	1	1
Utilization of Ketone Bodies	1	1	1	1	1	1
Ketone body metabolism	1	1	1	1	1	1

Lysosphingolipid and LPA receptors	1	1	1	1	1	1
Synaptic adhesion-like molecules	1	1	1	1	1	1
Intra-Golgi and retrograde Golgi-to-ER traffic	1	1	1	1	1	1
Transcription-Coupled Nucleotide Excision Repair (TC-NER)	1	1	1	1	1	1
Initiation of Nuclear Envelope Reformation	1	1	1	1	1	1
27-Hydroxylase Deficiency	1	1	1	1	1	1
Abasic sugar-phosphate removal via the single-nucleotide replacement pathway	1	1	1	1	1	1
Resolution of AP sites via the single-nucleotide replacement pathway	1	1	1	1	1	1
Opioid Signalling	1	1	1	1	1	1
Disassembly of the destruction complex and recruitment of AXIN to the membrane	1	1	1	1	1	1
Mitotic Prometaphase	1	1	1	1	1	1
VEGFR2 mediated vascular permeability	1	1	1	1	1	1
Antigen processing-Cross presentation	1	1	1	1	1	1
Signaling by NOTCH3	1	1	1	1	1	1
NADPH regeneration	1	1	1	1	1	1
Constitutive Signaling by NOTCH1 HD Domain Mutants	1	1	1	1	1	1
Erythrocytes take up oxygen and release carbon dioxide	1	1	1	1	1	1
Spry regulation of FGF signaling	1	1	1	1	1	1
Choline catabolism	1	1	1	1	1	1
DNA Damage Reversal	1	1	1	1	1	1
Transcriptional regulation by small RNAs	1	1	1	1	1	1
Regulation of FZD by ubiquitination	1	1	1	1	1	1
Activation of Matrix Metalloproteinases	1	1	1	1	1	1
Signaling by NOTCH1 HD Domain Mutants in Cancer	1	1	1	1	1	1
Host Interactions with Influenza Factors	1	1	1	1	1	1
Eukaryotic Translation Termination	1	1	1	1	1	1
APEX1-Independent Resolution of AP Sites via the Single Nucleotide Replacement Pathway	1	1	1	1	1	1

hypoxia and p53 in the cardiovascular system	1	1	1	1	1	1
JNK signaling in the CD4+ TCR pathway	1	1	1	1	1	1
Interferon gamma signaling	1	1	1	1	1	1
APOBEC3G mediated resistance to HIV-1 infection	1	1	1	1	1	1
Influenza Life Cycle	1	1	1	1	1	1
Peptide hormone metabolism	1	1	1	1	1	1
Hedgehog	1	1	1	1	1	1
Abnormal conversion of 2-oxoglutarate to 2-hydroxyglutarate	1	1	1	1	1	1
PIP3 activates AKT signaling	1	1	1	1	1	1
Diseases of metabolism	1	1	1	1	1	1
JAK-STAT signaling pathway - Homo sapiens (human)	1	1	1	1	1	1
multi-drug resistance factors	1	1	1	1	1	1
Effects of Nitric Oxide	1	1	1	1	1	1
PDGF	1	1	1	1	1	1
Tetrahydrobiopterin (BH4) synthesis_ recycling_ salvage and regulation	1	1	1	1	1	1
Rapoport-Luebering glycolytic shunt	1	1	1	1	1	1
MTF1 activates gene expression	1	1	1	1	1	1
Response to metal ions	1	1	1	1	1	1
Chromatin organization	1	1	1	1	1	1
5-Phosphoribose 1-diphosphate biosynthesis	1	1	1	1	1	1
skeletal muscle hypertrophy is regulated via akt-mtor pathway	1	1	1	1	1	1
Ubiquitin-dependent degradation of Cyclin D	1	1	1	1	1	1
Class C/3 (Metabotropic glutamate/pheromone receptors)	1	1	1	1	1	1
Fatty Acid Omega Oxidation	1	1	1	1	1	1
3-phosphoinositide biosynthesis	1	1	1	1	1	1
Metalloprotease DUBs	1	1	1	1	1	1
actions of nitric oxide in the heart	1	1	1	1	1	1
Striated Muscle Contraction	1	1	1	1	1	1
Abacavir transport and metabolism	1	1	1	1	1	1
heme degradation	1	1	1	1	1	1

S1P4 pathway	1	1	1	1	1	1
Signaling by Retinoic Acid	1	1	1	1	1	1
sumoylation as a mechanism to modulate ctbp-dependent gene responses	1	1	1	1	1	1
Synthesis And Processing Of GAG_ GAGPOL Polyproteins	1	1	1	1	1	1
D-myo-inositol (1_4_5)-trisphosphate biosynthesis	1	1	1	1	1	1
GPVI-mediated activation cascade	1	1	1	1	1	1
GDP-fucose biosynthesis	1	1	1	1	1	1
Viral Acute Myocarditis	1	1	1	1	1	1
VLDLR internalisation and degradation	1	1	1	1	1	1
catecholamine biosynthesis	1	1	1	1	1	1
glycogenolysis	1	1	1	1	1	1
Activated PKN1 stimulates transcription of AR (androgen receptor) regulated genes KLK2 and KLK3	1	1	1	1	1	1
Adrenaline signalling through Alpha-2 adrenergic receptor	1	1	1	1	1	1
Resolution of AP sites via the multiple-nucleotide patch replacement pathway	1	1	1	1	1	1
Resolution of Abasic Sites (AP sites)	1	1	1	1	1	1
Disorders of Folate Metabolism and Transport	1	1	1	1	1	1
Signaling by Ligand-Responsive EGFR Variants in Cancer	1	1	1	1	1	1
Alpha6 beta4 integrin-ligand interactions	1	1	1	1	1	1
Deactivation of the beta-catenin transactivating complex	1	1	1	1	1	1
Effects of PIP2 hydrolysis	1	1	1	1	1	1
Response to elevated platelet cytosolic Ca2+	1	1	1	1	1	1
CRMPs in Sema3A signaling	1	1	1	1	1	1
InlB-mediated entry of Listeria monocytogenes into host cell	1	1	1	1	1	1
RAF-MAP kinase cascade	1	1	1	1	1	1
Phase 2 - plateau phase	1	1	1	1	1	1
ethanol degradation II	1	1	1	1	1	1
Downregulation of ERBB2:ERBB3 signaling	1	1	1	1	1	1

RHO GTPases activate KTN1	1	1	1	1	1	1
Organic cation transport	1	1	1	1	1	1
Signaling by TGF-beta Receptor Complex	1	1	1	1	1	1
NOTCH2 Activation and Transmission of Signal to the Nucleus	1	1	1	1	1	1
Glycosaminoglycan metabolism	1	1	1	1	1	1
Termination of O-glycan biosynthesis	1	1	1	1	1	1
Linoleic acid (LA) metabolism	1	1	1	1	1	1
D-myo-inositol (1_4_5_6)-tetrakisphosphate biosynthesis	1	1	1	1	1	1
Cyclin A/B1/B2 associated events during G2/M transition	1	1	1	1	1	1
RUNX1 regulates transcription of genes involved in differentiation of myeloid cells	1	1	1	1	1	1
trefoil factors initiate mucosal healing	1	1	1	1	1	1
Fanconi anemia pathway - Homo sapiens (human)	1	1	1	1	1	1
lipoate biosynthesis and incorporation	1	1	1	1	1	1
Inflammatory mediator regulation of TRP channels - Homo sapiens (human)	1	1	1	1	1	1
cell to cell adhesion signaling	1	1	1	1	1	1
DARPP-32 events	1	1	1	1	1	1
classical complement pathway	1	1	1	1	1	1
Activation of Na-permeable kainate receptors	1	1	1	1	1	1
Assembly of the primary cilium	1	1	1	1	1	1
Ribosome biogenesis in eukaryotes - Homo sapiens (human)	1	1	1	1	1	1
Synthesis of PI	1	1	1	1	1	1
CDO in myogenesis	1	1	1	1	1	1
Myogenesis	1	1	1	1	1	1
Synthesis of Dolichyl-phosphate	1	1	1	1	1	1
IL2	1	1	1	1	1	1
Aurora A signaling	1	1	1	1	1	1
Neural Crest Differentiation	1	1	1	1	1	1
GPCR Adenosine A2A receptor	1	1	1	1	1	1

Cytokine-cytokine receptor interaction - Homo sapiens (human)	1	1	1	1	1	1
Interleukin-23 signaling	1	1	1	1	1	1
TGFBR2 Kinase Domain Mutants in Cancer	1	1	1	1	1	1
regulation of p27 phosphorylation during cell cycle progression	1	1	1	1	1	1
Frs2-mediated activation	1	1	1	1	1	1
lissencephaly gene (lis1) in neuronal migration and development	1	1	1	1	1	1
PTK6 Regulates RTKs and Their Effectors AKT1 and DOK1	1	1	1	1	1	1
Synthesis of UDP-N-acetyl-glucosamine	1	1	1	1	1	1
Visual signal transduction: Cones	1	1	1	1	1	1
Long-term potentiation - Homo sapiens (human)	1	1	1	1	1	1
lectin induced complement pathway	1	1	1	1	1	1
Rap1 signalling	1	1	1	1	1	1
Hedgehog _on_ state	1	1	1	1	1	1
RalA downstream regulated genes	1	1	1	1	1	1
Signalling to ERKs	1	1	1	1	1	1
Recognition of DNA damage by PCNA-containing replication complex	1	1	1	1	1	1
DNA Damage Response (only ATM dependent)	1	1	1	1	1	1
regulation of pgc-1a	1	1	1	1	1	1
Refsum Disease	1	1	1	1	1	1
Non-alcoholic fatty liver disease (NAFLD) - Homo sapiens (human)	1	1	1	1	1	1
tRNA processing in the nucleus	1	1	1	1	1	1
Asymmetric localization of PCP proteins	1	1	1	1	1	1
TAK1 activates NFkB by phosphorylation and activation of IKKs complex	1	1	1	1	1	1
ERK/MAPK targets	1	1	1	1	1	1
JNK (c-Jun kinases) phosphorylation and activation mediated by activated human TAK1	1	1	1	1	1	1
il-2 receptor beta chain in t cell activation	1	1	1	1	1	1
Viral myocarditis - Homo sapiens (human)	1	1	1	1	1	1
Renin-angiotensin system - Homo sapiens (human)	1	1	1	1	1	1
Cellular hexose transport	1	1	1	1	1	1

Type I diabetes mellitus - Homo sapiens (human)	1	1	1	1	1	1
Small cell lung cancer - Homo sapiens (human)	1	1	1	1	1	1
WNT5A-dependent internalization of FZD4	1	1	1	1	1	1
activated TAK1 mediates p38 MAPK activation	1	1	1	1	1	1
ras signaling pathway	1	1	1	1	1	1
GPCR signaling-G alpha i	1	1	1	1	1	1
Cytochrome P450 - arranged by substrate type	1	1	1	1	1	1
Synthesis of PIPs at the ER membrane	1	1	1	1	1	1
CHL1 interactions	1	1	1	1	1	1
Nef mediated downregulation of MHC class I complex cell surface expression	1	1	1	1	1	1
cdc25 and chk1 regulatory pathway in response to dna damage	1	1	1	1	1	1
SUMOylation	1	1	1	1	1	1
tRNA processing in the nucleus	1	1	1	1	1	1
HIV Life Cycle	1	1	1	1	1	1
RUNX2 regulates bone development	1	1	1	1	1	1
Ras signaling pathway - Homo sapiens (human)	1	1	1	1	1	1
GPCR signaling-G alpha q	1	1	1	1	1	1
role of mef2d in t-cell apoptosis	1	1	1	1	1	1
PI Metabolism	1	1	1	1	1	1
Breast cancer - Homo sapiens (human)	1	1	1	1	1	1
adp-ribosylation factor	1	1	1	1	1	1
Golgi Cisternae Pericentriolar Stack Reorganization	1	1	1	1	1	1
ErbB signaling pathway - Homo sapiens (human)	1	1	1	1	1	1
Interleukin-11 Signaling Pathway	1	1	1	1	1	1
Cell-cell junction organization	1	1	1	1	1	1
control of skeletal myogenesis by hdac and calcium/calmodulin-dependent kinase (camk)	1	1	1	1	1	1
TRAF6 mediated IRF7 activation in TLR7/8 or 9 signaling	1	1	1	1	1	1
Sema4D mediated inhibition of cell attachment and migration	1	1	1	1	1	1

GPCR signaling-G alpha s Epac and ERK	1	1	1	1	1	1
Mitochondrial translation initiation	1	1	1	1	1	1
il-10 anti-inflammatory signaling pathway	1	1	1	1	1	1
D-myo-inositol-5-phosphate metabolism	1	1	1	1	1	1
Progressive trimming of alpha-1_2-linked mannose residues from Man9/8/7GlcNAc2 to produce Man5GlcNAc2	1	1	1	1	1	1
N-glycan trimming and elongation in the cis-Golgi	1	1	1	1	1	1
CLEC7A (Dectin-1) signaling	1	1	1	1	1	1
GPCR signaling-cholera toxin	1	1	1	1	1	1
platelet amyloid precursor protein pathway	1	1	1	1	1	1
putrescine biosynthesis II	1	1	1	1	1	1
Receptor-ligand binding initiates the second proteolytic cleavage of Notch receptor	1	1	1	1	1	1
MAPK targets/ Nuclear events mediated by MAP kinases	1	1	1	1	1	1
multiple antiapoptotic pathways from igf-1r signaling lead to bad phos-phorylation	1	1	1	1	1	1
Deadenylation-dependent mRNA decay	1	1	1	1	1	1
Synthesis of IP3 and IP4 in the cytosol	1	1	1	1	1	1
Energy dependent regulation of mTOR by LKB1-AMPK	1	1	1	1	1	1
Adenylate cyclase inhibitory pathway	1	1	1	1	1	1
Inhibition of adenylate cyclase pathway	1	1	1	1	1	1
Transport of nucleosides and free purine and pyrimidine bases across the plasma membrane	1	1	1	1	1	1
Codeine Action Pathway	1	1	1	1	1	1
Base excision repair - Homo sapiens (human)	1	1	1	1	1	1
activation of csk by camp-dependent protein kinase inhibits signaling through the t cell receptor	1	1	1	1	1	1
Congenital Bile Acid Synthesis Defect Type II	1	1	1	1	1	1
role of -arrestins in the activation and targeting of map kinases	1	1	1	1	1	1
DNA Replication Pre-Initiation	1	1	1	1	1	1
D-myo-inositol (3_4_5_6)-tetrakisphosphate biosynthesis	1	1	1	1	1	1

1D-myo-inositol hexakisphosphate biosynthesis II (mammalian)	1	1	1	1	1	1
west nile virus	1	1	1	1	1	1
Gastric Cancer Network 2	1	1	1	1	1	1
basic mechanisms of sumoylation	1	1	1	1	1	1
Eicosanoid Synthesis	1	1	1	1	1	1
ErbB2/ErbB3 signaling events	1	1	1	1	1	1
Formyl peptide receptors bind formyl peptides and many other ligands	1	1	1	1	1	1
Deadenylation of mRNA	1	1	1	1	1	1
SEMA3A-Plexin repulsion signaling by inhibiting Integrin adhesion	1	1	1	1	1	1
tgf beta signaling pathway	1	1	1	1	1	1
Arachidonate production from DAG	1	1	1	1	1	1
dopamine degradation	1	1	1	1	1	1
Dual incision in TC-NER	1	1	1	1	1	1
GPCR signaling-pertussis toxin	1	1	1	1	1	1
anandamide degradation	1	1	1	1	1	1
triacylglycerol biosynthesis	1	1	1	1	1	1
Tamoxifen Metabolism Pathway	1	1	1	1	1	1
gamma-aminobutyric acid receptor life cycle pathway	1	1	1	1	1	1
PAR4-mediated thrombin signaling events	1	1	1	1	1	1
Apelin signaling pathway - Homo sapiens (human)	1	1	1	1	1	1
map kinase inactivation of smrt corepressor	1	1	1	1	1	1
d4gdi signaling pathway	1	1	1	1	1	1
Sphingolipid signaling pathway - Homo sapiens (human)	1	1	1	1	1	1
methylglyoxal degradation I	1	1	1	1	1	1
Synthesis of pyrophosphates in the cytosol	1	1	1	1	1	1
C-type lectin receptor signaling pathway - Homo sapiens (human)	1	1	1	1	1	1
e2f1 destruction pathway	1	1	1	1	1	1
Sodium-coupled sulphate_ di- and tri-carboxylate transporters	1	1	1	1	1	1
Validated nuclear estrogen receptor beta network	1	1	1	1	1	1
Synthesis of IPs in the ER lumen	1	1	1	1	1	1

CD40/CD40L signaling	1	1	1	1	1	1
Signaling by EGFR	1	1	1	1	1	1
GAB1 signalosome	1	1	1	1	1	1
deregulation of cdk5 in alzheimers disease	1	1	1	1	1	1
Intra-Golgi traffic	1	1	1	1	1	1
superpathway of D-myo-inositol (1_4_5)-trisphosphate metabolism	1	1	1	1	1	1
Catecholamine biosynthesis	1	1	1	1	1	1
2_-deoxy-α-D-ribose 1-phosphate degradation	1	1	1	1	1	1
Salivary secretion - Homo sapiens (human)	1	1	1	1	1	1
guanine and guanosine salvage	1	1	1	1	1	1
Signaling by PDGF	1	1	1	1	1	1
Scavenging by Class H Receptors	1	1	1	1	1	1
Metabolism of non-coding RNA	1	1	1	1	1	1
attenuation of gpcr signaling	1	1	1	1	1	1
Carboxyterminal post-translational modifications of tubulin	1	1	1	1	1	1
Endosomal Sorting Complex Required For Transport (ESCRT)	1	1	1	1	1	1
metabolism of anandamide an endogenous cannabinoid	1	1	1	1	1	1
Methadyl Acetate Action Pathway	1	1	1	1	1	1
the information processing pathway at the ifn beta enhancer	1	1	1	1	1	1
Cardiac muscle contraction - Homo sapiens (human)	1	1	1	1	1	1
Adrenergic signaling in cardiomyocytes - Homo sapiens (human)	1	1	1	1	1	1
CD28 dependent Vav1 pathway	1	1	1	1	1	1
PTEN Regulation	1	1	1	1	1	1
Phospholipase D signaling pathway - Homo sapiens (human)	1	1	1	1	1	1
Glutamate Neurotransmitter Release Cycle	1	1	1	1	1	1
NRIF signals cell death from the nucleus	1	1	1	1	1	1
PKMTs methylate histone lysines	1	1	1	1	1	1
Nef Mediated CD4 Down-regulation	1	1	1	1	1	1
ABC-family proteins mediated transport	1	1	1	1	1	1

rb tumor suppressor/checkpoint signaling in response to dna damage	1	1	1	1	1	1
NS1 Mediated Effects on Host Pathways	1	1	1	1	1	1
ECM proteoglycans	1	1	1	1	1	1
Activation of the pre-replicative complex	1	1	1	1	1	1
PTK6 Down-Regulation	1	1	1	1	1	1
Signaling by FGFR1	1	1	1	1	1	1
Bile acid and bile salt metabolism	1	1	1	1	1	1
Activation of GABAB receptors	1	1	1	1	1	1
Retinoic acid receptors-mediated signaling	1	1	1	1	1	1
Mitochondrial translation elongation	1	1	1	1	1	1
Serotonin and melatonin biosynthesis	1	1	1	1	1	1
Adrenoceptors	1	1	1	1	1	1
APC/C:Cdh1 mediated degradation of Cdc20 and other APC/C:Cdh1 targeted proteins in late mitosis/early G1	1	1	1	1	1	1
Condensation of Prophase Chromosomes	1	1	1	1	1	1
MicroRNAs in cancer - Homo sapiens (human)	1	1	1	1	1	1
Negative regulation of MET activity	1	1	1	1	1	1
PTK6 Regulates RHO GTPases_ RAS GTPase and MAP kinases	1	1	1	1	1	1
Signaling by Non-Receptor Tyrosine Kinases	1	1	1	1	1	1
internal ribosome entry pathway	1	1	1	1	1	1
E2F mediated regulation of DNA replication	1	1	1	1	1	1
Synthesis of PIPs at the Golgi membrane	1	1	1	1	1	1
Vitamin D (calciferol) metabolism	1	1	1	1	1	1
Longevity regulating pathway - Homo sapiens (human)	1	1	1	1	1	1
Cytosine methylation	1	1	1	1	1	1
Glucocorticoid Receptor Pathway	1	1	1	1	1	1
Regulation of TP53 Activity through Phosphorylation	1	1	1	1	1	1
purine deoxyribonucleosides degradation	1	1	1	1	1	1
Signaling by Retinoic Acid	1	1	1	1	1	1
Phosphatidylinositol Phosphate Metabolism	1	1	1	1	1	1

Protein export - Homo sapiens (human)	1	1	1	1	1	1
Ether lipid metabolism - Homo sapiens (human)	1	1	1	1	1	1
phenylethylamine degradation I	1	1	1	1	1	1
Association Between Physico-Chemical Features and Toxicity Associated Pathways	1	1	1	1	1	1
GABA synthesis	1	1	1	1	1	1
Reuptake of GABA	1	1	1	1	1	1
Beta-catenin phosphorylation cascade	1	1	1	1	1	1
Depolymerisation of the Nuclear Lamina	1	1	1	1	1	1
Autodegradation of the E3 ubiquitin ligase COP1	1	1	1	1	1	1
Glibenclamide Action Pathway	1	1	1	1	1	1
Stabilization of p53	1	1	1	1	1	1
homocarnosine biosynthesis	1	1	1	1	1	1
Phytochemical activity on NRF2 transcriptional activation	1	1	1	1	1	1
Selenocompound metabolism - Homo sapiens (human)	1	1	1	1	1	1
Kit receptor signaling pathway	1	1	1	1	1	1
p53-Dependent G1 DNA Damage Response	1	1	1	1	1	1
Axonal growth stimulation	1	1	1	1	1	1
Wnt signaling pathway - Homo sapiens (human)	1	1	1	1	1	1
Cardiac Progenitor Differentiation	1	1	1	1	1	1
p53-Dependent G1/S DNA damage checkpoint	1	1	1	1	1	1
putrescine degradation III	1	1	1	1	1	1
Enzymatic degradation of dopamine by COMT	1	1	1	1	1	1
adenine and adenosine salvage III	1	1	1	1	1	1
Electron Transport Chain (OXPHOS system in mitochondria)	1	1	1	1	1	1
Enzymatic degradation of Dopamine by monoamine oxidase	1	1	1	1	1	1
Dopamine clearance from the synaptic cleft	1	1	1	1	1	1
Aromatase Inhibitor Pathway (Multiple Tissues)_ Pharmacodynamics	1	1	1	1	1	1
Metabolism of serotonin	1	1	1	1	1	1
Serotonin clearance from the synaptic cleft	1	1	1	1	1	1

Sodium-coupled phosphate cotransporters	1	1	1	1	1	1
miR-517 relationship with ARCN1 and USP1	1	1	1	1	1	1
Ubiquitin Mediated Degradation of Phosphorylated Cdc25A	1	1	1	1	1	1
Transport of Mature Transcript to Cytoplasm	1	1	1	1	1	1
Condensation of Prometaphase Chromosomes	1	1	1	1	1	1
Ca2+ pathway	1	1	1	1	1	1
eukaryotic protein translation	1	1	1	1	1	1
Phenytoin Pathway_ Pharmacokinetics	1	1	1	1	1	1
Circadian entrainment - Homo sapiens (human)	1	1	1	1	1	1
ethanol degradation IV	1	1	1	1	1	1
Signaling by NOTCH2	1	1	1	1	1	1
Ras activation upon Ca2+ influx through NMDA receptor	1	1	1	1	1	1
Thermogenesis - Homo sapiens (human)	1	1	1	1	1	1
Regulation of expression of SLITs and ROBOs	1	1	1	1	1	1
CREB phosphorylation through the activation of Ras	1	1	1	1	1	1
TRP channels	1	1	1	1	1	1
propionyl-CoA degradation	1	1	1	1	1	1
2-oxobutanoate degradation	1	1	1	1	1	1
7-(3-amino-3-carboxypropyl)-wyosine biosynthesis	1	1	1	1	1	1
Phase I biotransformations_ non P450	1	1	1	1	1	1
putrescine biosynthesis I	1	1	1	1	1	1
RAF-independent MAPK1-3 activation	1	1	1	1	1	1
Cholesterol biosynthesis	1	1	1	1	1	1
urate biosynthesis/inosine 5_-phosphate degradation	1	1	1	1	1	1
Glycogen synthesis	1	1	1	1	1	1
Synthesis of PIPs at the plasma membrane	1	1	1	1	1	1
PI5P Regulates TP53 Acetylation	1	1	1	1	1	1
Regulation of TP53 Activity through Acetylation	1	1	1	1	1	1
Negative regulation of the PI3K/AKT network	1	1	1	1	1	1
2-oxoglutarate decarboxylation to succinyl-CoA	1	1	1	1	1	1

cell cycle: g2/m checkpoint	1	1	1	1	1	1
Mitochondrial translation	1	1	1	1	1	1
Signaling by EGFRvIII in Cancer	1	1	1	1	1	1
Signaling by EGFR in Cancer	1	1	1	1	1	1
aspirin blocks signaling pathway involved in platelet activation	1	1	1	1	1	1
MET in type 1 papillary renal cell carcinoma	1	1	1	1	1	1
Detoxification of Reactive Oxygen Species	1	1	1	1	1	1
C-type lectin receptors (CLRs)	1	1	1	1	1	1
BMAL1-CLOCK_NPAS2 activates circadian gene expression	1	1	1	1	1	1
Trafficking of GluR2-containing AMPA receptors	1	1	1	1	1	1
RHO GTPases activate PKNs	1	1	1	1	1	1
Dezocine Action Pathway	1	1	1	1	1	1
Synthesis of PIPs at the early endosome membrane	1	1	1	1	1	1
chaperones modulate interferon signaling pathway	1	1	1	1	1	1
NCAM1 interactions	1	1	1	1	1	1
SLIT2:ROBO1 increases RHOA activity	1	1	1	1	1	1
mevalonate pathway	1	1	1	1	1	1
superpathway of geranylgeranyldiphosphate biosynthesis I (via mevalo-nate)	1	1	1	1	1	1
Activation of AMPA receptors	1	1	1	1	1	1
Ubiquinone and other terpenoid-quinone biosynthesis - Homo sapiens (human)	1	1	1	1	1	1
Uncoating of the HIV Virion	1	1	1	1	1	1
GABA B receptor activation	1	1	1	1	1	1
Unblocking of NMDA receptor_ glutamate binding and activation	1	1	1	1	1	1
bile acid biosynthesis_ neutral pathway	1	1	1	1	1	1
Translesion synthesis by REV1	1	1	1	1	1	1
GABA receptor activation	1	1	1	1	1	1
Synthesis of PIPs at the late endosome membrane	1	1	1	1	1	1
S-adenosyl-L-methionine biosynthesis	1	1	1	1	1	1

Carnitine synthesis	1	1	1	1	1	1
fructose 2_6-bisphosphate synthesis	1	1	1	1	1	1
Adenylate cyclase activating pathway	1	1	1	1	1	1
G-protein mediated events	1	1	1	1	1	1
Regulation of nuclear SMAD2/3 signaling	1	1	1	1	1	1
IRAK1 recruits IKK complex upon TLR7/8 or 9 stimulation	1	1	1	1	1	1
mRNA Capping	1	1	1	1	1	1
ALK2 signaling events	1	1	1	1	1	1
NADH repair	1	1	1	1	1	1
Sulindac Metabolic Pathway	1	1	1	1	1	1
Glycerophospholipid catabolism	1	1	1	1	1	1
PI Metabolism	1	1	1	1	1	1
mTORC1-mediated signalling	1	1	1	1	1	1
Cdc20:Phospho-APC/C mediated degradation of Cyclin A	1	1	1	1	1	1
PKA activation in glucagon signalling	1	1	1	1	1	1
superpathway of melatonin degradation	1	1	1	1	1	1
FCERI mediated NF-kB activation	1	1	1	1	1	1
Synthesis of PS	1	1	1	1	1	1
oxidative ethanol degradation III	1	1	1	1	1	1
Nuclear Envelope Reassembly	1	1	1	1	1	1
Oxidative Stress Induced Senescence	1	1	1	1	1	1
Terminal pathway of complement	1	1	1	1	1	1
WNT-Ncore	1	1	1	1	1	1
Regulation of RUNX1 Expression and Activity	1	1	1	1	1	1
Plasmalogen biosynthesis	1	1	1	1	1	1
TFAP2A acts as a transcriptional repressor during retinoic acid induced cell differentiation	1	1	1	1	1	1
AlphaE beta7 integrin cell surface interactions	1	1	1	1	1	1
Calcium signaling pathway - Homo sapiens (human)	1	1	1	1	1	1
Energy dependent regulation of mTOR by LKB1-AMPK	1	1	1	1	1	1

Regulation of PTEN stability and activity	1	1	1	1	1	1
Medium chain acyl-coa dehydrogenase deficiency (MCAD)	1	1	1	1	1	1
G alpha (12/13) signalling events	1	1	1	1	1	1
Phosphate bond hydrolysis by NUDT proteins	1	1	1	1	1	1
Transcriptional regulation by the AP-2 (TFAP2) family of transcription factors	1	1	1	1	1	1
chrebp regulation by carbohydrates and camp	1	1	1	1	1	1
Calcium signaling in the CD4+ TCR pathway	1	1	1	1	1	1
histidine degradation	1	1	1	1	1	1
G alpha (z) signalling events	1	1	1	1	1	1
Vasopressin regulates renal water homeostasis via Aquaporins	1	1	1	1	1	1
IL12-mediated signaling events	1	1	1	1	1	1
Membrane binding and targetting of GAG proteins	1	1	1	1	1	1
Integration of provirus	1	1	1	1	1	1
Translesion synthesis by POLK	1	1	1	1	1	1
IL3	1	1	1	1	1	1
caspase cascade in apoptosis	1	1	1	1	1	1
VEGFR1 specific signals	1	1	1	1	1	1
Vif-mediated degradation of APOBEC3G	1	1	1	1	1	1
HDR through Homologous Recombination (HRR) or Single Strand Annealing (SSA)	1	1	1	1	1	1
CDT1 association with the CDC6:ORC:origin complex	1	1	1	1	1	1
Assembly of the pre-replicative complex	1	1	1	1	1	1
M/G1 Transition	1	1	1	1	1	1
Erythrocytes take up carbon dioxide and release oxygen	1	1	1	1	1	1
Sympathetic Nerve Pathway (Pre- and Post- Ganglionic Junction)	1	1	1	1	1	1
glutamine degradation/glutamate biosynthesis	1	1	1	1	1	1
IL2 signaling events mediated by PI3K	1	1	1	1	1	1
Inactivation_ recovery and regulation of the phototransduction cascade	1	1	1	1	1	1
The phototransduction cascade	1	1	1	1	1	1

superpathway of cholesterol biosynthesis	1	1	1	1	1	1
Steroid hormone biosynthesis - Homo sapiens (human)	1	1	1	1	1	1
PI5P_ PP2A and IER3 Regulate PI3K/AKT Signaling	1	1	1	1	1	1
Translesion synthesis by POLI	1	1	1	1	1	1
Cristae formation	1	1	1	1	1	1
Sympathetic Nerve Pathway (Neuroeffector Junction)	1	1	1	1	1	1
Displacement of DNA glycosylase by APEX1	1	1	1	1	1	1
superpathway of inositol phosphate compounds	1	1	1	1	1	1
Regulation of lipid metabolism by Peroxisome proliferator-activated receptor alpha (PPARalpha)	1	1	1	1	1	1
Warfarin Pathway_ Pharmacodynamics	1	1	1	1	1	1
ascorbate recycling (cytosolic)	1	1	1	1	1	1
Tamoxifen Pathway_ Pharmacokinetics	1	1	1	1	1	1
Fluoropyrimidine Pathway_ Pharmacokinetics	1	1	1	1	1	1
Bisphosphonate Pathway_ Pharmacodynamics	1	1	1	1	1	1
Taxane Pathway_ Pharmacokinetics	1	1	1	1	1	1
Selective Serotonin Reuptake Inhibitor Pathway_ Pharmacodynamics	1	1	1	1	1	1
Nicotine Pathway (Dopaminergic Neuron)_ Pharmacodynamics	1	1	1	1	1	1
D-glucuronate degradation	1	1	1	1	1	1
Benzodiazepine Pathway_ Pharmacodynamics	1	1	1	1	1	1
Methotrexate Pathway_ Pharmacokinetics	1	1	1	1	1	1
Leukotriene modifiers pathway_ Pharmacodynamics	1	1	1	1	1	1
Acetaminophen Pathway_ Pharmacokinetics	1	1	1	1	1	1
Nicotine Pathway_ Pharmacokinetics	1	1	1	1	1	1
ACE Inhibitor Pathway_ Pharmacodynamics	1	1	1	1	1	1
Beta-agonist/Beta-blocker Pathway_ Pharmacodynamics	1	1	1	1	1	1
Etoposide Pathway_ Pharmacokinetics/Pharmacodynamics	1	1	1	1	1	1
Long chain acyl-CoA dehydrogenase deficiency (LCAD)	1	1	1	1	1	1
Levomethadyl Acetate Action Action Pathway	1	1	1	1	1	1
Intracellular Signalling Through Adenosine Receptor A2b and Adenosine	1	1	1	1	1	1

Excitatory Neural Signalling Through 5-HTR 4 and Serotonin	1	1	1	1	1	1
Disopyramide Action Pathway	1	1	1	1	1	1
Procainamide (Antiarrhythmic) Action Pathway	1	1	1	1	1	1
Fosphenytoin (Antiarrhythmic) Action Pathway	1	1	1	1	1	1
UDP-N-acetyl-D-glucosamine biosynthesis II	1	1	1	1	1	1
Intracellular Signalling Through Adenosine Receptor A2a and Adenosine	1	1	1	1	1	1
Sepiapterin reductase deficiency	1	1	1	1	1	1
Galactosemia III	1	1	1	1	1	1
Galactosemia II (GALK)	1	1	1	1	1	1
Agents Acting on the Renin-Angiotensin System Pathway_ Pharmacody-namics	1	1	1	1	1	1
Mycophenolic Acid Metabolism Pathway	1	1	1	1	1	1
Bopindolol Action Pathway	1	1	1	1	1	1
Timolol Action Pathway	1	1	1	1	1	1
Carteolol Action Pathway	1	1	1	1	1	1
Intracellular Signalling Through Prostacyclin Receptor and Prostacyclin	1	1	1	1	1	1
Hydrolysis of LPE	1	1	1	1	1	1
Citalopram Action Pathway	1	1	1	1	1	1
Imipramine Action Pathway	1	1	1	1	1	1
Bile Acid Biosynthesis	1	1	1	1	1	1
Mitochondrial translation termination	1	1	1	1	1	1
D-Arginine and D-Ornithine Metabolism	1	1	1	1	1	1
Levallorphan Action Pathway	1	1	1	1	1	1
Dimethylthiambutene Action Pathway	1	1	1	1	1	1
Ethylmorphine Action Pathway	1	1	1	1	1	1
Pentazocine Action Pathway	1	1	1	1	1	1
Naltrexone Action Pathway	1	1	1	1	1	1
Naloxone Action Pathway	1	1	1	1	1	1
Dihydromorphine Action Pathway	1	1	1	1	1	1
Minus-strand DNA synthesis	1	1	1	1	1	1

Nuclear signaling by ERBB4	1	1	1	1	1	1
Bevantolol Action Pathway	1	1	1	1	1	1
Practolol Action Pathway	1	1	1	1	1	1
Transport of glycerol from adipocytes to the liver by Aquaporins	1	1	1	1	1	1
Clopidogrel Metabolism Pathway	1	1	1	1	1	1
ALKBH2 mediated reversal of alkylation damage	1	1	1	1	1	1
melatonin degradation I	1	1	1	1	1	1
Cerebrotendinous Xanthomatosis (CTX)	1	1	1	1	1	1
Zellweger Syndrome	1	1	1	1	1	1
Capecitabine Action Pathway	1	1	1	1	1	1
Excitatory Neural Signalling Through 5-HTR 7 and Serotonin	1	1	1	1	1	1
Excitatory Neural Signalling Through 5-HTR 6 and Serotonin	1	1	1	1	1	1
Vitamin K Metabolism	1	1	1	1	1	1
Hypophosphatasia	1	1	1	1	1	1
Dobutamine Action Pathway	1	1	1	1	1	1
Isoprenaline Action Pathway	1	1	1	1	1	1
Arbutamine Action Pathway	1	1	1	1	1	1
Amiodarone Action Pathway	1	1	1	1	1	1
Levobunolol Action Pathway	1	1	1	1	1	1
Metipranolol Action Pathway	1	1	1	1	1	1
Degradation of Superoxides	1	1	1	1	1	1
Pantoprazole Action Pathway	1	1	1	1	1	1
Rabeprazole Action Pathway	1	1	1	1	1	1
mRNA decay by 3_ to 5_ exoribonuclease	1	1	1	1	1	1
Omeprazole Action Pathway	1	1	1	1	1	1
Lansoprazole Action Pathway	1	1	1	1	1	1
Mexiletine Action Pathway	1	1	1	1	1	1
Lidocaine (Antiarrhythmic) Action Pathway	1	1	1	1	1	1
L-dopachrome biosynthesis	1	1	1	1	1	1
fatty acid α-oxidation	1	1	1	1	1	1

Pterine Biosynthesis	1	1	1	1	1	1
Quinidine Action Pathway	1	1	1	1	1	1
ALKBH3 mediated reversal of alkylation damage	1	1	1	1	1	1
Reversal of alkylation damage by DNA dioxygenases	1	1	1	1	1	1
DNA Damage Reversal	1	1	1	1	1	1
Thyroid hormone synthesis	1	1	1	1	1	1
Endosomal/Vacuolar pathway	1	1	1	1	1	1
Betaxolol Action Pathway	1	1	1	1	1	1
Atenolol Action Pathway	1	1	1	1	1	1
Respiratory electron transport	1	1	1	1	1	1
Long-term depression - Homo sapiens (human)	1	1	1	1	1	1
Hypusine synthesis from eIF5A-lysine	1	1	1	1	1	1
Alprenolol Action Pathway	1	1	1	1	1	1
Trifunctional protein deficiency	1	1	1	1	1	1
coenzyme A biosynthesis	1	1	1	1	1	1
Carnitine palmitoyl transferase deficiency (II)	1	1	1	1	1	1
Very-long-chain acyl coa dehydrogenase deficiency (VLCAD)	1	1	1	1	1	1
Citalopram Metabolism Pathway	1	1	1	1	1	1
Nicotine Metabolism Pathway	1	1	1	1	1	1
Clopidogrel Action Pathway	1	1	1	1	1	1
Synthesis of bile acids and bile salts via 7alpha-hydroxycholesterol	1	1	1	1	1	1
Nicotine Action Pathway	1	1	1	1	1	1
Paclitaxel Action Pathway	1	1	1	1	1	1
Vincristine Action Pathway	1	1	1	1	1	1
Vinblastine Action Pathway	1	1	1	1	1	1
Vinorelbine Action Pathway	1	1	1	1	1	1
Capecitabine Metabolism Pathway	1	1	1	1	1	1
Glycerol Phosphate Shuttle	1	1	1	1	1	1
Betaine Metabolism	1	1	1	1	1	1
Nalbuphine Action Pathway	1	1	1	1	1	1

Ketobemidone Action Pathway	1	1	1	1	1	1
Beta Oxidation of Very Long Chain Fatty Acids	1	1	1	1	1	1
Fatty Acid Elongation In Mitochondria	1	1	1	1	1	1
Lidocaine (Local Anaesthetic) Action Pathway	1	1	1	1	1	1
L-kynurenine degradation	1	1	1	1	1	1
Chloroprocaine Action Pathway	1	1	1	1	1	1
Cocaine Action Pathway	1	1	1	1	1	1
Dibucaine Action Pathway	1	1	1	1	1	1
Levobupivacaine Action Pathway	1	1	1	1	1	1
Bupivacaine Action Pathway	1	1	1	1	1	1
Gastric Acid Production	1	1	1	1	1	1
Muscle/Heart Contraction	1	1	1	1	1	1
Diltiazem Action Pathway	1	1	1	1	1	1
Propranolol Action Pathway	1	1	1	1	1	1
Pindolol Action Pathway	1	1	1	1	1	1
Erlotinib Action Pathway	1	1	1	1	1	1
Levorphanol Action Pathway	1	1	1	1	1	1
Propoxyphene Action Pathway	1	1	1	1	1	1
Tramadol Action Action Pathway	1	1	1	1	1	1
Bupranolol Action Pathway	1	1	1	1	1	1
Diphenoxylate Action Pathway	1	1	1	1	1	1
Nizatidine Action Pathway	1	1	1	1	1	1
Ranitidine Action Pathway	1	1	1	1	1	1
Short Chain Acyl CoA Dehydrogenase Deficiency (SCAD Deficiency)	1	1	1	1	1	1
Methadone Action Pathway	1	1	1	1	1	1
Oxycodone Action Pathway	1	1	1	1	1	1
Mitochondrial ABC transporters	1	1	1	1	1	1
Prilocaine Action Pathway	1	1	1	1	1	1
Procaine Action Pathway	1	1	1	1	1	1
Proparacaine Action Pathway	1	1	1	1	1	1

Heroin Action Pathway	1	1	1	1	1	1
Fatty acid Metabolism	1	1	1	1	1	1
Vitamin B6 Metabolism	1	1	1	1	1	1
Catecholamine Biosynthesis	1	1	1	1	1	1
Nucleotide Sugars Metabolism	1	1	1	1	1	1
proline degradation	1	1	1	1	1	1
Nebivolol Action Pathway	1	1	1	1	1	1
sarcosine oncometabolite pathway	1	1	1	1	1	1
Amlodipine Action Pathway	1	1	1	1	1	1
Gemcitabine Action Pathway	1	1	1	1	1	1
Prednisolone Action Pathway	1	1	1	1	1	1
Ethanol Degradation	1	1	1	1	1	1
Type II Na+/Pi cotransporters	1	1	1	1	1	1
Glutaric Aciduria Type I	1	1	1	1	1	1
Ethylmalonic Encephalopathy	1	1	1	1	1	1
Prednisolone Metabolism Pathway	1	1	1	1	1	1
Nitrendipine Action Pathway	1	1	1	1	1	1
Nisoldipine Action Pathway	1	1	1	1	1	1
Nimodipine Action Pathway	1	1	1	1	1	1
Intracellular Signalling Through LHCGR Receptor and Luteinizing Hormone/Choriogonadotropin	1	1	1	1	1	1
Ibutilide Action Pathway	1	1	1	1	1	1
Tocainide Action Pathway	1	1	1	1	1	1
Intracellular Signalling Through Histamine H2 Receptor and Histamine	1	1	1	1	1	1
Mitochondrial Beta-Oxidation of Short Chain Saturated Fatty Acids	1	1	1	1	1	1
Mitochondrial Beta-Oxidation of Medium Chain Saturated Fatty Acids	1	1	1	1	1	1
Mitochondrial Beta-Oxidation of Long Chain Saturated Fatty Acids	1	1	1	1	1	1
Dopa-responsive dystonia	1	1	1	1	1	1
Hyperphenylalaninemia due to 6-pyruvoyltetrahydropterin synthase deficiency (ptps)	1	1	1	1	1	1

Metal ion SLC transporters	1	1	1	1	1	1
Nevirapine Metabolism Pathway	1	1	1	1	1	1
Short-chain 3-hydroxyacyl-CoA dehydrogenase deficiency (SCHAD)	1	1	1	1	1	1
Thyroxine biosynthesis	1	1	1	1	1	1
Tenofovir Action Pathway	1	1	1	1	1	1
Chemokine signaling pathway	1	1	1	1	1	1
Alfentanil Action Pathway	1	1	1	1	1	1
Oxymorphone Action Pathway	1	1	1	1	1	1
Hydrocodone Action Pathway	1	1	1	1	1	1
Hydromorphone Action Pathway	1	1	1	1	1	1
Sufentanil Action Pathway	1	1	1	1	1	1
Remifentanil Action Pathway	1	1	1	1	1	1
Fentanyl Action Pathway	1	1	1	1	1	1
dTMP de novo biosynthesis (mitochondrial)	1	1	1	1	1	1
Taurine and Hypotaurine Metabolism	1	1	1	1	1	1
Pantothenate and CoA Biosynthesis	1	1	1	1	1	1
Selenoamino Acid Metabolism	1	1	1	1	1	1
Betazole Action Pathway	1	1	1	1	1	1
Roxatidine acetate Action Pathway	1	1	1	1	1	1
Metiamide Action Pathway	1	1	1	1	1	1
Isradipine Action Pathway	1	1	1	1	1	1
Aflatoxin activation and detoxification	1	1	1	1	1	1
Nifedipine Action Pathway	1	1	1	1	1	1
Felodipine Action Pathway	1	1	1	1	1	1
Nadolol Action Pathway	1	1	1	1	1	1
valine degradation	1	1	1	1	1	1
Pirenzepine Action Pathway	1	1	1	1	1	1
Carvedilol Action Pathway	1	1	1	1	1	1
Labetalol Action Pathway	1	1	1	1	1	1
Repaglinide Action Pathway	1	1	1	1	1	1

Nateglinide Action Pathway	1	1	1	1	1	1
Threonine and 2-Oxobutanoate Degradation	1	1	1	1	1	1
Phytanic Acid Peroxisomal Oxidation	1	1	1	1	1	1
Carnitine-acylcarnitine translocase deficiency	1	1	1	1	1	1
Pyruvaldehyde Degradation	1	1	1	1	1	1
3-Methylthiofentanyl Action Pathway	1	1	1	1	1	1
Ketone Body Metabolism	1	1	1	1	1	1
Riboflavin Metabolism	1	1	1	1	1	1
Butyrate Metabolism	1	1	1	1	1	1
Thiamine Metabolism	1	1	1	1	1	1
EGF-Core	1	1	1	1	1	1
Malaria - Homo sapiens (human)	1	1	1	1	1	1
NHR	1	1	1	1	1	1
Norepinephrine Neurotransmitter Release Cycle	1	1	1	1	1	1
Selenoamino acid metabolism	1	1	1	1	1	1
Androgen and estrogen biosynthesis and metabolism	1	1	1	1	1	1
Di-unsaturated fatty acid beta-oxidation	1	1	1	1	1	1
myo-inositol de novo biosynthesis	1	1	1	1	1	1
Lipoate metabolism	1	1	1	1	1	1
Mono-unsaturated fatty acid beta-oxidation	1	1	1	1	1	1
Omega-6 fatty acid metabolism	1	1	1	1	1	1
Putative anti-Inflammatory metabolites formation from EPA	1	1	1	1	1	1
Saturated fatty acids beta-oxidation	1	1	1	1	1	1
Squalene and cholesterol biosynthesis	1	1	1	1	1	1
Phytanic acid peroxisomal oxidation	1	1	1	1	1	1
Vitamin B1 (thiamin) metabolism	1	1	1	1	1	1
Vitamin B6 (pyridoxine) metabolism	1	1	1	1	1	1
Vitamin H (biotin) metabolism	1	1	1	1	1	1
Formation of annular gap junctions	1	1	1	1	1	1
IL-5 Signaling Pathway	1	1	1	1	1	1

Sphingolipid pathway	1	1	1	1	1	1
Inositol Phosphate Metabolism	1	1	1	1	1	1
Glycine Metabolism	1	1	1	1	1	1
Resolution of D-Loop Structures	1	1	1	1	1	1
Gliclazide Action Pathway	1	1	1	1	1	1
Nicotine Metabolism	1	1	1	1	1	1
nitric oxide signaling pathway	1	1	1	1	1	1
Nicotine Activity on Dopaminergic Neurons	1	1	1	1	1	1
Asparagine N-linked glycosylation	1	1	1	1	1	1
Processing of Capped Intron-Containing Pre-mRNA	1	1	1	1	1	1
Apoptosis	1	1	1	1	1	1
Respiratory electron transport_ ATP synthesis by chemiosmotic coupling_ and heat production by uncoupling proteins.	1	1	1	1	1	1
Dopaminergic Neurogenesis	1	1	1	1	1	1
Gene Silencing by RNA	1	1	1	1	1	1
Semaphorin interactions	1	1	1	1	1	1
Carnitine Synthesis	1	1	1	1	1	1
Threonine catabolism	1	1	1	1	1	1
Signaling by Insulin receptor	1	1	1	1	1	1
Signaling by Rho GTPases	1	1	1	1	1	1
Signaling by ROBO receptors	1	1	1	1	1	1
Transport of glycerol from adipocytes to the liver by Aquaporins	1	1	1	1	1	1
Downregulation of TGF-beta receptor signaling	1	1	1	1	1	1
fatty acid biosynthesis initiation	1	1	1	1	1	1
Cholesterol Biosynthesis Pathway	1	1	1	1	1	1
Opioid Signalling	1	1	1	1	1	1
Nucleotide Excision Repair	1	1	1	1	1	1
Thyroxine (Thyroid Hormone) Production	1	1	1	1	1	1
Genes targeted by miRNAs in adipocytes	1	1	1	1	1	1
threonine degradation	1	1	1	1	1	1

miR-targeted genes in adipocytes - TarBase	1	1	1	1	1	1
Iron metabolism in placenta	1	1	1	1	1	1
SREBF and miR33 in cholesterol and lipid homeostasis	1	1	1	1	1	1
miRs in Muscle Cell Differentiation	1	1	1	1	1	1
Leptin signaling pathway	1	1	1	1	1	1
Follicle Stimulating Hormone (FSH) signaling pathway	1	1	1	1	1	1
Eukaryotic Translation Initiation	1	1	1	1	1	1
Factors involved in megakaryocyte development and platelet production	1	1	1	1	1	1
Interferon alpha-beta signaling	1	1	1	1	1	1
3-phosphoinositide degradation	1	1	1	1	1	1
MAPK targets- Nuclear events mediated by MAP kinases	1	1	1	1	1	1
Mitotic G1-G1-S phases	1	1	1	1	1	1
Mitotic G2-G2-M phases	1	1	1	1	1	1
mRNA Capping	1	1	1	1	1	1
Neurotransmitter clearance	1	1	1	1	1	1
Neurotransmitter uptake and metabolism In glial cells	1	1	1	1	1	1
mTOR signalling	1	1	1	1	1	1
Peroxisomal lipid metabolism	1	1	1	1	1	1
Platelet Aggregation (Plug Formation)	1	1	1	1	1	1
Protein folding	1	1	1	1	1	1
Circadian Clock	1	1	1	1	1	1
Sotalol Action Pathway	1	1	1	1	1	1
Costimulation by the CD28 family	1	1	1	1	1	1
Effects of PIP2 hydrolysis	1	1	1	1	1	1
Eukaryotic Translation Elongation	1	1	1	1	1	1
Intrinsic Pathway for Apoptosis	1	1	1	1	1	1
EPO signaling	1	1	1	1	1	1
biotin-carboxyl carrier protein assembly	1	1	1	1	1	1
NCAM signaling for neurite out-growth	1	1	1	1	1	1
stathmin and breast cancer resistance to antimicrotubule agents	1	1	1	1	1	1

heme biosynthesis from uroporphyrinogen-III I	1	1	1	1	1	1
Familial Hypercholanemia (FHCA)	1	1	1	1	1	1
Mitochondrial protein import	1	1	1	1	1	1
Fcgamma receptor (FCGR) dependent phagocytosis	1	1	1	1	1	1
alpha-linolenic (omega3) and linoleic (omega6) acid metabolism	1	1	1	1	1	1
DAG and IP3 signaling	1	1	1	1	1	1
Regulation of Hypoxia-inducible Factor (HIF) by oxygen	1	1	1	1	1	1
Epinephrine Action Pathway	1	1	1	1	1	1
Deadenylation-dependent mRNA decay	1	1	1	1	1	1
Voltage gated Potassium channels	1	1	1	1	1	1
Transcriptional regulation of white adipocyte differentiation	1	1	1	1	1	1
Transcriptional activity of SMAD2-SMAD3-SMAD4 heterotrimer	1	1	1	1	1	1
Mitotic Metaphase and Anaphase	1	1	1	1	1	1
Fc epsilon receptor (FCERI) signaling	1	1	1	1	1	1
Esomeprazole Action Pathway	1	1	1	1	1	1
Thymic Stromal LymphoPoietin (TSLP) Signaling Pathway	1	1	1	1	1	1
Metastatic brain tumor	1	1	1	1	1	1
Glial Cell Differentiation	1	1	1	1	1	1
CDP-diacylglycerol biosynthesis	1	1	1	1	1	1
miRNA Biogenesis	1	1	1	1	1	1
Congenital Bile Acid Synthesis Defect Type III	1	1	1	1	1	1
Oncostatin M Signaling Pathway	1	1	1	1	1	1
Alpha 6 Beta 4 signaling pathway	1	1	1	1	1	1
NAD Biosynthesis II (from tryptophan)	1	1	1	1	1	1
Bile acid and bile salt metabolism	1	1	1	1	1	1
Negative regulation of FGFR1 signaling	1	1	1	1	1	1
Nifedipine Activity	1	1	1	1	1	1
EBV LMP1 signaling	1	1	1	1	1	1
Common Pathways Underlying Drug Addiction	1	1	1	1	1	1
Arachidonic acid metabolism	1	1	1	1	1	1

ATF6 (ATF6-alpha) activates chaperone genes	1	1	1	1	1	1
Growth hormone receptor signaling	1	1	1	1	1	1
O-glycosylation of TSR domain-containing proteins	1	1	1	1	1	1
MHC class II antigen presentation	1	1	1	1	1	1
Host Interactions of HIV factors	1	1	1	1	1	1
Cell-extracellular matrix interactions	1	1	1	1	1	1
S Phase	1	1	1	1	1	1
CRH	1	1	1	1	1	1
Translocation of SLC2A4 (GLUT4) to the plasma membrane	1	1	1	1	1	1
Signaling by ERBB2	1	1	1	1	1	1
Signaling by ERBB4	1	1	1	1	1	1
Binding and Uptake of Ligands by Scavenger Receptors	1	1	1	1	1	1
ERKs are inactivated	1	1	1	1	1	1
mRNA Splicing - Minor Pathway	1	1	1	1	1	1
Selenium Metabolism and Selenoproteins	1	1	1	1	1	1
Mammary gland development pathway - Embryonic development (Stage 1 of 4)	1	1	1	1	1	1
Mammary gland development pathway - Puberty (Stage 2 of 4)	1	1	1	1	1	1
Mammary gland development pathway - Involution (Stage 4 of 4)	1	1	1	1	1	1
Mammary gland development pathway - Pregnancy and lactation (Stage 3 of 4)	1	1	1	1	1	1
Regulation of TP53 Activity through Acetylation	1	1	1	1	1	1
Bladder Cancer	1	1	1	1	1	1
IL1 and megakaryocytes in obesity	1	1	1	1	1	1
Aryl Hydrocarbon Receptor Pathway	1	1	1	1	1	1
Liver X Receptor Pathway	1	1	1	1	1	1
Pregnane X Receptor pathway	1	1	1	1	1	1
Lipid storage and perilipins in skeletal muscle	1	1	1	1	1	1
Reverse Transcription of HIV RNA	1	1	1	1	1	1
glycerol degradation	1	1	1	1	1	1

Synthesis and Degradation of Ketone Bodies	1	1	1	1	1	1
Triacylglyceride Synthesis	1	1	1	1	1	1
Formation of the cornified envelope	1	1	1	1	1	1
Melatonin metabolism and effects	1	1	1	1	1	1
eIF5A regulation in response to inhibition of the nuclear export system	1	1	1	1	1	1
RAC1-PAK1-p38-MMP2 Pathway	1	1	1	1	1	1
MAPK6-MAPK4 signaling	1	1	1	1	1	1
Transcriptional regulation by RUNX1	1	1	1	1	1	1
Signaling by FGFR4	1	1	1	1	1	1
Signaling by FGFR3	1	1	1	1	1	1
Signaling by FGFR2	1	1	1	1	1	1
Macroautophagy	1	1	1	1	1	1
TP53 Regulates Metabolic Genes	1	1	1	1	1	1
transcription factor creb and its extracellular signals	1	1	1	1	1	1
RHO GTPases Activate ROCKs	1	1	1	1	1	1
RORA activates gene expression	1	1	1	1	1	1
TET1_2_3 and TDG demethylate DNA	1	1	1	1	1	1
RHO GTPases Activate Formins	1	1	1	1	1	1
phosphoinositides and their downstream targets	1	1	1	1	1	1
Activated PKN1 stimulates transcription of AR (androgen receptor) regulated genes KLK2 and KLK3	1	1	1	1	1	1
taurine biosynthesis	1	1	1	1	1	1
Base-Excision Repair_ AP Site Formation	1	1	1	1	1	1
Ovarian Infertility Genes	1	1	1	1	1	1
Hedgehog ligand biogenesis	1	1	1	1	1	1
NOTCH1 regulation of human endothelial cell calcification	1	1	1	1	1	1
Synthesis_ secretion_ and deacylation of Ghrelin	1	1	1	1	1	1
Abnormal conversion of 2-oxoglutarate to 2-hydroxyglutarate	1	1	1	1	1	1
G Protein Signaling Pathways	1	1	1	1	1	1
Preimplantation Embryo	1	1	1	1	1	1

DNA Double Strand Break Response	1	1	1	1	1	1
Amine-derived hormones	1	1	1	1	1	1
Early Phase of HIV Life Cycle	1	1	1	1	1	1
Beta-catenin independent WNT signaling	1	1	1	1	1	1
Gene Silencing by RNA	1	1	1	1	1	1
nicotine degradation III	1	1	1	1	1	1
Class I MHC mediated antigen processing & presentation	1	1	1	1	1	1
trans-Golgi Network Vesicle Budding	1	1	1	1	1	1
Surfactant metabolism	1	1	1	1	1	1
Degradation of AXIN	1	1	1	1	1	1
Composition of Lipid Particles	1	1	1	1	1	1
Olfactory bulb development and olfactory learning	1	1	1	1	1	1
Photodynamic therapy-induced AP-1 survival signaling.	1	1	1	1	1	1
Photodynamic therapy-induced NFE2L2 (NRF2) survival signaling	1	1	1	1	1	1
Photodynamic therapy-induced unfolded protein response	1	1	1	1	1	1
IL-1 signaling pathway	1	1	1	1	1	1
Pathways Affected in Adenoid Cystic Carcinoma	1	1	1	1	1	1
Ropivacaine Action Pathway	1	1	1	1	1	1
Interleukin-1 Induced Activation of NF-kappa-B	1	1	1	1	1	1
Wnt-beta-catenin Signaling Pathway in Leukemia	1	1	1	1	1	1
Hypothesized Pathways in Pathogenesis of Cardiovascular Disease	1	1	1	1	1	1
Simplified Interaction Map Between LOXL4 and Oxidative Stress Pathway	1	1	1	1	1	1
Lysosomal oligosaccharide catabolism	1	1	1	1	1	1
Striated Muscle Contraction	1	1	1	1	1	1
KSRP (KHSRP) binds and destabilizes mRNA	1	1	1	1	1	1
Metabolism of folate and pterines	1	1	1	1	1	1
Regulation of TP53 Expression and Degradation	1	1	1	1	1	1
Cardiac conduction	1	1	1	1	1	1
PI3K-AKT-mTOR - VitD3 Signalling	1	1	1	1	1	1
tumor suppressor arf inhibits ribosomal biogenesis	1	1	1	1	1	1

Resolution of D-loop Structures through Synthesis-Dependent Strand Annealing (SDSA)	1	1	1	1	1	1
rRNA modification in the nucleus and cytosol	1	1	1	1	1	1
Activated NOTCH1 Transmits Signal to the Nucleus	1	1	1	1	1	1
Long-chain-3-hydroxyacyl-coa dehydrogenase deficiency (LCHAD)	1	1	1	1	1	1
ERK Pathway in Huntington_s Disease	1	1	1	1	1	1
T-Cell antigen Receptor (TCR) pathway during Staphylococcus aureus infection	1	1	1	1	1	1
Cannabinoid receptor signaling	1	1	1	1	1	1
Regulation of Apoptosis by Parathyroid Hormone-related Protein	1	1	1	1	1	1
Simplified Depiction of MYD88 Distinct Input-Output Pathway	1	1	1	1	1	1
ESC Pluripotency Pathways	1	1	1	1	1	1
Steroid hormones	1	1	1	1	1	1
Serotonin and anxiety	1	1	1	1	1	1
IL-4 Signaling Pathway	1	1	1	1	1	1
Mevalonate pathway	1	1	1	1	1	1
miR-509-3p alteration of YAP1-ECM axis	1	1	1	1	1	1
H19 action Rb-E2F1 signaling and CDK-Beta-catenin activity	1	1	1	1	1	1
Role of Osx and miRNAs in tooth development	1	1	1	1	1	1
Protein alkylation leading to liver fibrosis	1	1	1	1	1	1
MAP kinase cascade	1	1	1	1	1	1
Steatosis AOP	1	1	1	1	1	1
cGMP-PKG signaling pathway - Homo sapiens (human)	1	1	1	1	1	1
MTF1 activates gene expression	1	1	1	1	1	1
Pyrophosphate hydrolysis	1	1	1	1	1	1
Fructose metabolism	1	1	1	1	1	1
Cellular hexose transport	1	1	1	1	1	1
RAB geranylgeranylation	1	1	1	1	1	1
Pentose phosphate pathway	1	1	1	1	1	1
TBC-RABGAPs	1	1	1	1	1	1

HSP90 chaperone cycle for steroid hormone receptors (SHR)	1	1	1	1	1	1
Interconversion of nucleotide di- and triphosphates	1	1	1	1	1	1
Glycogen metabolism	1	1	1	1	1	1
Cargo recognition for clathrin-mediated endocytosis	1	1	1	1	1	1
Phase I - Functionalization of compounds	1	1	1	1	1	1
Transcriptional regulation by the AP-2 (TFAP2) family of transcription factors	1	1	1	1	1	1
Plasmalogen biosynthesis	1	1	1	1	1	1
regulation of ck1/cdk5 by type 1 glutamate receptors	1	1	1	1	1	1
Ion channel transport	1	1	1	1	1	1
Antimicrobial peptides	1	1	1	1	1	1
Creatine metabolism	1	1	1	1	1	1
Synthesis of PA	1	1	1	1	1	1
Resolution of D-loop Structures through Holliday Junction Intermediates	1	1	1	1	1	1
Ketone body metabolism	1	1	1	1	1	1
Uptake and function of diphtheria toxin	1	1	1	1	1	1
Lactose synthesis	1	1	1	1	1	1
Regulation of RUNX1 Expression and Activity	1	1	1	1	1	1
Signaling by MET	1	1	1	1	1	1
Cilium Assembly	1	1	1	1	1	1
IRAK1 recruits IKK complex	1	1	1	1	1	1
Plasma lipoprotein assembly_ remodeling_ and clearance	1	1	1	1	1	1
RUNX1 regulates genes involved in megakaryocyte differentiation and platelet function	1	1	1	1	1	1
Miscellaneous transport and binding events	1	1	1	1	1	1
Fibrin Complement Receptor 3 Signaling Pathway	1	1	1	1	1	1
tRNA splicing	1	1	1	1	1	1
HDR through Homologous Recombination (HRR)	1	1	1	1	1	1
molybdenum cofactor biosynthesis	1	1	1	1	1	1

Phenylalanine_ tyrosine and tryptophan biosynthesis - Homo sapiens (human)	1	1	1	1	1	1
Neurotransmitter Disorders	1	1	1	1	1	1
Ras Signaling	1	1	1	1	1	1
Vitamin B6-dependent and responsive disorders	1	1	1	1	1	1
IL11	1	1	1	1	1	1

Table S6-7 enrichment_results_impala_EQ3_1vs2

pathway_name	P_genes	Q_genes	P_metabolites	Q_metabolites	P_joint	Q_joint
Metabolism	1.20E-05	0.0549	0.00309	1	6.68E-07	0.000667
Metabolism of proteins	0.000137	0.185	0.127	1	0.000209	0.069
EGFR1	8.66E-05	0.185	1	1	8.66E-05	0.078
Immune System	0.000161	0.185	1	1	0.00157	0.104
Signaling by Rho GTPases	0.000465	0.356	0.75	1	0.00313	0.558
Innate Immune System	0.000445	0.356	1	1	0.00388	0.578
Nuclear Receptors Meta-Pathway	0.000852	0.558	1	1	0.000852	0.476
Gene and protein expression by JAK-STAT signaling after Interleukin-12 stimulation	0.00101	0.578	1	1	0.00101	0.476
Metabolism of carbohydrates	0.00192	0.874	0.105	1	0.00191	0.185
Signal Transduction	0.00209	0.874	0.597	1	0.0096	1
Metabolism of RNA	0.00187	0.874	0.875	1	0.0121	1
Biochemical Pathways Part I	1	1	0.000168	0.716	0.000168	0.624
Neutrophil degranulation	0.00284	1	1	1	0.00284	0.646
Insulin	0.00391	1	1	1	0.00391	0.716
insulin Mam	0.00391	1	1	1	0.00391	1
Proteoglycans in cancer - Homo sapiens (human)	0.00391	1	1	1	0.00391	1
NRF2 pathway	0.00403	1	1	1	0.00403	1
Post-translational protein modification	0.00271	1	0.563	1	0.0114	1
ABC transporters - Homo sapiens (human)	1	1	0.00166	1	0.0123	1
Developmental Biology	0.00456	1	0.375	1	0.0126	1

Transcriptional Regulation by TP53	0.00403	1	0.5	1	0.0145	1
Cell Cycle Checkpoints	0.0156	1	1	1	0.0156	1
Leukocyte transendothelial migration - Homo sapiens (human)	0.0156	1	1	1	0.0156	1
Amino Acid metabolism	0.966	1	0.00248	1	0.0169	1
Human metabolism overview	1	1	0.0171	1	0.0171	1
Central carbon metabolism in cancer - Homo sapiens (human)	0.125	1	0.0214	1	0.0185	1
Hippo signaling pathway - Homo sapiens (human)	0.0234	1	1	1	0.0234	1
VEGFA-VEGFR2 Signaling Pathway	0.0254	1	1	1	0.0254	1
Metabolism of amino acids and derivatives	0.6	1	0.00671	1	0.0262	1
Tight junction - Homo sapiens (human)	0.0268	1	1	1	0.0268	1
RHO GTPase Effectors	0.00628	1	0.75	1	0.03	1
a6b1 and a6b4 Integrin signaling	0.0313	1	1	1	0.0313	1
Signaling events mediated by VEGFR1 and VEGFR2	0.0313	1	1	1	0.0313	1
downregulated of mta-3 in er-negative breast tumors	0.0313	1	1	1	0.0313	1
Integrated Breast Cancer Pathway	0.0313	1	1	1	0.0313	1
RNA Polymerase II Transcription	0.0115	1	0.5	1	0.0353	1
Role of Calcineurin-dependent NFAT signaling in lymphocytes	0.0391	1	1	1	0.0391	1
PI3K-Akt signaling pathway - Homo sapiens (human)	0.0419	1	1	1	0.0419	1
Axon guidance	0.0187	1	0.375	1	0.0419	1
Ebola Virus Pathway on Host	0.042	1	1	1	0.042	1
Glycolysis / Gluconeogenesis - Homo sapiens (human)	0.00763	1	1	1	0.0448	1
Vitamin B12 Metabolism	0.0313	1	0.25	1	0.0457	1
Gene expression (Transcription)	0.00794	1	1	1	0.0463	1
RhoA signaling pathway	0.0469	1	1	1	0.0469	1
LKB1 signaling events	0.0469	1	1	1	0.0469	1
TNFalpha	0.0479	1	1	1	0.0479	1
miR-targeted genes in leukocytes - TarBase	0.0479	1	1	1	0.0479	1
Amine compound SLC transporters	1	1	0.0488	1	0.0488	1
Vitamin D Receptor Pathway	0.0488	1	1	1	0.0488	1
Post-translational modification: synthesis of GPI-anchored proteins	0.0547	1	1	1	0.0547	1

Adherens junction - Homo sapiens (human)	0.0547	1	1	1	0.0547	1
Oocyte meiosis - Homo sapiens (human)	0.0547	1	1	1	0.0547	1
Membrane Trafficking	0.0107	1	1	1	0.059	1
Integrin-linked kinase signaling	0.0625	1	1	1	0.0625	1
GPCR signaling-cholera toxin	0.0625	1	1	1	0.0625	1
Carbohydrate digestion and absorption - Homo sapiens (human)	1	1	0.0625	1	0.0625	1
pentose phosphate pathway	0.0625	1	1	1	0.0625	1
p38 signaling mediated by MAPKAP kinases	0.0625	1	1	1	0.0625	1
FoxO family signaling	0.0625	1	1	1	0.0625	1
G2/M DNA damage checkpoint	0.0625	1	1	1	0.0625	1
G2/M Checkpoints	0.0625	1	1	1	0.0625	1
Peroxisome - Homo sapiens (human)	0.0625	1	1	1	0.0625	1
Peptide ligand-binding receptors	0.0625	1	1	1	0.0625	1
Hepatitis C - Homo sapiens (human)	0.0625	1	1	1	0.0625	1
Cysteine and methionine metabolism - Homo sapiens (human)	0.0371	1	0.312	1	0.0633	1
Pentose Phosphate Pathway	0.0313	1	0.375	1	0.0638	1
Glucose-6-phosphate dehydrogenase deficiency	0.0313	1	0.375	1	0.0638	1
Ribose-5-phosphate isomerase deficiency	0.0313	1	0.375	1	0.0638	1
Transaldolase deficiency	0.0313	1	0.375	1	0.0638	1
Cell Cycle	0.0159	1	0.75	1	0.0648	1
The citric acid (TCA) cycle and respiratory electron transport	0.0313	1	0.383	1	0.0649	1
Viral carcinogenesis - Homo sapiens (human)	0.0674	1	1	1	0.0674	1
L13a-mediated translational silencing of Ceruloplasmin expression	0.0676	1	1	1	0.0676	1
miR-targeted genes in lymphocytes - TarBase	0.0691	1	1	1	0.0691	1
Metabolism of lipids	0.0181	1	0.733	1	0.0706	1
Glycolysis and Gluconeogenesis	0.0166	1	0.812	1	0.0716	1

Table S6-8b differential abundance in OC of proteins in impacted pathways (joint analysis)

athway	Gene	log2FC(OC1vs3)
Biological oxidations	**ADH5**	-0.461955121
Biological oxidations	SULT1A1	-0.081857484
Biological oxidations	CMBL	-0.025696322
Biological oxidations	CNDP2	-0.169728243
Biological oxidations	GSTP1	-0.244477177
Biological oxidations	GCLC	-0.19616332
Biological oxidations	BPNT1	-0.50538059
Biological oxidations	COMT	-1.253649193
Biological oxidations	ESD	-0.572131017
Biological oxidations	GSTM3	-0.567137926
Biological oxidations	HSP90AB1	-0.181804247
Biological oxidations	AKR1A1	-0.521130784
Biological oxidations	ABHD14B	-0.030154879
Biological oxidations	ALDH2	-1.740970054
Biological oxidations	TPMT	-0.44646877
Biological oxidations	AHCY	-0.342424948
Cellular responses to stress	EEF1A1	-0.584186662
Cellular responses to stress	STIP1	-0.227325234
Cellular responses to stress	**GSTP1**	-0.244477177
Cellular responses to stress	UBA52	-0.56264169
Cellular responses to stress	HSPA8	-0.040015987
Cellular responses to stress	P4HB	-0.130908045
Cellular responses to stress	PRDX1	0.079494291
Cellular responses to stress	GPX1	-0.027806156
Cellular responses to stress	EHMT1	-0.733202728
Cellular responses to stress	SOD1	-1.32947E-05
Cellular responses to stress	PRDX2	0.288294606
Cellular responses to stress	PRDX5	-0.654602069
Cellular responses to stress	SERPINH1	-0.023967053

Cellular responses to stress	HSPA1B	0.332135449
Cellular responses to stress	HSPA1L	-0.782702761
Cellular responses to stress	HSPA2	-1.098617006
Cellular responses to stress	YWHAE	-0.026348434
Cellular responses to stress	HSPA4	-0.153271187
Cellular responses to stress	HSPA5	-0.215020617
Cellular responses to stress	HSPA6	-0.464705228
Cellular responses to stress	FKBP4	-0.065549673
Cellular responses to stress	HSPA9	-0.941051019
Cellular responses to stress	HSPB1	-0.026840004
Cellular responses to stress	PRDX6	0.022805961
Cellular responses to stress	VCP	-0.247401608
Cellular responses to stress	HSP90AA1	-0.119311243
Cellular responses to stress	PGR	-0.283094143
Cellular responses to stress	HSP90AB1	-0.181804247
Cellular responses to stress	TXN	-0.139915362
EGFR	RPLP0	-1.622601242
EGFR	KRT18	0.532455503
EGFR	MYO6	-0.161782418
EGFR	KIAA1217	0.197866408
EGFR	ANXA4	-0.221868523
EGFR	CSTB	-0.709759021
EGFR	EEF1A1	-0.584186662
EGFR	PGAM1	-0.468100438
EGFR	RPS2	-0.735239887
EGFR	CLTC	-0.110048171
EGFR	LDHA	-0.666815508
EGFR	ANXA2	-0.066673901
EGFR	AHNAK	-0.722285923
EGFR	IQGAP1	-0.437717098
EGFR	TKT	-0.392120777

EGFR	S100A10	-0.450436617
EGFR	S100A11	-0.524093587
EGFR	EPPK1	-0.373392312
EGFR	CDH1	-0.288124075
EGFR	ALDOA	0.094877154
EGFR	**ITGB4**	-0.630294167
EGFR	MVP	-0.602269316
EGFR	CFL1	-0.120754082
EGFR	PEBP1	-0.188771067
EGFR	ANXA1	-0.162080636
EGFR	KRT8	-0.520489786
EGFR	VCL	-0.100053317
EGFR	MYH9	-0.060815779
EGFR	PFN1	-0.26552506
EGFR	ACTR2	1.109122485
EGFR	TLN1	-0.185504188
EGFR	FLNB	-0.515881508
EGFR	STIP1	-0.227325234
EGFR	CLTA	0.134502662
EGFR	CDC42	-0.133886647
EGFR	ACTN4	-0.157529641
EGFR	TAGLN2	-0.028676414
EGFR	PDLIM1	0.2663088
EGFR	WASL	0.109509251
EGFR	ACTR3	0.212629308
EGFR	ALB	-0.4031327
EGFR	GSN	0.367776272
EGFR	PLEC	-3.353136521
EGFR	CBLB	-0.692515925
Gene and protein expression by JAK-STAT signaling after Interleukin-12 stimulation	RPLP0	-1.622601242

Gene and protein expression by JAK-STAT signaling after Interleukin-12 stimulation	ANXA2	-0.066673901
Gene and protein expression by JAK-STAT signaling after Interleukin-12 stimulation	CFL1	-0.120754082
Gene and protein expression by JAK-STAT signaling after Interleukin-12 stimulation	CDC42	-0.133886647
Gene and protein expression by JAK-STAT signaling after Interleukin-12 stimulation	**LCP1**	-0.623435078
Gene and protein expression by JAK-STAT signaling after Interleukin-12 stimulation	TCP1	-0.16166513
Gene and protein expression by JAK-STAT signaling after Interleukin-12 stimulation	PPIA	-0.037388918
Gene and protein expression by JAK-STAT signaling after Interleukin-12 stimulation	SOD1	-1.32947E-05
Gene and protein expression by JAK-STAT signaling after Interleukin-12 stimulation	TALDO1	-0.521132053
Gene and protein expression by JAK-STAT signaling after Interleukin-12 stimulation	CA1	-0.077725967

Table S6-8b differential abundance in OC of metabolites in impacted pathways (joint analysis)

Column1	Metabo-lites	Name	log2FC(OC1vs3)
Biological oxidations	**1004**	Phosphoric acid	1.092805
Biological oxidations	750	Glycine	-0.06685
Biological oxidations	33032	Glutamic acid	0.104083
Biological oxidations	5862	Cysteine	0.073015
Biological oxidations	243	Benzoic acid	0.459337
Biological oxidations	3893	Lauric acid	0.328612
Biological oxidations	94715	Glucuronic acid	0.454688
Biological oxidations	7405	5-Oxoproline	0.637694
Cellular responses to stress	**1110**	Succinic acid	-0.0611
Cellular responses to stress	51	2-Ketoglutaric acid	0.328762
Cellular responses to stress	**1004**	Phosphoric acid	1.092805
Gene expression (Transcription)	**1110**	Succinic acid	-0.0611
Gene expression (Transcription)	33032	Glutamic acid	0.104083
Gene expression (Transcription)	51	2-Ketoglutaric acid	0.328762
Gene expression (Transcription)	1004	Phosphoric acid	1.092805
Generic Transcription Pathway	**33032**	Glutamic acid	0.104083
Generic Transcription Pathway	1004	Phosphoric acid	1.092805
Glycolysis / Gluconeogenesis	**107689**	Lactic acid	0.239245
Glycolysis / Gluconeogenesis	5793	Glucose	0.575084
Glycolysis / Gluconeogenesis	1060	Pyruvic acid	0.534754
Immune System	**1004**	Phosphoric acid	1.092805
Metabolic reprogramming in colon cancer	**311**	Citric acid	0.728172
Metabolic reprogramming in colon cancer	439167	Ribose 5-phosphate	-0.1762
Metabolic reprogramming in colon cancer	107689	Lactic acid	0.239245
Metabolic reprogramming in colon cancer	1060	Pyruvic acid	0.534754

Metabolic reprogramming in colon cancer	750	Glycine	-0.06685
Metabolic reprogramming in colon cancer	51	2-Ketoglutaric acid	0.328762
Metabolic reprogramming in colon cancer	444972	Fumaric acid	0.20274
Metabolic reprogramming in colon cancer	525	Malic acid	0.192412
Metabolism	**311**	Citric acid	0.728172
Metabolism	18950	Mannose	-0.23222
Metabolism	753	Glycerol	0.111351
Metabolism	440995	Lactose	1.039342
Metabolism	1174	Uracil	0.523595
Metabolism	985	Palmitic acid	0.382639
Metabolism	750	Glycine	-0.06685
Metabolism	6306	Isoleucine	-0.1574
Metabolism	3893	Lauric acid	0.328612
Metabolism	94715	Glucuronic acid	0.454688
Metabolism	439167	Ribose 5-phosphate	-0.1762
Metabolism	7405	5-Oxoproline	0.637694
Metabolism	700	2-Aminoethanol	0.182196
Metabolism	107689	Lactic acid	0.239245
Metabolism	243	Benzoic acid	0.459337
Metabolism	1176	Urea	0.733166
Metabolism	760	Glyoxylic acid	0.325168
Metabolism	5960	Aspartic acid	-0.48643
Metabolism	439258	Cystathionine	0.728488
Metabolism	6912	Xylitol	0.996198
Metabolism	1110	Succinic acid	-0.0611
Metabolism	6057	Tyrosine	0.149945
Metabolism	5950	Alanine	-0.4088

Metabolism	1088	Sarcosine	-0.02407
Metabolism	6106	Leucine	0.505591
Metabolism	444972	Fumaric acid	0.20274
Metabolism	757	Glycolic acid	-0.38301
Metabolism	1004	Phosphoric acid	1.092805
Metabolism	5984	Fructose	0.884417
Metabolism	107812	Hypotaurine	-0.55682
Metabolism	1060	Pyruvic acid	0.534754
Metabolism	439194	Glyceric acid	0.199412
Metabolism	33032	Glutamic acid	0.104083
Metabolism	51	2-Ketoglutaric acid	0.328762
Metabolism	6036	Galactose	0.338039
Metabolism	239	3-Aminopropanoic acid	0.562807
Metabolism	5779	Ribose	-0.93597
Metabolism	5281	Stearic acid	0.329851
Metabolism	5862	Cysteine	0.073015
Metabolism	892	Inositol	-0.16909
Metabolism	439260	Norepinephrine	-0.07602
Metabolism	6262	Ornithine	-0.75966
Metabolism	1015	O-Phosphoethanola-mine	0.939234
Metabolism of amino acids and derivatives	**6262**	Ornithine	-0.75966
Metabolism of amino acids and derivatives	750	Glycine	-0.06685
Metabolism of amino acids and derivatives	6306	Isoleucine	-0.1574
Metabolism of amino acids and derivatives	1176	Urea	0.733166
Metabolism of amino acids and derivatives	760	Glyoxylic acid	0.325168

Metabolism of amino acids and derivatives	5960	Aspartic acid	-0.48643
Metabolism of amino acids and derivatives	6057	Tyrosine	0.149945
Metabolism of amino acids and derivatives	1110	Succinic acid	-0.0611
Metabolism of amino acids and derivatives	439258	Cystathionine	0.728488
Metabolism of amino acids and derivatives	5950	Alanine	-0.4088
Metabolism of amino acids and derivatives	1088	Sarcosine	-0.02407
Metabolism of amino acids and derivatives	6106	Leucine	0.505591
Metabolism of amino acids and derivatives	444972	Fumaric acid	0.20274
Metabolism of amino acids and derivatives	757	Glycolic acid	-0.38301
Metabolism of amino acids and derivatives	1004	Phosphoric acid	1.092805
Metabolism of amino acids and derivatives	107812	Hypotaurine	-0.55682
Metabolism of amino acids and derivatives	1060	Pyruvic acid	0.534754
Metabolism of amino acids and derivatives	33032	Glutamic acid	0.104083
Metabolism of amino acids and derivatives	51	2-Ketoglutaric acid	0.328762
Metabolism of amino acids and derivatives	239	3-Aminopropanoic acid	0.562807
Metabolism of amino acids and derivatives	5862	Cysteine	0.073015

Metabolism of amino acids and derivatives	439260	Norepinephrine	-0.07602
Metabolism of carbohydrates	**311**	Citric acid	0.728172
Metabolism of carbohydrates	18950	Mannose	-0.23222
Metabolism of carbohydrates	753	Glycerol	0.111351
Metabolism of carbohydrates	439167	Ribose 5-phosphate	-0.1762
Metabolism of carbohydrates	1004	Phosphoric acid	1.092805
Metabolism of carbohydrates	5984	Fructose	0.884417
Metabolism of carbohydrates	6912	Xylitol	0.996198
Metabolism of carbohydrates	1060	Pyruvic acid	0.534754
Metabolism of carbohydrates	439194	Glyceric acid	0.199412
Metabolism of carbohydrates	33032	Glutamic acid	0.104083
Metabolism of carbohydrates	51	2-Ketoglutaric acid	0.328762
Metabolism of carbohydrates	94715	Glucuronic acid	0.454688
Metabolism of carbohydrates	440995	Lactose	1.039342
Metabolism of carbohydrates	6036	Galactose	0.338039
Metabolism of carbohydrates	5960	Aspartic acid	-0.48643
Metabolism of carbohydrates	5779	Ribose	-0.93597
Metabolism of lipids	**311**	Citric acid	0.728172
Metabolism of lipids	753	Glycerol	0.111351
Metabolism of lipids	700	2-Aminoethanol	0.182196
Metabolism of lipids	1004	Phosphoric acid	1.092805
Metabolism of lipids	985	Palmitic acid	0.382639
Metabolism of lipids	750	Glycine	-0.06685
Metabolism of lipids	33032	Glutamic acid	0.104083
Metabolism of lipids	51	2-Ketoglutaric acid	0.328762
Metabolism of lipids	5281	Stearic acid	0.329851
Metabolism of lipids	1110	Succinic acid	-0.0611
Metabolism of lipids	892	Inositol	-0.16909
Metabolism of lipids	1015	O-Phosphoethanolamine	0.939234

Metabolism of proteins	**18950**	Mannose	-0.23222
Metabolism of proteins	1004	Phosphoric acid	1.092805
Metabolism of proteins	1060	Pyruvic acid	0.534754
Metabolism of proteins	750	Glycine	-0.06685
Metabolism of proteins	33032	Glutamic acid	0.104083
Metabolism of proteins	5862	Cysteine	0.073015
Metabolism of proteins	6306	Isoleucine	-0.1574
Metabolism of proteins	5960	Aspartic acid	-0.48643
Metabolism of proteins	6057	Tyrosine	0.149945
Metabolism of proteins	379	Octanoic acid	0.801524
Metabolism of proteins	5950	Alanine	-0.4088
Metabolism of proteins	6106	Leucine	0.505591
Phase II - Conjugation of compounds	**94715**	Glucuronic acid	0.454688
Phase II - Conjugation of compounds	1004	Phosphoric acid	1.092805
Phase II - Conjugation of compounds	750	Glycine	-0.06685
Phase II - Conjugation of compounds	33032	Glutamic acid	0.104083
Phase II - Conjugation of compounds	5862	Cysteine	0.073015
Phase II - Conjugation of compounds	243	Benzoic acid	0.459337
Phase II - Conjugation of compounds	7405	5-Oxoproline	0.637694
RNA Polymerase II Transcription	**33032**	Glutamic acid	0.104083
RNA Polymerase II Transcription	1004	Phosphoric acid	1.092805
Signal Transduction	**6262**	Ornithine	-0.75966
Signal Transduction	753	Glycerol	0.111351
Signal Transduction	1004	Phosphoric acid	1.092805
Signal Transduction	107689	Lactic acid	0.239245
Signal Transduction	1060	Pyruvic acid	0.534754
Signal Transduction	750	Glycine	-0.06685
Signal Transduction	5281	Stearic acid	0.329851
Signal Transduction	3893	Lauric acid	0.328612
Signal Transduction	33032	Glutamic acid	0.104083
Signal Transduction	1110	Succinic acid	-0.0611

Signal Transduction	11005	Myristic acid	-0.06268
Signal Transduction	51	2-Ketoglutaric acid	0.328762
Signal Transduction	985	Palmitic acid	0.382639
Signal Transduction	439260	Norepinephrine	-0.07602
Signal Transduction	8892	Caproic acid	0.613227
Signal Transduction	5988	Sucrose	0.208571

Table S6-8.c Proteins in the epithelial growth factor receptor (EGFR1) pathway.

Path-way	Gene	log2FC(OC1vs3)	Log2FC(NONvsPREG)	Trends of discussed proteins
EGFR1	ITGB4	-0.63029	-0.18355	
EGFR1	S100A10	-0.45044	-0.25727	
EGFR1	S100A11	-0.52409	-0.24169	
EGFR1	FLNB	-0.51588	-0.08339	
EGFR1	PEBP1	-0.18877	-0.15321	
EGFR1	KRT8	-0.52049	-0.13364	
EGFR1	MYH9	-0.06082	-0.10988	
EGFR1	TKT	-0.39212	-0.26492	
EGFR1	EPPK1	-0.37339	-0.23248	
EGFR1	RPLP0	-1.6226	-1.64123	
EGFR1	**KRT18**	**0.532456**	**-1.62982**	**lower in good embryos and at OC3**
EGFR1	PDLIM1	0.266309	0.059882	
EGFR1	MYO6	-0.16178	-1.38882	
EGFR1	RPS2	-0.73524	-0.47644	
EGFR1	ANXA1	-0.16208	-0.1531	
EGFR1	ANXA2	-0.06667	-0.41436	
EGFR1	CFL1	-0.12075	-0.15604	
EGFR1	AHNAK	-0.72229	-0.38611	
EGFR1	ANXA4	-0.22187	-0.74195	
EGFR1	TLN1	-0.1855	-0.09468	
EGFR1	CLTA	0.134503	-0.05987	
EGFR1	CLTC	-0.11005	-0.47524	
EGFR1	**CSTB**	**-0.70976**	**-0.73884**	**lower in good embryos and higher at OC3**
EGFR1	GSN	0.367776	0.708319	
EGFR1	ACTN4	-0.15753	-0.02493	

EGFR1	STIP1	-0.22733	-0.07429	
EGFR1	**ALB**	**-0.40313**	**0.311389**	**higher in good embryos and at OC3**
EGFR1	TAGLN2	-0.02868	0.046614	
EGFR1	**PLEC**	**-3.35314**	**0.82575**	**higher in good embryos and at OC3**
EGFR1	**KIAA1217**	**0.197866**	**-1.27964**	**lower in good embryos and at OC3**
EGFR1	PFN1	-0.26553	-0.10886	
EGFR1	WASL	0.109509	0.074823	
EGFR1	ALDOA	0.094877	-0.1873	
EGFR1	LDHA	-0.66682	-0.41988	
EGFR1	**CBLB**	**-0.69252**	**0.983516**	**higher in good embryos and at OC3**
EGFR1	CDC42	-0.13389	-0.05502	
EGFR1	CDH1	-0.28812	-0.19979	
EGFR1	MVP	-0.60227	-0.17915	
EGFR1	PGAM1	-0.4681	-0.49507	
EGFR1	ACTR3	0.212629	0.154175	
EGFR1	**ACTR2**	**1.109122**	**-0.1015**	**lower in good embryos and at OC3**
EGFR1	VCL	-0.10005	-0.11923	
EGFR1	IQGAP1	-0.43772	-0.2842	
EGFR1	EEF1A1	-0.58419	-0.70752	

Table S6-9 Univariate analysis of ULF according to EQ1 embryo classification of REIMS features in negative ionisation mode.

FDRcorr	p	MW	Column1	Potential id
0.00090751	>0.001	539.6951	Gr3>all	None
0.00140161	0.005	626.6677	Gr3>all	None
0.00288648	>0.001	535.7748	Gr3>all	None
0.003	0.001	533.7749	Gr3>all	None
0.016	0.003	655.6149	Gr3>(1c,2-16)	5 candidates
0.043	0.007	825.5636	Gr3>all	Many
0.04999084	0.01	181.0208	Gr3<(1c=216)	2-methyl-1,3-thiazolidine-2-carboxamide
0.19	0.022	599.6497	NS	
0.19	0.023	593.7315	NS	
0.26	0.038	597.6531	NS	
0.00414367	0.09	624.6703	NS	
0.00414367	0.014	564.716	NS	
0.00416313	0.019	566.7119	NS	
0.00428122	0.019	1128.61	NS	
0.00608721	0.15	682.6269	NS	
0.00614137	0.087	651.6882	NS	
0.00620309	0.00098306	572.6311	NS	
0.00889328	0.00142349	508.7549	NS	
0.01389071	0.00226742	678.4923	NS	
0.01389071	0.00225714	678.7061	NS	
0.01464662	0.00241402	736.6637	NS	
0.01520787	0.00253063	506.7565	NS	
0.01769041	0.00297176	384.7109	NS	
0.01919969	0.00325573	790.7008	NS	
0.02239045	0.00383228	324.7554	NS	

0.02782447	0.00480645	709.6478	NS
0.02812154	0.04	390.8445	NS
0.02862979	0.04	243.9629	NS
0.02912725	0.035	446.6611	NS
0.03062952	0.00551298	363.8261	NS
0.03062952	0.14	848.6588	NS
0.03667705	0.073	794.4069	NS
0.03775004	0.04	386.7066	NS
0.03970566	0.07	591.7329	NS
0.04127559	0.13	444.664	NS
0.04232915	0.09	680.4885	NS
0.04766125	0.089	707.5063	NS
0.04766125	0.093	411.7286	NS
0.04909755	0.11	583.6026	NS
0.04909755	0.086	676.7088	NS
0.12	0.011	550.9904	NS
0.05072055	0.01012803	208.8395	NS
0.05391694	0.01085174	644.7677	NS
0.05993325	0.01215762	270.7928	NS
0.06254254	0.01278603	618.7534	NS
0.06316271	0.01301292	388.7031	NS
0.06415877	0.01331981	326.7532	NS
0.06551489	0.01370517	763.6838	NS
0.06612604	0.01393782	353.7707	NS
0.06898885	0.01465056	355.7671	NS
0.07086561	0.01516142	266.7989	NS
0.07533786	0.01623764	875.6808	NS
0.07567849	0.01643099	622.5318	NS
0.07682522	0.01680171	268.7954	NS
0.07886346	0.01737246	272.79	NS

0.08281468	0.0183741	559.7809	NS
0.0844277	0.01886578	1240.602	NS
0.08451835	0.01915392	155.9496	NS
0.08451835	0.01902476	620.7518	NS
0.08483254	0.0194005	96.91983	NS
0.08483254	0.01949401	703.7278	NS
0.08544834	0.01977093	471.6825	NS
0.08723289	0.02032208	295.8139	NS
0.08843567	0.02074244	504.6192	NS
0.09013532	0.02128393	469.6863	NS
0.09098163	0.02219861	92.92608	NS
0.09098163	0.02187557	293.8167	NS
0.09098163	0.0223489	529.64	NS
0.09098163	0.02226975	531.6375	NS
0.09098163	0.02188132	761.6858	NS
0.09098163	0.02229807	815.7227	NS
0.09264427	0.02290413	527.6441	NS
0.09498292	0.02363283	846.6607	NS
0.09806371	0.02455478	1155.624	NS
0.09818649	0.02474113	705.7262	NS
0.09910593	0.02512987	468.1563	NS
0.10312472	0.02631233	179.8993	NS
0.1035734	0.02659095	560.7955	NS
0.10529583	0.02720003	154.8752	NS
0.10686447	0.0277746	701.512	NS
0.11013667	0.0287996	506.6158	NS
0.11301812	0.02973218	1325.577	NS
0.11536175	0.03053156	900.699	NS
0.12037208	0.03204835	995.3561	NS
0.12622512	0.03380673	384.1823	NS

0.14434974	0.03888979	383.1797	NS
0.15765839	0.04297503	995.298	NS
0.15765839	0.04284043	612.6213	NS
0.18196784	0.04988976	448.7998	NS
0.1835841	0.05062383	645.7722	NS
0.1886606	0.05232267	442.6681	NS
0.19024474	0.05306351	391.8063	NS
0.19156174	0.05373443	338.9772	NS
0.19252572	0.05430995	444.0953	NS
0.19388014	0.05499928	225.866	NS
0.19977577	0.05698833	150.8853	NS
0.2005004	0.05751279	235.8594	NS
0.20056228	0.05784839	788.7028	NS
0.20649547	0.05988696	452.2774	NS
0.21315574	0.06215635	421.1306	NS
0.21659357	0.06350208	865.5443	NS
0.23048692	0.06794068	215.8763	NS
0.23620016	0.0699991	954.2307	NS
0.23865684	0.07110536	94.92291	NS
0.24723715	0.0740536	152.8816	NS
0.24945446	0.07511307	171.9436	NS
0.2537481	0.07680806	446.0926	NS
0.25444729	0.07809753	905.7243	NS
0.25444729	0.07768705	476.7849	NS
0.25444729	0.07822943	1070.649	NS
0.27201308	0.0843084	356.1534	NS
0.27201308	0.08449218	616.5384	NS
0.27438622	0.08566416	186.1204	NS

Table S7-1a,b Earle's salts and TCM 199 medium composition

a Earle's salts

Components	**g/l**
Calcium Chloride•2 H2O	0.265
Magnesium sulfate (anhydrous)	0.098
Potassium chloride	0.4
Sodium chloride	6.8
Sodium phosphate monobasic (anhydrous)	0.122
D-glucose	1
Phenol red•Na	0.011

b TCM199

Component	**g/l**
Inorganic salts	
Calcium Chloride	0.1396
Ferric Nitrate • $9H_2O$	0.0007
Magnesium Sulfate (anhydrous)	0.0977
Potassium Chloride	0.4
Potassium Phosphate Monobasic	0.06
Sodium Acetate (anhydrous)	0.05
Sodium Chloride	8
Sodium Phosphate Dibasic (anhydrous)	0.0479
Amino Acids	
L-Alanine	0.025
L-Arginine • HCl	0.07
L-Aspartic Acid	0.03

L-Cysteine • HCl • H_2O	0.0001
L-Cystine • 2HCl	0.026
L-Glutamic Acid	0.0668
L-Glutamine	0.1
Glycine	0.05
L-Histidine • HCl • H_2O	0.0219
Hydroxy-L-Proline	0.01
L-Isoleucine	0.02
L-Leucine	0.06
L-Lysine • HCl	0.07
L-Methionine	0.015
L-Phenylalanine	0.025
L-Proline	0.04
L-Serine	0.025
L-Threonine	0.03
L-Tryptophan	0.01
L-Tyrosine • 2Na • $2H_2O$	0.0577
L-Valine	0.025
Vitamins	
Ascorbic Acid • Na	0.00006
D-Biotin	0.00001
Calciferol	0.0001
Choline Chloride	0.0005
Folic Acid	0.00001
Menadione (sodium bisulfite)	0.00002
myo-Inositol	0.00005
Niacinamide	0.00003

Nicotinic Acid	0.00003
p-Aminobenzoic Acid	0.00005
D-Pantothenic Acid (hemicalcium)	0.00001
Pyridoxal • HCl	0.00003
Pyridoxine • HCl	0.00003
Retinol Acetate	0.0001
Riboflavin	0.00001
DL-α-Tocopherol Phosphate • Na	0.00001
Thiamine • HCl	0.00001
Other	
Adenine Sulfate	0.01
Adenosine Triphosphate • 2Na	0.001
Adenosine Monophosphate • Na	0.0002
Cholesterol	0.0002
Deoxyribose	0.0005
Glucose	1
Glutathione (reduced)	0.00005
Guanine • HCl	0.0003
Hypoxanthine	0.0003
Phenol Red • Na	0.0213
Polyoxyethylenesorbitan Monooleate (TWEEN 80)	0.02
Ribose	0.0005
Thymine	0.0003
Uracil	0.0003
Xanthine • Na	0.0003

Table S7-2 Exp. E1, E2, E3: raw data - number of embryos classified by stage and grade in each run (replicate).

Run	Treatment	No. oocytes in IVC	No. of 1-cells	No. of TM D5	No. <8 cells	No. deg(>8 cells)	Total Devel-opment (No.TMs & B) on Day 7	Total No. of blastocysts on Day 7	No. of G1,2 Bs on Day 7	No. of additional B on D8 (dev. from TMs on D7)
E1-1	Overall	136	4	CysC: Exp E1, run (replicate) 1						
E1-1	LSOF + PVA (Control)	25		10	4	1	20	15	5	6
E1-1	Lab Std+BSA	23		5	2	9	12	11	6	1
E1-1	0µg/ml CysC	25		5	6	8	11	2	2	4
E1-1	0.1µg/ml CysC	25		6	10	3	12	7	6	0
E1-1	10µg/ml CysC	25		10	8	4	13	8	2	3
E1-2	Overall	167	6	CysC: Exp E1, run (replicate) 2						
E1-2	LSOF + PVA (Control)	30		13	4	1	25	20	9	0
E1-2	Lab Std+BSA	22		12	0	3	19	19	9	0
E1-2	0µg/ml CysC	30		6	9	4	17	10	3	6
E1-2	0.1µg/ml CysC	30		11	6	8	16	15	11	0
E1-2	10µg/ml CysC	30		9	5	6	19	11	9	5
E1-3	Overall	215	9	CysC: Exp E1, run (replicate) 3						
E1-3	LSOF + PVA (Control)	54		30	4	16	34	31	28	3
E1-3	0.1µg/ml Cystatin C	53		22	16	5	32	30	18	0
E1-3	1.0µg/ml Cystatin C	54		30	18	5	31	30	15	1
E1-3	10µg/ml Cystatin C	54		22	0	31	23	13	10	0
E2-1	Overall	295	19	CatB: Exp E2, run (replicate) 1						
E2-1	LSOF + PVA (Control)	38		9	13	7	18	13	10	1
E2-1	0ng/ml Cathepsin (water added)	42		15	14	5	24	16	11	4
E2-1	15ng/ml Cathepsin	42		13	9	12	21	18	9	3

E2-1	30ng/ml Cathepsin	42		10	15	5	22	20	13	1
E2-1	60ng/ml Cathepsin	42		10	13	6	23	19	11	0
E2-1	90ng/ml Cathepsin	43		10	17	13	12	9	7	2
E2-2	Overall	243	15	CatB: Exp E2, run (replicate) 2						
E2-2	LSOF + PVA (Control)	27		7	5	7	15	11	8	2
E2-2	0ng/ml Cathepsin (water added)	37		6	9	7	19	10	5	6
E2-2	15ng/ml Cathepsin	37		7	4	9	24	19	12	3
E2-2	30ng/ml Cathepsin	37		6	11	6	20	17	14	2
E2-2	60ng/ml Cathepsin	37		4	13	8	16	8	4	2
E2-2	90ng/ml Cathepsin	36		9	4	7	26	19	12	3
E2-3	Overall	182	13	CatB: Exp E2, run (replicate) 3						
E2-3	LSOF + PVA (Control)	30		17	4	6	21	18	10	1
E2-3	0ng/ml Cathepsin (water added)	30		11	5	10	16	14	11	1
E2-3	15ng/ml Cathepsin	31		12	9	9	11	8	4	0
E2-3	30ng/ml Cathepsin	30		10	5	8	19	18	10	0
E2-3	60ng/ml Cathepsin	30		9	10	6	15	11	7	3
E2-3	90ng/ml Cathepsin	31		9	8	9	13	11	9	0
E3-1	Overall	212	15	Pyruvate kinase M: Exp E3, run (replicate) 1						
E3-1	LSOF+PVA-DNP (Control)	53		n/a	6	12	35	30	18	6
E3-1	0.1µg/ml Pyruvate Kinase	52		n/a	10	7	37	28	14	7
E3-1	1.0µg/ml Pyruvate Kinase	53		n/a	7	14	32	27	15	7

E3-1	10µg/ml Pyruvate Kinase	54		n/a	8	7	37	26	11	8
E3-2	Overall	175	15	Pyruvate kinase M: Exp E3, run (replicate) 2						
E3-2	LSOF+PVA-DNP (Control)	45		n/a	0	19	26	20	9	6
E3-2	0.1µg/ml Pyruvate Kinase	44		n/a	0	22	20	15	4	3
E3-2	1.0µg/ml Pyruvate Kinase	42		n/a	17	4	20	18	9	3
E3-2	10µg/ml Pyruvate Kinase	44		n/a	8	12	24	17	12	3
E3-3	Overall	198	11	Pyruvate kinase M: Exp E3, run (replicate) 3						
E3-3	LSOF+PVA-DNP (Control)	48		n/a	12	9	27	19	9	3
E3-3	0.1µg/ml Pyruvate Kinase	50		n/a	0	18	32	22	22	2
E3-3	1.0µg/ml Pyruvate Kinase	50		n/a	8	8	19	15	10	6
E3-3	10µg/ml Pyruvate Kinase	50		n/a	8	9	33	20	13	13

Table S7-3 Embryo development parameters reported in experiments conducting *in vitro* embryo culture.

Study	Cleavage day 2 (%)	B/oocytes day 7 (%)	TM-B/cleaved day 7 (%)	B/cleaved day 7 (%)	B1-2/cleaved day 7 (%)
Matoba et al. 2010	50	15			
Matoba et al. 2014	80	22			
Zullo et al. 2016a	78		50		42-46
Zullo et al. 2016b	76		38-53		34-46±8.7
Sang et al. 2020	61	14-33			
Lopes et al. 2020	86	26			
Hill et al. 2008	60		40	30	
Leroy et al. 2005	76	22-33		29-43	
Azari-Dolatabad et al. 2019	87	30			
Gilardi et al. 2004	21-67	24-38		Mar-45	
AVERAGE	**73**	**25**	**44**	**31**	**39**

Table S7-4a General linear models analysis: Exp E1 (CysC)

Outcome var	Factor	Estimate	Std. Error	t value	P(>|t|)
TM_D5	(Intercept)	-0.58368	0.229615	-2.54199	0.038552
TM_D5	df$Group_protCys_0.1	-0.43579	0.299324	-1.45592	0.188752
TM_D5	df$Group_protCys_10	0.681535	0.382692	1.780896	0.11814
TM_D5	$NH_4HCO_3$1	-0.97909	0.344798	-2.83961	0.025059
TM_D5	Run2	0.352952	0.257221	1.372176	0.212362
TM_D5	Run3	0.663298	0.306716	2.162579	0.067351
TM_B_D7	(Intercept)	0.84089	0.271842	3.093299	0.017486
TM_B_D7	df$Group_protCys_0.1	-0.88948	0.354371	-2.51001	0.040396
TM_B_D7	df$Group_protCys_10	0.20614	0.453071	0.454984	0.662896
TM_B_D7	$NH_4HCO_3$1	-1.14448	0.408208	-2.80368	0.026384
TM_B_D7	Run2	0.634292	0.304524	2.082894	0.075761
TM_B_D7	Run3	-0.01383	0.363122	-0.0381	0.970675
B_D7	(Intercept)	0.135266	0.30521	0.443191	0.671001
B_D7	df$Group_protCys_0.1	-0.84662	0.397869	-2.12789	0.07089
B_D7	df$Group_protCys_10	0.778473	0.508683	1.530369	0.169779
B_D7	$NH_4HCO_3$1	-2.21515	0.458313	-4.83328	0.001892
B_D7	Run2	1.024282	0.341904	2.995822	0.02006
B_D7	Run3	0.431026	0.407694	1.05723	0.325521
B1,2_D7	(Intercept)	-1.17524	0.215305	-5.45847	0.000947
B1,2_D7	df$Group_protCys_0.1	-0.13807	0.28067	-0.49192	0.637824
B1,2_D7	df$Group_protCys_10	0.570035	0.358842	1.588539	0.156188
B1,2_D7	$NH_4HCO_3$1	-1.51045	0.323309	-4.67185	0.002283
B1,2_D7	Run2	0.731807	0.24119	3.034149	0.019003
B1,2_D7	Run3	0.843908	0.287601	2.934302	0.02189

<8 cells	(Intercept)	-2.12889	1.222405	-1.74156	0.125123
<8 cells	df$Group_protCys_0.1	2.388666	1.593514	1.498993	0.177553
<8 cells	df$Group_protCys_10	-1.58354	2.037341	-0.77726	0.462461
<8 cells	$NH_4HCO_3$1	1.758912	1.835603	0.95822	0.369869
<8 cells	Run2	-1.26001	1.369367	-0.92014	0.388107
<8 cells	Run3	-2.14939	1.632866	-1.31633	0.229526
Deg_>8 cells	(Intercept)	-1.96081	0.640731	-3.06027	0.018317
Deg_>8 cells	df$Group_protCys_0.1	0.072965	0.83525	0.087357	0.932834
Deg_>8 cells	df$Group_protCys_10	0.119015	1.067885	0.11145	0.914388
Deg_>8 cells	$NH_4HCO_3$1	0.793871	0.962143	0.825108	0.436522
Deg_>8 cells	Run2	-0.2917	0.717762	-0.4064	0.696584
Deg_>8 cells	Run3	0.689435	0.855877	0.80553	0.447009

Table S7-4b General linear models analysis: Exp E2 (CatB)

Outcome var	Factor	Estimate	Std. Error	t value	Pr(>|t|)
TM_D5	(Intercept)	-0.84955	0.176301	-4.81876	0.000537
TM_D5	df$Group_protzCath_15	-0.53955	0.236533	-2.28108	0.043453
TM_D5	df$Group_protzCath_30	-0.31667	0.236533	-1.33878	0.207653
TM_D5	df$Group_protzCath_60	-0.03819	0.236533	-0.16146	0.874661
TM_D5	df$Group_protzCath_90	-0.0943	0.236533	-0.39868	0.697762
TM_D5	Run4	-0.48599	0.193128	-2.51641	0.028658
TM_D5	Run5	0.486121	0.193128	2.517086	0.028623
TM_B_D7	(Intercept)	-0.07547	0.269353	-0.28019	0.784532
TM_B_D7	df$Group_protzCath_15	-0.15526	0.361375	-0.42964	0.675754
TM_B_D7	df$Group_protzCath_30	0.161336	0.361375	0.446452	0.663932
TM_B_D7	df$Group_protzCath_60	-0.0846	0.361375	-0.23411	0.819201
TM_B_D7	df$Group_protzCath_90	0.029672	0.361375	0.082108	0.936036
TM_B_D7	Run4	0.366655	0.295061	1.242641	0.239838
TM_B_D7	Run5	0.180117	0.295061	0.610441	0.553972
B_D7	(Intercept)	-0.50745	0.285831	-1.77535	0.103478
B_D7	df$Group_protzCath_15	-0.28976	0.383483	-0.75561	0.465756
B_D7	df$Group_protzCath_30	0.451698	0.383483	1.177882	0.263699

B_D7	df$Group_prot-zCath_60	-0.01259	0.383483	-0.03282	0.974406
B_D7	df$Group_prot-zCath_90	-0.15515	0.383483	-0.40459	0.693536
B_D7	Run4	0.06301	0.313113	0.201238	0.844185
B_D7	Run5	0.251883	0.313113	0.804449	0.438179
B1,2_D7	(Intercept)	-1.01806	0.256337	-3.97159	0.00219
B1,2_D7	df$Group_prot-zCath_15	-0.4964	0.343912	-1.44341	0.176774
B1,2_D7	df$Group_prot-zCath_30	0.299101	0.343912	0.869704	0.403041
B1,2_D7	df$Group_prot-zCath_60	-0.33861	0.343912	-0.98457	0.345994
B1,2_D7	df$Group_prot-zCath_90	-0.20033	0.343912	-0.58251	0.571972
B1,2_D7	Run4	0.013414	0.280803	0.04777	0.962756
B1,2_D7	Run5	0.151541	0.280803	0.53967	0.600179
<8 cells	(Intercept)	-0.85857	0.263274	-3.26112	0.007584
<8 cells	df$Group_prot-zCath_15	0.533339	0.353219	1.509937	0.159238
<8 cells	df$Group_prot-zCath_30	0.233326	0.353219	0.660571	0.522481
<8 cells	df$Group_prot-zCath_60	-0.16646	0.353219	-0.47127	0.646654
<8 cells	df$Group_prot-zCath_90	0.093965	0.353219	0.266025	0.79514
<8 cells	Run4	-0.63612	0.288402	-2.20566	0.049593
<8 cells	Run5	-0.54558	0.288402	-1.89174	0.085132
Deg_>8 cells	(Intercept)	-1.3828	0.184137	-7.50964	1.19E-05

Deg_>8 cells	df$Group_prot-zCath_15	-0.33072	0.247046	-1.33871	2.08E-01
Deg_>8 cells	df$Group_prot-zCath_30	-0.38025	0.247046	-1.53918	1.52E-01
Deg_>8 cells	df$Group_prot-zCath_60	0.205331	0.247046	0.831146	4.24E-01
Deg_>8 cells	df$Group_prot-zCath_90	-0.22564	0.247046	-0.91334	3.81E-01
Deg_>8 cells	Run4	0.172758	0.201712	0.856456	4.10E-01
Deg_>8 cells	Run5	0.461093	0.201712	2.285895	4.31E-02

Table S7-4c General linear models analysis: Exp E3 (PKM)

Outcome var	Factor	Estimate	Std. Er-ror	t value	Pr(>|t|)
TM_B_D7	(Intercept)	0.769545	0.192803	3.991355	0.007189
TM_B_D7	df$Group_prot-PKM_0.1	0.172845	0.22263	0.776379	0.467018
TM_B_D7	df$Group_prot-PKM_1	-0.46453	0.22263	-2.08656	0.081987
TM_B_D7	df$Group_prot-PKM_10	-0.01973	0.22263	-0.08864	0.932253
TM_B_D7	Run7	-0.6371	0.192803	-3.30443	0.016318
TM_B_D7	Run9	-0.44158	0.192803	-2.29034	0.061915
B_D7	(Intercept)	0.231949	0.149311	1.55346	0.171305
B_D7	df$Group_prot-PKM_0.1	-0.1626	0.17241	-0.94308	0.382044
B_D7	df$Group_prot-PKM_1	-0.23898	0.17241	-1.38612	0.215026

B_D7	df$Group_prot-PKM_10	-0.14867	0.17241	-0.86229	0.421649
B_D7	Run7	-0.50256	0.149311	-3.36586	0.01512
B_D7	Run9	-0.57358	0.149311	-3.84153	0.008544
B1,2_D7	(Intercept)	-0.99014	0.419329	-2.36125	0.056188
B1,2_D7	df$Group_prot-PKM_0.1	0.058378	0.484199	0.120565	0.907971
B1,2_D7	df$Group_prot-PKM_1	-0.0325	0.484199	-0.06712	0.948663
B1,2_D7	df$Group_prot-PKM_10	-0.02532	0.484199	-0.05229	0.959992
B1,2_D7	Run7	-0.50225	0.419329	-1.19774	0.276185
B1,2_D7	Run9	-0.04494	0.419329	-0.10717	0.918151
<8 cells	(Intercept)	-2.86628	1.940437	-1.47713	0.190108
<8 cells	df$Group_prot-PKM_0.1	2.500062	2.240624	1.115789	0.307196
<8 cells	df$Group_prot-PKM_1	2.81354	2.240624	1.255695	0.255911
<8 cells	df$Group_prot-PKM_10	-0.97596	2.240624	-0.43557	0.678379
<8 cells	Run7	-2.71982	1.940437	-1.40165	0.210572
<8 cells	Run9	-1.04859	1.940437	-0.54039	0.608389
Deg_>8 cells	(Intercept)	-1.27574	0.499914	-2.55192	0.043378
Deg_>8 cells	df$Group_prot-PKM_0.1	-0.44976	0.577251	-0.77914	0.465511
Deg_>8 cells	df$Group_prot-PKM_1	-0.64179	0.577251	-1.1118	0.308777
Deg_>8 cells	df$Group_prot-PKM_10	0.176353	0.577251	0.305505	0.770303

Deg_>8 cells	Run7	0.618095	0.499914	1.236403	0.26251
Deg_>8 cells	Run9	0.200471	0.499914	0.40101	0.702303